Springer Series in Materials Science 241

Kwang Soo Cho

Viscoelasticity of Polymers

Theory and Numerical Algorithms

Springer

Springer Series in Materials Science

Volume 241

The Springer Series in Materials Science covers the complete spectrum of materials physics, including fundamental principles, physical properties, materials theory and design. Recognizing the increasing importance of materials science in future device technologies, the book titles in this series reflect the state-of-the-art in understanding and controlling the structure and properties of all important classes of materials.

More information about this series at http://www.springer.com/series/856

Kwang Soo Cho

Viscoelasticity of Polymers

Theory and Numerical Algorithms

Springer

Kwang Soo Cho
Polymer Science and Engineering
Kyungpook National University
Daegu
Korea, Republic of (South Korea)

ISSN 0933-033X ISSN 2196-2812 (electronic)
Springer Series in Materials Science
ISBN 978-94-017-7562-5 ISBN 978-94-017-7564-9 (eBook)
DOI 10.1007/978-94-017-7564-9

Library of Congress Control Number: 2016932346

Printed on acid-free paper

This Springer imprint is published by SpringerNature
The registered company is Springer Science+Business Media B.V. Dordrecht

To my wife (Minjee Kim) and son (Hanwhi Cho) who are the delayers of my research and the prime movers of my life

Preface

Viscoelasticity or rheology is important in polymer science and engineering because it plays a crucial role in production and characterization of polymeric materials. Understanding the viscoelasticity of polymers requires knowledge of various disciplines such as continuum mechanics, thermodynamics, advanced applied mathematics, polymer physics, and statistical mechanics. Rheology of polymers is studied by the researchers from various fields such as polymer scientists, mechanical engineers, chemical engineers, physicists, and chemists. Hence, it is hard to expect that a newcomer to the field of polymer viscoelasticity would be familiar with such diverse disciplines. From this viewpoint, one may feel the necessity of a book which addresses basic sciences for polymer viscoelasticity as possible as many. Examples of such comprehensive books of rheology are "Dynamics of Polymeric Liquids, volume I and II" written by Bird and coauthors, and "Engineering Rheology" written by Tanner. The book of Bird and coauthors does not contain numerical methods for nonlinear viscoelastic flows while the book of Tanner deals with it. Even though both books are comprehensive rheology books, in the author's opinion, the former is focused on development of constitutive equation while the latter is oriented to the application of constitutive equation to polymer processing. Because it is practically impossible to write a comprehensive book of rheology which contains everything of rheology, most famous books of rheology have their own orientation indicating authors' expertise, with addressing sufficient amount of basic knowledges. The author intends to write a comprehensive rheology book with the orientation to the identification of the rheological properties of polymers from their experimental data. This has been one of the themes of the author's research for recent 10 years.

Any single book cannot satisfy all readers because each reader has different backgrounds and different maturity in their knowledge. When the author was a master-degree student, he thought that Larson's book, "Constitutive Equations of Polymer Melts and Solutions," is not good because it is so compact. However, when he read the book after his Ph.D., he recognized that it is one of well-made rheology books. The present book assumes the readers to have strong background

of engineering mathematics of undergraduate level. The readers do not have to be familiar with tensor analysis because it is given in the book. This book is designed for experimental rheologists, who are strong in mathematics, as well as for students, who want to be familiar with theoretical rheology.

The book consists of three parts. The first part provides fundamental principles which should be necessary to understand the other parts: linear and nonlinear viscoelasticity. This part briefly addresses necessary mathematics, continuum mechanics and thermodynamics, statistical mechanics and polymer physics.

As the book is oriented to the rheological identification of polymers from the experimental data, the second part of linear viscoelasticity contains basic numerical methods which are useful for viscoelastic spectrum, time–temperature superposition, and application of linear viscoelastic principles to polymeric systems. Different from previous rheology books, this part is devoted to numerical algorithms of data processing which is expected to be helpful for experimentalists.

The last part starts from theory of nonlinear constitutive equation in order to explain large amplitude oscillatory shear (LAOS). The last chapter on LAOS is one of the most remarkable features of this book which makes the book different from previous well-made books of rheology.

The author appreciates for the help of a number of persons: his teachers, colleagues, students, and family. Without their help, this book could not have been written. Professor Jinyoung Park, Dongchoon Hyun, Dongyoon Lee, and Dr. Jung-Eun Bae are thankful for the review of the manuscript. Several parts of the book have resulted from the research with my old student, Dr. Jung-Eun Bae. Work cannot be in isolation. The author owes the present work to his teachers who taught him. Especially, Prof. Sangyong Kim made him to recognize the pleasure of academic career. The author cannot forget his students because his research results included in the book cannot be obtained without their assistance. This book was supported by Kyungpook National University Research Fund 2011.

Daegu, Korea Kwang Soo Cho

Contents

Part I Fundamental Principles

1 Preliminary Mathematics 3
1 Vector Space 3
1.1 Definition of Vector Space 3
1.2 Linear Combination and Basis 5
1.3 Dual Space 8
2 Inner Product Space 10
2.1 Generalization of Inner Product 10
2.2 Generalization of Distance 12
2.3 Orthogonalized Basis 13
2.4 Application of Orthogonal Polynomials 20
2.5 Summation Convention 23
3 Coordinate System and Basis 26
3.1 How to Construct a Coordinate System 26
3.2 Cylindrical and Spherical Coordinate Systems 32
3.3 Change of Coordinate Systems 34
4 Vector Analysis 37
4.1 Vector Algebra 37
4.2 Differentiation of Vector 39
4.3 Integration of Vector and Scalar 44
5 Tensor Analysis 54
5.1 Polyadic Notation of Linear Transform 54
5.2 Tensor Algebra 58
5.3 Tensor Calculus 70
6 Fourier and Laplace Transforms 74
6.1 The Dirac Delta Function 75
6.2 Fourier Transform and Its Inversion 78
6.3 Dirac Delta Function Revisited 83
6.4 Laplace Transform and Its Inversion 84
References 90

2 Continuum Thermomechanics 93
1 Kinematics 94
1.1 Material and Spatial Coordinates 94
1.2 Strain 96
1.3 Deformation of Area and Volume 100
1.4 Rate of Deformation 101
1.5 Relative Deformation Gradient 104
2 Balance Equations 110
2.1 Mass Balance 110
2.2 Momentum Balance 112
2.3 Energy Balance: The First Law of Thermodynamics 118
2.4 Balance Equations in Terms of Flux 121
3 Classical Constitutive Equations 124
3.1 Elasticity 124
3.2 Viscous Fluids 131
3.3 Viscoelastic Models 136
4 Thermodynamics 146
4.1 Equilibrium Thermodynamics 146
4.2 Classical Irreversible Thermodynamics 154
4.3 Theory of Internal Variables 160
5 Principle of Constitutive Equation 166
5.1 Upper-Convective Maxwell Model 166
5.2 Principle of Material Frame Indifference 169
References 175

3 Statistical Mechanics 177
1 Probability Theory 178
1.1 Moments and Cumulants 179
1.2 Statistical Independence 181
1.3 The Central Limit Theorem 182
1.4 Gaussian Distribution 185
2 Equilibrium Statistical Mechanics 188
2.1 Ensemble Theory 188
2.2 Fluctuations and Equivalence of Ensembles 196
2.3 The Equipartition Theorem and the Virial Theorem 204
3 Brownian Motion 211
3.1 Langevin Equation 211
3.2 Diffusion Equation 214
3.3 Liouville Equation 216
3.4 Generalized Langevin Equation 219
3.5 The Fokker–Planck Equation 223
References 229

4 Polymer Physics 231
1 Polymer Structure 231
1.1 Definition of Polymer 231
1.2 Structure of a Single Polymer Chain 233
1.3 Structure of Assembly of Polymer Chains 236
2 Chain Conformation and Size of Polymer Chain 239
2.1 Size of Polymer Chain 239
2.2 Chain Models and Universality 242
2.3 Size Distribution 250
2.4 Molecular Weight and Molecular Weight Distribution 254
3 Polymer Solution 260
3.1 Polymer Concentration 260
3.2 Concentration Regimes 261
3.3 Entanglement 264
4 Rubber Elasticity 267
4.1 Thermodynamics of Rubber 268
4.2 Statistical Mechanical Theory 269
4.3 Phenomenological Models 272
References 280

Part II Linear Viscoelasticity

5 Theory of Linear Viscoelasticity 285
1 Fundamental Theory 285
1.1 The Origin of Viscoelasticity 285
1.2 The Boltzmann Superposition Principle 287
1.3 Dynamic Experiment 293
1.4 The Kramers–Kronig Relations 298
1.5 Thermodynamic Analysis 299
2 Measurement of Linear Viscoelasticity 302
2.1 Devices and Instruments 302
2.2 Preliminary Tests 303
2.3 Inertia Effect in Stress-Controlled Rheometer 310
2.4 Diffusion Wave Spectroscopy 313
3 Phenomenological Models 316
3.1 Spring–Dashpot Models Revisited 316
3.2 Parsimonious Models 321
3.3 Models Based on Fractional Derivatives 327
4 Molecular Theories 332
4.1 Dynamic Equation 332
4.2 The Stress of Polymeric Fluid 337
4.3 The Rouse Model 338
4.4 The Zimm Model 344

4.5 The Doi–Edwards Model 344
4.6 Modification of the Doi–Edwards Model 353
References 357

6 Numerical Methods 361
1 Polynomial Regression 362
1.1 Basics 362
1.2 Use of Orthogonal Polynomials. 363
1.3 B-Spline Regression 366
2 Nonlinear Regression 369
2.1 Basics 369
2.2 The Levenberg–Marquardt Algorithm 370
2.3 Example I 371
2.4 Example II 374
3 Padé Approximation. 377
3.1 Basics 377
3.2 Application to the FENE Model 379
3.3 Application to Discrete Spectrum 380
4 Numerical Integration and Differentiation 382
4.1 Error Analysis of Integration of Experimental Data 383
4.2 Numerical Differentiation with Regularization 385
5 Discrete Fourier Transform 392
5.1 Fourier Series 392
5.2 Discrete Fourier Transform. 393
References 395

7 Viscoelastic Spectrum 397
1 Fundamentals 397
1.1 Importance of Spectrum 397
1.2 The Fuoss–Kirkwood Relations. 398
1.3 Ill-Posedness of Spectrum 406
1.4 Some Important Equations and Inequalities. 408
2 Algorithms for Continuous Spectrum 411
2.1 Regularization Method. 411
2.2 Fixed-Point Iteration 414
2.3 Power Series Approximation. 416
2.4 Other Algorithms 422
2.5 Comparison of Algorithms 425
3 Algorithms for Discrete Spectrum 427
3.1 Nonlinear Least Squares. 427
3.2 The Padé–Laplace Methods 429
3.3 Approximation from Continuous Spectrum 430
References 434

8 Time-Temperature Superposition 437
1 Fundamentals of TTS 437
1.1 Phenomenology of TTS 437
1.2 Temperature Dependence of Shift Factor 442
1.3 Molecular Explanation of TTS 445
2 Geometric Interpretation 447
2.1 Geometric Analogy to TTS 447
2.2 New Master Curve 448
2.3 Application of Numerical Differentiation 452
3 Algorithms for TTS 454
3.1 Nonlinear Regression Method 454
3.2 Minimization of Arc Length 455
References 456

9 Applications to Polymer Systems 459
1 Interconversion of Various Experimental Data 459
1.1 Static Data to Dynamic Data 459
1.2 Laplace Transform from Dynamic Data 467
2 Polymer Melts and Solutions 468
2.1 Monodisperse Linear Polymer in Molten State 468
2.2 Polydisperse Polymer Melts 473
2.3 Polymer Solution 477
3 Immiscible Blend of Polymers 479
3.1 Mixture of Newtonian Fluids 480
3.2 The Gramespacher and Meissner Model 481
3.3 The Palierne Model 483
3.4 Comparison of the GM and the Palierne Models 483
References 485

Part III Nonlinear Viscoelasticity

10 Nonlinear Constitutive Equations 491
1 Rheometrics 491
1.1 Shear Flow 492
1.2 Measurement of Steady Viscoelastic Functions 496
1.3 Simple Elongational Flow 505
2 Models Based on Expansion 508
2.1 Rivlin–Ericksen Expansion 508
2.2 Green–Rivlin Expansion 510
3 Generalization of Linear Viscoelastic Models 513
3.1 Oldroyd Generalization 513
3.2 K-BKZ Model 516

4 Models Based on Speculation of Structure 521
4.1 Spring-Dumbbell Models 521
4.2 Temporary Network Approaches 532
4.3 Multimode Versions 534
5 Thermodynamic Theory 537
5.1 Leonov Model 537
5.2 Thermodynamic Analysis of Other Models 541
References 542

11 Large Amplitude Oscillatory Shear 545
1 Introduction to LAOS 545
1.1 Phenomenology of LAOS 545
1.2 Overview of LAOS Research 546
2 Methods of Analysis 549
2.1 FT-Rheology 549
2.2 Stress and Strain Decomposition 553
2.3 Scaling Theory of LAOS 563
3 Analytical Solution of LAOS 571
3.1 Convected Maxwell Models 572
3.2 Time–Strain Separable K-BKZ Model 582
3.3 Nonseparable Maxwell Models 583
4 Semi-analytical Method for LAOS 592
References 597

Appendix: Functional Derivative 601

Index 609

Part I
Fundamental Principles

Chapter 1
Preliminary Mathematics

Abstract This chapter addresses mathematical preliminaries necessary to understand polymer viscoelasticity assuming that the readers are familiar with engineering mathematics of sophomore. Analysis of vector and tensor is the majority of this chapter, which is necessary to understand constitutive theories of polymer viscoelasticity as well as the theory of polymer physics. Since the knowledge of functional analysis is also needed to understand numerical methods to be used for the processing of viscoelastic data, the vectors and tensors in this chapter include not only physical quantities but also generalized ones called abstract vectors. Because of this purpose, the analysis of vector and tensor starts from the notion of vector space which is an abstraction of physical vector. As for linear viscoelastic theory, both Fourier and Laplace transforms are frequently used. Since this book is not a text of mathematics, rigorous proofs will not be seriously considered. For the proofs, the readers should refer the related references.

1 Vector Space

1.1 Definition of Vector Space

Vector is defined as a quantity having both magnitude and direction as described in undergraduate text books. Although this definition is simple and intuitive, it is not convenient for the application to more general cases. Hence, we will adopt the abstraction of vector which is helpful for the description of the analysis of nonlinear viscoelasticity and the numerical methods of viscoelastic characterization in a unified manner.

One of the most intuitive examples of vector is a displacement vector which points from a position to another position. The sum of two displacement vectors is the vector obtained by parallelogram rule. This rule works for velocity and acceleration obtained by the differentiation of position vector which can be considered as a displacement vector issuing from the origin. Geometric consideration shows easily that velocity and acceleration follows the sum rule of displacement vector.

K.S. Cho, *Viscoelasticity of Polymers*, Springer Series
in Materials Science 241, DOI 10.1007/978-94-017-7564-9_1

However, experiment is needed to prove that force follows the sum rule of displacement vectors, though force has both magnitude and direction. The experimental proof is as simple as to show that when three forces exerted on a point are in equilibrium, the geometric sum of any set of two forces is equal to the opposite of the other force. Here, the opposite of a force is the vector having the same magnitude but opposite direction. Then, one becomes to know that every physical quantity considered as a vector follows the sum rule of displacement vector. As for displacement vector, scalar multiplication is defined as the replacement of the magnitude of the vector by the multiplication of the magnitude by the scalar but maintaining direction. These two binary operations can be used as the generalization of vector.

A set having the two binary operations called addition and scalar multiplication is called a vector space when the two binary operations satisfy the followings and the elements of the set are called vectors.

[1] Addition is commutative:

$$\mathbf{a}+\mathbf{b}=\mathbf{b}+\mathbf{a} \tag{1.1}$$

[2] As for three arbitrary vectors **u**, **v**, **w**, addition is associative:

$$(\mathbf{u}+\mathbf{v})+\mathbf{w}=\mathbf{u}+(\mathbf{v}+\mathbf{w}) \tag{1.2}$$

[3] The zero vector **0** is a unique vector such that for any vector **a**,

$$\mathbf{a}+\mathbf{0}=\mathbf{a} \tag{1.3}$$

[4] For every element of the set, there exists a unique vector $-\mathbf{a}$ such that

$$\mathbf{a}+(-\mathbf{a})=\mathbf{0} \tag{1.4}$$

[5] For any real number c and arbitrary vectors **a** and **b,** the scalar multiplication satisfies

$$c(\mathbf{a}+\mathbf{b})=c\mathbf{a}+c\mathbf{b} \tag{1.5}$$

[6] For any real numbers c and k, scalar multiplication on **a** satisfies

$$(c+k)\mathbf{a}=c\mathbf{a}+k\mathbf{a} \tag{1.6}$$

[7] Associate rule for scalar multiplication is valid for any two scalars c and k and a vector **a**:

$$c(k\mathbf{a})=(ck)\mathbf{a} \tag{1.7}$$

[8] Real number, unity is the identity of the scalar multiplication:

$$1\mathbf{a} = \mathbf{a} \tag{1.8}$$

Note that it is assumed that addition of any two elements of the set is also an element of the set and scalar multiplication of a vector also belongs to the set. More generally, complex number can replace the role of real number. However, we will not treat complex vector space, here, which involves complex number as scalar, because the complex vector is not relevant in mechanics of viscoelasticity.

It is easy to know that the set of continuous functions satisfies the definition of vector space and so does the set of matrices with the same form. Then, continuous function and matrix can be considered as abstract vector.

An example of a vector space, consider pairs of n real numbers denoted by $\mathbf{x} = (x_1, x_2, \ldots, x_n)$. Denote the set of all pairs of n real numbers as E^n. The set is a vector space when addition and scalar multiplication are defined as

$$\begin{aligned} \mathbf{x} + \mathbf{y} &= (x_1 + y_1, x_2 + y_2, \ldots, x_n + y_n) \in E^n \\ c\mathbf{x} &= (cx_1, cx_2, \ldots, cx_n) \in E^n \end{aligned} \tag{1.9}$$

It is easy to prove that E^n satisfies Eqs. (1.1)–(1.8). The vector space E^n is called n-dimensional Euclidean space. An $N \times M$ matrix is considered as a vector of E^{NM}, too.

1.2 Linear Combination and Basis

When m vectors, say, $\mathbf{a}_1, \ldots, \mathbf{a}_m$ are members of a vector space, a vector $\mathbf{x}$ is called a linear combination of the vectors $\mathbf{a}_1, \ldots, \mathbf{a}_m$, if there exist scalars $c_1, c_2, \ldots, c_m$ such that

$$\mathbf{x} = c_1\mathbf{a}_1 + \cdots + c_m\mathbf{a}_m \tag{1.10}$$

When making all of $c_1, c_2, \ldots, c_m$ zero is the only way to make the vector $\mathbf{x}$ of Eq. (1.10) the zero vector, the vectors $\mathbf{a}_1, \ldots, \mathbf{a}_m$ are said to be independent.

Suppose that N vectors $\mathbf{a}_1, \ldots, \mathbf{a}_N$ of a vector space are independent. If any set consisting of the N vectors $\mathbf{a}_1, \ldots, \mathbf{a}_N$ and any other vector of the vector space is not independent, then the N vector $\mathbf{a}_1, \ldots, \mathbf{a}_N$ are called the bases of the vector space. Then, any vector $\mathbf{b}$ and the N vectors $\mathbf{a}_1, \ldots, \mathbf{a}_N$ are not independent. This implies that there exists nonzero real numbers among $c_1, c_2, \ldots, c_{N+1}$ such that

$$c_1\mathbf{a}_1 + \cdots + c_N\mathbf{a}_N + c_{N+1}\mathbf{b} = \mathbf{0} \tag{1.11}$$

If $c_{N+1} = 0$, then Eq. (1.11) means

$$c_1\mathbf{a}_1 + \cdots + c_N\mathbf{a}_N = \mathbf{0} \tag{1.12}$$

and then it is contradictory to the premise that $\mathbf{a}_1, \ldots, \mathbf{a}_N$ are independent. Hence, c_{N+1} must not be zero. Finally, we can express $\mathbf{b}$ as a linear combination of the bases $\mathbf{a}_1, \ldots, \mathbf{a}_N$:

$$\mathbf{b} = -\frac{c_1}{c_{N+1}}\mathbf{a}_1 - \cdots - \frac{c_N}{c_{N+1}}\mathbf{a}_N \tag{1.13}$$

Equation (1.13) implies that any vector of the vector space can be expressed by a linear combination of the base vectors $\mathbf{a}_1, \ldots, \mathbf{a}_N$. That is, an arbitrary vector $\mathbf{v}$ of the vector space can be expressed by

$$\mathbf{v} = \sum_{n=1}^{N} v_n\mathbf{a}_n \tag{1.14}$$

The scalars v_n are called the components of the vector $\mathbf{v}$ with respect to the base vectors of $\{\mathbf{a}_1, \ldots, \mathbf{a}_N\}$. Equation (1.14) implies that basis $\{\mathbf{a}_1, \ldots, \mathbf{a}_N\}$ spans the vector space because any vector can be expressed by a linear combination of the base vectors.

A set of base vectors is called simply basis and a base vector is called a base. There are a number of ways to choose a basis. However, it can be proven that the number of base vectors is not different from each other. The number of base vectors is called the dimension of the vector space. In summary, base vectors have two properties:

[1] Base vectors are linearly independent.
[2] Any vector is expressed by a linear combination of base vectors.

When a set of base vectors of a vector space is known, the two properties of base vectors imply the components of a vector are uniquely determined. Assume that $\{\mathbf{a}_1, \ldots, \mathbf{a}_N\}$ is the set of the base vectors and a vector $\mathbf{v}$ can be expressed by two sets of components as follows:

$$\mathbf{v} = \sum_{n=1}^{N} v_n\mathbf{a}_n = \sum_{n=1}^{N} v'_n\mathbf{a}_n \tag{1.15}$$

Then, Eq. (1.15) leads to

$$\sum_{n=1}^{N} \left(v_n - v'_n\right)\mathbf{a}_n = \mathbf{0} \tag{1.16}$$

Since base vectors are linearly independent, it is clear that for all n, $v_n = v'_n$ which proves that components of a vector are uniquely determined. However, this does not mean that two sets of components of a vector with respect to two different sets of base vectors are identical.

For physical vector in 3-dimensional space, these theoretical tools such as linear independence and base vectors look unnecessarily complicate. However, these concepts are very convenient and necessary when abstract vectors such as continuous functions are considered. The approaches based on vector space can be met in several fields of applied mathematics as well as quantum mechanics. See Atkinson and Han (2000) for numerical methods, and Luenberger (1969) for optimization theory, Kreyszig (1978) for functional analysis, and Prugovecki (2006) for quantum mechanics.

A vector space can have a number of base vectors. A new set of N vectors can be generated by linear combination of a set of base vectors $A = \{\mathbf{a}_1, \ldots, \mathbf{a}_N\}$ as follows:

$$\mathbf{b}_i = \sum_{k=1}^{N} Q_{ik}\mathbf{a}_k \quad (i = 1, 2, \ldots, N) \tag{1.17}$$

where coefficients Q_{ik} are assumed to form an invertible matrix. Consider a linear combination from $B = \{\mathbf{b}_1, \ldots, \mathbf{b}_N\}$: $\mathbf{u} \equiv c_1\mathbf{b}_1 + \cdots + c_N\mathbf{b}_N$. If the vector $\mathbf{u}$ is the zero vector, then we have

$$\mathbf{u} = \sum_{i=1}^{N} c_i\mathbf{b}_i = \sum_{i=1}^{N} c_i \left(\sum_{k=1}^{N} Q_{ik}\mathbf{a}_k \right) = \sum_{k=1}^{N} \left(\sum_{i=1}^{N} Q_{ik}c_i \right) \mathbf{a}_k = \mathbf{0} \tag{1.18}$$

Equation (1.18) implies that for all k

$$\sum_{i=1}^{N} Q_{ik}c_i = 0 \tag{1.19}$$

Since the matrix Q_{ik} is invertible, Eq. (1.19) uniquely determines $c_i = 0$ for all i. Hence, the set $\{\mathbf{b}_i\}$ is linearly independent. Let P_{mn} be the inverse matrix of Q_{ik}. Then, we have

$$\mathbf{a}_i = \sum_{k=1}^{N} P_{ik}\mathbf{b}_k \quad (i = 1, 2, \ldots, N) \tag{1.20}$$

Substitution of Eq. (1.20) into Eq. (1.14) proves that any vector $\mathbf{v}$ can be expressed by a linear combination of $B = \{\mathbf{b}_1, \ldots, \mathbf{b}_N\}$. Detailed proofs are found in Ames (1970).

1.3 Dual Space

Consider a linear mapping $\widetilde{\phi}$ from a vector space V to real numbers. It is a real-valued function of a vector of V with satisfying the following properties:

$$\widetilde{\phi}(\mathbf{u}+\mathbf{v}) = \widetilde{\phi}(\mathbf{u}) + \widetilde{\phi}(\mathbf{v}), \quad \widetilde{\phi}(\alpha\mathbf{u}) = \alpha\widetilde{\phi}(\mathbf{u}) \tag{1.21}$$

where α is an arbitrary real number and $\mathbf{u}$ and $\mathbf{v}$ are arbitrary vectors of V. The linear mapping $\widetilde{\phi}$ is called linear functional. If a set of linear functionals on V satisfies the conditions of vector space, then the set is denoted by V^* and called the dual space of the vector space V.

Here, the addition of any two functionals $\widetilde{\phi} \in V^*$ and $\widetilde{\eta} \in V^*$ is defined as

$$\left(\widetilde{\phi} + \widetilde{\eta}\right)(\mathbf{u}) \equiv \widetilde{\phi}(\mathbf{u}) + \widetilde{\eta}(\mathbf{u}) \tag{1.22}$$

Then, it is clear that $\widetilde{\phi} + \widetilde{\eta} \in V^*$. For any real number α, scalar multiplication is defined as

$$\left(\alpha\widetilde{\phi}\right)(\mathbf{u}) \equiv \alpha\widetilde{\phi}(\mathbf{u}) \tag{1.23}$$

Of course, we know that $\alpha\widetilde{\phi} \in V^*$. The zero functional is defined a mapping from V to 0 for any elements of V. Then, it is not difficult to show that the set of linear functional V^* is a vector space.

Let $\{\mathbf{b}_i\}$ be a set of base vectors of N-dimensional vector space V. Consider N linear functionals $\widetilde{\phi}^{(i)}$ defined as $\widetilde{\phi}^{(i)}(\mathbf{b}_k) = \delta_{ik}$ where δ_{ik} is the *Kronecker's delta* which is unity whenever $i = k$ and zero otherwise. Then, it is easy to show that the set $\{\widetilde{\phi}^{(i)}\}$ is the base of V^*. The first step is to show that $\{\widetilde{\phi}^{(i)}\}$ is linearly independent and the second step is to show that $\{\widetilde{\phi}^{(i)}\}$ generates any linear functional that belongs to V^*. The linear independence of $\{\widetilde{\phi}^{(i)}\}$ means that if a linear combination of $\{\widetilde{\phi}^{(i)}\}$ for any vector $\mathbf{v}$ of V is zero:

$$\sum_{k=1}^{N} c_k \widetilde{\phi}^{(k)}(\mathbf{v}) = 0 \tag{1.24}$$

then all coefficients c_k are zero. Substitution of a base vector $\mathbf{b}_i$ of V to Eq. (1.24) gives $c_i = 0$. Thus, the set $\{\widetilde{\phi}^{(i)}\}$ is linearly independent. For any vector $\mathbf{v}$ whose components are v_k, a linear functional $\widetilde{\phi}$ satisfies

$$\widetilde{\phi}(\mathbf{v}) = \widetilde{\phi}\left(\sum_{k=1}^{N} v_k \mathbf{b}_k\right) = \sum_{k=1}^{N} v_k \widetilde{\phi}(\mathbf{b}_k) \tag{1.25}$$

Equation (1.25) implies that if N values of $\widetilde{\phi}(\mathbf{b}_i)$ are known, then the value of $\widetilde{\phi}(\mathbf{v})$ is determined. Consider a functional $\widetilde{\psi}$ which is a linear functional such that

$$\widetilde{\psi}(\mathbf{v}) = \sum_{k=1}^{N} \widetilde{\phi}(\mathbf{b}_k)\widetilde{\phi}^{(k)}(\mathbf{v}) \tag{1.26}$$

Then, we know that $\psi(\mathbf{b}_i) = \widetilde{\phi}(\mathbf{b}_i)$ from the definition of $\widetilde{\phi}^{(i)}$. It is clear that the functional $\widetilde{\psi}(\mathbf{v})$ is identical to $\widetilde{\phi}(\mathbf{v})$ because the two linear functionals have the same value for any vector $\mathbf{v}$.

The Dirac delta function is one of the most important applications of linear functional. Consider the vector space F of continuous functions defined on the interval $(-\infty, \infty)$. One may define linear functional by using the following integral transform

$$\widetilde{\phi}[f(x)] = \int_{-\infty}^{\infty} \phi(x) f(x) \mathrm{d}x \tag{1.27}$$

where $f(x)$ is a vector of F and $\phi(x)$ is the function given by the functional $\widetilde{\phi}$. The function $\phi(x)$ can be considered as the kernel function from the viewpoint of integral transform. Fourier transform is a linear functional for functions $f(x)$ which satisfies

$$\int_{-\infty}^{\infty} |f(x)| \mathrm{d}x < \infty \tag{1.28}$$

and the kernel function is given by $\phi(x) = \exp(-\mathrm{i}qx)$ where $\mathrm{i} = \sqrt{-1}$. One may imagine that any linear functional corresponds to its own kernel function: the one-to-one correspondence between linear functional and function. The existence of the correspondence can be proved when the inner product is defined over the vector space of functions. It will be treated later. The Dirac delta function is the kernel function of the linear functional which maps $f(x) \in F$ to $f(0)$:

$$\widetilde{\delta}[f(x)] = \int_{-\infty}^{\infty} \delta(x) f(x) \mathrm{d}x = f(0) \tag{1.29}$$

However, the Dirac delta function $\delta(x)$ cannot be defined at $x = 0$. Hence, new name for something like function is necessary. The name is distribution (Zemanian 1987). Note that $\delta(x)$ works always under integration. Thus, the Dirac delta function can be said to be a linear functional.

Problem 1

[1] Show that the following sets are vector space if addition and scalar multiplication are suitably defined.

[a] Set of $N \times M$ matrix,
[b] Set of polynomials of order N,
[c] Set of linear functionals from physical vectors.

[2] Show that the followings are linearly independent.

[a] $\{\sin \omega t, \sin 2\omega t, \sin 3\omega t, \ldots, \sin N\omega t\}$
[b] $\left\{1, x, x^2, x^3, \ldots, x^N\right\}$

[3] When $B = \{\mathbf{b}_1, \mathbf{b}_2, \ldots, \mathbf{b}_N\} \subset V$ is a linearly independent set of vector space V, show that any subset of B is also linearly independent.

[4] If $\{\mathbf{a}_1, \mathbf{a}_2, \ldots, \mathbf{a}_N\}$ is a base of vector space V and $\{\mathbf{b}_1, \mathbf{b}_2, \ldots, \mathbf{b}_M\}$ is also a base of the same vector space, then show that $M = N$.

[5] If a subset of a vector space V is also a vector space, then it is called subspace. Consider two subspace V_1 and V_2 of V. Show that the following set is a vector space.

$$V_1 + V_2 \equiv \{\mathbf{v} | \mathbf{v} = \mathbf{v}_1 + \mathbf{v}_2; \mathbf{v}_1 \in V_1, \mathbf{v}_2 \in V_2\}$$

[6] Show that the intersection of two subspace is a vector space.

[7] V_1 and V_2 are subspaces of V whose dimension is finite. When the dimension of a vector space U is denoted by $\dim(U)$, show that

$$\dim(V_1 + V_2) = \dim(V_1) + \dim(V_2) - \dim(V_1 \cap V_2)$$

2 Inner Product Space

2.1 Generalization of Inner Product

In physics, the inner product of two vectors is defined as the product of three terms: the magnitudes of the two vectors and the cosine of the angle between the two vectors. Hence, the inner product can be considered as a mapping from two vectors to a real number. It is assumed that the readers are familiar with the inner product of physics. Then, it is clear that

$$\begin{aligned} \mathbf{a}\cdot\mathbf{b} &= \mathbf{b}\cdot\mathbf{a} \\ (\mathbf{a}+\mathbf{b})\cdot\mathbf{c} &= \mathbf{a}\cdot\mathbf{c}+\mathbf{b}\cdot\mathbf{c} \\ (k\mathbf{a})\cdot\mathbf{b} &= k(\mathbf{a}\cdot\mathbf{b}) \\ \mathbf{a}\cdot\mathbf{a} &\geq 0 \end{aligned} \tag{2.1}$$

where **a**, **b**, and **c** are arbitrary vectors and k is an arbitrary real number. Note that $\mathbf{a}\cdot\mathbf{a}=0$ is valid only when $\mathbf{a}=\mathbf{0}$. Furthermore, we know that the magnitude of a vector **a** is given by

$$\|\mathbf{a}\| = \sqrt{\mathbf{a}\cdot\mathbf{a}} \tag{2.2}$$

Generalization of inner product can be done by the replacement of the physical vectors in Eq. (2.1) by abstract ones of arbitrary vector space. In other words, we define inner product as a binary operation satisfying Eq. (2.1). The notation $\langle \mathbf{a}, \mathbf{b}\rangle$ instead of $\mathbf{a}\cdot\mathbf{b}$ would be used in order to emphasize that the inner product under consideration is a generalized one. There are a number of definitions of inner product available for a given vector space.

Consider a vector space consisting of integrable functions on the interval of $[a, b]$. Then, one of the simplest inner product might be defined as

$$\langle f, g\rangle \equiv \int_a^b f(x)g(x)w(x)\mathrm{d}x \tag{2.3}$$

where $w(x)$ is nonnegative over the interval and called weight function. It is easy to show that Eq. (2.3) satisfies Eq. (2.1).

As for $N \times N$ matrix, one may define inner product as follows:

$$\langle \mathbf{A}, \mathbf{B}\rangle \equiv \sum_{i=1}^{N}\sum_{k=1}^{N} a_{ik}b_{ik} \tag{2.4}$$

where **A** and **B** are $N \times N$ matrices and a_{ik} and b_{ik} are their components, respectively. It is also easy to show that Eq. (2.4) satisfies Eq. (2.1).

A vector space with inner product is called inner product space and the magnitude of vector is called *norm*. Metric space is a vector space equipped with the definition of norm. Since the norm of vector can be defined from inner product, inner product space is a metric space. If every *Cauchy sequence* of vectors of an inner product space converges in the space, then the space is called *Hilbert space* irrespective of the dimension of the space. A sequence of vectors $\{\mathbf{x}_k\}$ is a Cauchy sequence when it satisfies the condition that if for any positive real number $\varepsilon > 0$, there exists a positive integer N such that for all positive integers $m, n > N$, then the magnitude of $\mathbf{x}_m - \mathbf{x}_n$ is smaller than ε. Since we can take linear combinations of base vectors as a sequence, and any vector of the Hilbert space can be expressed by

a linear combination of base vectors, it is clear that any inner product space of finite dimension is a Hilbert space. However, all inner product spaces of infinite dimension are not Hilbert spaces. Further information on metric and Hilbert spaces are found in Kreyszig (1978), Luenberger (1969), and Prugovecki (2006).

2.2 Generalization of Distance

The distance between two positions is equal to the magnitude of the displacement vector connecting the two positions. The magnitude of a geometric vector can be obtained by the inner product as shown in Eq. (2.2). Then, the distance in a metric space can be defined as the norm of the difference between two vectors of the metric space.

The notion of distance in our daily life is summarized with *the nonnegativity of distance* that the distance between any two vectors is nonnegative; *the symmetry of distance* that the distance from **a** to **b** is equal to that from **b** to **a**; *the triangle inequality* that the sum of distances from **a** to **b** and from **b** to **c** is not less than the distance between **a** and **c**. If the distance between **a** and **b** is denoted by $g(\mathbf{a}, \mathbf{b})$, then the three axioms are expressed by

$$\begin{aligned} &g(\mathbf{a}, \mathbf{b}) \geq 0 \\ &g(\mathbf{a}, \mathbf{b}) = g(\mathbf{b}, \mathbf{a}) \\ &g(\mathbf{a}, \mathbf{b}) + g(\mathbf{b}, \mathbf{c}) \geq g(\mathbf{a}, \mathbf{c}) \end{aligned} \tag{2.5}$$

As for inner product space, one can define the distance from inner product as $g(\mathbf{a}, \mathbf{b}) \equiv \sqrt{\langle \mathbf{a} - \mathbf{b}, \mathbf{a} - \mathbf{b} \rangle}$. Then, it is not difficult to show that the definition of distance satisfies Eq. (2.5) except the triangle inequality. The Cauchy–Schwarz inequality is necessary to prove the triangle inequality. For any generalized inner product which satisfies Eq. (2.1), the following is valid:

$$\langle \mathbf{a}, \mathbf{a} \rangle \langle \mathbf{b}, \mathbf{b} \rangle \geq \langle \mathbf{a}, \mathbf{b} \rangle^2 \tag{2.6}$$

where **a** and **b** are arbitrary vectors of an inner product space. Because of the last inequality of Eq. (2.1), for any real number t, we have

$$\langle \mathbf{a} + t\mathbf{b}, \mathbf{a} + t\mathbf{b} \rangle \geq 0 \tag{2.7}$$

Applying the properties of inner product, Eq. (2.7) can be rewritten as

$$\langle \mathbf{b}, \mathbf{b} \rangle t^2 + 2\langle \mathbf{a}, \mathbf{b} \rangle t + \langle \mathbf{a}, \mathbf{a} \rangle \geq 0 \tag{2.8}$$

Since Eq. (2.8) is valid for any real number, the discriminant must not be positive:

$$\frac{D}{4} = \langle \mathbf{a}, \mathbf{b} \rangle^2 - \langle \mathbf{a}, \mathbf{a} \rangle \langle \mathbf{b}, \mathbf{b} \rangle \leq 0 \tag{2.9}$$

Note that Eq. (2.9) is identical to Eq. (2.6).

As for physical vector, the Cauchy–Schwarz inequality is straightforward because of the definition of the inner product in physics such that

$$\langle \mathbf{a}, \mathbf{b} \rangle = \mathbf{a} \cdot \mathbf{b} = \|\mathbf{a}\| \|\mathbf{b}\| \cos\theta \tag{2.10}$$

where θ is the angle between the two vectors. Note that $-1 \leq \cos\theta \leq 1$ for any θ. Analogy to the inner product of physical vectors, the angle between two abstract vectors might be defined as

$$\cos\theta \equiv \frac{\langle \mathbf{a}, \mathbf{b} \rangle}{\sqrt{\langle \mathbf{a}, \mathbf{a} \rangle} \sqrt{\langle \mathbf{b}, \mathbf{b} \rangle}} \tag{2.11}$$

Let us move back to the problem of the triangle inequality of distance. Since distance is not negative, the triangle inequality is equivalent to

$$[g(\mathbf{a}, \mathbf{b}) + g(\mathbf{b}, \mathbf{c})]^2 \geq [g(\mathbf{a}, \mathbf{c})]^2 \tag{2.12}$$

Replace the distance function by the corresponding inner product. Then, we have

$$\begin{aligned} [g(\mathbf{a},\ \mathbf{b}) + g(\mathbf{b}, \mathbf{c})]^2 &\geq \langle \mathbf{a} - \mathbf{b}, \mathbf{a} - \mathbf{b} \rangle + \langle \mathbf{b} - \mathbf{c}, \mathbf{b} - \mathbf{c} \rangle + 2\langle \mathbf{a} - \mathbf{b}, \mathbf{b} - \mathbf{c} \rangle \\ &= \langle (\mathbf{a} - \mathbf{b}) + (\mathbf{b} - \mathbf{c}), (\mathbf{a} - \mathbf{b}) + (\mathbf{b} - \mathbf{c}) \rangle = \langle \mathbf{a} - \mathbf{c}, \mathbf{a} - \mathbf{c} \rangle \\ &= [g(\mathbf{a}, \mathbf{c})]^2 \end{aligned} \tag{2.13}$$

Then, the proof is completed.

2.3 *Orthogonalized Basis*

Vector spaces considered in this book are usually assumed as inner product space or Hilbert space. From inner product, one can consider the notion of orthogonality such that the inner product of two nonzero vector is zero. As for physical vectors, orthogonality implies that the directions of the two vectors are perpendicular to each other. Hence, orthogonality is an abstraction of the perpendicularity of geometry. Whenever we consider physical vectors, orthogonality is identical to perpendicularity.

In general, two base vectors do not have to be orthogonal. However, mutually orthogonal base vectors are more convenient. Consider N mutually orthogonal

vectors of an inner product space of finite dimension. These vectors are linearly independent if N is not larger than the dimension of the inner product space. Mutually orthogonal vectors $\{\mathbf{u}_1, \mathbf{u}_2, \ldots, \mathbf{u}_N\}$ are said to be vectors such that $\langle \mathbf{u}_i, \mathbf{u}_k \rangle = 0$ for any pair of i and k whenever the two indices are not same. If a linear combination of these vectors is the zero vector:

$$c_1\mathbf{u}_1 + c_2\mathbf{u}_2 + \cdots + c_N\mathbf{u}_N = \mathbf{0} \tag{2.14}$$

then taking inner product with $\mathbf{u}_i$ on both sides of Eq. (2.14) gives $c_i\langle \mathbf{u}_i, \mathbf{u}_i \rangle = 0$. The property of inner product results in $c_i = 0$ for any i. Thus, these N vectors are linearly independent. It is not difficult to show that contradiction occurs whenever N is larger than the dimension of the space. If N is equal to the dimension of the space, it is clear that the N mutually orthogonal vectors are base vectors.

Mutually orthogonal base vectors are called orthonormal base vectors when every member of the base vectors has the magnitude of unity. If we have mutually orthogonal base vectors $\{\mathbf{u}_1, \mathbf{u}_2, \ldots, \mathbf{u}_N\}$, then we can define N vectors such that

$$\mathbf{e}_i = \frac{1}{\sqrt{\langle \mathbf{u}_i, \mathbf{u}_i \rangle}}\mathbf{u}_i \quad \text{for} \quad i = 1, 2, \ldots, N \tag{2.15}$$

From Eq. (2.15), it is straightforward that

$$\langle \mathbf{e}_i, \mathbf{e}_k \rangle = \mathbf{e}_i \cdot \mathbf{e}_k = \delta_{ik} \tag{2.16}$$

where δ_{ik} is called Kronecker's delta which is unity when $i = k$ and zero otherwise. Orthonormal base vectors are more convenient than mutually orthogonal ones because any vector can be expressed by

$$\mathbf{v} = \sum_{k=1}^{N} \langle \mathbf{v}, \mathbf{e}_k \rangle \mathbf{e}_k = \sum_{k=1}^{N} (\mathbf{v} \cdot \mathbf{e}_k)\mathbf{e}_k \tag{2.17}$$

When orthonormal base is used, inner product of any two vectors is expressed by

$$\langle \mathbf{a}, \mathbf{b} \rangle = \mathbf{a} \cdot \mathbf{b} = \sum_{k=1}^{N} a_k b_k \tag{2.18}$$

where a_k and b_k are kth components of $\mathbf{a}$ and $\mathbf{b}$, respectively, with respect to the orthonormal base.

Then, how can we obtain an orthonormal base from a given base? Suppose that we have a basis $\{\mathbf{b}_1, \mathbf{b}_2, \ldots, \mathbf{b}_N\}$, which do not have to be mutually orthogonal. Since a member of an orthogonal basis $\{\mathbf{e}_1, \mathbf{e}_2, \ldots, \mathbf{e}_N\}$ is also a vector, it can be expressed by a linear combination of $\{\mathbf{b}_1, \mathbf{b}_2, \ldots, \mathbf{b}_N\}$:

$$\mathbf{e}_i = \sum_{k=1}^{N} Q_{ik}\mathbf{b}_k \tag{2.19}$$

With the help of Eq. (2.16), we have

$$\left\langle \sum_{n=1}^{N} Q_{in}\mathbf{b}_n, \sum_{m=1}^{N} Q_{km}\mathbf{b}_m \right\rangle = \sum_{n=1}^{N}\sum_{m=1}^{N} Q_{in}Q_{km}\langle \mathbf{b}_n, \mathbf{b}_m\rangle = \delta_{ik} \tag{2.20}$$

Since we know $\langle \mathbf{b}_n, \mathbf{b}_m\rangle$ for any pair of n and m, Eq. (2.20) is a set of N^2 nonlinear equations for N^2 unknowns Q_{ik}. This is a quite complicate problem. The *Gram–Schmidt orthogonalization* is a simpler method to find Q_{ik} in a systematic way.

2.3.1 The Gram–Schmidt Orthogonalization

The first step of the Gram–Schmidt orthogonalization is to find a mutually orthogonal bias, say $\{\mathbf{u}_1, \mathbf{u}_2, \ldots, \mathbf{u}_N\}$ from a given basis $\{\mathbf{b}_1, \mathbf{b}_2, \ldots, \mathbf{b}_N\}$. The next step is the normalization of the mutually orthogonal basis by $\mathbf{e}_i = \mathbf{u}_i/\|\mathbf{u}_i\|$.

Set $\mathbf{u}_1 = \mathbf{b}_1$ and $\mathbf{u}_2 = \mathbf{b}_2 + q_1^{(2)}\mathbf{u}_1$. Then, there is only one unknown $q_1^{(2)}$ which could be determined by the orthogonality condition of $\langle \mathbf{u}_1, \mathbf{u}_2\rangle = 0$. Then, we know that

$$q_1^{(2)} = -\frac{\langle \mathbf{b}_2, \mathbf{b}_1\rangle}{\langle \mathbf{b}_1, \mathbf{b}_1\rangle} = -\frac{\langle \mathbf{b}_2, \mathbf{u}_1\rangle}{\langle \mathbf{u}_1, \mathbf{u}_1\rangle} \tag{2.21}$$

Since there are two orthogonal conditions such that $\langle \mathbf{u}_1, \mathbf{u}_3\rangle = 0$ and $\langle \mathbf{u}_2, \mathbf{u}_3\rangle = 0$, one may construct $\mathbf{u}_3$ by $\mathbf{u}_3 = \mathbf{b}_3 + q_2^{(3)}\mathbf{u}_2 + q_1^{(3)}\mathbf{u}_1$. The unknowns $q_2^{(3)}$ and $q_1^{(3)}$ can be determined by solving the following set of linear equations:

$$\begin{aligned} \langle \mathbf{u}_1, \mathbf{u}_1\rangle q_1^{(3)} + \langle \mathbf{u}_1, \mathbf{u}_2\rangle q_2^{(3)} &= -\langle \mathbf{u}_1, \mathbf{u}_3\rangle \\ \langle \mathbf{u}_2, \mathbf{u}_1\rangle q_1^{(3)} + \langle \mathbf{u}_2, \mathbf{u}_2\rangle q_2^{(3)} &= -\langle \mathbf{u}_2, \mathbf{u}_3\rangle \end{aligned} \tag{2.22}$$

Since $\langle \mathbf{u}_k, \mathbf{u}_k\rangle > 0$ because $\mathbf{u}_k \neq \mathbf{0}$ for any k, Eq. (2.22) must have a unique solution and we have

$$\mathbf{u}_3 = \mathbf{b}_3 - \frac{\langle \mathbf{b}_3, \mathbf{u}_2\rangle}{\langle \mathbf{u}_2, \mathbf{u}_2\rangle}\mathbf{u}_2 - \frac{\langle \mathbf{b}_3, \mathbf{u}_1\rangle}{\langle \mathbf{u}_1, \mathbf{u}_1\rangle}\mathbf{u}_1 \tag{2.23}$$

Similar procedure can be applied to $\mathbf{u}_n$ for $n > 3$ and we have

$$\mathbf{u}_n = \mathbf{b}_n - \sum_{k=1}^{n-1} \frac{\langle \mathbf{b}_n, \mathbf{u}_k\rangle}{\langle \mathbf{u}_k, \mathbf{u}_k\rangle}\mathbf{u}_k \tag{2.24}$$

Since this procedure gives mutually orthogonal basis $\{\mathbf{u}_1, \mathbf{u}_2, \ldots, \mathbf{u}_N\}$, finally we have orthonormal basis:

$$\mathbf{e}_i = \frac{1}{\|\mathbf{u}_i\|}\mathbf{u}_i \tag{2.25}$$

The Gram–Schmidt orthogonalization implies that any inner product space can have orthonormal basis. We know that finite-order polynomials have the basis $B_N = \{1, x, \ldots, x^N\}$. Suppose that the inner product space of polynomial is equipped with the inner product defined by

$$\langle p(x), q(x)\rangle = \int_a^b p(x)q(x)w(x)\mathrm{d}x \tag{2.26}$$

where the weight function $w(x)$ is positive for the whole interval of $a < x < b$.

First, consider the case of $a = 0$, $b = L > 0$, and $w(x) = 1$, then the mutually orthogonal basis $M_N = \{Q_0(x), Q_1(x), \ldots, Q_N(x)\}$ from the basis B_N is given by

$$Q_0(x) = 1; \quad Q_1(x) = x - \frac{1}{2}L; \quad Q_2(x) = x^2 - Lx + \frac{1}{6}L^2; \quad \ldots \tag{2.27}$$

Note that $M_N \subset M_{N+m}$ when $m > 0$.

2.3.2 Orthogonal Polynomials

There are several named orthogonal polynomials which have different definitions of inner product. The Legendre polynomials construct an orthogonal basis for $a = -1$, $b = 1$ and $w(x) = 1$. Some of the Legendre polynomials are

$$\begin{aligned} &P_0(x) = 1; \quad P_1(x) = x; \quad P_2(x) = 2^{-1}\left(3x^2 - 1\right); \\ &P_3(x) = 2^{-1}\left(5x^3 - 3x\right); \quad P_4(x) = 2^{-3}\left(35x^4 - 30x^2 + 3\right); \\ &P_5(x) = 2^{-3}\left(63x^5 - 70x^3 + 15x\right); \quad \ldots \end{aligned} \tag{2.28}$$

Although the Gram–Schmidt orthogonalization is easy to be understood and is a systematic way, the calculation procedures are tedious and time-consuming. As for the Legendre polynomials, the following recursive equation is valid:

$$P_{n+1}(x) = \frac{2n+1}{n+1}xP_n(x) - \frac{n}{n+1}P_{n-1}(x) \quad \text{for} \quad n \geq 1 \tag{2.29}$$

Note that $P_0(x) = 1$ and $P_1(x) = x$ are needed as initial conditions for the recursive Eq. (2.29). The recursive equations are more convenient than the Gram–

Schmidt orthogonalization. As for the Legendre polynomials, the following orthogonal conditions are valid:

$$\int_{-1}^{1} P_m(x)\, P_n(x)\mathrm{d}x = \frac{2}{2n+1}\delta_{mn} \tag{2.30}$$

When $a = -1$, $b = 1$ and $w(x) = 1/\sqrt{1-x^2}$ is used, the Chebyshev polynomials of the first kind are obtained. Some of the Chebyshev polynomials of the first kind are

$$\begin{aligned} &T_0(x) = 1; \quad T_1(x) = x; \quad T_2(x) = 2x^2 - 1; \\ &T_3(x) = 4x^3 - 3x; \quad T_4(x) = 8x^4 - 8x^2 + 1; \\ &T_5(x) = 16x^5 - 20x^3 + 5x; \ldots \end{aligned} \tag{2.31}$$

The recursive equation for the Chebyshev polynomial of the first kind is given as

$$T_{n+1}(x) = 2xT_n(x) - T_{n-1}(x) \quad \text{for } n \geq 1 \tag{2.32}$$

with the initial conditions of $T_0(x) = 1$ and $T_1(x) = x$. The orthogonal conditions are given as

$$\int_{-1}^{1} \frac{T_m(x)\, T_n(x)}{\sqrt{1-x^2}}\mathrm{d}x = \begin{cases} 0 & \text{for } m \neq n \\ \pi & \text{for } m = n = 0 \\ \frac{1}{2}\pi & \text{for } m = n \neq 0 \end{cases} \tag{2.33}$$

It is noteworthy that the Chebyshev polynomial of the first kind is useful in analysis of large amplitude oscillatory shear (LAOS) because it has the following properties:

$$\begin{aligned} &T_n(\cos\theta) = \cos(n\theta) \\ &T_n(x) = T_n(n \arccos x) = \cosh(n \arccos \mathrm{h}x) \end{aligned} \tag{2.34}$$

See Chap. 11. Furthermore, the Chebyshev polynomial of the first kind is also useful in various fields of numerical methods. Polynomial regression is one of the most representative applications of the polynomial.

The Chebyshev polynomial of the second kind $U_n(x)$ is defined over the same interval, but its weight function is $w(x) = \sqrt{1-x^2}$. Its recursive equation is the same as that of the first kind while the initial conditions are given as $U_0(x) = 1$ and $U_1(x) = 2x$.

The Hermite polynomials are an orthogonal basis for $a = -\infty$, $b = \infty$ and $w(x) = \exp(-x^2)$. Some of the Hermite polynomials are

$$\begin{aligned} &H_0(x) = 1; \quad H_1(x) = 2x; \quad H_2(x) = 4x^2 - 2; \\ &H_3(x) = 8x^3 - 12x; \quad H_4(x) = 16x^4 - 48x^2 + 12; \\ &H_5(x) = 32x^5 - 160x^3 + 120x; \ldots \end{aligned} \tag{2.35}$$

The recursive equation is given as

$$H_{n+1}(x) = 2xH_n(x) - 2nH_{n-1}(x) \quad \text{for } n \geq 1 \tag{2.36}$$

The initial conditions are $H_0(x) = 1$ and $H_1(x) = 2x$, and the orthogonal conditions are given as

$$\int_{-\infty}^{\infty} H_m(x)H_n(x)e^{-x^2}\mathrm{d}x = 2^n\sqrt{\pi}\,n!\delta_{mn} \tag{2.37}$$

The Laguerre polynomials are an orthogonal basis for $a = 0$, $b = \infty$ and $w(x) = \exp(-x)$. Since the interval of the polynomial is identical to that of Laplace transform, it is applied to numerical inversion of Laplace transform (Cohen 2007). Some of the Laguerre polynomials are

$$\begin{aligned} &L_0(x) = 1; \quad L_1(x) = -x + 1; \quad L_2(x) = \frac{1}{2}\left(x^2 - 4x + 2\right); \\ &L_3(x) = \frac{1}{6}\left(-x^3 + 9x^2 - 18x + 6\right); \\ &L_4(x) = \frac{1}{24}\left(x^4 - 16x^3 + 72x^2 - 96x + 24\right); \ \ldots \end{aligned} \tag{2.38}$$

The recursive equation of the Laguerre polynomials are given as

$$L_{n+1}(x) = \frac{(2n + 1 - x)L_n(x) - nL_{n-1}(x)}{n+1} \tag{2.39}$$

with the initial conditions of $L_0(x) = 1$ and $L_1(x) = 1 - x$.

Polynomial regression by using orthogonal polynomials plays an important role in the data processing of both linear and nonlinear viscoelasticity. Most orthogonal polynomials originate from solution of differential equations. These differential equations belong to Sturm–Liouville equations. See Arfken and Weber (2001) for further study. Table 1 is the list of some orthogonal polynomials which are popularly used in various fields of science.

2.3.3 Dual Basis

For any basis of N-dimensional inner product space, say $B = \{\mathbf{g}_1, \mathbf{g}_2, \ldots, \mathbf{g}_N\}$, we can define its dual basis $\overline{B} = \left\{\mathbf{g}^1, \mathbf{g}^2, \ldots, \mathbf{g}^N\right\}$ which satisfies

Table 1 List of orthogonal polynomials

Name	Interval	Weight function	Recursive equation
Legendre	$-1<x<1$	1	$P_{n+1}(x)=\frac{2n+1}{n+1}xP_n(x)-\frac{n}{n+1}P_{n-1}(x)$ $P_0(x)=1,\ P_1(x)=x$
Chebyshev I	$-1<x<1$	$\frac{1}{\sqrt{1-x^2}}$	$T_{n+1}(x)=2xT_n(x)-T_{n-1}(x)$ $T_0(x)=1,\ T_1(x)=x$
Chebyshev II	$-1<x<1$	$\sqrt{1-x^2}$	$U_{n+1}(x)=2xU_n(x)-U_{n-1}(x)$ $U_0(x)=1,\ U_1(x)=2x$
Hermite	$-\infty<x<\infty$	$\exp(-x^2)$	$H_{n+1}(x)=2xH_n(x)-2nH_{n-1}(x)$ $H_0(x)=1,\ H_1(x)=2x$
Laguerre	$0<x<\infty$	$\exp(-x)$	$L_{n+1}(x)=\frac{(2n+1-x)L_n(x)-nL_{n-1}(x)}{n+1}$ $L_0(x)=1,\ L_1(x)=1-x$

$$\left\langle \mathbf{g}_i, \mathbf{g}^k \right\rangle = \delta_i^k \tag{2.40}$$

If Eq. (2.40) holds, the second basis is called the dual basis of the first. Reversely, the first basis is also the dual basis of the second. Note that we have used superscript in order to distinguish the dual base vector from the original base vector and δ_i^k is another notation of the Kronecker's delta. Question on dual basis is how we can determine the dual basis from a given basis. Since $\mathbf{g}^i$ is a vector, it can be expressed by a linear combination of the original basis as follows:

$$\mathbf{g}^i = \sum_{k=1}^{N} g^{ik}\mathbf{g}_k \tag{2.41}$$

where ik of g^{ik} means superscript not exponent. The definition of dual basis, Eq. (2.40) gives

$$\sum_{k=1}^{N} g^{ik}g_{km} = \delta_m^i \tag{2.42}$$

where

$$g_{km} \equiv \left\langle \mathbf{g}_k, \mathbf{g}_m \right\rangle \tag{2.43}$$

It is easy to show that the matrix formed by g_{km} is invertible because $\mathbf{g}_k$ is linearly independent. Thus, it can be concluded that g^{ik} is the component of the inverse of the matrix of g_{ik}. Since the inverse of a matrix is determined uniquely, the dual basis of a basis is uniquely determined and always exists. The notion of dual basis is important in curvilinear coordinate systems (Sect. 3) as well as objective time-derivative for nonlinear viscoelastic constitutive equations (Sect. 4 in Chap. 10).

2.4 Application of Orthogonal Polynomials

Since we are equipped with how to define distance in abstract vector space, consider an inner product space V consisting of continuous functions defined on the interval of $a<x<b$. Note that Nth-order polynomial, P_N spanned by $B_N = \{1, x, \ldots, x^N\}$ is also an inner product space included in V. When $f(x) \in V$, we want to find the best approximation of P_N. It is a problem to determine coefficients $\{a_k\}$ which minimize the distance $\|f(x) - p_N(x)\|$ where

$$p_N(x) = a_0 + a_1 x + a_2 x^2 + \cdots + a_N x^N \tag{2.44}$$

Since it is equivalent to minimize $\chi^2 \equiv \|f(x) - p_N(x)\|^2$, we express χ^2 in terms of inner product:

$$\chi^2 = \langle p_N(x), p_N(x)\rangle - 2\langle p_N(x), f(x)\rangle + \langle f(x), f(x)\rangle \tag{2.45}$$

Let any basis of P_N be denoted by $C_N = \{\phi_0(x), \phi_1(x), \ldots, \phi_N(x)\}$. Then, Eq. (2.44) is equivalent to

$$p_N(x) = \sum_{k=0}^{N} c_k \phi_k(x) \tag{2.46}$$

When $\phi_k(x) = x^k$, we know $a_k = c_k$. Equation (2.45) can be rewritten in terms of $\phi_k(x)$ as follows:

$$\chi^2 = \sum_{i=0}^{N}\sum_{k=0}^{N} \langle \phi_i(x), \phi_k(x)\rangle c_i c_k - 2\sum_{k=0}^{N} \langle \phi_k(x), f(x)\rangle c_k + \langle f(x), f(x)\rangle \tag{2.47}$$

Since χ^2 is a quadraction for c_k, the minimization implies $\partial\chi^2/\partial c_n = 0$. Then, we have a system of $N+1$ linear equations such that

$$\sum_{k=0}^{N} S_{ik} c_k = b_i \tag{2.48}$$

where $S_{ik} \equiv \langle \phi_i(x), \phi_k(x)\rangle$ is a symmetric matrix and $b_i \equiv \langle \phi_i(x), f(x)\rangle$. When we use orthogonal polynomial such that

$$\langle \phi_i(x), \phi_k(x)\rangle = \delta_{ik} \tag{2.49}$$

the solution of Eq. (2.48) is given as

$$c_n = \langle f(x), \phi_n(x)\rangle \tag{2.50}$$

Thus, the coefficients depend on the corresponding inner product.

To obtain the coefficients $\{a_n\}$ from $\{c_n\}$, we need the relations between the basis B_N and an orthonormal basis. It is noteworthy that there exists invertible matrix such that

$$\phi_n(x) = \sum_{k=0}^{N} \gamma_{nk} x^k \quad \text{for } n = 0, 1, 2, \ldots, N \tag{2.51}$$

where $\phi_k(x)$ is considered as an orthogonal polynomial. Substitution of Eq. (2.51) into Eq. (2.46) yields

$$p_N(x) = \sum_{k=0}^{N} \left(\sum_{n=0}^{N} \gamma_{nk} c_n \right) x^k \tag{2.52}$$

and

$$a_k = \sum_{n=0}^{N} \gamma_{nk} c_n \tag{2.53}$$

The Taylor series expansion is one of the most well-known approximations of a function. Consider the problem to obtain an approximation of e^x over the interval of $-1 \le x \le 1$ to the third order. The Maclaurin series is the Taylor series about $x = 0$. The Maclaurin series gives

$$e^x \approx 1 + x + \frac{x^2}{2} + \frac{x^3}{6} \tag{2.54}$$

Using normalized Chebyshev polynomial of the first kind gives

$$e^x \approx 2.24404\, \widehat{T}_0(x) + 1.41664\, \widehat{T}_1(x) + 0.340269\, \widehat{T}_2(x) + 0.055568\, \widehat{T}_3(x) \tag{2.55}$$

Note that $\widehat{T}_n(x)$ is the normalized Chebyshev polynomial of the first kind such that

$$\begin{aligned} \widehat{T}_0(x) &= \tfrac{1}{\sqrt{\pi}} & \widehat{T}_1(x) &= \sqrt{\tfrac{2}{\pi}} x \\ \widehat{T}_2(x) &= \sqrt{\tfrac{2}{\pi}} (2x^2 - 1) & \widehat{T}_3(x) &= \sqrt{\tfrac{2}{\pi}} (4x^3 - 3x) \end{aligned} \tag{2.56}$$

It is noteworthy that

$$\left\langle e^x, \widehat{T}_n(x) \right\rangle = \int_{-1}^{1} \frac{e^x\, \widehat{T}_n(x)}{\sqrt{1 - x^2}} \mathrm{d}x = \begin{cases} \sqrt{\pi} I_n(1) & \text{for } n = 0 \\ \sqrt{2\pi} I_n(1) & \text{for } n = 1, 2, 3 \end{cases} \tag{2.57}$$

where $I_n(x)$ is the modified Bessel function of the first kind. Application of Eq. (2.56) to Eq. (2.55) gives

$$e^x \approx 0.9946 + 0.9973x + 0.5430x^2 + 0.1773x^3 \tag{2.58}$$

Using normalized Legendre polynomial gives

$$e^x \approx \frac{e - e^{-1}}{\sqrt{2}}\widehat{P}_0(x) + \frac{\sqrt{6}}{e}\widehat{P}_1(x) + \sqrt{\frac{5}{2}}\left(e - 7e^{-1}\right)\widehat{P}_2(x) + \sqrt{\frac{7}{2}}\left(37e^{-1} - 5e\right)\widehat{P}_3(x) \tag{2.59}$$

where

$$\begin{aligned} \widehat{P}_0(x) &= \frac{1}{\sqrt{2}} & \widehat{P}_1(x) &= \sqrt{\frac{3}{2}}x \\ \widehat{P}_2(x) &= \sqrt{\frac{5}{8}}(3x^2 - 1) & \widehat{P}_3(x) &= \sqrt{\frac{7}{8}}(5x^3 - 3x) \end{aligned} \tag{2.60}$$

Application of Eq. (2.60) to Eq. (2.59) yields

$$e^x \approx 0.9963 + 0.9980x + 0.5367x^2 + 0.1761x^3 \tag{2.61}$$

Figure 1 compares relative errors of the three third-order approximations: Eqs. (2.54), (2.58), and (2.61). The relative errors are defined here as

$$\text{Relative Error} = 1 - \frac{\text{Approximation}}{\text{Exact Value}} \tag{2.62}$$

The approximations by using orthogonal polynomials show similar behavior of relative errors whose absolute value is less than about 2 % over the whole interval

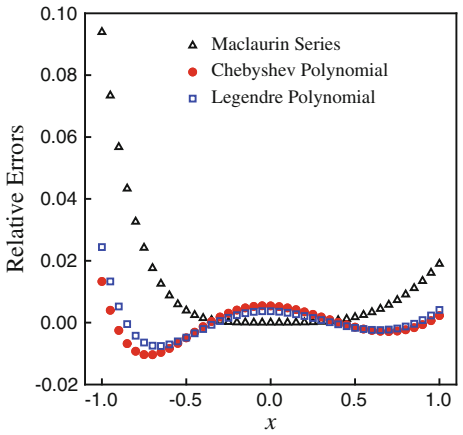

Fig. 1 Comparison of the Maclaurin series with the economized power series by using orthogonal polynomials

of $-1<x<1$. On the other hand, the Maclaurin series shows much higher errors when $|x|>0.5$. The economized power series from Chebyshev polynomial looks better than those from Legendre polynomial.

When polynomial regression is considered, the function $f(x)$ of Eq. (2.45) is replaced by experimental data y_α, independent variable x by x_α and the inner product by the summation over data as follows:

$$\chi^2 = \sum_{\alpha=1}^{M} \left[y_\alpha - \sum_{k=0}^{N} c_k \phi_k(x_\alpha) \right]^2 \tag{2.63}$$

where M is the number of data and $\phi_k(x)$ is the kth orthogonal polynomial or x^k. In this case, we do not consider that $\phi_k(x)$ is normalized. The minimization of Eq. (2.63) is reduced to Eq. (2.48) again while the matrix S_{ik} and column vector b_i should be modified as follows:

$$S_{ik} = \sum_{\alpha=1}^{M} \phi_i(x_\alpha)\, \phi_k(x_\alpha), \quad b_i = \sum_{\alpha=1}^{M} y_\alpha \phi_i(x_\alpha) \tag{2.64}$$

When orthogonal polynomial is used for $\phi_k(x)$, the matrix S_{ik} becomes a diagonal-dominated matrix. In other words, the absolute values of off-diagonal components become much smaller than those of diagonal components. However, $S_{ik} \le S_{im}$ for $k<m$ when $\phi_k(x) = x^k$. In this case, the matrix is no longer diagonal-dominant and solving Eq. (2.48) is apt to face a numerical problem due to ill-conditioned matrix (Atkinson and Han 2000; Atkinson 1978).

Economized power series was applied to obtain the analytical solution of the K-BKZ model for LAOS by Cho et al. (2010). They needed a power series approximation of the damping function of the K-BKZ model. See Problem 2[6].

2.5 Summation Convention

A vector $\mathbf{v}$ of N-dimensional vector space can be expressed by a linear combination of an orthonormal basis $\{\mathbf{e}_n\}$ as follows:

$$\mathbf{v} = \sum_{k=1}^{N} v_k \mathbf{e}_k \tag{2.65}$$

When the dimension N is known, using the summation symbol Σ is not convenient. Because the index k appears two times in Eq. (2.65), the omission of the symbol Σ makes notation much simpler. A new summation convention to be used here is called Einstein's convention such that

$$\mathbf{v} = \sum_{k=1}^{N} v_k \mathbf{e}_k = v_k \mathbf{e}_k \tag{2.66}$$

The twice-repeated index in a single term implies the summation over the index from 1 to the dimension N. To minimize unnecessary confusion, repetition of index more than twice is excluded. Hence, $a_{ik}b_k c_k$ does not mean summation on k.

By this notation, Eq. (2.48) can be rewritten as

$$S_{ik}c_k = b_i \tag{2.67}$$

Both Eqs. (2.48) and (2.67) express N linear equations because Eq. (2.67) implies that the equation works for any i. The index k meaning summation is called dummy index, while the index i is called free index. The following examples help the readers be familiar with the summation convention:

$$\mathbf{u} \cdot \mathbf{v} = \langle u_i \mathbf{b}_i, v_k \mathbf{b}_k \rangle = u_i v_k \langle \mathbf{b}_i, \mathbf{b}_k \rangle = \sum_{i=1}^{N} \sum_{k=1}^{N} u_i v_k \langle \mathbf{b}_i, \mathbf{b}_k \rangle \tag{2.68}$$

$$\begin{aligned} \delta_{ik}\delta_{kj} &= \sum_{k=1}^{N} \delta_{ik}\delta_{kj} = \delta_{ij} \\ A_{ik}\delta_{k1} &= A_{i1} \\ \delta_{kk} &= \delta_{11} + \delta_{22} + \delta_{33} + \cdots + \delta_{NN} = N \end{aligned} \tag{2.69}$$

Problem 2

[1] Consider an inner product space V with finite dimension and its subspaces V_1 and V_2. If the intersection of the two subspaces is $\{\mathbf{0}\}$, then show that a vector $\mathbf{v}_1 \in V_1$ and a vector $\mathbf{v}_2 \in V_2$ are orthogonal.

[2] Show that mutually orthogonal vectors are linearly independent.

[3] Consider a vector space that is spanned by column vectors $[\ 1 \quad -1 \quad 0\ ]^T$, $[\ 0 \quad 2 \quad 1\ ]^T$ and $[\ 1 \quad -1 \quad 1\ ]^T$. Find orthonormal basis from the basis by using the Gram–Schmidt orthogonalization.

[4] For vectors of an inner product space, show that the following is valid:

$$\|\mathbf{u}+\mathbf{v}\|^2 + \|\mathbf{u}-\mathbf{v}\|^2 = 2\|\mathbf{u}\|^2 + 2\|\mathbf{v}\|^2 \tag{2.a}$$

[5] Consider two sequences $\{\mathbf{u}_1, \mathbf{u}_2, \ldots, \mathbf{u}_n, \ldots\}$ and $\{\mathbf{v}_1, \mathbf{v}_2, \ldots, \mathbf{v}_n, \ldots\}$ which belong to an inner product space V. If the sequence $\{\mathbf{u}_n\}$ has the limit $\mathbf{u}_\infty \in V$ such that $\|\mathbf{u}_\infty - \mathbf{u}_n\|$ goes to zero as n increases and so does $\{\mathbf{v}_n\}$, then show that the sequence defined by $\langle \mathbf{u}_n,\ \mathbf{v}_n \rangle$ has the limit $\langle \mathbf{u}_\infty, \mathbf{v}_\infty \rangle$.

[6] Find sixth-order economized power series of $f(x) = (1+x^2)^{-1}$ over the interval of $-2 < x < 2$.

[7] Show that the Legendre polynomials satisfy the following differential equation:

$$\frac{\mathrm{d}}{\mathrm{d}x}\left[\left(1-x^2\right)\frac{\mathrm{d}P_n(x)}{\mathrm{d}x}\right]+n(n+1)P_n(x)=0 \tag{2.b}$$

[8] Show the following identities.

[a] $\dfrac{1}{\sqrt{1-2xt+t^2}}=\sum_{n=0}^{\infty}P_n(x)t^n$

[b] $\dfrac{1-tx}{1-2tx+t^2}=\sum_{n=0}^{\infty}T_n(x)t^n$

[c] $\exp(2xt-t^2)=\sum_{n=0}^{\infty}\dfrac{H_n(x)}{n!}t^n$

[9] Explain the following equations. Assume that index runs from 1 to 3.

[a] $(x_{i\alpha}-\overline{x}\delta_{i\alpha})(x_{k\alpha}-\overline{x}\delta_{k\alpha})$

[b] $A_{ik}x_ix_k$

[10] Suppose that index runs from 1 to 3. The permutation symbol is defined as

$$\varepsilon_{ikn}=\frac{(i-k)(k-n)(n-i)}{2} \tag{2.c}$$

[a] If $T_{ik}=T_{ki}$, then show that $\varepsilon_{ipq}T_{pq}=0$.

[b] Show that $\varepsilon_{ipq}\varepsilon_{ipq}=6$.

[c] Show that $\varepsilon_{ikm}\varepsilon_{pqm}=\delta_{ip}\delta_{kq}-\delta_{iq}\delta_{kp}$.

[11] Prove that

[a] If $T_{ik}=-T_{ki}$, then $T_{ik}x_ix_k=0$.

[b] If $W_{ik}=-W_{ki}$ and $S_{ik}=S_{ki}$, then $S_{ik}W_{ik}=0$

[12] We define

$$G_{ikpq}=\lambda\delta_{ik}\delta_{pq}+\mu\left(\delta_{ip}\delta_{kq}+\delta_{iq}\delta_{kp}\right)+\gamma\left(\delta_{ip}\delta_{kq}-\delta_{iq}\delta_{kp}\right) \tag{2.d}$$

where λ, μ, and γ are constant. When $T_{ik}=T_{ki}$ and $E_{ik}=E_{ki}$, calculate $T_{ik}=G_{ikpq}E_{pq}$.

3 Coordinate System and Basis

3.1 How to Construct a Coordinate System

From now on, we will devote to physical vectors. We will consider only 3-dimensional inner product space of physical vectors. Since most physical vectors are related to geometric vectors such as position and velocity, we start from how to quantify position. One of the simplest way to treat position as a mathematical entity is to construct three mutually perpendicular axes at the origin. The origin divides each axis to two parts: positive and negative parts. Let the three unit vectors parallel to the three axes be denoted by $\mathbf{e}_1$, $\mathbf{e}_2$, and $\mathbf{e}_3$. The direction of each unit vector is chosen as the one from the origin to positive part. Since these three unit vectors are mutually perpendicular, they are linearly independent. From our intuition, we know that a position can be described uniquely by three numbers. This allows us to write a position vector $\mathbf{r}$ as

$$\mathbf{r} = x_1\mathbf{e}_1 + x_2\mathbf{e}_2 + x_3\mathbf{e}_3 = x_k\mathbf{e}_k \tag{3.1}$$

where the absolute value of component x_k implies the minimum distance from the position $\mathbf{r}$ to kth axis. The sign of x_k is positive when the vertical line from the position to kth axis meets the positive part of the axis. Since the three orthogonal unit vectors span any position as shown in Eq. (3.1), these vectors form an orthonormal basis. Thus, coordinate system can be considered as a mapping from a geometric point to a pair of three real numbers.

Equation (3.1) can be interpreted in different manners. When x_1 is considered as a variable with fixing $x_2 = x_3 = 0$, Eq. (3.1) is the equation of the straight line passing the origin in the direction of $\mathbf{e}_1$. Similarly, Eq. (3.1) becomes the equation of the straight line passing the origin in the direction of $\mathbf{e}_k$ when x_k is considered as a variable with fixing the other two coordinates fixed. Generalizing this reasoning further, consider the following vector equation:

$$\mathbf{p} = \mathbf{r} + \xi_k\mathbf{u}_k \tag{3.2}$$

where $\mathbf{u}_1$, $\mathbf{u}_2$ and $\mathbf{u}_3$ are linearly independent and constant, and $\mathbf{r}$ is a position vector under consideration. When two of ξ_1, ξ_2, and ξ_3 are fixed at zero and the other is allowed to vary, Eq. (3.2) becomes the straight line passing the point $\mathbf{r}$. When ξ_i is chosen as a variable, the direction of the line is parallel to the vector $\mathbf{u}_i$. Since $\mathbf{u}_1$, $\mathbf{u}_2$, and $\mathbf{u}_3$ are linearly independent, Eq. (3.2) can be converted to three straight lines which do not meet each other anywhere except the point $\mathbf{r}$. These three lines are called coordinate lines. Every position $\mathbf{r}$ has three coordinate lines and is identified by the intersection of the three coordinate lines. Varying $\mathbf{r}$, the space can be filled with coordinate lines. The three vectors $\mathbf{u}_1$, $\mathbf{u}_2$, and $\mathbf{u}_3$ are tangent vectors of the corresponding coordinate lines at the position $\mathbf{r}$ because

$$\mathbf{u}_i = \frac{\partial \mathbf{p}}{\partial \xi_i} \tag{3.3}$$

The three numbers ξ_1, ξ_2, and ξ_3 are coordinates of $\mathbf{p}$ relative to $\mathbf{r}$.

Consider a plane passing the position $\mathbf{r}$. When the normal vector of the plane is denoted by $\mathbf{n}$, any point on the plane, say $\mathbf{p}$, satisfies following equation:

$$(\mathbf{p} - \mathbf{r}) \cdot \mathbf{n} = 0 \tag{3.4}$$

There are infinitely many planes expressed by Eq. (3.4). Among these planes, we are interested in the planes where one of the three relative coordinates is fixed and the others are free to vary, say $\xi_i = 0$. Then, Eqs. (3.2) and (3.4) lead us to

$$\left(\xi_\alpha \mathbf{u}_\alpha + \xi_\beta \mathbf{u}_\beta\right) \cdot \mathbf{n}_i = 0 \,(\text{no sum on } \alpha \,\text{and}\, \beta) \tag{3.5}$$

Note that $\alpha \neq i$, $\beta \neq i$ and $\alpha \neq \beta$. The normal vector $\mathbf{n}_i$ for $\xi_i = 0$ must be perpendicular to both $\mathbf{u}_\alpha$ and $\mathbf{u}_\beta$ because ξ_α and ξ_β are arbitrary real numbers. Such normal vector must be parallel to $\mathbf{u}_\alpha \times \mathbf{u}_\beta$. Then, we can choose

$$\mathbf{n}_1 = \gamma_1 \mathbf{u}_2 \times \mathbf{u}_3, \quad \mathbf{n}_2 = \gamma_2 \mathbf{u}_3 \times \mathbf{u}_1, \quad \mathbf{n}_3 = \gamma_3 \mathbf{u}_1 \times \mathbf{u}_2 \tag{3.6}$$

where γ_i is proportional coefficient. Since $\mathbf{u}_1 \cdot (\mathbf{u}_2 \times \mathbf{u}_3) \neq 0$ for any three vectors of linear independence, we can choose

$$\gamma_1 = \gamma_2 = \gamma_3 = \frac{1}{\mathbf{u}_1 \cdot (\mathbf{u}_2 \times \mathbf{u}_3)} \tag{3.7}$$

Then, we know $\mathbf{u}_i \cdot \mathbf{n}_k = \delta_{ik}$. It is interesting that these properties of $\{\mathbf{n}_i\}$ are those of the dual basis of $\{\mathbf{u}_i\}$. Furthermore, it is not difficult to show that position $\mathbf{r}$ is the intersection of the three flat planes obtained by substitution of $\xi_1 = 0$, $\xi_2 = 0$ and $\xi_3 = 0$ into Eq. (3.2).

From elementary calculus, it is known that $f(\mathbf{p}) = 0$, where $f(\mathbf{p})$ is a real-valued function and is a mathematical expression of a surface in three-dimensional space. It is also known that the gradient of f at a point $\mathbf{p}$ on the surface is a vector perpendicular to the surface at the point $\mathbf{p}$. Thus, the normal vector $\mathbf{n}_i$ is parallel to $\nabla f_i(\mathbf{p})$, the gradient of $f_i(\mathbf{p}) = \xi_i$. Note that for a function $f(\mathbf{p})$, the total differential of the function is given as

$$\mathrm{d}f = f(\mathbf{p} + \mathrm{d}\mathbf{p}) - f(\mathbf{p}) = \frac{\partial f}{\partial \xi_k} \mathrm{d}\xi_k = \nabla f \cdot \mathrm{d}\mathbf{p} \tag{3.8}$$

Note that ∇f of Eq. (3.8) is the gradient of f at $\mathbf{p}$. With the help of Eq. (3.2), we know that $\mathrm{d}\mathbf{p} = \mathrm{d}\xi_k \mathbf{u}_k$. Then, Eq. (3.8) gives

$$\frac{\partial f}{\partial \xi_k} \mathrm{d}\xi_k = (\mathbf{u}_k \cdot \nabla f)\, \mathrm{d}\xi_k \tag{3.9}$$

Since Eq. (3.9) holds for arbitrary $\mathrm{d}\xi_k$, we have

$$\frac{\partial f}{\partial \xi_k} = \mathbf{u}_k \cdot \nabla f \tag{3.10}$$

Note that the right-hand side of Eq. (3.10) is the directional derivative in the direction of $\mathbf{u}_k$. Replacement of f by ξ_i gives

$$\mathbf{u}_k \cdot \nabla \xi_i = \frac{\partial \xi_i}{\partial \xi_k} = \delta_{ik} \tag{3.11}$$

Since there exists uniquely the set of vectors $\{\mathbf{n}_i\}$ satisfying $\mathbf{n}_i \cdot \mathbf{u}_k = \delta_{ik}$ for a given set of linearly independent vectors $\{\mathbf{u}_k\}$, it is concluded that the three vectors $\nabla \xi_i$ are identical to the three vectors $\mathbf{n}_i$ of Eq. (3.6):

$$\mathbf{n}_i = \nabla \xi_i \tag{3.12}$$

Coordinate surfaces are defined as the surfaces characterized by $\xi_i = 0$.

When $\{\mathbf{u}_i\}$ is a set of unit vectors which are mutually orthogonal, it is clear that $\mathbf{u}_i = \mathbf{n}_i$. In other words, dual basis is identical to the original basis. If $\{\mathbf{u}_i\}$ is not an orthonormal basis, then $\mathbf{u}_i = \mathbf{n}_i$ may not be valid. A coordinate system with a set of orthonormal vectors $\{\mathbf{u}_i\}$ is called rectangular coordinate system or Cartesian coordinate system. There are infinitely many rectangular coordinate systems because it is possible to choose infinitely many $\{\mathbf{u}_i\}$. For rectangular coordinate system, notation $\mathbf{e}_i$ will be used instead of $\mathbf{u}_i$ in order to emphasize the fact that $\mathbf{e}_i \cdot \mathbf{e}_k = \delta_{ik}$ and the dual basis of $\{\mathbf{e}_i\}$ is itself.

Why are such complicate notions necessary? It is because we want to construct a curvilinear coordinate system. We first consider coordinate lines instead of base vectors when a curvilinear coordinate system is constructed. Imagine that the space is filled with infinitely many coordinate lines. The condition of coordinate lines is that only three coordinate lines intersect at a point in the space and they cannot meet again at any different point. Let us call it *the intersection condition of coordinate lines*. If the three coordinate lines are straight and intersect perpendicularly at any point of the space, the coordinate system is a rectangular coordinate system. If a coordinate line is not straight, then the coordinate system is curvilinear. Can this way to construct a coordinate system describe any point in the space uniquely? The answer is yes if all coordinate lines satisfy the conditions mentioned above.

Categorize all coordinate lines into three types: ξ_1-lines, ξ_2-lines, and ξ_3-lines. The classification is that every coordinate line passing at a point is assigned to one of the three types without any duplication. Thus, every point has its own three coordinate lines with different types. With this, it is concluded that any two different coordinate lines with the same type cannot intersect. Let us call it *the parallelism of*

coordinate line. However, it does not mean that two different points cannot belong to the same coordinate line. There must be infinitely many points in a coordinate lines. Without loss of generality, consider a coordinate line which belongs to the type of ξ_1-lines and two different points A and B on the ξ_1-line. The point A has its own ξ_2-line and ξ_3-line and so does the point B. If the two ξ_2-lines of A and B are identical, the contradiction of the intersection condition of coordinate lines is recognized. It is because the ξ_1-line and the ξ_2-line intersect twice at two different points of A and B. The same is valid for ξ_3-line. Finally, it can be concluded that every point is determined uniquely by a particular set of three coordinate lines of different types.

Since any line can be parameterized by real number (Kreyszig 2011), every point has a unique set of three real numbers called coordinates. Each real number is the parameter of corresponding coordinate line.

Now move to the method for determining the basis naturally imbedded in a coordinate system. One of the most natural ways is to use the tangent vector of coordinate line as shown in Eq. (3.3). Since all coordinate systems have three types of coordinate lines, there exist tangent vectors of three kinds according to the coordinate lines of three types. The magnitude of each tangent vector depends on how to parameterize the coordinate line. In general, the three tangent vectors depend on positions where the tangents are taken. The three tangent vectors at a point are linearly independent because of the intersection condition and the parallelism of coordinate lines. Hence, these tangent vectors at a point can be chosen as a basis. The members of this basis are called *tangent base vectors* (Aris 1962).

The tangent base vectors of a rectangular coordinate system are constant vectors irrespective of position because every coordinate line is straight. Since coordinate lines at a point intersect perpendicularly, the tangent base vectors are mutually orthogonal. If the parameterization of coordinate lines is taken to be consistent with length scale, the three tangent base vectors have the same magnitude of unity. Hence, it is conventional to define a rectangular coordinate system as the one that have orthonormal basis. All coordinate systems with straight coordinate lines are not rectangular coordinate system because straight coordinate lines can be chosen in order that intersection is made by angles different from rectangular angle. Such coordinate systems are called oblique linear coordinate systems which are convenient in crystallography.

Let x_k be a coordinate of rectangular coordinate system. Then, we are interested in one-to-one mapping such that

$$\xi^i = \xi^i(x_1, x_2, x_3) \tag{3.13}$$

where i is not power but superscript. The three functions ξ^i of rectangular coordinates have different values for different sets of rectangular coordinates because Eq. (3.13) is a one-to-one mapping. Since (x_1, x_2, x_3) determines a point uniquely, so does (ξ^1, ξ^2, ξ^3). Hence, it can be said that (ξ^1, ξ^2, ξ^3) is also a set of

coordinates. Let us call $\{\xi^i\}$ generalized coordinate system. Then, there exists the inverse mapping such that

$$x_k = x_k\left(\xi^1, \xi^2, \xi^3\right) \tag{3.14}$$

When two of ξ^is are fixed, Eq. (3.14) is a curve parameterized by the other ξ. Hence, Eq. (3.14) can be used to define three coordinate lines. Since a position $\mathbf{p}$ is expressed by $\mathbf{p} = x_k \mathbf{e}_k$, the tangent base vectors of ξ^i-coordinate system is given by

$$\mathbf{g}_i = \frac{\partial \mathbf{p}}{\partial \xi^i} = \frac{\partial x_k}{\partial \xi^i}\mathbf{e}_k \tag{3.15}$$

The tangent base vectors are called *contravariant base vectors*.

Coordinate surface was discussed previously. From Eq. (3.13), $\xi^i - c = 0$ is a coordinate surface where c is a given real number. Then, we can define gradient vector of coordinate surface as follows:

$$\mathbf{g}^i = \nabla \xi^i = \frac{\partial \xi^i}{\partial x_m}\mathbf{e}_m \tag{3.16}$$

It is interesting to investigate the inner product of tangent base vector and gradient vector:

$$\begin{aligned} \mathbf{g}_i \cdot \mathbf{g}^k &= \left(\frac{\partial x_p}{\partial \xi^i}\mathbf{e}_p\right) \cdot \left(\frac{\partial \xi^k}{\partial x_q}\mathbf{e}_q\right) = \frac{\partial x_p}{\partial \xi^i}\frac{\partial \xi^k}{\partial x_q}\mathbf{e}_p \cdot \mathbf{e}_q \\ &= \frac{\partial x_p}{\partial \xi^i}\frac{\partial \xi^k}{\partial x_q}\delta_{pq} = \frac{\partial x_p}{\partial \xi^i}\frac{\partial \xi^k}{\partial x_p} \\ &= \frac{\partial \xi^k}{\partial \xi^i} = \delta_{ik} \end{aligned} \tag{3.17}$$

Here, chain rule of differentiation was used. Equation (3.17) implies that the gradient vectors are dual basis of tangent basis. The dual base vectors $\mathbf{g}^i$ are called *covariant base vectors*.

From Eq. (3.17), it is also known that the matrix $\partial \xi^i / \partial x_k$ is the inverse of the matrix $\partial x_i / \partial \xi^k$. This existence of inverse implies that the Jacobian of the mapping of Eq. (3.13) is not zero:

$$\det\left(\frac{\partial \xi^i}{\partial x_k}\right) \neq 0 \tag{3.18}$$

Such transform of coordinate is called *proper transform* (Sokolnikoff 1964).

Since a coordinate system has base vectors of two kinds, there are two ways to express a vector:

$$\mathbf{v} = v^k \mathbf{g}_k = v_k \mathbf{g}^k \tag{3.19}$$

The components denoted by superscript v^k and subscript v_k are called covariant and contravariant components of a vector $\mathbf{v}$, respectively. Note that using Eq. (3.17) gives

$$v^i = \mathbf{g}^i \cdot \mathbf{v} \quad \text{and} \quad v_i = \mathbf{g}_i \cdot \mathbf{v} \tag{3.20}$$

The magnitude of a vector $\mathbf{v}$ is given by the square root of $\mathbf{v} \cdot \mathbf{v}$ as follows:

$$\|\mathbf{v}\| = \sqrt{\mathbf{v} \cdot \mathbf{v}} = \sqrt{(v_i \mathbf{g}^i) \cdot (v^k \mathbf{g}_k)} = \sqrt{v_i v^i} \tag{3.21}$$

We have more two different ways to express $\|\mathbf{v}\|$ such that

$$\|\mathbf{v}\| = \sqrt{(v_i \mathbf{g}^i) \cdot (v_k \mathbf{g}^k)} = \sqrt{g^{ik} v_i v_k} \tag{3.22}$$

and

$$\|\mathbf{v}\| = \sqrt{(v^i \mathbf{g}_i) \cdot (v^k \mathbf{g}_k)} = \sqrt{g_{ik}\, v^i v^k} \tag{3.23}$$

where

$$g^{ik} = \mathbf{g}^i \cdot \mathbf{g}^k \quad \text{and} \quad g_{ik} = \mathbf{g}_i \cdot \mathbf{g}_k \tag{3.24}$$

It is easily understood that two matrices g^{ik} and g_{ik} are symmetric. Since the magnitude of vector is nonnegative real number, it is clear that the followings are valid for any real numbers of v_i and v^i:

$$v_i v^i \geq 0, \quad g^{ik} v_i v_k \geq 0 \quad \text{and} \quad g_{ik} v^i v^k \geq 0 \tag{3.25}$$

Inequalities (3.25) imply that g^{ik} and g_{ik} are positive definite. Since g^{ik} and g_{ik} are involved in the magnitude of vector, they are called metric matrices.

Since contravariant base vector $\mathbf{g}_i$ is a vector, it can be expressed by a linear combination of covariant base vectors such that $\mathbf{g}_i = \gamma_{ik} \mathbf{g}^k$. Application of Eq. (3.24) gives $\gamma_{ik} = g_{ik}$. Similarly $\mathbf{g}^i = \gamma^{ik} \mathbf{g}_k$ gives $\gamma^{ik} = g^{ik}$. Then, we know that metric matrix converts contravariant base vector to covariant base vector and vice versa:

$$\mathbf{g}^i = g^{ik} \mathbf{g}_k \quad \text{and} \quad \mathbf{g}_i = g_{ik} \mathbf{g}^k \tag{3.26}$$

Furthermore, it is not difficult to show that

$$v^i = g^{ik} v_k \quad \text{and} \quad v_i = g_{ik} v^k \tag{3.27}$$

where v^i and v_i are, respectively, covariant and contravariant components of a vector $\mathbf{v} = v^i \mathbf{g}_i = v_i \mathbf{g}^i$.

3.2 Cylindrical and Spherical Coordinate Systems

Among curvilinear coordinate systems, cylindrical and spherical coordinate systems are representative and frequently used in engineering problems. The definition of cylindrical coordinate system is given by

$$r = \sqrt{x^2 + y^2}, \quad \phi = \arctan \frac{y}{x}, \quad z = z \tag{3.28}$$

where $x = x_1$, $y = x_2$, and $z = x_3$ are rectangular coordinates and $r = \xi^1$, $\phi = \xi^2$, and $z = \xi^3$ are cylindrical coordinates. Equation (3.28) allows the following inverse mapping:

$$x = r \cos \phi, \quad y = r \sin \phi, \quad z = z \tag{3.29}$$

The contravariant and covariant base vectors of cylindrical coordinate system are given by

$$\mathbf{g}_1 = \cos \phi \mathbf{e}_1 + \sin \phi \mathbf{e}_2; \quad \mathbf{g}_2 = -r \sin \phi \mathbf{e}_1 + r \cos \phi \mathbf{e}_2; \quad \mathbf{g}_3 = \mathbf{e}_3 \tag{3.30}$$

and

$$\mathbf{g}^1 = \cos \phi \, \mathbf{e}_1 + \sin \phi \, \mathbf{e}_2; \quad \mathbf{g}^2 = -\frac{\sin \phi}{r} \mathbf{e}_1 + \frac{\cos \phi}{r} \mathbf{e}_2; \quad \mathbf{g}^3 = \mathbf{e}_3 \tag{3.31}$$

Equations (3.30) and (3.31) reveal that both contravariant and covariant basis are orthogonal ones: If $i \neq k$, then $\mathbf{g}_i \cdot \mathbf{g}_k = \mathbf{g}^i \cdot \mathbf{g}^k = 0$. Furthermore, $\mathbf{g}_i$ is parallel to $\mathbf{g}^k$. Because of these properties of cylindrical coordinate system, it is more convenient to use the following orthonormal basis:

$$\begin{aligned} \mathbf{e}_r &= \mathbf{g}_1 = \mathbf{g}^2 = \cos \phi \, \mathbf{e}_1 + \sin \phi \, \mathbf{e}_2 \\ \mathbf{e}_\phi &= \frac{1}{r} \mathbf{g}_2 = r \mathbf{g}^2 = -\sin \phi \, \mathbf{e}_1 + \cos \phi \, \mathbf{e}_2 \\ \mathbf{e}_z &= \mathbf{g}_1 = \mathbf{g}^1 = \mathbf{e}_3 \end{aligned} \tag{3.32}$$

Cylindrical coordinate system is more convenient than rectangular coordinate system when a mathematical problem has axial symmetry. On the other hand, spherical coordinate system is more convenient when point symmetry is involved. Spherical coordinate system is defined as

$$r = \sqrt{x^2 + y^2 + z^2}, \quad \theta = \arctan\frac{z}{\sqrt{x^2 + y^2}}, \quad \phi = \arctan\frac{y}{x} \tag{3.33}$$

The inverse mapping of Eq. (3.33) is given as

$$x = r\cos\phi\sin\theta, \quad y = r\sin\phi\sin\theta, \quad z = r\cos\theta \tag{3.34}$$

The contravariant and covariant base vectors of spherical coordinate system is given as

$$\begin{aligned}
\mathbf{g}_1 &= \cos\phi\sin\theta\,\mathbf{e}_1 + \sin\phi\sin\theta\,\mathbf{e}_2 + \cos\theta\,\mathbf{e}_3 \\
\mathbf{g}_2 &= r\cos\phi\cos\theta\,\mathbf{e}_1 + r\sin\phi\cos\theta\,\mathbf{e}_2 - r\sin\theta\,\mathbf{e}_3 \\
\mathbf{g}_3 &= -r\sin\phi\sin\theta\,\mathbf{e}_1 + r\cos\phi\sin\theta\,\mathbf{e}_2
\end{aligned} \tag{3.35}$$

and

$$\mathbf{g}^1 = \mathbf{g}_1, \quad \mathbf{g}^2 = \frac{1}{r^2}\mathbf{g}_2, \quad \mathbf{g}^3 = \frac{1}{r^2\sin^2\theta}\mathbf{g}_3 \tag{3.36}$$

Note that $\xi^1 = r$, $\xi^2 = \theta$ and $\xi^3 = \phi$ were used. Just as cylindrical coordinate system, we have $\mathbf{g}_i \cdot \mathbf{g}_k = \mathbf{g}^i \cdot \mathbf{g}^k = 0$ whenever $i \neq k$. Then, it is also convenient to use orthonormal basis such that

$$\begin{aligned}
\mathbf{e}_r &= \mathbf{g}_1 = \mathbf{g}^1 = \cos\phi\sin\theta\,\mathbf{e}_1 + \sin\phi\sin\theta\,\mathbf{e}_2 + \cos\theta\,\mathbf{e}_3 \\
\mathbf{e}_\theta &= \frac{1}{r}\mathbf{g}_2 = r\mathbf{g}^2 = \cos\phi\cos\theta\,\mathbf{e}_1 + \sin\phi\cos\theta\,\mathbf{e}_2 - \sin\theta\,\mathbf{e}_3 \\
\mathbf{e}_\phi &= \frac{1}{r\sin\theta}\mathbf{g}_3 = r\sin\theta\,\mathbf{g}^3 = -\sin\phi\,\mathbf{e}_1 + \cos\phi\,\mathbf{e}_2
\end{aligned} \tag{3.37}$$

It is interesting that $\mathbf{e}_\phi$ and longitude angle ϕ of spherical coordinate system are identical to $\mathbf{e}_\phi$ and ϕ of cylindrical coordinate system, respectively. Note that the radial distance of spherical coordinate system is denoted by r which is the same symbol used for the distance from z axis in this book, while symbol ρ is used for the radial distance in another book (Arfken 2001).

3.3 Change of Coordinate Systems

Consider two generalized coordinate systems such as $\{\xi^i\}$ and $\{\overline{\xi}^i\}$. Since both ξ^i and $\overline{\xi}^i$ are one-to-one mappings from the same rectangular coordinate system, composition of mappings gives

$$\overline{\xi}^i = \overline{\xi}^i(x_1, x_2, x_3) = \overline{\xi}^i\left(x_1\left(\{\xi^k\}\right), x_2\left(\{\xi^k\}\right), x_3\left(\{\xi^k\}\right)\right) = \overline{\xi}^i\left(\xi^1, \xi^2, \xi^3\right) \quad (3.38)$$

Equation (3.38) implies the existence of the mapping from $\{\xi^i\}$ to $\{\overline{\xi}^i\}$ and the inverse mapping from $\{\overline{\xi}^i\}$ to $\{\xi^i\}$ because the two coordinates are proper. Hence, we can write

$$\xi^i = \xi^i\left(\overline{\xi}^1, \overline{\xi}^2, \overline{\xi}^3\right), \quad \overline{\xi}^i = \overline{\xi}^i\left(\xi^1, \xi^2, \xi^3\right) \quad (3.39)$$

Let the contravariant and covariant base vectors of $\{\xi^i\}$ be denoted by $\{\mathbf{g}_i\}$ and $\{\mathbf{g}^i\}$, respectively. Similarly, $\{\overline{\mathbf{g}}_i\}$ and $\{\overline{\mathbf{g}}^i\}$ are the contravariant and covariant base vectors of $\{\overline{\xi}^i\}$. Then, chain rule of differentiation gives

$$\overline{\mathbf{g}}_i = \frac{\partial x_m}{\partial \overline{\xi}^i}\mathbf{e}_m = \frac{\partial x_m}{\partial \xi^k}\frac{\partial \xi^k}{\partial \overline{\xi}^i}\mathbf{e}_m = \frac{\partial \xi^k}{\partial \overline{\xi}^i}\mathbf{g}_k \quad (3.40)$$

and

$$\overline{\mathbf{g}}^i = \frac{\partial \overline{\xi}^i}{\partial x_m}\mathbf{e}_m = \frac{\partial \overline{\xi}^i}{\partial \xi^k}\frac{\partial \xi^k}{\partial x_m}\mathbf{e}_m = \frac{\partial \overline{\xi}^i}{\partial \xi^k}\mathbf{g}^k \quad (3.41)$$

Note that chain rule of differentiation gives

$$\frac{\partial \xi^i}{\partial \overline{\xi}^m}\frac{\partial \overline{\xi}^m}{\partial \xi^k} = \frac{\partial \xi^i}{\partial \xi^k} = \delta^i_k \quad (3.42)$$

where $\delta^i_k = \delta_{ik}$ is used to emphasize that contravariant and covariant components are represented by subscript and superscript, respectively. Equation (3.42) implies that $\partial \xi^i / \partial \overline{\xi}^k$ is the inverse of $\partial \overline{\xi}^i / \partial \xi^k$ and vice versa. Then, Eqs. (3.40) and (3.41) can be rewritten as

$$\mathbf{g}_i = \frac{\partial \overline{\xi}^k}{\partial \xi^i}\overline{\mathbf{g}}_k \quad \text{and} \quad \mathbf{g}^i = \frac{\partial \xi^i}{\partial \overline{\xi}^k}\overline{\mathbf{g}}^k \quad (3.43)$$

Since a vector $\mathbf{v}$ can be expressed by Eq. (3.19), we have

$$\mathbf{v} = v^i \mathbf{g}_i = v^i \frac{\partial \overline{\xi}^k}{\partial \xi^i} \overline{\mathbf{g}}_k = \overline{v}^k \overline{\mathbf{g}}_k = v_i \mathbf{g}^i = v_i \frac{\partial \xi^i}{\partial \overline{\xi}^k} \overline{\mathbf{g}}^k = \overline{v}_k \overline{\mathbf{g}}^k \tag{3.44}$$

where $\overline{v}^k$ and $\overline{v}_k$ are the covariant and contravariant components of $\mathbf{v}$ in $\overline{\xi}$-coordinate system. Then, we obtain the transform rule for component of vector as follows:

$$\overline{v}^i = \frac{\partial \overline{\xi}^i}{\partial \xi^k} v^k \quad \text{and} \quad \overline{v}_i = \frac{\partial \xi^k}{\partial \overline{\xi}^i} v_k \tag{3.45}$$

As a special case, consider two rectangular coordinate systems $\{x_i\}$ and $\{\overline{x}_i\}$ with the common origin. Then, the transform rule for basis is given by

$$\mathbf{e}_i = \frac{\partial \overline{x}_k}{\partial x_i} \overline{\mathbf{e}}_k \quad \text{and} \quad \overline{\mathbf{e}}_i = \frac{\partial x_k}{\partial \overline{x}_i} \mathbf{e}_k \tag{3.46}$$

Since base vectors of rectangular coordinate system are constant, the matrix of partial derivatives $\partial \overline{x}_k / \partial x_i$ and its inverse are constant matrices. Furthermore, it is valid that

$$\frac{\partial \overline{x}_m}{\partial x_i} \frac{\partial \overline{x}_m}{\partial x_k} = \frac{\partial x_m}{\partial \overline{x}_i} \frac{\partial x_m}{\partial \overline{x}_k} = \delta_{ik} \tag{3.47}$$

because $\overline{\mathbf{e}}_i \cdot \overline{\mathbf{e}}_k = \mathbf{e}_i \cdot \mathbf{e}_k = \delta_{ik}$. Since the inverse matrix is uniquely determined, we have

$$\frac{\partial \overline{x}_i}{\partial x_k} = \frac{\partial x_i}{\partial \overline{x}_k} \tag{3.48}$$

This implies that the transpose matrix of $\partial \overline{x}_k / \partial x_i$ is its inverse. Such matrix is called orthogonal matrix.

Problem 3

[1] Express the intersection point between a flat plane $\{\mathbf{x} | \, \mathbf{n} \cdot (\mathbf{x} - \mathbf{p}) = 0\}$ and a straight line $\{\mathbf{x} | \mathbf{x} = \mathbf{q} + \mathbf{v}\, t, t \in \mathrm{R}\}$ in terms of $\mathbf{n}$, $\mathbf{p}$, $\mathbf{q}$, and $\mathbf{v}$.

[2] When the condition $\xi_i = 0$ is posed to Eq. (3.2), show that Eq. (3.5) is equivalent to the condition.

[3] If Eq. (3.13) is linear equations such as $\xi^i = Q^{ik} x_k$, then find covariant and contravariant bases in terms of the orthonormal basis of the rectangular coordinate system.

[4] Suppose that the contravariant base vectors of a coordinate system satisfy

$$\mathbf{g}_i \cdot \mathbf{g}_k = \begin{cases} 0 & \text{for } i \neq k \\ h_i & \text{for } i = k \end{cases} \tag{3.a}$$

Then, express the covariant base vectors in terms of h_i and the contravariant base vectors.

[5] Derive

$$\mathbf{e}_i = \frac{\partial \xi^k}{\partial x_i}\mathbf{g}_k = \frac{\partial x_i}{\partial \xi_k}\mathbf{g}^k \tag{3.b}$$

[6] Consider two rectangular coordinate systems equipped with orthonormal basis $\{\mathbf{e}_i\}$ and $\{\overline{\mathbf{e}}_i\}$. Prove that

$$\frac{\partial x_k}{\partial \overline{x}_i} = \overline{\mathbf{e}}_i \cdot \mathbf{e}_k$$

[7] Prove that $g^{ik}x_i x_k \geq 0$ for arbitrary real numbers x_i with $i = 1, 2, 3$.

[8] Consider cylindrical coordinate system with $\xi^1 = r$, $\xi^2 = \phi$, and $\xi^3 = z$ and calculate the coefficients Γ^m_{ik} such that

$$\frac{\partial \mathbf{g}_i}{\partial \xi^k} = \Gamma^m_{ik}\mathbf{g}_m$$

[9] For two rectangular coordinates, a vector can be expressed by $\mathbf{v} = v_i\mathbf{e}_i = \overline{v}_k\overline{\mathbf{e}}_k$. Find the relation between v_i and $\overline{v}_k$ by using Eq. (3.46).

[10] A position vector $\mathbf{x} = x_k\mathbf{e}_k$ can be expressed in terms of cylindrical coordinates as follows:

$$\mathbf{x} = r\mathbf{e}_r + z\mathbf{e}_z \tag{3.c}$$

From Eq. (3.c), we can obtain

$$\mathrm{d}\mathbf{x} = \mathrm{d}r\,\mathbf{e}_r + r\mathrm{d}\phi\,\mathbf{e}_\phi + \mathrm{d}z\mathbf{e}_z \tag{3.d}$$

Prove Eqs. (3.c) and (3.d).

[11] As for spherical coordinate system, derive the followings:

$$\begin{aligned} \mathbf{e}_1 &= \sin\theta\cos\phi\,\mathbf{e}_r + \cos\theta\cos\phi\,\mathbf{e}_\theta - \sin\phi\,\mathbf{e}_\phi \\ \mathbf{e}_2 &= \sin\theta\sin\phi\,\mathbf{e}_r + \cos\theta\sin\phi\,\mathbf{e}_\theta + \cos\phi\,\mathbf{e}_\phi \\ \mathbf{e}_1 &= \cos\theta\,\mathbf{e}_r - \sin\theta\,\mathbf{e}_\theta \end{aligned} \tag{3.e}$$

[12] Consider a change of coordinates from a rectangular coordinate system to another rectangular coordinate system. Show that for any i and k, $|\partial\overline{x}_i/\partial x_k| \leq 1$.

[13] Express $\partial\overline{x}_i/\partial x_k$ of the Problem [12] in terms of the inner products of $\{\mathbf{e}_i\}$ and $\{\overline{\mathbf{e}}_i\}$. Note that $\mathbf{e}_i$ can be expressed by using a linear combination of $\{\overline{\mathbf{e}}_k\}$ and vice versa.

4 Vector Analysis

4.1 Vector Algebra

Before moving to vector calculus, it is worthwhile to study vector algebra which is helpful for understanding vector calculus. Various vector identities will be introduced here, assuming that the readers know the definition and properties of vector product.

As for right-handed rectangular coordinate system, the orthogonal basis satisfies

$$\mathbf{e}_1 \times \mathbf{e}_2 = \mathbf{e}_3, \quad \mathbf{e}_2 \times \mathbf{e}_3 = \mathbf{e}_1, \quad \mathbf{e}_3 \times \mathbf{e}_1 = \mathbf{e}_2 \tag{4.1}$$

It is interesting that Eq. (4.1) can be rewritten as

$$\mathbf{e}_p \times \mathbf{e}_q = \varepsilon_{pqk}\mathbf{e}_k \tag{4.2}$$

where ε_{ikm} is called permutation symbol or Levi-Civita symbol such that

$$\varepsilon_{ikm} = \frac{(i-k)(k-m)(m-i)}{2} \tag{4.3}$$

Equation (4.3) implies that $\varepsilon_{ikm} = 0$ if any duplication of index occurs and $\varepsilon_{ikm} = \pm 1$ otherwise. When all the three indexes are different, the sign of ε_{ikm} is determined by the number of permutation to make the arrange of the indexes *ikm* be 123. Odd permutations assign -1 while even permutations 1. Taking examples, we have

$$\varepsilon_{123} = \varepsilon_{312} = \varepsilon_{231} = 1; \quad \varepsilon_{213} = \varepsilon_{321} = \varepsilon_{132} = -1 \tag{4.4}$$

Using the permutation symbol provides an easier way to calculate the vector product of two vectors, $\mathbf{a} = a_m\mathbf{e}_m$ and $\mathbf{b} = b_n\mathbf{e}_n$ as follows:

$$\mathbf{a} \times \mathbf{b} = (a_m\mathbf{e}_m) \times (b_n\mathbf{e}_n) = a_m b_n \mathbf{e}_m \times \mathbf{e}_n = \varepsilon_{imn} a_m b_n \mathbf{e}_i \tag{4.5}$$

There are a few identities related to vector product. The identities often appear in various calculations of vector and tensor. Consider three arbitrary vectors, say **a**, **b**, and **c**. One often meets a problem to calculate $(\mathbf{b} \times \mathbf{c}) \times \mathbf{a}$. Vector $\mathbf{b} \times \mathbf{c}$ is perpendicular to both **b** and **c**. Use the notation $\mathbf{n} = \mathbf{b} \times \mathbf{c}$. Then, we can decompose the vector **a** as follows:

$$\mathbf{a} = \nu\mathbf{n} + \beta\mathbf{b} + \gamma\mathbf{c} \tag{4.6}$$

Using Eq. (4.6) gives

$$(\mathbf{b} \times \mathbf{c}) \times \mathbf{a} = \beta\mathbf{b} \times \mathbf{n} + \gamma\mathbf{c} \times \mathbf{n} \tag{4.7}$$

Since $\mathbf{n}$ is perpendicular to both $\mathbf{b}$ and $\mathbf{c}$, it is clear that both $\mathbf{b} \times \mathbf{n}$ and $\mathbf{c} \times \mathbf{n}$ must be spanned by $\mathbf{b}$ and $\mathbf{c}$. Hence, the vector $(\mathbf{b} \times \mathbf{c}) \times \mathbf{a}$ must be a linear combination of $\mathbf{b}$ and $\mathbf{c}$. Since $(\mathbf{b} \times \mathbf{c}) \times \mathbf{a}$ is linear in $\mathbf{a}$, $\mathbf{b}$, and $\mathbf{c}$, it is a reasonable assumption that

$$(\mathbf{b} \times \mathbf{c}) \times \mathbf{a} = \alpha_1(\mathbf{b} \cdot \mathbf{a})\mathbf{c} + \alpha_2(\mathbf{c} \cdot \mathbf{a})\mathbf{b} \tag{4.8}$$

Two coefficients α_1 and α_2 should be determined. Taking inner product with $\mathbf{a}$ on both sides of Eq. (4.8), the left side is zero since it is perpendicular to $\mathbf{a}$.

$$0 = \alpha_1(\mathbf{b} \cdot \mathbf{a})(\mathbf{c} \cdot \mathbf{a}) + \alpha_2(\mathbf{c} \cdot \mathbf{a})(\mathbf{b} \cdot \mathbf{a}) \tag{4.9}$$

This implies that $\alpha_1 = -\alpha_2 \equiv \alpha$. Since Eq. (4.8) must hold for arbitrary vectors, putting $\mathbf{a} = \mathbf{e}_2$, $\mathbf{b} = \mathbf{e}_2$ and $\mathbf{c} = \mathbf{e}_3$ gives

$$\alpha(\mathbf{e}_2 \cdot \mathbf{e}_2)\,\mathbf{e}_3 - \alpha(\mathbf{e}_3 \cdot \mathbf{e}_2)\,\mathbf{e}_2 = \mathbf{e}_3 \tag{4.10}$$

Hence, the coefficient α must be unity and we have

$$(\mathbf{b} \times \mathbf{c}) \times \mathbf{a} = (\mathbf{b} \cdot \mathbf{a})\,\mathbf{c} - (\mathbf{c} \cdot \mathbf{a})\,\mathbf{b} \tag{4.11}$$

This identity can be easily memorized if it is called BAC-CAB rule (Arfken 2001). Applying Eq. (4.5) to Eq. (4.11), we have an identity relating the permutation symbol and Kronecker's delta:

$$\varepsilon_{ijk}\varepsilon_{pqk} = \delta_{ip}\delta_{jq} - \delta_{iq}\delta_{jp} \tag{4.12}$$

From elementary calculus, we know well that the magnitude of vector product is the area of the parallelogram spanned by the two vectors. Hence, the absolute value of the triple product $\mathbf{a} \cdot (\mathbf{b} \times \mathbf{c})$ is the volume of the parallelepiped spanned by the three vectors. Consider a point represented by curvilinear coordinate system. There are three infinitesimal vectors which are tangent to the corresponding coordinate lines:

$$\mathbf{t}_1 \equiv \mathrm{d}\xi^1\mathbf{g}_1, \quad \mathbf{t}_2 \equiv \mathrm{d}\xi^2\mathbf{g}_2, \quad \mathbf{t}_3 \equiv \mathrm{d}\xi^3\mathbf{g}_3 \tag{4.13}$$

We are interested in the volume of the parallelepiped spanned by the three infinitesimal tangent vectors:

$$\mathrm{d}V = \mathbf{t}_1 \cdot (\mathbf{t}_2 \times \mathbf{t}_3) = \mathbf{g}_1 \cdot (\mathbf{g}_2 \times \mathbf{g}_3)\, \mathrm{d}\xi^1 \mathrm{d}\xi^2 \mathrm{d}\xi^3 \tag{4.14}$$

Application of Eq. (3.15) gives

$$\begin{aligned} \mathrm{d}V &= \left(\frac{\partial x_m}{\partial \xi^1}\mathbf{e}_m\right) \cdot \left[\left(\frac{\partial x_n}{\partial \xi^2}\mathbf{e}_n\right) \times \left(\frac{\partial x_k}{\partial \xi^3}\mathbf{e}_k\right)\right] \mathrm{d}\xi^1 \mathrm{d}\xi^2 \mathrm{d}\xi^3 \\ &= \varepsilon_{mnk} \frac{\partial x_m}{\partial \xi^1} \frac{\partial x_n}{\partial \xi^2} \frac{\partial x_k}{\partial \xi^3}\, \mathrm{d}\xi^1 \mathrm{d}\xi^2 \mathrm{d}\xi^3 = \det\left(\frac{\partial x_i}{\partial \xi^k}\right) \mathrm{d}\xi^1 \mathrm{d}\xi^2 \mathrm{d}\xi^3 \end{aligned} \tag{4.15}$$

Note that Eq. (4.15) includes the formula for determination of 3×3 matrix such that

$$\det(F_{ik}) = \varepsilon_{ijk} F_{1i} F_{2j} F_{3k} = \varepsilon_{ijk} F_{i1} F_{j2} F_{k3} \tag{4.16}$$

4.2 Differentiation of Vector

Consider a sufficiently smooth function of position $f(\mathbf{x})$. The position $\mathbf{x}$ can be expressed in various ways depending on coordinate systems. Consider the case of generalized coordinate system such that $f(\mathbf{x}) = f\left(\xi^1, \xi^2, \xi^3\right)$. Then, the total differential of f is given by

$$\mathrm{d}f = \frac{\partial f}{\partial \xi^k} \mathrm{d}\xi^k \tag{4.17}$$

From elementary calculus, it is known that the total differential is the inner product of gradient of the function and infinitesimal difference of position vector:

$$\mathrm{d}f = \nabla f \cdot \mathrm{d}\mathbf{x} \tag{4.18}$$

Since the position vector x can be expressed by $\mathbf{x} = x_k \mathbf{e}_k$, the infinitesimal difference is given by

$$\mathrm{d}\mathbf{x} = \mathrm{d}x_k \mathbf{e}_k = \frac{\partial x_k}{\partial \xi^i} \mathrm{d}\xi^i \mathbf{e}_k = \mathrm{d}\xi^i \mathbf{g}_i \tag{4.19}$$

where Eq. (3.15) was used. Since ∇f is a vector, we can express ∇f in terms of a linear combination of covariant base vector:

$$\nabla f = f_k \mathbf{g}^k \tag{4.20}$$

Substitution of Eqs. (4.19) and (4.20) into Eq. (4.18) yields

$$\mathrm{d}f = \left(f_k \mathbf{g}^k\right) \cdot \left(\mathrm{d}\xi^i \mathbf{g}_i\right) = f_i \mathrm{d}\xi^i \tag{4.21}$$

Comparison of Eq. (4.21) with Eq. (4.17) illustrates

$$\nabla f = \frac{\partial f}{\partial \xi^k} \mathbf{g}^k \tag{4.22}$$

Elementary calculus defines the gradient of a function as follows:

$$\nabla f = \frac{\partial f}{\partial x_k} \mathbf{e}_k \tag{4.23}$$

Application of chain rule of differentiation gives

$$\nabla f = \frac{\partial f}{\partial \xi^i} \frac{\partial \xi^i}{\partial x_k} \mathbf{e}_k = \frac{\partial f}{\partial \xi^i} \mathbf{g}^i \tag{4.24}$$

where Eq. (3.16) was used. Hence, we obtained the same equation again.

Since vector-differential operators such as curl and divergence can be expressed by vector operation on vectors with del operator $\nabla = \mathbf{e}_k(\partial/\partial x_k)$, it is important to express the del operator in generalized coordinate system. The learning from gradient gives

$$\nabla = \mathbf{g}^k \frac{\partial}{\partial \xi^k} \tag{4.25}$$

Then, the divergent of a vector $\mathbf{v} = v^i \mathbf{g}_i$ is given by

$$\nabla \cdot \mathbf{v} = \left(\mathbf{g}^k \frac{\partial}{\partial \xi^k}\right) \cdot \left(v^i \mathbf{g}_i\right) = \mathbf{g}^k \cdot \frac{\partial v^i \mathbf{g}_i}{\partial \xi^k} = \frac{\partial v^i}{\partial \xi^k} \mathbf{g}^k \cdot \mathbf{g}_i + v^i \mathbf{g}^k \cdot \frac{\partial \mathbf{g}_i}{\partial \xi^k} \tag{4.26}$$

It is noteworthy that the partial derivative of $\partial \mathbf{g}_i / \partial \xi^k$ is not the zero vector because base vectors of general coordinate system depend on position in general. Hence, we have to evaluate the partial derivative. Using Eq. (3.15) gives

$$\frac{\partial \mathbf{g}_i}{\partial \xi^k} = \frac{\partial}{\partial \xi^k} \left(\frac{\partial x_m}{\partial \xi^i} \mathbf{e}_m\right) = \frac{\partial^2 x_m}{\partial \xi^i \partial \xi^k} \mathbf{e}_m \tag{4.27}$$

Then, application of Eq. (3.16) gives

$$\mathbf{g}^k \cdot \frac{\partial \mathbf{g}_i}{\partial \xi^k} = \frac{\partial^2 x_m}{\partial \xi^i \partial \xi^k} \left(\frac{\partial \xi^k}{\partial x_n} \mathbf{e}_n \right) \cdot \mathbf{e}_m = \frac{\partial^2 x_m}{\partial \xi^i \partial \xi^k} \frac{\partial \xi^k}{\partial x_m} \tag{4.28}$$

Then finally, we have

$$\nabla \cdot \mathbf{v} = \frac{\partial v^i}{\partial \xi^i} + v^i \frac{\partial^2 x_m}{\partial \xi^i \partial \xi^k} \frac{\partial \xi^k}{\partial x_m} \tag{4.29}$$

These analyses illustrate that vector differentiation in generalized coordinate system needs formula of partial derivatives of base vectors with respective generalized coordinates. Followings are summary of such partial derivatives:

$$\frac{\partial \mathbf{g}_i}{\partial \xi^k} = \Gamma^m_{ik} \mathbf{g}_m = \Gamma_{mik} \mathbf{g}^m \tag{4.30}$$

and

$$\frac{\partial \mathbf{g}^i}{\partial \xi^k} = -\Gamma^i_{mk} \mathbf{g}^m = -\Gamma^i_{nk} g^{nm} \mathbf{g}_m \tag{4.31}$$

where

$$\Gamma^m_{ik} = \mathbf{g}_m \cdot \frac{\partial \mathbf{g}_i}{\partial \xi^k} = \frac{\partial^2 x_p}{\partial \xi^i \partial \xi^k} \frac{\partial \xi^m}{\partial x_p} = \Gamma^m_{ki} \tag{4.32}$$

and

$$\Gamma_{mik} = \mathbf{g}_m \cdot \frac{\partial \mathbf{g}_i}{\partial \xi^k} = \frac{\partial^2 x_p}{\partial \xi^m \partial \xi^i} \frac{\partial x_p}{\partial \xi^k} = \Gamma_{imk} \tag{4.33}$$

The coefficients Γ_{mik} and Γ^m_{ik} are called the Christoffel symbols of the first kind and of the second kind, respectively.

For evaluation of curl, we need to know the vector product of base vectors. Note that $\{\mathbf{g}_i\}$ are dual basis of $\{\mathbf{g}^i\}$. Then, learning from (3.1), the reader easily recognized that

$$\mathbf{g}^1 = \frac{\mathbf{g}_2 \times \mathbf{g}_3}{\mathbf{g}_1 \cdot (\mathbf{g}_2 \times \mathbf{g}_3)}, \quad \mathbf{g}^2 = \frac{\mathbf{g}_3 \times \mathbf{g}_1}{\mathbf{g}_1 \cdot (\mathbf{g}_2 \times \mathbf{g}_3)}, \quad \mathbf{g}^3 = \frac{\mathbf{g}_1 \times \mathbf{g}_2}{\mathbf{g}_1 \cdot (\mathbf{g}_2 \times \mathbf{g}_3)} \tag{4.34a}$$

and

$$\mathbf{g}_1 = \frac{\mathbf{g}^2 \times \mathbf{g}^3}{\mathbf{g}^1 \cdot (\mathbf{g}^2 \times \mathbf{g}^3)}, \quad \mathbf{g}_2 = \frac{\mathbf{g}^3 \times \mathbf{g}^1}{\mathbf{g}^1 \cdot (\mathbf{g}^2 \times \mathbf{g}^3)}, \quad \mathbf{g}_3 = \frac{\mathbf{g}^1 \times \mathbf{g}^2}{\mathbf{g}^1 \cdot (\mathbf{g}^2 \times \mathbf{g}^3)} \tag{4.34b}$$

It is not difficult to derive

$$g \equiv \det(g_{ik}) \geq 0 \tag{4.35}$$

and

$$\sqrt{g} = \mathbf{g}_1 \cdot (\mathbf{g}_2 \times \mathbf{g}_3) = \frac{1}{\mathbf{g}^1 \cdot (\mathbf{g}^2 \times \mathbf{g}^3)} \tag{4.36}$$

Then, with the help of Eqs. (4.34a, b), we have

$$\mathbf{g}_i \times \mathbf{g}_k = \varepsilon_{ikm}\sqrt{g}\mathbf{g}^m, \quad \mathbf{g}^i \times \mathbf{g}^k = \frac{\varepsilon_{ikm}}{\sqrt{g}}\mathbf{g}_m \tag{4.37}$$

Substitution of (3.26) into the right-hand sides of Eq. (4.37) gives

$$\mathbf{g}_i \times \mathbf{g}_k = \varepsilon_{ikm}\sqrt{g}g^{mn}\mathbf{g}_n, \quad \mathbf{g}^i \times \mathbf{g}^k = \frac{\varepsilon_{ikm}}{\sqrt{g}}g_{mn}\mathbf{g}^n \tag{4.38}$$

Similarly, we have

$$\begin{aligned} \mathbf{g}_i \times \mathbf{g}^k &= g^{kn}\varepsilon_{inm}\sqrt{g}\,\mathbf{g}^m = \varepsilon_{inm}g^{kn}g^{mj}\sqrt{g}\,\mathbf{g}_j; \\ \mathbf{g}^i \times \mathbf{g}_k &= g_{kq}\frac{\varepsilon_{iqm}}{\sqrt{g}}\mathbf{g}_m = g_{kq}g_{mp}\frac{\varepsilon_{iqm}}{\sqrt{g}}\mathbf{g}^p \end{aligned} \tag{4.39}$$

Now we are equipped with every thing necessary to calculate curl of vector. Application of Eqs. (4.30) and (4.39) gives

$$\begin{aligned} \nabla \times \mathbf{v} &= \left(\mathbf{g}^i \frac{\partial}{\partial \xi^i}\right) \times \left(v^k \mathbf{g}_k\right) = \frac{\partial v^k}{\partial \xi^i}\mathbf{g}^i \times \mathbf{g}_k + v^k \mathbf{g}^i \times \frac{\partial \mathbf{g}_k}{\partial \xi^i} \\ &= \left(\frac{\partial v^k}{\partial \xi^i} + v^p \Gamma^k_{pi}\right) g_{kq}\frac{\varepsilon_{iqm}}{\sqrt{g}}\mathbf{g}_m \end{aligned} \tag{4.40}$$

Although use of the generalized coordinate gives quite complicate equation as shown in Eqs. (4.24), (4.29), and (4.40), it becomes dramatically simplified when geometry of mathematical problem has symmetry. These equations are important not only because most engineering and physical problems are reduced partial differential equations which are consist of curl and divergence of vector of scalar fields but also because nonlinear constitutive theory of viscoelasticity requires generalized coordinate systems. These equations will be helpful especially in Chap. 8. When

generalized coordinate system under consideration is orthogonal curvilinear coordinate system such as cylindrical and spherical ones, these equations become simpler. In addition to gradient, curl and divergence, Laplacian ∇^2 is one of the most important differential operators in vector analysis. Laplacian is the divergence of gradient. Followings are useful.

4.2.1 Cylindrical Coordinate System

$$\nabla = \mathbf{e}_r \frac{\partial}{\partial r} + \mathbf{e}_\phi \frac{1}{r}\frac{\partial}{\partial \phi} + \mathbf{e}_z \frac{\partial}{\partial z} \tag{4.41}$$

$$\nabla f = \frac{\partial f}{\partial r}\mathbf{e}_r + \frac{1}{r}\frac{\partial f}{\partial \phi}\mathbf{e}_\phi + \frac{\partial f}{\partial z}\mathbf{e}_z \tag{4.42}$$

$$\nabla^2 f = \frac{1}{r}\frac{\partial}{\partial r}\left(r\frac{\partial f}{\partial r}\right) + \frac{1}{r^2}\frac{\partial^2 f}{\partial \phi^2} + \frac{\partial^2 f}{\partial z^2} \tag{4.43}$$

$$\nabla \cdot \mathbf{v} = \frac{1}{r}\frac{\partial (r v_r)}{\partial r} + \frac{1}{r}\frac{\partial v_\phi}{\partial r} + \frac{\partial v_z}{\partial z} \tag{4.44}$$

$$\nabla \times \mathbf{v} = \left(\frac{1}{r}\frac{\partial v_z}{\partial \phi} - \frac{\partial v_\phi}{\partial z}\right)\mathbf{e}_r + \left(\frac{\partial v_r}{\partial z} - \frac{\partial v_z}{\partial \rho}\right)\mathbf{e}_\phi + \frac{1}{r}\left[\frac{\partial (r v_\phi)}{\partial r} - \frac{\partial v_r}{\partial \phi}\right]\mathbf{e}_z \tag{4.45}$$

$$\mathbf{v} = v_r \mathbf{e}_r + v_\phi \mathbf{e}_\phi + v_z \mathbf{e}_z \tag{4.46}$$

4.2.2 Spherical Coordinate System

$$\nabla = \mathbf{e}_r \frac{\partial}{\partial r} + \mathbf{e}_\theta \frac{1}{r}\frac{\partial}{\partial \theta} + \mathbf{e}_\phi \frac{1}{r \sin\theta}\frac{\partial}{\partial \phi} \tag{4.47}$$

$$\nabla f = \frac{\partial f}{\partial r}\mathbf{e}_r + \frac{1}{r}\frac{\partial f}{\partial \theta}\mathbf{e}_\theta + \frac{1}{r \sin\theta}\frac{\partial f}{\partial \phi}\mathbf{e}_\phi \tag{4.48}$$

$$\nabla^2 f = \frac{1}{r^2}\frac{\partial}{\partial r}\left(r^2\frac{\partial f}{\partial \rho}\right) + \frac{1}{r^2 \sin^2\theta}\left[\sin\theta \frac{\partial}{\partial \theta}\left(\sin\theta \frac{\partial f}{\partial \theta}\right) + \frac{\partial^2 f}{\partial \phi^2}\right] \tag{4.49}$$

$$\nabla \cdot \mathbf{v} = \frac{1}{r^2}\frac{\partial (r^2 v_r)}{\partial r} + \frac{1}{r \sin\theta}\left(\frac{\partial v_\theta \sin\theta}{\partial \theta} + \frac{\partial v_\phi}{\partial \phi}\right) \tag{4.50}$$

$$\nabla \times \mathbf{v} = \frac{1}{r\sin\theta}\left[\frac{\partial}{\partial\theta}\left(v_\phi \sin\theta\right) - \frac{\partial v_\theta}{\partial\phi}\right]\mathbf{e}_r + \frac{1}{r}\left[\frac{1}{\sin\theta}\frac{\partial v_r}{\partial\phi} - \frac{\partial}{\partial r}\left(rv_\phi\right)\right]\mathbf{e}_\phi + \frac{1}{r}\left[\frac{\partial}{\partial r}(rv_\theta) - \frac{\partial v_r}{\partial\theta}\right]\mathbf{e}_\phi \tag{4.51}$$

where

$$\mathbf{v} = v_r\mathbf{e}_r + v_\theta\mathbf{e}_\theta + v_\phi\mathbf{e}_\phi \tag{4.52}$$

4.3 Integration of Vector and Scalar

Integration can be said to sum infinitely many terms which are divided infinitely small for easier calculations. As an example, consider the calculation of the area of a circle. The circle can be divided into N isosceles triangles. It is easier to calculate the area of the triangles. As N increases, the area of the triangle becomes smaller. However, the total area of the triangles converges to the area of the circle. This notion can be applied to various integrations involving vector and scalar such as line, surface, and volume integrations.

4.3.1 Line Integral

We are interested in an integral of vector over a curve. In physics, calculation of work is a representative example of line integrals. Suppose that force is given as a vector-valued function of position and the route of particle motion is given as a vector-valued function of time. Then, the work is calculated by

$$W = \int_{\mathbf{p}}^{\mathbf{q}} \mathbf{f}(\mathbf{x}) \cdot \mathrm{d}\mathbf{x} \tag{4.53}$$

where $\mathbf{f}(\mathbf{x})$ is the force field, $\mathbf{x}$ is the position on the curve and $\mathbf{p}$ and $\mathbf{q}$ are initial and final positions, respectively. If the curve is divided to sufficiently small segments, say $\mathrm{d}\mathbf{x}$, then they can be considered as straight line segments. It is a reasonable assumption that $\mathbf{f}(\mathbf{x})$ is a nearly constant vector on the line segment. Then, the integral can be evaluated by

$$W = \lim_{N\to\infty} \sum_{n=1}^{N} \mathbf{f}\left(\frac{\mathbf{x}_n + \mathbf{x}_{n-1}}{2}\right) \cdot (\mathbf{x}_n - \mathbf{x}_{n-1}) \tag{4.54}$$

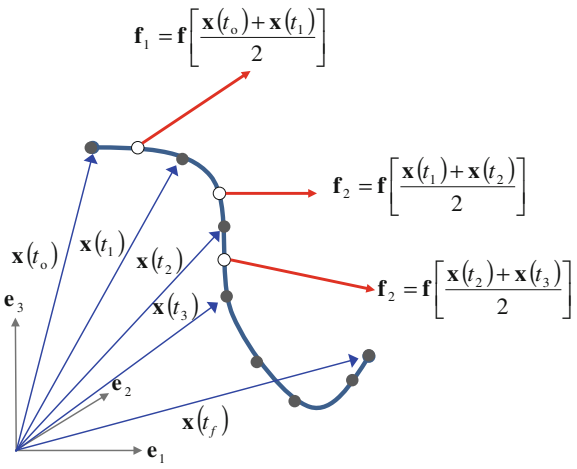

Fig. 2 Partition of line

where $\mathbf{x}_0 = \mathbf{p}$, $\mathbf{x}_N = \mathbf{q}$ and $\mathbf{x}_n$ are points on the curve. Partition of curve is illustrated in Fig. 2.

Any curve can be parameterized by a real number. If the parameterization is known with $\mathbf{x}(t_o) = \mathbf{p}$, $\mathbf{x}(t_f) = \mathbf{q}$ and $t_o \leq t \leq t_f$, then Eq. (4.53) can be replaced by

$$W = \int_{t_o}^{t_f} \mathbf{f}[\mathbf{x}(t)] \cdot \mathbf{v}(t)\, dt \tag{4.55}$$

where $\mathbf{v}(t) = d\mathbf{x}/dt$.

With this notion, one can evaluate the following line integral, too:

$$B = \int_{t_o}^{t_f} \mathbf{b}(t) \times d\mathbf{x}(t) \tag{4.56}$$

4.3.2 Surface Integral

Now we move to integration over surface. In order to do that, we need a way to partition a surface. One of the most elegant methods to describe a surface is to use a mapping from two-dimensional plane to three-dimensional space. Surface of sphere, as an example, can be characterized by longitude ϕ angle and latitude angle θ. It is clear that $0 \leq \phi < 2\pi$ and $0 \leq \theta < \pi$. When the center of a sphere is the origin, a point of the sphere $\mathbf{x}$ can be expressed in terms of θ and ϕ as follows:

$$\mathbf{x} = R\cos\phi\sin\theta\,\mathbf{e}_1 + R\sin\phi\sin\theta\,\mathbf{e}_2 + R\cos\theta\,\mathbf{e}_3 = R\mathbf{e}_r \tag{4.57}$$

where R is the radius of the sphere. This is the parameterization of surface.

For generalization, consider a set of two-dimensional plane U. Let the coordinates of U be denoted by p and q. Parameterization of surface is to find a one-to-one mapping from U to three-dimensional space V such that

$$\mathbf{x}(p,\ q) = x_k(p,\ q)\,\mathbf{e}_k \tag{4.58}$$

In general, any surface cannot be expressed by a single expression of Eq. (4.58). However, if a surface is divided to parts of finite numbers, Eq. (4.58) can be applied for each part with different functions $x_k(p, q)$. Consider union of several two-dimensional sets such that

$$U = \bigcup_{n=1}^{N} U_n \tag{4.59}$$

Consider also a mapping from U_n to a set S_n in three-dimensional space such that

$$\mathbf{x}^{(n)}(p, q) = x_k^{(n)}(p, q)\,\mathbf{e}_k \tag{4.60}$$

Then, patch of a surface S is defined as the set of mappings of Eq. (4.60) if the whole surface S is the union of S_n:

$$S = \bigcup_{n=1}^{N} S_n \tag{4.61}$$

It is known that any surface has at least a patch (O'Neill 2006).

A finite portion of surface S_n can be filled with coordinate lines of two kinds: p-lines and q-lines. The p-line is defined as a curve that is obtained from a member of the patch of the surface, say Eq. (4.60) when q is fixed at a certain value. The q-line can be defined similarly. Now S_n can be partitioned by partitioning U_n. One of the simplest partition of U_n is to divide U_n to small rectangles whose sides have the length of dp and dq. The boundaries of these rectangles are mapped into the two coordinate lines in three-dimensional space. Then, the surface looks like a collection of small tiles. Since both dp and dq are infinitesimal, each tile can be considered as a small piece of flat plane. We want to express the normal vectors and areas of the small tiles mathematically. Figure 3 illustrates partition of surface.

We can define tangent vectors of the two coordinate lines as

$$\mathbf{t}_p = \frac{\partial \mathbf{x}}{\partial p}; \quad \mathbf{t}_q = \frac{\partial \mathbf{x}}{\partial q} \tag{4.62}$$

It is not difficult to show that the two tangent vectors are linearly independent. Since each tile is a parallelogram spanned by the two vectors such as d$p\mathbf{t}_p$ and d$q\,\mathbf{t}_q$, the area of the tile da is given by

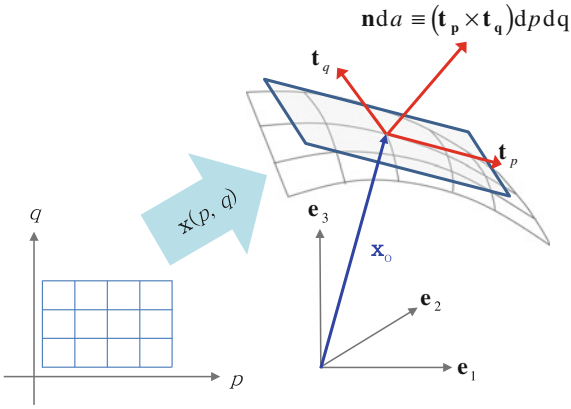

Fig. 3 Partition of surface

$$\mathrm{d}a = \left\|\mathbf{t}_p \times \mathbf{t}_q\right\| \mathrm{d}p\,\mathrm{d}q \tag{4.63}$$

Furthermore, the normal vector is proportional to the vector product of the two tangent vectors. Then, we can define area vector as follows:

$$\mathrm{d}\mathbf{a} \equiv \left(\mathbf{t}_p \times \mathbf{t}_q\right) \mathrm{d}p\,\mathrm{d}q \tag{4.64}$$

When a region is enveloped by a surface, the direction of surface normal vector is conventionally chosen outward. This convention can be satisfied by the choice of two coordinate p and q. Now we are equipped with everything to evaluate the following integrals:

$$SI_1 = \iint_{\partial\Omega} \mathbf{b} \cdot \mathrm{d}\mathbf{a}; \tag{4.65a}$$

$$SI_2 = \iint_{\partial\Omega} \mathbf{b} \times \mathrm{d}\mathbf{a}; \tag{4.65b}$$

$$SI_3 = \iint_{\partial\Omega} \mathbf{f}\,\mathrm{d}a; \tag{4.65c}$$

$$SI_4 = \iint_{\partial\Omega} f\,\mathrm{d}\mathbf{a}; \tag{4.65d}$$

where $\partial\Omega$ is the region of surface over which integration is carried. The surface integral SI_1 is scalar, whereas SI_2, SI_3, and SI_4 are vectors. By using Eqs. (4.63) and (4.64), these surface integrals are reduced to double integrals over the intervals of p and q.

4.3.3 Volume Integral

One of the simplest partitions of three-dimensional region is to divide the region to rectangular cubes. Let the three sides of cubes be aligned parallel to the axis of a rectangular coordinate system. Then, volume of each cube is given by

$$\mathrm{d}V = \mathrm{d}x\mathrm{d}y\mathrm{d}z \tag{4.66}$$

Then, volume integral is reduced to triple integral. Although this partition is simple, the evaluation of volume integral happens to be very difficult when the boundary of the region does not fit rectangular coordinate system.

If a region of integral fits a generalized coordinate system, the boundary of the region is easily expressed by

$$a_k < \xi^k < b_k \quad \text{with } k = 1, 2, 3 \tag{4.67}$$

In this case, it is rather difficult to partition the region. If choosing coordinate lines with spacing by $\mathrm{d}\xi^k$, very small parallelepiped are spanned by three vectors: $\mathbf{g}_1\mathrm{d}\xi^1$, $\mathbf{g}_2\mathrm{d}\xi^2$ and $\mathbf{g}_3\mathrm{d}\xi^3$. The volume of the infinitesimal parallelepiped is given by

$$\mathrm{d}V = |\mathbf{g}_1 \cdot (\mathbf{g}_2 \times \mathbf{g}_3)|\, \mathrm{d}\xi^1\mathrm{d}\xi^2\mathrm{d}\xi^3 \tag{4.68}$$

It is not difficult to arrange the coordinates in order that $\mathbf{g}_1 \cdot (\mathbf{g}_2 \times \mathbf{g}_3) > 0$. Right-handed coordinate system is the one that satisfies $\mathbf{g}_1 \cdot (\mathbf{g}_2 \times \mathbf{g}_3) > 0$. Then, the following volume integrals carried in the curvilinear coordinate system become triple integral over the three generalized coordinates.

$$VI_1 = \iiint_{\Omega} f(\mathbf{x})\, \mathrm{d}V; \tag{4.69a}$$

$$VI_2 = \iiint_{\Omega} \mathbf{b}(\mathbf{x})\, \mathrm{d}V \tag{4.69b}$$

4.3.4 Divergence Theorem

Here, we will illustrate the divergence theorem which relates surface integral to volume integral. This theorem is as useful as integration by parts of single-variable functions. The word "illustrate" is used because following analysis is not a rigorous proof. The illustration requires coordinate systems. To maximize generality, use of generalized coordinate system is recommendable. However, generalized coordinate

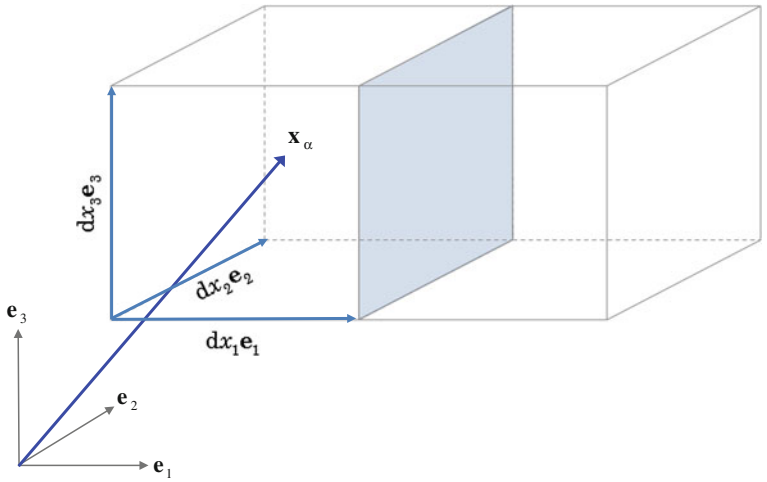

Fig. 4 Infinitesimal volume element for the illustration of the divergence theorem

system results in complicate calculation which might be an obstacle when student readers understand the theorem. To make it insightful, the complicate equations should be simplified. Hence, we shall use rectangular coordinate system. Of course, the same results can be obtained with generalized coordinate system, too.

A three-dimensional region of any shape can be partitioned by coordinate surfaces with spacing by dx_k. Then, we can obtain infinitesimal cubes spanned by three tangent vectors $dx_1\mathbf{e}_1$, $dx_2\mathbf{e}_2$, and $dx_3\mathbf{e}_3$ as shown in Fig. 4. Let the center of the αth cube be denoted by $\mathbf{x}_\alpha$. The cube has six flat surfaces whose normal vectors are $\pm\mathbf{e}_k$. Symbol $a_{(\pm i)}$ denotes the surface whose normal vector is $\pm\mathbf{e}_i$. Note that the area of $a_{(\pm 1)}$ is $da_{(\pm 1)} = dx_2 dx_3$. In general, we have

$$da_{(\pm i)} = \frac{dV}{dx_i} \tag{4.70}$$

where dV is the volume of the cube, which is given by $dx_1 dx_2 dx_3$. The center of $a_{(\pm i)}$ is given by

$$\mathbf{r}^{(\alpha)}_{(\pm i)} = \mathbf{x}_\alpha \pm \frac{1}{2} dx_i \mathbf{e}_i \,(\text{no sum on } i) \tag{4.71}$$

Consider a vector field $\mathbf{b}(\mathbf{x})$. We are interested in the sum such that

$$I_\alpha \equiv \sum_{k=1}^{3} \left[\mathbf{b}\left(\mathbf{r}^{(\alpha)}_{(+k)}\right) \cdot \mathbf{e}_k + \mathbf{b}\left(\mathbf{r}^{(\alpha)}_{(-k)}\right) \cdot (-\mathbf{e}_k) \right] da_{(k)} \tag{4.72}$$

Using Taylor expansion, Eq. (4.72) becomes simpler as follows:

$$I_\alpha = \sum_{k=1}^{3}\left[b_k\left(\mathbf{x}_\alpha + \frac{1}{2}\mathrm{d}x_k\mathbf{e}_k\right) - b_k\left(\mathbf{x}_\alpha - \frac{1}{2}\mathrm{d}x_k\mathbf{e}_k\right)\right]\frac{\mathrm{d}V}{\mathrm{d}x_k} = \sum_{k=1}^{3}\left.\frac{\partial b_k}{\partial x_k}\right|_{\mathbf{x}_\alpha}\mathrm{d}V \\ = (\nabla\cdot\mathbf{b})_{\mathbf{x}_\alpha}\mathrm{d}V \tag{4.73}$$

Summing I_α over the whole region, we have

$$\sum_{\alpha=1} I_\alpha = \iiint_\Omega \nabla\cdot\mathbf{b}\mathrm{d}V \tag{4.74}$$

If the αth cube is interior to the region Ω, then it has six neighbors and share one of its faces with one of the neighbors. However, the normal vectors of the common face of two adjacent cubes have opposite direction. Then, I_α is canceled by neighborhood. If the αth cube is located on the boundary of Ω, then it has at least one face without sharing. Note that Eq. (4.72) has six inner products of vector field **b** and area vector of each face. Then, canceling by neighborhood gives a surface integral such that

$$\sum_{\alpha=1} I_\alpha = \iint_{\partial\Omega}\mathbf{b}\cdot\mathrm{d}\mathbf{a} \tag{4.75}$$

Combination of Eqs. (4.74) and (4.75) yields the divergence theorem:

$$\iint_{\partial\Omega}\mathbf{b}\cdot\mathrm{d}\mathbf{a} = \iiint_\Omega \nabla\cdot\mathbf{b}\,\mathrm{d}V \tag{4.76}$$

Sometimes surface integral happens to be more difficult than volume integral. Then, the divergence theorem is powerful in calculation. However, one of the most important roles of the divergence theorem is to develop a mathematical theory in various fields of physics and engineering. Examples are derivation of various balance equations in continuum thermomechanics and molecular theories based on probability distribution function which fades away at remote places in the space of random variables.

There are various modifications of the divergence theorem. Consider a vector fields which is factorized by the product of a scalar field and a vector field such that $\mathbf{v} = f\mathbf{u}$. Application of the divergence theorem gives

$$\iiint_\Omega (\mathbf{u}\cdot\nabla f + f\nabla\cdot\mathbf{u})\,\mathrm{d}V = \iint_{\partial\Omega} f\mathbf{u}\cdot\mathrm{d}\mathbf{a} \tag{4.77}$$

If $\mathbf{u} = \nabla g$, then Eq. (4.77) becomes

$$\iiint_{\Omega} \left(\nabla g \cdot \nabla f + f\nabla^2 g\right) \mathrm{d}V = \iint_{\partial\Omega} f\nabla g \cdot \mathrm{d}\mathbf{a} \tag{4.78}$$

Interchange of f and g gives

$$\iiint_{\Omega} \left(\nabla g \cdot \nabla f + g\nabla^2 f\right) \mathrm{d}V = \iint_{\partial\Omega} g\nabla f \cdot \mathrm{d}\mathbf{a} \tag{4.79}$$

Subtraction of Eq. (4.78) by Eq. (4.79) gives

$$\iiint_{\Omega} \left(f\nabla^2 g - g\nabla^2 f\right) \mathrm{d}V = \iint_{\partial\Omega} \left(f\nabla g - g\nabla f\right) \cdot \mathrm{d}\mathbf{a} \tag{4.80}$$

Equations (4.78) and (4.79) are called Green's first identity, and Eq. (4.80) is named Green's second identity. Green's second identity is used in proving the uniqueness of the solution of Laplace equation $\nabla^2\psi = 0$.

4.3.5 Stokes Theorem

Consider a piece of surface Σ and its boundary $\partial\Sigma$. The surface can be partitioned by p-coordinate and q-coordinate lines as shown in Fig. 5. The q values of two adjacent p-lines are different by dq and the p values of two adjacent q-lines by dp. By this partition, the surface is a collection of infinitesimal parallelograms spanned by two vectors $\mathbf{t}_p \mathrm{d}p$ and $\mathbf{t}_q \mathrm{d}q$.

Let the center of the αth parallelogram be denoted by $\mathbf{x}_\alpha = \mathbf{x}(p_\alpha, q_\alpha)$. The positions of the four corner points of the αth parallelogram are given in terms of $\mathbf{x}_\alpha$ and the corresponding patch $\mathbf{x}(p, q)$:

$$\begin{aligned} \mathbf{r}_1^{(\alpha)} &= \mathbf{x}\left(p_\alpha - \frac{1}{2}\mathrm{d}p, q_\alpha - \frac{1}{2}\mathrm{d}q\right); \quad \mathbf{r}_2^{(\alpha)} = \mathbf{x}\left(p_\alpha + \frac{1}{2}\mathrm{d}p, q_\alpha - \frac{1}{2}\mathrm{d}q\right); \\ \mathbf{r}_3^{(\alpha)} &= \mathbf{x}\left(p_\alpha + \frac{1}{2}\mathrm{d}p, q_\alpha + \frac{1}{2}\mathrm{d}q\right); \quad \mathbf{r}_4^{(\alpha)} = \mathbf{x}\left(p_\alpha - \frac{1}{2}\mathrm{d}p, q_\alpha + \frac{1}{2}\mathrm{d}q\right); \end{aligned} \tag{4.81}$$

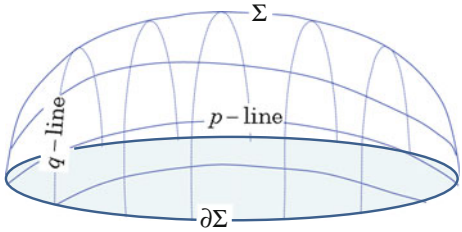

Fig. 5 Partition of the surface Σ which is bounded by the loop ∂Σ

Now, we are interested in

$$I_\alpha = \mathbf{b}_1 \cdot \left(\mathbf{r}_2^{(\alpha)} - \mathbf{r}_1^{(\alpha)}\right) + \mathbf{b}_2 \cdot \left(\mathbf{r}_3^{(\alpha)} - \mathbf{r}_2^{(\alpha)}\right) + \mathbf{b}_3 \cdot \left(\mathbf{r}_4^{(\alpha)} - \mathbf{r}_3^{(\alpha)}\right) + \mathbf{b}_4 \cdot \left(\mathbf{r}_1^{(\alpha)} - \mathbf{r}_4^{(\alpha)}\right) \tag{4.82}$$

where $\mathbf{b}_k = \mathbf{b}(\mathbf{x}_k)$ with

$$\begin{aligned} \mathbf{x}_1 &= \frac{1}{2}\left(\mathbf{r}_1^{(\alpha)} + \mathbf{r}_2^{(\alpha)}\right); \quad \mathbf{x}_2 = \frac{1}{2}\left(\mathbf{r}_2^{(\alpha)} + \mathbf{r}_3^{(\alpha)}\right); \\ \mathbf{x}_3 &= \frac{1}{2}\left(\mathbf{r}_3^{(\alpha)} + \mathbf{r}_4^{(\alpha)}\right); \quad \mathbf{x}_4 = \frac{1}{2}\left(\mathbf{r}_4^{(\alpha)} + \mathbf{r}_1^{(\alpha)}\right) \end{aligned} \tag{4.83}$$

Using Taylor expansion again gives

$$\begin{aligned} I_\alpha &= \left[\left(\mathbf{t}_p \cdot \mathbf{e}_i\right)\frac{\partial b_k}{\partial x_i}\left(\mathbf{t}_q \cdot \mathbf{e}_k\right) - \left(\mathbf{t}_q \cdot \mathbf{e}_i\right)\frac{\partial b_k}{\partial x_i}\left(\mathbf{t}_p \cdot \mathbf{e}_k\right)\right] \mathrm{d}p\mathrm{d}q \\ &= \left(\nabla \times \mathbf{b}\right) \cdot \left(\mathbf{t}_p \times \mathbf{t}_q\right) \mathrm{d}p\mathrm{d}q \\ &= \left(\nabla \times \mathbf{b}\right) \cdot \mathrm{d}\mathbf{a}_\alpha \end{aligned} \tag{4.84}$$

where all derivatives are those at $\mathbf{x}_\alpha$. Derivation from the first line to the second line of Eq. (4.84) requires an identity related to skew-symmetric tensor which will be studied in the next sections.

Summing I_α over all infinitesimal parallelograms, we have a surface integral such that

$$\sum_{\alpha=1} I_\alpha = \iint_\Sigma \left(\nabla \times \mathbf{b}\right) \cdot \mathrm{d}\mathbf{a} \tag{4.85}$$

On the other hand, Eq. (4.82) is a line integral along the boundary line of the αth infinitesimal parallelogram. Summing I_α results in cancelation of the contributions from the common line segments shared by two adjacent parallelograms, which gives

$$\sum_{\alpha=1} I_\alpha = \int_{\partial\Sigma} \mathbf{b} \cdot \mathrm{d}\mathbf{r} \tag{4.86}$$

Finally, we arrive at the famous theorem of Stokes:

$$\int_{\partial\Sigma} \mathbf{b} \cdot \mathrm{d}\mathbf{r} = \iint_\Sigma \left(\nabla \times \mathbf{b}\right) \cdot \mathrm{d}\mathbf{a} \tag{4.87}$$

It must be noted that the boundary of the surface $\partial\Sigma$ is a closed loop.

Stokes theorem is a mathematical basis of Faraday's law of induction. It is also useful in calculation of irrotational flow whose velocity field $\mathbf{v}$ satisfies $\nabla \times \mathbf{v} = \mathbf{0}$. Equation (4.87) implies that when a force field is irrotational, then the work done by the force over any closed loop will be zero. This is equivalent to the existence of a scalar field whose gradient is the force field. The scalar field ψ is called potential when the following is satisfied

$$\mathbf{b} = -\nabla\psi \tag{4.88}$$

The minus sign is adopted in order that the sum of kinetic energy and potential becomes conserved.

Problem 4

[1] If an unknown vector $\mathbf{x}$ satisfies $\mathbf{a} \times \mathbf{x} = \mathbf{b}$ and $\mathbf{a} \cdot \mathbf{x} = \beta$ for known vector $\mathbf{a}$ and $\mathbf{b}$ and a known real number β, express $\mathbf{x}$ in terms of $\mathbf{a}$, $\mathbf{b}$, and β.

[2] Prove the identity:

$$(\mathbf{a} \times \mathbf{b}) \times (\mathbf{c} \times \mathbf{d}) = [\mathbf{a} \cdot (\mathbf{b} \times \mathbf{d})]\mathbf{c} - [\mathbf{a} \cdot (\mathbf{b} \times \mathbf{c})]\mathbf{d} \tag{4.a}$$

[3] If $\mathbf{n}$ is a given unit vector, then prove that any vector $\mathbf{a}$ can be expressed as follows:

$$\mathbf{a} = (\mathbf{a} \cdot \mathbf{n})\,\mathbf{n} + \mathbf{n} \times (\mathbf{a} \times \mathbf{n}) \tag{4.b}$$

[4] Derive Eq. (4.12) from the identity of Eq. (4.11).

[5] Derive Eqs. (4.30) and (4.31).

[6] Derive Eqs. (4.34a, b)–(4.37), and (4.39).

[7] Derive Eqs. (4.43)–(4.45).

[8] Derive Eqs. (4.49)–(4.51).

[9] Prove following identities.

$$\nabla f[g(\mathbf{x})] = f'[g(\mathbf{x})]\nabla g \quad \text{where } f'(x) = \frac{\mathrm{d}f}{\mathrm{d}x}; \tag{4.c}$$

$$\nabla \times \nabla f = \mathbf{0}; \tag{4.d}$$

$$\nabla \cdot (\nabla \times \mathbf{b}) = 0; \tag{4.e}$$

$$\nabla \times (\nabla \times \mathbf{b}) = \nabla(\nabla \cdot \mathbf{b}) - \nabla^2\mathbf{b}; \tag{4.f}$$

$$\nabla^2(\nabla \cdot \mathbf{b}) = \nabla \cdot \left(\nabla^2\mathbf{b}\right); \tag{4.g}$$

$$\nabla^2(\nabla \times \mathbf{b}) = \nabla \times \left(\nabla^2\mathbf{b}\right) \tag{4.h}$$

[10] Prove following identity.

$$\iiint_{\Omega} \mathbf{c} \cdot (\nabla \times \mathbf{b})\, \mathrm{d}V = \iint_{\partial\Omega} (\mathbf{b} \times \mathbf{c}) \cdot \mathrm{d}\mathbf{a} \tag{4.i}$$

where $\mathbf{c}$ is a constant vector.

5 Tensor Analysis

The second-order tensor is a linear transform from a physical vector to another physical vector. Linear algebra lets us know that linear transforms form a vector space if scalar multiplication and addition are defined over the set of linear transform. Thus, third-order tensor can be defined as a linear transform from a vector to a second-order tensor or from a second-order tensor to a vector. Higher-order tensor also can be defined. There are several ways to express tensor. Here, polyadic notation is preferred.

5.1 Polyadic Notation of Linear Transform

Consider an experiment that is aimed at measuring the electric dipole moment $\mathbf{p} = p_i \mathbf{e}_i$ of a molecule in a coordinate system. For the measurement, suppose that an electric field $\mathbf{E} = E_k \mathbf{e}_k$ is applied to the molecule and the following relation is obtained:

$$p_i = A_{ik} E_k \tag{5.1}$$

where the coefficients A_{ik} are independent of the electric field. This relation looks like that there exists a mapping from electric field to electric dipole moment vector. Since electric dipole moment is responsive to electric field, the component-wise Eq. (5.1) must be a facet of a linear transform from electric field vector to dipole moment vector. Hence, we want to find the linear transform from Eq. (5.1). Since $p_i = \mathbf{e}_i \cdot \mathbf{p}$ and $E_k = \mathbf{e}_k \cdot \mathbf{E}$, we want to rewrite Eq. (5.1) as follows:

$$\mathbf{p} = p_i \mathbf{e}_i = A_{ik} (\mathbf{e}_k \cdot \mathbf{E})\, \mathbf{e}_i \tag{5.2}$$

Motivated from Eq. (5.2), one may invent a mathematical entity called dyadic which is a pair of two vectors. For given two vectors $\mathbf{a}$ and $\mathbf{b}$, dyadic is denoted by $\mathbf{ab}$ and is equipped with the following properties as an operator. For any vector $\mathbf{x}$,

$$\mathbf{ab} \cdot \mathbf{x} = (\mathbf{b} \cdot \mathbf{x})\mathbf{a}; \quad \mathbf{x} \cdot \mathbf{ab} = (\mathbf{a} \cdot \mathbf{x})\mathbf{b} \tag{5.3}$$

Then, the dyadic **ab** plays the role of a linear transform because for any two vectors **x** and **y** with arbitrary real numbers α and β, the followings hold:

$$\begin{aligned}\mathbf{ab}\cdot(\alpha\mathbf{x}+\beta\mathbf{y}) &= \alpha(\mathbf{b}\cdot\mathbf{x})\mathbf{a}+\beta(\mathbf{b}\cdot\mathbf{y})\mathbf{a} = \alpha\mathbf{ab}\cdot\mathbf{x}+\beta\mathbf{ab}\cdot\mathbf{y};\\ (\alpha\mathbf{x}+\beta\mathbf{y})\cdot\mathbf{ab} &= \alpha(\mathbf{x}\cdot\mathbf{a})\mathbf{b}+\beta(\mathbf{y}\cdot\mathbf{a})\mathbf{b} = \alpha\mathbf{x}\cdot\mathbf{ab}+\beta\mathbf{y}\cdot\mathbf{ab}\end{aligned} \tag{5.4}$$

Linear transform is a mapping from vector space to vector space. The word "linear" implies that when the argument is any linear combination of vectors of domain, then the image of the linear transform is the linear combination of the images of each vector with the same coefficients as shown in Eq. (5.4).

Using zero vector **0**, one can define the dyadic which maps any vector to the zero vector: $\mathbf{O}\equiv\mathbf{00}$. Then, we know that $\mathbf{O}\cdot\mathbf{x}=\mathbf{x}\cdot\mathbf{O}=\mathbf{0}$. From two dyadics **ab** and **cd**, a new linear transform can be defined as $\gamma_1\mathbf{ab}+\gamma_2\mathbf{cd}$ where γ_1 and γ_2 are arbitrary real numbers. The new linear transform, say $\mathbf{N}=\gamma_1\mathbf{ab}+\gamma_2\mathbf{cd}$, is defined to satisfy

$$\begin{aligned}\mathbf{N}\cdot\mathbf{x} &= \gamma_1(\mathbf{b}\cdot\mathbf{x})\mathbf{a}+\gamma_2(\mathbf{d}\cdot\mathbf{x})\mathbf{c};\\ \mathbf{x}\cdot\mathbf{N} &= \gamma_1(\mathbf{x}\cdot\mathbf{a})\mathbf{b}+\gamma_2(\mathbf{x}\cdot\mathbf{c})\mathbf{d}\end{aligned} \tag{5.5}$$

Equation (5.5) includes the definitions of addition and scalar multiplication. It is clear that the scalar multiplication of a dyadic with zero is the zero dyadic or the zero linear transform **O**. Then, it is not difficult to show that linear combination of dyadics form the vector space of linear transform.

Denote the set of all linear transforms from a physical vector to another physical vector by T. Then, any member of T can be expressed by

$$\mathbf{T}=T_{ik}\mathbf{e}_i\mathbf{e}_k \tag{5.6}$$

It is not difficult to show that the elementary dyadics $\mathbf{e}_i\mathbf{e}_k$ form a basis of T. Furthermore, any linear transform can be expressed by Eq. (5.6).

The notion of dyadic can be applied to Eq. (5.2). Define polarizability as a linear transform such that

$$\mathbf{A}=A_{ik}\mathbf{e}_i\mathbf{e}_k \tag{5.7}$$

Equation (5.2) is recovered by application of **A** to electric field $\mathbf{E}=E_m\mathbf{e}_m$. However, it cannot be said that the experimental confirmation of Eq. (5.1) in a single coordinate system implies the existence of the linear transform **A**. Consider another rectangular coordinate system different from the original one. Let the basis of another coordinate system be $\{\overline{\mathbf{e}}_k\}$. Then, we have

$$\overline{\mathbf{e}}_i=\frac{\partial x_k}{\partial\overline{x}_i}\mathbf{e}_k \tag{5.8a}$$

and

$$\mathbf{e}_i = \frac{\partial \overline{x}_k}{\partial x_i}\overline{\mathbf{e}}_k \tag{5.8b}$$

Application of Eqs. (5.8a, b) to Eq. (5.2) yields

$$\mathbf{p} = A_{ik}\left(\frac{\partial \overline{x}_n}{\partial x_k}\overline{\mathbf{e}}_n \cdot \mathbf{E}\right)\frac{\partial \overline{x}_m}{\partial x_i}\overline{\mathbf{e}}_m \tag{5.9}$$

Since $\overline{E}_k = \overline{\mathbf{e}}_k \cdot \mathbf{E}$ and $\overline{p}_a = \overline{\mathbf{e}}_a \cdot \mathbf{p}$, Eq. (5.9) can be rewritten as

$$\overline{p}_a = \frac{\partial \overline{x}_a}{\partial x_i}\frac{\partial \overline{x}_n}{\partial x_k}A_{ik}\overline{E}_n \tag{5.10}$$

Application of Eqs. (5.8a, b) to Eq. (5.7) yields

$$\mathbf{A} = A_{ab}\mathbf{e}_a\mathbf{e}_b = \frac{\partial \overline{x}_i}{\partial x_a}\frac{\partial \overline{x}_k}{\partial x_b}A_{ab}\overline{\mathbf{e}}_i\overline{\mathbf{e}}_k = \overline{A}_{ik}\overline{\mathbf{e}}_i\overline{\mathbf{e}}_k \tag{5.11}$$

The experimental proof for the existence of $\mathbf{A}$ of Eq. (5.7) is to show that

$$\overline{A}_{ik} = \frac{\partial \overline{x}_i}{\partial x_a}\frac{\partial \overline{x}_k}{\partial x_b}A_{ab} \tag{5.12}$$

holds for any pair of rectangular coordinate systems. If Eq. (5.12) does not hold, then A_{ik} is not a component of tensor $\mathbf{A}$. Equation (5.12) is the rule of coordinate transform for second-order tensor. Since the physical meaning of $\mathbf{A}$ is how strong electric dipole moment is generated by a given electric field, it is a characteristic of a molecule. Hence, it is a physical quantity.

Tensor is a linear transform that represents a physical quantity. Polarizability tensor $\mathbf{A}$ is a second-order tensor because its transform rule, Eq. (5.12) requires two transform matrix $\partial \overline{x}_i/\partial x_k$. Following this naming, vector is called the first-order tensor because its transform rule requires only one $\partial \overline{x}_i/\partial x_k$, whereas scalar is called zero-order tensor because it requires no transform matrix. We can define third-order tensor and higher-order tensors. Although third-order tensor is rarely used in rheology, fourth-order tensor is important because viscosity and modulus are examples of fourth-order tensor. *N*th-order tensor can be expressed as a linear combination of *N*-acids of base vectors

$$\mathbf{T} = T_{n_1 n_2 \ldots n_N}\mathbf{e}_{n_1}\mathbf{e}_{n_2}\ldots\mathbf{e}_{n_N} \tag{5.13}$$

We use the following notation for second-order and fourth-order tensors

$$\mathbf{T}\cdot\mathbf{E}=(T_{im}\mathbf{e}_i\mathbf{e}_m)\cdot(E_{nk}\mathbf{e}_n\mathbf{e}_k)=T_{im}E_{nk}(\mathbf{e}_m\cdot\mathbf{e}_n)\,\mathbf{e}_i\mathbf{e}_k=T_{im}E_{mk}\mathbf{e}_i\mathbf{e}_k; \tag{5.14a}$$

$$\mathbf{T}:\mathbf{E}=T_{im}E_{nk}(\mathbf{e}_i\cdot\mathbf{e}_n)\,(\mathbf{e}_m\cdot\mathbf{e}_k)=T_{ik}E_{ik}; \tag{5.14b}$$

$$\mathbf{T}\cdot\cdot\,\mathbf{E}=T_{im}E_{nk}(\mathbf{e}_i\cdot\mathbf{e}_k)\,(\mathbf{e}_m\cdot\mathbf{e}_n)=T_{km}E_{mk}; \tag{5.14c}$$

$$\mathbf{G}:\mathbf{E}=\left(G_{ikpq}\mathbf{e}_i\mathbf{e}_k\mathbf{e}_p\mathbf{e}_q\right):(E_{mn}\mathbf{e}_m\mathbf{e}_n)=G_{ikpq}E_{pq}\mathbf{e}_i\mathbf{e}_k; \tag{5.14d}$$

$$\mathbf{E}:\mathbf{G}=(E_{mn}\mathbf{e}_m\mathbf{e}_n):\left(G_{ikpq}\mathbf{e}_i\mathbf{e}_k\mathbf{e}_p\mathbf{e}_q\right)=G_{ikpq}E_{ik}\mathbf{e}_p\mathbf{e}_q \tag{5.14e}$$

Equation (5.14a) implies that the product of two second-order tensors is also a second-order tensor. Let $\mathbf{C}=\mathbf{T}\cdot\mathbf{E}$. Since both $\mathbf{T}$ and $\mathbf{E}$ are linear transforms, the tensor C can be interpreted as the composition of the two linear transforms. To show this, consider $\mathbf{v}=\mathbf{E}\cdot\mathbf{u}$ and $\mathbf{w}=\mathbf{T}\cdot\mathbf{v}$ where $\mathbf{u}=u_a\mathbf{e}_a$. Equation (5.14a) gives

$$\mathbf{w}=\mathbf{T}\cdot(\mathbf{E}\cdot\mathbf{u})=(T_{im}\mathbf{e}_i\mathbf{e}_m)\cdot(E_{nk}u_k\mathbf{e}_n)=T_{im}E_{mk}u_k\mathbf{e}_i \tag{5.15}$$

On the other hand, we have

$$\mathbf{C}\cdot\mathbf{u}=(\mathbf{T}\cdot\mathbf{E})\cdot\mathbf{u}=(T_{im}E_{mk}\mathbf{e}_i\mathbf{e}_k)\cdot(u_a\mathbf{e}_a)=T_{im}E_{mk}u_k\mathbf{e}_i \tag{5.16}$$

The equivalence of Eqs. (5.15) and (5.16) proves not only that $\mathbf{C}$ is the composite linear transform of $\mathbf{T}$ and $\mathbf{E}$ but also that

$$\mathbf{T}\cdot(\mathbf{E}\cdot\mathbf{u})=(\mathbf{T}\cdot\mathbf{E})\cdot\mathbf{u} \tag{5.17}$$

In general, the products of the second-order tensors with single dot such as $\mathbf{A}\cdot\mathbf{B}\cdot\mathbf{C}\ldots\mathbf{G}$ satisfies associate rule:

$$\mathbf{A}\cdot(\mathbf{B}\cdot\mathbf{C})=(\mathbf{A}\cdot\mathbf{B})\cdot\mathbf{C} \tag{5.18}$$

Table 2 summarizes various tensors and their rule of coordinate transform. It is a convention that second-order tensor is usually called tensor if context does not give rise to any confusion.

Table 2 Tensors and coordinate transform

Order	Polyadics	Number of components	Coordinate transform
First	$\mathbf{v}=v_i\mathbf{e}_i$	3^1	$\overline{v}_i=\frac{\partial\overline{x}_i}{\partial x_k}v_k$
Second	$\mathbf{T}=T_{ik}\mathbf{e}_i\mathbf{e}_k$	3^2	$\overline{T}_{ik}=\frac{\partial\overline{x}_i}{\partial x_m}\frac{\partial\overline{x}_k}{\partial x_n}T_{mn}$
Third	$\mathbf{H}=H_{ikn}\mathbf{e}_i\mathbf{e}_k\mathbf{e}_n$	3^3	$\overline{H}_{ikn}=\frac{\partial\overline{x}_i}{\partial x_p}\frac{\partial\overline{x}_k}{\partial x_q}\frac{\partial\overline{x}_n}{\partial x_r}H_{pqr}$
Fourth	$\mathbf{G}=G_{ijkl}\mathbf{e}_i\mathbf{e}_j\mathbf{e}_k\mathbf{e}_l$	3^4	$\overline{G}_{ijkl}=\frac{\partial\overline{x}_i}{\partial x_p}\frac{\partial\overline{x}_j}{\partial x_q}\frac{\partial\overline{x}_k}{\partial x_r}\frac{\partial\overline{x}_l}{\partial x_s}G_{pqrs}$

5.2 Tensor Algebra

5.2.1 Tensor Components with Respect to Generalized Basis

Just as vector, tensor can be expressed by linear combinations of various bases. When generalized coordinates are used, there are two kinds of basis: covariant and contravariant basis. Hence, vector has two ways of representation, second-order tensor has four ways, third-order tensor has eight ways, and so on:

$$\mathbf{v} = v^i \mathbf{g}_i = v_k \mathbf{g}^k; \tag{5.19a}$$

$$\mathbf{T} = T^{ik}\mathbf{g}_i\mathbf{g}_k = T_{ik}\mathbf{g}^i\mathbf{g}_k = T_i^{\cdot k}\mathbf{g}^i\mathbf{g}_k = T_{\cdot k}^{i}\mathbf{g}_i\mathbf{g}^k; \tag{5.19b}$$

$$\mathbf{H} = H_{ikm}\mathbf{g}^i\mathbf{g}^k\mathbf{g}^m = H^{ikm}\mathbf{g}_i\mathbf{g}_k\mathbf{g}_m = H_{\cdot km}^{i}\mathbf{g}_i\mathbf{g}^k\mathbf{g}^m = \cdots \tag{5.19c}$$

Since $\mathbf{g}_i \cdot \mathbf{g}^k = \delta_i^k$, it is easily understood that

$$v^i = \mathbf{g}^i \cdot \mathbf{v}, \quad v_i = \mathbf{g}_i \cdot \mathbf{v}; \tag{5.20a}$$

$$\begin{aligned} T^{ik} &= \mathbf{g}^i \cdot \mathbf{T} \cdot \mathbf{g}^k; \quad T_{i\cdot}^{\cdot k} = \mathbf{g}_i \cdot \mathbf{T} \cdot \mathbf{g}^k; \\ T_{\cdot k}^{i\cdot} &= \mathbf{g}^i \cdot \mathbf{T} \cdot \mathbf{g}_k; \quad T_{ik} = \mathbf{g}_i \cdot \mathbf{T} \cdot \mathbf{g}_k \end{aligned} \tag{5.20b}$$

Let the Cartesian components of $\mathbf{T}$ be denoted by $T_{ik}^{(c)}$ in order to distinguish it from the contravariant components T_{ik}. If context does not give rise to any confusion, then we shall use T_{ik} as the Cartesian components of $\mathbf{T}$. Then, the relation between Cartesian and generalized components can be obtained in a simple way:

$$T_{ik}^{(c)} = \mathbf{e}_i \cdot \mathbf{T} \cdot \mathbf{e}_k = \mathbf{e}_i \cdot \left(T_{pq}\mathbf{g}^p\mathbf{g}^q\right) \cdot \mathbf{e}_k = T_{pq}(\mathbf{e}_i \cdot \mathbf{g}^p)\,(\mathbf{e}_k \cdot \mathbf{g}^q) = \frac{\partial \xi^p}{\partial x_i}\frac{\partial \xi^q}{\partial x_k}T_{pq}; \tag{5.21a}$$

$$T_{ik}^{(c)} = \mathbf{e}_i \cdot \left(T^{pq}\mathbf{g}_p\mathbf{g}_q\right) \cdot \mathbf{e}_k = \frac{\partial x_i}{\partial \xi^p}\frac{\partial x_k}{\partial \xi^q}T^{pq} \tag{5.21b}$$

The rest relations are left as exercise.

We have learned how generalized base vectors are related according to change of coordinates. Here Eqs. (3.40) and (3.41) are applied to Eq. (5.20b) in order to obtain the relation between the components of second-order tensors of two different generalized coordinate systems:

$$\overline{T}_{ik} = \overline{\mathbf{g}}_i \cdot \mathbf{T} \cdot \overline{\mathbf{g}}_k = \left(\frac{\partial \xi^p}{\partial \overline{\xi}^i}\mathbf{g}_p\right) \cdot \mathbf{T} \cdot \left(\frac{\partial \xi^q}{\partial \overline{\xi}^k}\mathbf{g}_q\right) = \frac{\partial \xi^p}{\partial \overline{\xi}^i}\frac{\partial \xi^q}{\partial \overline{\xi}^k}\mathbf{g}_p \cdot \mathbf{T} \cdot \mathbf{g}_q = \frac{\partial \xi^p}{\partial \overline{\xi}^i}\frac{\partial \xi^q}{\partial \overline{\xi}^k}T_{pq} \tag{5.22}$$

Similar method gives

$$\overline{T}^{ik} = \frac{\partial \overline{\xi}^i}{\partial \xi^p} \frac{\partial \overline{\xi}^k}{\partial \xi^q} T^{pq} \tag{5.23}$$

5.2.2 Symmetric and Skew-Symmetric Tensors

For any second-order tensor $\mathbf{T}$, we can define its transpose tensor, $\mathbf{T}^T$, which satisfies

$$\mathbf{u} \cdot \mathbf{T} \cdot \mathbf{v} = \mathbf{v} \cdot \mathbf{T}^T \cdot \mathbf{u} \tag{5.24}$$

for any two vectors $\mathbf{u}$ and $\mathbf{v}$. It is clear that $\mathbf{T}^T = T_{ik}\mathbf{e}_k\mathbf{e}_i = T_{ki}\mathbf{e}_i\mathbf{e}_k$ when $\mathbf{T} = T_{ik}\mathbf{e}_i\mathbf{e}_k$. Equation (5.24) implies that the transpose tensor of the tensor is itself:

$$\left(\mathbf{T}^T\right)^T = \mathbf{T} \tag{5.25}$$

The followings are identities related to transpose tensors:

$$(a\mathbf{T} + b\mathbf{S})^T = a\mathbf{T}^T + b\mathbf{S}^T; \tag{5.26a}$$

$$(\mathbf{T} \cdot \mathbf{S})^T = \mathbf{S}^T \cdot \mathbf{T}^T; \tag{5.26b}$$

$$\mathbf{T} \cdot \mathbf{u} = \mathbf{u} \cdot \mathbf{T}^T \tag{5.26c}$$

where $\mathbf{T}$ and $\mathbf{S}$ are arbitrary second-order tensors, a and b are arbitrary real numbers, and $\mathbf{u}$ is an arbitrary vector.

A tensor $\mathbf{S}$ is called symmetric tensor when $\mathbf{S} = \mathbf{S}^T$ and a tensor $\mathbf{W}$ is called skew-symmetric tensor (or antisymmetric tensor) when $\mathbf{W} = -\mathbf{W}^T$. A skew-symmetric tensor has 3 nonzero Cartesian components because $W_{ik} = -W_{ki}$. Then, one may imagine the existence of a vector $\mathbf{w} = w_k\mathbf{e}_k$ such that

$$\mathbf{W} \cdot \mathbf{x} = \mathbf{w} \times \mathbf{x} \tag{5.27}$$

for any vector $\mathbf{x} = x_k\mathbf{e}_k$. The vector $\mathbf{w}$ is called the axial vector of $\mathbf{W}$. Using a Cartesian coordinate system, Eq. (5.27) yields

$$W_{ik} = -\varepsilon_{ikm} w_m \tag{5.28}$$

Using the identity $\varepsilon_{ikm}\varepsilon_{ikn} = 2\delta_{mn}$, we have

$$w_i = -\frac{1}{2}\varepsilon_{ipq}W_{pq} \tag{5.29}$$

As for a skew-symmetric tensor $\mathbf{W}$ and two any vector $\mathbf{u}$ and $\mathbf{v}$, the following is always valid.

$$\mathbf{u}\cdot\mathbf{W}\cdot\mathbf{v} = \mathbf{w}\cdot(\mathbf{v}\times\mathbf{u}) \tag{5.30}$$

Since $\mathbf{A} - \mathbf{A}^T$ is a skew-symmetric tensor for any tensor $\mathbf{A}$, Eq. (5.30) implies that

$$\mathbf{u}\cdot\mathbf{A}\cdot\mathbf{v} - \mathbf{v}\cdot\mathbf{A}\cdot\mathbf{u} = \mathbf{a}\cdot(\mathbf{v}\times\mathbf{u}) \tag{5.31}$$

where $\mathbf{a}$ is the axial vector of $\mathbf{A} - \mathbf{A}^T$.

For a vector field $\mathbf{b}(\mathbf{x})$, the differential of $\mathbf{b}$ is given by

$$\mathrm{d}\mathbf{b} = (\nabla\mathbf{b})^T\cdot\mathrm{d}\mathbf{x} = \frac{\partial b_i}{\partial x_k}\mathrm{d}x_k\mathbf{e}_i \tag{5.32}$$

Note that

$$\nabla\mathbf{b} = \left(\mathbf{e}_i\frac{\partial}{\partial x_i}\right)(b_k\mathbf{e}_k) = \frac{\partial b_k}{\partial x_i}\mathbf{e}_i\mathbf{e}_k \tag{5.33}$$

The axial vector of $\nabla\mathbf{b} - (\nabla\mathbf{b})^T$ is given by

$$-\frac{1}{2}\varepsilon_{ipq}\left(\frac{\partial b_q}{\partial x_p} - \frac{\partial b_p}{\partial x_q}\right)\mathbf{e}_i = -\varepsilon_{ipq}\frac{\partial b_q}{\partial x_p}\mathbf{e}_i = -\nabla\times\mathbf{b} \tag{5.34}$$

Replacement of $\mathbf{A}$ and $\mathbf{a}$ of Eq. (5.31) by $\nabla\mathbf{b}$ and $-\nabla\times\mathbf{b}$, respectively, gives

$$\mathbf{u}\cdot\nabla\mathbf{b}\cdot\mathbf{v} - \mathbf{v}\cdot\nabla\mathbf{b}\cdot\mathbf{u} = (\nabla\times\mathbf{b})\cdot(\mathbf{u}\times\mathbf{v}) \tag{5.35}$$

Application of Eq. (5.35) to Eq. (4.84) proves the Stokes theorem.

Any tensor $\mathbf{A}$ can be decomposed to symmetric and skew-symmetric parts as follows:

$$\mathbf{A} = \frac{1}{2}\left(\mathbf{A} + \mathbf{A}^T\right) + \frac{1}{2}\left(\mathbf{A} - \mathbf{A}^T\right) \tag{5.36}$$

It is clear that the first term of the right-hand side is a symmetric tensor and the last term is a skew-symmetric tensor.

5.2.3 The Identity Tensor

If for any vector $\mathbf{v}$, a tensor maps $\mathbf{v}$ to itself, then the tensor is called the identity tensor and is denoted by $\mathbf{I}$:

$$\mathbf{I} \cdot \mathbf{v} = \mathbf{v} \cdot \mathbf{I} = \mathbf{v} \tag{5.37}$$

Since the identity tensor is a tensor, it can be expressed by $\mathbf{I} = I_{mn}\mathbf{e}_m\mathbf{e}_n$. Determination of I_{mn} can be done by:

$$I_{mn} = \mathbf{e}_m \cdot \mathbf{I} \cdot \mathbf{e}_n = \mathbf{e}_m \cdot \mathbf{e}_n = \delta_{mn} \tag{5.38}$$

It must be emphasized that Eq. (5.36) is valid for any orthonormal basis. Hence, it is clear that

$$\mathbf{I} = \mathbf{e}_k\mathbf{e}_k = \bar{\mathbf{e}}_m\bar{\mathbf{e}}_m \tag{5.39}$$

From the definitions of covariant and contravariant base vectors, the identity tensor can be rewritten in terms of covariant or contravariant base vectors (see Problem [5] of Sect. 3):

$$\mathbf{I} = g^{ik}\mathbf{g}_i\mathbf{g}_k = g_{ik}\mathbf{g}^i\mathbf{g}^k = \mathbf{g}^k\mathbf{g}_k = \mathbf{g}_k\mathbf{g}^k \tag{5.40}$$

5.2.4 Orthogonal Tensors

If a tensor $\mathbf{P}$ satisfies $\mathbf{P} \cdot \mathbf{P}^T = \mathbf{P}^T \cdot \mathbf{P} = \mathbf{I}$, then the tensor is called *orthogonal tensor*. Consider two orthonormal basis $\{\mathbf{e}_i\}$ and $\{\bar{\mathbf{e}}_i\}$. Equation (5.8a) can be rewritten as

$$\bar{\mathbf{e}}_i = \mathbf{Q} \cdot \mathbf{e}_i \tag{5.41}$$

where

$$\mathbf{Q} = \frac{\partial x_p}{\partial \bar{x}_q}\mathbf{e}_p\mathbf{e}_q \tag{5.42}$$

It is clear that

$$\mathbf{Q}^T \cdot \mathbf{Q} = \left(\frac{\partial x_p}{\partial \bar{x}_i}\mathbf{e}_i\mathbf{e}_p\right) \cdot \left(\frac{\partial x_m}{\partial \bar{x}_k}\mathbf{e}_m\mathbf{e}_k\right) = \frac{\partial x_m}{\partial \bar{x}_i}\frac{\partial x_m}{\partial \bar{x}_k}\mathbf{e}_i\mathbf{e}_k \tag{5.43}$$

Since $\overline{\mathbf{e}}_i \cdot \overline{\mathbf{e}}_k = \mathbf{e}_i \cdot \mathbf{e}_k$, we have

$$\overline{\mathbf{e}}_i \cdot \overline{\mathbf{e}}_k = (\mathbf{Q} \cdot \mathbf{e}_i) \cdot (\mathbf{Q} \cdot \mathbf{e}_k) = \left(\mathbf{e}_i \cdot \mathbf{Q}^T\right) \cdot (\mathbf{Q} \cdot \mathbf{e}_k) = \mathbf{e}_i \cdot \left(\mathbf{Q}^T \cdot \mathbf{Q}\right) \cdot \mathbf{e}_k = \delta_{ik} \quad (5.44)$$

Then, Eq. (5.44) implies that $\mathbf{Q}^T \cdot \mathbf{Q} = \mathbf{I}$. It also implies that

$$\frac{\partial x_m}{\partial \overline{x}_i} \frac{\partial x_m}{\partial \overline{x}_k} = \delta_{ik} \quad (5.43a)$$

Similarly, we can derive that

$$\frac{\partial \overline{x}_m}{\partial x_i} \frac{\partial \overline{x}_m}{\partial x_k} = \delta_{ik} \quad (5.43b)$$

5.2.5 Inverse Tensor

One of important features of the identity tensor is the product with second-order tensor. For any second-order tensor $\mathbf{T}$, the following is valid

$$\mathbf{I} \cdot \mathbf{T} = \mathbf{T} \cdot \mathbf{I} = \mathbf{T} \quad (5.45)$$

For a second-order tensor $\mathbf{T}$, if there is a second-order tensor $\mathbf{T}^{-1}$ such that

$$\mathbf{T} \cdot \mathbf{T}^{-1} = \mathbf{T}^{-1} \cdot \mathbf{T} = \mathbf{I} \quad (5.46)$$

then the tensor $\mathbf{T}^{-1}$ is unique and called the *inverse tensor* of $\mathbf{T}$. If a tensor $\mathbf{T}$ has the inverse, the tensor is called an *invertible tensor*. Consider a representation of an invertible tensor, $\mathbf{T} = T_{ik}^{(c)} \mathbf{e}_i \mathbf{e}_k$. Suppose that the matrix $T_{ik}^{(c)}$ has the inverse matrix $S_{ik}^{(c)}$. Then, we can construct a tensor $\mathbf{S} = S_{ik}^{(c)} \mathbf{e}_i \mathbf{e}_k$ in the same coordinate system. It is quite easy to check $\mathbf{T} \cdot \mathbf{S} = \mathbf{S} \cdot \mathbf{T} = \delta_{ik} \mathbf{e}_i \mathbf{e}_k$. Using coordinate change yields

$$\mathbf{S} = \frac{\partial \overline{x}_m}{\partial x_i} \frac{\partial \overline{x}_n}{\partial x_k} S_{ik}^{(c)} \overline{\mathbf{e}}_m \overline{\mathbf{e}}_n; \quad \mathbf{T} = \frac{\partial \overline{x}_m}{\partial x_i} \frac{\partial \overline{x}_n}{\partial x_k} T_{ik}^{(c)} \overline{\mathbf{e}}_m \overline{\mathbf{e}}_n \quad (5.47)$$

Then, we have

$$\overline{S}_{ik}^{(c)} \overline{T}_{km}^{(c)} = \overline{T}_{ik}^{(c)} \overline{S}_{km}^{(c)} = \delta_{im} \quad (5.48)$$

Thus, if the components matrix of a tensor is invertible in a rectangular coordinate system, then so does the component matrix in another rectangular coordinate system. Since inverse matrix is determined uniquely, it can be said that inverse tensor also is determined uniquely.

When a tensor is expressed by $\mathbf{T} = T^{ik}\mathbf{g}_i\mathbf{g}_k$, we want to find a tensor $\mathbf{S} = S_{mn}\mathbf{g}^m\mathbf{g}^n$ which satisfies $\mathbf{S}\cdot\mathbf{T} = \mathbf{T}\cdot\mathbf{S} = \mathbf{I}$. Note that

$$\mathbf{S}\cdot\mathbf{T} = S_{ik}T^{kn}\mathbf{g}^i\mathbf{g}_n; \quad \mathbf{T}\cdot\mathbf{S} = T^{ik}S_{kn}\mathbf{g}^i\mathbf{g}_n; \tag{5.49}$$

Since $\mathbf{I} = \mathbf{g}^i\mathbf{g}_i$, $S_{ik}T^{kn} = T^{ik}S_{kn} = \delta^i_n$ should be valid. Hence, the component matrix S_{ik} should be the inverse of T^{ik}.

5.2.6 Tensor Invariants

The double product of two tensors $\mathbf{T}:\mathbf{E} = T_{ik}E_{ik}$ shown in Eq. (5.14b) looks like a bilinear functional from two tensors to a real number. If Eq. (5.14b) is a real functional of tensors, the value $T_{ik}E_{ik}$ must be invariant for the same tensors irrespective of coordinate systems. To show this, we use Eq. (5.45):

$$\overline{T}_{ik}\overline{E}_{ik} = \frac{\partial\overline{x}_i}{\partial x_m}\frac{\partial\overline{x}_k}{\partial x_n}T_{mn}\frac{\partial\overline{x}_i}{\partial x_p}\frac{\partial\overline{x}_k}{\partial x_q}E_{pq} = \frac{\partial\overline{x}_i}{\partial x_m}\frac{\partial\overline{x}_i}{\partial x_p}\frac{\partial\overline{x}_k}{\partial x_n}\frac{\partial\overline{x}_k}{\partial x_q}T_{mn}E_{pq} \tag{5.50}$$

Application of Eq. (5.43) gives

$$\overline{T}_{ik}\overline{E}_{ik} = T_{mn}E_{mn} = T_{ik}E_{ik} \tag{5.51}$$

Hence, $f(\mathbf{T},\mathbf{E}) = \mathbf{T}:\mathbf{E}$ is a scalar-valued function of tensor. Similarly, we can show that $g(\mathbf{T},\mathbf{E}) = \mathbf{T}\cdot\cdot\mathbf{E}$ is also a scalar-valued function of tensor. In general, scalars made of inner product of tensors such as $\mathbf{T}:\mathbf{E}$ and $\mathbf{T}\cdot\cdot\mathbf{E}$ are independent of coordinate change. The scalar quantities are called tensor invariants.

One of the most important tensor invariants is trace of a tensor which is defined as

$$\mathrm{tr}(\mathbf{T}) = \mathbf{I}:\mathbf{T} = \mathbf{I}\cdot\cdot\mathbf{T} \tag{5.52}$$

As for nonnegative integer, we define

$$\mathbf{T}^0 = \mathbf{I}; \quad \mathbf{T}^1 = \mathbf{T}; \quad \mathbf{T}^2 = \mathbf{T}\cdot\mathbf{T}; \cdots \mathbf{T}^n = \underbrace{\mathbf{T}\cdot\mathbf{T}\cdot\mathbf{T}\cdots\mathbf{T}}_{n\ \text{times}} \tag{5.53}$$

Then, $f(\mathbf{T}) = \mathrm{tr}(\mathbf{T}^n)$ is a scalar-valued function of tensor. There are several identities related to trace of tensor:

$$\mathrm{tr}(a\mathbf{T} + b\mathbf{S}) = a\,\mathrm{tr}(\mathbf{T}) + b\,\mathrm{tr}(\mathbf{S}); \tag{5.54a}$$

$$\mathrm{tr}\left(\mathbf{T}^T\right) = \mathrm{tr}(\mathbf{T}); \tag{5.54b}$$

$$\mathrm{tr}(\mathbf{T}\cdot\mathbf{S}) = \mathrm{tr}(\mathbf{S}\cdot\mathbf{T}) = \mathbf{T}:\mathbf{S}^T \tag{5.54c}$$

In matrix algebra, determinant is a function from $N \times N$ matrix to a real number. Since a tensor is represented by a 3×3 matrix, the determinant of a tensor $\mathbf{T}$ is defined as the determinant of the component matrix and denoted by $\det(\mathbf{T})$. Furthermore, $\det(\mathbf{T})$ has the same value irrespective of coordinate change. Thus, $f(\mathbf{T}) = \det(\mathbf{T})$ is a scalar-valued function of tensor. Determinant of tensor can be calculated by the determinant of a component matrix of the tensor in a coordinate system, $\det(\mathbf{T}) = \varepsilon_{mnl}T_{1m}T_{2n}T_{3l}$. Hence, determinant of tensor satisfies the properties of the determinant of 3×3 matrix:

$$\det(\mathbf{I}) = 1; \tag{5.55a}$$

$$\det\left(\mathbf{T}^T\right) = \det(\mathbf{T}); \tag{5.55b}$$

$$\det(\mathbf{T}\cdot\mathbf{S}) = \det(\mathbf{T})\ \det(\mathbf{S}); \tag{5.55c}$$

$$\det\left(\mathbf{T}^{-1}\right) = \frac{1}{\det(\mathbf{T})} \tag{5.55d}$$

5.2.7 The Cayley–Hamilton Theorem

Eigenvalue problem for a tensor $\mathbf{T}$ is to find a vector $\mathbf{v}$ and a number λ such that

$$\mathbf{T}\cdot\mathbf{v} = \lambda\mathbf{v} \tag{5.56}$$

Here, the vector $\mathbf{v}$ is called an eigenvector of $\mathbf{T}$ and the number λ is called eigenvalue. In a Cartesian coordinate system, Eq. (5.56) is equivalent to

$$(T_{ik} - \lambda\delta_{ik})\, v_k = 0 \tag{5.57}$$

where v_k is the kth component of eigenvector $\mathbf{v}$. The trivial solution of Eq. (5.57) is $\mathbf{v} = v_k\mathbf{e}_k = \mathbf{0}$. The condition for the existence of nonzero eigenvector is

$$\det(T_{ik} - \lambda\delta_{ik}) = 0 \tag{5.58}$$

Equation (5.58) is a cubic equation for λ such that

$$P_{\mathbf{T}}(\lambda) \equiv \lambda^3 - I_1\lambda^2 + I_2\lambda - I_3 = 0 \tag{5.59}$$

where

$$\begin{aligned} I_1 &= T_{kk} = \mathrm{tr}(\mathbf{T}); \\ I_2 &= \frac{1}{2}(T_{ii}T_{kk} - T_{ik}T_{ki}) = \frac{1}{2}\left\{[\mathrm{tr}(\mathbf{T})]^2 - \mathrm{tr}(\mathbf{T}^2)\right\}; \\ I_3 &= \det(T_{ik}) = \det(\mathbf{T}) \end{aligned} \tag{5.60}$$

Since Eq. (5.58) is equivalent to $\det(\mathbf{T} - \lambda\mathbf{I}) = 0$ and determinant of tensor is a tensor invariant, it is easily understood that I_1, I_2 and I_3 are also tensor invariant. They are called principal invariants of tensor $\mathbf{T}$. Hence, the following notation is also used:

$$I_{\mathbf{T}} = I_1, \quad II_{\mathbf{T}} = I_2, \quad III_{\mathbf{T}} = I_3 \tag{5.61}$$

This notation is used to emphasize that these invariants are obtained from the tensor $\mathbf{T}$.

When an eigenvalue is found, then Eq. (5.56) gives nonzero eigenvectors corresponding to the eigenvalue. Since Eq. (5.57) is a homogeneous equation for v_k, the magnitude of eigenvector cannot be determined uniquely. In other words, eigenvalue problem is to find the direction of vector corresponding to the eigenvalue. Hence, we shall consider only unit eigenvector for convenience. If necessary, it will be mentioned that the eigenvector under consideration is not a unit vector.

Symmetric tensor is very important in continuum mechanics. It can be proved that any symmetric tensor has distinct three real roots for the characteristic equation of (5.59). Then, two eigenvectors with different eigenvalues of symmetric tensor are orthogonal to each other. Suppose $\lambda_1 \neq \lambda_2$. Then, Eq. (5.56) gives

$$\mathbf{v}_2 \cdot (\mathbf{T} \cdot \mathbf{v}_1) = \lambda_1 \mathbf{v}_2 \cdot \mathbf{v}_1; \quad \mathbf{v}_1 \cdot (\mathbf{T} \cdot \mathbf{v}_2) = \lambda_2 \mathbf{v}_1 \cdot \mathbf{v}_2 \tag{5.62}$$

where $\mathbf{v}_1$ and $\mathbf{v}_2$ are the eigenvectors corresponding to λ_1 and λ_2, respectively. Since $\mathbf{T}$ is symmetric, $\mathbf{v}_1 \cdot \mathbf{T} \cdot \mathbf{v}_2 = \mathbf{v}_2 \cdot \mathbf{T} \cdot \mathbf{v}_1$, which implies that

$$(\lambda_1 - \lambda_2)\mathbf{v}_1 \cdot \mathbf{v}_2 = 0 \tag{5.63}$$

This results in the orthogonality of the two eigenvectors: $\mathbf{v}_1 \cdot \mathbf{v}_2 = 0$ because $\lambda_1 \neq \lambda_2$.

Since a symmetric tensor has three distinct real eigenvalues, it must have three mutually orthogonal eigenvectors. Then, we can construct an orthonormal base consisting of the three eigenvectors. Let the basis be denoted by $\{\mathbf{v}_k\}$. Equation (5.56) implies that $\mathbf{v}_i \cdot \mathbf{T} \cdot \mathbf{v}_k = \lambda_i$ when $i = k$ and $\mathbf{v}_i \cdot \mathbf{T} \cdot \mathbf{v}_k = 0$ when $i \neq k$. This allows us to write

$$\mathbf{T} = \lambda_1 \mathbf{v}_1 \mathbf{v}_1 + \lambda_2 \mathbf{v}_2 \mathbf{v}_2 + \lambda_3 \mathbf{v}_3 \mathbf{v}_3 \tag{5.64}$$

This is called spectral decomposition, which implies that the component matrix of a symmetric tensor can be diagonalized as shown in Eq. (5.64) when coordinate

systems is suitably chosen. The axis of the diagonalization is called the principal axis.

Since any symmetric tensor can be expressed as Eq. (5.64). It is clear that for any nonnegative integer n,

$$\mathbf{T}^n = \sum_{k=1}^{3} (\lambda_k)^n \mathbf{v}_k \mathbf{v}_k \tag{5.65}$$

From Eq. (5.59), we can derive

$$\mathbf{T}^3 - I_\mathbf{T}\mathbf{T}^2 + II_\mathbf{T}\mathbf{T} - III_\mathbf{T}\mathbf{I} = \sum_{k=1}^{3} P_\mathbf{T}(\lambda_k)\, \mathbf{v}_k \mathbf{v}_k = \mathbf{0} \tag{5.66}$$

because of Eq. (5.59). Consider a two-dimensional tensor such that

$$\mathbf{B} = B_{11}\mathbf{e}_1\mathbf{e}_1 + B_{22}\mathbf{e}_2\mathbf{e}_2 + B_{12}\mathbf{e}_1\mathbf{e}_2 + B_{21}\mathbf{e}_2\mathbf{e}_1 \tag{5.67}$$

where $B_{\alpha\beta}$ are arbitrary real numbers. The principal invariants of $\mathbf{B}$ is easily calculated as follows:

$$I_\mathbf{B} = B_{11} + B_{22}; \quad II_\mathbf{B} = B_{11}B_{22} - B_{12}B_{21}; \quad III_\mathbf{B} = 0 \tag{5.68}$$

Furthermore, the two-dimensional tensor $\mathbf{B}$ satisfies

$$\mathbf{B}^3 - I_\mathbf{B}\mathbf{B}^2 + II_\mathbf{B}\mathbf{A} - III_\mathbf{B}\mathbf{I} = \mathbf{0} \tag{5.69}$$

because the tensor satisfies

$$\mathbf{B}^2 - I_\mathbf{B}\mathbf{B} + II_\mathbf{B}(\mathbf{I} - \mathbf{e}_3\mathbf{e}_3) = \mathbf{0} \tag{5.70}$$

Thus, the readers may conclude that any tensor $\mathbf{T}$ satisfies

$$\mathbf{T}^3 - I_1\mathbf{T}^2 + I_2\mathbf{T} - I_3\mathbf{I} = \mathbf{0} \tag{5.71}$$

If we set $P_\mathbf{T}(\lambda) = \lambda^3 - I_1\lambda^2 + I_2\lambda - \lambda^0$ which is the polynomial of Eq. (5.59), then Eq. (5.71) is equivalent to $P(\mathbf{T}) = \mathbf{0}$. Equation (5.71) holds for any second-order tensor, which is called the *Cayley–Hamilton theorem*.

The proof of the Cayley–Hamilton theorem may be done by the substitution of $T_{ik}\mathbf{e}_i\mathbf{e}_k$ to Eq. (5.71), which needs a long and tedious calculation. Although elegant proofs are found in text books of linear algebra and tensor analysis, these also require a long series of theorems. Hence, the proof of the Cayley–Hamilton theorem is omitted here.

Usefulness of the Cayley–Hamilton theorem is to allow us to calculate $\mathbf{T}^n$ in terms of $\mathbf{T}^2$, $\mathbf{T}$ and $\mathbf{I}$ with principal invariants of $\mathbf{T}$. Some examples are

$$\mathbf{T}^3 = I_1\mathbf{T}^2 - I_2\mathbf{T} + I_3\mathbf{I}; \quad \mathbf{T}^4 = \left(I_1^2 - I_2\right)\mathbf{T}^2 - I_1I_2\mathbf{T} + (I_1 + 1)\, I_3\mathbf{I} \tag{5.72}$$

In general, we have

$$\mathbf{T}^n = f_2^{(n)}(I_1, I_2, I_3)\,\mathbf{T}^2 + f_1^{(n)}(I_1, I_2, I_3)\mathbf{T} + f_0^{(n)}(I_1, I_2, I_3)\mathbf{I} \tag{5.73}$$

The functions $f_k^{(n)}$ can be determined iteratively by using the Cayley–Hamilton theorem.

5.2.8 Quadratic Form

Given a second-order tensor $\mathbf{T}$, a quadratic function of a vector $\mathbf{x}$ can be defined by

$$f_{\mathbf{T}}(\mathbf{x}) = \mathbf{x} \cdot \mathbf{T} \cdot \mathbf{x} \tag{5.74}$$

A scalar-valued function defined by Eq. (5.74) is called quadratic form of tensor $\mathbf{T}$. If $f_{\mathbf{T}}(\mathbf{x}) > 0$ for any nonzero vector $\mathbf{x}$, the tensor $\mathbf{T}$ is called a positive definite tensor.

Consider a tensor defined by $\mathbf{S} = \sigma_1\mathbf{e}_1\mathbf{e}_1 + \sigma_2\mathbf{e}_2\mathbf{e}_2$ with $\sigma_1 > 0$ and $\sigma_2 > 0$. The tensor $\mathbf{S}$ is not positive definite because $f_{\mathbf{S}}(\mathbf{x}) > 0$ is not valid for $\mathbf{x} = x\mathbf{e}_3$. An example of a positive definite tensor is $\mathbf{B} = \mathbf{F} \cdot \mathbf{F}^T$ (or $\mathbf{C} = \mathbf{F}^T \cdot \mathbf{F}$) where $\mathbf{F}$ is an invertible tensor. It is easy to show the tensor is positive definite:

$$f_{\mathbf{B}}(\mathbf{x}) = \mathbf{x} \cdot \left(\mathbf{F} \cdot \mathbf{F}^T\right) \cdot \mathbf{x} = (\mathbf{x} \cdot \mathbf{F}) \cdot \left(\mathbf{F}^T \cdot \mathbf{x}\right) = \left(\mathbf{F}^T \cdot \mathbf{x}\right) \cdot \left(\mathbf{F}^T \cdot \mathbf{x}\right) > 0 \tag{5.75}$$

Note that if $\mathbf{F}$ is invertible, then so is $\mathbf{F}^T$ and that $\mathbf{F}^T \cdot \mathbf{x} \neq \mathbf{0}$ whenever $\mathbf{x} \neq \mathbf{0}$. Thus, $f_{\mathbf{B}}(\mathbf{x})$ is always positive whenever $\mathbf{x} \neq \mathbf{0}$ because $f_{\mathbf{B}}(\mathbf{x})$ is the square of the magnitude of the vector $\mathbf{F}^T \cdot \mathbf{x}$.

If a symmetric tensor is positive definite, the tensor follows Eq. (5.64) and all eigenvalues λ_k are positive. Then, using Eq. (5.64) implies that there exists a symmetric positive tensor such that $\mathbf{T} = \mathbf{U}^2$ and

$$\mathbf{U} = \sqrt{\lambda_1}\,\mathbf{v}_1\mathbf{v}_1 + \sqrt{\lambda_2}\,\mathbf{v}_2\mathbf{v}_2 + \sqrt{\lambda_3}\,\mathbf{v}_3\mathbf{v}_3 \tag{5.76}$$

Theses theorems will be used in kinematics of continuum mechanics for understanding finite deformation of viscoelastic materials.

5.2.9 Tensor Functions

Using the definition (5.53) gives the exponential function of tensor such that

$$\exp(\mathbf{T}) \equiv \sum_{n=0}^{\infty} \frac{1}{n!} \mathbf{T}^n \tag{5.77}$$

When applying Eq. (5.73) to Eq. (5.77), we use the following definitions such that

$$\begin{aligned} f_2^{(0)} &= f_1^{(0)} = 0\,; \quad f_0^{(0)} = 1\,; \\ f_2^{(1)} &= f_0^{(1)} = 0\,; \quad f_1^{(1)} = 1\,; \\ f_1^{(2)} &= f_0^{(2)} = 0\,; \quad f_2^{(2)} = 1 \end{aligned} \tag{5.78}$$

Then, Eq. (5.77) becomes

$$\exp(\mathbf{T}) = \left(\sum_{n=0}^{\infty} \frac{f_2^{(n)}}{n!} \right) \mathbf{T}^2 + \left(\sum_{n=0}^{\infty} \frac{f_1^{(n)}}{n!} \right) \mathbf{T} + \left(\sum_{n=0}^{\infty} \frac{f_0^{(n)}}{n!} \right) \mathbf{I} \tag{5.79}$$

Hence, the existence of exponential function of tensor requires the convergence of the infinite series in the right-hand side of Eq. (5.79). It is known that the convergences hold. When $\mathbf{T}$ is a symmetric tensor, the spectral decomposition of $\mathbf{T}$, Eq. (5.64) gives

$$\exp(\mathbf{T}) = \sum_{k=1}^{3} \exp(\lambda_k)\, \mathbf{v}_k \mathbf{v}_k \tag{5.80}$$

If a function $f(x)$ can be expanded as the Taylor series with infinite radius of convergence, we can define

$$f(\mathbf{T}) = \sum_{n=0}^{\infty} \frac{f^{(n)}(0)}{n!} \mathbf{T}^n \tag{5.81}$$

As for a symmetric tensor, we have

$$f(\mathbf{T}) = \sum_{k=1}^{3} f(\lambda_k)\, \mathbf{v}_k \mathbf{v}_k \tag{5.82}$$

As for the exponential function of Eq. (5.77), the following identities hold:

$$\exp(a\mathbf{T} + b\mathbf{S}) = \exp(a\mathbf{T}) \cdot \exp(b\mathbf{S}); \tag{5.83a}$$

$$\exp(\mathbf{T}) \cdot \exp(-\mathbf{T}) = \exp(-\mathbf{T}) \cdot \exp(\mathbf{T}) = \mathbf{I} \tag{5.83b}$$

It must be noted that Eq. (5.83a) assumes that $\mathbf{T}$ and $\mathbf{S}$ commute: $\mathbf{T} \cdot \mathbf{S} = \mathbf{S} \cdot \mathbf{T}$. Then, we can define $\exp(\mathbf{0}) = \mathbf{I}$.

Consider a tensor-valued function of time, $\mathbf{W}(t)$ which is a mapping from real number to tensor. The following differential equation of tensor appears in rheology:

$$\frac{\mathrm{d}\mathbf{W}}{\mathrm{d}t} - \mathbf{H}\cdot\mathbf{W} - \mathbf{W}\cdot\mathbf{H}^T = \mathbf{S}(t) \tag{5.84}$$

where $\mathbf{H}$ is a constant tensor and $\mathbf{S}(t)$ is a given tensor-valued function of time. To solve the differential equation, introduce

$$\mathbf{K}(t) = \exp(-t\mathbf{H})\cdot\mathbf{W}\cdot\exp\left(-t\mathbf{H}^T\right) \tag{5.85}$$

Then, it is clear that

$$\frac{\mathrm{d}\mathbf{K}}{\mathrm{d}t} = e^{-t\mathbf{H}}\cdot\left(\frac{\mathrm{d}\mathbf{W}}{\mathrm{d}t} - \mathbf{H}\cdot\mathbf{W} - \mathbf{W}\cdot\mathbf{H}^T\right)\cdot e^{-t\mathbf{H}^T} \tag{5.86}$$

Combining Eq. (5.84) with Eq. (5.86), we have

$$\frac{\mathrm{d}\mathbf{K}}{\mathrm{d}t} = e^{-t\mathbf{H}}\cdot\mathbf{S}(t)\cdot e^{-t\mathbf{H}^T} \tag{5.87}$$

Integration gives

$$\mathbf{K}(t) - \mathbf{K}(0) = \int_0^t e^{-\tau\mathbf{H}}\cdot\mathbf{S}(\tau)\cdot e^{-\tau\mathbf{H}^T}\mathrm{d}\tau \tag{5.88}$$

Since $\mathbf{K}(0) = \mathbf{W}(0)$, application of Eqs. (5.83a, b) gives

$$\mathbf{W}(t) = e^{t\mathbf{H}}\cdot\mathbf{W}(0)\cdot e^{t\mathbf{H}^T} + \int_0^t e^{-(\tau-t)\mathbf{H}}\cdot\mathbf{S}(\tau)\cdot e^{-(\tau-t)\mathbf{H}^T}\mathrm{d}\tau \tag{5.89}$$

We can find an analogy with the solution of the ordinary differential equation such that

$$\frac{\mathrm{d}w}{\mathrm{d}t} + hw = b(t) \tag{5.90}$$

5.2.10 Isotropic Tensors

Isotropic tensor is a tensor whose components are not dependent on coordinate change. When a tensor are expressed by $\mathbf{T} = T_{ik}\mathbf{e}_i\mathbf{e}_k = \overline{T}_{ik}\overline{\mathbf{e}}_i\overline{\mathbf{e}}_k$, *isotropic tensor*

means $T_{ik} = \overline{T}_{ik}$ for any pair of basis. Without any proof, we state isotropic tensors of second, third, and fourth order:

$$\text{2nd order tensor} \quad \mathbf{U}^{(2)} = \lambda \mathbf{I} \tag{5.91a}$$

$$\text{3rd order tensor} \quad \mathbf{U}^{(3)} = \lambda \varepsilon_{ikm} \mathbf{e}_i \mathbf{e}_k \mathbf{e}_m \tag{5.91b}$$

$$\text{4th order tensor} \quad \mathbf{U}^{(4)} = \left(\alpha \delta_{ik}\delta_{pq} + \beta \delta_{ip}\delta_{kq} + \gamma \delta_{iq}\delta_{kp}\right) \mathbf{e}_i \mathbf{e}_k \mathbf{e}_p \mathbf{e}_q \tag{5.91c}$$

where α, β, γ, and λ are all arbitrary real numbers.

Isotropic tensor-valued function $\mathbf{G}(\mathbf{T})$ is defined as the one which satisfies

$$\mathbf{G}\left(\mathbf{Q} \cdot \mathbf{T} \cdot \mathbf{Q}^T\right) = \mathbf{Q} \cdot \mathbf{G}(\mathbf{T}) \cdot \mathbf{Q}^T \tag{5.92}$$

where $\mathbf{Q}$ is an arbitrary orthogonal tensor. It is known that when the domain of the isotropic tensor is the set of symmetric tensors, then

$$\mathbf{G}(\mathbf{T}) = \gamma_0 \mathbf{I} + \gamma_1 \mathbf{T} + \gamma_2 \mathbf{T}^2 \tag{5.93}$$

where γ_k are functions of principal invariants of $\mathbf{T}$. The proof is found in Haupt (2000).

5.3 Tensor Calculus

Consider a vector field $\mathbf{v} = v_k(\mathbf{x})\,\mathbf{e}_k$. The differential of the vector field is given by

$$\mathrm{d}\mathbf{v} = \mathbf{v}(\mathbf{x} + \mathrm{d}\mathbf{x}) - \mathbf{v}(\mathbf{x}) = \mathrm{d}v_i \mathbf{e}_i = \frac{\partial v_i}{\partial x_k} \mathrm{d}x_k \mathbf{e}_i \tag{5.94}$$

Then, one may introduce a tensor called gradient of $\mathbf{v}$ such that

$$\mathrm{d}\mathbf{v} = \operatorname{grad} \mathbf{v} \cdot \mathrm{d}\mathbf{x} \tag{5.95}$$

Comparison of Eqs. (5.94) with (5.95) gives

$$\operatorname{grad} \mathbf{v} = \frac{\partial v_i}{\partial x_k} \mathbf{e}_i \mathbf{e}_k \tag{5.96}$$

Using the symbol del, we have

$$\operatorname{grad} \mathbf{v} = (\nabla \mathbf{v})^T \tag{5.97}$$

Note that $\nabla\mathbf{v}$ is the dyadic of vector-differential operator ∇ and vector $\mathbf{v}$:

$$\nabla\mathbf{v} = \left(\mathbf{e}_i \frac{\partial}{\partial x_i}\right)(v_k \mathbf{e}_k) = \frac{\partial v_k}{\partial x_i}\mathbf{e}_i\mathbf{e}_k = (\operatorname{grad}\mathbf{v})^T \tag{5.98}$$

It is interesting that the gradient of scalar-valued function of vector is a vector field while that of vector-valued function of vector is a tensor field.

Note that gradients of scalar and vector can be derived from total differentials. Another method is to use directional derivative. Consider a scalar field and its directional derivative

$$\frac{\mathrm{d}}{\mathrm{d}t} f(\mathbf{x} + t\mathbf{h})\bigg|_{t=0} = \nabla f \cdot \mathbf{h} \tag{5.99}$$

As for a vector field, we have

$$\frac{\mathrm{d}}{\mathrm{d}t}\mathbf{v}(\mathbf{x} + t\mathbf{h})\bigg|_{t=0} = (\nabla\mathbf{v})^T \cdot \mathbf{h} \tag{5.100}$$

where $\mathbf{h}$ is an arbitrary vector. Then, we can extend this notion to a scalar-valued function of tensor:

$$\frac{\mathrm{d}}{\mathrm{d}t} f(\mathbf{T} + t\mathbf{H})\bigg|_{t=0} = \frac{\partial f}{\partial T_{ik}} H_{ik} = \frac{\partial f}{\partial \mathbf{T}} : \mathbf{H} = \operatorname{tr}\left(\frac{\partial f}{\partial \mathbf{T}} \cdot \mathbf{H}^T\right) \tag{5.101}$$

For simplicity, we used the notation such that

$$\frac{\partial f}{\partial \mathbf{T}} = \frac{\partial f}{\partial T_{ik}}\mathbf{e}_i\mathbf{e}_k \tag{5.102}$$

Then, we can define the gradient of f by $\partial f/\partial\mathbf{T}$. Application of Eq. (5.101) gives

$$\frac{\partial \operatorname{tr}(\mathbf{T}^n)}{\partial \mathbf{T}} = n\left(\mathbf{T}^T\right)^{n-1} \tag{5.103}$$

where n is a positive integer. To derive Eq. (5.103), the following is needed:

$$(\mathbf{T} + t\mathbf{H})^n = \mathbf{T}^n + t\sum_{k=0}^{n-1} \mathbf{T}^k \cdot \mathbf{H} \cdot \mathbf{T}^{n-1-k} + \mathbf{O}\left(t^2\right) \tag{5.104}$$

where $\mathbf{O}(t^2)$ is the terms that can be factorized by t^2.

Taking trace on both sides of Eq. (5.71), we have

$$\det(\mathbf{T}) = \frac{1}{6}\left\{ [\mathrm{tr}(\mathbf{T})]^3 - 3\mathrm{tr}(\mathbf{T})\,\mathrm{tr}\left(\mathbf{T}^2\right) + 2\mathrm{tr}\left(\mathbf{T}^3\right)\right\} \tag{5.105}$$

Then, using Eq. (5.103) gives

$$\frac{\partial}{\partial \mathbf{T}}\det(\mathbf{T}) = \det(\mathbf{T})\,\mathbf{T}^{-T} \tag{5.106}$$

where

$$\mathbf{T}^{-T} = \left(\mathbf{T}^{-1}\right)^T = \left(\mathbf{T}^T\right)^{-1} \tag{5.107}$$

With the help of Eqs. (5.103) and (5.106), we can derive

$$\frac{\partial I_\mathbf{B}}{\partial \mathbf{B}} = \mathbf{I}; \quad \frac{\partial II_\mathbf{B}}{\partial \mathbf{B}} = I_\mathbf{B}\mathbf{I} - \mathbf{B}^T; \quad \frac{\partial III_\mathbf{B}}{\partial \mathbf{B}} = III_\mathbf{B}\mathbf{B}^{-T} \tag{5.108}$$

Equation (5.108) is useful when we study constitutive equation of isotropic nonlinear elastic materials.

Divergence theorem studied in Sect. 4 can be applied to the definition of the divergence of second-order tensor. Substitution of $\mathbf{b} = \mathbf{c}\cdot\mathbf{T}$ into Eq. (4.76) gives

$$\mathbf{c}\cdot\left(\iint_{\partial\Omega}\mathbf{T}\cdot\mathrm{d}\mathbf{a} - \iiint_{\Omega}\nabla\cdot\mathbf{T}^T\mathrm{d}V\right) = \mathbf{0} \tag{5.109}$$

where $\mathbf{c}$ is assumed to be an arbitrary constant vector. The identity (5.109) implies that

$$\iint_{\partial\Omega}\mathbf{T}\cdot\mathrm{d}\mathbf{a} = \iiint_{\Omega}\mathrm{div}\,\mathbf{T}\,\mathrm{d}V \tag{5.110}$$

where

$$\mathrm{div}\,\mathbf{T} \equiv \nabla\cdot\mathbf{T}^T = \left(\mathbf{e}_i\frac{\partial}{\partial x_i}\right)\cdot\left(T_{pq}\mathbf{e}_q\mathbf{e}_p\right) = \frac{\partial T_{pi}}{\partial x_i}\mathbf{e}_p \tag{5.111}$$

Note that divergence of tensor is defined by Eq. (5.111).

Problem 5

[1] Prove the identity $\varepsilon_{ikm}\varepsilon_{ikn} = 2\delta_{mn}$

[2] Using Eqs. (5.8a, b) and (5.42) show that $\mathbf{Q} = \bar{\mathbf{e}}_k\mathbf{e}_k$.

[3] Show that $\mathrm{tr}(\mathbf{S}\cdot\mathbf{W}) = 0$ for any symmetric tensor $\mathbf{S}$ and any skew-symmetric tensor $\mathbf{W}$.

[4] Derive Eqs. (5.54a–c).
[5] Derive Eqs. (5.60).
[6] Derive Eqs. (5.69) and (5.70).
[7] Derive Eqs. (5.83a, b).
[8] Show that $\left(e^{\mathbf{A}}\right)^T = e^{\mathbf{A}^T}$
[9] Show that $\mathbf{C} = \mathbf{F}^T \cdot \mathbf{F}$ is symmetric and positive definite tensor, whenever $\mathbf{F}$ is invertible.
[10] Consider any linearly independent vectors $\mathbf{u}$, $\mathbf{v}$, and $\mathbf{w}$ and invertible tensor $\mathbf{F}$. Show that

$$\mathbf{F}^T \cdot [(\mathbf{F} \cdot \mathbf{u}) \times (\mathbf{F} \cdot \mathbf{v})] = \det(\mathbf{F})\, \mathbf{u} \times \mathbf{v} \tag{5.a}$$

and

$$\frac{(\mathbf{F} \cdot \mathbf{u}) \cdot [(\mathbf{F} \cdot \mathbf{v}) \times (\mathbf{F} \cdot \mathbf{w})]}{\mathbf{u} \cdot (\mathbf{v} \times \mathbf{w})} = \det(\mathbf{F}) \tag{5.b}$$

See Gurtin et al. (2010).
[11] Prove that $\mathrm{tr}\left(\mathbf{P}^{-1} \cdot \mathbf{A} \cdot \mathbf{P}\right) = \mathrm{tr}(\mathbf{A})$.
[12] For a given tensor $\mathbf{B} = \mathbf{b}_k \mathbf{b}_k$, show that

$$\begin{aligned} I_{\mathbf{B}} &= \sum_{k=1}^{3} \mathbf{b}_k \cdot \mathbf{b}_k; \\ II_{\mathbf{B}} &= \|\mathbf{b}_1 \times \mathbf{b}_2\|^2 + \|\mathbf{b}_2 \times \mathbf{b}_3\|^2 + \|\mathbf{b}_3 \times \mathbf{b}_1\|^2; \\ III_{\mathbf{B}} &= [\mathbf{b}_1 \cdot (\mathbf{b}_2 \times \mathbf{b}_3)]^2 \end{aligned} \tag{5.c}$$

See Cho (2009).
[13] Scalar-valued function of tensor is given by $f(\mathbf{B}) = \phi(I_{\mathbf{B}}, II_{\mathbf{B}}, III_{\mathbf{B}})$. Assume that $\mathbf{B}$ is symmetric. Then, derive

$$\frac{\partial f}{\partial \mathbf{B}} = (f_1 + I_{\mathbf{B}} f_2)\, \mathbf{I} - f_2 \mathbf{B} + III_{\mathbf{B}} f_3 \mathbf{B}^{-1} \tag{5.d}$$

where

$$f_1 = \frac{\partial \phi}{\partial I_{\mathbf{B}}}, \quad f_2 = \frac{\partial \phi}{\partial II_{\mathbf{B}}}, \quad f_3 = \frac{\partial \phi}{\partial III_{\mathbf{B}}} \tag{5.e}$$

See Gurtin et al. (2010), Haupt (2000), and Drozdov (1996).
[14] Using the divergence theorem, show that

$$\iint_{\partial\Omega} \mathbf{v} \times \mathrm{d}\mathbf{a} = -\iiint_{\partial\Omega} \nabla \times \mathbf{v} \mathrm{d}V \tag{5.f}$$

[15] Consider a function of vector $f(\mathbf{h},\ t)$ which satisfies

$$\frac{\partial f}{\partial t} = -\nabla_{\mathbf{h}} \cdot \{(\mathbf{L} \cdot \mathbf{h}) f - \alpha \nabla_{\mathbf{h}} f + \beta \mathbf{h} f\} \tag{5.g}$$

where $\mathbf{L}$ is a constant second-order tensor and α and β are constants. Furthermore, assume that

$$f \geq 0, \quad \lim_{\|\mathbf{h}\| \to \infty} \|\mathbf{h}\|^n f = 0, \quad \int_{-\infty}^{\infty} \int_{-\infty}^{\infty} \int_{-\infty}^{\infty} f(\mathbf{h}, t)\ \mathrm{d}h_1 \mathrm{d}h_2 \mathrm{d}h_3 = 1 \tag{5.h}$$

where $n = 0,\ 1,\ 2$. Then, derive the differential equation of $\mathbf{T}(t)$ which is defined by

$$\mathbf{T}(t) \equiv \int_{-\infty}^{\infty} \int_{-\infty}^{\infty} \int_{-\infty}^{\infty} \mathbf{h}\mathbf{h} f(\mathbf{h}, t)\ \mathrm{d}h_1 \mathrm{d}h_2 \mathrm{d}h_3 \tag{5.i}$$

See Bird et al. (1987).

[16] Consider a function of vector $f(\mathbf{x})$ which satisfies

$$f[t\mathbf{x} + (1-t)\,\mathbf{y}] \leq t f(\mathbf{x}) + (1-t) f(\mathbf{y}) \tag{5.j}$$

where $\mathbf{x}$ and $\mathbf{y}$ are arbitrary vectors and t is any real number. Then, show that the Hessian tensor defined by $\mathbf{H} \equiv \nabla\nabla f$ is positive definite.
See Luenberger (1969).

[17] Show that for any skew-symmetric tensor $\mathbf{W}$ and any vector $\mathbf{x}$,

$$\mathbf{x} \cdot \mathbf{W} \cdot \mathbf{x} = 0 \tag{5.k}$$

6 Fourier and Laplace Transforms

Fourier and Laplace transforms are linear mappings from a function space to another function space. The mappings are known as one-to-one. They are useful not only in solving differential equations but also in finding physical insights. In linear rheology, Fourier and Laplace transforms play the role of connecting different measurements, which results in overcoming the limitation of rheological measurements.

6.1 The Dirac Delta Function

Before studying Fourier and Laplace transforms, it is worthwhile to study the Dirac delta function because it is an important mathematical tool in integral transforms.

When a density distribution $\rho(\mathbf{x})$ is given, the total mass of a region Ω can be calculated by the volume integral of the density distribution over the region:

$$M = \iiint_{\Omega} \rho(\mathbf{x})\, dV \tag{6.1}$$

Consider mass points that are distributed at $\{\mathbf{r}_i\}$ with the mass of $\{m_i\}$. If the total number of mass points is N, the total mass of the particle system is given by

$$M = \sum_{i=1}^{N} m_i \tag{6.2}$$

Equation (6.1) contains the information on the spatial distribution of mass through $\rho(\mathbf{x})$ while Eq. (6.2) does not include the density field. Equation (6.2) cannot describe the region where mass points are distributed although we have the information of $\{m_i\}$ and $\{\mathbf{r}_i\}$. Hence, it is necessary to invent a mathematical entity which can describe the spatial distribution of mass point.

Consider a function $\eta_\varepsilon(\mathbf{x};\ \mathbf{r}_i)$ which has nonzero value near a point $\mathbf{r}_i$ and zero outside of the neighborhood of $\mathbf{r}_i$. Furthermore, the function should satisfy

$$\iiint \eta_\varepsilon(\mathbf{x};\ \mathbf{r}_i)\, dV = 1 \tag{6.3}$$

In Eq. (6.3), the integration region is over the whole space though it is not designated under the symbol of integration. The linear dimension of the neighborhood is assumed to be a small positive number ε. A mathematical invention to express the small region might be the open ball defined as

$$B_\varepsilon(\mathbf{r}_i) \equiv \{\, \mathbf{x} \,|\, \|\mathbf{x} - \mathbf{r}_i\| < \varepsilon \} \tag{6.4}$$

Then, we can say that

$$\iiint \eta_\varepsilon(\mathbf{x};\ \mathbf{r}_i)\, dV = \iiint_{B_\varepsilon(\mathbf{r}_i)} \eta_\varepsilon(\mathbf{x};\ \mathbf{r}_i)\, dV = 1 \tag{6.5}$$

because $\eta_\varepsilon(\mathbf{x};\ \mathbf{r}_i) = 0$ outside of $B_\varepsilon(\mathbf{r}_i)$. Let $\eta_\varepsilon(\mathbf{x})$ be denoted by $\eta_\varepsilon(\mathbf{x};\ \mathbf{0})$. Then, we know that $\eta_\varepsilon(\mathbf{x} - \mathbf{r}_i) = \eta_\varepsilon(\mathbf{x};\ \mathbf{r}_i)$. Let us call $\eta_\varepsilon(\mathbf{x})$ seed function.

Using the notion of seed function, we can express the density distribution by

$$\rho(\mathbf{x}) = \sum_{i=1}^{N} m_i \eta_\varepsilon(\mathbf{x} - \mathbf{r}_i) \tag{6.6}$$

Integration of Eq. (6.6) must give the total mass of Eq. (6.2). Hence, Eq. (6.6) seems to be a distribution of mass. This approach is often found in molecular theories (Evans and Morris 2008). However, if two particles happen to satisfy $\|\mathbf{r}_i - \mathbf{r}_k\| < \varepsilon$, the distribution deviates from our notion for mass distribution. Thus, we need a function defined under the limit of $\varepsilon \to 0$. For simplicity, we first consider the case of one-dimension.

Lesson from Eqs. (6.4) and (6.5) may define the one-dimensional seed function as

$$\eta_\varepsilon(x) = \frac{1}{\varepsilon}\eta\left(\frac{x}{\varepsilon}\right) \tag{6.7}$$

where $\eta(x)$ is any function which has positive finite value near $x = 0$ and satisfies

$$\int_{-\infty}^{\infty} \eta(x)\mathrm{d}x = 1, \quad \eta(-x) = \eta(x) \tag{6.8}$$

Thus, as ε goes to zero, the value of $\eta_\varepsilon(x)$ at $x = 0$ goes to the inifinite while the width of the nonzero region of $\eta_\varepsilon(x)$ goes to zero. There are several examples of seed functions. However, Fourier transform prefers

$$\eta_\varepsilon(x) = \frac{1}{\sqrt{2\pi\varepsilon}}\exp\left(-\frac{x^2}{2\varepsilon}\right) \tag{6.9}$$

Note that ε of Eq. (6.7) is replaced by $\sqrt{\varepsilon}$ in Eq. (6.9) because of simplicity. One of the simplest seed function might be

$$\eta_\varepsilon(x) = \begin{cases} \varepsilon^{-1} & -\frac{1}{2}\varepsilon < x < \frac{1}{2}\varepsilon \\ 0 & \text{otherwise} \end{cases} \tag{6.10}$$

The Dirac delta function is defined as

$$\int_{-\infty}^{\infty} \delta(x) f(x)\,\mathrm{d}x = \lim_{\varepsilon\to 0} \int_{-\infty}^{\infty} \eta_\varepsilon(x) f(x)\,\mathrm{d}x \tag{6.11}$$

instead of

$$\delta(x) = \lim_{\varepsilon\to 0} \eta_\varepsilon(x) \tag{6.12}$$

Note that $f(x)$ is any function in Eq. (6.11). Because Eq. (6.12) diverges to inifinite at $x = 0$, the Dirac delta function is defined by Eq. (6.11) instead of Eq. (6.12). As ε goes to zero, the function $\eta_\varepsilon(x)$ increases by the order of ε^{-1}, while the width of the nonzero region of $\eta_\varepsilon(x)$ decreases by the order of ε. Then, the value of $f(x)$ is maintained as $f(0)$ in the nonzero region. Hence, we have

$$\int_{-\infty}^{\infty} \delta(x) f(x)\, \mathrm{d}x = f(0) \tag{6.13}$$

Thus, the Dirac delta function is a linear functional from function $f(x)$ to real number $f(0)$. However, we use it as a function.

One-dimensional Dirac delta function has the following properties:

$$\delta(-x) = \delta(x); \tag{6.14a}$$

$$\delta(ax) = \frac{\delta(x)}{|a|}; \tag{6.14b}$$

$$\int_{-\infty}^{\infty} \delta(x - x_\mathrm{o}) f(x) \mathrm{d}x = f(x_\mathrm{o}) \tag{6.14c}$$

$$\int_{-\infty}^{\infty} \frac{\mathrm{d}\delta(x)}{\mathrm{d}x} f(x)\, \mathrm{d}x = \left.\frac{\mathrm{d}f}{\mathrm{d}x}\right|_{x=0} \tag{6.14d}$$

N-dimensional version of the Dirac delta function can be defined as

$$\delta(x_1, x_2, \ldots, x_N) = \delta(x_1)\delta(x_2)\ldots\delta(x_N) \tag{6.15}$$

For simplicity, N-dimensional vector is denoted by $\mathbf{x} = (x_1,\ x_2, \ldots, x_N)$ and N-dimensional volume element by $\mathrm{d}^N\mathbf{x} = \mathrm{d}x_1\mathrm{d}x_2\ldots\mathrm{d}x_N$. Then, we have

$$\int f(\mathbf{x})\, \delta(\mathbf{x})\, \mathrm{d}^N\mathbf{x} = f(\mathbf{0}) \tag{6.16}$$

In three-dimensional space, the electric field $\mathbf{E}(\mathbf{x})$ generated by a charge q located at $\mathbf{r}$ is given as

$$\mathbf{E} = \frac{q}{4\pi\varepsilon_\mathrm{o}} \frac{\mathbf{x} - \mathbf{r}}{\|\mathbf{x} - \mathbf{r}\|^3} \tag{6.17}$$

where ε_o is the permittivity in free space. Gauss law gives

$$\nabla \cdot \mathbf{E} = \frac{\rho_e(\mathbf{x})}{\varepsilon_o} \tag{6.18}$$

Note that the charge density $\rho_e(\mathbf{x})$ of a point charge must be

$$\rho_e(\mathbf{x}) = q\delta(\mathbf{x} - \mathbf{r}) \tag{6.19}$$

Combination of the Coulomb's law and the Gauss' law gives

$$\delta(\mathbf{x} - \mathbf{r}) = -\frac{1}{4\pi}\nabla^2 \frac{1}{\|\mathbf{x} - \mathbf{r}\|} \tag{6.20}$$

where ∇ is the del operator with respect to $\mathbf{x}$. More rigorous discussion on Eq. (6.20) is found in Marsden and Tromba (2003).

6.2 *Fourier Transform and Its Inversion*

6.2.1 *N*-Dimensional Fourier Transform

N-dimensional Fourier transform is used in analysis of chain conformation which is related to the entropic force exerted on a chain. Statistics of polymer conformation has an analogy to Brownian motion, stochastic process. Characteristic function of probability distribution is an example of the application of Fourier transform of multidimension. Another important application is scattering experiment of polymer fluids. See Rubinstein and Colby (2003), Doi and Edwards (1986), and Doi (1996).

Consider a scalar-valued function of *N*-dimensional vector $f(\mathbf{x})$ satisfying

$$\int |f(\mathbf{x})|\, \mathrm{d}^N\mathbf{x} < \infty \tag{6.21}$$

Equation (6.21) implies that

$$\lim_{\|\mathbf{x}\| \to \infty} f(\mathbf{x}) = 0 \tag{6.22}$$

For the functions, the Fourier transform is defined by

$$\widehat{F}[f(\mathbf{x})] = \hat{f}(\mathbf{k}) = \int f(\mathbf{x})\, e^{-\mathrm{i}\mathbf{k}\cdot\mathbf{x}} \mathrm{d}^N\mathbf{x} \tag{6.23}$$

where $\mathbf{k}$ is also N-dimensional vector, $\mathrm{i} = \sqrt{-1}$, and $\mathbf{k} \cdot \mathbf{x}$ is the inner product of two N-dimensional vectors such that

$$\mathbf{k} \cdot \mathbf{x} = \sum_{n=1}^{N} k_n x_n \tag{6.24}$$

Because of Eq. (6.21), the integral of Eq. (6.23) is finite. Thus, the function $\hat{f}(\mathbf{k})$ exists.

From the definition, it is clear that Fourier transform is a linear mapping from a function space to another function space. According to Krantz (1992), the inverse Fourier transform can be derived by using the seed function defined as

$$G_\varepsilon(\mathbf{x}) = \exp\left(-\frac{\varepsilon}{2}\mathbf{x} \cdot \mathbf{x}\right) \tag{6.25}$$

Then, the Fourier transform of $G_\varepsilon(\mathbf{x})$ is given by

$$\widehat{G}_\varepsilon(\mathbf{k}) = \left(\frac{2\pi}{\varepsilon}\right)^{N/2} G_{\varepsilon^{-1}}(\mathbf{k}) = \left(\frac{2\pi}{\varepsilon}\right)^{N/2} \exp\left(-\frac{\mathbf{k} \cdot \mathbf{k}}{2\varepsilon}\right) \tag{6.26}$$

Using Eq. (6.9), we can define

$$\eta_\varepsilon(\mathbf{x}) = \eta_\varepsilon(x_1)\, \eta_\varepsilon(x_2) \ldots \eta_\varepsilon(x_N) \tag{6.27}$$

Then, Eq. (6.26) can be rewritten as

$$\widehat{G}_\varepsilon(\mathbf{x}) = (2\pi)^N \eta_\varepsilon(\mathbf{x}) \tag{6.28}$$

Now define an integral transform such that

$$\widehat{F}^{-1}\left[\hat{f}(\mathbf{k})\right] \equiv \frac{1}{(2\pi)^N} \int \hat{f}(\mathbf{k})\, e^{\mathrm{i}\mathbf{k}\cdot\mathbf{x}} \mathrm{d}^N\mathbf{k} \tag{6.29}$$

Since $G_\varepsilon(\mathbf{x})$ goes to unity as ε goes to zero, Eq. (6.29) becomes

$$\widehat{F}^{-1}\left[\hat{f}(\mathbf{k})\right] = \lim_{\varepsilon \to 0} \frac{1}{(2\pi)^N} \int \hat{f}(\mathbf{k})\, G_\varepsilon(\mathbf{k})\, e^{\mathrm{i}\mathbf{k}\cdot\mathbf{x}} \mathrm{d}^N\mathbf{k} \tag{6.30}$$

Substituting Eq. (6.23) into Eq. (6.30) and changing the order of integration gives

$$\begin{aligned} \widehat{F}^{-1}\left[\hat{f}(\mathbf{k})\right] &= \lim_{\varepsilon \to 0} \frac{1}{(2\pi)^N} \int f(\mathbf{r})\, \widehat{G}_\varepsilon(\mathbf{r} - \mathbf{x})\, \mathrm{d}^N\mathbf{r} \\ &= \lim_{\varepsilon \to 0} \int f(\mathbf{r})\, \eta_\varepsilon(\mathbf{r} - \mathbf{x})\, \mathrm{d}^N\mathbf{r} \\ &= f(\mathbf{x}) \end{aligned} \tag{6.31}$$

Hence, the integral transform $\widehat{F}^{-1}$ is the inverse Fourier transform. In summary, we have

$$\hat{f}(\mathbf{k}) = \int f(\mathbf{x})\, e^{-\mathrm{i}\mathbf{k}\cdot\mathbf{x}} \mathrm{d}^N\mathbf{x}, \quad f(\mathbf{x}) = \frac{1}{(2\pi)^N} \int \hat{f}(\mathbf{k})\, e^{\mathrm{i}\mathbf{k}\cdot\mathbf{x}} \mathrm{d}^N\mathbf{k} \tag{6.32}$$

6.2.2 One-Dimensional Fourier Transform

One-dimensional Fourier transform is important in linear rheology because it provides the relation between static response function and dynamic response function. Static response functions are relaxation modulus and creep compliance which are measured from static loading, while dynamic response functions are storage and loss moduli which are measured from sinusoidal loading. See Ferry (1980).

If N of Eq. (6.32) is replaced by 1, then 1-dimensional Fourier transform pair is obtained by

$$\hat{f}(\omega) = \int_{-\infty}^{\infty} f(t)\, e^{-\mathrm{i}\omega t} \mathrm{d}t\,; \quad f(t) = \frac{1}{2\pi} \int_{-\infty}^{\infty} \hat{f}(\omega)\, e^{\mathrm{i}\omega t} \mathrm{d}\omega \tag{6.33}$$

Of course, the two functions must satisfy

$$\int_{-\infty}^{\infty} |f(t)|\, \mathrm{d}t < \infty, \quad \int_{-\infty}^{\infty} \left|\hat{f}(\omega)\right| \mathrm{d}\omega < \infty \tag{6.34}$$

where both $f(t)$ and $\hat{f}(\omega)$ are assumed to be complex-valued function of real variable, which implies

$$|f(t)| = \sqrt{f(t)\overline{f(t)}} \tag{6.35}$$

In Eq. (6.35), $\overline{f(t)}$ is the complex conjugate of $f(t)$.

From complex analysis, it is known that $e^{\mathrm{i}\theta} = \cos\theta + \mathrm{i}\sin\theta$, which is called Euler's formula. If $f(t)$ is a real-valued and even function, we have

$$\hat{f}(\omega) = \int_{-\infty}^{\infty} f(t)\, \cos\omega t\, \mathrm{d}t - \mathrm{i} \int_{-\infty}^{\infty} f(t)\, \sin\omega t\, \mathrm{d}t \tag{6.36}$$

Since $f(t)$ is an even function of t and $\sin\omega t$ is an odd function of t, the last integral of the right-hand side of Eq. (6.36) becomes zero. Then, Eq. (6.36) becomes

$$\hat{f}(\omega) = 2\int_0^\infty f(t)\,\cos\omega t\,\mathrm{d}t \tag{6.37a}$$

Equation (6.37a) implies that $\hat{f}(\omega)$ is real and an even function such that $\hat{f}(-\omega) = \hat{f}(\omega)$ because $\cos\omega t$ is an even function of ω. Similarly, if $f(t)$ is real and an odd function, then we have

$$\hat{f}(\omega) = -2\mathrm{i}\int_0^\infty f(t)\,\sin\omega t\,\mathrm{d}t \tag{6.37b}$$

This implies that $\hat{f}(\omega)$ is purely imaginary and an odd function such that $\hat{f}(-\omega) = -\hat{f}(\omega)$.

Euler's formula gives the inverse Fourier transform as follows:

$$f(t) = \frac{1}{2\pi}\int_{-\infty}^{\infty}\hat{f}(\omega)\cos\omega t\mathrm{d}\omega + \frac{\mathrm{i}}{2\pi}\int_{-\infty}^{\infty}\hat{f}(\omega)\sin\omega t\mathrm{d}\omega \tag{6.38}$$

If $\hat{f}(\omega)$ is real and even, then

$$f(t) = \frac{1}{\pi}\int_0^\infty \hat{f}(\omega)\cos\omega t\mathrm{d}\omega \tag{6.39a}$$

If $\hat{f}(\omega)$ is purely imaginary and odd, then

$$f(t) = \frac{\mathrm{i}}{\pi}\int_0^\infty \hat{f}(\omega)\sin\omega t\mathrm{d}\omega \tag{6.39b}$$

In linear rheology, a response function such as relaxation modulus has to obey

$$\chi(t) = \begin{cases} G(t) \geq 0 & \text{for } t \geq 0 \\ 0 & \text{for } t < 0 \end{cases} \tag{6.40}$$

because of causality. Assume that $G(t)$ is a monotonic decreasing function. From $\chi(t)$ we can define even and odd functions such that

$$\chi_{\mathrm{Even}}(t) = \begin{cases} \frac{1}{2}G(t) \geq 0 & \text{for } t \geq 0 \\ \frac{1}{2}G(-t) \geq 0 & \text{for } t < 0 \end{cases}; \tag{6.41a}$$

$$\chi_{\text{Odd}}(t) = \begin{cases} \frac{1}{2}G(t) \geq 0 & \text{for } t \geq 0 \\ -\frac{1}{2}G(-t) \leq 0 & \text{for } t < 0 \end{cases} \tag{6.41b}$$

Then, we have

$$\hat{\chi}(\omega) = \chi'(\omega) - \mathrm{i}\chi''(\omega) \tag{6.42}$$

where

$$\chi'(\omega) = 2\int_0^\infty \chi_{\text{Even}}(t)\cos\omega t \mathrm{d}t = \int_0^\infty G(t)\cos\omega t \mathrm{d}t \tag{6.43a}$$

and

$$\chi''(\omega) = 2\int_0^\infty \chi_{\text{Odd}}(t)\sin\omega t \mathrm{d}t = \int_0^\infty G(t)\sin\omega t \mathrm{d}t \tag{6.43b}$$

Equations (6.43a) and (6.43b) are obtained by using the properties of real-valued functions such as Eqs. (6.37a) and (6.37b). Inverse Fourier transform is given by

$$G(t) = \frac{2}{\pi}\int_0^\infty \chi'(\omega)\cos\omega t \mathrm{d}\omega = \frac{2}{\pi}\int_0^\infty \chi''(\omega)\sin\omega t \mathrm{d}\omega \tag{6.44}$$

One-dimensional Fourier transform has several properties which are very useful in many fields of physical science. These properties are introduced below without proof.

$$\widehat{F}\left[\frac{\mathrm{d}f}{\mathrm{d}t}\right] = \mathrm{i}\omega\hat{f}(\omega); \tag{6.45a}$$

$$\widehat{F}\left[\frac{\mathrm{d}^2 f}{\mathrm{d}t^2}\right] = -\omega^2\hat{f}(\omega); \tag{6.45b}$$

$$\widehat{F}\left[\int_a^t f(\tau)d\tau\right] = \frac{\hat{f}(\omega)}{\mathrm{i}\omega} + 2\pi F(a)\delta(\omega) \quad \text{with } f(t) = \frac{\mathrm{d}F}{\mathrm{d}t}; \tag{6.45c}$$

$$\widehat{F}[f(ct)] = -\frac{1}{c}\hat{f}\left(\frac{\omega}{c}\right); \tag{6.45d}$$

$$\widehat{F}[f(t+c)] = e^{ic\omega}\hat{f}(\omega); \tag{6.45e}$$

$$\widehat{F}[e^{at}f(t)] = \hat{f}(\omega + ia) \tag{6.45f}$$

6.2.3 Convolution Theorem

In Fourier transform, convolution of two functions is defined as

$$h(t) = (f^* g)(t) \equiv \int_{-\infty}^{\infty} f(\tau)g(t-\tau)d\tau \tag{6.46}$$

Assume that the three functions $f(t)$, $g(t)$, and $h(t)$ have their own Fourier transforms. Application of Eq. (6.32) gives

$$\hat{h}(\omega) = \hat{f}(\omega)\hat{g}(\omega) \tag{6.47}$$

Equation (6.47) can be derived by the change of the order of integration. Equations (6.46) and (6.47) are called the *convolution theorem*.

Equation (6.46) becomes the Fredholm integral equation of the first kind if the function $f(t)$ should be determined from the kernel function $g(t-\tau)$ and data function $h(t)$. Then, the convolution theorem lead us to

$$f(t) = \frac{1}{2\pi}\int_{-\infty}^{\infty} \frac{\hat{h}(\omega)}{\hat{g}(\omega)} e^{i\omega t} d\omega \tag{6.48}$$

The Fredholm integral equation of the first kind is found in linear viscoelasticity and linear dielectrics. In linear rheology, relaxation time spectrum is the solution of the Fredholm integral equation of the first kind. Use of Eq. (6.48) was applied to the problem of linear dielectrics by Fuoss and Kirkwood (1941), and their method can be applied to linear rheology of polymer, too Davies and Anderssen (1997) and Lee et al. (2015).

6.3 *Dirac Delta Function Revisited*

From the properties of the Dirac delta function, it is clear that it has well-defined Fourier transform such that

$$\hat{\delta}(\omega) = \int_{-\infty}^{\infty} \delta(t) e^{-i\omega t} dt = 1 \tag{6.49}$$

Since $\hat{\delta}(\omega) = 1$, Eq. (6.33) gives

$$\delta(t) = \frac{1}{2\pi} \int_{-\infty}^{\infty} e^{i\omega t} d\omega \tag{6.50}$$

which is the Fourier transform representation of the Dirac delta function.

N-dimensional delta function can be expressed by Fourier transform, too. If **x** and **k** are *N*-dimensional vector, then the *N*-dimensional delta function is given by

$$\delta(\mathbf{x}) = \frac{1}{(2\pi)^N} \int e^{i\mathbf{k}\cdot\mathbf{x}} d^N\mathbf{k} \tag{6.51}$$

Equation (6.51) is very useful in treating multidimensional probability density function. Its diverse applications are found in the statistics for polymer chain conformation (Doi and Edwards 1986), the distribution approaches of equilibrium statistical mechanics (McQuarrie 2000), and the derivation of momentum balance equation in terms of molecular motion (Evans and Morris 2008; Zuvarev 1974).

6.4 *Laplace Transform and Its Inversion*

6.4.1 Definition and Applications

Laplace transform is a powerful method in solving linear ordinary differential equations with constant coefficients because it converts a differential equation to an algebraic equation. Since one-dimensional linear viscoelastic models are linear ordinary differential equations, the calculation of strain and stress becomes easier when Laplace transform is used.

The definition of Laplace transform is given as

$$\widetilde{L}[f(t)] = \widetilde{f}(s) \equiv \int_0^{\infty} f(t) e^{-st} dt \tag{6.52}$$

Usually, the variable s is considered as real number. It can be, however, considered as complex number sometimes. When $s > 0$, the kernel function e^{-st} is a decreasing function of time. Hence, it is not necessary to require that

$$\int_0^\infty |f(t)|\mathrm{d}t < \infty \tag{6.53}$$

However, if $|f(t)|$ increases faster than e^{st}, the Laplace transform of $f(t)$ cannot exist. Thus, the domain of Laplace transform is larger than that of Fourier transform.

Just as Fourier transform, Laplace transform is also a linear mapping from a function space to another function space. Hence, we have

$$\widetilde{L}[af(t) + bg(t)] = a\widetilde{L}[f(t)] + b\widetilde{L}[g(t)] \tag{6.54}$$

for any real numbers a and b. One of the most important features of Laplace transform is

$$\widetilde{L}\left[\frac{\mathrm{d}^n f}{\mathrm{d}t^n}\right] = s^n\widetilde{f}(s) - \sum_{k=1}^{n} s^{n-k}\frac{\mathrm{d}^{n-k}f}{\mathrm{d}t^{n-k}}\bigg|_{t=0} \tag{6.55}$$

Just as Fourier transform, Laplace transform also has the convolution theorem. Suppose that three functions $h(t), f(t)$ and $g(t)$ have their own Laplace transforms. Furthermore, suppose that

$$h(t) = (f * g)(t) = \int_0^t f(t-\tau)g(\tau)\mathrm{d}\tau \tag{6.56}$$

It is not difficult to show that for any two functions $f(t)$ and $g(t)$

$$\int_0^t f(t-\tau)g(\tau)\mathrm{d}\tau = \int_0^t f(\tau)g(t-\tau)\mathrm{d}\tau \tag{6.57}$$

The right-hand side of Eq. (6.56) is called the convolution of f and g. Note that the convolution of Laplace transform has a little difference from that of Fourier transform. Compare Eq. (6.56) with Eq. (6.46). Then, the convolution theorem of Laplace transform reads

$$\widetilde{h}(s) = \widetilde{f}(s)\widetilde{g}(s) \tag{6.58}$$

Since the poof of the convolution theorem is found in several textbooks, we omit it.

Combination of Eqs. (6.54) and (6.55) converts a differential equation to an algebraic equation. Consider a linear differential equation which are found in linear viscoelastic models:

$$\sum_{n=0}^{M} a_n \frac{\mathrm{d}^n \sigma}{\mathrm{d}t^n} = \sum_{n=0}^{N} b_n \frac{\mathrm{d}^n \gamma}{\mathrm{d}t^n} \tag{6.59}$$

where a_n and b_n are constants and one of $\sigma(t)$ and $\gamma(t)$ is assumed to be given. Note that in Eq. (6.56), we used the notation such that

$$f(t) = \frac{\mathrm{d}^0 f}{\mathrm{d}t^0} \tag{6.60}$$

Application of Laplace transform gives

$$P(s)\widetilde{\sigma}(s) - \Pi(s) = Q(s)\widetilde{\gamma}(s) - \Omega(s) \tag{6.61}$$

where

$$\begin{aligned} P(s) &= \sum_{n=0}^{M} a_n s^n; \quad \Pi(s) = \sum_{n=0}^{M} \left(a_n \sum_{k=1}^{n} \sigma^{(n-k)}(0) \right); \\ Q(s) &= \sum_{n=0}^{N} b_n s^n; \quad \Omega(s) = \sum_{n=0}^{N} \left(b_n \sum_{k=1}^{n} \sigma^{(n-k)}(0) \right) \end{aligned} \tag{6.62}$$

Suppose that $\gamma(t)$ is given. Then, we have

$$\widetilde{\sigma}(s) = \widetilde{H}(s)\widetilde{\gamma}(s) + \widetilde{T}(s) \tag{6.63}$$

where

$$\widetilde{H}(s) = \frac{Q(s)}{P(s)}; \tag{6.64}$$

$$\widetilde{T}(s) = \frac{\Pi(s) - \Omega(s)}{P(s)} \tag{6.65}$$

If we have a method to invert Laplace transform, the convolution theorem gives the solution of Eq. (6.59) in the form of convolution:

$$\sigma(t) = \int_0^t H(t-\tau)\gamma(\tau)\mathrm{d}\tau + T(t) \tag{6.66}$$

The last term of the right-hand side of Eq. (6.66) is originated from initial conditions. Applications of Laplace transform to rheology are found in Tschoegl (1989), Riande et al. (2000), and Valko and Abate (2004).

6.4.2 Inverse Laplace Transform

The necessary condition of Fourier transform is that a function $g(t)$ should go to zero as t goes to infinite. However, convergence condition of Laplace transform is weaker than that of Fourier transform as mentioned earlier. If we express a function $f(t)$ which has its Laplace transform, by $f(t) = e^{\gamma t} g(t)$ for a positive real γ, the function $g(t)$ satisfies the condition of Fourier transform. Using inverse Fourier transform gives

$$g(t) = \frac{1}{2\pi} \int_{-\infty}^{\infty} \hat{g}(\omega) e^{i\omega t} d\omega = \frac{1}{2\pi} \int_{-\infty}^{\infty} \left[\int_{-\infty}^{\infty} g(\tau) e^{-i\omega\tau} d\tau \right] e^{i\omega t} d\omega \tag{6.67}$$

Since Laplace transform considers the interval of $t \geq 0$, we can say that

$$f(t) = \begin{cases} e^{\gamma t} g(t) & t \geq 0 \\ 0 & t < 0 \end{cases} \tag{6.68}$$

Generality is not lost even if setting $g(t) = 0$ when $t < 0$. Then, Eq. (6.67) can be rewritten as

$$g(t) = \frac{1}{2\pi} \int_{-\infty}^{\infty} \left[\int_{0}^{\infty} g(\tau) e^{-i\omega\tau} d\tau \right] e^{i\omega t} d\omega \tag{6.69}$$

Since $f(t) = e^{\gamma t} g(t)$, we have

$$f(t) = \frac{e^{\gamma t}}{2\pi} \int_{-\infty}^{\infty} \left[\int_{0}^{\infty} f(\tau) e^{-\gamma\tau} e^{-i\omega\tau} d\tau \right] e^{i\omega t} d\omega \tag{6.70}$$

Setting $s = \gamma + i\omega$, Eq. (6.70) becomes

$$f(t) = \frac{1}{2\pi i} \int_{\gamma - i\infty}^{\gamma + i\infty} \tilde{f}(s) e^{st} ds \tag{6.71}$$

The integral is the contour integral on the complex plane as shown in Fig. 6. When finite number of simple poles are inside of the loop of Fig. 6, the residue theorem can be used to evaluate the integral (Arfken and Weber 2001). In general, it is difficult to evaluate the integral analytically. Thus, hundreds of numerical algorithms have been developed (Cohen 2007). Some algorithms are available in MATLAB (Valsa and Brancik 1998).

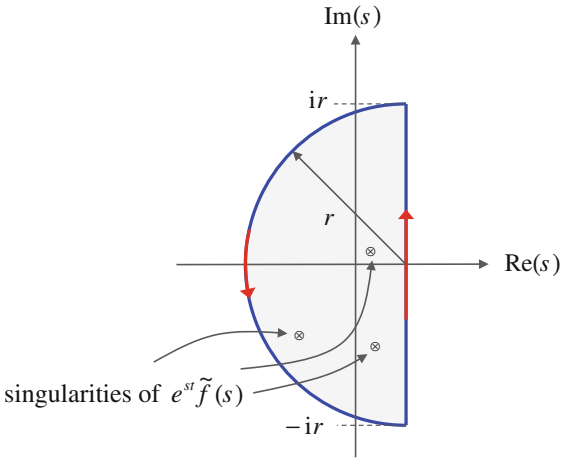

Fig. 6 Contour of inverse Laplace transform

Problem 6

[1] Derive followings

$$\int_{-\infty}^{\infty} e^{-ax^2+bx}\mathrm{d}x = \sqrt{\frac{\pi}{a}}\exp\left(\frac{b^2}{4a}\right) \quad \text{for } a > 0 \tag{6.a}$$

[2] The $N \times N$ matrix A_{ik} is symmetric and positive definite:

$$A_{ik} = A_{ki} \quad \text{and} \quad A_{ik}x_i x_k > 0 \quad \text{for any non-zero vector } \mathbf{x} \tag{6.b}$$

Then, derive

$$\int \exp(-A_{ik}x_i x_k)\mathrm{d}^N\mathbf{x} = \frac{(2\pi)^{N/2}}{\sqrt{\det(A_{ik})}} \tag{6.c}$$

[3] Derive Eq. (6.26).

[4] When $g(\nu)$ is given, solve the integral equation:

$$g(\nu) = \int_{-\infty}^{\infty} \frac{f(t)}{\cosh(\nu - t)}\mathrm{d}t \tag{6.d}$$

See Fuoss and Kirkwood (1941) and Davies and Anderssen (1997).

[5] Solve the integro-differential equation:

$$\begin{aligned} &\mu \frac{\mathrm{d}^2\gamma}{\mathrm{d}t^2} + \int_0^t G(t-\tau)\frac{\mathrm{d}\gamma}{\mathrm{d}\tau}\mathrm{d}\tau = \sigma_\mathrm{o}\sin\omega t; \\ &G(t) = G_\infty + (G_\mathrm{o} - G_\infty)e^{-t/\lambda}; \\ &\gamma(0) = \left.\frac{\mathrm{d}\gamma}{\mathrm{d}t}\right|_{t=0} = 0 \end{aligned} \tag{6.e}$$

See Baravian and Quemada (1998) and Kim et al. (2015).

[6] Find the Fourier and Laplace transforms of $G(t)$ which are given by

$$G(t) = \begin{cases} 0 & t<0 \\ \sum_{n=1}^{N} G_n e^{-t/\lambda_n} & t \geq 0 \end{cases} \tag{6.f}$$

Compare $\widetilde{G}(\mathrm{i}\omega)$ with $\widehat{G}(\omega)$.

[7] Prove the following properties of Laplace transform
Initial Value Theorem

$$f(0^+) = \lim_{s\to\infty} s\widetilde{f}(s) \tag{6.g}$$

Final Value Theorem

$$f(\infty) = \lim_{s\to 0} s\widetilde{f}(s) \tag{6.h}$$

[8] Using Laplace transform and Fourier transform, show that

$$\int_{-\infty}^{\infty} \frac{\sin x}{x}\mathrm{d}x = \pi \tag{6.i}$$

[9] Show that

$$\delta(x) = \lim_{a\to 0} \frac{1}{a\pi}\mathrm{sinc}\frac{x}{a} \tag{6.j}$$

where

$$\mathrm{sinc}x = \frac{\sin x}{x} \tag{6.k}$$

References

D.B. Ames, *Fundamentals of Linear Algebra* (International Textbook Company, Scranton, 1970)

R. Aris, *Vectors, Tensors, and the Basic Equations of Fluid Mechanics* (Dover, New York, 1962)

G.B. Arfken, H.J. Weber, *Mathematical Methods for Physicists* (Harcourt Sci. & Tech., 2001)

K. Atkinson, *An Introduction to Numerical Analysis* (Wiley, New York, 1978)

K. Atkinson, W. Han, *Theoretical Numerical Analysis,* 3rd edn. (Springer, New York, 2000)

C. Baravian, D. Quemada, Using instrumental inertia in controlled stress rheometry. Rheol. Acta **37**, 223–233 (1998)

R.B. Bird, C.F. Curtiss, R.C. Armstrong, O. Hassager, *Dynamics of Polymeric Liquids*. Kinetic Theory, vol. 2 (Wiley, New York, 1987)

K.S. Cho, Vector decomposition of the evolution equations of the conformation tensor of Maxwellian Fluids. Korea-Australia Rheol. J. **21**, 143–146 (2009)

K.S. Cho, K.-W. Song, G.-S. Chang, Scaling relations in nonlinear viscoelastic behavior of aqueous PEO solutions under large amplitude oscillatory shear flow. J. Rheol. **54**, 27–63 (2010)

A.M. Cohen, *Numerical Methods for Laplace Transform Inversion* (Springer, New York, 2007)

A.R. Davies, R.S. Anderssen, Sampling localization in determining the relaxation spectrum. J. Nonnewton. Fluid Mech. **73**, 163–179 (1997)

M. Doi, S.F. Edwards, *The Theory of Polymer Dynamics* (Oxford, 1986)

M. Doi, *Introduction to Polymer Physics* (Clarendon Press, Oxford, 1996)

A.D. Drozdov, *Finite Elasticity and Viscoelasticity* (World Scientific, Singapore, 1996)

D.J. Evans, G. Morris, *Statistical Mechanics of Nonequilibrium Liquids* (Cambridge University Press, Cambridge, 2008)

J.D. Ferry, *Viscoelastic Properties of Polymers* (Wiley, New York, 1980)

R.M. Fuoss, J.G. Kirkwood, Electrical properties of solids. VIII. Dipole moments in polyvinyl chloride-diphenyl systems. J. Am. Chem. Soc. **63**, 385–394 (1941)

M.E. Gurtin, E. Fried, L. Anand, *The Mechanics and Thermodynamics of Continua* (Cambridge, 2010)

P. Haupt, *Continuum Mechanics and Theory of Materials* (Springer, New York, 2000)

M.K. Kim, J.-E. Bae, N. Kang, K.S. Cho, Extraction of viscoelastic functions from creep data with ringing. J. Rheol. **59**, 237–252 (2015)

S.G. Krantz, *Partial Differential Equations and Complex Analysis* (CRC Press, Cleveland, 1992)

E. Kreyszig, *Introductory Functional Analysis with Applications* (Wiley, New York, 1978)

E. Kreyszig, *Advanced Engineering Mathematics*, 10th edn. (Wiley, New York, 2011)

S. Lee, J.-E. Bae, K.S. Cho, Complex decomposition method for relaxation time spectrum, in *Annual European Rheology Conference*, Nantes, 2015

D.G. Luenberger, *Optimization by Vector Space Methods* (Wiley, New York, 1969)

J.E. Marsden, A.J. Tromba, *Vector Calculus*, 5th edn. (W. H. Freeman and Company, New York, 2003)

D.A. McQuarrie, *Statistical Mechanics* (University Science Books, Sausalito, 2000)

B. O'Neill, *Elementary Differential Geometry*, 2nd edn. (Academic Press, New York, 2006)

E. Prugovecki, *Quantum Mechanics in Hilbert Space* (Dover, New York, 2006)

E. Riande, R. Díaz-Calleja, M.G. Prolongo, R.M. Masegosa, C. Salom, *Polymer Viscoelasticity, Stress and Strain in Practice* (Marcel Dekker, New York, 2000)

M. Rubinstein, R.H. Colby, *Polymer Physics* (Oxford University Press, Oxford, 2003)

I.S. Sokolnikoff, *Tensor Analysis*, 2nd edn. (Wiley, New York, 1964)

N.W. Tschoegl, *The Phenomenological Theory of Linear Viscoelastic Behavior* (Springer, New York, 1989)

P.P. Valko, J. Abate, Numerical Laplace inversion in rheological characterization. J. Nonnewton. Fluid Mech. **116**, 395–406 (2004)
J. Valsa, L. Brancik, Approximate formulae for numerical inversion of Laplace transform. Int. J. Num. Model. **11**, 153–166 (1998)
A.H. Zemanian, *Distribution Theory and Transform Analysis* (Dover, New York, 1987)
D.N. Zuvarev, *Nonequilibrium Statistical Thermodynamics* (Consultants Bureau, New York, 1974)

Chapter 2
Continuum Thermomechanics

Abstract The core of this chapter is continuum mechanics and the principle of constitutive equation. Equilibrium and nonequilibrium thermodynamics are also included because these disciplines are necessary to understand the principle of constitutive equation. The introduction to some classical constitutive equations is also addressed for eaiser understanding of the principle of constitutive equation.

Materials consist of atoms and molecules. Although materials are collection of discrete particles, it is more convenient to treat them as a continuum because the constituent particles are extremely small and the number of the particles is hugely large. Continuum is an uncountable set of points which are continuously distributed. It is assumed that there exist points between any pair of points in the continuum. Hence, continuum can be considered a subset of three-dimensional Euclidian space, E^3 (O'Neill 2006). The point of continuum is called material particle. However, it does not mean a physical particle such as atom and molecule. The material particle is as small as a point from macroscopic viewpoint, while it is so large to contain a number of molecules from microscopic viewpoint.

A macroscopic quantity is assigned to individual material particles and is interpreted as an average over the molecules in the material particle. This means that the macroscopic quantity is related to a function of microscopic quantities which varies faster in both time and space than the macroscopic quantity. Through averaging process, the faster variations of microscopic quantities are canceled mutually, and then, the average of the function of microscopic quantities becomes a smoothly varying function of both space and time (Callen 1985). This is the reason why the macroscopic quantity can be described by a field.

K.S. Cho, *Viscoelasticity of Polymers*, Springer Series
in Materials Science 241, DOI 10.1007/978-94-017-7564-9_2

1 Kinematics

1.1 Material and Spatial Coordinates

When classical mechanics is described in terms of particles, the main object is to predict the position of each particle as a function of time. The curves describing the motion of particles can be denoted by $\mathbf{x}_\alpha(t)$ where the subscript indicates the particles. In the case of discrete particle system, the index α is an integer. However, in the case of continuum, integer cannot be used as an indicator of material particles because there is no one-to-one correspondence between integers and material particles.

Imagine that we observe how a lump of materials moves. Since we can construct a coordinate system and have a clock, we can assign every material particle to a coordinate at every time. If we choose a time as the reference time among the interval of observation, then we can identify each material particle by the coordinate at the reference time. The coordinate at the reference time is an indicator of material particle and is called *material coordinate*. Let the material coordinate be denoted by the vector $\tilde{\mathbf{x}}$. As time flows, each material particle moves and is found at $\mathbf{x}$ at the time of t. If we collect all positions at corresponding time, then we have a mapping from $\tilde{\mathbf{x}}$ to $\mathbf{x}$ at every moment:

$$\mathbf{x} = \boldsymbol{\chi}(\tilde{\mathbf{x}}, t) \tag{1.1}$$

Equation (1.1) can be interpreted as the path of the material particle $\tilde{\mathbf{x}}$ as a function of time, which is a spatial curve from the viewpoint of geometry. When time t is fixed, Eq. (1.1) describes the distribution of material particles at time t. The distribution is called *configuration*. The configuration at the reference time is called the *reference configuration*, while the configuration at the present time t is called the *current configuration*. The current configuration is called *deformed configuration* if the body of material is considered to be deformed.

When Newton's second law is written in terms of particle position, it is the equation of motion whose solution is the path of particle motion. From the solution, we can calculate the force exerted on the particle at every moment. Thus, if we know Eq. (1.1), then we come to know everything needed in mechanics. How to obtain Eq. (1.1) will be studied later. For a while, it is assumed that Eq. (1.1) is known.

From the definition of material coordinate, it is clear that when time is the reference time τ, the following is valid:

$$\tilde{\mathbf{x}} = \boldsymbol{\chi}(\tilde{\mathbf{x}}, \tau) \tag{1.2}$$

In continuum mechanics, it is basically assumed that any material particle cannot be created nor annihilated. Then, the mapping Eq. (1.1) is one to one at every moment. Then, we can assume that the mapping has its inverse such that

$$\tilde{\mathbf{x}} = \boldsymbol{\chi}^{-1}(\mathbf{x}, t) \tag{1.3}$$

Since Eq. (1.1) is the path of material particle $\tilde{\mathbf{x}}$, the velocity $\mathbf{v}$ of $\tilde{\mathbf{x}}$ is determined by

$$\mathbf{v} = \frac{\partial \boldsymbol{\chi}(\tilde{\mathbf{x}}, t)}{\partial t} \tag{1.4}$$

Here, the time derivative is the partial differentiation with respect to t at fixed $\tilde{\mathbf{x}}$. Then, the velocity is a vector-valued function of material coordinate and time. Hence, we can write the velocity as follows:

$$\mathbf{v} = \tilde{\mathbf{v}}(\tilde{\mathbf{x}}, t) \tag{1.5}$$

Substitution of Eqs. (1.3)–(1.5) yields

$$\mathbf{v} = \tilde{\mathbf{v}}\left(\boldsymbol{\chi}^{-1}(\mathbf{x}, t), t\right) \equiv \mathbf{v}(\mathbf{x}, t) \tag{1.6}$$

Equation (1.5) implies that physical quantity $\mathbf{v}$ is described in terms of material coordinate, while Eq. (1.6) implies that the same quantity is described in terms of current coordinate $\mathbf{x}$. The former is called *Lagrangian description* or *material description*, and the latter is called *Eulerian description* or *spatial description*.

Lagrangian description of continuum is a direct translation of the Newtonian mechanics of particle because Eq. (1.4) is equivalent to the time derivative of $\mathbf{x}_\alpha(t)$. On the other hand, Eulerian description is more abstract but is more convenient. Since material particle is extremely small in macroscopic scale, it is practically impossible to trace individual material particles experimentally. However, observation of material at a fixed point in space is easier than tracing the material particles. Hence, a kind of translation is necessary when formulating a physical law by Eulerian description.

Acceleration vector is important because it is related to force through the second law of Newtonian mechanics. It is the time derivative of velocity such that

$$\mathbf{a} = \frac{\partial \tilde{\mathbf{v}}}{\partial t} \tag{1.7}$$

Note that Eq. (1.7) is the partial derivative of time at fixed material coordinate. Hence, it is called *material time derivative*. The material time derivative can be calculated easily if the function to be differentiated is expressed in terms of material

coordinate and time. The time derivative of Eq. (1.6) at fixed $\mathbf{x}$ is not the genuine acceleration which can be related to the force exerted on the material particle. Chain rule of differentiation provides the material time derivative from the function expressed in Eulerian description:

$$\mathbf{a} = \frac{\partial \mathbf{v}}{\partial t} + \mathbf{v} \cdot \nabla \mathbf{v} \tag{1.8}$$

where the partial differentiation of time is the one at fixed spatial coordinate $\mathbf{x}$ and the del operator means the differentiation with respect to spatial coordinate. Hence, we define a differential operator called material time derivative as

$$\frac{\mathrm{d}}{\mathrm{d}t} = \frac{\partial}{\partial t} + \mathbf{v} \cdot \nabla \tag{1.9}$$

1.2 Strain

1.2.1 Concept of Strain

If any pair of material particles of a continuum maintains the same distance during motion, the continuum is called *rigid body*. Motion of the rigid body consists of only translation and rotation. Hence, there is no pure deformation in the rigid body. Equation (1.1) describes the motion of material particles. If a continuum body is not a rigid body, then Eq. (1.1) consists of translation, rotation, and pure deformation.

Strain is a measure of pure deformation. Experience of daily life gives a measure of deformation for string such as

$$\varepsilon = \frac{l - l_\mathrm{o}}{l_\mathrm{o}} \tag{1.10}$$

where l and l_o are the lengths of string after and before a deformation, respectively. The intuitive strain of string ε is in the interval of $-1 < \varepsilon < \infty$. No deformation is represented by $\varepsilon = 0$. Negative strain means contraction, whereas positive strain means elongation. Various measures of strain can be suggested:

$$\lambda = \frac{l}{l_\mathrm{o}}; \quad h = \log \lambda \tag{1.11}$$

However, these strain measures cannot describe three-dimensional deformation. Consider a cylinder which has a small arrow on its lateral surface. The arrow is assumed to be in the direction of the axis of the cylinder. When exerting a

combination of elongation and twist on the cylinder, the deformed arrow has a different direction and length from the original arrow. Hence, a three-dimensional strain measure can describe the change of both direction and length unlike the strain measures of Eqs. (1.10) and (1.11).

1.2.2 Deformation Gradient

Consider a pair of two material coordinates $\tilde{\mathbf{x}}_1$ and $\tilde{\mathbf{x}}_2$. Assume that they are very close to each other. Then, we can write

$$\mathrm{d}\tilde{\mathbf{x}} = \tilde{\mathbf{x}}_2 - \tilde{\mathbf{x}}_1 \tag{1.12}$$

When $\mathbf{x}_k = \boldsymbol{\chi}(\tilde{\mathbf{x}}_k, t)$, we have

$$\mathrm{d}\mathbf{x} \equiv \boldsymbol{\chi}(\tilde{\mathbf{x}}_2, t) - \boldsymbol{\chi}(\tilde{\mathbf{x}}_1, t) = \mathbf{F} \cdot \mathrm{d}\tilde{\mathbf{x}} \tag{1.13}$$

where

$$\mathbf{F} = \widetilde{\nabla}\boldsymbol{\chi} \tag{1.14}$$

In Eq. (1.14), $\widetilde{\nabla}$ means the differentiation with respect to material coordinate and ∇ represents the differentiation with respect to spatial coordinate. Equation (1.13) implies that *deformation gradient* $\mathbf{F}$ does not contain translational motion because the contributions from translational motion are same for every material particle. However, rotational motion is still imbedded in deformation gradient $\mathbf{F}$.

1.2.3 Polar Decomposition

The existence of the inverse mapping, Eq. (1.3), implies that the deformation gradient is invertible. The theorem of *polar decomposition* is that any invertible tensor $\mathbf{F}$ can be decomposed to

$$\mathbf{F} = \mathbf{R} \cdot \mathbf{U} = \mathbf{V} \cdot \mathbf{R} \tag{1.15}$$

where $\mathbf{R}$ is an orthogonal tensor and both $\mathbf{U}$ and $\mathbf{V}$ are symmetric and positive definite tensors, respectively. Furthermore, the decomposition is unique.

It is clear that both $\mathbf{B} = \mathbf{F} \cdot \mathbf{F}^T$ and $\mathbf{C} = \mathbf{F}^T \cdot \mathbf{F}$ are symmetric and positive definite, respectively. Then, there exist two symmetric and positive definite tensors such that

$$\mathbf{B} = \mathbf{V}^2 \quad \text{and} \quad \mathbf{C} = \mathbf{U}^2 \tag{1.16}$$

because of the spectral decomposition theorem of symmetric and positive definite tensors. The two tensors **U** and **V** are uniquely determined from the deformation tensor **F**. The proof of polar decomposition can be done by showing that $\mathbf{F} \cdot \mathbf{U}^{-1}$ and $\mathbf{V}^{-1} \cdot \mathbf{F}$ are orthogonal tensors and they are identical. The proof of polar decomposition is found in Haupt (2000) and other books of advanced continuum mechanics.

1.2.4 Cauchy–Green Strains

It is not difficult to show that any rotational motion can be determined by an orthogonal tensor whose determinant is positive. Then, polar decomposition provides a way to find a strain measure which excludes both translational and rotational motions. The candidates are

$$\mathbf{B} = \mathbf{F} \cdot \mathbf{F}^T \tag{1.17a}$$

and

$$\mathbf{C} = \mathbf{F}^T \cdot \mathbf{F} \tag{1.17b}$$

The tensor **B** and **C** are called *left Cauchy–Green tensor* and *right Cauchy–Green tensor*, respectively. When deformation gradient represents only rotational motion, **F** must be an orthogonal tensor. Then, Eq. (1.17a) implies that $\mathbf{B} = \mathbf{C} = \mathbf{I}$. Of course, both **U** and **V** can be used as strain measures. However, calculations of **B** and **C** are easier than those of **U** and **V**, which is why **B** and **C** are preferred rather than **U** and **V**.

Consider a line element imbedded in the reference configuration $\mathrm{d}\tilde{\mathbf{x}} = \mathrm{d}\tilde{l}\mathbf{n}$ where **n** is the unit vector and $\mathrm{d}\tilde{l}$ is the length of the material line element. The material line element becomes $\mathrm{d}\mathbf{x} = \mathbf{F} \cdot \mathrm{d}\tilde{\mathbf{x}}$ after deformation. Then, the length of the deformed line element is given by

$$(\mathrm{d}l)^2 = \mathrm{d}\mathbf{x} \cdot \mathrm{d}\mathbf{x} = \mathrm{d}\tilde{\mathbf{x}} \cdot \mathbf{C} \cdot \mathrm{d}\tilde{\mathbf{x}} = \left(\mathrm{d}\tilde{l}\right)^2 \mathbf{n} \cdot \mathbf{C} \cdot \mathbf{n} \tag{1.18}$$

Arrangement of Eq. (1.18) yields

$$\lambda_n^2 \equiv \left(\frac{\mathrm{d}l}{\mathrm{d}\tilde{l}}\right)^2 = \mathbf{n} \cdot \mathbf{C} \cdot \mathbf{n} \tag{1.19}$$

Hence, the diagonal component of **C** is the square of the ratio of deformed length to undeformed length when the line element is in the direction of the axis of the coordinate of the reference configuration.

Consider two material line elements which are mutually orthogonal: $\mathrm{d}\tilde{\mathbf{x}}_1 = \mathrm{d}\tilde{l}\mathbf{n}_1$, $\mathrm{d}\tilde{\mathbf{x}}_2 = \mathrm{d}\tilde{l}\mathbf{n}_2$, and $\mathbf{n}_1 \cdot \mathbf{n}_2 = 0$. When $\mathrm{d}\mathbf{x}_k$ indicates the deformed line element of $\mathrm{d}\tilde{\mathbf{x}}_k$, we have

$$\mathrm{d}\mathbf{x}_1 \cdot \mathrm{d}\mathbf{x}_2 = \mathrm{d}\tilde{\mathbf{x}}_1 \cdot \mathbf{C} \cdot \mathrm{d}\tilde{\mathbf{x}}_2 = \left(\mathrm{d}\tilde{l}\right)^2 \mathbf{n}_1 \cdot \mathbf{C} \cdot \mathbf{n}_2 \tag{1.20}$$

Note that the angle θ_{12} between $\mathrm{d}\mathbf{x}_1$ and $\mathrm{d}\mathbf{x}_2$ is given by

$$\cos\theta_{12} = \frac{\mathrm{d}\mathbf{x}_1 \cdot \mathrm{d}\mathbf{x}_2}{\sqrt{\mathrm{d}\mathbf{x}_1 \cdot \mathrm{d}\mathbf{x}_1}\sqrt{\mathrm{d}\mathbf{x}_2 \cdot \mathrm{d}\mathbf{x}_2}} = \frac{\mathbf{n}_1 \cdot \mathbf{C} \cdot \mathbf{n}_2}{\sqrt{\mathbf{n}_1 \cdot \mathbf{C} \cdot \mathbf{n}_1}\sqrt{\mathbf{n}_2 \cdot \mathbf{C} \cdot \mathbf{n}_2}} \tag{1.21}$$

Equation (1.21) implies that the off-diagonal component $\mathbf{n}_1 \cdot \mathbf{C} \cdot \mathbf{n}_2$ is related to the distortion of shape if both $\mathrm{d}\tilde{\mathbf{x}}_1$ and $\mathrm{d}\tilde{\mathbf{x}}_2$ do not conduct length change.

Both $\mathbf{B}$ and $\mathbf{C}$ are three-dimensional generalization of λ of Eq. (1.11). Since the two Cauchy–Green tensors are symmetric and positive definite, $\log \mathbf{B}$ and $\log \mathbf{C}$ can be defined. These strain measures are generalization of h of Eq. (1.11).

1.2.5 Infinitesimal Strain

For rigid solid, small deformation is more interesting. A convenient measure of strain is *infinitesimal strain* which is also called *engineering strain*. When deformation is infinitesimal, the difference between the reference and deformed configuration is very small. Then, we are interested in *displacement vector* field defined as

$$\mathbf{u}(\tilde{\mathbf{x}}, t) = \mathbf{x}(\tilde{\mathbf{x}}, t) - \tilde{\mathbf{x}} \tag{1.22}$$

Then, the gradient of displacement vector field is given by

$$\left(\widetilde{\nabla}\mathbf{u}\right)^T = \mathbf{F} - \mathbf{I} \tag{1.23}$$

Expression of $\mathbf{C}$ in terms of $\mathbf{u}$ is given by

$$\mathbf{C} = \left[\mathbf{I} + \left(\widetilde{\nabla}\mathbf{u}\right)^T\right]^T \cdot \left[\mathbf{I} + \left(\widetilde{\nabla}\mathbf{u}\right)^T\right] = \mathbf{I} + 2\mathbf{E} + \widetilde{\nabla}\mathbf{u} \cdot \left(\widetilde{\nabla}\mathbf{u}\right)^T \tag{1.24}$$

where

$$\mathbf{E} = \frac{1}{2}\left[\widetilde{\nabla}\mathbf{u} + \left(\widetilde{\nabla}\mathbf{u}\right)^T\right] \tag{1.25}$$

When deformation is infinitesimally small, the second-order term of Eq. (1.24) can be neglected. Then, we have

$$\mathbf{E} \approx \frac{1}{2}(\mathbf{C} - \mathbf{I}) \tag{1.26}$$

Consider $\mathrm{d}\tilde{\mathbf{x}} = \mathrm{d}\tilde{l}\mathbf{n}$ as before. Since $\mathrm{d}l + \mathrm{d}\tilde{l} \approx 2\mathrm{d}\tilde{l}$ for infinitesimal deformation, we have

$$\frac{(\mathrm{d}l)^2 - (\mathrm{d}\tilde{l})^2}{(\mathrm{d}\tilde{l})^2} = \frac{(\mathrm{d}l - \mathrm{d}\tilde{l})(\mathrm{d}l + \mathrm{d}\tilde{l})}{(\mathrm{d}\tilde{l})^2} \approx 2\frac{\mathrm{d}l - \mathrm{d}\tilde{l}}{\mathrm{d}\tilde{l}} \tag{1.27}$$

On the other hand, the left-hand side of Eq. (1.27) is equal to

$$\frac{(\mathrm{d}l)^2 - (\mathrm{d}\tilde{l})^2}{(\mathrm{d}\tilde{l})^2} = \frac{\mathrm{d}\mathbf{x} \cdot \mathrm{d}\mathbf{x} - \mathrm{d}\tilde{\mathbf{x}} \cdot \mathrm{d}\tilde{\mathbf{x}}}{\mathrm{d}\tilde{\mathbf{x}} \cdot \mathrm{d}\tilde{\mathbf{x}}} = \mathbf{n} \cdot \mathbf{C} \cdot \mathbf{n} - 1 \approx 2\mathbf{n} \cdot \mathbf{E} \cdot \mathbf{n} \tag{1.28}$$

Then, we have

$$\mathbf{n} \cdot \mathbf{E} \cdot \mathbf{n} = \frac{(\mathrm{d}l + \mathrm{d}\tilde{l})(\mathrm{d}l - \mathrm{d}\tilde{l})}{2(\mathrm{d}\tilde{l})^2} = \frac{\mathrm{d}l - \mathrm{d}\tilde{l}}{\mathrm{d}\tilde{l}} \tag{1.29}$$

Here, we used the approximation of $\mathrm{d}l + \mathrm{d}\tilde{l} \approx 2\mathrm{d}\tilde{l}$. Equation (1.29) implies that $\mathbf{E}$ can be considered as the generalization of ε of Eq. (1.10). Application of Eqs. (1.26)–(1.21) yields

$$\cos\theta_{12} \approx \mathbf{n}_1 \cdot \mathbf{E} \cdot \mathbf{n}_2 \tag{1.30}$$

Hence, the off-diagonal components of infinitesimal strain have the same meaning with those of $\mathbf{C}$.

Compared with infinitesimal strain, $\mathbf{B}$ and $\mathbf{C}$ are called finite strains. When rubbery materials are considered, finite strains must be used.

1.3 Deformation of Area and Volume

Consider an area element $\mathrm{d}\tilde{\mathbf{a}}$ in the reference configuration. From Eq. (4.64) in Chap. 1, we know that

$$\mathrm{d}\tilde{\mathbf{a}} = (\tilde{\mathbf{t}}_p \times \tilde{\mathbf{t}}_q)\mathrm{d}p\mathrm{d}p \tag{1.31}$$

Since the two tangent vectors $\tilde{\mathbf{t}}_p$ and $\tilde{\mathbf{t}}_q$ are imbedded in a surface in the reference configuration, the two vectors become

$$\mathbf{t}_p = \mathbf{F} \cdot \tilde{\mathbf{t}}_p \quad \text{and} \quad \mathbf{t}_q = \mathbf{F} \cdot \tilde{\mathbf{t}}_q \tag{1.32}$$

Then, the area element in a deformed configuration becomes

$$\mathrm{d}\mathbf{a} = \mathbf{t}_p \times \mathbf{t}_q \, \mathrm{d}p\mathrm{d}q \tag{1.33}$$

Now, we will use the identity Eq. (5.a) in Chap. 1 of Problem 5

$$\mathbf{F}^T \cdot [(\mathbf{F} \cdot \mathbf{u}) \times (\mathbf{F} \cdot \mathbf{v})] = \det(\mathbf{F})\mathbf{u} \times \mathbf{v} \tag{1.34}$$

Note that $\tilde{\mathbf{t}}_p$ and $\tilde{\mathbf{t}}_q$ are linearly independent. If setting $\mathbf{u} = \tilde{\mathbf{t}}_p$ and $\mathbf{v} = \tilde{\mathbf{t}}_p$, then Eqs. (1.31), (1.33), and (1.34) give

$$\mathrm{d}\mathbf{a} = \det(\mathbf{F})\mathbf{F}^{-T} \cdot \mathrm{d}\tilde{\mathbf{a}} \tag{1.35}$$

For right-handed coordinate system, the volume element is given by the triple scalar product of three tangent vectors of coordinate:

$$\mathrm{d}\widetilde{V} = \tilde{\mathbf{g}}_1 \cdot (\tilde{\mathbf{g}}_2 \times \tilde{\mathbf{g}}_3)\mathrm{d}\tilde{\xi}^1\mathrm{d}\tilde{\xi}^2\mathrm{d}\tilde{\xi}^3 \tag{1.36}$$

As before, the tilde implies the reference configuration. Since deformation can be understood as a coordinate change, the chain rule of differentiation gives

$$\mathbf{g}_k = \mathbf{F} \cdot \tilde{\mathbf{g}}_k \tag{1.37}$$

Then, the deformed volume element is given by

$$\mathrm{d}V = (\mathbf{F} \cdot \tilde{\mathbf{g}}_1) \cdot [(\mathbf{F} \cdot \tilde{\mathbf{g}}_2) \times (\mathbf{F} \cdot \tilde{\mathbf{g}}_3)]\mathrm{d}\tilde{\xi}^1\mathrm{d}\tilde{\xi}^2\mathrm{d}\tilde{\xi}^3 = \det(\mathbf{F})\mathrm{d}\widetilde{V} \tag{1.38}$$

Here, Eq. (5.d) in Chap. 1 of Problem 5 is used.

1.4 Rate of Deformation

1.4.1 Deformation Rate Tensor and Spin Tensor

Now, we are interested in quantitative description of how fast deformation occurs. The velocity gradient in Lagrangian description is given by

$$\mathrm{d}\mathbf{v} = \left(\widetilde{\nabla}\tilde{\mathbf{v}}\right)^T \cdot \mathrm{d}\tilde{\mathbf{x}} \tag{1.39}$$

Using the chain rule of differentiation, we have the identity such that

$$\frac{\mathrm{d}\mathbf{F}}{\mathrm{d}t} = \left(\tilde{\nabla}\tilde{\mathbf{v}}\right)^T = (\nabla\mathbf{v})^T \cdot \mathbf{F} \tag{1.40}$$

Note that

$$\left(\tilde{\nabla}\tilde{\mathbf{v}}\right)^T = \frac{\partial \tilde{v}_i}{\partial \tilde{x}_k}\mathbf{e}_i\mathbf{e}_k; \quad (\nabla\mathbf{v})^T = \frac{\partial v_i}{\partial x_k}\mathbf{e}_i\mathbf{e}_k \tag{1.41}$$

Combining the above three equations, we have

$$\mathrm{d}\mathbf{v} = (\nabla\mathbf{v})^T \cdot \mathrm{d}\mathbf{x} \tag{1.42}$$

We call the *velocity gradient* in Eulerian description just velocity gradient and denote it by

$$\mathbf{L} \equiv (\nabla\mathbf{v})^{\mathrm{T}} \tag{1.43}$$

Then, the material time derivative of deformation gradient is given by

$$\dot{\mathbf{F}} \equiv \frac{\mathrm{d}\mathbf{F}}{\mathrm{d}t} = \mathbf{L} \cdot \mathbf{F} \tag{1.44}$$

This identity is important in the development of the nonlinear viscoelastic constitutive equations.

We shall show that the total differential of velocity field $\mathrm{d}\mathbf{v}$ is the material time derivative of the infinitesimal difference $\mathrm{d}\mathbf{x}$ in the current configuration. Consider the total differential of $\mathbf{v}$:

$$\mathrm{d}\mathbf{v} = \mathbf{v}(\mathbf{x} + \mathrm{d}\mathbf{x}, t) - \mathbf{v}(\mathbf{x}, t) = \tilde{\mathbf{v}}(\tilde{\mathbf{x}} + \mathrm{d}\tilde{\mathbf{x}}, t) - \mathbf{v}(\tilde{\mathbf{x}}, t) \tag{1.45}$$

The first equality is the Eulerian description, and the second is the Lagrangian description. From the definition of velocity, we obtain

$$\mathrm{d}\mathbf{v} = \frac{\mathrm{d}}{\mathrm{d}t}[\mathbf{x}(\tilde{\mathbf{x}} + \mathrm{d}\tilde{\mathbf{x}}, t) - \mathbf{x}(\tilde{\mathbf{x}}, t)] = \frac{\mathrm{d}}{\mathrm{d}t}\mathrm{d}\mathbf{x} \tag{1.46}$$

and

$$\mathrm{d}\mathbf{v} = \frac{\mathrm{d}}{\mathrm{d}t}(\mathbf{F} \cdot \mathrm{d}\tilde{\mathbf{x}}) = \frac{\mathrm{d}\mathbf{F}}{\mathrm{d}t} \cdot \mathrm{d}\tilde{\mathbf{x}} = \frac{\mathrm{d}\mathbf{F}}{\mathrm{d}t} \cdot \left(\mathbf{F}^{-1} \cdot \mathrm{d}\mathbf{x}\right) = \dot{\mathbf{F}} \cdot \mathbf{F}^{-1} \cdot \mathrm{d}\mathbf{x} \tag{1.47}$$

In Eq. (1.47), it is used that $\mathrm{d}\tilde{\mathbf{x}}$ can be considered as constant vector with respect to material time differentiation. Comparison of Eq. (1.42) with Eq. (1.47) gives Eq. (1.44) again. This result is not more important than Eq. (1.46) because

Eq. (1.46) gives a new insight on velocity gradient. The infinitesimal arc length in the current configuration can be defined as $(\mathrm{d}l)^2 = \mathrm{d}\mathbf{x} \cdot \mathrm{d}\mathbf{x}$. Then, we have

$$\frac{1}{2}\frac{\mathrm{d}}{\mathrm{d}t}(\mathrm{d}l)^2 = \mathrm{d}l\frac{\mathrm{d}}{\mathrm{d}t}\mathrm{d}l = \mathrm{d}\mathbf{x} \cdot \frac{\mathrm{d}}{\mathrm{d}t}\mathrm{d}\mathbf{x} = \mathrm{d}\mathbf{x} \cdot \mathrm{d}\mathbf{v} = \mathrm{d}\mathbf{x} \cdot \mathbf{L} \cdot \mathrm{d}\mathbf{x} \tag{1.48}$$

The last term is the quadratic form of velocity gradient. The Problem 5 (McQuarrie 2000), Eq. (5.k), in Chap. 1 let us know that

$$\frac{\mathrm{d}}{\mathrm{d}t}(\mathrm{d}l)^2 = \mathrm{d}\mathbf{x} \cdot \mathbf{D} \cdot \mathrm{d}\mathbf{x} \tag{1.49}$$

where $\mathbf{D}$ is the symmetric part of velocity gradient and is called *deformation rate tensor*. The unique decomposition of tensor shown in Eq. (5.36) in Chap. 1 gives

$$\mathbf{D} = \frac{1}{2}\left(\mathbf{L} + \mathbf{L}^T\right) \quad \text{and} \quad \mathbf{W} = \frac{1}{2}\left(\mathbf{L} - \mathbf{L}^T\right) \tag{1.50}$$

The skew-symmetric tensor $\mathbf{W}$ is called *spin tensor*.

Differential geometry of a curve illustrates that when the curve is parameterized by its arc length, the tangent vector $\mathrm{d}\mathbf{x}/\mathrm{d}l$ is a unit vector. Then, Eq. (1.49) becomes

$$\frac{1}{\mathrm{d}l}\frac{\mathrm{d}}{\mathrm{d}t}\mathrm{d}l = \frac{\mathrm{d}}{\mathrm{d}t}\log(\mathrm{d}l) = \frac{\mathrm{d}\mathbf{x}}{\mathrm{d}l} \cdot \mathbf{D} \cdot \frac{\mathrm{d}\mathbf{x}}{\mathrm{d}l} \tag{1.51}$$

Thus, $\mathbf{D}$ indicates how fast the infinitesimal line element is extended or contracted. More detailed analysis is found in Aris (1962).

With the help of Eq. (1.44) and the polar decomposition, we have

$$\mathbf{L} = \dot{\mathbf{F}} \cdot \mathbf{F}^{-1} = \dot{\mathbf{V}} + \mathbf{V} \cdot \left(\dot{\mathbf{R}} \cdot \mathbf{R}^T\right) \cdot \mathbf{V}^{-1} \tag{1.52}$$

Note that $\dot{\mathbf{V}} = \mathrm{d}\mathbf{V}/\mathrm{d}t$ is symmetric because $\mathbf{V}$ is symmetric and the last term in the right-hand side of Eq. (1.52) is skew-symmetric because of skew-symmetric $\dot{\mathbf{R}} \cdot \mathbf{R}^T$. Equation (1.50) gives

$$\mathbf{D} = \frac{\mathrm{d}\mathbf{V}}{\mathrm{d}t} \tag{1.53}$$

and

$$\mathbf{W} = \mathbf{V} \cdot \left(\frac{\mathrm{d}\mathbf{R}}{\mathrm{d}t} \cdot \mathbf{R}^T\right) \cdot \mathbf{V}^{-1} \tag{1.54}$$

Note that the polar decomposition implies that $\mathbf{U}$ and $\mathbf{V}$ represent pure deformation. Thus, Eq. (1.53) also means that $\mathbf{D}$ represents deformation rate as shown in

Eq. (1.51). When the motion of continuum is pure rotation, the deformation gradient becomes an orthogonal tensor. Putting $\mathbf{F} = \mathbf{R}$ into Eq. (1.52), we have $\mathbf{L} = \dot{\mathbf{R}} \cdot \mathbf{R}^T$. The tensors $\mathbf{V}$ and $\mathbf{V}^{-1}$ in $\mathbf{W}$ play the role that pure deformation is canceled when $\mathbf{W}$ transforms $d\mathbf{x}$ to $\mathbf{W} \cdot d\mathbf{x}$. In other words, $\mathbf{W}$ is related to the rotation only. Hence, we call $\mathbf{W}$ spin tensor. Furthermore, for any vector $\mathbf{x}$, the following is an identity:

$$\mathbf{W} \cdot \mathbf{x} = -(\nabla \times \mathbf{v}) \times \mathbf{x} \tag{1.55}$$

This implies that the curl of velocity represents the rotation in flow.

It is interesting that the representative strain tensors $\mathbf{B}$ and $\mathbf{C}$ have different forms of material time derivatives:

$$\dot{\mathbf{B}} = \mathbf{L} \cdot \mathbf{B} + \mathbf{B} \cdot \mathbf{L}^T \tag{1.56}$$

and

$$\dot{\mathbf{C}} = 2\mathbf{F}^T \cdot \mathbf{D} \cdot \mathbf{F} \tag{1.57}$$

1.5 Relative Deformation Gradient

1.5.1 Relativity of Deformation

If the macroscopic properties of a continuum are functions of the states of the body, then we can choose the reference configuration in a definite manner. For an example, the lowest energy state may give the reference configuration. Solid was believed as such a material body. As for such solids, we often experience a state of material in equilibrium without deformation. It is not much difficult to control the state of the solid materials in order to choose the reference configuration at will. However, a tiny perturbation makes fluid flow. Although it is difficult to find the well-defined reference configuration of fluid, imagination of the concrete reference configuration allows us to describe mechanical phenomena well if we are equipped with mathematical tools such as material time derivative and if it is a reasonable assumption that the macroscopic properties of the fluid are functions of suitable state variables. However, if the macroscopic properties depend on not only current state but also how materials experience the variation of state in past, the choice of reference configuration loses a foundation. The reference configuration becomes relative. Viscoelastic materials are ones that their history determines their present just as human.

The use of the current configuration as the reference one is more convenient in the description of viscoelastic deformation, because viscoelastic behavior is

determined by the effects of past deformation. Effect of far past is less than that of near past, which is called *fading memory*.

1.5.2 Relative Deformation Measures

As before, $\mathbf{x}$ is the position vector of a material particle at current time and the position of the particle at time τ is denoted by $\hat{\mathbf{x}}$. The configuration characterized by $\hat{\mathbf{x}}$ shall be called past configuration. Then, we have a one-to-one mapping such that

$$\hat{\mathbf{x}} = \boldsymbol{\chi}_t(\mathbf{x}, \tau), \quad \mathbf{x} = \boldsymbol{\chi}_t(\mathbf{x}, t) = \boldsymbol{\chi}_t^{-1}(\hat{\mathbf{x}}, \tau) \tag{1.58}$$

Note that the subscript t emphasizes that the configuration at t is the reference configuration.

The use of Eq. (1.58) gives *relative deformation gradient* defined by

$$\mathbf{F}_t(\tau) = (\nabla \hat{\mathbf{x}})^T \tag{1.59}$$

Equation (1.59) also means that

$$\mathrm{d}\hat{\mathbf{x}} = \mathbf{F}_t(\tau) \cdot \mathrm{d}\mathbf{x}; \quad \mathrm{d}\mathbf{x} = \mathbf{F}_t^{-1}(\tau) \cdot \mathrm{d}\hat{\mathbf{x}} \tag{1.60}$$

Application of polar decomposition to relative deformation gradient gives

$$\mathbf{F}_t(\tau) = \mathbf{R}_t(\tau) \cdot \mathbf{U}_t(\tau) = \mathbf{V}_t(\tau) \cdot \mathbf{R}_t(\tau) \tag{1.61}$$

Of course, it is clear that

$$\mathbf{F}_t(t) = \mathbf{R}_t(t) = \mathbf{U}_t(t) = \mathbf{V}_t(t) = \mathbf{I} \tag{1.62}$$

This is the result from that the current configuration is chosen as the reference configuration. Deformation measures such as $\mathbf{F}$, $\mathbf{U}$, and $\mathbf{V}$ are defined from the reference configuration represented by $\tilde{\mathbf{x}}$ and those such as $\mathbf{F}_t$ $\mathbf{U}_t$, and $\mathbf{V}_t$ are given from the current configuration. Carefully considering the definitions of the deformation measures, it can be understood that they represent the quantitative description of deformation relative to the reference configurations under consideration. Hence, Eq. (1.62) holds. If we denote t_R as the reference time of $\mathbf{F}$, $\mathbf{U}$, and $\mathbf{V}$, then we have

$$\mathbf{F}(t_R) = \mathbf{R}(t_R) = \mathbf{U}(t_R) = \mathbf{V}(t_R) = \mathbf{I} \tag{1.63}$$

As we did in Sect. 1.2, we can define the various strain measures such as

$$\mathbf{B}_t(\tau) = \mathbf{F}_t(\tau) \cdot \mathbf{F}_t^T(\tau) \tag{1.64a}$$

and

$$\mathbf{C}_t(\tau) = \mathbf{F}_t^T(\tau) \cdot \mathbf{F}_t(\tau) \tag{1.64b}$$

The *relative Finger deformation tensor* is defined as $\mathbf{C}_t^{-1}(\tau)$, and the *relative Piola deformation tensor* is defined as $\mathbf{B}_t^{-1}(\tau)$.

1.5.3 Velocity Gradient Revisited

The velocity of a material particle is the time derivative of $\hat{\mathbf{x}}(\mathbf{x}, \tau)$ at fixed $\mathbf{x}$ and can be denoted by $\hat{\mathbf{v}}(\mathbf{x}, \tau)$. Then, the velocity at present is $\mathbf{v}(\mathbf{x}, t) = \hat{\mathbf{v}}(\mathbf{x}, t)$. The velocity gradient at time of τ is given by $\mathbf{L}(\mathbf{x}, \tau) = (\nabla \hat{\mathbf{v}})^T$. Replacement of τ by t gives the velocity gradient at present time. The time derivative of relative deformation gradient is given by

$$\frac{\partial}{\partial \tau}\mathbf{F}_t(\tau) = \frac{\partial}{\partial \tau}\frac{\partial \hat{x}_i}{\partial x_k}\mathbf{e}_i\mathbf{e}_k = \frac{\partial \hat{v}_i}{\partial x_k}\mathbf{e}_i\mathbf{e}_k = \mathbf{L}(\mathbf{x}, \tau) \tag{1.65}$$

Equation (1.65) implies that although $\mathbf{F}_t(t) = \mathbf{I}$, the time derivative of relative deformation gradient at present time is the velocity gradient at present time:

$$\left.\frac{\partial}{\partial \tau}\mathbf{F}_t(\tau)\right|_{\tau=t} = \mathbf{L}(\mathbf{x}, t) \tag{1.66}$$

Application of the polar decomposition of Eq. (1.61) gives

$$\mathbf{L}(\mathbf{x}, t) = \left[\mathbf{R}_t(\tau) \cdot \frac{\partial \mathbf{U}_t(\tau)}{\partial \tau} + \frac{\partial \mathbf{R}_t(\tau)}{\partial \tau} \cdot \mathbf{U}_t(\tau)\right]_{t=\tau} = \dot{\mathbf{U}}_t(t) + \dot{\mathbf{R}}_t(t) \tag{1.67}$$

where Eq. (1.62) is used. It is noteworthy that the time derivatives of $\mathbf{F}_t(\tau)$, $\mathbf{U}_t(\tau)$, $\mathbf{V}_t(\tau)$, and $\mathbf{R}_t(\tau)$ at $\tau = t$ may not be the identity tensor even though Eq. (1.62) is valid. Since $\mathbf{R}_t(\tau)$ is an orthogonal tensor, its time derivative with respect to τ must be skew-symmetric [see Problem 1 (Huang 1963)]. Compared with Eqs. (1.53) and (1.54), we have

$$\mathbf{D} = \dot{\mathbf{U}}_t(t) = \left.\frac{\partial \mathbf{U}_t}{\partial \tau}\right|_{\tau=t} = \frac{\mathrm{d}\mathbf{V}}{\mathrm{d}t} \tag{1.68}$$

and

$$\mathbf{W} = \dot{\mathbf{R}}_t(t) = \left.\frac{\partial \mathbf{R}_t}{\partial \tau}\right|_{\tau=t} = \mathbf{V} \cdot \left(\frac{\mathrm{d}\mathbf{R}}{\mathrm{d}t} \cdot \mathbf{R}^T\right) \cdot \mathbf{V}^{-1} \tag{1.69}$$

This confirms again that the deformation rate tensor is the rate of pure deformation and the spin tensor is the rate of rotation.

1.5.4 Rivlin–Ericksen Tensor

Strain measure $\mathbf{C}_t$ defined in Eq. (1.64b) is a function of past time τ. One may want to estimate $\mathbf{C}_t$ in terms of the deformation quantities at present time. It can be done by the Taylor expansion such as

$$\mathbf{C}_t(\mathbf{x},\tau) = \mathbf{C}_t(\mathbf{x},t) + \sum_{n=1}^{\infty} \frac{1}{n!} \left(\frac{\partial^n \mathbf{C}_t}{\partial \tau^n} \right)_{\tau=t} (\tau - t)^n \tag{1.70}$$

The *Rivlin–Ericksen tensors* are defined as

$$\mathbf{A}_n(\mathbf{x},t) \equiv \left(\frac{\partial^n \mathbf{C}_t}{\partial \tau^n} \right)_{\tau=t} \tag{1.71}$$

The use of Eqs. (1.63) and (1.71) gives

$$\mathbf{C}_t(\mathbf{x},\tau) = \mathbf{I} + (\tau - t)\mathbf{A}_1 + \frac{(\tau - t)^2}{2}\mathbf{A}_2 + \cdots \tag{1.72}$$

From the definition of $\mathbf{C}_t$, it is clear that

$$\left(\mathrm{d}\hat{l}\right)^2 \equiv \mathrm{d}\hat{\mathbf{x}} \cdot \mathrm{d}\hat{\mathbf{x}} = \mathrm{d}\mathbf{x} \cdot \mathbf{C}_t \cdot \mathrm{d}\mathbf{x} \tag{1.73}$$

Differentiation of Eq. (1.73) with respect to τ at a fixed $\mathbf{x}$ gives

$$\frac{\partial^n}{\partial \tau^n} \left(\mathrm{d}\hat{l}\right)^2 = \mathrm{d}\mathbf{x} \cdot \frac{\partial^n \mathbf{C}_t}{\partial \tau^n} \cdot \mathrm{d}\mathbf{x} \tag{1.74}$$

Substitution of $\tau = t$ gives

$$\left[\frac{\partial^n}{\partial \tau^n} \left(\mathrm{d}\hat{l}\right)^2 \right]_{\tau=t} = \frac{\mathrm{d}^n}{\mathrm{d}t^n} (\mathrm{d}l)^2 = \mathrm{d}\mathbf{x} \cdot \mathbf{A}_n \cdot \mathrm{d}\mathbf{x} \tag{1.75}$$

where

$$\left(\mathrm{d}\hat{l}\right)^2_{\tau=t} = (\mathrm{d}l)^2 = \mathrm{d}\mathbf{x} \cdot \mathrm{d}\mathbf{x} \tag{1.76}$$

is used. Note that Eqs. (1.48) and (1.49) give

$$\frac{\mathrm{d}}{\mathrm{d}t}\mathrm{d}\mathbf{x} = \mathrm{d}\mathbf{v} = \mathbf{L}\cdot\mathrm{d}\mathbf{x} \tag{1.77}$$

Finally, we have

$$\begin{aligned}\frac{\mathrm{d}^{n+1}}{\mathrm{d}t^{n+1}}\mathrm{d}\mathbf{x}\cdot\mathrm{d}\mathbf{x} &= \mathrm{d}\mathbf{x}\cdot\mathbf{A}_{n+1}\cdot\mathrm{d}\mathbf{x} = \frac{\mathrm{d}}{\mathrm{d}t}\mathrm{d}\mathbf{x}\cdot\mathbf{A}_n\cdot\mathrm{d}\mathbf{x}\\ &= \mathrm{d}\mathbf{x}\cdot\left(\mathbf{L}^T\cdot\mathbf{A}_n + \frac{\mathrm{d}\mathbf{A}_n}{\mathrm{d}t} + \mathbf{A}_n\cdot\mathbf{L}\right)\cdot\mathrm{d}\mathbf{x}\end{aligned} \tag{1.78}$$

Comparison of Eq. (1.75) with Eq. (1.78) yields

$$\mathbf{A}_{n+1} = \frac{\mathrm{d}\mathbf{A}_n}{\mathrm{d}t} + \mathbf{L}^T\cdot\mathbf{A}_n + \mathbf{A}_n\cdot\mathbf{L} \tag{1.79}$$

Equation (1.79) holds when n is any positive integers. For $n = 1$, we have

$$\frac{\mathrm{d}}{\mathrm{d}t}\mathrm{d}\mathbf{x}\cdot\mathrm{d}\mathbf{x} = \mathrm{d}\mathbf{x}\cdot\left(\mathbf{L}+\mathbf{L}^T\right)\cdot\mathrm{d}\mathbf{x} = \mathrm{d}\mathbf{x}\cdot\mathbf{A}_1\cdot\mathrm{d}\mathbf{x} \tag{1.80}$$

Hence, we know that

$$\mathbf{A}_1 = 2\mathbf{D} \tag{1.81}$$

If $\mathbf{A}_n$ is symmetric, then $\mathbf{A}_{n+1}$ is also symmetric. It can be proved easily by the use of Eq. (1.79). Since $\mathbf{A}_1$ is symmetric, mathematical induction gives all the Rivlin–Ericksen tensors are symmetric.

Problem 1

[1] Simple shear is a motion defined by

$$\mathbf{x} = \tilde{\mathbf{x}} + \gamma(t)(\tilde{\mathbf{x}}\cdot\mathbf{n})\mathbf{m} \tag{1.a}$$

where γ is called shear strain, $\mathbf{m}$ and $\mathbf{n}$ are constant unit vectors, and $\mathbf{m}\cdot\mathbf{n} = 0$. Let $\mathbf{k} = \mathbf{m}\times\mathbf{n}$. Then, $\mathbf{m}$, $\mathbf{n}$, and $\mathbf{k}$ form an orthonormal basis. Calculate $\mathbf{F}$, $\mathbf{B}$, $\mathbf{C}$, $\mathbf{U}$, $\mathbf{V}$, $\mathbf{R}$, $\mathbf{L}$, $\mathbf{D}$, and $\mathbf{W}$.

[2] Prove that $\mathrm{tr}(\mathbf{E}) \approx \left(\mathrm{d}V - \mathrm{d}\widetilde{V}\right)/\mathrm{d}\widetilde{V}$ for infinitesimal deformation.

[3] Show that $I_{\mathbf{B}} = I_{\mathbf{C}}$, $II_{\mathbf{B}} = II_{\mathbf{C}}$, and $III_{\mathbf{B}} = III_{\mathbf{C}}$.

[4] Prove that

$$(I_{\mathbf{U}})^2 = I_{\mathbf{C}} + 2II_{\mathbf{U}};\quad (II_{\mathbf{U}})^2 = II_{\mathbf{C}} + I_{\mathbf{U}}\sqrt{III_{\mathbf{U}}};\quad (III_{\mathbf{U}})^2 = III_{\mathbf{C}} \tag{1.b}$$

[5] Consider the unit vector $\mathbf{n}$ which is in the direction of the rotation axis. Then, it is not difficult to find a unit vector $\mathbf{m}$ which is perpendicular to $\mathbf{n}$. From the two unit vectors, define $\mathbf{k} = \mathbf{m} \times \mathbf{n}$. It is clear that the three unit vectors form an orthonormal basis. Then, show that the following tensor is an orthogonal tensor.

$$\mathbf{Q} = \mathbf{nn} + \cos\theta(\mathbf{mm} + \mathbf{kk}) + \sin\theta(\mathbf{km} - \mathbf{mk}) \tag{1.c}$$

[6] Show that $\dot{\mathbf{R}} \cdot \mathbf{R}^T$ is skew-symmetric. Use $\mathbf{R} \cdot \mathbf{R}^T = \mathbf{I}$.

[7] Consider the velocity field given as $\mathbf{v} = r\omega(z)\mathbf{e}_z$ where cylindrical coordinate system is assumed and find deformation rate tensor $\mathbf{D}$.

[8] Prove that

$$\frac{\mathrm{d}}{\mathrm{d}t}\mathrm{d}V = (\nabla \cdot \mathbf{v})\mathrm{d}\widetilde{V} \tag{1.d}$$

[9] Consider the case that the reference configuration uses generalized basis $\{\tilde{\mathbf{g}}^k\}$ and the current configuration uses generalized basis $\{\mathbf{g}_k\}$. Then, show that deformation gradient is given by

$$\mathbf{F} = \frac{\partial \xi^i}{\partial \tilde{\xi}^k}\mathbf{g}_i\tilde{\mathbf{g}}^k \tag{1.e}$$

[10] Prove that

$$\frac{\mathrm{d}\mathbf{F}^{-1}}{\mathrm{d}t} = -\mathbf{F}^{-1} \cdot \mathbf{L} \tag{1.f}$$

[11] Prove Eq. (1.47).

[12] Show that time derivative of any orthogonal tensor is skew-symmetric.

[13] Show that the Rivlin–Ericksen tensors are symmetric.

[14] Show that

$$\mathbf{F}_t(\tau) = \mathbf{F}(\tilde{\mathbf{x}}, \tau) \cdot \mathbf{F}^{-1}(\tilde{\mathbf{x}}, t) \tag{1.g}$$

[15] Derive

$$\frac{\mathrm{d}}{\mathrm{d}t}\mathbf{F}_t(\tau) = -\mathbf{F}_t(\tau) \cdot \mathbf{L}(t) \tag{1.h}$$

[16] Derive

$$\frac{\mathrm{d}}{\mathrm{d}t}\mathbf{C}_t(\tau) + \mathbf{L}^T(t) \cdot \mathbf{C}_t(\tau) + \mathbf{C}_t(\tau) \cdot \mathbf{L}(t) = \mathbf{0} \tag{1.i}$$

[17] Derive

$$\frac{\mathrm{d}}{\mathrm{d}t}\mathbf{C}_t^{-1}(\tau) - \mathbf{L}(t)\cdot\mathbf{C}_t^{-1}(\tau) - \mathbf{C}_t^{-1}(\tau)\cdot\mathbf{L}^T(t) = \mathbf{0} \tag{1.j}$$

2 Balance Equations

We shall deal with four balance equations of mass, linear momentum, angular momentum, and energy for single-component materials. As for multicomponent versions, refer to De Groot (1984). Entropy balance equation will be discussed in Sect. 4.

2.1 Mass Balance

It is the basic assumption of continuum theory that there exists a scalar field called mass density such that

$$M = \iiint_{\widetilde{\Omega}} \tilde{\rho}(\tilde{\mathbf{x}}, t)\mathrm{d}\widetilde{V} \tag{2.1}$$

where M is the total mass of material particles in the region of $\widetilde{\Omega}$. Note that $\widetilde{\Omega}$ is the region in the reference configuration. Since all material particles in $\widetilde{\Omega}$ move to the region Ω at time t, mass conservation law implies

$$M = \iiint_{\Omega} \rho(\mathbf{x}, t)\mathrm{d}V \tag{2.2}$$

No mass change during any motion gives

$$\frac{\mathrm{d}M}{\mathrm{d}t} = \frac{\mathrm{d}}{\mathrm{d}t}\iiint_{\Omega} \rho(\mathbf{x}, t)\mathrm{d}V = \iiint_{\Omega}\left(\frac{\mathrm{d}\rho}{\mathrm{d}t}\mathrm{d}V + \rho\frac{\mathrm{d}}{\mathrm{d}t}\mathrm{d}V\right) = 0 \tag{2.3}$$

Application of Eq. (1.d) of Problem 1 gives

$$\iiint_{\Omega}\left[\frac{\mathrm{d}\rho}{\mathrm{d}t} + (\nabla\cdot\mathbf{v})\rho\right]\mathrm{d}V = 0 \tag{2.4}$$

Since Eqs. (2.1) and (2.2) hold for arbitrary subset of the reference configuration, it is clear that

$$\frac{\mathrm{d}\rho}{\mathrm{d}t} + (\nabla \cdot \mathbf{v})\rho = 0 \tag{2.5}$$

Application of Eq. (1.9), the definition of material time derivative, gives

$$\frac{\partial \rho}{\partial t} = -\nabla \cdot (\rho \mathbf{v}) \tag{2.6}$$

Equations (2.5) and (2.6) are called continuity equation or mass balance equation.

When volume does not vary during motion, the motion is called incompressible. Incompressible condition is equivalent to constant density field. Compared with gas, compression of liquid requires huge pressure. Hence, incompressible condition is a good approximation for flow of liquid. Rubbery material is observed as incompressible material because its change in shape is easier than the volumetric change for moderate loading. Then, application of constant density to Eq. (2.5) or (2.6) gives

$$\nabla \cdot \mathbf{v} = 0 \tag{2.7}$$

Similar approximation can be used for liquid fluids. If flow field is given by $\mathbf{v} = v(x, y, t)\mathbf{e}_3$, Eq. (2.7) holds. Hence, it can be said that incompressible condition can be considered as a material property for certain materials. It is noteworthy that certain special deformation of compressible material may not change volume.

The most important feature of mass balance equation is that it holds for every material. This feature holds for the balance equation to be introduced later. Hence, these balance equations are called governing equations, too.

2.1.1 Reynolds Transport Theorem

Consider $\boldsymbol{\phi}(\mathbf{x}, t)$ is a tensorial quantity of any order. Then, the corresponding quantity for the region Ω can be given by

$$\boldsymbol{\Phi}(\mathbf{x}, t) = \iiint_{\Omega} \rho(\mathbf{x}, t)\boldsymbol{\phi}(\mathbf{x}, t)\mathrm{d}V \tag{2.8}$$

Then, the material time derivative of $\boldsymbol{\Phi}(\mathbf{x}, t)$ is given by

$$\begin{aligned}\frac{\mathrm{d}}{\mathrm{d}t}\boldsymbol{\Phi}(\mathbf{x}, t) &= \frac{\mathrm{d}}{\mathrm{d}t}\iiint_{\Omega} \rho(\mathbf{x}, t)\boldsymbol{\phi}(\mathbf{x}, t)\mathrm{d}V = \iiint_{\Omega} \left[\frac{\mathrm{d}\rho}{\mathrm{d}t}\boldsymbol{\phi}\,\mathrm{d}V + \rho\frac{\mathrm{d}\boldsymbol{\phi}}{\mathrm{d}t}\mathrm{d}V + \rho\boldsymbol{\phi}\frac{\mathrm{d}}{\mathrm{d}t}\mathrm{d}V\right] \\ &= \iiint_{\Omega} \left\{\rho\frac{\mathrm{d}\boldsymbol{\phi}}{\mathrm{d}t} + \left[\frac{\mathrm{d}\rho}{\mathrm{d}t} + (\nabla \cdot \mathbf{v})\rho\right]\boldsymbol{\phi}\right\}\mathrm{d}V\end{aligned} \tag{2.9}$$

Here, Eq. (1.d) was used. Application of the mass balance equation, Eq. (2.5), gives

$$\frac{\mathrm{d}}{\mathrm{d}t}\iiint_{\Omega}\rho\,\phi\,\mathrm{d}V=\iiint_{\Omega}\rho\frac{\mathrm{d}\phi}{\mathrm{d}t}\mathrm{d}V \tag{2.10}$$

This identity is called the *Reynolds transport theorem*. This theorem is very important because it will be used when we derive various balance equations.

2.2 Momentum Balance

2.2.1 Linear Momentum Balance

There are two kinds of forces exerted on a material body: *contact force* and *body force*. The action of contact force is carried through the contact surface, while that of body force is carried at a distance. The representative body forces are gravitational and electrostatic forces.

Newton's second law implies that the total force exerted on a body is the time rate of the total linear momentum of the body. This holds for any part of the whole body. The mathematical expression of the second law of Newtonian mechanics is given by

$$\frac{\mathrm{d}}{\mathrm{d}t}\iiint_{\Omega}\rho\mathbf{v}\,\mathrm{d}V=\iint_{\partial\Omega}\mathbf{t}\,\mathrm{d}a+\iiint_{\Omega}\rho\mathbf{b}\,\mathrm{d}V \tag{2.11}$$

where $\mathbf{t}$ is the contact force per unit area, called *stress vector*, and $\mathbf{b}$ is the body force per unit mass. The left side can be expanded as follows:

$$\frac{\mathrm{d}}{\mathrm{d}t}\iiint_{\Omega}\rho\mathbf{v}\,\mathrm{d}V=\iiint_{\Omega}\rho\frac{\mathrm{d}\mathbf{v}}{\mathrm{d}t}\mathrm{d}V \tag{2.12}$$

Here, we used the Reynolds transport theorem.

Cauchy proved that there exists a second-order tensor called *stress* such that

$$\mathbf{t}=\mathbf{T}\cdot\mathbf{n} \tag{2.13}$$

where $\mathbf{n}$ is the unit vector normal to the surface element $\mathrm{d}a$. Then, the surface integral of Eq. (2.11) becomes

$$\iint_{\partial\Omega}\mathbf{t}\,\mathrm{d}a=\iint_{\partial\Omega}\mathbf{T}\cdot\mathbf{n}\mathrm{d}a=\iint_{\partial\Omega}\mathbf{T}\cdot\mathrm{d}\mathbf{a}=\iiint_{\Omega}\mathrm{div}\,\mathbf{T}\,\mathrm{d}V \tag{2.14}$$

Substitution of Eqs. (2.12) and (2.14) into Eq. (2.11) yields

$$\iiint_{\Omega} \left[\rho \frac{\mathrm{d}\mathbf{v}}{\mathrm{d}t} - \operatorname{div} \mathbf{T} - \rho \mathbf{b} \right] \mathrm{d}V = \mathbf{0} \tag{2.15}$$

Since this must be valid for any region Ω, the integrand of Eq. (2.15) must be the zero vector:

$$\rho \frac{\mathrm{d}\mathbf{v}}{\mathrm{d}t} = \operatorname{div} \mathbf{T} + \rho \mathbf{b}, \tag{2.16}$$

which is the local form (or differential form) of linear momentum balance. This equation is also valid for any materials.

The two governing equations are actually four scalar equations because the continuity equation is a scalar equation, while the linear momentum balance equation is a vector equation. However, these equations contain thirteen unknown fields: one for mass density field; three for velocity vector field; and nine for stress tensor field. Only four equations cannot determine the thirteen unknown fields uniquely. Hence, we need nine more equations. The nine equations correspond to *constitutive equation* which relates stress tensor to deformation. The constitutive equation is a tensor equation and will be discussed in Sect. 3. Different from governing equations, the constitutive equation represents material properties.

2.2.2 Stress Tensor

To understand what stress is, we consider a body of materials as a collection of molecules. If forces exerting on the body do not give rise to any deformation, then the body moves as a rigid body. Assume that a tiny probe is installed in the body and it can detect any variation of the force field around the point where the probe is installed. The probe averages out the variation whose wavelength is shorter than the size of material particle hypothesized in continuum theory and also does the variation whose frequency is higher than the inverse of the minimum characteristic time concerned in continuum theory. Then, it can be said that the tiny probe can detect the variation of the force field in the scale of continuum theory. Let us call the force field in the scale of continuum theory the macroscopic force field. On the other hand, microscopic force field is the object to be averaged by the probe.

The microscopic force field varies due to the changes in intermolecular potential and momentum rates of molecules. These changes must be deeply related to the changes in relative positions of molecules, which is deformation in terminology of continuum theory. Thus, stress cannot be generated without any deformation.

Consider a small volume Ω in a deformed body and divide the volume into two parts: A and B. The volume Ω is enveloped by the surface $\partial\Omega$. The surface $\partial\Omega$ is the union of $\partial\Omega_A$ and $\partial\Omega_B$ which belong to A and B, respectively. Suppose that the two subsets A and B are distinguished by the flat plane $\partial\Omega_{AB}$ between the subsets. Suppose that a macroscopic force field is distributed on $\partial\Omega$. Then, force exerted on $\partial\Omega_A$ results in the force exerted on $\partial\Omega_{AB}$ of B. Let the force on $\partial\Omega_{AB}$ of B be denoted by $\delta\mathbf{f}_{AB}$. The force on $\partial\Omega_B$ generates the force $\delta\mathbf{f}_{BA}$ on $\partial\Omega_{AB}$ of A. The action–reaction law implies that $\delta\mathbf{f}_{AB} = -\delta\mathbf{f}_{BA}$. It is assumed that there exists the limit such that

$$\mathbf{t}(\mathbf{x}, t, \mathbf{n}) = \lim_{\delta a \to 0} \frac{\delta \mathbf{f}_{AB}}{\delta a} \tag{2.17a}$$

where $\mathbf{x}$ is the center of $\partial\Omega_{AB}$, δa is the area of $\partial\Omega_{AB}$, and $\mathbf{n}$ is the unit normal vector of $\partial\Omega_{AB}$, whose direction is outward from B. Similarly, we have

$$\mathbf{t}(\mathbf{x}, t, -\mathbf{n}) = \lim_{\delta a \to 0} \frac{\delta \mathbf{f}_{BA}}{\delta a} \tag{2.17b}$$

The action–reaction law gives

$$\mathbf{t}(\mathbf{x}, t, -\mathbf{n}) = -\mathbf{t}(\mathbf{x}, t, \mathbf{n}) \tag{2.18}$$

The force field $\mathbf{t}(\mathbf{x}, t, \mathbf{n})$ is called *stress vector*.

Cauchy proved that

$$\mathbf{t}(\mathbf{x}, t, \mathbf{n}) = \mathbf{T}(\mathbf{x}, t) \cdot \mathbf{n} \tag{2.19}$$

by the use of the tiny tetrahedron as shown in Fig. 1.

The tetrahedron shown in Fig. 1 has four flat planes whose normal vectors are $-\mathbf{e}_1$, $-\mathbf{e}_2$, $-\mathbf{e}_3$, and $\mathbf{n}$. We can choose $\mathbf{n}$ freely. The plane of $-\mathbf{e}_1$ is the projection of the plane of $\mathbf{n}$ on the x_2x_3 plane. Hence, if the area of the plane of $\mathbf{n}$ is Δa, then the

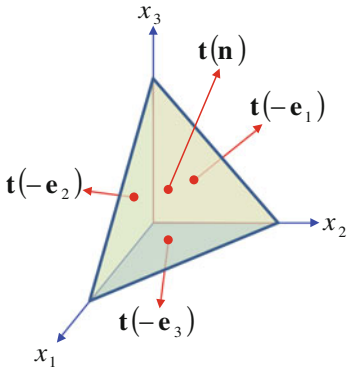

Fig. 1 Cauchy's tetrahedron

area Δa_1 of the plane of $-\mathbf{e}_1$ is given by $(\mathbf{n}\cdot\mathbf{e}_1)\Delta a$. Similarly, the area Δa_k of the plane of $-\mathbf{e}_k$ is given by $(\mathbf{n}\cdot\mathbf{e}_k)\Delta a$. The volume of the tetrahedron can be calculated by $\Delta V = \frac{1}{3}h\Delta a$ where h is the height of the tetrahedron from the plane of $\mathbf{n}$. Then, the force balance for the tetrahedron is given by

$$\rho\Delta V\frac{\mathrm{d}\mathbf{v}}{\mathrm{d}t} = \mathbf{t}(\mathbf{n}) + \sum_{k=1}^{3}\mathbf{t}(-\mathbf{e}_k)\Delta a(\mathbf{n}\cdot\mathbf{e}_k) + \rho\mathbf{g}\Delta V \tag{2.20}$$

If taking $\Delta V \to 0$ which means $\Delta a \to 0$ and $h \to 0$, we have

$$\mathbf{t}(\mathbf{n}) + \sum_{k=1}^{3}\mathbf{t}(-\mathbf{e}_k)(\mathbf{n}\cdot\mathbf{e}_k) = \mathbf{0} \tag{2.21}$$

Using Eq. (2.18), we have

$$\mathbf{t}(\mathbf{n}) = \mathbf{t}(\mathbf{e}_k)(\mathbf{e}_k\cdot\mathbf{n}) \tag{2.22}$$

where summation convention was used as before. Since $\mathbf{t}(\mathbf{e}_k)$ is a vector, we can write

$$\mathbf{t}(\mathbf{e}_k) = T_{ik}\mathbf{e}_i \tag{2.23}$$

Substitution of Eq. (2.23) into Eq. (2.22) gives

$$\mathbf{t}(\mathbf{n}) = T_{ik}\mathbf{e}_i\mathbf{e}_k\cdot\mathbf{n} \tag{2.24}$$

Equation (2.13) is proven.

When a force is exerted on small area, the effect of the force on the body is larger than that of the same force exerted on larger area. Even though force vector and area are fixed, the effect of the force can be different depending on the orientation of the surface. Thus, the effect of force exerted on a body differs depending on both the area and orientation of the contact surface. Hence, we can consider a piece of surface as a vector when we consider the effect of force on a body. We want the effect of force to be represented by the force normalized by oriented area (area vector). Although a vector cannot be divided by another vector, we can use

$$\mathbf{f} = \mathbf{T}\cdot\mathbf{a} \tag{2.25}$$

where $\mathbf{f}$ is the force vector, $\mathbf{a}$ is the area vector, and the second-order tensor $\mathbf{T}$ is the normalized effect of the force. Hence, stress has the dimension of force per unit area. When dividing both sides of Eq. (2.25) by the area $a = \|\mathbf{a}\|$ and taking $a \to 0$, Eq. (2.13) is recovered.

2.2.3 Angular Momentum Balance

When linear momentum and position of a particle are given, respectively, as $\mathbf{p}$ and $\mathbf{x}$, the angular momentum of the particle is given by $\mathbf{l} = \mathbf{x} \times \mathbf{p}$. The torque of the particle is the time rate of angular momentum. Then, we have

$$\frac{\mathrm{d}\mathbf{l}}{\mathrm{d}t} = \frac{\mathrm{d}}{\mathrm{d}t}(\mathbf{x} \times \mathbf{p}) = \mathbf{x} \times \mathbf{f} \tag{2.26}$$

Note that the time rate of angular momentum is equal to the moment of force.

Consider a body denoted by Ω. The total angular momentum is given by

$$\mathbf{L} = \iiint_{\Omega} \mathbf{x} \times \rho \mathbf{v} \, \mathrm{d}V \tag{2.27}$$

Continuum version of the moment of force is given by

$$\mathbf{M} = \iint_{\partial\Omega} \mathbf{x} \times \mathbf{t} \, \mathrm{d}a + \iiint_{\Omega} \mathbf{x} \times \rho \mathbf{b} \, \mathrm{d}V \tag{2.28}$$

Then, we have the continuum version of Eq. (2.26):

$$\frac{\mathrm{d}\mathbf{L}}{\mathrm{d}t} = \iiint_{\Omega} \mathbf{x} \times \rho \frac{\mathrm{d}\mathbf{v}}{\mathrm{d}t} \mathrm{d}V = \mathbf{M} \tag{2.29}$$

Note that $\mathrm{d}\mathbf{x}/\mathrm{d}t = \mathbf{v}$ and $\mathbf{v} \times \mathbf{v} = \mathbf{0}$. Equation (2.27) can be derived by the use of the Reynolds transport theorem.

In Sect. 5, we have learned that a vector product can be replaced by the corresponding skew-symmetric tensor [see Eqs. (5.27) and (5.28) in Chap. 1]. Then, we have

$$\mathbf{x} \times \mathbf{t} = \mathbf{G} \cdot \mathbf{t} = \mathbf{G} \cdot \mathbf{T} \cdot \mathbf{n} \tag{2.30}$$

Note that Eq. (2.13) is used and the skew-symmetric tensor $\mathbf{G}$ is given by

$$\mathbf{G} = G_{ik} \mathbf{e}_i \mathbf{e}_k = -\varepsilon_{ikp} x_p \mathbf{e}_i \mathbf{e}_k \tag{2.31}$$

Then, the divergence theorem gives

$$\begin{aligned} \iint_{\partial\Omega} \mathbf{x} \times \mathbf{t} \, \mathrm{d}S &= \iiint_{\Omega} \mathrm{div}(\mathbf{G} \cdot \mathbf{T}) \mathrm{d}V = \iiint_{\Omega} \nabla \cdot \left(\mathbf{T}^T \cdot \mathbf{G}^T\right) \mathrm{d}V \\ &= \iiint_{\Omega} \left[\mathbf{G} \cdot \left(\nabla \cdot \mathbf{T}^T\right) + \frac{\partial G_{ik}}{\partial x_j} T_{kj} \mathbf{e}_i \right] \mathrm{d}V \end{aligned} \tag{2.32}$$

Note that

$$\frac{\partial G_{ik}}{\partial x_j} T_{kj} = -\varepsilon_{ikp} \frac{\partial x_p}{\partial x_j} T_{kj} = -\varepsilon_{ikp} T_{kp} \tag{2.33}$$

With the help of Eqs. (2.32) and (2.33), Eq. (2.29) can be rewritten by

$$\iiint_{\Omega} \mathbf{G} \cdot \left(\rho \frac{\mathrm{d}\mathbf{v}}{\mathrm{d}t} - \nabla \cdot \mathbf{T}^T - \rho \mathbf{b} \right) \mathrm{d}V = - \iiint_{\Omega} \varepsilon_{ikp} T_{kp} \mathbf{e}_i \mathrm{d}V \tag{2.34}$$

The left side of Eq. (2.34) is zero vector because of the equation of linear momentum balance. Hence, we have

$$\varepsilon_{ikp} T_{kp} = 0 \tag{2.35}$$

Equation (2.35) is equivalent to $T_{ik} = T_{ki}$. Finally, we come to know that the symmetry of stress tensor is the consequence from angular momentum conservation.

2.2.4 Piola–Kirchhoff Stress

The stress $\mathbf{T}$ is called *Cauchy stress* or *true stress*. Cauchy stress is a linear transform from the outward normal vector $\mathbf{n}$ of the current configuration to the stress vector which is exerted on the infinitesimal surface element of the current configuration. With the help of Eq. (1.37), we have

$$\mathbf{t}\,\mathrm{d}a = \mathbf{T} \cdot \mathrm{d}\mathbf{a} = \widetilde{\mathbf{P}} \cdot \mathrm{d}\tilde{\mathbf{a}} \tag{2.36}$$

where

$$\widetilde{\mathbf{P}} \equiv \det(\mathbf{F}) \mathbf{T} \cdot \mathbf{F}^{-T} \tag{2.37}$$

The tensor $\widetilde{\mathbf{P}}$ is called *Piola–Kirchhoff stress of the 1st kind*, which is a linear transform from the infinitesimal surface element of the reference configuration to the force exerted on the infinitesimal surface element of the current configuration. Note that $\widetilde{\mathbf{P}}$ is not symmetric, while Cauchy stress $\mathbf{T}$ is symmetric. *Piola–Kirchhoff stress of the 2nd kind* is defined by

$$\widetilde{\mathbf{T}} = \mathbf{F}^{-1} \cdot \widetilde{\mathbf{P}} = \det(\mathbf{F}) \mathbf{F}^{-1} \cdot \mathbf{T} \cdot \mathbf{F}^{-T} \tag{2.38}$$

Note that $\widetilde{\mathbf{T}}^T = \widetilde{\mathbf{T}}$ from the definition.

2.3 Energy Balance: The First Law of Thermodynamics

2.3.1 Heat Transfer

There are three ways of heat transfer: conduction, convection, and radiation. Conduction occurs through mediation of materials irrespective of solid and fluid. Convection occurs by flow in fluid. On the other hand, radiation does not need any mediation of materials because it transfers energy through propagation of electromagnetic wave. Since convection is an energy transfer coupled with flow motion, we consider conduction and radiation here.

Since materials absorb and radiate electromagnetic wave, the net energy rate $\dot{Q}_{\text{rad}}$ for only radiation is given by

$$\dot{\mathrm{Q}}_{\text{rad}} = \iiint_{\Omega} \rho r \, \mathrm{d}V \tag{2.39}$$

where r is a scalar field representing the rate of the energy gain per unit mass by absorbance and radiation of electromagnetic wave.

According to Fourier, the heat flux of conduction is given in terms of temperature gradient:

$$\mathbf{q} = -\kappa \nabla T \tag{2.40}$$

where $\mathbf{q}$ is the *heat flux*, κ is the *heat conductivity*, and T is the absolute temperature. Then, net energy rate $\dot{Q}_{\text{cond}}$ for only heat conduction is given by

$$\dot{Q}_{\text{cond}} = -\iint_{\partial\Omega} \mathbf{q} \cdot \mathrm{d}\mathbf{a} \tag{2.41}$$

2.3.2 Energy Balance

When a body of continuum exchanges mechanical work and heat with its surroundings, the rate of the net energy gain of the body $\mathrm{d}E/\mathrm{d}t$ is given by

$$\frac{\mathrm{d}E}{\mathrm{d}t} = \frac{\mathrm{d}W}{\mathrm{d}t} + \frac{\mathrm{d}Q}{\mathrm{d}t} \tag{2.42}$$

where $\mathrm{d}W/\mathrm{d}t$ is the rate of mechanical work given to the body and $\mathrm{d}Q/\mathrm{d}t$ is the rate of heat gain.

The rate of mechanical work is called the mechanical power which can be calculated by

$$\frac{\mathrm{d}W}{\mathrm{d}t} = \iint_{\partial\Omega} \mathbf{t}\cdot\mathbf{v}\,\mathrm{d}a + \iiint_{\Omega} \rho\mathbf{b}\cdot\mathbf{v}\,\mathrm{d}V \tag{2.43}$$

Application of Eq. (2.13) gives

$$\frac{\mathrm{d}W}{\mathrm{d}t} = \iiint_{\Omega} \mathrm{tr}(\mathbf{L}\cdot\mathbf{T})\mathrm{d}V + \iiint_{\Omega} \mathbf{v}\cdot(\nabla\cdot\mathbf{T} + \rho\mathbf{b})\mathrm{d}V \tag{2.44}$$

Here, we used divergence theorem and symmetry of stress tensor. The use of Eq. (2.16) gives

$$\frac{\mathrm{d}W}{\mathrm{d}t} = \frac{\mathrm{d}K}{\mathrm{d}t} + \iiint_{\Omega} \mathrm{tr}(\mathbf{L}\cdot\mathbf{T})\mathrm{d}V \tag{2.45}$$

where K is the kinetic energy of the body:

$$K = \iiint_{\Omega} \frac{\rho}{2}\mathbf{v}\cdot\mathbf{v}\,\mathrm{d}V \tag{2.46}$$

Note that the Reynolds transport theorem gives

$$\frac{\mathrm{d}K}{\mathrm{d}t} = \iiint_{\Omega} \rho\mathbf{v}\cdot\frac{\mathrm{d}\mathbf{v}}{\mathrm{d}t}\mathrm{d}V \tag{2.47}$$

We define stress power as the second term in the right-hand side of Eq. (2.45). Note that

$$\mathrm{tr}(\mathbf{L}\cdot\mathbf{T}) = \mathrm{tr}(\mathbf{D}\cdot\mathbf{T}) = \mathrm{tr}(\mathbf{T}\cdot\mathbf{D}) = \mathrm{tr}(\mathbf{T}\cdot\mathbf{L}) = \mathbf{T}:\mathbf{D} \tag{2.48}$$

It is clear that the rate of heat gain $\mathrm{d}Q/\mathrm{d}t$ is the sum of $\dot{Q}_{\mathrm{cond}}$ and $\dot{Q}_{\mathrm{rad}}$. Then, we have

$$\frac{\mathrm{d}E}{\mathrm{d}t} = \frac{\mathrm{d}K}{\mathrm{d}t} + \iiint_{\Omega} \mathbf{T}:\mathbf{D}\,\mathrm{d}V - \iiint_{\Omega} \nabla\cdot\mathbf{q}\,\mathrm{d}V + \iiint_{\Omega} \rho r\,\mathrm{d}V \tag{2.49}$$

The total energy E can be considered as the sum of the kinetic energy and the energy stored in the material called *internal energy*:

$$E = U + K \tag{2.50}$$

where U is the internal energy. For the internal energy U, we can define internal energy density u such that

$$U = \iiint_{\Omega} \rho u \, \mathrm{d}V \tag{2.51}$$

Substitution of Eq. (2.50) into Eq. (2.49) and rearrangement give

$$\iiint_{\Omega} \left[\rho \frac{\mathrm{d}u}{\mathrm{d}t} + \nabla \cdot \mathbf{q} - \rho r - \mathbf{T} : \mathbf{D} \right] \mathrm{d}V = 0 \tag{2.52}$$

Since Eq. (2.52) is valid for arbitrary region of Ω, it can be concluded that

$$\rho \frac{\mathrm{d}u}{\mathrm{d}t} = -\nabla \cdot \mathbf{q} + \rho r + \mathbf{T} : \mathbf{D} \tag{2.53}$$

The term including stress, $\mathbf{T} : \mathbf{D}$, is called *stress power*. Equation (2.53) implies that the rate of internal energy is equal to the sum of the rate of net gain of heat and the stress power. The first law of equilibrium thermodynamics reads

$$\mathrm{d}u = \mathrm{d}q + \mathrm{d}w \tag{2.54}$$

where $\mathrm{d}u$ is the differential of internal energy, $\mathrm{d}q$ is the infinitesimal heat entering the system, and $\mathrm{d}w$ is the infinitesimal work done on the system. Comparison of Eq. (2.53) with Eq. (2.54) tells us that the stress power and the rate of heat gain correspond to $\mathrm{d}w$ and $\mathrm{d}q$, respectively.

As for rigid body with constant heat capacity, it is clear that

$$\mathbf{T} : \mathbf{D} = 0; \quad \mathrm{d}u = c_V \mathrm{d}T \tag{2.55}$$

where c_V is the *specific heat capacity* at constant volume. In this case, rigid body implies $c_\mathrm{V} = c_\mathrm{P}$, too. Of course, c_P is the specific heat capacity at constant pressure. Then, with the help of Eq. (2.40), Eq. (2.53) becomes

$$\frac{\partial T}{\partial t} = \frac{\kappa}{\rho c_\mathrm{P}} \nabla^2 T + \frac{r}{c_\mathrm{P}} \tag{2.56}$$

It is usual that r depends on position and time through temperature. Then, Eq. (2.56) is a nonlinear equation of temperature because r is proportional to T^4 (the Stefan–Boltzmann law). At a moderate temperature, it is a good approximation the term involving r is negligible compared with other terms in Eq. (2.56). Then, we obtain a diffusion equation of temperature such that

$$\frac{\partial T}{\partial t} = \frac{\kappa}{\rho c_\mathrm{P}} \nabla^2 T \tag{2.57}$$

As for deformable body, we need the second law and suitable constitutive equation for internal energy to derive temperature equation similar to Eqs. (2.56) and (2.57). This will be discussed when we study irreversible thermodynamics.

2.4 Balance Equations in Terms of Flux

We have derived several balance equations on the basis of the motion of material particles. The same equations can be derived from another basis called flux (Deen 1998; Bird 2002; De Groot 1984). Although the use of flux in the derivation of balance equation is easily understood and is made of direct parlance to physical meaning, physical quantities may need their ways to finding the corresponding fluxes. Furthermore, it is additionally necessary to consider source term. However, the use of flux provides a unified way to balance equations of various physical quantities. Therefore, we give general forms of balance equation in terms of flux and then interpret the balance equations derived before from the viewpoint of flux.

Consider a physical quantity, say Φ which is defined by

$$\Phi = \iiint_{\widehat{\Omega}} \rho\phi \, \mathrm{d}\widehat{V} \tag{2.58}$$

where $\widehat{\Omega}$ represents an arbitrary region fixed in space, ϕ is the field such that $\rho\phi$ is the density of Φ, ρ is the mass density, and $\mathrm{d}\widehat{V}$ is the infinitesimal volume element of $\widehat{\Omega}$. Thus, $\mathrm{d}\widehat{V}$ is independent of time. Hence, the rate of Φ is given by

$$\frac{\mathrm{d}\Phi}{\mathrm{d}t} = \iiint_{\widehat{\Omega}} \left(\frac{\partial}{\partial t} \rho\phi \right) \mathrm{d}\widehat{V} \tag{2.59}$$

Introduction of flux and source gives

$$\frac{\mathrm{d}\Phi}{\mathrm{d}t} = -\iint_{\partial\widehat{\Omega}} \mathbf{J}_\phi \cdot \widehat{\mathbf{n}} \mathrm{d}\widehat{S} + \iiint_{\widehat{\Omega}} \Pi_\phi \mathrm{d}\widehat{V}; \quad \frac{\partial \rho\phi}{\partial t} = -\mathrm{div}\mathbf{J}_\phi + \Pi_\phi \tag{2.60}$$

where $\mathbf{J}_\phi$ is the flux of the physical quantity Φ (or ϕ) and Π_ϕ is the source term. The minus sign of surface integral is originated from the convention that unit normal vector $\widehat{\mathbf{n}}$ of surface element is given by the outward normal vector. Equation (2.60) is the general form of balance equations.

Equation (2.4), the balance equation of mass, can be obtained when $\phi = 1$ and the flux and the source are identified by

$$\mathbf{J}_\rho = \rho\mathbf{v}; \quad \Pi_\rho = 0 \tag{2.61}$$

Since mass is conserved, it is obvious that the source term of mass is zero. When linear momentum balance is considered, we know that $\phi = \mathbf{v}$ and

$$\mathbf{J}_{\mathbf{v}} = \rho \mathbf{v}\mathbf{v} - \mathbf{T}; \quad \Pi_{\mathbf{v}} = \rho \mathbf{b} \tag{2.62}$$

Equation (2.50) leads us to that the energy density is given by

$$\rho\varepsilon = \rho u + \frac{1}{2}\rho \|\mathbf{v}\|^2 \tag{2.63}$$

Since energy is conserved, it is obvious that the source term of energy must be zero. Then, the flux and source term of energy are given by

$$\mathbf{J}_{\varepsilon} = \rho\varepsilon \mathbf{v} + \mathbf{q}_T - \mathbf{T} \cdot \mathbf{v}; \quad \Pi_{\varepsilon} = 0 \tag{2.64}$$

where $\mathbf{q}_T$ is the total heat flux which includes heat transfer by both conduction and radiation:

$$\nabla \cdot \mathbf{q}_T = \nabla \cdot \mathbf{q} - \rho r \tag{2.65}$$

From Eq. (2.65), thermal energy density or heat energy density ρq can be defined as

$$Q = \iiint_{\Omega} \rho q \, \mathrm{d}V \tag{2.66}$$

and

$$\rho \frac{\mathrm{d}q}{\mathrm{d}t} = -\nabla \cdot \mathbf{q}_T \tag{2.67}$$

Then, energy balance equation can be rewritten by

$$\frac{\partial \rho\varepsilon}{\partial t} + \nabla \cdot \mathbf{J}_{\varepsilon} = 0 \tag{2.68}$$

or

$$\frac{\mathrm{d}u}{\mathrm{d}t} = \frac{\mathrm{d}q}{\mathrm{d}t} - \hat{p}\frac{\mathrm{d}v}{\mathrm{d}t} + v\mathbf{T}' : \mathbf{L} \tag{2.69}$$

where v is the specific volume such that $v = \rho^{-1}$, $\hat{p} = -\frac{1}{3}\mathrm{tr}(\mathbf{T})$, and $\mathbf{T}'$ is the deviatoric stress such that $\mathbf{T} = -\hat{p}\mathbf{I} + \mathbf{T}'$.

Note that the conservative quantities such as mass and energy have no source term, whereas the nonconservative quantity such as linear momentum has nonzero source term. This viewpoint suggests that the entropy of nonequilibrium has the following formal balance equation:

$$\rho \frac{\mathrm{d}s}{\mathrm{d}t} = -\nabla \cdot \mathbf{J}_s + \Pi_s \tag{2.70}$$

The second law of thermodynamics demands the nonnegativeness of the source term of entropy: $\Pi_s \geq 0$. The essence of irreversible thermodynamics is to find the formulation of flux and source term of entropy in terms of measurable field variables. This will be discussed in Sect. 4.

It is noteworthy that the flux of momentum is a second-order tensor and the flux of mass is a vector, which implies that if a physical quantity is an nth-order tensor, then the corresponding flux is a tensorial quantity with the order of $n+1$. Meanwhile, the source term has the same order as the physical quantity.

Problem 2

[1] Derive Eq. (2.29) by use the Reynolds transport theorem.

[2] Derive

$$\rho(\mathbf{x}, t) = \frac{\tilde{\rho}(\tilde{\mathbf{x}}, t_R)}{\det(\mathbf{F})} \tag{2.a}$$

where ρ is the mass density field in the current configuration, $\tilde{\rho}$ is the mass density in the reference configuration, and t_R is the reference time.

[3] Derive the equation of motion in terms of Piola–Kirchhoff stress of the first kind.

[4] The case of $\mathbf{T} = T_{11}\mathbf{e}_1\mathbf{e}_1 + T_{22}\mathbf{e}_2\mathbf{e}_2 + T_{12}(\mathbf{e}_1\mathbf{e}_2 + \mathbf{e}_2\mathbf{e}_1)$ is called the state of plane stress. Suppose that the body is in the state of plane stress and in equilibrium: $\nabla \cdot \mathbf{T} = \mathbf{0}$. Show the existence of $\psi(x_1, x_2)$ such that

$$\frac{\partial^2 \psi}{\partial x_2^2} = T_{11}; \quad \frac{\partial^2 \psi}{\partial x_1^2} = T_{22}; \quad \frac{\partial^2 \psi}{\partial x_1 \partial x_2} = -T_{12} \tag{2.b}$$

[5] Show that

$$\mathrm{tr}(\mathbf{T} \cdot \mathbf{L}) = \mathrm{tr}\left(\mathbf{V}^{-1} \cdot \mathbf{T} \cdot \frac{\mathrm{d}\mathbf{V}}{\mathrm{d}t}\right) \tag{2.c}$$

[6] Suppose that a material satisfies

$$\frac{\mathrm{d}f(\mathbf{B})}{\mathrm{d}t} = \mathrm{tr}(\mathbf{T} \cdot \mathbf{L}) \tag{2.d}$$

Then, show that

$$\mathbf{T} = 2\mathbf{B} \cdot \frac{\partial f}{\partial \mathbf{B}} \tag{2.e}$$

[7] Derive that

$$\mathrm{tr}(\mathbf{T}\cdot\mathbf{L}) = \frac{1}{\det(\mathbf{F})}\mathrm{tr}\left(\widetilde{\mathbf{P}}\cdot\frac{\mathrm{d}\mathbf{F}}{\mathrm{d}t}\right) \tag{2.f}$$

[8] Derive Eq. (2.53) by the use of Eqs. (2.60) and (2.64).

3 Classical Constitutive Equations

From the viewpoint of rheology, materials can be classified into four groups: elastic body; viscous fluid; plastic body; and viscoelastic body. Stress of elastic body is a function of strain, which means that a current stress is uniquely determined by a strain at the present time. Viscous fluid is a body whose stress is a function of deformation rate and independent of strain. Stress of plastic material is determined by the path of deformation but independent of the deformation rate. This dependence on deformation path implies that different stresses occur when a given strain is conducted by different paths of deformation. For example, the two deformation paths such as the twist after an extension and the extension after a twist give different stresses even if the final strains are same. Since stress of plastic body is independent of the deformation rate, the same stress is obtained from two deformation histories with the same deformation path but different duration times. Stress of viscoelastic material is determined by the history of deformation. Hence, stress of viscoelastic material may depend on both the rate and the path of deformation. Different from plastic body, stress of viscoelastic body may be different for the deformation histories with the same deformation path but different duration times.

In this section, we shall introduce three kinds of classical constitutive equations: those of isotropic linear elastic body; viscous fluid; and linear viscoelastic body. These examples are helpful to understand more advanced theories of constitutive equations for polymeric materials. Some of them are practically important, and the others are conceptually important.

3.1 Elasticity

3.1.1 Constitutive Equation of Linear Elastic Body

Consider only infinitesimal deformation which means that infinitesimal strain is sufficient in describing stress. Isotropic linear elastic constitutive equation is an idealization of material. The constitutive equation is based on the assumptions such that

[1] Material properties are isotropic.
[2] Stress depends linearly only on current infinitesimal strain.

When stress is a linear function of infinitesimal strain, we can write the stress as follows:

$$T_{ik} = C_{ikmn} e_{mn} \tag{3.1}$$

where T_{ik} is the component of the stress tensor, C_{ikmn} is the component of fourth-order tensor called *modulus*, and e_{mn} is the component of infinitesimal strain.

Although fourth-order tensor has 81 components, the modulus tensor has only 21 independent components for fully anisotropic materials (Sadd 2009). However, the modulus of isotropic materials has only two independent components. Since material is isotropic, the modulus tensor must be isotropic fourth-order tensor such as

$$C_{ikmn} = \lambda \delta_{ik} \delta_{mn} + G(\delta_{im}\delta_{kn} + \delta_{in}\delta_{km}) + \beta(\delta_{im}\delta_{kn} - \delta_{in}\delta_{km}) \tag{3.2}$$

Application of Eq. (3.2) to Eq. (3.1) gives

$$T_{ik} = \lambda e_{mm} \delta_{ik} + 2G\, e_{ik} \tag{3.3}$$

Since $e_{ik} = e_{ki}$, the term involving β disappears irrespective of strain tensor. Hence, isotropic linear elastic body has only two independent modulus components.

3.1.2 Moduli of Isotropic Linear Elasticity

Problem 1 [2] provides that the trace of strain is the volumetric strain. Hydrostatic pressure $T_{ik} = p\delta_{ik}$ gives only change of volume without shape change. Taking trace on both sides of Eq. (3.3), we have

$$(3\lambda + 2G) e_{\mathrm{V}} = T_{mm} = 3p \tag{3.4}$$

where $e_V = e_{mm}$. *Bulk modulus* K is defined as the slope in the plot of p as a function of e_{V}. Then, we have

$$K = \lambda + \frac{2}{3} G \tag{3.5}$$

An example of simple shear is $\mathbf{x} = \tilde{\mathbf{x}} + \gamma x_2 \mathbf{e}_1$. As for this deformation, the volume does not change, but only the shape of material changes. The infinitesimal strain for the *simple shear* is given by

$$\mathbf{E} = \frac{\gamma}{2}(\mathbf{e}_1\mathbf{e}_2 + \mathbf{e}_2\mathbf{e}_1) \tag{3.6}$$

Application of Eq. (3.6) to Eq. (3.3) gives

$$\mathbf{T} = \tau(\mathbf{e}_1\mathbf{e}_2 + \mathbf{e}_2\mathbf{e}_1) \tag{3.7}$$

where

$$\tau = G\gamma \tag{3.8}$$

Note that γ and τ are called shear strain and *shear stress*, respectively. Hence, G is called *shear modulus* which represents the resistance to shear. Deviatoric strain $\mathbf{E}'$ is defined as

$$\mathbf{E}' = \mathbf{E} - \frac{1}{3}\mathrm{tr}(\mathbf{E})\mathbf{I} \tag{3.9}$$

Equation (3.9) immediately indicates that the deviatoric strain is traceless:

$$\mathrm{tr}(\mathbf{E}') = 0 \tag{3.10}$$

Then, Eq. (3.3) can be rewritten in terms of K and G as follows:

$$\mathbf{T} = Ke_{\mathrm{V}}\mathbf{I} + 2G\mathbf{E}' \tag{3.11}$$

The isotropic term of Eq. (3.11) corresponds to the stress due to volume change, while the term of deviatoric strain corresponds to the stress due to shape change.

One of the most convenient test methods for elastic material is *simple elongation*. If elongation axis is $\mathbf{e}_1$, then only nonzero component of stress is T_{11}. Then, we have only three nonzero components of strain:

$$e_{11} = \frac{\lambda + G}{G(3\lambda + 2G)}T_{11}; \quad e_{22} = e_{33} = -\frac{\lambda}{\lambda + G}e_{11} \tag{3.12}$$

Young's modulus is the slope in the plot of T_{11} against e_{11}. Hence, we have

$$E = \frac{G(3\lambda + 2G)}{\lambda + G} \tag{3.13}$$

Simple elongation test provides the measurement of Young's modulus as well as *Poisson's ratio* defined as

$$\nu = -\frac{e_{22}}{e_{11}} = \frac{\lambda}{2(\lambda + G)} \tag{3.14}$$

The constitutive equation can be rewritten in terms of E and ν as follows:

$$\begin{aligned} e_{11} &= \frac{T_{11} - \nu(T_{22} + T_{33})}{E}; \quad e_{22} = \frac{T_{22} - \nu(T_{33} + T_{11})}{E}; \\ e_{33} &= \frac{T_{33} - \nu(T_{11} + T_{22})}{E}; \quad e_{12} = \frac{T_{12}}{2G}; \quad e_{23} = \frac{T_{23}}{2G}; \quad e_{31} = \frac{T_{31}}{2G} \end{aligned} \tag{3.15}$$

Bulk modulus and shear modulus can be expressed in terms of Young's modulus and Poisson's ratio as follows:

$$K = \frac{E}{3(1-2\nu)}; \quad G = \frac{E}{2(1+\nu)} \tag{3.16}$$

As Poisson's ratio goes to $\frac{1}{2}$, bulk modulus goes to infinity, which means that volume cannot be changed for any deformation. However, G goes to $\frac{1}{3}E$ as ν approaches to $\frac{1}{2}$. Hence, a material with $K \gg G$ behaves as *incompressible solid*. Rubber has Poisson's ratio very close to $\frac{1}{2}$.

3.1.3 Positiveness of Moduli

Deformation gives rise to the increase of the internal energy of linear elastic body. The minimum internal energy must be achieved at $\mathbf{E} = \mathbf{0}$. Strain energy density is the difference between the internal energies per unit volume of deformed and undeformed configurations. Then, the strain energy density can be calculated by integrating the differential equation such as

$$\mathrm{d}f = \mathbf{T} : \mathrm{d}\mathbf{E} \tag{3.17}$$

This is the infinitesimal work per unit volume.

It is a reasonable assumption that higher strain gives rise to higher strain energy density. Mathematical expression of this notion is

$$f(t_1\mathbf{E}) \geq f(t_2\mathbf{E}) \tag{3.18}$$

where $\mathbf{E}$ is arbitrary and $t_1 \geq t_2$ are arbitrary positive real numbers. The strain energy density must be an even function of strain such that $f(\mathbf{E}) = f(-\mathbf{E})$. We can expand $f(t\mathbf{E})$ as follows:

$$f(t\mathbf{E}) = f(\mathbf{0}) + t\left(\frac{\partial f}{\partial \mathbf{E}}\right)_{\mathbf{E}=\mathbf{0}} : \mathbf{E} + \frac{t^2}{2}\mathbf{E} : \left(\frac{\partial^2 f}{\partial \mathbf{E}\partial \mathbf{E}}\right)_{\mathbf{E}=\mathbf{0}} : \mathbf{E} + \cdots \tag{3.19}$$

Since Eq. (3.17) implies $\mathbf{T} = \partial f/\partial \mathbf{E}$, $\mathbf{E} = \mathbf{0}$ implies $(\partial f/\partial \mathbf{E})_{\mathbf{E}=\mathbf{0}} = \mathbf{0}$. Then, the inequality of Eq. (3.18) implies that

$$f(t_1\mathbf{E}) - f(t_2\mathbf{E}) = \frac{t_1^2 - t_2^2}{2}\mathbf{E} : \mathbf{C} : \mathbf{E} \geq 0 \tag{3.20}$$

where

$$\left(\frac{\partial^2 f}{\partial \mathbf{E}\partial \mathbf{E}}\right)_{\mathbf{E}=\mathbf{0}} = \left(\frac{\partial f}{\partial e_{ik}\partial e_{mn}}\right)_{\mathbf{E}=\mathbf{0}} \mathbf{e}_i\mathbf{e}_k\mathbf{e}_m\mathbf{e}_n = C_{ikmn}\mathbf{e}_i\mathbf{e}_k\mathbf{e}_m\mathbf{e}_n = \mathbf{C} \tag{3.21}$$

Since $t_1 > t_2$, we have

$$\mathbf{E} : \mathbf{C} : \mathbf{E} = C_{ikmn}e_{ik}e_{mn} \geq 0 \tag{3.22}$$

The inequality must hold for any strain. Note that $\mathbf{E}$ is arbitrary. Hence, Eq. (3.22) implies the modulus tensor is positive definite. Equation (3.22) can be rewritten for isotropic linear elastic body as follows:

$$\mathbf{E} : \mathbf{C} : \mathbf{E} = K(e_{\mathrm{V}})^2 + 2G\mathbf{E}' : \mathbf{E}' \geq 0 \tag{3.23}$$

Note that $(e_{\mathrm{V}})^2 > 0$ and $\mathbf{E}' : \mathbf{E}' \geq 0$. Since we can render volume strain to be zero while deviatoric strain is not zero tensor, the inequality gives $G > 0$. Similarly, isotropic stress such as $\mathbf{T} = p\mathbf{I}$ gives $e_{\mathrm{V}} \neq 0$ and $\mathbf{E}' = \mathbf{0}$. Then, we have $K > 0$. Then, it is not difficult to show that $E > 0$, $\lambda > 0$, and

$$-1 < \nu < \frac{1}{2} \tag{3.24}$$

3.1.4 Navier Equation

Modulus of most practical materials is so high that their deformation is nearly independent of gravitation. Hence, neglection of body force is usually chosen. When deformed elastic body rests in equilibrium, we have the equilibrium equation such as

$$\nabla \cdot \mathbf{T} = 0 \tag{3.25}$$

When deformation is infinitesimal, $\mathbf{x} \approx \tilde{\mathbf{x}}$ holds. Then, we can use $\widetilde{\nabla} \approx \nabla$. Hence, Eq. (1.25) can be rewritten by

$$\mathbf{E} = \frac{1}{2}\left[\nabla\mathbf{u} + (\nabla\mathbf{u})^T\right] \tag{3.26}$$

Then, we can express the equilibrium equation in terms of displacement vector:

$$\nabla(\nabla \cdot \mathbf{u}) + \frac{G}{\lambda + G}\nabla^2 \mathbf{u} = \mathbf{0} \tag{3.27}$$

Equation (3.27) is *Navier equation*.

If body force is not neglected, then the Navier equation becomes

$$\nabla^2 \mathbf{u} + \frac{1}{1-2\nu}\nabla(\nabla \cdot \mathbf{u}) = -\frac{2(1+\nu)}{E}\rho \mathbf{b} \tag{3.28}$$

Here, λ and G are replaced by E and ν. A vector identity

$$\nabla(\nabla \cdot \mathbf{u}) = \nabla^2 \mathbf{u} + \nabla \times (\nabla \times \mathbf{u}) \tag{3.29}$$

gives

$$\nabla^2 \mathbf{u} + \frac{1}{2(1-\nu)}\nabla \times (\nabla \times \mathbf{u}) = -\frac{(1+\nu)(1-2\nu)}{E(1-\nu)}\rho \mathbf{b} \tag{3.30}$$

If displacement field $\mathbf{u}$ is irrotational, then Eq. (3.30) gives

$$\nabla^2 \mathbf{u} = -\frac{(1+\nu)(1-2\nu)}{E(1-\nu)}\rho \mathbf{b} \tag{3.31}$$

Equation (3.31) is three independent Poisson's equations. When body force is neglected, the Navier equation is reduced to Laplace equation.

Applications of Navier equation to several elastostatic problems are found in various texts of elasticity such as Sadd (2009) and Landau (1986).

3.1.5 Nonlinear Elasticity

Stress of elastic material is an algebraic function of strain. When deformation is infinitesimal, it is clear that the stress is a function of infinitesimal strain. However, there is no obvious reference to choose a finite strain among various finite strains in nonlinear elasticity. The *principle of material frame-indifference*, which will be explained in Sect. 5, might be helpful for this problem. However, for a while, we assume that appropriate strain measure is $\mathbf{B} = \mathbf{F} \cdot \mathbf{F}^T$. For simplicity, we consider only isotropic materials.

Since we are interested in only isotropic material, the learning from Sect. 5.3 gives

$$\mathbf{T} = G_0 \mathbf{I} + G_1 \mathbf{B} + G_2 \mathbf{B}^2 \tag{3.32}$$

where G_0, G_1 and G_2 are functions of principal invariants of $\mathbf{B}$. Cauchy elastic materials are the ones whose stress is expressed by Eq. (3.32). It is known that the work done by stress of Eq. (3.32) may depend on deformation path (Ogden 1984).

Consider the stress power shown in Eq. (2.53). We are interested in the condition that allows the stress power to be time derivative of a scalar function. Exploiting properties of trace, we have

$$\mathrm{tr}(\mathbf{T}\cdot\mathbf{L}) = \mathrm{tr}\left(\mathbf{T}\cdot\frac{\mathrm{d}\mathbf{F}}{\mathrm{d}t}\cdot\mathbf{F}^{-1}\right) = \mathrm{tr}\left(\mathbf{T}\cdot\frac{\mathrm{d}\mathbf{V}}{\mathrm{d}t}\cdot\mathbf{V}^{-1}\right) = \mathrm{tr}\left(\mathbf{V}^{-1}\cdot\mathbf{T}\cdot\frac{\mathrm{d}\mathbf{V}}{\mathrm{d}t}\right) \tag{3.33}$$

Here, Eq. (1.46) was used. Consider a scalar-valued function of $\mathbf{V}$ of Eq. (1.15) such that

$$\mathbf{T} = \mathbf{V}\cdot\frac{\partial\Phi}{\partial\mathbf{V}} \tag{3.34}$$

Since $\mathbf{V}$ is symmetric tensor, substitution of Eq. (3.34) into Eq. (3.33) yields

$$\mathrm{tr}(\mathbf{T}\cdot\mathbf{L}) = \frac{\partial\Phi}{\partial\mathbf{V}}:\frac{\mathrm{d}\mathbf{V}}{\mathrm{d}t} = \frac{\mathrm{d}\Phi}{\mathrm{d}t} \tag{3.35}$$

Thus, Eq. (3.34) is the condition that the stress power must be material time derivative of a scalar-valued function of $\mathbf{V}$. If the scalar function of Eq. (3.34) is a function of $\mathbf{V}$, then it is also a function of $\mathbf{B} = \mathbf{V}^2 = \mathbf{F}\cdot\mathbf{F}^T$. Note that $\mathbf{B}$ is much more convenient than $\mathbf{V}$ because $\mathbf{B}$ does not require complicate polar decomposition. Then, Eq. (3.34) becomes

$$\mathbf{T} = 2\mathbf{B}\cdot\frac{\partial\Phi}{\partial\mathbf{B}} \tag{3.36}$$

Equations (3.34) and (3.36) are known as the constitutive equations of Green elasticity or hyperelasticity.

If material is isotropic, the scalar function Φ must be a function of principal invariants of $\mathbf{B}$. Then, Eq. (3.36) can be rewritten by

$$\mathbf{T} = 2(III_{\mathbf{B}}\Phi_3 + II_{\mathbf{B}}\Phi_2)\mathbf{I} + 2\Phi_1\mathbf{B} - 2III_{\mathbf{B}}\Phi_2\mathbf{B}^{-1} \tag{3.37}$$

where

$$\Phi_1 = \frac{\partial\Phi}{\partial I_{\mathbf{B}}};\quad \Phi_2 = \frac{\partial\Phi}{\partial II_{\mathbf{B}}};\quad \Phi_3 = \frac{\partial\Phi}{\partial III_{\mathbf{B}}} \tag{3.38}$$

If material is incompressible, then it is clear that $III_{\mathbf{B}} = 1$ and Eq. (3.37) becomes

$$\mathbf{T} = -p\mathbf{I} + 2\left(\frac{\partial \Phi}{\partial I_{\mathbf{B}}}\mathbf{B} - \frac{\partial \Phi}{\partial I_{\mathbf{B}^{-1}}}\mathbf{B}^{-1}\right) \tag{3.39}$$

Note that p cannot be determined by constitutive equation because volume is preserved. The pressure p can be determined by boundary condition. The *Cayley–Hamilton theorem* with $III_{\mathbf{B}} = 1$ gives

$$I_{\mathbf{B}} = II_{\mathbf{B}^{-1}}; \quad II_{\mathbf{B}} = I_{\mathbf{B}^{-1}} \tag{3.40}$$

Mechanical behavior of rubber can be approximated to isotropic incompressible elasticity.

3.2 Viscous Fluids

3.2.1 Constitutive Equation of Viscous Fluids

Normal fluids are isotropic. Since stress of viscous fluid is a function of deformation rate, the most general form should be

$$\mathbf{T} = \beta_o\mathbf{I} + \beta_1\mathbf{D} + \beta_2\mathbf{D}^2 \tag{3.41}$$

where β_k are functions of principal invariants of deformation rate tensor $\mathbf{D}$. The linearization of Eq. (3.41) gives the constitutive equation of *Newtonian fluid*. Although $I_{\mathbf{D}} = \mathrm{tr}(\mathbf{D}) = \nabla \cdot \mathbf{v}$ is a linear function of $\mathbf{D}$, the other principal invariants are not linear functions of $\mathbf{D}$. If $\beta_2 \neq 0$, Eq. (3.41) cannot be linearized. Then, Newtonian fluids are obtained from Eq. (3.41) whenever $\beta_2 = 0$, $\beta_2 \equiv 2\eta_s$ is a constant, and β_o is given by

$$\beta_o = -p + \eta_b(\nabla \cdot \mathbf{v}) \tag{3.42}$$

Here, pressure p is a function of mass density and temperature, which is given from the equation of state. Viscosities η_b and η_s are called, respectively, bulk and shear viscosities. Finally, the stress of Newtonian fluid is given by

$$\mathbf{T} = -p\mathbf{I} + \eta_b(\nabla \cdot \mathbf{v})\mathbf{I} + 2\eta_s\mathbf{D} \tag{3.43}$$

Note that the deviatoric stress is given by

$$\mathbf{T}' = 2\eta_s\left[\mathbf{D} - \frac{\mathrm{tr}(\mathbf{D})}{3}\mathbf{I}\right] = 2\eta_s\mathbf{D}' \tag{3.44}$$

No flow implies that stress becomes hydrostatic pressure which must be determined by the equation of the state of the fluid. Hence, p in Eq. (3.43) is the pressure of equilibrium thermodynamics. All fluid cannot sustain its shape without a container, and such isotropic term is necessary. The stress without $-p\mathbf{I}$ is called extra stress which is generated by flow. Extra stress is denoted and defined as

$$\mathbf{T}_{\mathrm{ex}} = \mathbf{T} + p\mathbf{I} = \eta_{\mathrm{b}}(\nabla \cdot \mathbf{v})\mathbf{I} + 2\eta_{\mathrm{s}}\mathbf{D} \tag{3.45}$$

Thermodynamic analysis will show that shear viscosity must be positive, while the sum of bulk viscosity and two-thirds of shear viscosity must be positive.

3.2.2 Navier–Stokes Equation

Consider only Newtonian fluids. Substitution of Eq. (3.43) into equation of motion (2.16) yields

$$\rho\left(\frac{\partial \mathbf{v}}{\partial t} + \mathbf{v} \cdot \nabla \mathbf{v}\right) = -\nabla p + (\eta_{\mathrm{b}} + \eta_{\mathrm{s}})\nabla(\nabla \cdot \mathbf{v}) + \eta_{\mathrm{s}}\nabla^2 \mathbf{v} \tag{3.46}$$

Equation (3.46) is called *Navier–Stokes equation* which is actually three nonlinear partial differential equations with four unknown functions. This equation should be solved with continuity equation so that the number of equations is equal to that of unknown functions.

Liquids behave like *incompressible fluid* in moderate conditions. Hence, it is a good approximation that

$$\nabla \cdot \mathbf{v} = 0 \tag{3.47}$$

Application of Eq. (3.47) gives

$$\rho\left(\frac{\partial \mathbf{v}}{\partial t} + \mathbf{v} \cdot \nabla \mathbf{v}\right) = -\nabla p + \eta_{\mathrm{s}}\nabla^2 \mathbf{v} \tag{3.48}$$

It is the *Navier–Stokes equation* of incompressible fluids. Since the density of incompressible fluid is a constant and the hydrostatic pressure cannot be given from the equation of state, the four equations of Eqs. (3.47) and (3.48) have four unknown functions: three components of velocity and hydrostatic pressure.

Since both Eqs. (3.46) and (3.48) are difficult to be solved exactly, several approximations have been developed. These approximations are based on dimensional analysis because nondimensionalization makes it easier to compare the magnitudes of various quantities such as velocity, density, viscosity, pressure, and gravitation. Consider the following nondimensionalizations:

$$\mathbf{x} = l_c\bar{\mathbf{x}}; \quad \nabla = \frac{1}{l_c}\overline{\nabla}; \quad \mathbf{v} = v_c\bar{\mathbf{v}}; \quad \mathbf{b} = g\bar{\mathbf{b}}; \quad t = t_c\bar{t}; \quad p = p_c\bar{p} \tag{3.49}$$

where bar and subscript c indicate dimensionless quantity and characteristic quantity, respectively. Note that g is the acceleration of gravity. Characteristic quantities are chosen among the quantities to represent the system (Deen 1998). Then, Eq. (3.48) can be rewritten in terms of dimensionless quantities as follows:

$$\mathrm{Re}\left(\frac{1}{\mathrm{St}}\frac{\partial\bar{\mathbf{v}}}{\partial\bar{t}} + \bar{\mathbf{v}}\cdot\overline{\nabla}\cdot\bar{\mathbf{v}}\right) = -\left(\frac{l_c p_c}{\eta_s v_c}\right)\overline{\nabla}\bar{p} + \overline{\nabla}^2\bar{\mathbf{v}} + \frac{\mathrm{Re}}{\mathrm{Fr}}\bar{\mathbf{b}} \tag{3.50}$$

where dimensionless numbers Re, Sr, and Fr are defined as

$$\mathrm{Re} = \frac{\rho v_c l_c}{\eta_s}; \quad \mathrm{St} = \frac{t_c v_c}{l_c}; \quad \mathrm{Fr} = \frac{v_c^2}{g l_c} \tag{3.51}$$

Note that Re is the *Reynolds number* which represents the ratio of inertial force to viscous force, St is the *Strouhal number* which indicates the ratio of the time intrinsic for flow to the convection time, and Fr is the *Froude number* which corresponds to the ratio of inertial force to gravitational force.

If Sr is much larger than other dimensionless quantities, then the time derivative term can be neglected. Then, the velocity can be considered as the one independent of time. If Re is much smaller than Fr, then the effect of body force can be neglected. The body force is usually neglected in the flow of polymer melts, because their viscosity is much higher.

There are two ways to select the characteristic pressure: *viscous pressure scale* and *inertial pressure scale*. The former is given by

$$p_c = \frac{\eta_s v_c}{l_c} \tag{3.52}$$

and the latter is given by

$$p_c = \rho v_c^2 \tag{3.53}$$

If viscous scale is used, then the incompressible Navier–Stokes equation becomes

$$\frac{\partial\bar{\mathbf{v}}}{\partial\bar{t}} + \mathrm{St}\bar{\mathbf{v}}\cdot\overline{\nabla}\cdot\bar{\mathbf{v}} = -\frac{\mathrm{St}}{\mathrm{Re}}\overline{\nabla}\bar{p} + \frac{\mathrm{St}}{\mathrm{Re}}\overline{\nabla}^2\bar{\mathbf{v}} + \frac{\mathrm{St}}{\mathrm{Fr}}\bar{\mathbf{b}} \tag{3.54}$$

If the characteristic time t_c is chosen as

$$t_c = \frac{\rho l_c^2}{\eta_s}, \tag{3.55}$$

then we have

$$\mathrm{St} = \mathrm{Re} \tag{3.56}$$

Hence, Eq. (3.54) becomes

$$\frac{\partial \bar{\mathbf{v}}}{\partial \bar{t}} + \mathrm{Re}\,\bar{\mathbf{v}} \cdot \overline{\nabla} \cdot \bar{\mathbf{v}} = -\overline{\nabla}\bar{p} + \overline{\nabla}^2 \bar{\mathbf{v}} + \frac{\mathrm{Re}}{\mathrm{Fr}} \bar{\mathbf{b}} \tag{3.57}$$

Taking the limit $\mathrm{Re} \to 0$, we have

$$\frac{\partial \bar{\mathbf{v}}}{\partial \bar{t}} = -\overline{\nabla}\bar{p} + \overline{\nabla}^2 \bar{\mathbf{v}} \tag{3.58}$$

This equation is effective for suspensions consisting of tiny particles and incompressible Newtonian fluid. The *Stokes flow* is the flow that Eq. (3.58) is a good approximation. Equation (3.58) is a set of linear partial differential equations because the convection term $\bar{\mathbf{v}} \cdot \overline{\nabla} \bar{\mathbf{v}}$ is removed. Various solution methods for Eq. (3.58) are found in Kim and Karrila (2005).

3.2.3 Viscous Model for Polymer Melts

Since polymer melts have very high viscosity, it is usual to use $\mathrm{Re} = 0$. However, the viscosity of polymer melt is not constant even though the temperature dependence of the viscosity is not considered. Shear viscosity of polymer melt is a function of deformation rate tensor. Since polymer melt is considered as incompressible fluid, the first principal invariant of $\mathbf{D}$ is zero. For simplicity, if the third invariant is neglected, then the viscosity becomes the scalar-valued function of only the second invariant. It is more convenient to use *shear rate* $\dot{\gamma} \geq 0$ defined below rather than the second invariant:

$$\dot{\gamma} = \sqrt{4|II_{\mathbf{D}}|} \tag{3.59}$$

Note that in simple shear flow, deformation rate tensor is usually given by

$$\mathbf{D} = g(\mathbf{ab} + \mathbf{ba}) \tag{3.60}$$

where g is a function of position and time, $\mathbf{a}$ is the unit vector along the *flow direction*, and $\mathbf{b}$ is the unit vector in the direction where the magnitude of velocity varies (Tanner 2002). The direction of $\mathbf{b}$ is called *gradient direction*, and the third direction other than $\mathbf{a}$ and $\mathbf{b}$ is called *vorticity direction*. Then, Eq. (3.59) implies that

$$\dot{\gamma} = |g| \tag{3.61}$$

Note that shear flow is the one that satisfies $\mathbf{a} \cdot \mathbf{b} = 0$.

In polymer processing, it is usual to use the following viscous fluid model:

$$\mathbf{T} = -p\mathbf{I} + 2\eta(\dot{\gamma})\mathbf{D} \tag{3.62}$$

with

$$\eta(\dot{\gamma}, T) = \frac{\eta_o(T)}{\{1 + [\eta_o(T)\dot{\gamma}/\sigma_o]^a\}^b} \tag{3.63}$$

Here, the viscosity model (3.63) is called the Carreau–Yasuda model (Bird et al. 1987). The *Carreau–Yasuda model* has four parameters at constant temperature. Note that Eq. (3.63) implies that

$$\lim_{\dot{\gamma}\to 0} \eta(\dot{\gamma}, T) = \eta_o(T) \tag{3.64}$$

Hence, η_o is called the *zero-shear viscosity*. When $\eta_o\dot{\gamma}\sigma_o^{-1} \ll 1$, Eq. (3.62) behaves like the constitutive equation of incompressible Newtonian fluid.

Viscosity of most liquids depends on temperature. The temperature dependence of liquid agrees well, in most cases, with

$$\eta_o(T) = \eta_\infty \exp\left(\frac{T_a}{T}\right) \tag{3.65}$$

where both η_∞ and T_a are positive material parameters. The activation energy of flow is defined by

$$T_a = \frac{E_a}{R} \tag{3.66}$$

where R is the gas constant whose value is about 8.314 J K^{-1} mol^{-1}.

Adopting Eq. (3.65), the Carreau–Yasuda model becomes 6-parameter model. One of the most important features of the Carreau–Yasuda model is temperature–shear rate superposition. The plot of $\eta/\eta_o(T)$ against $\dot{\gamma}/\dot{\gamma}_o$ is nearly independent of temperature. Note that

$$\dot{\gamma}_o = \frac{\sigma_o}{\eta_o(T)} \tag{3.67}$$

The zero-shear viscosity of polymer melt is also dependent on molecular weight of polymer. It is known that

$$\frac{\eta_o(M, T)}{\eta_o(M_C, T)} = \begin{cases} \frac{M}{M_C} & \text{for } M \le M_C \\ \left(\frac{M}{M_C}\right)^{3.4} & \text{for } M \ge M_C \end{cases} \tag{3.68}$$

where M_C and M are, respectively, the *critical molecular weight* and *weight-average molecular weight* (Chap. 4). Hence, we can confirm experimentally the T-M-$\dot{\gamma}$ superposition from the plot of $\eta/\eta_o(T)$ against $\dot{\gamma}/\dot{\gamma}_o$. Since the critical molecular weight depends on kinds of polymers, it can be considered as material constant. Equation (3.68) is nearly independent of molecular weight distribution.

It is difficult to obtain sufficiently many viscosity data for the identification of Eq. (3.63). Hence, the use of the above superposition principle is very effective in the determination of the material parameters. This will be discussed in Part II.

It is difficult to obtain isothermal viscosity data whose shear rates are so wide to identify Eq. (3.63). Usual range of shear rate is $\eta_o\dot{\gamma}\sigma_o^{-1} \gg 1$. In this region of shear rate, Eq. (3.63) is approximated by

$$\eta = \frac{K}{\dot{\gamma}^n} \tag{3.69}$$

This is the two-parameter model called the *power law fluid model*.

It is worthwhile to mention that shear viscosity of polymer melts or polymer solutions is calculated by

$$\eta = \frac{\sigma}{\dot{\gamma}} \tag{3.70}$$

where σ is the shear stress measured from steady simple shear flow. There are several methods to measure the shear viscosity of polymeric fluid, which will be discussed in Part III. Since shear stress must not be a decreasing function of shear rate, it is clear that $0 < n < 1$ as well as $0 < ab < 1$. Both Eqs. (3.63) and (3.70) represent that the shear viscosity is a decreasing function of shear rate. Hence, most polymeric fluids are *shear-thinning fluids*.

3.3 Viscoelastic Models

3.3.1 Spring–Dashpot Models

Stress of polymeric materials depends on both strain and strain rate because the materials are viscoelastic. Before the birth of the society of rheology, the materials have been studied and modeled. At that time, solids were considered as linear elastic body (called *Hookean body*) whose stress is linear function of strain, whereas fluids were considered as linear viscous fluid (called Newtonian fluid) whose stress is linear function of strain rate. Since spring can be represented for linear elastic solids and dashpot for linear viscous fluids, it is a natural way to model linear viscoelasticity by the combinations of spring and dashpot.

The *Maxwell model* is a one-dimensional model that a spring and a dashpot are connected in a series. When the modulus of the spring is denoted by $G_M > 0$ and the viscosity of the dashpot by $\eta_M > 0$, the one-dimensional stress σ is given by

$$\sigma = G_M \gamma_e = \eta_M \frac{d\gamma_v}{dt} \tag{3.71}$$

where γ_e is the strain of the spring and γ_v is the strain of the dashpot. Since the two mechanical elements are connected in a series, it is clear that the total strain is given by

$$\gamma = \gamma_e + \gamma_v \tag{3.72}$$

Combining Eqs. (3.71) and (3.72), we have

$$\frac{d\sigma}{dt} + \frac{G_M}{\eta_M}\sigma = G_M \frac{d\gamma}{dt} \tag{3.73}$$

Since the units of G_M and η_M are Pa and Pa-s, respectively, we can define relaxation time such that

$$\lambda_M = \frac{\eta_M}{G_M} \tag{3.74}$$

The general solution of Eq. (3.73) is given by

$$\sigma(t) = \sigma(t_o)\exp\left(-\frac{t - t_o}{\lambda}\right) + \int_{t_o}^{t} G(t-\tau)\frac{d\gamma}{d\tau}d\tau \tag{3.75}$$

where the relaxation modulus $G(t)$ is defined by

$$G(t) = G_M \exp\left(-\frac{t}{\lambda_M}\right) \tag{3.76}$$

If we know the time when stress is zero, say it is t_o, Eq. (3.75) becomes simpler:

$$\sigma(t) = \int_{t_o}^{t} G(t-\tau)\frac{d\gamma}{d\tau}\,d\tau \tag{3.77}$$

However, because stress of viscoelastic material is determined by deformation history, it is difficult to know when stress is zero. Setting $t_o \to -\infty$, Eq. (3.75) becomes independent of initial condition:

$$\sigma(t) = \int_{-\infty}^{t} G(t-\tau)\frac{\mathrm{d}\gamma}{\mathrm{d}\tau}\,\mathrm{d}\tau \tag{3.78}$$

Equation (3.78) is valid even if $\sigma(-\infty) \neq 0$.

Equation (3.78) with Eq. (3.76) is the constitutive equation of the Maxwell model. If strain is given by $\gamma(t) = \gamma_o \Theta(t)$ where $\Theta(t)$ is the *unit step function* defined by

$$\Theta(t) = \begin{cases} 1 & \text{for} \quad t \geq 0 \\ 0 & \text{for} \quad t < 0 \end{cases} \tag{3.79}$$

The test by the step strain is called stress relaxation. The derivative of the unit step function is the *Dirac delta function*:

$$\frac{\mathrm{d}\Theta}{\mathrm{d}t} = \delta(t) \tag{3.80}$$

Then, stress is given by

$$\sigma(t) = G(t)\gamma_o = G_M \gamma_o \exp\left(-\frac{t}{\lambda_M}\right) \tag{3.81}$$

Equation (3.81) implies that stress becomes smaller as time increases. This tendency qualitatively agrees with the experimental results of viscoelastic materials. Only two material parameters G_M and λ_M cannot fit experimental data.

It is interesting that the stress of Eq. (3.81) at $t = -1$ is larger than the stress at $t = 0$. It is ridiculous because strain was zero for $t < 0$. How can we remove this contradiction?

In Eq. (3.78), $t - \tau$ implies the interval between the time at which stress is measured and the time at which strain was given. Hence, $G(t - \tau)$ represents the weight of the effect of deformation given before $t - \tau$. It is a reasonable reasoning that the effects from far past must be smaller than those from near past. This notion is called *fading memory*. The principle of fading memory insists that relaxation modulus must be a decreasing function of time. Furthermore, the stress at present time cannot be affected by the strain which will be given in future. This is called *principle of causality*. If $t - \tau$ is less than zero, then τ is the time of future. The principle of causality insists that $G(t) = 0$ for $t < 0$. Thus, Eq. (3.76) must be replaced by

$$G(t) = G_M e^{-t/\lambda_M}\Theta(t) \tag{3.82}$$

The *Voigt model* (or *Kelvin–Voigt model*) is the one in which spring and dashpot are connected in parallel. Because of parallel connection, both mechanical elements have the same strain. Then, the total stress is given by

$$\sigma = G_V \gamma + \eta_V \frac{d\gamma}{dt} \tag{3.83}$$

This one-dimensional constitutive equation easily gives stress when strain is given. As for stress relaxation test, the stress is easily calculated as follows:

$$\sigma(t) = G_V \gamma_o \Theta(t) + \eta_V \gamma_o \delta(t) \tag{3.84}$$

Compared with Eq. (3.81), the stress of the Voigt model does not decrease just as that of elastic material. Only difference from linear elasticity is the last term containing the Dirac delta function. This term is not detectable in any experiment. At any way, Eq. (3.84) implies that the relaxation modulus of the Voigt model is given by

$$G(t) = G_V \Theta(t) + \eta_V \delta(t) \tag{3.85}$$

Equation (3.83) is a linear differential equation of strain. The general solution is given by

$$\gamma(t) = \exp\left(-\frac{t - t_o}{\tau_V}\right)\gamma(t_o) + \int_{t_o}^{t} \frac{1}{\eta_V} \exp\left(-\frac{t - \tau}{\tau_V}\right)\sigma(\tau)d\tau \tag{3.86}$$

where the *retardation time* of the Voigt model $\tau_V = \eta_V / G_V$. Application of integration by parts gives

$$\gamma(t) = e^{-(t-t_o)/\tau_V}\left[\gamma(t_o) - \frac{\sigma(t_o)}{G_V}\right] + \frac{\sigma(t)}{G_V} - \int_{t_o}^{t} \frac{1}{G_V} \exp\left(-\frac{t - \tau}{\tau_V}\right)\frac{d\sigma}{d\tau}d\tau \tag{3.87}$$

Just as before, we take $t_o \to -\infty$ to remove the effect of initial condition. Then, we have

$$\gamma(t) = \int_{-\infty}^{t} J(t - \tau)\frac{d\sigma}{d\tau}d\tau \tag{3.88}$$

where $J(t)$ is called *creep compliance* and is given by

$$J(t) = \frac{1 - e^{-t/\tau_V}}{G_V}\Theta(t) \tag{3.89}$$

The unit step function was introduced to Eq. (3.89) because of the principle of causality.

In creep experiment, strain is measured as a function of time under the stress controlled by $\sigma(t) = \sigma_o \Theta(t)$. When creep test is done, the strain of elastic materials does not vary, while the strain of the Voigt model depends on time as follows:

$$\gamma(t) = \sigma_o J(t) \Theta(t) \tag{3.90}$$

As time goes to infinity, strain of Eq. (3.90) approaches to σ_o / G_V which is the strain of the spring of the Voigt model when the spring is exerted by the stress σ_o. This implies that the growth of the creep strain is retarded. Because of this retardation of strain, the characteristic time in Eq. (3.89), τ_V, is called *retardation time*.

Although the Maxwell model and the Voigt model are successful in the description of a few viscoelastic phenomena, the agreement is qualitative, not quantitative. Furthermore, the creep behavior of the Maxwell model and the relaxation behavior of the Voigt model are disappointing. Improvement is expected when more mechanical elements are involved in modeling.

The *standard solid model* is the parallel connection of the Maxwell model with a spring whose modulus is G_1. Then, the one-dimensional constitutive equation becomes

$$\lambda \frac{d\sigma}{dt} + \sigma = \eta_2 \left(1 + \frac{G_1}{G_2}\right) \frac{d\gamma}{dt} + G_1 \gamma \tag{3.91}$$

where η_2 and G_2 are viscosity and modulus of the Maxwell model, respectively. The differential equation can be replaced again by Eq. (3.78), but the relaxation modulus is given by

$$G(t) = \left[G_1 + G_2 \exp\left(-\frac{t}{\lambda}\right)\right] \Theta(t) \tag{3.92}$$

with

$$\lambda = \frac{\eta_2}{G_2} \tag{3.93}$$

The *Jeffreys model* is the connection of the Voigt model with a dashpot of η_1 in a series. Then, the one-dimensional constitutive equation is given by

$$\frac{d\sigma}{dt} + \frac{G_2}{\eta_1 + \eta_2} \sigma = \frac{\eta_1}{\eta_1 + \eta_2} G_2 \frac{d\gamma}{dt} + \frac{\eta_1 \eta_2}{\eta_1 + \eta_2} \frac{d^2\gamma}{dt^2} \tag{3.94}$$

where η_2 and G_2 are viscosity and modulus of the Voigt model, respectively. The Jeffreys model describes the creep behavior of polymeric fluid well, while the standard solid model describes the relaxation behavior of polymeric solid well. The creep compliance of the Jeffreys model is given by

$$J(t) = \left(\frac{t}{\eta_0} + \frac{1 - e^{-t/\tau}}{G_2}\right)\Theta(t) \tag{3.95}$$

where the retardation time is given by

$$\tau = \frac{\eta_2}{G_2} \tag{3.96}$$

3.3.2 Generalization of One-Dimensional Models

However, these two 3-element models still suffer from quantitative disagreement with experimental data even though a quite large improvement is achieved compared with the 2-element models. The *generalized Maxwell model* is the parallel connection of N different Maxwell elements with a single spring. The generalized Maxwell model gives better fitting of relaxation data as N increases. Similarly, connection of N different Voigt elements and a single dashpot in a series gives better fitting of creep data as N increases. This is called the *generalized Voigt model*. The relaxation modulus of N-mode Maxwell model is given by

$$G(t) = \left(G_\infty + \sum_{k=1}^{N} G_k e^{-t/\lambda_k}\right)\Theta(t) \tag{3.97}$$

where kth-mode relaxation time is defined as $\lambda_k = \eta_k/G_k$. The N-mode Voigt model has the creep compliance such as

$$J(t) = \left(\frac{t}{\eta_o} + \sum_{k=1}^{N} \frac{1 - e^{-t/\tau_k}}{G_k}\right)\Theta(t) \tag{3.98}$$

where kth-mode retardation time is defined as $\tau_k = \eta_k/G_k$.

The generalized Maxwell and Voigt models can be generalized further by the introduction of relaxation and retardation spectra. The summation in Eqs. (3.97) and (3.98) is replaced by integration:

$$G(t) = \int_{-\infty}^{\infty} H(\lambda) e^{-t/\lambda} \mathrm{d}\log\lambda \tag{3.99}$$

and

$$J(t) = \int_{-\infty}^{\infty} L(\tau)\left(1 - e^{-t/\tau}\right)\mathrm{d}\log\tau \tag{3.100}$$

Note that these integral equations adopt logarithmic scale to make the *relaxation time spectrum* $H(\lambda)$ have the dimension of modulus and to make the *retardation time spectrum* $L(\tau)$ have the dimension of compliance. The two spectra cannot be measured directly because they are conceptual quantities. We shall show that the relaxation time spectrum is uniquely determined in Part II. Similar approaches can be applied to the uniqueness of retardation time spectrum. Equations (3.99) and (3.100) are the *Fredholm integral equation of the first kind* (Arfken 2001). How to solve this integral equation will be discussed in Part II, too.

From various spring–dashpot models (Tschoegl 1989), we know that all linear viscoelastic models satisfy Eqs. (3.78) and (3.88). The two equations are known as the *Boltzmann superposition principle*. This will be proved in Part II. Then, the modeling of relaxation modulus or creep compliance is more effective than the design of multielement spring–dashpot models. A parsimonious modeling is to model the Laplace transform of creep compliance:

$$\frac{1}{s\widetilde{G}(s)} = \frac{1}{\eta_o s} + \frac{J_1}{[1+(\tau_1 s)^{\alpha_1}]^{\beta_1}} + \frac{J_2}{[1+(\tau_2 s)^{\alpha_2}]^{\beta_2}} \tag{3.101}$$

where $\widetilde{G}(s)$ is the Laplace transform of relaxation modulus (Marin and Graessley 1977). Equation (3.101) agrees very well with experimental data of polymer melts with narrow molecular weight distribution when $\beta_1 = \beta_2 = 1$. Another parsimonious model is

$$G(t) = G_\infty + G_1 \exp\left(-\left(\frac{t}{\lambda}\right)^{\beta}\right) \tag{3.102}$$

It is known as *Kohlrausch–Williams–Watts (KWW) equation* (Riande 2000).

An interesting generalization is to apply fractional derivative to spring–dashpot models (Smit and de Vries 1970). Although the spring–dashpot models contain derivatives of integer order, the *fractional models* use *fractional derivative* which is defined as (Bagley and Torvik 1983)

$$\frac{\mathrm{d}^\alpha f(t)}{\mathrm{d}t^\alpha} = \frac{1}{\Gamma(1-\alpha)}\frac{\mathrm{d}}{\mathrm{d}t}\int_0^t \frac{f(\tau)}{(t-\tau)^\alpha}\mathrm{d}\tau, \quad 0<\alpha<1 \tag{3.103}$$

3.3.3 Concept of Internal Variable

Consider the Maxwell model. The strains of the spring and the dashpot cannot be controlled separately. The mechanical work on the model is stored in the spring element. The mechanical work per unit volume done on the Maxwell material is given by

$$dW = \sigma d\gamma = \sigma d\gamma_e + \sigma d\gamma_v \tag{3.104}$$

Hence, we have

$$\frac{dW}{dt} = G_M \gamma_e \frac{d\gamma_e}{dt} + \eta_M \left(\frac{d\gamma_v}{dt}\right)^2 \tag{3.105}$$

Here, we used $\sigma = \sigma_e = \sigma_v$ and $\gamma = \gamma_e + \gamma_v$. When $U_e \equiv \frac{1}{2} G_M \gamma_e^2$, Eq. (3.105) becomes

$$\frac{dU_e}{dt} = G_M \gamma_e \frac{d\gamma_e}{dt}, \tag{3.106}$$

Then, for arbitrary interval of time, we have

$$W \equiv \int_{t_o}^{t} \frac{dW}{dt} dt' = U_e(\gamma_e(t)) - U_e(\gamma_e(t_o)) + \int_{t_o}^{t} \eta_M \left(\frac{d\gamma_v}{dt'}\right)^2 dt' \tag{3.107}$$

The last term in the right-hand side of Eq. (3.107) is always positive and an increasing function of time t if viscosity η_M is positive. Meanwhile, the first two terms in the right-hand side represent the difference of a scalar function of strain γ_e. Hence, it can be said that a part of mechanical work done on the Maxwell material is stored. The stored energy can be considered as the increase in the Helmholtz free energy of the material. Then, one may think that the thermodynamics of the Maxwell model cannot be described by the use of only strain and temperature.

It was known that irreversible thermodynamics of viscoelastic materials cannot be described completely by the use of only the state variables of equilibrium thermodynamics and their gradients. Additional state variables needed for viscoelastic materials are called *internal variables* (Coleman and Gurtin 1967; Maugin and Muschik 1994; Muschik 1990). The internal variables were motivated from the internal strain such as spring strain. The irreversible thermodynamics for viscoelasticity will be discussed in Sect. 4.

3.3.4 Generalization of Three-Dimensional Model

Linear mechanical behaviors of materials are observed when deformation is infinitesimal. Then, application of infinitesimal strain and the Boltzmann superposition principle allows us to write

$$\mathbf{T} = \int_{-\infty}^{t} \mathbf{C}(t - \tau) \frac{d\mathbf{E}}{d\tau} d\tau \tag{3.108}$$

where $\mathbf{C}$ is a fourth-order tensor-valued function of time. If the material is isotropic, the fourth-order tensor, relaxation modulus can be written by

$$\mathbf{C}(t) = \left[\Lambda(t)\delta_{ik}\delta_{pq} + G(t)\left(\delta_{ip}\delta_{kq} + \delta_{iq}\delta_{kp}\right)\right]\mathbf{e}_i\mathbf{e}_k\mathbf{e}_p\mathbf{e}_q \tag{3.109}$$

Since $\Lambda(t)$ the time-dependent version of λ in Eq. (3.3) and $G(t)$ corresponds to time-dependent shear modulus, we can define time-dependent bulk modulus and write

$$\mathbf{T} = \int_{-\infty}^{t} K(t-\tau)\frac{\mathrm{d}e_{\mathrm{V}}}{\mathrm{d}\tau}\mathrm{d}\tau\,\mathbf{I} + 2\int_{-\infty}^{t} G(t-\tau)\frac{\mathrm{d}\mathbf{E}'}{\mathrm{d}\tau}\mathrm{d}\tau \tag{3.110}$$

This is the three-dimensional extension of Eq. (3.78). If we are interested in incompressible viscoelastic fluids, then Eq. (3.110) can be rewritten by

$$\mathbf{T} = -p\,\mathbf{I} + 2\int_{-\infty}^{t} G(t-\tau)\mathbf{D}(\tau)\mathrm{d}\tau \tag{3.111}$$

Note that when deformation is infinitesimal, the time derivative of infinitesimal strain is the deformation rate tensor and the deformation rate tensor of incompressible fluid is traceless.

3.3.5 Generalization of Nonlinear Viscoelasticity

One may figure nonlinear version of the Maxwell model such as

$$\lambda_{\mathrm{M}}\frac{\mathrm{d}\mathbf{T}'}{\mathrm{d}t} + \mathbf{T}' = 2\eta_{\mathrm{M}}\mathbf{D}; \tag{3.112}$$

$$\mathbf{T} = -p\mathbf{I} + \mathbf{T}' \tag{3.113}$$

Here, incompressible fluid is assumed. The one-dimensional strain rate is replaced by deformation rate tensor, and the ordinary time derivative is replaced by the material time derivative. Although this extension seems plausible, various problems arise. One of the most important problems is related to the time rate of stress. The use of the material time derivative gives rise to the ambiguity in physical meaning of stress rate. Besides, mechanical behavior of material must be independent of observer. These problems can be solved with the principle of material frame-indifference which will be discussed in Sect. 5.

Applying integration by parts, Eq. (3.78) can be rewritten by

$$\sigma(t) = \int_{-\infty}^{t} \mu(t-\tau)\gamma(\tau)\mathrm{d}\tau \tag{3.114}$$

where $\mu(t)$ is called the *memory function* defined as

$$\mu(t) = -\frac{\mathrm{d}G}{\mathrm{d}t} \geq 0 \tag{3.115}$$

Then, one may want to replace the one-dimensional strain by the finite strain, say $\mathbf{H}(t)$ for convenience:

$$\mathbf{T} = -p\mathbf{I} + \int_{-\infty}^{t} \mu(t-\tau)\mathbf{H}(\tau)\mathrm{d}\tau \tag{3.116}$$

In this approach, we have to determine which strain measure is suitable. Furthermore, we have to investigate whether the principle of material frame-indifference is satisfied by Eq. (3.116).

There are two branches in the development of nonlinear viscoelastic constitutive equations: differential types based on Eq. (3.112) and integral types based on Eq. (3.116). These will be studied in Part III. When boundary value problem is considered, the differential-type constitutive equation is more convenient than the integral-type one in numerical implementation.

Problem 3

[1] From Eq. (3.3), derive

$$e_{ik} = \frac{1}{2G}\left(T_{ik} - \frac{\lambda}{3\lambda + 2G} T_{mm}\delta_{ik}\right) \tag{3.a}$$

[2] Derive Eq. (3.15)

[3] Show that

$$E = \frac{9KG}{3K+G}; \quad \nu = \frac{3K-2G}{2(3K+G)} \tag{3.b}$$

[4] Consider a spherical shell whose outer and inner radii are R_{out} and R_{in}, respectively. The shell contains a fluid with pressure of p_{in}. The pressure of surroundings is p_{out}. Because of symmetry, it can be assumed that the displacement field is given by

$$\mathbf{u} = u(r)\mathbf{e}_r \tag{3.c}$$

where spherical coordinate system is used. Find displacement field and stress tensor.

[5] Derive the constitutive equation of linear isotropic body, Eq. (3.11), from that of isotropic hyperelastic body, Eq. (3.36).

[6] Derive Eq. (3.39) from Eq. (3.37) by the use of the Cayley–Hamilton theorem.

[7] Derive Eq. (3.42).

[8] Derive Eq. (3.50).

[9] Derive Eq. (3.57).

[10] It is known that

$$s\widetilde{G}(s)\big|_{s=\mathrm{i}\omega} = G'(\omega) + \mathrm{i}G''(\omega) \tag{3.d}$$

Derive storage and loss moduli, $G'(\omega)$ and $G''(\omega)$ from Eq. (3.101) as for $\beta_1 = \beta_2 = 1$.

[11] When $\mathbf{H}(\tau) = \mathbf{C}_t(\tau)$ and $\mu(t) = (G_\mathrm{o}/\lambda)\exp(-t/\lambda)\Theta(t)$, show that stress of Eq. (3.116) satisfies

$$\mathbf{T}' + \lambda\left(\frac{\mathrm{d}\mathbf{T}'}{\mathrm{d}t} - \mathbf{L}\cdot\mathbf{T}' - \mathbf{T}'\cdot\mathbf{L}^T\right) = 2G_\mathrm{o}\lambda\mathbf{D} \tag{3.e}$$

4 Thermodynamics

4.1 Equilibrium Thermodynamics

We shall not treat theories of equilibrium thermodynamics in detail because this book is not a text of thermodynamics. However, we shall review some features of equilibrium thermodynamics, which are necessary in the development of viscoelastic constitutive equations of polymers. The readers of this book are assumed familiar with the theory of equilibrium thermodynamics provided in sophomore courses such as physical chemistry in departments of chemistry and chemical engineering, thermodynamics in department of mechanical engineering, and thermal physics in department of physics.

4.1.1 Thermodynamic Space and Processes

Thermodynamics is a macroscopic science of energy transform. Energy transfer occurs in the form of work and heat. As shown in Sect. 2.3, internal energy can be considered as an invention for the purpose of energy conservation. Energy transfers to a system of materials give rise to the changes in two forms of energy: internal energy and kinetic energy as shown in Eq. (2.53).

Most forms of energy can be related to work. Originally, work is a line integration of force field over the path on which material particle moves. As a simplified example, differential work is given by $\mathrm{d}W = \phi \mathrm{d}\xi$ where ϕ is a force field and $\mathrm{d}\xi$ is the differential of the coordinate that describes the path. Dividing the differential work by $\mathrm{d}t$, we can have the equation of power: $\mathrm{d}W/\mathrm{d}t = \phi v$ where $v = \mathrm{d}\xi/\mathrm{d}t$. Then, we can find an analogy from stress power: $\mathbf{T} : \mathbf{D} = T_{ik}D_{ik}$ if we match stress to generalized force and deformation rate to generalized velocity. Then, component-wise form of differential work can be generalized by

$$\mathrm{d}W = \sum_{k=1}^{N} \phi_k \mathrm{d}\xi_k \tag{4.1}$$

After kinetic energy is canceled in energy balance equation, the following are left:

$$\mathrm{d}U = \sum_{k=1}^{N} \phi_k \mathrm{d}\xi_k + \mathrm{d}Q \tag{4.2}$$

where $\mathrm{d}Q$ is the differential heat. Equation (4.2) implies that internal energy varies according to the variation of N generalized coordinates and heat. Hence, one may imagine that internal energy is determined by $N+1$ independent variables.

It is a traditional notion in physics that physical phenomena can be described exactly by variables of finite number. The variables are called state variables. It is believed that a thermodynamic system can be fully identified by a set of state variables. If a system with a given set of values of state variables comes to have different set of values of state variables, then the system is said to experience a thermodynamic process. Then, we can imagine an analogy that a system is equivalent to a point which moves in the thermodynamic space whose coordinates are the state variables. A trajectory of the point (the system) is called *thermodynamic process* or simply process.

The first law of energy conservation gives us a clue that the number of state variables might be $N + 1$. Theory of equilibrium thermodynamics reads that if Eq. (4.2) holds, then only $N + 1$ *state variables* describe the thermodynamic phenomena in equilibrium uniquely. From Eq. (4.2), N generalized coordinates $\{\xi_k\}$ can be chosen as state variables. The other state variable, which is related to heat transfer, could be chosen from the second law of thermodynamics. For a while, we

accept the axiom such that in equilibrium, there are $N + 1$ state variables even though the $N + 1$th state variables are not obviously known yet.

In thermodynamics, surroundings are the universe except the system. If we are interested in surroundings rather than the system, the surroundings can be considered as a system and then the system can be considered as surroundings. The distinction depends on our interest. The state of surrounding is called external condition.

If external condition maintains constant values, then the state variables of the system approach to certain constant values. Equilibrium state is the state represented by the constant values of state variables. Relaxation time is the characteristic time needed for the completion of the variation of state variables. If external conditions vary from one constant set of values to another constant set of values in a time, say external time, much longer than the relaxation time, then the changes in state variables look like immediate transition from one equilibrium to another equilibrium. If the difference between the two external conditions is infinitesimally small and if the external time is much longer than the relaxation time, then state variables change with maintaining equilibrium. The reverse of the process is believed to restore the states of both the system and its surroundings. Such process is called reversible process. It is expected that reversible process requires extremely slow progress. Hence, reversible process is considered as quasi-static process. Otherwise, a process is called irreversible process.

4.1.2 Existence of Entropy and Absolute Temperature

Consider only reversible processes from a given equilibrium state. Adiabatic process is a process without heat transfer. Then, Eq. (4.2) becomes

$$\mathrm{d}U - \sum_{k=1}^{N} \phi_k \mathrm{d}\xi_k = 0 \tag{4.3}$$

We can consider a thermodynamic space which is constructed by $\{\xi_k\}$ and U. Then, Eq. (4.3) represents a curve in the thermodynamic space. It is natural to adopt U as the $N + 1$th coordinate. For a given state denoted by $\mathbf{x}_\mathrm{o} = \left(U^{(\mathrm{o})}, \xi_1^{(\mathrm{o})} \ldots, \xi_N^{(\mathrm{o})}\right)$, there are infinitely many adiabatic curves passing the state $\mathbf{x}_\mathrm{o}$. Analogy of state variables to coordinates in thermodynamic space allows us to rewrite Eq. (4.3) as follows:

$$\mathbf{n} \cdot \mathrm{d}\mathbf{x} = 0 \tag{4.4}$$

where

$$\mathbf{n} = (\eta, \eta\phi_1, \eta\phi_2, \ldots, \eta\phi_N) \tag{4.5}$$

and

$$\mathrm{d}\mathbf{x} = (\mathrm{d}U, \mathrm{d}\xi_1, \mathrm{d}\xi_2, \ldots, \mathrm{d}\xi_N) \tag{4.6}$$

Note that η is a function of the state variables. We can imagine a surface element whose points satisfy Eq. (4.4). Then, the vector $\mathbf{n}$ is perpendicular to the surface element. The surface element can be expressed by a function:

$$f(\mathbf{x}) = f(U, \xi_1, \xi_2, \ldots, \xi_N) = \sigma \tag{4.7}$$

The variable σ can be determined by the substitution of $\mathbf{x}_0$ into Eq. (4.4). Adiabatic surface is the surface represented by Eq. (4.7). Consider the notions of coordinate system in Sect. 3. Then, two adjacent adiabatic surfaces must be parallel to each other because of the parallelism of coordinate. Note that all adiabatic curves passing $\mathbf{x}_o$ cannot meet any point on adjacent adiabatic surface. Then, we can take σ as a new thermodynamic coordinate whenever N coordinates are taken on adiabatic surface. Furthermore, we can take σ in order to satisfy

$$\left(\frac{\partial\sigma}{\partial U}\right)_{\{\xi_k\}} > 0 \tag{4.8}$$

Then, we can find a function such that

$$U = U(\sigma, \xi_1, \xi_2, \ldots, \xi_N) \tag{4.9}$$

We define

$$\tau = \left(\frac{\partial U}{\partial\sigma}\right)_{\{\xi_k\}} > 0 \tag{4.10}$$

The inequality holds because of Eq. (4.8). Note that adiabatic process implies $\mathrm{d}\sigma = 0$ because of the definition of σ. Then, the total differential of internal energy is given by

$$\mathrm{d}U = \sum_{k=1}^{N} \phi_k \mathrm{d}\xi_k + \tau\mathrm{d}\sigma \tag{4.11}$$

Comparison of Eq. (4.11) with Eq. (4.2) gives

$$\mathrm{d}Q = \tau\mathrm{d}\sigma \tag{4.12}$$

It must be noted that Eq. (4.12) holds whenever the process is reversible because Eq. (4.12) was derived from the assumption that only reversible processes are considered. Now, it is the time to find the physical meanings of σ and τ.

Consider a system which is the union of two subsystems 1 and 2. As for the two subsystems, we can define τ_k and σ_k with $k = 1$ and 2. Then, we can also define $\phi_k^{(1)}$ and $\xi_k^{(1)}$ for the subsystem 1 and $\phi_k^{(2)}$ and $\xi_k^{(2)}$ for the subsystem 2. The differential heat must satisfy

$$\mathrm{d}Q = \mathrm{d}Q_1 + \mathrm{d}Q_2 \tag{4.13}$$

where $\mathrm{d}Q_1$ and $\mathrm{d}Q_2$ are the differential heats given to subsystems 1 and 2, respectively. Then, the definitions of σ and τ give

$$\mathrm{d}Q = \tau \mathrm{d}\sigma = \tau_1 \mathrm{d}\sigma_1 + \tau_2 \mathrm{d}\sigma_2 \tag{4.14}$$

This differential equation means

$$\sigma = \sigma(\sigma_1, \sigma_2) \tag{4.15}$$

Note that σ_1 depends on $\{\xi_k^{(1)}\}$ but is independent of $\{\xi_k^{(2)}\}$. Similarly, σ_2 depends on $\{\xi_k^{(2)}\}$ but is independent of $\{\xi_k^{(1)}\}$. Equation (4.14) gives

$$\left(\frac{\partial \sigma}{\partial \sigma_1}\right)_{\sigma_2} = \frac{\tau_1}{\tau} = f_1(\sigma_1, \sigma_2); \quad \left(\frac{\partial \sigma}{\partial \sigma_1}\right)_{\sigma_2} = \frac{\tau_1}{\tau} = f_1(\sigma_1, \sigma_2) \tag{4.16}$$

Then, we have

$$\tau = \frac{\tau_1}{f_1(\sigma_1, \sigma_2)} = \frac{\tau_2}{f_2(\sigma_1, \sigma_2)} \tag{4.17}$$

We have empirical temperature scale such as Celsius or Fahrenheit scales. Since σ is related to heat, it is reasonable that σ, σ_1, and σ_2 depend on empirical temperature T'. Then, we can rewrite Eq. (4.15) as follows:

$$\sigma = \sigma\left(T', \left\{\xi_k^{(1)}\right\}, \left\{\xi_k^{(2)}\right\}\right) \tag{4.18}$$

When the two subsystems are in thermal equilibrium, we can write

$$\tau_1 = \tau_1(T', \sigma_1); \quad \tau_2 = \tau_2(T', \sigma_2) \tag{4.19}$$

It is assumed that the functional relations of the subsystems must hold for the total system. Then, we have

$$\tau = \tau(T', \sigma_1, \sigma_2) = \tau(T', \sigma(\sigma_1, \sigma_2)) \tag{4.20}$$

Then, Eq. (4.16) gives

$$f_1(\sigma_1\sigma_2) = \frac{\tau_1(T', \sigma_1)}{\tau(T', \sigma)}; \quad f_2(\sigma_1\sigma_2) = \frac{\tau_2(T', \sigma_1)}{\tau(T', \sigma)} \tag{4.21}$$

It is possible to eliminate T' dependence whenever there exists a function of the empirical temperature $T(T')$ such that

$$\tau_1 = T(T')\psi_1(\sigma_1); \quad \tau_2 = T(T')\psi_2(\sigma_2); \quad \tau = T(T')\psi(\sigma) \tag{4.22}$$

Consider a monotonically increasing function of σ, say $\psi(\sigma)$. Then, we can invent

$$S = \psi(\sigma); \quad T = \frac{\mathrm{d}\sigma}{\mathrm{d}S}\tau \tag{4.23}$$

Then, it is clear that

$$\mathrm{d}Q = \tau \mathrm{d}\sigma = T\mathrm{d}S \tag{4.24}$$

From Eq. (4.10), we know that τ, τ_1, and τ_2 are positive. Hence, we can assume that $\psi(\sigma) > 0$, $\psi_1(\sigma_1) > 0$, and $\psi_2(\sigma_2) > 0$. Then, we have

$$\tau_1 \mathrm{d}\sigma_1 = T(T')\mathrm{d}S_1; \quad \tau_2 \mathrm{d}\sigma_2 = T(T')\mathrm{d}S_2; \quad \tau \mathrm{d}\sigma = T(T')\mathrm{d}S \tag{4.25}$$

where

$$\frac{\mathrm{d}S_1}{\mathrm{d}\sigma_1} = \psi_1(\sigma_1); \quad \frac{\mathrm{d}S_2}{\mathrm{d}\sigma_2} = \psi_2(\sigma_2); \quad \frac{\mathrm{d}S}{\mathrm{d}\sigma} = \psi(\sigma) \tag{4.26}$$

Application of Eq. (4.25) to Eq. (4.14) gives

$$\mathrm{d}S = \mathrm{d}S_1 + \mathrm{d}S_2 \tag{4.27}$$

If we scale T to make correspondence to ideal gas temperature, then T becomes the absolute temperature and S can be defined as entropy. However, Eq. (4.27) does not imply

$$S = S_1 + S_2 \tag{4.28}$$

If any system has the same entropy at $T = 0$, which is the third law of equilibrium thermodynamics, then Eq. (4.28) holds. Equation (4.28) implies that entropy is an

extensive quantity. Extensive quantity satisfies the definition of the homogenous function of the first order:

$$S(\lambda U, \lambda\xi_1, \lambda\xi_2, \ldots, \lambda\xi_N) = \lambda S(U, \xi_1, \xi_2, \ldots, \xi_N) \tag{4.29}$$

for any positive real number λ.

The second law is an empirical law. We have derived S and T from the analogy of state variables to coordinates. The parallelism of coordinates implies that near a given state, there must be infinitely many states which cannot be connected to the given state through any adiabatic curve. This is called *inaccessible statement of Caratheodory*. The approach introduced above was developed by C. Caratheodory (Ma 1985). Although the way of Caratheodory shows the existence of entropy in a generalized manner, it is far from the empirical notion, the maximization of entropy.

4.1.3 Clausius Inequality

Originally, the Clausius inequality was derived from the Carnot engine. Refer (Huang 1963) for the detail of the inequality. The inequality states that

$$\oint_C \frac{\mathrm{d}Q}{T} \leq 0 \tag{4.30}$$

where the integral symbol represents a cycling process irrespective of reversibility. This is called the *Clausius inequality*. In Huang (1963), any cyclic process is assumed to be decomposed to tiny cyclic processes consisting of isothermal and adiabatic processes in thermodynamic space. Then, it is questionable what the absolute temperature T is in an irreversible process. From the original derivation of Clausius, the temperature T must be the one of the heat reservoirs. A number of theoretical problems are involved in the inequality. Hence, Callen took the following axioms on entropy (Callen 1985):

[1] Entropy is a concave function of state variables

$$S = S(U, \xi_1, \xi_2, \ldots, \xi_N) \tag{4.31}$$

[2] Partial derivative of entropy with respect to internal energy is positive

$$\left(\frac{\partial S}{\partial U}\right)_{\{\xi_k\}} > 0 \tag{4.32}$$

[3] Entropy is a positively homogeneous function of degree 1 as shown in Eq. (4.29).

Concave function implies that for any two states $\mathbf{x}_1$ and $\mathbf{x}_2$,

$$S(t\mathbf{x}_1 + (1-t)\mathbf{x}_2) \geq tS(\mathbf{x}_1) + (1-t)S(\mathbf{x}_2) \tag{4.33}$$

where t is any real number in the interval of $0 \leq t \leq 1$. Then, it can be proved that the internal energy U is a positively homogeneous function of degree 1 and ϕ_k and T are positively homogeneous functions of degree 0. Equivalently, temperature and generalized forces are intensive properties. Concavity of entropy results in convexity of internal energy, too.

4.1.4 Thermodynamic Potentials

Although equilibrium thermodynamics started from imperfect foundation, axiomatic unification of equilibrium thermodynamics agrees well with experimental results. Any counter example has not been found. This makes beginners feel much difficulty in understanding thermodynamics. Hence, we adopt the result of the Clausius inequality:

$$\mathrm{d}S \geq \frac{\mathrm{d}Q}{T} \tag{4.34}$$

Equation (4.2) illustrates that $T^{-1}\mathrm{d}Q = T^{-1}(\mathrm{d}U - \mathrm{d}W)$. Then, Eqs. (4.2) and (4.34) give the following inequalities:

$$\mathrm{d}S \geq \frac{\mathrm{d}U}{T} - \sum_{k=1}^{N} \frac{\phi_k}{T}\mathrm{d}\xi_k; \tag{4.35a}$$

$$\mathrm{d}U \leq T\mathrm{d}S + \sum_{k=1}^{N} \phi_k \mathrm{d}\xi_k; \tag{4.35b}$$

$$\mathrm{d}H \equiv \mathrm{d}\left(U - \sum_{k=1}^{N} \phi_k \xi_k\right) \leq T\mathrm{d}S - \sum_{k=1}^{N} \xi_k \mathrm{d}\phi_k; \tag{4.35c}$$

$$\mathrm{d}F \equiv \mathrm{d}(U - TS) \leq -S\mathrm{d}T + \sum_{k=1}^{N} \phi_k \mathrm{d}\xi_k; \tag{4.35d}$$

$$\mathrm{d}G \equiv \mathrm{d}(H - TS) \leq -S\mathrm{d}T - \sum_{k=1}^{N} \xi_k \mathrm{d}\phi_k \tag{4.35e}$$

Here, H is the *enthalpy*, F is the *Helmholtz free energy*, and G is the *Gibbs free energy*. The equalities of Eqs. (4.35a) hold whenever the process is reversible.

Equations (4.35a) illustrate that the Helmholtz free energy is a state function of system temperature and mechanical coordinates $\{\xi_k\}$, while the internal energy is a state function of entropy and mechanical coordinates. This is the result from *Legendre transform* (McQuarrie 2000).

Furthermore, spontaneous process occurs in the direction to the decrease of system's Helmholtz energy under the constraint of fixed temperature and mechanical coordinates. Similar analysis can be done for the internal energy, the enthalpy, and the Gibbs free energy. Hence, U, H, F, and G can play the role of entropy, the indicator of spontaneous process under the corresponding constraints.

These thermodynamic functions are called thermodynamic potential because important thermodynamic properties are obtained from the partial derivatives of them as shown in Eq. (4.35a). Entropy can be obtained from the partial derivatives of free energies:

$$S = -\left(\frac{\partial F}{\partial T}\right)_{\{\xi_k\}} = -\left(\frac{\partial G}{\partial T}\right)_{\{\phi_k\}} \tag{4.36}$$

Here, it must be noted that the two partial differentiations with respect to temperature are different because different state variables are fixed in the partial derivatives: F for mechanical coordinate and G for generalized forces.

4.2 Classical Irreversible Thermodynamics

4.2.1 Basic Assumptions

Classical irreversible thermodynamics (CIT) is based on local equilibrium hypothesis, which means every material particles can be considered as a tiny system in equilibrium (De Groot 1984). This does not mean the equilibrium of the whole system. Although all material particles are in equilibrium, each material particle may have different states. Each equilibrium state is assumed to be fully described by state variables such as strain and internal energy. For isotropic fluids, thermodynamic space consists of specific volume (volume per unit mass) and internal energy. Therefore, classical irreversible thermodynamics is founded on the same thermodynamic space of equilibrium thermodynamics.

It was known that classical irreversible thermodynamics is successful in describing the mechanical phenomena involving classical constitutive equations such as the Fourier conduction law, viscous fluids, and elastic solids. Since stress of viscous fluid is independent of current strain except volume change, the thermodynamic state of viscous fluids can be identified by internal energy and specific volume.

The specific volume can be replaced by density because $\bar{v} = \rho^{-1}$. Then, each material particle is assumed to have entropy field such that

$$s = \tilde{s}(\tilde{\mathbf{x}}, t) = s(u, \rho) \quad \text{(for fluid)} \tag{4.37}$$

and

$$s = s(u, \mathbf{B}) \quad \text{(for solid)} \tag{4.38}$$

Note that deformation gradient $\mathbf{F}$ contains both pure deformation and rigid body motion of rotation, while $\mathbf{B} = \mathbf{F} \cdot \mathbf{F}^T$ or $\mathbf{C} = \mathbf{F}^T \cdot \mathbf{F}$ represents only pure deformation. Hence, it is reasonable that $\mathbf{B}$ (or $\mathbf{C}$) is more appropriate than $\mathbf{F}$ as a thermodynamic state variable. Fundamentally, the use of $\mathbf{B}$ (or $\mathbf{C}$) is supported by the principle of material frame-indifference, which will be discussed in Sect. 5.

We start from fluid. The local equilibrium hypothesis gives

$$\mathrm{d}s = \frac{\partial s}{\partial u}\mathrm{d}u + \frac{\partial s}{\partial \rho}\mathrm{d}\rho \tag{4.39}$$

Note that since thermodynamic space is given by (u, ρ), we do not use the notation of Eq. (4.36) for convenience if there is no confusion. The total differentials in Eq. (4.39) are assumed to be replaced by material time derivative. Hence, Eq. (4.39) can be rewritten by

$$\frac{\mathrm{d}s}{\mathrm{d}t} = \frac{\partial s}{\partial u}\frac{\mathrm{d}u}{\mathrm{d}t} + \frac{\partial s}{\partial \rho}\frac{\mathrm{d}\rho}{\mathrm{d}t} \tag{4.40}$$

From the equilibrium thermodynamics, we know that

$$\left(\frac{\partial S}{\partial U}\right)_V = \frac{1}{T}; \quad \left(\frac{\partial S}{\partial V}\right)_U = \frac{p}{T} \tag{4.41}$$

Then, local equilibrium hypothesis leads to the use of

$$\frac{\partial s}{\partial u} = \frac{1}{T}; \quad \frac{\partial s}{\partial \rho} = \frac{p}{\rho^2 T} \tag{4.42}$$

Since both internal energy per unit mass u and mass density ρ are fields, the use of Eqs. (2.5) and (2.53) gives

$$\rho\frac{\mathrm{d}s}{\mathrm{d}t} = (-\nabla \cdot \mathbf{q} + \rho r + \mathbf{T} : \mathbf{D})\frac{1}{T} - (\nabla \cdot \mathbf{v})\frac{p}{T} \tag{4.43}$$

where Eq. (4.42) was used. The main purpose of the local equilibrium hypothesis is to derive an inequality in terms of field variables, which represents the second law. The inequality is called the Clausius–Duhem inequality.

As for solid, we can take thermodynamic space as the pair of internal energy and deformation gradient. Then, similar procedure leads to

$$\rho \frac{\mathrm{d}s}{\mathrm{d}t} = (-\nabla \cdot \mathbf{q} + \rho r + \mathbf{T} : \mathbf{D}) \frac{1}{T} + \rho \frac{\partial s}{\partial \mathbf{B}} : \frac{\mathrm{d}\mathbf{B}}{\mathrm{d}t} \tag{4.44}$$

4.2.2 Entropy Balance Equation

In order to rewrite the Clausius inequality in terms of field variables, we define entropy production S_{irr} such that

$$\mathrm{d}S = \frac{\mathrm{d}Q}{T} + \mathrm{d}S_{\mathrm{irr}} \tag{4.45}$$

Compared with the Clausius inequality Eq. (4.34), it is clear that for any thermodynamic process,

$$\mathrm{d}S_{\mathrm{irr}} \geq 0 \tag{4.46}$$

The equality holds if and only if the thermodynamic process is reversible.

We consider an arbitrary region Ω of a continuum, and the entropy of the region is assumed to be calculated by

$$S = \iiint_{\Omega} \rho s \, \mathrm{d}V \tag{4.47}$$

Similarly, we define *entropy production* per unit mass as

$$S_{\mathrm{irr}} = \iiint_{\Omega} \rho s_{\mathrm{irr}} \mathrm{d}V \tag{4.48}$$

Then, the differential heat term in Eq. (4.45) can be generalized as follows:

$$\frac{\mathrm{d}S}{\mathrm{d}t} = \frac{\mathrm{d}S_{\mathrm{irr}}}{\mathrm{d}t} - \iint_{\partial\Omega} \frac{1}{T} \mathbf{q} \cdot \mathrm{d}\mathbf{a} + \iiint_{\Omega} \frac{\rho r}{T} \mathrm{d}V \tag{4.49}$$

Differential form of Eq. (4.49) is obtained by the substitution of Eqs. (4.47) and (4.48) into Eq. (4.49) and application of the Reynolds transport theorem:

$$\rho \frac{\mathrm{d}s}{\mathrm{d}t} = -\nabla \cdot \left(\frac{\mathbf{q}}{T} \right) + \frac{\rho r}{T} + \rho \frac{\mathrm{d}s_{\mathrm{irr}}}{\mathrm{d}t} \tag{4.50}$$

Note that the first two terms in the right-hand side of Eq. (4.50) correspond to dQ/T of Eq. (4.34), which can be interpreted as the entropy transfer by heat transfer. On the other hand, the last term is the entropy production because it was introduced to make the Clausius inequality be the entropy balance equation. In order to emphasize this correspondence, we introduce the notation such that

$$\nabla \cdot \mathbf{j}_s = \nabla \cdot \left(\frac{\mathbf{q}}{T}\right) - \frac{\rho r}{T} \tag{4.51}$$

Here, $\mathbf{j}_s$ is defined as the entropy flux which consists of two fluxes such that

$$\mathbf{j}_s = \frac{\mathbf{q}}{T} + \mathbf{j}_{\text{rad}} \tag{4.52}$$

where

$$\nabla \cdot \mathbf{j}_{\text{rad}} = -\frac{\rho r}{T} \tag{4.53}$$

Although the vector field $\mathbf{j}_{\text{rad}}$ may not be determined uniquely from the given density, temperature, and r, it must not give rise to any significant problem because we will always use $\mathbf{j}_{\text{rad}}$ only through its divergence.

With the help of Eq. (4.50), the Clausius inequality in Eq. (4.46) can be rewritten by

$$\rho \frac{\mathrm{d}s_{\text{irr}}}{\mathrm{d}t} = \rho \frac{\mathrm{d}s}{\mathrm{d}t} + \nabla \cdot \mathbf{j}_s \geq 0 \tag{4.54}$$

Equation (4.54) is called the *Clausius–Duhem inequality*. Since the entropy production is the source term from the flux formalism of balance equation, the second law is the positiveness of entropy source.

4.2.3 Application of Entropy Balance

If Eq. (4.43) is substituted to Eq. (4.54), then this inequality can be written in terms of measurable field variables

$$\rho \frac{\mathrm{d}s_{\text{irr}}}{\mathrm{d}t} = \frac{1}{T}(\mathbf{T} : \mathbf{D} - \nabla \cdot \mathbf{q} + \rho r) - (\nabla \cdot \mathbf{v})\frac{p}{T} + \nabla \cdot \mathbf{j}_s \geq 0 \tag{4.55}$$

Stress can be decomposed into isotropic and deviatoric parts as follows:

$$\mathbf{T} = \mathbf{T}' + \frac{\mathrm{tr}(\mathbf{T})}{3}\mathbf{I} \tag{4.56}$$

Note that $\mathrm{tr}(\mathbf{T}') = 0$. Then, we know that

$$\mathbf{T} : \mathbf{D} = \mathbf{T}' : \mathbf{D} + \frac{1}{3}\mathrm{tr}(\mathbf{T})\ \mathrm{tr}(\mathbf{D}) \tag{4.57}$$

Since $\mathrm{tr}(\mathbf{D}) = \nabla \cdot \mathbf{v}$, application of Eq. (4.57) to Eq. (4.55) gives the Clausius inequality such that

$$\rho T \frac{\mathrm{d}s_{\mathrm{irr}}}{\mathrm{d}t} = \mathbf{T}' : \mathbf{D}' + (\nabla \cdot \mathbf{v})\left[\frac{\mathrm{tr}(\mathbf{T})}{3} + p\right] - \frac{\mathbf{q} \cdot \nabla T}{T} \geq 0 \tag{4.58}$$

Note that the following identity is used in Eq. (4.58):

$$\mathbf{T}' : \mathbf{D} = \mathbf{T}' : \left[\mathbf{D}' + \tfrac{1}{3}\mathrm{tr}(\mathbf{D})\mathbf{I}\right] = \mathbf{T}' : \mathbf{D}' \tag{4.59}$$

Since ∇T, $\mathbf{D}'$, and $\mathrm{tr}(\mathbf{D}) = \nabla \cdot \mathbf{v}$ can be given independently, it is obvious that

$$\mathbf{T}' : \mathbf{D}' \geq 0 \tag{4.60}$$

$$(\nabla \cdot \mathbf{v})\left[\frac{\mathrm{tr}(\mathbf{T})}{3} + p\right] \geq 0 \tag{4.61}$$

and

$$-\frac{\mathbf{q} \cdot \nabla T}{T} \geq 0 \tag{4.62}$$

The constitutive equation of Newtonian fluid is given by Eq. (3.43). Application of Eq. (3.43) to Eqs. (4.60) and (4.61) results in thermodynamic constraints on the phenomenological constitutive equation:

$$\eta_{\mathrm{s}} > 0; \eta_{\mathrm{b}} > -\frac{2}{3}\eta_{\mathrm{s}} \tag{4.63}$$

Assuming that heat conduction follows the Fourier law Eq. (2.40), Eq. (4.62) gives

$$\kappa > 0 \tag{4.64}$$

These results illustrate that the constitutive equations of Newtonian fluid and Fourier conduction law agree with the second law if the material constants satisfy Eqs. (4.63) and (4.64).

Now, turn to the case of solid. Substitution of Eq. (4.44) into Eq. (4.51) yields

$$\rho T \frac{\mathrm{d}s_{\mathrm{irr}}}{\mathrm{d}t} = -\frac{\mathbf{q}\cdot\nabla T}{T} + \left(\mathbf{T} + 2T\mathbf{B}\cdot\rho\frac{\partial s}{\partial \mathbf{B}}\right) : \mathbf{D} \tag{4.65}$$

Here, the following identity was used:

$$\frac{\mathrm{d}\mathbf{B}}{\mathrm{d}t} = \mathbf{L}\cdot\mathbf{B} + \mathbf{B}\cdot\mathbf{L}^T \tag{4.66}$$

Since $\mathbf{D}$ and ∇T can be given independently, Eq. (4.65) implies that

$$\mathbf{T} = -2T\,\mathbf{B}\cdot\rho\frac{\partial s}{\partial \mathbf{B}} \tag{4.67}$$

and Eq. (4.62). Equation (4.67) implies that if entropy as a function of u and $\mathbf{B}$ is known, then the Cauchy stress can be obtained by the gradient of entropy with respect to $\mathbf{B}$.

It is noteworthy that $\partial s/\partial \mathbf{B}$ of Eq. (4.67) is made of partial derivatives at fixed internal energy. Experiment at a fixed internal energy is extremely difficult to be implemented, whereas experiment at constant temperature is practical.

4.2.4 The Clausius–Duhem Inequality in Terms of Free Energy

As shown in Eq. (4.35a), the Clausius inequality can be rewritten in terms of Helmholtz free energy. We define

$$F = \iiint_{\Omega} \rho f \,\mathrm{d}V \tag{4.68}$$

and

$$f = u - Ts \tag{4.69}$$

Then, it is not difficult to show that f is a function of temperature and mass density for fluids. Similarly, as for solid, f is a function of temperature and deformation gradient. Hence, we have

$$f = \begin{cases} f(T,\rho) & \text{for fluid} \\ f(T,\mathbf{B}) & \text{for solid} \end{cases} \tag{4.70}$$

and the Clausius inequality is given by

$$\rho T \frac{\mathrm{d}s_{\mathrm{irr}}}{\mathrm{d}t} = -\frac{\mathbf{q}\cdot\nabla T}{T} + \mathbf{T}' : \mathbf{D}' + (\nabla\cdot\mathbf{v})\left[p + \frac{\mathrm{tr}(\mathbf{T})}{3}\right] \geq 0; \tag{4.71}$$

$$\rho T \frac{\mathrm{d}s_{\mathrm{irr}}}{\mathrm{d}t} = \left(\mathbf{T} - 2\mathbf{B}\cdot\rho\frac{\partial f}{\partial \mathbf{B}}\right) : \mathbf{D} - \frac{\mathbf{q}\cdot\nabla T}{T} \geq 0 \tag{4.72}$$

Note that Eq. (4.71) is identical to Eq. (4.58). Because of the independence of $\mathbf{D}$ and $\nabla\theta$, Eq. (4.72) is split into two inequalities and we have

$$\mathbf{T} = 2\mathbf{B}\cdot\rho\frac{\partial f}{\partial \mathbf{B}} \tag{4.73}$$

Note that $\partial f/\partial \mathbf{B}$ is made of the partial derivatives at constant temperature, while $\partial s/\partial \mathbf{B}$ of Eq. (4.67) consists of those at constant internal energy. Therefore, we have

$$\left(\frac{\partial f}{\partial \mathbf{B}}\right)_T = -T\left(\frac{\partial s}{\partial \mathbf{B}}\right)_u \tag{4.74}$$

It is worthy to compare Eq. (4.73) with the constitutive equation of hyperelasticity, as in Eq. (3.36). The strain energy function $\Phi(\mathbf{B}, T)$ is easily identified by $\rho f(\mathbf{B}, T)$ for incompressible elastic materials. As for compressible elastic body, the determination of free energy from strain energy function needs some carefulness. It is reasonable to assume that mass density of homogeneous material is constant at the reference configuration. Then, we have

$$\frac{\partial \tilde{\rho} f}{\partial \mathbf{B}} = \sqrt{\det(\mathbf{B})}\frac{\partial \Phi}{\partial \mathbf{B}} \tag{4.75}$$

where Eq. (2.a) and $\det(\mathbf{F}) = \sqrt{\det(\mathbf{B})}$ were used. Then, Eq. (4.75) provides free energy from an experimentally determined strain free energy.

4.3 *Theory of Internal Variables*

4.3.1 General Theory

When thermodynamic state space is identical to that of equilibrium thermodynamics, it is difficult to describe the irreversible thermodynamics of viscoelastic material. Although the *rational thermodynamics* is constructed to describe

viscoelasticity by introducing the principle of fading memory, it is known that the rational thermodynamics suffers from a few problems (Jou 1996). In order to overcome the demerits of the rational thermodynamics, it is necessary to extend the thermodynamic space of state variables. *Extended irreversible thermodynamics* is to adopt the thermodynamic space as the union of the equilibrium thermodynamic space and fluxes. However, this extended thermodynamic space is not convenient in the development of viscoelastic constitutive equations. The other extended thermodynamic space can be constructed by introducing *internal variables*.

Consider linear viscoelastic models made of spring and dashpot. As an example, consider the Maxwell model. The total strain is the sum of strains of spring and dashpot. It can be said that both strains of spring and dashpot are internal strain or internal variables. In the principle of the model, if a spring strain is given, then dashpot strain is determined by the difference between the total strain and the spring strain and vice versa. However, it is not possible to determine both internal strains independently by any experiment. Furthermore, it is impossible to control the internal variables, while the total strain is both measurable and controllable. As for further information of internal variable, refer to Coleman and Gurtin (1967), Valanis (1971), and Maugin (1999).

Here, we consider a generalization of internal variables more than the internal strains of spring–dashpot models. According to Maugin (1999), internal variables may be measureable but cannot be controlled. This means that we cannot design any experiment to make the internal variables have desired values at will. Thermodynamic theory of internal variables provides a way to restrict the forms of the evolution equations (or kinetic equations) of internal variables as well as any needed constitutive equations. Basic assumptions of the thermodynamics of internal variables are listed below:

[1] Thermodynamic space consists of the state variables of equilibrium thermodynamics and the internal variables of finite number.
[2] Each internal variable has its own evolution equation.
[3] Thermodynamic potentials such as free energies are function of state variables mentioned in [1].
[4] Internal variables are measurable but not controllable.

For simplicity, consider the case that internal variable is a second-order tensor $\mathbf{X}$. Then, the thermodynamic space is given by $(u, \mathbf{B}, \mathbf{X}, \nabla T)$ for solid. According to Coleman and Gurtin (1967), it is not necessary to use local equilibrium hypothesis in the identification of

$$\frac{1}{T} = \left(\frac{\partial s}{\partial u}\right)_{\mathbf{B},\mathbf{X},\nabla T} \tag{4.76}$$

However, the use of the local equilibrium hypothesis does not give rise to significant difference. The use of $(T, \mathbf{B}, \mathbf{X}, \nabla T)$ is more convenient than that of $(u, \mathbf{B}, \mathbf{X}, \nabla T)$. Then, principle of equipresence (Jou 1996; Truesdell 2004) gives

$$f = f(T, \mathbf{B}, \mathbf{X}, \nabla T); \tag{4.77}$$

$$s = s(T, \mathbf{B}, \mathbf{X}, \nabla T); \tag{4.78}$$

$$\mathbf{T} = \mathbf{T}(T, \mathbf{B}, \mathbf{X}, \nabla T); \tag{4.79}$$

$$\mathbf{q} = \mathbf{q}(T, \mathbf{B}, \mathbf{X}, \nabla T); \tag{4.80}$$

$$\frac{\mathrm{d}\mathbf{X}}{\mathrm{d}t} = \mathbf{G}(T, \mathbf{B}, \mathbf{X}, \nabla T); \tag{4.81}$$

Then, the material time derivative of free energy is given by

$$\frac{\mathrm{d}f}{\mathrm{d}t} = \frac{\mathrm{d}u}{\mathrm{d}t} - s\frac{\mathrm{d}T}{\mathrm{d}t} - T\frac{\mathrm{d}s}{\mathrm{d}t} = \frac{\partial f}{\partial T}\frac{\mathrm{d}T}{\mathrm{d}t} + \frac{\partial f}{\partial \mathbf{B}} : \frac{\mathrm{d}\mathbf{B}}{\mathrm{d}t} + \frac{\partial f}{\partial \mathbf{X}} : \frac{\mathrm{d}\mathbf{X}}{\mathrm{d}t} \tag{4.82}$$

With the help of Eq. (2.53), we have

$$\rho T\frac{\mathrm{d}s_{\mathrm{irr}}}{\mathrm{d}t} = -\frac{\mathbf{q}\cdot\nabla T}{T} + \mathbf{T} : \mathbf{D} - \rho\left(\frac{\mathrm{d}f}{\mathrm{d}t}\right)_T \geq 0 \tag{4.83}$$

where

$$\rho\left(\frac{\mathrm{d}f}{\mathrm{d}t}\right)_T = \left(2\rho\mathbf{B}\cdot\frac{\partial f}{\partial \mathbf{B}}\right) : \mathbf{D} + \rho\frac{\partial f}{\partial \mathbf{X}} : \mathbf{G} \tag{4.84}$$

Smart mathematical trick of Coleman and Gurtin (1967) gives

$$\mathbf{T} = 2\rho\mathbf{B}\cdot\frac{\partial f}{\partial \mathbf{B}}, \tag{4.85}$$

$$s = -\frac{\partial f}{\partial T}, \tag{4.86}$$

$$\frac{\partial f}{\partial \nabla T} = \mathbf{0}, \tag{4.87}$$

and

$$\rho\frac{\partial f}{\partial \mathbf{X}} : \mathbf{G} + \frac{\mathbf{q}\cdot\nabla T}{T} \leq 0 \tag{4.88}$$

From Eq. (4.87), it is obvious that free energy, entropy, and stress are independent of temperature gradient (Coleman and Gurtin 1967). Then, constitutive theory is to specify the structures of functions such as $f(T, \mathbf{B}, \mathbf{X})$, $\mathbf{G}(T, \mathbf{B}, \mathbf{X}, \nabla T)$, and $\mathbf{q}(T, \mathbf{B}, \mathbf{X}, \nabla T)$. Equations (4.83) and (4.86) play the role of constraints of the functions.

4.3.2 Application to One-Dimensional Model

Consider the Maxwell model. This intuitive model implicitly says that $G_M > 0$ and $\eta_M > 0$. We shall show that these inequalities hold because of the second law. It is natural that free energy is related to energy storage. Then, one may think of free energy as a function of elastic strain such that

$$f = \frac{G_M}{2}\gamma_e^2 + f_o(T) = \frac{G_M}{2}(\gamma - \gamma_v)^2 + f_o(T) \tag{4.89}$$

where G_M is considered as a function of temperature. There are two cases of thermodynamic space: (T, γ, γ_e) and (T, γ, γ_v).

As for isothermal deformation, we know that $\nabla T = \mathbf{0}$. Then, the second law of Eq. (4.83) becomes

$$\sigma\frac{d\gamma}{dt} - G_M\gamma_e\frac{d\gamma_e}{dt} \geq 0 \tag{4.90}$$

or

$$\sigma\frac{d\gamma}{dt} - G_M(\gamma - \gamma_v)\left(\frac{d\gamma}{dt} - \frac{d\gamma_v}{dt}\right) \geq 0 \tag{4.91}$$

One may suggest one of the simplest evolution equations of internal variable as

$$\frac{d\gamma_v}{dt} = \frac{\gamma_e}{\lambda_M} = \frac{\gamma - \gamma_v}{\lambda_M} \tag{4.92}$$

Equation (4.92) is identical to

$$\frac{d\gamma_e}{dt} = \frac{d\gamma}{dt} - \frac{\gamma_e}{\lambda_M} \tag{4.93}$$

because $\gamma_e = \gamma - \gamma_v$.

Substitution of Eq. (4.93) into Eq. (4.90) gives

$$(\sigma - G_M\gamma_e)\frac{d\gamma}{dt} + \frac{G_M}{\lambda}\gamma_e^2 \geq 0 \tag{4.94}$$

Since $d\gamma/dt$ and γ_e can be given independently, it can be concluded that

$$\sigma = G_M\gamma_e \tag{4.95}$$

and

$$\frac{G_{\mathrm{M}}}{\lambda_{\mathrm{M}}} > 0 \tag{4.96}$$

The same results are obtained by the substitution of Eq. (4.92) into Eq. (4.91).

One-dimensional version of Eq. (4.88) is given by

$$G_{\mathrm{M}}(\gamma - \gamma_{\mathrm{v}})\frac{\mathrm{d}\gamma_{\mathrm{v}}}{\mathrm{d}t} \leq 0 \tag{4.97}$$

Substitution of Eq. (4.92) into Eq. (4.97) gives

$$-\frac{G_{\mathrm{M}}}{\lambda_{\mathrm{M}}}(\gamma - \gamma_{\mathrm{v}})^2 \leq 0 \tag{4.98}$$

Then, we obtain Eq. (4.96) again.

4.3.3 Temperature Equation

Energy balance equation, Eq. (2.53), is not convenient to predict temperature field because it does not contain time derivative of temperature. From equilibrium thermodynamics, we know that specific heat capacity at constant volume is given by

$$c_{\mathrm{V}} = -T\frac{\partial^2 f}{\partial T^2} \tag{4.99}$$

We can consider entropy as a function of temperature, strain, and internal variables: $s = s(T, \mathbf{B}, \mathbf{X})$. Then, we have

$$\begin{aligned}\frac{\mathrm{d}s}{\mathrm{d}t} &= \frac{c_{\mathrm{V}}}{T}\frac{\mathrm{d}T}{\mathrm{d}t} + \left(\frac{\partial s}{\partial \mathbf{B}}\right)_{T,\mathbf{X}} : \frac{\mathrm{d}\mathbf{B}}{\mathrm{d}t} + \left(\frac{\partial s}{\partial \mathbf{X}}\right)_{T,\mathbf{B}} : \frac{\mathrm{d}\mathbf{X}}{\mathrm{d}t} \\ &= \frac{c_{\mathrm{V}}}{T}\frac{\mathrm{d}T}{\mathrm{d}t} - \left[\frac{\partial}{\partial \mathbf{B}}\left(\frac{\partial f}{\partial T}\right)_{\mathbf{B},\mathbf{X}}\right]_{T,\mathbf{X}} : \frac{\mathrm{d}\mathbf{B}}{\mathrm{d}t} - \left[\frac{\partial}{\partial \mathbf{X}}\left(\frac{\partial f}{\partial T}\right)_{\mathbf{B},\mathbf{X}}\right]_{T\mathbf{B}} : \frac{\mathrm{d}\mathbf{X}}{\mathrm{d}t}\end{aligned} \tag{4.100}$$

Here, Eqs. (4.86) and (4.97) were used. The last two terms of Eq. (4.98) can be rewritten by

$$\left[\frac{\partial}{\partial T}\left(\frac{\mathrm{d}f}{\mathrm{d}t}\right)_T\right]_{\mathbf{B},\mathbf{X}} = \left[\frac{\partial}{\partial \mathbf{B}}\left(\frac{\partial f}{\partial T}\right)_{\mathbf{B},\mathbf{X}}\right]_{T,\mathbf{X}} : \frac{\mathrm{d}\mathbf{B}}{\mathrm{d}t} + \left[\frac{\partial}{\partial \mathbf{X}}\left(\frac{\partial f}{\partial T}\right)_{\mathbf{B},\mathbf{X}}\right]_{T\mathbf{B}} : \frac{\mathrm{d}\mathbf{X}}{\mathrm{d}t} \tag{4.101}$$

Then, we can write simply

$$\frac{\mathrm{d}s}{\mathrm{d}t} = \frac{c_\mathrm{V}}{T}\frac{\mathrm{d}T}{\mathrm{d}t} - \frac{\partial}{\partial T}\left(\frac{\mathrm{d}f}{\mathrm{d}t}\right)_T \tag{4.102}$$

With the help of Eqs. (4.51), (4.53), and (4.83), Eq. (4.102) can be rewritten by

$$\rho c_\mathrm{V}\frac{\mathrm{d}T}{\mathrm{d}t} = -\nabla\cdot\mathbf{q} + \rho r + \mathbf{T}:\mathbf{D} + \rho T^2\frac{\partial}{\partial T}\left[\frac{1}{T}\left(\frac{\mathrm{d}f}{\mathrm{d}t}\right)_T\right] \tag{4.103}$$

If f is known as a function of state variables and if the evolution equations of both $\mathbf{B}$ and internal variable $\mathbf{X}$, then Eq. (4.103) allows us to calculate temperature field.

The first and second terms in the right-hand side of Eq. (4.103) represent heat transfer, and the third term indicates stress power. It can be shown that the last term is the rate of internal energy at constant temperature (see Problem [1]). Hence, Eq. (4.103) becomes

$$\rho c_\mathrm{V}\frac{\mathrm{d}T}{\mathrm{d}t} = -\nabla\cdot\mathbf{q} + \rho r + \mathbf{T}:\mathbf{D} - \rho\left(\frac{\mathrm{d}u}{\mathrm{d}t}\right)_T \tag{4.104}$$

The stress power can be interpreted as the effect of mechanical work on deformation of material. The last term of Eq. (4.104) can be interpreted as the rate of energy storage in the material. Hence, the last two terms imply that temperature is altered by the part of mechanical work, which is obtained by excluding the kinetic energy and energy storage in the material from the total mechanical work.

Problem 4

[1] In equilibrium thermodynamics, the following equation is known as the Gibbs–Helmholtz equation:

$$U = -T^2\left[\frac{\partial}{\partial T}\left(\frac{F}{T}\right)\right]_v; \tag{4.a}$$

$$H = -T^2\left[\frac{\partial}{\partial T}\left(\frac{G}{T}\right)\right]_p \tag{4.b}$$

Derive Eqs. (4.a) and (4.b).

[2] The van der Waals equation is an empirical equation of state such that

$$p = \frac{RT}{\overline{V}-b} - \frac{a}{\overline{V}^2} \tag{4.c}$$

where R is the gas constant, $\overline{V}$ is the molar volume, and a and b are material parameters. Derive the Helmholtz free energy from Eq. (4.c). Note that the Helmholtz free energy of ideal gas can be derived by $p\overline{V} = RT$ as follows:

$$F^{IG}\left(\overline{V}, T, n\right) = -nRT\log\left(T^{3/2}\overline{V}\right) + nc^{\mathrm{IG}}T \tag{4.d}$$

where n is the mole number of molecules and c^{IG} is the integration constant. Eq. (4.d) was derived by the integration of

$$p = -\left(\frac{\partial F^{\mathrm{IG}}}{\partial \overline{V}}\right)_{T,n} \tag{4.e}$$

[3] Derive Eqs. (4.58) and (4.65)
[4] Derive Eqs. (4.72) and (4.83).
[5] Derive Eqs. (4.103) and (4.104).

5 Principle of Constitutive Equation

5.1 Upper-Convective Maxwell Model

In Sect. 3, it was mentioned that the material time derivative of stress is not appropriate. Consider that we are interested in the generalization of the one-dimensional Maxwell model. One may imagine that every material particle is assigned to identical Maxwell model but different orientation. Here, the orientation of the Maxwell model implies the principal axis of the stress. As shown in Fig. 2, the Maxwell element flows along the path of the corresponding material particle.

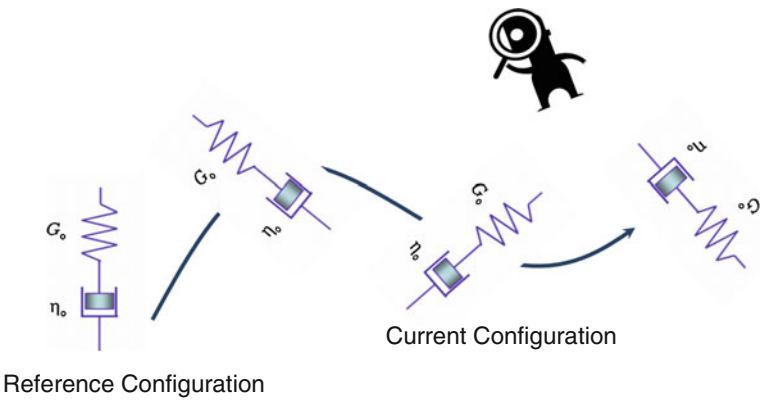

Fig. 2 Convection of Maxwell element in flow

The convective motion of the Maxwell element includes translation, rotation, and pure deformation.

However, the observer cannot see the motion in detail. The observer can detect only the stress field as a function of time in a fixed frame of coordinate system. The stress observed at time of t can be written by

$$\mathbf{T}(t) = T_{ik}(t)\,\mathbf{e}_i\mathbf{e}_k \tag{5.1}$$

where the base vectors $\{\mathbf{e}_i\}$ are those of the fixed frame of coordinate. If the stress is expressed in terms of the basis imbedded in the convective motion of material particles, which must be aligned in the orientation of the Maxwell model, then we have

$$\mathbf{T}(t) = \widetilde{T}^{ik}(t)\,\mathbf{g}_i(t)\,\mathbf{g}_k(t) \tag{5.2}$$

where $\{\mathbf{g}^i\}$ are the basis imbedded in the flow. The material time derivative of the stress tensor is given by

$$\frac{\mathrm{d}\mathbf{T}}{\mathrm{d}t} = \frac{\mathrm{d}T_{ik}}{\mathrm{d}t}\mathbf{e}_i\mathbf{e}_k = \frac{\mathrm{d}\widetilde{T}^{ik}}{\mathrm{d}t}\mathbf{g}_i\mathbf{g}_k + \widetilde{T}^{ik}\frac{\mathrm{d}\mathbf{g}_i}{\mathrm{d}t}\mathbf{g}_k + \widetilde{T}^{ik}\mathbf{g}_i\frac{\mathrm{d}\mathbf{g}_k}{\mathrm{d}t} \tag{5.3}$$

However, the origin of the stress is the extension of the Maxwell element. Hence, the Maxwell model must be

$$\lambda_{\mathrm{M}}\frac{\mathrm{d}\widetilde{T}^{ik}}{\mathrm{d}t}\mathbf{g}_i\mathbf{g}_k + \widetilde{T}^{ik}\mathbf{g}_i\mathbf{g}_k = 2\eta_{\mathrm{M}}\mathbf{D} \tag{5.4}$$

This is the correct three-dimensional extension of the Maxwell model. We have to find the basis $\{\mathbf{g}^i\}$ at each time for using Eq. (5.4), which is not convenient. We need a translation of the component-wise time derivative in terms of easily measurable field quantities. In order to do that, we have to know how to construct the convective basis $\{\mathbf{g}^i\}$ from the orthonormal basis $\{\mathbf{e}_i\}$.

The motion of material particles, Eq. (1.1), can be interpreted as a coordinate transform. The covariant base vector of the reference configuration is given by

$$\tilde{\mathbf{g}}_i = \frac{\partial\tilde{\mathbf{x}}}{\partial\tilde{x}_i} \tag{5.5}$$

Then, the covariant base vector of the current configuration is given by

$$\mathbf{g}_i = \frac{\partial\mathbf{x}}{\partial\tilde{x}_i} = \mathbf{F}\cdot\tilde{\mathbf{g}}_i \tag{5.6}$$

As for contravariant basis, we know that

$$\tilde{\mathbf{g}}_i \cdot \tilde{\mathbf{g}}^k = \mathbf{g}_i \cdot \mathbf{g}^k = \delta_i^k \tag{5.7}$$

Hence, it is obvious that

$$\mathbf{F} = \mathbf{g}_k \tilde{\mathbf{g}}^k; \tag{5.8a}$$

$$\mathbf{F}^{-1} = \tilde{\mathbf{g}}_k \mathbf{g}^k \tag{5.8b}$$

With the help of Eq. (5.8a), we obtain

$$\mathbf{g}^k = \mathbf{F}^{-T} \cdot \tilde{\mathbf{g}}^k \tag{5.9}$$

For simplicity, take the Cartesian coordinate system of the observer as the coordinate system of the reference coordinate system. This simplification gives

$$\tilde{\mathbf{g}}_i = \tilde{\mathbf{g}}^i = \mathbf{e}_i, \tag{5.10}$$

$$\mathbf{g}_i = \mathbf{F} \cdot \mathbf{e}_i, \tag{5.11}$$

and

$$\mathbf{g}^i = \mathbf{F}^{-T} \cdot \mathbf{e}_i \tag{5.12}$$

From Eq. (5.3), application of Eq. (5.11) gives

$$\overset{\triangledown}{\mathbf{T}} \equiv \frac{\mathrm{d}\widetilde{T}^{ik}}{\mathrm{d}t} \mathbf{g}_i \mathbf{g}_k = \frac{\mathrm{d}\mathbf{T}}{\mathrm{d}t} - \mathbf{L} \cdot \mathbf{T} - \mathbf{T} \cdot \mathbf{L}^T \tag{5.13}$$

Equation (5.13) is the definition of the *upper-convective time derivative*, and the modified Maxwell model of Eq. (5.4) is called the *upper-convective Maxwell model* (*UCM*):

$$\lambda_{\mathrm{M}} \overset{\triangledown}{\mathbf{T}} + \mathbf{T} = 2\eta_{\mathrm{M}} \mathbf{D} \tag{5.14}$$

This is a three-dimensional extension of the Maxwell model. However, this extension is not general but is a model-based extension. We need more general principle for constitutive model which is not based on a particular model.

It is noteworthy that the process of reasoning the UCM exploits the notion that the constitutive equation must be independent of the observer. We need to know how differently various tensorial quantities are recognized by different observers.

5.2 *Principle of Material Frame Indifference*

5.2.1 Change of Observer

Consider two observers: The observer 1 is fixed, while the observer 2 moves with translation and rotation as shown in Fig. 3. The two observers are assumed to share the same coordinate system when they see the reference configuration. For simplicity, we consider only Cartesian coordinate system. Since the motion of the observer 2 is that of rigid body, the origin of the observer 2 can be described by a vector-valued function $\mathbf{c}(t)$, while the basis of observer 2 can be described by

$$\mathbf{u}_i(t) = \mathbf{Q}(t) \cdot \mathbf{e}_i \tag{5.15}$$

where $\mathbf{Q}(t) = Q_{mn}\mathbf{e}_m\mathbf{e}_n$ is an orthogonal tensor which has the initial condition of $\mathbf{Q}(t=0) = \mathbf{I}$ and $\{\mathbf{e}_i\}$ are the basis of the observer 1.

A material particle is seen as $\mathbf{x}$ by the observer 1, while the same material particle is seen as $\mathbf{x}^*$ by the observer 2. Then, we have

$$\mathbf{x}^* = \mathbf{x} - \mathbf{c}(t) \tag{5.16}$$

The same material particle has different coordinates depending on the observers as follows:

$$\text{Observer 1} \quad x_i = \mathbf{e}_i \cdot \mathbf{x} \tag{5.17}$$

$$\text{Observer 2} \quad x_i^* = \mathbf{u}_i \cdot \mathbf{x}^* \tag{5.18}$$

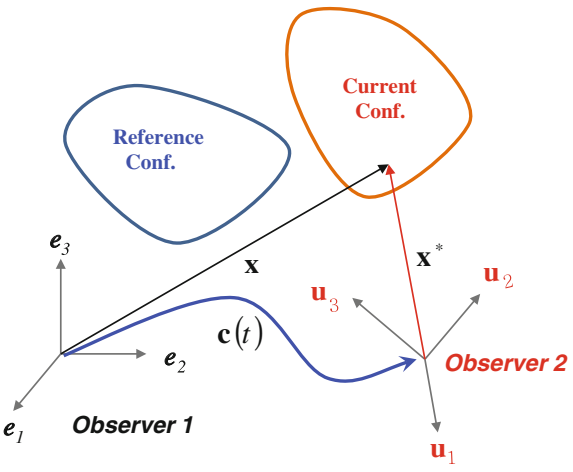

Fig. 3 Two observers

With the help of Eqs. (5.5) and (5.16), we can find the relation between the two coordinates

$$x_i^* = Q_{ki}x_k + \bar{c}_i \tag{5.19}$$

Here, we introduced $\bar{c}_i = -Q_{ki}c_k$ for the simplification of notation. Equation (5.19) can be rewritten by

$$\mathbf{x}^* = \mathbf{Q}^T \cdot \mathbf{x} + \bar{\mathbf{c}} \tag{5.20}$$

Note that both x_k and x_i^* are real-valued functions of material coordinates and time. Here, we introduced the asterisk symbol in order to denote the tensorial quantity recognized by the observer 2. Since the component of deformation gradient tensor is seen by the observer 1 as $F_{ik} = \partial x_i/\partial \tilde{x}_k$, that of deformation gradient tensor seen by the observer 2 is

$$F_{ik}^* = \frac{\partial x_i^*}{\partial \tilde{x}_k} = Q_{mi}\frac{\partial x_m}{\partial \tilde{x}_k} = Q_{mi}F_{mk} \tag{5.21}$$

Here, Eq. (5.19) was used. Note that $\mathbf{F}^* = F_{ik}^*\mathbf{e}_i\mathbf{e}_k$. Equation (5.21) can be rewritten by

$$\mathbf{F}^* = \mathbf{Q}^T \cdot \mathbf{F} \tag{5.22}$$

From Eq. (5.22), we obtain the following:

$$\mathbf{B}^* = \mathbf{Q}^T \cdot \mathbf{B} \cdot \mathbf{Q}; \tag{5.23}$$

$$\mathbf{C}^* = \mathbf{C} \tag{5.24}$$

From Eq. (5.19), we can calculate the velocity as follows:

$$\begin{aligned} \mathbf{v}^* &= \frac{\mathrm{d}}{\mathrm{d}t}x_i^*\mathbf{e}_i = \left(\frac{\mathrm{d}Q_{ki}}{\mathrm{d}t}x_k + Q_{ki}v_k + \frac{\mathrm{d}\bar{c}_i}{\mathrm{d}t}\right)\mathbf{e}_i \\ &= \frac{\mathrm{d}\mathbf{Q}^T}{\mathrm{d}t} \cdot \mathbf{x} + \mathbf{Q}^T \cdot \mathbf{v} + \frac{\mathrm{d}\bar{\mathbf{c}}}{\mathrm{d}t} \end{aligned} \tag{5.25}$$

Differentiation of $\mathbf{v}^*$ with respect to $\mathbf{x}^*$ gives

$$\mathbf{L}^* = \mathbf{Q}^T \cdot \mathbf{L} \cdot \mathbf{Q} + \mathbf{Q}^T \cdot \frac{\mathrm{d}\mathbf{Q}}{\mathrm{d}t} \tag{5.26}$$

Then, we also have

$$\mathbf{D}^* = \mathbf{Q}^T \cdot \mathbf{D} \cdot \mathbf{Q} \tag{5.27}$$

Because of the identity such that

$$\frac{\mathrm{d}\mathbf{I}}{\mathrm{d}t} = \mathbf{Q}^T \cdot \frac{\mathrm{d}\mathbf{Q}}{\mathrm{d}t} + \frac{\mathrm{d}\mathbf{Q}^T}{\mathrm{d}t} \cdot \mathbf{Q} = \mathbf{0} \tag{5.28}$$

As for spin tensor, we have

$$\mathbf{W}^* = \mathbf{Q}^T \cdot \mathbf{W} \cdot \mathbf{Q} + \mathbf{Q}^T \cdot \frac{\mathrm{d}\mathbf{Q}}{\mathrm{d}t} \tag{5.29}$$

Infinitesimal difference of $\mathbf{x}^*$ is given by $\mathrm{d}\mathbf{x}^* = \mathbf{x}^*(\tilde{\mathbf{x}} + \mathrm{d}\tilde{\mathbf{x}}, t) - \mathbf{x}^*(\tilde{\mathbf{x}}, t)$. Then, Eq. (5.20) gives

$$\mathrm{d}\mathbf{x}^* = \mathbf{Q}^T \cdot \mathrm{d}\mathbf{x} = \mathbf{Q}^T \cdot \mathbf{F} \cdot \mathrm{d}\tilde{\mathbf{x}} = \mathbf{F}^* \cdot \mathrm{d}\tilde{\mathbf{x}} \tag{5.30}$$

If two arbitrary vectors $\mathbf{u}$ and $\mathbf{w}$ follow $\mathbf{u}^* = \mathbf{Q}^T \cdot \mathbf{u}$ and $\mathbf{w}^* = \mathbf{Q}^T \cdot \mathbf{w}$, then it is obvious that

$$\mathbf{u}^* \times \mathbf{w}^* = \mathbf{Q}^T \cdot (\mathbf{u} \times \mathbf{w}) \tag{5.31}$$

and

$$\mathbf{u}^* \mathbf{w}^* = \mathbf{Q}^T \cdot (\mathbf{u}\mathbf{w}) \cdot \mathbf{Q} \tag{5.32}$$

Furthermore, if a tensor $\mathbf{A}$ obeys $\mathbf{A}^* = \mathbf{Q}^T \cdot \mathbf{A} \cdot \mathbf{Q}$, then we know that when $\mathbf{w} = \mathbf{A} \cdot \mathbf{u}$,

$$\mathbf{A}^* \cdot \mathbf{u}^* = \mathbf{Q}^T \cdot (\mathbf{A} \cdot \mathbf{u}) = \mathbf{w}^* \tag{5.33}$$

With the help of Eqs. (1.33), (5.30), and (5.31), the differential area element satisfies the following identity:

$$\mathrm{d}\mathbf{a}^* = \mathbf{Q}^T \cdot \mathrm{d}\mathbf{a} \tag{5.34}$$

Since the stress vector issuing from a material point, it is obvious that $\mathbf{t}^* = \mathbf{Q}^T \cdot \mathbf{t}$. Then, Eq. (5.33) leads to

$$\mathbf{t}^\circ = \mathbf{T}^* \cdot \mathrm{d}\mathbf{a}^* \tag{5.35}$$

and

$$\mathbf{T}^* = \mathbf{Q}^T \cdot \mathbf{T} \cdot \mathbf{Q} \tag{5.36}$$

5.2.2 Objective Vector and Tensor

So far, we discussed the consequences of the change of observers. Some vectors follow the relation $\mathbf{u}^* = \mathbf{Q}^T \cdot \mathbf{u}$, while others do not. Similarly, some tensors follow the relation $\mathbf{A}^* = \mathbf{Q}^T \cdot \mathbf{A} \cdot \mathbf{Q}$, while others do not. The *Eulerian objective vectors and tensors* are defined as the ones such that

$$\mathbf{u}^* = \mathbf{Q}^T(t) \cdot \mathbf{u} \tag{5.37}$$

and

$$\mathbf{A}^* = \mathbf{Q}^T(t) \cdot \mathbf{A} \cdot \mathbf{Q}(t) \tag{5.38}$$

Meanwhile, right Cauchy–Green tensor $\mathbf{C}$ and Piola–Kirchhoff stress of the 2nd kind are invariant for the change of observer. Note that

$$\left(\mathbf{F}^{-1}\right)^* = \mathbf{F}^{-1} \cdot \mathbf{Q}(t); \quad \left(\mathbf{F}^{-T}\right)^* = \mathbf{Q}^T(t) \cdot \mathbf{F}^{-T} \tag{5.39}$$

Equation (5.39) immediately gives

$$\begin{aligned} \widetilde{\mathbf{T}}^* &= \det(\mathbf{F}^*)\left(\mathbf{F}^{-1}\right)^* \cdot \mathbf{T}^* \cdot \left(\mathbf{F}^{-T}\right)^* \\ &= \det(\mathbf{F})\, \mathbf{F}^{-1} \cdot \mathbf{Q} \cdot \mathbf{Q}^T \cdot \mathbf{T} \cdot \mathbf{Q} \cdot \mathbf{Q}^T \cdot \mathbf{F}^{-T} \\ &= \widetilde{\mathbf{T}} \end{aligned} \tag{5.40}$$

We define *Lagrangian objective tensors* as $\mathbf{A}^* = \mathbf{A}$.

The definition of relative deformation gradient tensor, Eq. (1.59), implies that

$$\mathbf{F}_t(\tau) = \mathbf{F}(\tau) \cdot \mathbf{F}^{-1}(t) \tag{5.41}$$

The use of Eq. (5.22) gives

$$\mathbf{F}_t^*(\tau) = \mathbf{Q}^T(\tau) \cdot \mathbf{F}_t(\tau) \cdot \mathbf{Q}(t) \tag{5.42}$$

Consequently, Eq. (1.66) gives

$$\mathbf{B}_t^*(\tau) = \mathbf{Q}^T(\tau) \cdot \mathbf{B}_t(\tau) \cdot \mathbf{Q}(\tau) \tag{5.43}$$

and

$$\mathbf{C}_t^*(\tau) = \mathbf{Q}^T(t) \cdot \mathbf{C}_t(\tau) \cdot \mathbf{Q}(t) \tag{5.44}$$

In summary, the objective tensors are Cauchy stress tensor $\mathbf{T}$, left Cauchy–Green tensor $\mathbf{B}$, right relative Cauchy–Green tensor $\mathbf{C}_t(\tau)$, relative finger tensor $\mathbf{C}_t^{-1}(\tau)$, and deformation rate tensor $\mathbf{D}$. It is obvious that the identity tensor $\mathbf{I}$ is both Eulerian and Lagrangian objective tensors.

5.2.3 Principle of Material Frame Indifference

Several classical constitutive equations are introduced in Sect. 3. Since Cauchy stress is an Eulerian objective tensor, the formulation of stress tensor, constitutive equation, must obey the transform rule of Eulerian objective tensor. Since $\mathbf{I}$, $\mathbf{B}$, and $\mathbf{D}$ are Eulerian objective tensors, it is obvious that the constitutive equations of Newtonian fluid and hyperelasticity follow the transform rule. The *principle of material frame-indifference* states that constitutive formulation must follow the transform rule (Truesdell and Noll 2004). If Piola–Kirchhoff stress of the 2nd kind is considered, then the formulation must consist of Lagrangian objective terms.

As for upper-convective Maxwell model, it obeys the principle of material frame-indifference. To show this, we have to show that the upper-convective time derivative satisfies

$$\overset{\nabla}{\mathbf{T}}{}^* = \mathbf{Q}^T(t) \cdot \overset{\nabla}{\mathbf{T}} \cdot \mathbf{Q}(t) \tag{5.45}$$

Note that

$$\frac{\mathrm{d}}{\mathrm{d}t}\left(\mathbf{Q}^T \cdot \mathbf{T} \cdot \mathbf{Q}\right) = \mathbf{Q}^T \cdot \frac{\mathrm{d}\mathbf{T}}{\mathrm{d}t} \cdot \mathbf{Q} + \frac{\mathrm{d}\mathbf{Q}^T}{\mathrm{d}t} \cdot \mathbf{T} \cdot \mathbf{Q} + \mathbf{Q}^T \cdot \mathbf{T} \cdot \frac{\mathrm{d}\mathbf{Q}}{\mathrm{d}t} \tag{5.46}$$

and

$$(\mathbf{L} \cdot \mathbf{T} + \mathbf{T} \cdot \mathbf{L})^* = \mathbf{Q}^T \cdot (\mathbf{L} \cdot \mathbf{T} + \mathbf{T} \cdot \mathbf{L}) \cdot \mathbf{Q} - \frac{\mathrm{d}\mathbf{Q}^T}{\mathrm{d}t} \cdot \mathbf{T} \cdot \mathbf{Q} - \mathbf{Q}^T \cdot \mathbf{T} \cdot \frac{\mathrm{d}\mathbf{Q}}{\mathrm{d}t} \tag{5.47}$$

Here, we used

$$\frac{\mathrm{d}\mathbf{Q}}{\mathrm{d}t} = -\mathbf{Q} \cdot \frac{\mathrm{d}\mathbf{Q}^T}{\mathrm{d}t} \cdot \mathbf{Q}; \quad \frac{\mathrm{d}\mathbf{Q}^T}{\mathrm{d}t} = -\mathbf{Q}^T \cdot \frac{\mathrm{d}\mathbf{Q}}{\mathrm{d}t} \cdot \mathbf{Q}^T \tag{5.48}$$

Equation (5.45) is immediately obtained by the application of Eqs. (5.46) and (5.47) to the definition of the upper-convective time derivative. Hence, the UCM

model follows the principle of material frame-indifference. Such constitutive model is called objective constitutive equation.

Note that *objective time derivatives* obey Eq. (5.45). It is known that the following time derivatives are also objective:

$$\overset{\Delta}{\mathbf{T}} \equiv \frac{\mathrm{d}\mathbf{T}}{\mathrm{d}t} + \mathbf{L}^T \cdot \mathbf{T} + \mathbf{T} \cdot \mathbf{L} \tag{5.49}$$

and

$$\overset{\mathrm{O}}{\mathbf{T}} \equiv \frac{\mathrm{d}\mathbf{T}}{\mathrm{d}t} - \mathbf{W} \cdot \mathbf{T} + \mathbf{T} \cdot \mathbf{W} \tag{5.50}$$

Equation (5.49) is the *lower-convective time derivative*, and Eq. (5.50) is the *Jaumann time derivative*. Object time derivatives satisfy the principle of material frame-indifference.

Problem 5

[1] Derive Eqs. (2.a) and (2.b).
[2] Derive Eq. (5.14).
[3] Derive Eq. (5.26).
[4] Derive Eq. (5.39).
[5] Derive Eq. (5.46).
[6] Show that the lower-convective time derivative and the Jaumann time derivative are objective.
[7] Show that

$$\mathbf{R}^* = \mathbf{Q}^T \cdot \mathbf{R}; \tag{5.a}$$

$$\mathbf{U}^* = \mathbf{U}; \tag{5.b}$$

$$\mathbf{V}^* = \mathbf{Q}^T \cdot \mathbf{V} \cdot \mathbf{Q} \tag{5.c}$$

[8] Show that for any tensor field,

$$\overset{\mathrm{O}}{\mathbf{A}} = \frac{1}{2}\left(\overset{\nabla}{\mathbf{A}} + \overset{\Delta}{\mathbf{A}}\right) \tag{5.d}$$

[9] Consider a vector field obeying

$$\frac{\mathrm{d}\mathbf{u}}{\mathrm{d}t} = \mathbf{L} \cdot \mathbf{u} - \zeta \mathbf{D} \cdot \mathbf{u} \tag{5.e}$$

where ζ is a positive constant. Then, derive that

$$\overset{\nabla}{\mathbf{G}} + \zeta(\mathbf{D}\cdot\mathbf{G} + \mathbf{G}\cdot\mathbf{D}) = \mathbf{0} \tag{5.f}$$

where $\mathbf{G} = \mathbf{uu}$.

References

G.B. Arfken, H.J. Weber, *Mathematical Methods for Physicists* (Harcourt Sci. & Tech., 2001)

R. Aris, *Vectors, Tensors, and the Basic Equations of Fluid Mechanics* (Dover, New York, 1962)

R.L. Bagley, P.J. Torvik, A theoretical basis for the application of fractional calculus to viscoelasticity. J. Rheol. **27**, 201–210 (1983)

R.B. Bird, R.C. Armstrong, O. Hassager, *Dynamics of Polymeric Liquids Vol. 1. Fluid Mechanics*, vol. 1 (Wiley, London, 1987)

R.B. Bird, W.E. Stewart, E.N. Lightfoot, *Transport Phenomena*, 2nd edn. (Wiley, London, 2002)

H.B. Callen, *Thermodynamics and Introduction to Thermostatistics*, 2nd edn. (Wiley, London, 1985)

B.D. Coleman, M.E. Gurtin, Thermodynamics with internal variables. J. Chem. Phys. **47**, 597–613 (1967)

W.E. Deen, *Analysis of Transport Phenomena* (Oxford University Press, Oxford, 1998)

S.R. De Groot, P. Mazur, *Non-Equilibrium Thermodynamics* (Dover, 1984)

P. Haupt, *Continuum Mechanics and Theory of Materials* (Springer, Berlin, 2000)

K. Huang, *Statistical Mechanics* (Wiley, London, 1963)

D. Jou, J. Casas-Vázquez, G. Lebon, *Extended Irreversible Thermodynamics* (Springer, Berlin, 1996)

S. Kim, S.J. Karrila, *Microhydrodynamics Principles and Selected Applications* (Dover, New York, 2005)

L.D. Landau, E.M. Lifshitz, *Theory of Elasticity*, 3rd edn. (Pergamon Press, Oxford, 1986)

S.-K. Ma, *Statistical Mechanics* (World Scientific, Singapore, 1985)

G. Marin, W.W. Graessley, Viscoelastic properties of high molecular weight polymers in the molten state I. Study of narrow molecular weight distribution samples. Rheol. Acta **16**, 527–533 (1977)

G.A. Maugin, *The Thermomechanics of Nonlinear Irreversible Behavior*s (World Scientific, Singapore, 1999)

G.A. Maugin, W. Muschik, Thermodynamics with internal variables. Part I. General concepts. J. Non-Equilib. Thermodyn. **19**, 217–249 (1994)

D.A. McQuarrie, *Statistical Mechanics* University (Science Books, 2000)

W. Muschik, Internal variables in non-equilibrium thermodynamics. J. Non-Equilib. Thermodyn. **15**, 127–137 (1990)

R.W. Ogden, *Non-linear Elastic Deformations* (Dover, New York, 1984)

B. O'Neill, *Elementary Differential Geometry*, 2nd edn. (Academic Press, New York, 2006)

E. Riande, R. Díaz-Calleja, M.G. Prolongo, R.M. Masegosa, C. Salom, *Polymer Viscoelasticity, stress and strain in practice* (Marcel Dekker, New York, 2000)

M.H. Sadd, *Elasticity, Theory, Applications, and Numerics*, 2nd edn. (Academic Press, New York, 2009)

W. Smit, H. de Vries, Rheological models containing fractional derivatives. Rheol. Acta **9**, 525–534 (1970)

R.I. Tanner, *Engineering Rheology,* 2nd edn. (Oxford University Press, Oxford, 2002)
C. Truesdell, W. Noll, *The Non-Linear Field Theories of Mechanics,* 3rd edn. (Springer, Berlin, 2004)
N.W. Tschoegl, *The Phenomenological Theory of Linear Viscoelastic Behavior* (Springer, Berlin, 1989)
K.C. Valanis, A theory of viscoplasticity without a yield surface: part I. General theory. Arch. Mech. **23**, 517–533 (1971)

Chapter 3
Statistical Mechanics

Abstract This chapter is included because statistical mechanical theories play an important role in molecular theories of polymer viscoelasticity. Hence, this chapter is a brief review of statistical mechanics which is focused on the explanation of stress in terms of molecular interactions. Section 1 addresses probability theory which will be used in the other sections. Section 2 is devoted to equilibrium statistical mechanics based on classical mechanics because quantum effect is rare in polymer viscoelasticity. Section 3 deals with Brownian motion which is the core of polymer motion in solution and molten states.

Statistical mechanics plays an important role in the development of molecular theories of polymer rheology. Equilibrium statistical mechanics is necessary for the molecular theory of rubber elasticity because it is based on the statistical mechanical theory of chain conformation. Molecular theory of polymer viscoelasticity is also based on the statistical mechanics of Brownian motion. Hence, we shall introduce a brief summary of the statistical mechanical theories for easier understanding the molecular theory of polymer viscoelasticity.

Statistical mechanics is classified as the background mechanics. If it is based on classical mechanics, then it is called classical statistical mechanics. On the other hand, quantum statistical mechanics is based on quantum mechanics. This classification reflects the main purpose of statistical mechanics that explains the macroscopic phenomena in terms of molecular motions. Of course, quantum statistical mechanics is more fundamental than classical statistical mechanics. Classical statistical mechanics can be considered as a good approximation of quantum statistical mechanics. However, classical statistical mechanics is sufficient in this book because the quantum effect is negligible in most of the physical phenomena related to polymer.

State variables in classical mechanics are positions and momenta of all constituent particles of the system. Here, the particles mean molecules or atoms. These state variables are called microstate variables compared with the state variables of thermodynamics, which are macrostate variables. Although the microstate variables are deterministic from the viewpoint of classical mechanics, extremely large degree

K.S. Cho, *Viscoelasticity of Polymers*, Springer Series
in Materials Science 241, DOI 10.1007/978-94-017-7564-9_3

of freedom can be treated by neither the second law of Newtonian mechanics nor the Hamilton equation of motion. Hence, statistical mechanics adopts statistical treatment for motions of the particles. When N-particle system is considered, lack of information on the microstate variables of the surroundings makes us see the phenomena occurring in the system as stochastic processes. In addition, it is practically impossible to specify all initial conditions of the microstate variables of the system as well as those of the surroundings. Therefore, we need some knowledge of probability theory which is essential in statistical mechanics. The readers who want more are recommended to read the textbooks of statistical mechanics such as Huang (1963), Chandler (1987), McQuarrie (2000), Schwabl (2006) and Tuckerman (2010). Although analytical mechanics is necessary to understand classical statistical mechanics, we omit the review of analytical mechanics such as Lagrangian and Hamiltonian mechanics in this book. If necessary, read Landau and Lifshitz (1976), Thornton and Marion (2004).

1 Probability Theory

Statistical mechanics deals with probability distribution of huge number of state variables. Let the distribution function denoted by $P(\{\xi_k\})$, where $\{\xi_k\}$ are *microstate variables*. When N-particle system is considered, we can say that $\{\xi_k\}$ consists of $3N$ components of the positions of N particles $\{\mathbf{r}_1, \mathbf{r}_2, \ldots, \mathbf{r}_N\}$ and $3N$ components of the momenta of N particles $\{\mathbf{p}_1, \mathbf{p}_2, \ldots, \mathbf{p}_N\}$. Therefore, the number of microstate variables is $6N$ and $\{\xi_k\} = \{\mathbf{r}_1, \ldots, \mathbf{r}_N, \mathbf{p}_1, \ldots, \mathbf{p}_N\}$. The *phase space* is the $6N$-dimensional space formed by the microstate variables. For simplicity, we use the notation such that

$$\Gamma = \{\xi_k\}; \quad \mathrm{d}\Gamma = \mathrm{d}\xi_1 \mathrm{d}\xi_2 \ldots \mathrm{d}\xi_{6N} \tag{1.1}$$

The *Hamiltonian* of the N-particle system is given by the sum of kinetic and potential energies of the particles in the system:

$$H = \sum_{\alpha=1}^{N} \frac{\mathbf{p}_\alpha \cdot \mathbf{p}_\alpha}{2m_\alpha} + U(\{\mathbf{r}_\alpha\}) \tag{1.2}$$

where $m_\alpha, \mathbf{p}_\alpha$, and $\mathbf{r}_\alpha$ are, respectively, mass, momentum, and position of the αth particle. Note that the Hamiltonian becomes the total mechanical energy when the potential energy $U(\{\mathbf{r}_\alpha\})$ is not dependent explicitly on time (Landau and Lifshitz 1976; Thornton and Marion 2004). Equation (1.2) is an example that a macroscopic quantity is a function of microstate variable: $E = H(\Gamma)$. Lack of our knowledge on the initial conditions of the system and surroundings makes $\{\xi_k\}$ be stochastic random variables although the evolution of microstate variables is deterministic according to the Law of Newtonian mechanics. Due to the same reason, the total mechanical energy E is also a stochastic random variable. The observed mechanical

energy must be the average of the Hamiltonian Eq. (1.2). If the probability distribution $P(\Gamma, t)$ is given, the average is calculated by

$$E(t) = \langle H(\Gamma) \rangle = \int H(\Gamma) P(\Gamma, t) \mathrm{d}\Gamma \tag{1.3}$$

Similarly, Eq. (1.3) can be applied to the average of any macroscopic quantity represented by a function of microstate variables:

$$A(t) = \left\langle \widehat{A}(\Gamma) \right\rangle = \int \widehat{A}(\Gamma) P(\Gamma, t) \mathrm{d}\Gamma \tag{1.4}$$

Most interesting macroscopic quantities, say A, have their functions of microstate variables, say $\widehat{A}(\Gamma)$. Therefore, if we know every thing about the probability distribution $P(\Gamma, t)$, then it can be said that every problem about statistical mechanics is solved. What is measured by experiment is not the probability distribution but the average such as Eq. (1.4).

1.1 Moments and Cumulants

Hereafter, we shall introduce the brief summary of probability theory because the theory is helpful to understand equilibrium statistical mechanics as well as nonequilibrium statistical mechanics. For simplicity, consider the case of a single random variable ξ. When dynamics is not interesting, the probability distribution is expressed by $P(\xi)$. The nth moment of the probability distribution is defined as

$$\mu_n \equiv \langle \xi^n \rangle = \int_{-\infty}^{\infty} \xi^n P(\xi) \mathrm{d}\xi \tag{1.5}$$

Note that the probability distribution function of Eq. (1.5), called probability density function, must not be negative for any value of ξ. With the normalization condition, we know that

$$P(\xi) \geq 0; \quad \mu_0 = \int_{-\infty}^{\infty} P(\xi) \mathrm{d}\xi = 1 \tag{1.6}$$

Equation (1.6) immediately results in

$$\lim_{|\xi| \to \infty} P(\xi) = 0 \tag{1.7}$$

Hence, we know that the Fourier transform of the probability distribution exists as:

$$\hat{P}(q) = \left\langle e^{-\mathrm{i}q\xi} \right\rangle = \int_{-\infty}^{\infty} e^{\mathrm{i}q\xi} P(\xi)\mathrm{d}\xi \tag{1.8}$$

The Fourier transform is called the *characteristic function*. The uniqueness of the Fourier transform implies that the probability distribution can be uniquely determined from a given characteristic function. Note that the Taylor series expansion of the characteristic function is given by

$$\hat{P}(q) = \sum_{n=0}^{\infty} \frac{(-\mathrm{i}q)^n}{n!} \langle \xi^n \rangle \tag{1.9}$$

Equation (1.9) implies that if we know every moment, then we can determine the probability distribution. On the other hand, if we know the characteristic function, then we can calculate nth moment as follows:

$$\mu_n = \langle \xi^n \rangle = \mathrm{i}^n \left(\frac{\mathrm{d}\hat{P}}{\mathrm{d}q} \right)_{q=0} \tag{1.10}$$

Cumulant generating function is defined as

$$\hat{K}(q) = \log \hat{P}(q) \tag{1.11}$$

Assume that $\hat{K}(q)$ can be expanded as

$$\hat{K}(q) = \sum_{n=0}^{\infty} \frac{(-\mathrm{i}q)^n}{n!} \kappa_n \tag{1.12}$$

where κ_n is the nth cumulant. According to Pourahmadi (1984), it is known that if $\exp\left(\sum_{k=0}^{\infty} a_k q^k\right) = \sum_{k=0}^{\infty} c_k q^k$ then

$$c_{n+1} = \sum_{k=0}^{n} \left(1 - \frac{k}{n+1}\right) a_{n+1-k} c_k, \quad n = 0, 1, 2, \ldots \tag{1.13}$$

Replacing c_n by $(-\mathrm{i})^n \mu_n / n!$ and a_n by $(-\mathrm{i})^n \kappa_n / n!$, we have

$$\mu_{n+1} = \sum_{p=0}^{n} \binom{n}{p} \mu_{n-p} \kappa_{p+1} \tag{1.14}$$

Conversion of Eq. (1.14) gives (Berberan-Santos 2007)

$$\kappa_{n+1} = \mu_{n+1} - \sum_{p=0}^{n-1} \binom{n}{p} \mu_{n-p} \kappa_{p+1} \tag{1.15}$$

Note that $\kappa_0 = 0$ while $\mu_0 = 1$. The first three cumulants are given as:

$$\kappa_1 = \mu_1; \quad \kappa_2 = \mu_2 - \mu_1^2 = \sigma^2; \quad \kappa_3 = 2\mu_1^3 - 3\mu_1\mu_2 + \mu_3 \tag{1.16}$$

where σ is the standard deviation.

1.2 Statistical Independence

Consider two continuous random variables x_1 and x_2. We are interested in the probability that $x_1 \in I_1 = (a_1, b_1)$ and $x_2 \in I_2 = (a_2, b_2)$. Then, the *joint probability density function* $P(x_1, x_2)$ is defined as

$$\Pr(x_1 \in I_1 \text{ and } x_2 \in I_2) = \int_{a_2}^{b_2} \int_{a_1}^{b_1} P(x_1, x_2) \mathrm{d}x_1 \mathrm{d}x_2 \tag{1.17}$$

The *marginal distribution function* is the probability density function defined by

$$P_1(x_1) = \int_{-\infty}^{\infty} P(x_1, x_2) \mathrm{d}x_2 \quad \text{or} \quad P_2(x_2) = \int_{-\infty}^{\infty} P(x_1, x_2) \mathrm{d}x_1 \tag{1.18}$$

Note that $P_1(x_1)$ is the probability distribution of x_1 for any value of x_2. The meaning of $P_2(x_2)$ is understood in the same way.

The probability of $x_1 \in I_1$ whenever $x_2 \in I_2$ is a *conditional probability* such that

$$\Pr(x_1 \in I_1 | x_2 \in I_2) = \frac{\int_{a_2}^{b_2} \int_{a_1}^{b_1} P(x_1, x_2) \mathrm{d}x_1 \mathrm{d}x_2}{\int_{a_2}^{b_2} \int_{-\infty}^{\infty} P(x_1, x_2) \mathrm{d}x_1 \mathrm{d}x_2} = \frac{\int_{a_2}^{b_2} \int_{a_1}^{b_1} P(x_1, x_2) \mathrm{d}x_1 \mathrm{d}x_2}{\int_{a_2}^{b_2} P_2(x_2) \mathrm{d}x_2} \tag{1.19}$$

When we denote the event $x_k \in I_k$ by E_k, Eq. (1.19) can be rewritten by

$$\Pr(E_1 | E_2) = \frac{\Pr(E_1 \cap E_2)}{\Pr(E_2)} \tag{1.20}$$

The event E_k^C implies $x_k \notin I_k$. Then, it is obvious that $\Pr(E_k^C) = 1 - \Pr(E_k)$. If the event of x_2 does not influence the event of x_1, then the two conditional

probabilities $\Pr(E_1|E_2)$ and $\Pr(E_1|E_2^C)$ must be same. This case is called *statistical independence* of the two random variables. The statistical independence immediately results in

$$\frac{\Pr(E_1) - \Pr(E_1 \cap E_2)}{1 - \Pr(E_2)} = \frac{\Pr(E_1 \cap E_2)}{\Pr(E_2)} \tag{1.21}$$

Solving Eq. (1.21) for $\Pr(E_1 \cap E_2)$, we have

$$\Pr(E_1 \cap E_2) = \Pr(E_1)\Pr(E_2) \tag{1.22}$$

Since Eq. (1.22) holds for arbitrary intervals, statistical independence also results in

$$P(x_1 x_2) = P_1(x_1)P_2(x_2) \tag{1.23}$$

This can be expanded to the joint probability density function of N random variables. If N random variables are statistically independent, then factorization of the joint probability distribution holds the following:

$$P(x_1, x_2, \ldots, x_N) = \prod_{n=1}^{N} P_n(x_n) \tag{1.24}$$

Of course, $P_n(x_n)$ is defined as

$$P_n(x_n) = \prod_{k \neq n}^{N} \int_{-\infty}^{\infty} \mathrm{d}x_k P(x_1, x_2, \ldots, x_N) \tag{1.25}$$

1.3 The Central Limit Theorem

Consider statistically independent N random variables $\{x_k\}$. Assume that for $1 \leq k \leq N$, all the marginal distributions are identical:

$$P_k(x_k) = f(x_k) \tag{1.26}$$

We are interested in the probability distribution of y defined as

$$y = \frac{1}{\sqrt{N}} \sum_{k=1}^{N} x_k \tag{1.27}$$

The probability distribution function of y can be calculated from the joint probability density function by use of the Dirac delta function as follows:

$$\Phi_N(y) = \int_{-\infty}^{\infty} \cdots \int_{-\infty}^{\infty} \delta\left(y - \frac{1}{\sqrt{N}} \sum_{k=1}^{N} x_k\right) P(x_1, \ldots, x_N) \mathrm{d}x_1 \ldots \mathrm{d}x_N \tag{1.28}$$

Note that Eq. (1.28) holds irrespective of the statistical independence of the N random variables. The Dirac delta function extracts the events of Eq. (1.27) among the whole events of $-\infty < x_k < \infty$. This technique is often found in statistical mechanics and polymer physics. Using Eq. (6.50) in Chap. 1, Eq. (1.28) can be rewritten by

$$\Phi_N(y) = \frac{1}{2\pi} \int_{-\infty}^{\infty} \cdots \int_{-\infty}^{\infty} \left\{ \int_{-\infty}^{\infty} \exp\left[\mathrm{i}q \left(y - \frac{1}{\sqrt{N}} \sum_{k=1}^{N} x_k \right) \right] \mathrm{d}q \right\} P(x_1, \ldots, x_N) \mathrm{d}x_1 \ldots \mathrm{d}x_N \tag{1.29}$$

Changing the order of integration and using the statistical independence, we have

$$\Phi_N(y) = \frac{1}{2\pi} \int_{-\infty}^{\infty} \psi_N(q) e^{\mathrm{i}qy} \mathrm{d}q \tag{1.30}$$

where

$$\psi_N(q) = \left[\int_{-\infty}^{\infty} e^{-\mathrm{i}\frac{qx}{\sqrt{N}}} f(x) \mathrm{d}x \right]^N = \hat{f}^N\left(\frac{q}{\sqrt{N}}\right) \tag{1.31}$$

Since $\hat{f}(q)$ is the characteristic function of $f(x)$, we can replace $\hat{f}(q)$ by the cumulant generating function $\phi(q) = \log \hat{f}(q)$. Then, Eq. (1.30) becomes

$$\Phi_N(y) = \frac{1}{2\pi} \int_{-\infty}^{\infty} e^{N\phi\left(q/\sqrt{N}\right)} e^{\mathrm{i}qy} \mathrm{d}q \tag{1.32}$$

Equation (1.12) allows us to use

$$N\phi\left(\frac{q}{\sqrt{N}}\right) = \sum_{n=1}^{\infty} \frac{(-\mathrm{i})^n}{n!} \frac{\kappa_n}{N^{n/2-1}} q^n \tag{1.33}$$

The coefficients of q^n with $n > 2$ become negligible as N increases because the coefficients are proportional to $N^{1-n/2}$. Then, Eq. (1.33) can be approximated for large N by

$$N\phi\left(\frac{q}{\sqrt{N}}\right) \approx -\mathrm{i}\mu q - \frac{\sigma^2}{2}q^2 \tag{1.34}$$

where μ and σ are, respectively, mean and standard deviation of the distribution $f(x)$. Then, Eq. (1.32) can be approximated by

$$\Phi_N(y) \approx \frac{1}{2\pi}\int_{-\infty}^{\infty} \exp\left[\mathrm{i}(y-\mu)q - \frac{\sigma^2}{2}q^2\right]\mathrm{d}q = \sqrt{\frac{1}{2\pi\sigma^2}}\exp\left[-\frac{(y-\mu)^2}{2\sigma^2}\right] \tag{1.35}$$

It is noteworthy that Eq. (1.35) is based on the arbitrariness of the probability distribution $f(x)$. Hence, the *central limit theorem* is that the normalized sum of the statistically independent random variables with the identical probability density function comes to have the *Gaussian distribution function* of Eq. (1.35) as N is suitably large.

Consider a random variable x whose probability distribution function is given by $P_X(x)$. We are interested in a new random variable which is defined as $y = \phi(x)$, where the function $\phi(x)$ is a monotonically increasing function. Then, it is clear that

$$\Pr(a < x < b) = \Pr(\phi(a) < y < \phi(b)) \tag{1.36}$$

Note that Eq. (1.36) holds for arbitrary reals a and b. From Eq. (1.36), we shall derive the probability distribution $P_Y(y)$ of the new random variable y. Then, Eq. (1.36) results in

$$\begin{aligned}\int_{x-\frac{1}{2}\mathrm{d}x}^{x+\frac{1}{2}\mathrm{d}x} P_X(\xi)\mathrm{d}\xi = P_X(x)\mathrm{d}x &= \int_{\phi(x-\frac{1}{2}\mathrm{d}x)}^{\phi(x+\frac{1}{2}\mathrm{d}x)} P_Y(y)\mathrm{d}y \\ &= P_Y[\phi(x)]\frac{\mathrm{d}\phi}{\mathrm{d}x}\mathrm{d}x = P_Y(y)\frac{\mathrm{d}\phi}{\mathrm{d}x}\mathrm{d}x\end{aligned} \tag{1.37}$$

Then we have

$$P_Y(y) = \frac{P_X(x)}{\phi'(x)} = \frac{P_X\left(\phi^{-1}(y)\right)}{\phi'\left(\phi^{-1}(y)\right)} \tag{1.38}$$

where $\phi'(x) = \mathrm{d}\phi/\mathrm{d}x$ and $\phi^{-1}(y) = x$ are the inverse function of $\phi(x)$, which must exist because $\phi(x)$ is a monotonically increasing function.

When $\phi(x)$ is a monotonically decreasing function, the same procedure gives the following:

$$P_Y(y) = \frac{P_X(x)}{|\phi'(x)|} = \frac{P_X\left(\phi^{-1}(y)\right)}{\left|\phi'\left(\phi^{-1}(y)\right)\right|} \tag{1.39}$$

Return to Eq. (1.27). We are interested in a new random variable $z = \sqrt{N}\,y$. Equations (1.35) and (1.39) give the following:

$$P_N(z) = \sqrt{\frac{1}{2\pi N\sigma^2}} \exp\left[-\frac{\left(z - \sqrt{N}\mu\right)^2}{2N\sigma^2}\right] \tag{1.40}$$

This result implies that the sum of N statistically independent random variables follows the Gaussian distribution whose mean and standard deviation are, respectively, $\sqrt{N}\mu$ and $\sqrt{N}\sigma$.

The central limit theorem is important in statistics as well as various fields of physics such as Brownian motion and statistical theory of polymer chain conformation. Hence, it is necessary to study important characteristics of the Gaussian distribution.

1.4 Gaussian Distribution

The Gaussian distribution of Eq. (1.35) can be extended to n-dimensional case as follows:

$$P(\mathbf{x}) = A \exp\left[-\frac{1}{2}\mathbf{B}^{-1} : (\mathbf{x} - \bar{\mathbf{x}})(\mathbf{x} - \bar{\mathbf{x}})\right] \tag{1.41}$$

where $\mathbf{x} = (x_1, x_2, \ldots, x_n)$ is a n-dimensional random vector, $\bar{\mathbf{x}} = (\bar{x}_1, \bar{x}_2, \ldots, \bar{x}_n)$ is the mean, $\mathbf{B}^{-1}$ is a positive definite and symmetric $n \times n$ matrix, and A is the positive constant for the normalization condition:

$$A^{-1} = \sqrt{(2\pi)^n \det(\mathbf{B})} \tag{1.42}$$

This can be derived easily by using the diagonalization of $\mathbf{B}^{-1}$ and the Gaussian integral:

$$\int_{-\infty}^{\infty} e^{-ax^2} \mathrm{d}x = \sqrt{\frac{\pi}{a}} \tag{1.43}$$

We consider the case of $\bar{\mathbf{x}} = \mathbf{0}$ because the following results can be applied to the case of $\bar{\mathbf{x}} \neq \mathbf{0}$ by the transform $\mathbf{z} = \mathbf{x} - \bar{\mathbf{x}}$.

The characteristic function of the multivariate Gaussian distribution function is given by

$$\hat{P}(\mathbf{q}) = \left\langle e^{-\mathrm{i}\mathbf{q}\cdot\mathbf{x}} \right\rangle = \exp\left(-\frac{1}{2}\mathbf{q}\cdot\mathbf{B}\cdot\mathbf{q} \right) \tag{1.44}$$

Any moment of the Gaussian distribution can be calculated from the differentiation of the characteristic function as follows:

$$\left\langle x_1^{k_1} x_2^{k_2} \ldots x_n^{k_n} \right\rangle = \int x_1^{k_1} x_2^{k_2} \ldots x_n^{k_n} P(\mathbf{x}) \mathrm{d}\mathbf{x}^n = (-\mathrm{i})^m \left(\frac{\partial^m \hat{P}(\mathbf{q})}{\partial q_1^{k_1} \ldots \partial q_n^{k_n}} \right)_{\mathbf{q}=\mathbf{0}} \tag{1.45}$$

Equation (1.45) is called the *Wick's theorem*. Then, it is obvious that

$$\begin{aligned} \langle \mathbf{x} \rangle = \mathbf{0}; \quad \langle \mathbf{xx} \rangle = \mathbf{B}; \quad \langle \mathbf{xxx} \rangle = \mathbf{0}; \\ \langle \mathbf{xxxx} \rangle = \left(B_{ij}B_{kl} + B_{ik}B_{jl} + B_{il}B_{jk} \right) \mathbf{e}_i \mathbf{e}_j \mathbf{e}_k \mathbf{e}_l \end{aligned} \tag{1.46}$$

where $\mathbf{e}_i$ is the orthonormal n-dimensional vector.

If we use the notation such that $\langle \mathbf{xx} \rangle = \left\langle \mathbf{x}^2 \right\rangle$, $\langle \mathbf{xxx} \rangle = \left\langle \mathbf{x}^3 \right\rangle$, and so on, the Wick's theorem gives

$$\left\langle \mathbf{x}^{2n+1} \right\rangle = \mathbf{0} \quad \text{with} \quad n = 0, 1, \ldots \tag{1.47}$$

and we know that $\left\langle \mathbf{x}^{2n} \right\rangle$ is a combination of the components of $\mathbf{B}$.

Consider an analytic function $f(\mathbf{x})$, where $\mathbf{x}$ is the random variable of the Gaussian distribution of Eq. (1.41) with $\bar{\mathbf{x}} \neq \mathbf{0}$. Then, we are interested in $\langle \mathbf{x} f(\mathbf{x}) \rangle$. From the definition of the average, we have

$$\begin{aligned} \langle \mathbf{x} f(\mathbf{x}) \rangle &= \langle (\mathbf{x} - \bar{\mathbf{x}}) f(\mathbf{x}) \rangle + \bar{\mathbf{x}} \langle f(\mathbf{x}) \rangle \\ &= A \int \mathbf{h} f(\mathbf{x}) e^{-\frac{1}{2}\mathbf{h}\cdot\mathbf{B}^{-1}\cdot\mathbf{h}} \mathrm{d}\mathbf{x} + \bar{\mathbf{x}} \langle f(\mathbf{x}) \rangle \\ &= A\mathbf{B} \cdot \int \mathbf{B}^{-1} \cdot \mathbf{h} f(\mathbf{x}) e^{-\frac{1}{2}\mathbf{h}\cdot\mathbf{B}^{-1}\cdot\mathbf{h}} \mathrm{d}\mathbf{x} + \bar{\mathbf{x}} \langle f(\mathbf{x}) \rangle \\ &= -A\mathbf{B} \cdot \int f(\mathbf{h} + \bar{\mathbf{x}}) \left(\frac{\partial}{\partial \mathbf{h}} e^{-\frac{1}{2}\mathbf{h}\cdot\mathbf{B}^{-1}\cdot\mathbf{h}} \right) \mathrm{d}\mathbf{h} + \bar{\mathbf{x}} \langle f(\mathbf{x}) \rangle \end{aligned} \tag{1.48}$$

where

$$\mathbf{h} = \mathbf{x} - \bar{\mathbf{x}} \tag{1.49}$$

Note that

$$\frac{\partial}{\partial \mathbf{h}}\left[f(\mathbf{h}+\bar{\mathbf{x}})e^{-\frac{1}{2}\mathbf{h}\cdot\mathbf{B}^{-1}\cdot\mathbf{h}}\right] = \frac{\partial f(\mathbf{h}+\bar{\mathbf{x}})}{\partial \mathbf{h}}e^{-\frac{1}{2}\mathbf{h}\cdot\mathbf{B}^{-1}\cdot\mathbf{h}} + f(\mathbf{h}+\bar{\mathbf{x}})\left(\frac{\partial}{\partial \mathbf{h}}e^{-\frac{1}{2}\mathbf{h}\cdot\mathbf{B}^{-1}\cdot\mathbf{h}}\right) \tag{1.50}$$

Application of Eq. (1.50) to Eq. (1.48) yields

$$\langle \mathbf{x}f(\mathbf{x})\rangle = -A\mathbf{B}\cdot\int \frac{\partial}{\partial \mathbf{h}}\left[f(\mathbf{h}+\bar{\mathbf{x}})e^{-\frac{1}{2}\mathbf{h}\cdot\mathbf{B}^{-1}\cdot\mathbf{h}}\right]\mathrm{d}\mathbf{h} + \bar{\mathbf{x}}\langle f(\mathbf{x})\rangle + \mathbf{B}\cdot\left\langle\frac{\partial f}{\partial \mathbf{x}}\right\rangle \tag{1.51}$$

Since the first integral of the right-hand side can be replaced by the surface integral because of n-dimensional divergence theorem, it disappears because $e^{-\frac{1}{2}\mathbf{h}\cdot\mathbf{B}^{-1}\cdot\mathbf{h}}$ goes to zero as $\|\mathbf{h}\| \to \infty$. Furthermore, if $\bar{\mathbf{x}} \neq \mathbf{0}$ then

$$\mathbf{B} = \langle \mathbf{h}\mathbf{h}\rangle = \langle \mathbf{x}\mathbf{x}\rangle - \langle \mathbf{x}\rangle\langle \mathbf{x}\rangle = \langle \mathbf{x}\mathbf{x}\rangle - \overline{\mathbf{x}}\overline{\mathbf{x}} \tag{1.52}$$

Then, we can have a very useful equation such that

$$\langle \mathbf{x}f(\mathbf{x})\rangle = \bar{\mathbf{x}}\langle f(\mathbf{x})\rangle + \mathbf{B}\cdot\left\langle\frac{\partial f}{\partial \mathbf{x}}\right\rangle \tag{1.53}$$

Equation (1.53) is very useful in the derivation of the *Fokker–Planck equation* from the *Langevin equation* under the assumption that the random force is governed by the Gaussian distribution.

Problems 1

[1] Derive Eq. (1.23).

[2] Derive the following integrations for $a > 0$

$$\int_{-\infty}^{\infty} e^{-ax^2}\mathrm{d}x = \sqrt{\frac{\pi}{a}} \tag{1.a}$$

$$\int_{-\infty}^{\infty} e^{-ax^2+bx+c}\mathrm{d}x = \sqrt{\frac{\pi}{a}}\exp\left(\frac{b^2}{4a}+c\right) \tag{1.b}$$

[3] For the Gaussian distribution [Eq. (1.35)], prove that

$$\langle x^n\rangle = \begin{cases} 0 & \text{if } n \text{ is odd,} \\ \sigma^n(n-1)!! & \text{if } n \text{ is even} \end{cases} \tag{1.c}$$

where

$$(2k-1)!! = \sum_{p=1}^{k} (2p-1) \text{ double factorial} \tag{1.d}$$

[4] Derive Eq. (1.43).
[5] Derive Eq. (1.44).
[6] Show that

$$\mathbf{B} \cdot \int \frac{\partial}{\partial \mathbf{h}} \left[f(\mathbf{h} + \bar{\mathbf{x}}) e^{-\frac{1}{2}\mathbf{h}\cdot\mathbf{B}^{-1}\cdot\mathbf{h}} \right] \mathrm{d}\mathbf{h} = \mathbf{0} \tag{1.e}$$

2 Equilibrium Statistical Mechanics

2.1 Ensemble Theory

Statistical mechanics is to deal with mechanical system in terms of probability distributions. Consider a thermodynamic system which can be described by thermodynamic state variables of finite number. As mentioned before, the thermodynamic state variables are averages of certain functions of microstates. There is a huge number of microstates for given macrostates of finite number. Then, it is a natural question what the probability distribution is like if macrostates are fixed.

2.1.1 Microcanonical Ensemble

Consider the case that the number of molecules N, the volume of the system V, and the total mechanical energy E are given. It is clear that there are a huge number of systems that have the fixed values of N, V, and E. Set of such systems is called *microcanonical ensemble*. Even though such systems, members of microcanonical ensemble, share the same values of N, V, and E, they have different microstates which are points in phase space. Principle of *equal* a priori *probability* states that every point of the microcanonical ensemble has the same probability. Thus, the probability distribution of microcanonical ensemble is assumed to be uniform. Unfortunately, there is no mathematical proof of the principle.

The number of members of microcanonical ensemble can be calculated by

$$\Omega(N, V, E) = c \int \mathrm{d}\mathbf{p}_1 \ldots \int \mathrm{d}\mathbf{p}_N \int_V \mathrm{d}\mathbf{r}_1 \ldots \int_V \mathrm{d}\mathbf{r}_1 \delta(H_N(\Gamma) - E) \tag{2.1}$$

where the Hamiltonian in Eq. (2.1) is the one in Eq. (1.2) and c is the proportional coefficient. The proportional coefficient can be determined from quantum mechanical principles such as indistinguishability of particles and uncertainty principle (McQuarrie 2000):

$$c = \frac{1}{h^{3N} N!} \tag{2.2}$$

where h is the Planck's constant whose value is 6.626070×10^{-34} J s. It is noteworthy that Eq. (2.1) is proportional to the area of $6N-1$-dimensional surface at which the Hamiltonian has the same energy of E. It is convenient to absorb the correction fraction in $\mathrm{d}\Gamma$ by $\mathrm{d}\tilde{\Gamma} = (h^{3N} N!)^{-1} \mathrm{d}\mathbf{r}_1 \ldots \mathrm{d}\mathbf{r}_N \mathrm{d}\mathbf{p}_1 \ldots \mathrm{d}\mathbf{p}_N$. It is noteworthy that the newly defined differential volume of phase space is dimensionless. Hereafter, we use the notation $\mathrm{d}\tilde{\Gamma} = (h^{3N} N!)^{-1} \mathrm{d}\Gamma$. If the number of molecules N should be emphasized, then we use $\mathrm{d}\tilde{\Gamma}^N = (h^{3N} N!)^{-1} \mathrm{d}\Gamma^N$.

The function $\Omega(N, V, E)$ is called the *sum of state* or *partition function* of microcanonical ensemble. Since the principle of equal a priori probability means that any microstate on the equal energy surface is equally probable, the probability distribution is given by

$$P_{\mathrm{MC}}(\Gamma) = \frac{\delta(H(\Gamma) - E)}{\Omega(N, V, E)} \tag{2.3}$$

If we consider only microstates of the energy surface as the space for integration, then Eq. (2.3) can be rewritten by $P_{\mathrm{MC}}(S^{6N-1}) = 1/\Omega$, where S^{6N-1} denotes the points on the energy surface.

Boltzmann suggested the relation between entropy S and the phase volume Ω:

$$S = k_{\mathrm{B}} \log \Omega(N, V, E) \tag{2.4}$$

where k_{B} is the Boltzmann constant which is the gas constant R divided by the Avogadro's number N_{A}. The values of the constants are $k_{\mathrm{B}} \approx 1.381 \times 10^{-23}\,\mathrm{J\,K^{-1}}$, $R \approx 8.314\ \mathrm{J\,K^{-1}\,mol^{-1}}$, and $N_{\mathrm{Avo}} \approx 6.022 \times 10^{23}\,\mathrm{mol^{-1}}$. Unfortunately, Eq. (2.4) was not derived but introduced by genius intuition. However, the validity of Eq. (1.10) can be proved by its consistency with thermodynamics. Equation (2.4) satisfies the additivity of entropy and other features.

The total differential of entropy can be expressed from Eq. (2.4) as follows:

$$\mathrm{d}S = \left(\frac{\partial S}{\partial E}\right)_{N,V} \mathrm{d}E + \left(\frac{\partial S}{\partial V}\right)_{N,E} \mathrm{d}V + \left(\frac{\partial S}{\partial N}\right)_{V,E} \mathrm{d}N \tag{2.5}$$

If internal energy is interpreted by the total mechanical energy of molecules in the system, then connection of Eq. (2.5) with equilibrium thermodynamics provides the following:

$$\begin{aligned}\frac{1}{T} &= \left(\frac{\partial S}{\partial E}\right)_{N,V} = k_{\mathrm{B}} \frac{\partial \log \Omega(N,V,E)}{\partial E};\\ \frac{p}{T} &= \left(\frac{\partial S}{\partial V}\right)_{N,E} = k_{\mathrm{B}} \frac{\partial \log \Omega(N,V,E)}{\partial V};\\ \frac{\mu}{T} &= -\left(\frac{\partial S}{\partial N}\right)_{V,E} = -k_{\mathrm{B}} \frac{\partial \log \Omega(N,V,E)}{\partial N}\end{aligned} \tag{2.6}$$

where μ is the chemical potential. Since the partition function $\Omega(N,V,E)$ is calculated from molecular structure and motion, Eqs. (2.1), (2.4), and (2.6) provide the way to calculate macroscopic quantities from molecular motion.

Consider a continuously differentiable function $g : \mathrm{R}^N \to \mathrm{R}$, where R^N is the N-dimensional Euclidean space and R is the set of real number. The properties of the Dirac delta function are noteworthy such that

$$\int_{\mathrm{R}^N} f(\mathbf{x})\delta[g(\mathbf{x})]\mathrm{d}\mathbf{x} = \int_{g(\mathbf{x})=0} \frac{f(\mathbf{x})}{\|\nabla_N g\|}\mathrm{d}S^{N-1} \tag{2.7}$$

where $g(\mathbf{x}) = 0$ of the second integral implies that the integral is carried over the hypersurface $g(\mathbf{x}) = 0$ in R^N, $\mathrm{d}S^{N-1}$ is the area element on the hypersurface, and

$$\|\nabla_N g\| = \sqrt{\sum_{k=1}^{N}\left(\frac{\partial g}{\partial x_k}\right)^2} \quad \text{with} \quad \mathbf{x} = (x_1, x_2, \ldots, x_N) \tag{2.8}$$

Note that the dimension of the hypersurface is $N - 1$. Application of Eq. (2.7) to the partition function of microcanonical ensemble gives

$$\Omega = \int_{H(\Gamma)=E} \frac{\mathrm{d}\tilde{S}^{6N-1}}{\|\nabla_{6N} H\|} \tag{2.9}$$

where $\mathrm{d}\tilde{S}^{6N-1}$ contains the quantum mechanical correction $(h^{3N}N!)^{-1}$ and

$$\|\nabla_{6N} H\| = \sqrt{\sum_{k=1}^{N}\left[\left\|\frac{\partial H}{\partial \mathbf{r}_k}\right\|^2 + \left\|\frac{\partial H}{\partial \mathbf{p}_k}\right\|^2\right]} \tag{2.10}$$

Now we calculate $-k_{\mathrm{B}}\langle \log P_{\mathrm{MC}}\rangle_{\mathrm{MC}}$:

$$-k_{\mathrm{B}}\langle \log P_{\mathrm{MC}}\rangle_{\mathrm{MC}} = \frac{k_{\mathrm{B}}}{\Omega}\int_{H(\Gamma)=E} \frac{\log \Omega}{\|\nabla_{6N} H\|}\mathrm{d}\tilde{S}^{6N-1} = k_{\mathrm{B}} \log \Omega = S \tag{2.11}$$

Equation (2.11) means that the entropy is the ensemble average of the logarithm of the probability distribution of the ensemble. The formulation $S = -k_{\mathrm{B}}\langle \log P_{\mathrm{ens}} \rangle_{\mathrm{ens}}$ will be found in various ensembles. This type of entropy relation was invented from the research of communication called *information theory* (Shannon 1948). Application of information theory to statistical mechanics provides a systematic way for the description of equilibrium statistical mechanics irrespective of ensemble (Jaynes 1957a, b).

2.1.2 Canonical Ensemble

Consider the thermodynamic systems defined by N, V, and temperature of T. A huge number of systems with different microstates satisfy the constraints of N, V, and T. Set of such systems is called canonical ensemble. Constant temperature implies that the systems of canonical ensemble exchange energy with their surroundings. Hence, the members of canonical ensemble have different mechanical energies. We want to find the probability distribution function of canonical ensemble. Unfortunately, the general derivation has not been found. The most popular derivation assumes that the surrounding and the system are in thermal equilibrium which means that both the surrounding and the system of canonical ensemble have the same temperature. Furthermore, the union of the system and surrounding is a member of the microcanonical ensemble of N, V, and E. Since the surrounding is also a system, let the microstates of the system and surrounding be denoted, respectively, by Γ_A and Γ_B. Then, the union has the probability distribution such as

$$P_{\mathrm{MC}}(\Gamma_A, \Gamma_B) = \frac{\delta(E - H_A(\Gamma_A) - H_B(\Gamma_B))}{\Omega(N_A + N_B, V_A + V_B, E)} \tag{2.12}$$

Then, the probability distribution of the system is given by

$$P_{\mathrm{C}}(\Gamma_A) = \int P_{\mathrm{MC}}(\Gamma_A, \Gamma_B)\mathrm{d}\tilde{\Gamma}_B = \frac{\Omega_B(N_B, V_B, E - H_A(\Gamma_A))}{\Omega(N_A + N_B, V_A + V_B, E)} \tag{2.13}$$

Assume further that $H_A \ll E$. Then, Taylor expansion gives the following as

$$\log P_{\mathrm{C}}(\Gamma_A) = \log \frac{\Omega_B(E)}{\Omega(E)} - \frac{\partial \log \Omega_B(E)}{\partial E} H_A(\Gamma_A) \tag{2.14}$$

The partial derivative can be replaced by temperature according to Eq. (2.6):

$$P_{\mathrm{C}}(\Gamma_A) = \frac{\Omega_B(E)}{\Omega(E)} \exp\left[-\frac{H_A(\Gamma_A)}{k_{\mathrm{B}}T}\right] \tag{2.15}$$

Since $P_{\mathrm{C}}(\Gamma_A)$ is a probability density function, it must satisfy the normalization condition such that

$$\int P_{\mathrm{C}}(\Gamma_A)\mathrm{d}\tilde{\Gamma}_A = 1 \tag{2.16}$$

Then, it is clear that

$$P_{\mathrm{C}}(\Gamma_A) = \frac{e^{-\beta H_A(\Gamma_A)}}{Z} \tag{2.17}$$

where

$$Z = \int e^{-\beta H_A(\Gamma_A)}\mathrm{d}\tilde{\Gamma}_A \tag{2.18}$$

and

$$\beta = \frac{1}{k_{\mathrm{B}}T} \tag{2.19}$$

Note that the quantum mechanical correction is included in Eq. (2.18). The normalization factor $Z(N, V, T)$ is called the partition function of canonical ensemble.

The internal energy of the system of canonical ensemble is interpreted as the average of Hamiltonian such that

$$U = \langle H(\Gamma)\rangle_{\mathrm{C}} \equiv \int H(\Gamma)P_{\mathrm{C}}(\Gamma)\mathrm{d}\tilde{\Gamma} \tag{2.20}$$

From the definition of the partition function $Z(N, V, T)$, we have

$$U = -\frac{\partial}{\partial\beta}\log Z \tag{2.21}$$

Since $\beta = (k_{\mathrm{B}}T)^{-1}$, we know that

$$U = k_{\mathrm{B}}T^2\left(\frac{\partial \log Z}{\partial T}\right)_{N,V} \tag{2.22}$$

Equation (2.22) is analogs to the Gibbs–Helmholtz equation [see Eq. (4.a) in Chap. 1]:

$$U = -T^2\left(\frac{\partial}{\partial T}\frac{F}{T}\right)_{N,V} \tag{2.23}$$

Comparison of Eqs. (2.22) and (2.23) yields that Helmholtz free energy F is related to the partition function of canonical ensemble:

$$F = -k_{\mathrm{B}} T \log Z(N, V, T) \tag{2.24}$$

Then, the entropy can be calculated by the thermodynamic relation:

$$S = -\left(\frac{\partial F}{\partial T}\right)_{N,V} = k_{\mathrm{B}} \log Z + k_{\mathrm{B}} T \left(\frac{\partial \log Z}{\partial T}\right)_{N,V} \tag{2.25}$$

It is interesting that Eq. (2.25) gives

$$S = -k_{\mathrm{B}} \langle \log P_{\mathrm{C}} \rangle = -k_{\mathrm{B}} \int P_{\mathrm{C}}(\Gamma) \log P_{\mathrm{C}}(\Gamma) \mathrm{d}\tilde{\Gamma} \tag{2.26}$$

We found the consistency of the information theory of entropy in canonical ensemble.

2.1.3 Grand Canonical Ensemble

Now we are interested in the collection of systems defined by volume, temperature, and chemical potential μ. Such collection of system is called *grand canonical ensemble*. Since the system is defined by μ, it can be said that the systems of grand canonical ensemble can exchange molecules with surrounding.

In order to derive the probability distribution of grand canonical ensemble, consider a system of canonical ensemble. The system has two subsystems A and B. Assume that A is much smaller than B:

$$N_{\mathrm{A}} \ll N_{\mathrm{B}} \quad \text{and} \quad V_{\mathrm{A}} \ll V_{\mathrm{B}} \tag{2.27}$$

It is also assumed that the two subsystems can exchange molecules. The Hamiltonian of the system is the sum of those of subsystems:

$$H(\Gamma_A, \Gamma_B, N) = H(\Gamma_A, N_{\mathrm{A}}) + H(\Gamma_B, N_{\mathrm{B}}) \tag{2.28}$$

with $N = N_{\mathrm{A}} + N_{\mathrm{B}}$ and $V = V_{\mathrm{A}} + V_{\mathrm{B}}$. Since there is exchange of molecules, the partition function is calculated carefully. It is not important which molecule is in V_{A} or V_{B}. The partition function of the total system must contain the all possible cases of different N_{A}'s. The partition function is the sum over N_{A} from zero to N. Thus, we have

$$
\begin{aligned}
Z(N,V,T) &= \frac{1}{h^{3N}N!}\sum_{N_A=0}^{N}\frac{N!}{N_\mathrm{A}!N_\mathrm{B}!}\int\int e^{-\beta H(\Gamma_A)}e^{-\beta H(\Gamma_B)}\mathrm{d}\Gamma_A\mathrm{d}\Gamma_B \\
&= \sum_{N_\mathrm{A}=0}^{N}\left(\int e^{-\beta H(\Gamma_A)}\mathrm{d}\tilde{\Gamma}_\mathrm{A}\right)\left(\int e^{-\beta H(\Gamma_B)}\mathrm{d}\tilde{\Gamma}_\mathrm{B}\right) \\
&= \sum_{N_\mathrm{A}=0}^{N} Z(N_\mathrm{A},V_\mathrm{A},T)Z(N-N_\mathrm{A},V_\mathrm{B},T)
\end{aligned}
\tag{2.29}
$$

Since molecules are not distinguishable, the term $N!/(N_\mathrm{A}!N_\mathrm{B}!)$ was included in the first equality.

Since the probability distribution of the system A is given by the integration of $P_\mathrm{C}(\Gamma_\mathrm{A},\Gamma_\mathrm{B})$ over Γ_B, we have

$$
P_\mathrm{G}(\Gamma_\mathrm{A}) = \frac{Z(N-N_\mathrm{A},V_\mathrm{B},T)}{Z(N,V,T)}e^{-\beta H(\Gamma_A)} \tag{2.30}
$$

From Eq. (2.24), we know that

$$
\frac{Z(N-N_\mathrm{A},V_\mathrm{B},T)}{Z(N,V,T)} = \exp\{-\beta[F(N-N_\mathrm{A},V-V_\mathrm{A},T)-F(N,V,T)]\} \tag{2.31}
$$

Using Eq. (2.27), the following approximation is available:

$$
F(N-N_\mathrm{A},V-V_\mathrm{A},T)-F(N,V,T) \approx -N_\mathrm{A}\mu + pV_\mathrm{A} \tag{2.32}
$$

Then, we have the probability distribution of the system A:

$$
P_\mathrm{G}\left(\Gamma^N\right) = z^N e^{-\beta pV-\beta H(\Gamma)} = \frac{e^{\beta N\mu-\beta H(\Gamma)}}{e^{\beta pV}} \tag{2.33}
$$

where z is the fugacity defined by

$$
\mu = k_\mathrm{B}T\log z \tag{2.34}
$$

In Eq. (2.33), we dropped subscripts A, because the subsystem A is the system that we are interested in. Note that the subsystem A is the system that belongs to grand canonical ensemble and the subsystem B is the particle reservoir as well as the heat reservoir. It is easily understood that the ensemble average of a quantity $A(\Gamma,N)$ is given by

$$
\langle A\rangle_G = \sum_{N=0}^{\infty}\int A\left(\Gamma^N\right)\frac{z^N e^{-\beta H\left(\Gamma^N\right)}}{e^{\beta pV}}\mathrm{d}\tilde{\Gamma}^N \tag{2.35}
$$

We introduced superscript N for the volume element of phase space, because the number of momenta and positions changes according to the number of molecules.

Since the distribution P_{G} is the marginal distribution of the distribution P_{C} of the total system, it is obvious that

$$\sum_{N=0}^{\infty} \int P_{\mathrm{G}}\left(\Gamma^{N}\right) \mathrm{d}\tilde{\Gamma}^{N} = 1 \tag{2.36}$$

Thus, Eq. (2.33) can be rewritten by

$$P_{\mathrm{C}}\left(\Gamma^{N}\right) = \frac{z^{N} \exp\left[-\beta H\left(\Gamma^{N}\right)\right]}{\Xi(V, T, \mu)} \tag{2.37}$$

where $\Xi(V, T, \mu)$ is the partition function of grand canonical ensemble defined as

$$\Xi(V, T, \mu) \equiv \sum_{N=0}^{\infty} z^{N} \int e^{-\beta H\left(\Gamma^{N}\right)} \mathrm{d}\tilde{\Gamma}^{N} \tag{2.38}$$

Comparison of Eqs. (2.33) and (2.38) immediately gives

$$pV = k_{\mathrm{B}} T \log \Xi(V, T, \mu) \tag{2.39}$$

Theory of equilibrium thermodynamics gives

$$pV = G - U + TS = N\mu - U + TS \tag{2.40}$$

and

$$\mathrm{d}(pV) = N\mathrm{d}\mu + p\mathrm{d}V + S\mathrm{d}T \tag{2.41}$$

Comparison of Eqs. (2.39) and (2.41) gives

$$\left[\frac{\partial}{\partial V}\left(k_{\mathrm{B}} T \log \Xi\right)\right]_{\mu,T} = k_{\mathrm{B}} T \left(\frac{\partial \log \Xi}{\partial V}\right)_{\mu,T} = p; \tag{2.42}$$

$$\left[\frac{\partial}{\partial \mu}\left(k_{\mathrm{B}} T \log \Xi\right)\right]_{V,T} = k_{\mathrm{B}} T \left(\frac{\partial \log \Xi}{\partial \mu}\right)_{V,T} = N; \tag{2.43}$$

$$\left[\frac{\partial}{\partial T}\left(k_{\mathrm{B}} T \log \Xi\right)\right]_{\mu,V} = k_{\mathrm{B}} \log \Xi + k_{\mathrm{B}} T \left(\frac{\partial \log \Xi}{\partial T}\right)_{\mu,V} = S \tag{2.44}$$

From Eq. (2.38), the derivative of $\log \Xi$ with respective β gives

$$\frac{\partial \log \Xi}{\partial \beta} = -k_B T^2 \left(\frac{\partial \log \Xi}{\partial T} \right)_{V,\mu} = -\langle H \rangle_G + \mu \langle N \rangle_G \tag{2.45}$$

Comparison of Eq. (2.45) with Eq. (2.44) gives

$$-\langle H \rangle_G + \mu \langle N \rangle_G = pV - TS \tag{2.46}$$

As before, the ensemble average of Hamiltonian is interpreted again as the internal energy of the system. Then, comparison of Eq. (2.46) with Eq. (2.40) implies that the ensemble average of the number of molecules $\langle N \rangle_G$ can be interpreted as N, the number of molecules in equilibrium thermodynamics.

From Eq. (2.38), the derivative with respect to chemical potential gives

$$\begin{aligned} k_B T \left(\frac{\partial \log \Xi}{\partial \mu} \right)_{V,T} &= \frac{k_B T}{\Xi} \sum_{N=0}^{\infty} \beta N z^N \int e^{-\beta H(\Gamma^N)} d\tilde{\Gamma}^N \\ &= \sum_{N=0}^{\infty} \int N P_G(\Gamma^N) d\tilde{\Gamma}^N = \langle N \rangle_G \end{aligned} \tag{2.47}$$

which supports the result from Eq. (2.46).

It is interesting that the information theory of entropy is also valid in grand canonical ensemble:

$$\begin{aligned} -k_B \langle \log P_G \rangle_G &= -\frac{k_B}{\Xi} \sum_{N=0}^{\infty} z^N \int e^{-\beta H(\Gamma^N)} \left(N \log z - \beta H(\Gamma^N) - \log \Xi \right) d\tilde{\Gamma}^N \\ &= \frac{pV + U - N\mu}{T} = S \end{aligned} \tag{2.48}$$

2.2 *Fluctuations and Equivalence of Ensembles*

Various ensembles were addressed above. If different ensembles give different thermodynamic results, then statistical mechanics cannot be a theory of physics. We shall show that the various equilibrium ensembles are equivalent to each other because the fluctuations of thermodynamic quantities from each ensemble are negligible when the system under consideration is macroscopic.

2.2.1 Information Theory of Entropy

We have studied the formalism of statistical mechanics that the probability distribution of microcanonical ensemble is based on the principle of equal a priori probability and the probability distributions of other ensembles are derived from that of microcanonical ensemble and various approximations. Here, we introduce a new formalism of classical statistical mechanics based on the information theory (Jaynes 1957a, b). This formalism is more general and systematic than the previous one.

The new formalism starts from the definition of entropy such that

$$S = -k_{\mathrm{B}} \langle \log P \rangle \tag{2.49}$$

where P is the probability distribution of given ensemble and $\langle \cdots \rangle$ is the average for the ensemble. Equation (2.49) was derived for microcanonical, canonical, and grand canonical ensembles: Eqs. (2.11), (2.26), and (2.48). The information theory states that the probability distribution should be the one that maximizes the entropy of Eq. (2.49) subjected to some constraints. The constraints are the information of the probability distribution such as some moments of the probability distribution:

$$\left\langle H\left(\Gamma^N\right)\right\rangle = \sum_{N=0}^{\infty} \int H\left(\Gamma^N\right) P\left(\Gamma^N\right) \mathrm{d}\tilde{\Gamma}^N; \tag{2.50a}$$

$$\langle N \rangle = \sum_{N=0}^{\infty} \int N P\left(\Gamma^N\right) \mathrm{d}\tilde{\Gamma}^N; \tag{2.50b}$$

$$1 = \sum_{N=0}^{\infty} \int P\left(\Gamma^N\right) \mathrm{d}\tilde{\Gamma}^N \tag{2.50c}$$

If the number of molecules N is fixed just as canonical or microcanonical ensembles, then the second is not necessary because the number of molecules N is given independent of the probability distributions. Equation (2.50a) is not necessary for microcanonical ensemble because the energy is given independent of the probability distribution of microcanonical ensemble. However, the probability distribution of canonical ensemble needs, instead of Eq. (2.50a), the following:

$$\langle H(\Gamma) \rangle_{\mathrm{C}} = \int H\left(\Gamma^N\right) P_{\mathrm{C}}\left(\Gamma^N\right) \mathrm{d}\tilde{\Gamma}^N \tag{2.51}$$

Since the third constraint is the normalization condition of probability distribution function, the probability distributions of all ensembles should satisfy the constraint Eq. (2.50c).

Maximization or minimization of a function subject to constraints can be solved systematically by the use of the method of Lagrange multipliers (Marsden and Tromba 2003; Edgar and Himmelblau 1989). Application of the method of Lagrange multiplier to the maximization of entropy is given by

$$\delta\left(S+\gamma_H\langle H\rangle+\gamma_N\langle N\rangle+\gamma_1\sum_{N=0}^{\infty}\int P\left(\Gamma^N\right)\mathrm{d}\tilde{\Gamma}^N\right)=0 \tag{2.52}$$

Note that all multiplies such as γ_H, γ_N, and γ_1 are independent of the integration variables. We recommend Thornton and Marion (2004) and Arfken and Weber (2001) to the readers who are not familiar to the notation of variation.

In microcanonical ensemble, we consider the space of appropriate variables as the hypersurface of the same energy. Since N and E are fixed, the only constraint is the normalization condition:

$$\int P_{\mathrm{MC}}\left(S^{6N-1}\right)\frac{\mathrm{d}\tilde{S}^{6N-1}}{\|\nabla_{6N}H\|}=1 \tag{2.53}$$

Then, the variational equation, Eq. (2.52), becomes

$$\delta\left(-k_{\mathrm{B}}\int P_{\mathrm{MC}}\log P_{\mathrm{MC}}\frac{\mathrm{d}\tilde{S}^{6N-1}}{\|\nabla_{6N}H\|}+\gamma_1\int P_{\mathrm{MC}}\frac{\mathrm{d}\tilde{S}^{6N-1}}{\|\nabla_{6N}H\|}\right)=0 \tag{2.54}$$

Since the variation is originated from that of the probability distribution, note that

$$\begin{aligned}\delta\int P_{\mathrm{MC}}\log P_{\mathrm{MC}}\frac{\mathrm{d}\tilde{S}^{6N-1}}{\|\nabla_{6N}H\|}&=\int\left(\log P_{\mathrm{MC}}+1\right)\delta P_{\mathrm{MC}}\frac{\mathrm{d}\tilde{S}^{6N-1}}{\|\nabla_{6N}H\|}\\ \delta\int P_{\mathrm{MC}}\frac{\mathrm{d}\tilde{S}^{6N-1}}{\|\nabla_{6N}H\|}&=\int\delta P_{\mathrm{MC}}\frac{\mathrm{d}\tilde{S}^{6N-1}}{\|\nabla_{6N}H\|}\end{aligned} \tag{2.55}$$

Then, Eq. (2.54) becomes simpler as follows:

$$\int\left(-k_{\mathrm{B}}\log P_{\mathrm{MC}}-k_{\mathrm{B}}+\gamma_1\right)\delta P_{\mathrm{MC}}\frac{\mathrm{d}\tilde{S}^{6N-1}}{\|\nabla_{6N}H\|}=0 \tag{2.56}$$

Since the variation of the probability distribution is arbitrary, we have

$$P_{\mathrm{MC}}=\exp\left(\frac{\gamma_1-k_{\mathrm{B}}}{k_{\mathrm{B}}}\right) \tag{2.57}$$

on the energy surface. To determine the multiplier γ_1, Eq. (2.57) is substituted to the normalization condition. Then, we have

$$P_{\mathrm{MC}}=\frac{1}{\Omega(E,V,N)} \tag{2.58}$$

on the energy surface or

$$P_{\mathrm{MC}} = \frac{\delta(H(\Gamma) - E)}{\Omega(E, V, N)} \tag{2.59}$$

in the whole phase space.

In canonical ensemble, the constraints for the maximization of entropy are given as

$$\int P_{\mathrm{C}}(\Gamma)\mathrm{d}\tilde{\Gamma} = 1; \quad \int H(\Gamma)P_{\mathrm{C}}(\Gamma)\mathrm{d}\tilde{\Gamma} = \langle H \rangle = U \tag{2.60}$$

Then, the variational equation for canonical ensemble is given by

$$\int [-k_{\mathrm{B}}\delta(P_{\mathrm{C}} \log P_{\mathrm{C}}) + \gamma_{\mathrm{H}} H(\Gamma)\delta P_{\mathrm{C}} + \gamma_1 \delta P_{\mathrm{C}}]\mathrm{d}\tilde{\Gamma} = 0 \tag{2.61}$$

Equation (2.61) gives the probability distribution of canonical ensemble as follows:

$$\log P_{\mathrm{C}}(\Gamma) = \frac{\gamma_{\mathrm{H}} H(\Gamma) + \gamma_1 - k_{\mathrm{B}}}{k_{\mathrm{B}}} \tag{2.62}$$

The multiplier γ_H is determined by the thermodynamic relation as follows:

$$\left(\frac{\partial U}{\partial S}\right)_{V,N} = T = -\frac{1}{\gamma_H} \tag{2.63}$$

Application of the normalization condition determines the probability distribution:

$$P_{\mathrm{C}}(\Gamma) = \frac{e^{-\beta H(\Gamma)}}{Z(N, V, T)} \tag{2.64}$$

where

$$Z(N, V, T) = \int e^{-\beta H(\Gamma)}\mathrm{d}\tilde{\Gamma} \tag{2.65}$$

This is the result obtained previously from the union of the system and heat reservoir.

We will leave the problem for grand canonical ensemble as homework to the readers. The grand canonical ensemble requires the three constraints of Eqs. (2.50a–c).

2.2.2 Fluctuation

The probability distribution of an ensemble provides not only the thermodynamic properties as ensemble average but also the variances of thermodynamic properties. This cannot be done by classical thermodynamics which considers thermodynamic state variables deterministically. The probability distribution of canonical ensemble gives the variance of energy:

$$\sigma_{\mathrm{E}}^2 = \left\langle \left(E - \langle E \rangle_{\mathrm{C}}\right)^2 \right\rangle_{\mathrm{C}} = \frac{1}{Z}\int (H-U)^2 e^{-\beta H} \mathrm{d}\tilde{\Gamma} = k_{\mathrm{B}} T^2 \left(\frac{\partial U}{\partial T}\right)_{V,N} \tag{2.66}$$

The second equality is obtained from purely mathematical deduction. From the thermodynamics, we know that $(\partial U/\partial T)_{V,N} = C_{\mathrm{V}}$ where C_{V} is the heat capacity at constant volume. Since variance must not be negative, we have the following inequality:

$$k_{\mathrm{B}} T^2 C_{\mathrm{V}} = \sigma_{\mathrm{E}}^2 \geq 0 \tag{2.67}$$

Equation (2.67) shows that the heat capacity is not negative. Thus, the relative variance (coefficient of variation) is given by

$$\frac{\sigma_{\mathrm{E}}}{U} = \frac{\sqrt{k_{\mathrm{B}} T^2 C_{\mathrm{V}}}}{U} \tag{2.68}$$

We know that U and C_{V} are extensive properties and T is an intensive property. In the sequence, the relative variance is order of $N^{-1/2}$. Thus, in a typical macroscopic system, the relative deviation from mean energy is negligibly small. Hence, the average energy of canonical ensemble is exactly equivalent to the energy of microcanonical ensemble from the macroscopic viewpoints.

As for grand canonical ensemble, we can calculate the variance of the number of molecules. The result is

$$\sigma_{\mathrm{N}}^2 = k_{\mathrm{B}} T \left(\frac{\partial \langle N \rangle_{\mathrm{G}}}{\partial \mu}\right)_{V,T} \geq 0 \tag{2.69}$$

From thermodynamics, we know that

$$\left(\frac{\partial \mu}{\partial N}\right)_{V,T} = -\frac{V^2}{N^2}\left(\frac{\partial P}{\partial V}\right)_{N,T} = \frac{V \kappa_T}{N^2} \tag{2.70}$$

where κ_T is the isothermal compressibility which is an intensive property. Then, the relative deviation from the mean number of molecules is given by

$$\frac{\sigma_N}{N} = \sqrt{\frac{k_B T \kappa_T}{V}} \propto \frac{1}{\sqrt{N}} \tag{2.71}$$

Since only V is an extensive property in the right-hand side of Eq. (2.71), the relative deviation from the mean number of molecules in a macroscopic system is extremely small, too. This shows the equivalence between the grand canonical and canonical ensembles.

Although classical equilibrium thermodynamics deals with thermodynamic quantities deterministically and equilibrium statistical mechanics does them stochastically, the discrepancy between the two approaches disappears when the system size is macroscopic, $N \sim 10^{23}$. It is said that a system can be considered as a macroscopic if *thermodynamic limit* is valid. The thermodynamic limit is that N/V remains finite as both N and V go to infinite.

2.2.3 The Relations Between Partition Functions

The partition function of any ensemble can be considered as the number of systems in the ensemble. Since a system of an ensemble corresponds to a point of the phase space and the representative point is interpreted as microstate, the partition function is called the sum of states.

Canonical ensemble is the collection of systems with the same temperature while microcanonical ensemble is the collection of systems with the same energy. Let the number of systems of the same energy of E in canonical ensemble be $\mathsf{N}(E)$. Then, $\mathsf{N}(E)$ is proportional to the Boltzmann factor $e^{-\beta E}$. Since the partition function of microcanonical ensemble $\Omega(E)$ is equivalent to the number of systems with given E, N, and V, it can be said that

$$\mathsf{N}(E, N, V, T) = \Omega(E, V, N) e^{-\beta E} \tag{2.72}$$

Summing $\mathsf{N}(E)$ over for all possible energy E, the partition function of canonical ensemble is obtained:

$$Z(N, V, T) = \int_0^\infty \Omega(E, V, N) e^{-\beta E} \mathrm{d}E \tag{2.73}$$

Equation (2.73) implies that the partition function of canonical ensemble is the Laplace transform of that of microcanonical ensemble. It can be said that the partition function of microcanonical ensemble generates that of canonical ensemble. It is interesting that Eq. (2.38) implies that

$$\Xi(\mu, V, T) = \sum_{N=0}^{\infty} z^N Z(N, V, T) \tag{2.74}$$

Thus, it can be said that the partition function of grand canonical ensemble is generated from the partition function of canonical ensemble.

2.2.4 Generalized Ensembles

Although the three ensembles are representative and popular, there are a number of ensembles to be utilized. Here we introduce a generalized way to construct a new ensemble according to Chandler (1987).

We can summarize the equations of partition function and the probability distribution for ensembles studied as follows:

$$\frac{S}{k_B} = \langle \log P_{MC} \rangle_{MC} = -\log \Omega; \tag{2.75}$$

$$\frac{S}{k_B} = \langle \log P_C \rangle_C = -\log Z - \beta \langle H \rangle_C; \tag{2.76}$$

$$\frac{S}{k_B} = \langle \log P_G \rangle_G = -\log \Xi - \beta \langle H \rangle_G - \beta\mu \langle N \rangle_G \tag{2.77}$$

The three equations seem to be connected by a certain relation. Note that for E, V, and N, no fluctuation is permitted in microcanonical ensemble, while energy fluctuation is permitted in canonical ensemble and the number of molecules and energy can fluctuate in grand canonical ensemble. In the three equations for S/k_B, their first term is the minus of the logarithm of the partition function and the next terms are the linear combination of the product of the average of fluctuating quantities and their conjugates. The meaning of the conjugate can be explained in terms of total differential of S/k_B. In thermodynamics, the total differential of entropy is given by

$$\frac{dS}{k_B} = \beta dU + \beta p dV - \beta\mu dN \tag{2.78}$$

Equation (2.78) implies that internal energy U is conjugated with β, V is conjugated with βp, and N is conjugated with $-\beta\mu$. The Legendre transformation of $k_B^{-1}S$ by the replacement of U with its conjugated variable gives

$$d\left(\frac{S}{k_B} - \beta E\right) = d(-\beta F) = -E d\beta + \beta p dV - \beta\mu dN \tag{2.79}$$

Let $\Pi_{\mathrm{C}} = k_{\mathrm{B}}^{-1} S - \beta E$ and $\Pi_{\mathrm{MC}} = k_{\mathrm{B}}^{-1} S$. Then, compared with Eqs. (2.75)–(2.77), we have

$$\Pi_{\mathrm{MC}} = \frac{S}{k_{\mathrm{B}}} = \log \Omega \quad \text{and} \quad \Pi_{\mathrm{C}} = -\frac{F}{k_{\mathrm{B}} T} = \log Z \tag{2.80}$$

The logarithm of the partition function of microcanonical ensemble is the Legendre transformation of that of canonical ensemble by changing fluctuating quantity for its conjugate.

We can extend this reasoning from microcanonical ensemble to grand canonical ensemble. Compared with microcanonical ensemble, grand canonical ensemble permits the fluctuation of the number of molecules and energy. Consider the Legendre transformation of the logarithm of microcanonical ensemble from U and N to their conjugates β and $\beta\mu$. Then, we have

$$\mathrm{d} \log \Pi_{\mathrm{G}} = \mathrm{d}\left(\frac{S}{k_{\mathrm{B}}} - \beta U - \beta \mu N \right) = \mathrm{d}(\beta p V) = \mathrm{d} \log \Xi \tag{2.81}$$

From Eqs. (2.75) to (2.77), the logarithm of probability distribution can be constructed similarly

$$\begin{aligned} \log P_{\mathrm{MC}} &= -\log \Omega; \\ \log P_{\mathrm{C}} &= -\log Z - \beta H(\Gamma); \\ \log P_{\mathrm{G}} &= -\log \Xi - \beta H\left(\Gamma^N\right) - \beta \mu N \end{aligned} \tag{2.82}$$

Now we can apply this reasoning to finding a new ensemble. If we want the ensemble that permits the fluctuation of volume and energy, then we can construct the partition function and the probability distribution for the ensemble as follows:

$$\mathrm{d} \log \Pi_{\mathrm{PV}} = \mathrm{d}\left(\frac{S}{k_{\mathrm{B}}} - \beta U - \beta p V \right) = \mathrm{d}(-\beta G) = \log \Theta(N, p, \theta) \tag{2.83}$$

$$\log P_{\mathrm{PV}} = -\log \Theta - \beta H(\Gamma) - \beta p V \tag{2.84}$$

$$\Theta = \int_0^\infty \int e^{-\beta H(\Gamma) - \beta p V} \mathrm{d}\tilde{\Gamma} \mathrm{d}V \tag{12.85}$$

The ensemble is called isothermal–isobaric ensemble (McQuarrie 2000).

2.3 The Equipartition Theorem and the Virial Theorem

The phase space is a manifold of $6N$ dimension such that

$$\{\xi_k\} = \{\mathbf{r}_1, \ldots, \mathbf{r}_N, \mathbf{p}_1, \ldots, \mathbf{p}_N\} \tag{2.86}$$

The probability distribution function of canonical ensemble, say $P_{\mathrm{C}}(\{\xi_k\})$, is defined on the manifold. The normalization condition for the probability distribution can be written by

$$\int_{-\infty}^{\infty} \cdots \int_{-\infty}^{\infty} P_{\mathrm{C}}(\xi_1, \ldots, \xi_{6N}) \mathrm{d}\xi_1 \ldots \mathrm{d}\xi_{6N} = 1 \tag{2.87}$$

Equation (2.87) implies that for any ξ_k

$$\lim_{|\xi_k| \to \infty} P_{\mathrm{C}}(\xi_1, \ldots, \xi_{6N}) = 0 \tag{2.88}$$

Then, we have the identity:

$$\int_{-\infty}^{\infty} \frac{\partial}{\partial \xi_k} (\xi_i P_{\mathrm{C}}) \mathrm{d}\xi_k = [\xi_i P_{\mathrm{C}}(\xi_1, \ldots, \xi_{6N})]_{\xi_k = -\infty}^{\xi_k = \infty} = 0 \tag{2.89}$$

The left-hand side of Eq. (2.89) can be rewritten by

$$\int_{-\infty}^{\infty} \frac{\partial}{\partial \xi_k} (\xi_i P_{\mathrm{C}}) \mathrm{d}\xi_k = \int_{-\infty}^{\infty} \left(\delta_{ik} - \beta \xi_i \frac{\partial H}{\partial \xi_k} \right) P_{\mathrm{C}} \mathrm{d}\xi_k \tag{2.90}$$

The immediate consequence of Eq. (2.90) is given as

$$\left\langle \xi_i \frac{\partial H}{\partial \xi_k} \right\rangle_{\mathrm{C}} = k_{\mathrm{B}} T \delta_{ik} \tag{2.91}$$

This is called the *equipartition theorem* or classical virial theorem. Although we derive the equipartition theorem in canonical ensemble, the theorem can be derived in microcanonical ensemble, too (Huang 1963; Tuckerman 2010). From Eq. (1.2), the average kinetic energy of a molecule is given by

$$\left\langle \frac{m_\alpha}{2} \mathbf{v}_\alpha \cdot \mathbf{v}_\alpha \right\rangle = \frac{3}{2} k_{\mathrm{B}} T \tag{2.92}$$

One of the most important postulates in equilibrium statistical mechanics is the *ergodic hyperthesis* that in equilibrium, the ensemble average is equal to the time average such that

$$\langle A(\Gamma)\rangle_T = \frac{1}{\Delta t}\int_{t_o}^{t_o+\Delta t} A(\Gamma(t))\mathrm{d}t = \langle A(\Gamma)\rangle_{\text{ensemble}} \tag{2.93}$$

where t_o is arbitrarily given. This is the theoretical basis of molecular dynamics simulation (Tuckerman 2010). The virial theorem is that the time average of kinetic energy is given by

$$\langle K\rangle_T = -\frac{1}{2}\left\langle \sum_{\alpha=1}^{N} \mathbf{f}_\alpha \cdot \mathbf{r}_\alpha \right\rangle_T \tag{2.94}$$

where $\mathbf{f}_\alpha$ is the force exerted on the αth particle and we know that $\mathrm{d}\mathbf{p}_\alpha/\mathrm{d}t = \mathbf{f}_\alpha$ from the second law of Newtonian mechanics (Goldstein et al. 2001). Here we shall discuss generalized virial theorem.

To prove the virial theorem, we are interested in a tensor quantity such that

$$\mathbf{G} = \sum_{\alpha=1}^{N} \mathbf{p}_\alpha \mathbf{r}_\alpha \tag{2.95}$$

The average of the time derivative of $\mathbf{G}$ is given by

$$\left\langle \frac{\mathrm{d}\mathbf{G}}{\mathrm{d}t} \right\rangle_T = \left\langle \sum_{\alpha=1}^{N} \frac{\mathbf{p}_\alpha \mathbf{p}_\alpha}{m_\alpha} \right\rangle_T + \left\langle \sum_{\alpha=1}^{N} \mathbf{f}_\alpha \mathbf{r}_\alpha \right\rangle_T \tag{2.96}$$

The left-hand side of Eq. (2.96) can be written by

$$\left\langle \frac{\mathrm{d}\mathbf{G}}{\mathrm{d}t} \right\rangle_T = \lim_{\Delta t\to\infty} \frac{\mathbf{G}(t_o+\Delta t) - \mathbf{G}(t_o)}{\Delta t} \tag{2.97}$$

If the motion is periodic, then the left-hand side would be exactly zero whenever Δt is the period of the motion. Although the motion is not periodic, if the all particles remain in a finite region and the total energy is finite, then the time average vanishes for sufficiently long Δt. Then, the virial theorem of Eq. (2.94) is obtained by taking trace on both sides of Eq. (2.96).

Consider a material point (or particle) of continuum mechanics (see Chap. 2). The material point is the notion of macroscopic theory, which contains a huge number of molecules. However, here it is handled by a region of space with finite volume of Ω from the microscopic viewpoint. We can still use the assumption of

$\langle d\mathbf{G}/dt\rangle_T = 0$. The force exerted on the αth molecule (or microscopic particle) is specified in detail as follows:

$$\mathbf{f}_\alpha = \sum_{\gamma\neq\alpha}^{N} \mathbf{f}_{\alpha\gamma} + \mathbf{t}_\alpha \tag{2.98}$$

where $\mathbf{f}_{\alpha\gamma}$ is the internal force exerted on the αth microscopic particle by the γth microscopic particle and $\mathbf{t}_\alpha$ is the force exerted on the αth microscopic particle by the microscopic particles outside of the volume Ω.

Now we define a tensor quantity such that

$$\mathbf{G} = \sum_{\alpha=1}^{N} \mathbf{p}_\alpha(\mathbf{r}_\alpha - \tilde{\mathbf{x}}) \tag{2.99}$$

where $\tilde{\mathbf{x}}$ is the center of mass of the microscopic particles in Ω and it can be interpreted as the position of the material particle of continuum mechanics. The time average of the rate of $\mathbf{G}$ is given by

$$\left\langle \frac{d\mathbf{G}}{dt} \right\rangle_T = \left\langle \sum_{\alpha=1}^{N} \mathbf{f}_\alpha(\mathbf{r}_\alpha - \tilde{\mathbf{x}}) \right\rangle_T + \left\langle \sum_{\alpha=1}^{N} \frac{\mathbf{p}_\alpha \mathbf{p}_\alpha}{m_\alpha} \right\rangle_T \tag{2.100}$$

Note that the time derivative used here is the one along the motion of the material point $\tilde{\mathbf{x}}$. Hence, we know that

$$\frac{d\tilde{\mathbf{x}}}{dt} = \mathbf{0} \tag{2.101}$$

Then, Eq. (2.100) becomes

$$\left\langle \frac{d\mathbf{G}}{dt} \right\rangle_T = \langle \hat{\mathbf{V}} \rangle_T + \left\langle \sum_{\alpha=1}^{N} \frac{\mathbf{p}_\alpha \mathbf{p}_\alpha}{m_\alpha} \right\rangle_T = \mathbf{0} \tag{2.102}$$

where $\hat{\mathbf{V}}$ is the virial tensor defined as

$$\hat{\mathbf{V}} = \sum_{\alpha=1}^{N} \mathbf{f}_\alpha(\mathbf{r}_\alpha - \tilde{\mathbf{x}}) \tag{2.103}$$

Application of Eq. (2.98) allows us to decompose the virial tensor $\hat{\mathbf{V}}$ into two parts:

$$\hat{\mathbf{V}}_{\text{in}} = \sum_{\alpha=1}^{N} \sum_{\gamma\neq\alpha}^{N} \mathbf{f}_{\alpha\gamma}(\mathbf{r}_\alpha - \tilde{\mathbf{x}}) \tag{2.104}$$

and

$$\hat{\mathbf{V}}_{\text{wall}} = \sum_{\alpha=1}^{N} \mathbf{t}_\alpha(\mathbf{r}_\alpha - \tilde{\mathbf{x}}) \tag{2.105}$$

It is assumed that the interaction forces between different microscopic particles are short-range ones. In other words, the forces $\mathbf{t}_\alpha$ are effective only at the boundary of the region Ω. Then, we can introduce stress tensor and stress vector in the approximation of the wall virial tensor $\hat{\mathbf{V}}_{\text{wall}}$ as follows:

$$\left\langle \hat{\mathbf{V}}_{\text{wall}} \right\rangle_T \approx \oint_{\partial\Omega} \mathbf{t}(\mathbf{r} - \tilde{\mathbf{x}}) \mathrm{d}S = \oint_{\partial\Omega} (\mathbf{r} - \tilde{\mathbf{x}}) \cdot \mathbf{T} \cdot \mathrm{d}\mathbf{S} \tag{2.106}$$

Here we used the symmetry of stress $\mathbf{n} \cdot \mathbf{T} = \mathbf{T} \cdot \mathbf{n} = \mathbf{t}$ (see Chap. 2). Note that the vector $\mathbf{r}$ is on the boundary of Ω and the surface integral of Eq. (2.106) is carried on $\mathbf{r}$. Then, the divergence theorem and $\nabla_{\mathbf{r}}(\mathbf{r} - \tilde{\mathbf{x}}) = \mathbf{I}$ gives the following:

$$\left\langle \hat{\mathbf{V}}_{\text{wall}} \right\rangle_T = \int_\Omega (\mathbf{r} - \tilde{\mathbf{x}}) \nabla_{\mathbf{r}} \cdot \mathbf{T} \mathrm{d}V + \int_\Omega \mathbf{T} \mathrm{d}V \tag{2.107}$$

Here the del operator $\nabla_{\mathbf{r}}$ means the differentiation with respect to $\mathbf{r}$. Note that the size of Ω is sufficiently small from macroscopic viewpoint and the stress is a macroscopic quantity of continuum mechanics where the spatial variation of physical quantity has the characteristic length longer than the linear size of Ω. Hence, we can replace $\nabla_{\mathbf{r}}$ by ∇ which is the differential operator with respect to spatial coordinate of $\tilde{\mathbf{x}}$. Then, Eq. (2.107) becomes

$$\left\langle \hat{\mathbf{V}}_{\text{wall}} \right\rangle_T = \int_\Omega \mathbf{T} \mathrm{d}V \approx \Omega \mathbf{T} \tag{2.108}$$

It is because

$$\int_\Omega (\mathbf{r} - \tilde{\mathbf{x}}) \nabla_{\mathbf{r}} \cdot \mathbf{T} \mathrm{d}V \approx \int_\Omega (\mathbf{r} - \tilde{\mathbf{x}}) \nabla \cdot \mathbf{T} \mathrm{d}V = \left(\int_\Omega (\mathbf{r} - \tilde{\mathbf{x}}) \mathrm{d}V \right) \nabla \cdot \mathbf{T} = \mathbf{0} \tag{2.109}$$

Substitution of Eq. (2.108) into Eq. (2.101) gives

$$\mathbf{T} = -\frac{1}{\Omega} \left\langle \sum_{\alpha=1}^{N} \frac{\mathbf{p}_\alpha \mathbf{p}_\alpha}{m_\alpha} \right\rangle_T - \frac{1}{\Omega} \left\langle \hat{\mathbf{V}}_{\text{in}} \right\rangle_T \tag{2.110}$$

Assume the pair-wise additivity of intermolecular interaction potential (McQuarrie 2000). Then, the potential of Eq. (1.2) can be expressed by

$$U(\{\mathbf{r}_\alpha\}) = \sum_{\alpha=1}^{N}\sum_{\gamma\neq\alpha}^{N} u\left(r_{\alpha\gamma}\right) \tag{2.111}$$

where

$$r_{\alpha\gamma} = \left\|\mathbf{r}_{\alpha\gamma}\right\|; \quad \mathbf{r}_{\alpha\gamma} = \mathbf{r}_\alpha - \mathbf{r}_\gamma \tag{2.112}$$

Then, the intermolecular force $\mathbf{f}_{\alpha\gamma}$ is given by

$$\mathbf{f}_{\alpha\gamma} = -\frac{\partial u\left(r_{\alpha\gamma}\right)}{\partial \mathbf{r}_\alpha} = -\frac{1}{r_{\alpha\gamma}}\frac{\mathrm{d}u}{\mathrm{d}r_{\alpha\gamma}}\mathbf{r}_{\alpha\gamma} = \frac{1}{r_{\alpha\gamma}}\frac{\mathrm{d}u}{\mathrm{d}r_{\alpha\gamma}}\mathbf{r}_{\gamma\alpha} = -\mathbf{f}_{\gamma\alpha} \tag{2.113}$$

Then, the internal virial tensor $\hat{\mathbf{V}}_{\mathrm{in}}$ is given by

$$\hat{\mathbf{V}}_{\mathrm{in}} = \frac{1}{2}\sum_{\alpha=1}^{N}\sum_{\gamma\neq\alpha}^{N}\mathbf{f}_{\alpha\gamma}\mathbf{r}_{\alpha\gamma} = -\frac{1}{2}\sum_{\alpha=1}^{N}\sum_{\gamma\neq\alpha}^{N}\frac{1}{r_{\alpha\gamma}}\frac{\mathrm{d}u}{\mathrm{d}r_{\alpha\gamma}}\mathbf{r}_{\alpha\gamma}\mathbf{r}_{\alpha\gamma} \tag{2.114}$$

Here, we used

$$\sum_{\alpha=1}^{N}\sum_{\gamma\neq\alpha}^{N}\mathbf{f}_{\alpha\gamma} = \mathbf{0} \tag{2.115}$$

Finally we have the following:

$$\mathbf{T} = -\frac{1}{\Omega}\left\langle\sum_{\alpha=1}^{N}\frac{\mathbf{p}_\alpha\mathbf{p}_\alpha}{m_\alpha}\right\rangle_T + \frac{1}{2\Omega}\left\langle\sum_{\alpha=1}^{N}\sum_{\gamma\neq\alpha}^{N}\frac{1}{r_{\alpha\gamma}}\frac{\mathrm{d}u}{\mathrm{d}r_{\alpha\gamma}}\mathbf{r}_{\alpha\gamma}\mathbf{r}_{\alpha\gamma}\right\rangle_T \tag{2.116}$$

It is noteworthy that the time average fluctuates vigorously if Ω and Δt is too small, whereas sufficiently large Ω and Δt give smooth and slow variation. Equation (2.116) can be used for molecular dynamics simulation. Equation (2.116) was derived by Swenson (1983).

If we know nonequilibrium probability distribution such that

$$\frac{1}{\Omega\Delta t}\int_t^{t+\Delta t} A(\Gamma(t'))\mathrm{d}t' = \int A(\Gamma)P_{\mathrm{noneq}}(\Gamma,t)\mathrm{d}\Gamma \equiv \langle A\rangle_{\mathrm{noneq}}(t), \tag{2.117}$$

then the time averages of Eq. (2.116) can be replaced by the nonequilibrium ensemble averages.

$$\mathbf{T} = -\left\langle \sum_{\alpha=1}^{N} \frac{\mathbf{p}_\alpha \mathbf{p}_\alpha}{m_\alpha} \right\rangle + \frac{1}{2} \left\langle \sum_{\alpha=1}^{N} \sum_{\gamma \neq \alpha}^{N} \frac{1}{r_{\alpha\gamma}} \frac{\mathrm{d}u}{\mathrm{d}r_{\alpha\gamma}} \mathbf{r}_{\alpha\gamma} \mathbf{r}_{\alpha\gamma} \right\rangle \tag{2.118}$$

Equation (2.118) is important in rheology because it relates stress with microstates and intermolecular interaction potentials. Irving and Kirkwood derived not only Eq. (2.118) but also various balance equations in terms of microstates from the *Liouville equation* (Irving and Kirkwood 1950).

In equilibrium, we can replace the time averages by equilibrium ensemble averages. The stress tensor of fluid without flow becomes $\mathbf{T} = -p\mathbf{I}$. Then, taking trace on both sides of Eq. (2.118), we have

$$pV = \frac{1}{3} \left\langle \sum_{\alpha=1}^{N} \frac{\|\mathbf{p}_\alpha\|^2}{m_\alpha} \right\rangle - \frac{1}{6} \left\langle \sum_{\alpha=1}^{N} \sum_{\gamma \neq \alpha}^{N} \frac{\mathrm{d}u}{\mathrm{d}r_{\alpha\gamma}} r_{\alpha\gamma} \right\rangle \tag{2.119}$$

Note that no spatial variation of physical quantities in equilibrium allows to use macroscopic volume V. Since the first ensemble average of Eq. (2.119) is two times of the ensemble average of kinetic energy, application of the equipartition theorem gives pressure equation:

$$pV = Nk_\mathrm{B}T - \frac{1}{6} \left\langle \sum_{\alpha=1}^{N} \sum_{\gamma \neq \alpha}^{N} \frac{\mathrm{d}u}{\mathrm{d}r_{\alpha\gamma}} r_{\alpha\gamma} \right\rangle \tag{2.120}$$

Since the ideal gas has no intermolecular potential, Eq. (2.120) becomes the equation of state of ideal gas when $u = 0$. If radial distribution function $g(r)$ is known McQuarrie (2000), Eq. (2.120) becomes simpler:

$$\frac{p}{k_\mathrm{B}T} = \rho_N - \frac{\rho_N^2}{6k_\mathrm{B}T} \int_0^\infty r \frac{\mathrm{d}u}{\mathrm{d}r} g(r) 4\pi r^2 \mathrm{d}r \tag{2.121}$$

where $\rho_N = N/V$. The first term in the right-hand side is the one for the ideal gas and the second term represents the effect of intermolecular interactions.

Problems 2

[1] The volume of the n-dimensional sphere of radius of r is given by

$$V_n(r) = \int \cdots \int_{r^2 > \sum_{k=1}^{n} x_k^2} \mathrm{d}x_1 \ldots \mathrm{d}x_n = K_n r^n \tag{2.a}$$

To identify K_n, you can use the following identities

$$I_n = \int_{-\infty}^{\infty} \cdots \int_{-\infty}^{\infty} \exp\left(-\sum_{k=1}^{n} x_k^2\right) \mathrm{d}x_1 \ldots \mathrm{d}x_n = \sqrt{\pi^n}; \quad I_n = \int_0^{\infty} e^{-r^2} \frac{\mathrm{d}V_n}{\mathrm{d}r} \mathrm{d}r \tag{2.b}$$

Verify that

$$K_n = \sqrt{\left(\frac{2e\pi}{n}\right)^n} \tag{2.c}$$

[2] For ideal gas, derive

$$\Omega(E, V, N) = \frac{2\pi m (2\pi m E)^{\frac{3}{2}N-1}}{h^{3N} N! \Gamma\left(\frac{3}{2}N\right)} V^N \tag{2.d}$$

Here, m is the mass of the ideal gas.

[3] Derive the equation of state for ideal gas from Eq. (2.d).

[4] When the Hamiltonian of N-particle system is given by

$$H = \sum_{k=1}^{N} \frac{\mathbf{p}_k^2}{2m} + U(\{\mathbf{r}_n\}) \tag{2.e}$$

Show that

$$Z(N, V, T) = \frac{Q(N, V, T)}{\lambda^{3N} N!} \tag{2.f}$$

Where

$$\lambda = \sqrt{\frac{h^2}{2\pi m k_\mathrm{B} T}} \tag{2.g}$$

and

$$Q(N, V, T) = \int_V \cdots \int_V e^{-\beta U} \mathrm{d}\mathbf{r}_1 \ldots \mathrm{d}\mathbf{r}_N \tag{2.h}$$

[5] When $U(\{\mathbf{r}_k\}) = 0$ in Eq. (2.e) implies ideal gas. Derive the partition function Z of ideal gas and calculate the entropy.

[6] Diatomic molecule might be considered as two spheres that are connected as rigid body. Assume that the two spheres have the same mass of m and the

distance between them is fixed as a. Then, the Hamiltonian of the rigid diatomic molecule is given by

$$H = \sum_{k=1}^{N} \left[\frac{\mathbf{p}_k^2}{4M} + \frac{1}{2I} \left(p_{\theta,k}^2 + \frac{p_{\phi,k}^2}{\sin^2 \theta} \right) \right] \tag{2.i}$$

where M is the total mass, $M = 2m$, and I is the moment of inertia, $I = ma^2/2$. Show that

$$Z = (2\pi M k_B T)^{3N/2} \left(8\pi^2 I k_B T\right)^N V^N \tag{2.j}$$

Show that this ideal gas follows:

$$U = \frac{5N}{2} k_B T; \quad p = \frac{N k_B T}{V} \tag{2.k}$$

[7] Derive the Helmholtz free energy of ideal gas from the equation of state and compare it with the solution of Problem [5].

3 Brownian Motion

Consider a small particle with the diameter of a is suspended in fluid. Ceaseless motion of the molecules of the fluid makes them frequent random collision with the particle. The average magnitude of the force due to a single collision may be proportional to $k_B T$. This small force could give rise to motion of the particle if the mass of the particle is quite small. However, if the size of the particle is large enough to suffer from a number of almost simultaneous collisions in random directions, then the net force exerted on the particle could be canceled. On the other hand, if the size is also small enough, then the net force could not be canceled and the collisions could give rise to random motion of the particle. This random motion is called *Brownian motion*.

3.1 Langevin Equation

Mechanics of Brownian motion is important because it can be applied to various fields of physics including polymer rheology. It can explain diffusion phenomena as the consequence from thermal motion of molecules.

If the fluid is Newtonian fluid, then the motion of the particle suffers from the resistance force due to the viscosity of the fluid. Stokes calculated the friction force:

$$\mathbf{f}_{\text{vis}} = -\zeta \mathbf{v} \tag{3.1}$$

where $\mathbf{v}$ is the velocity of the Brownian particle and the friction coefficient is given by

$$\zeta = 6\pi\eta a \tag{3.2}$$

where η is the viscosity of the Newtonian fluid. Then, the equation of motion for the Brownian particle is given by

$$m\frac{\mathrm{d}\mathbf{v}}{\mathrm{d}t} = -\zeta \mathbf{v} + \mathbf{f}_R(t) \tag{3.3}$$

where $\mathbf{f}_R$ represents the impact force due to thermal motion of the fluid molecules. Equation (3.3) is called the *Langevin equation*. The random force $\mathbf{f}_R$ must be a random variable. If a random variable is a function of time, then it is called a stochastic variable. Since the direction of the random force must be random, it is a reasonable to assume that

$$\langle \mathbf{f}_R(t) \rangle = \mathbf{0} \tag{3.4}$$

Since the magnitude of $\mathbf{f}_R(t)$ is not zero, it is clear that $\langle \mathbf{f}_R(t)\mathbf{f}_R(t') \rangle \neq \mathbf{0}$. We are interested in the correlation tensor $\langle \mathbf{f}_R(t)\mathbf{f}_R(t') \rangle$. To specify the tensor, we need some assumptions. It is a reasonable assumption that the random variables $\mathbf{f}_R(t)$ and $\mathbf{f}_R(t')$ are statistically independent if $t \neq t'$. Then, the consequence of the statistical independence is $\langle \mathbf{f}_R(t)\mathbf{f}_R(t') \rangle = \mathbf{0}$ for $t \neq t'$. It is a daring assumption. However, if observation timescale is much longer than the average interval between the collisions, then this assumption is plausible. Then, we assume that

$$\langle \mathbf{f}_R(t)\mathbf{f}_R(t') \rangle = B\delta(t - t')\mathbf{I} \tag{3.5}$$

where B corresponds to the square of the average magnitude of the random force and $\boldsymbol{I}$ is the identity tensor.

Since we modeled the correlation tensor for the random force, we are now interested in the correlation tensor of the velocity vector of the Brownian particle. The general solution of Eq. (3.3) is given by

$$\mathbf{v}(t) = \frac{1}{m}\int_{-\infty}^{t} e^{-\zeta(t-\tau)/m}\mathbf{f}_R(\tau)\mathrm{d}\tau \tag{3.6}$$

Then, the velocity correlation tensor for $t = t'$ is given by

$$\langle \mathbf{v}(t)\mathbf{v}(t) \rangle = \frac{1}{m^2}\int_{-\infty}^{t}\int_{-\infty}^{t} e^{-\zeta(2t-\tau-\tau')/m}\langle \mathbf{f}_R(\tau)\mathbf{f}_R(\tau') \rangle \mathrm{d}\tau\mathrm{d}\tau' = \frac{B}{2m\zeta}\mathbf{I} \tag{3.7}$$

Application of the equipartition theorem gives

$$\mathrm{tr}(\langle \mathbf{v}(t)\mathbf{v}(t)\rangle) = \frac{3k_\mathrm{B}T}{m} = \frac{3B}{2m\zeta} \tag{3.8}$$

Hence, we know that

$$B = 2\zeta k_\mathrm{B}T \tag{3.9}$$

This result is called the *fluctuation-dissipation theorem* because B is the strength of fluctuating force (random force) and ζ represents the dissipation by the viscosity of the medium fluid (Zwanzig 2001).

For different times, the velocity correlation tensor is given by

$$\langle \mathbf{v}(t)\mathbf{v}(t')\rangle = \frac{k_\mathrm{B}T}{m} e^{-\zeta|t-t'|/m}\mathbf{I} \tag{3.10}$$

The absolute term $|t - t'|$ is originated from the order of integrations.

Now we are interested in mean square distance (MSD) of Brownian particle. Let the position of Brownian particle at time of t be denoted by $\mathbf{x}(t)$. Then, the position vector is related to the velocity vector of Eq. (3.6) as follows:

$$\mathbf{x}(t) = \mathbf{x}(0) + \int_0^t \mathbf{v}(s)\mathrm{d}s \tag{3.11}$$

MSD is calculated from Eq. (3.11):

$$\begin{aligned}\left\langle \|\mathbf{x}(t) - \mathbf{x}(0)\|^2 \right\rangle &= \int_0^t \int_0^t \langle \mathbf{v}(s)\cdot\mathbf{v}(\tau)\rangle \mathrm{d}\tau\mathrm{d}s = \frac{3k_\mathrm{B}T}{m}\int_0^t\int_0^t e^{-\zeta|\tau-s|/m}\mathrm{d}\tau\mathrm{d}s \\ &= \frac{6k_\mathrm{B}T}{\zeta}t - \frac{6k_\mathrm{B}Tm}{\zeta^2}\left(1 - e^{-\zeta t/m}\right)\end{aligned} \tag{3.12}$$

Note that for large time, we have

$$\left\langle \|\mathbf{x}(t) - \mathbf{x}(0)\|^2 \right\rangle = 6Dt \tag{3.13}$$

where

$$D = \frac{k_\mathrm{B}T}{\zeta} = \frac{k_\mathrm{B}T}{6\pi\eta a} \tag{3.14}$$

We will show that D in Eq. (3.14) is the diffusion constant and Eq. (3.14) is called the *Stokes–Einstein equation* which relates the diffusion constant with the viscosity of the medium.

3.2 Diffusion Equation

The random force of the Langevin function is a time-dependent random variable and the random variable is an indexed collection of random variable called stochastic process. Since the velocity of Brownian particle is a linear functional of the random force, Eq. (3.6), the velocity is also a stochastic random variable. Because of Eq. (3.11), the position of Brownian particle is also a stochastic variable.

Let the probability distribution of the position of Brownian particle be denoted by $P(\mathbf{x}, t)$. We start from the *Chapman–Kolmogorov equation* to derive the probability distribution $P(\mathbf{x}, t)$:

$$P(\mathbf{x}, t + \Delta t) = \int T(\mathbf{r}, \mathbf{x} - \mathbf{r}, \Delta t) P(\mathbf{x} - \mathbf{r}, t) \mathrm{d}\mathbf{r} \tag{3.15}$$

where transition probability distribution $T(\mathbf{r}, \mathbf{x}, \Delta t)$ represents the probability that a Brownian particle at $\mathbf{x}$ is moved by the displacement of $\mathbf{r}$ irrespective of the present time. Hence, Eq. (3.15) implies that the probability of the event of $(\mathbf{x}, t + \Delta t)$ can be determined from the probability of the event of $(\mathbf{x} - \mathbf{r}, t)$ and the transition probability distribution. Equation (3.15) also implies that future probability can be determined by the present probability without the knowledge of the whole history. To use Eq. (3.15), we need to know the function $T(\mathbf{r}, \mathbf{x}, \Delta t)$.

Since the random force is not correlated for two different times, it is reasonable to assume that the transition probability depends on only displacement vector: $T(\mathbf{r}, \mathbf{x}, \Delta t) = T(\mathbf{r}, \Delta t)$. Since the diffusing medium is isotropic, there is no preferred orientation of displacement. Then, we can reduce the function as $T(\mathbf{r}, \Delta t) = T(\|\mathbf{r}\|, \Delta t)$. Since $T(\mathbf{r}, \Delta t)$ is a probability distribution, the normalization condition is assumed. As for arbitrary function $f(\mathbf{r})$, we define the transition average as

$$\langle f(\mathbf{r}) \rangle_T = \int f(\mathbf{r}) T(\mathbf{r}, \Delta t) \mathrm{d}\mathbf{r} \tag{3.16}$$

Then, the Taylor series expansion of Eq. (3.15) is given as

$$\begin{aligned} P(\mathbf{x}, t) + \frac{\partial P}{\partial t} \Delta t &= \left\langle P(\mathbf{x}, t) - \nabla P \cdot \mathbf{r} + \frac{1}{2} \mathbf{r}\mathbf{r} : \nabla\nabla P \right\rangle_T \\ &= P(\mathbf{x}, t) \langle 1 \rangle_T - \langle \mathbf{r} \rangle_T \cdot \nabla P + \frac{1}{2} \langle \mathbf{r}\mathbf{r} \rangle_T : \nabla\nabla P \end{aligned} \tag{3.17}$$

Since $T(\mathbf{r})$ is a scalar-valued isotropic function of vector, it is obvious that

$$\langle 1 \rangle_T = 1; \quad \langle \mathbf{r} \rangle_T = \mathbf{0}; \quad \langle \mathbf{r}\mathbf{r} \rangle_T = \frac{b^2(\Delta t)}{3} \mathbf{I} \tag{3.18}$$

where

$$b^2(\Delta t) = \mathrm{tr}\left(\langle \mathbf{rr} \rangle_T\right) = \langle \mathbf{r} \cdot \mathbf{r} \rangle_T = 4\pi \int_0^\infty r^4 T(\mathbf{r}, \Delta t) \mathrm{d}r > 0 \tag{3.19}$$

Arrangement of Eq. (3.17) gives

$$\frac{\partial P}{\partial t} = \frac{b^2(\Delta t)}{6\Delta t} \nabla^2 P \tag{3.20}$$

Note that the square of the characteristic length of diffusion $b^2(\Delta t)$ is assumed as a linear function of Δt:

$$D = \frac{b^2(\Delta t)}{6\Delta t} \tag{3.21}$$

Note that the constant D is the diffusion constant.

A suspension of Brownian particles is assumed as the collection of statistically independent Brownian particles. Then, the number concentration $c(\mathbf{x}, t)$ is given by

$$c(\mathbf{x}, t) = \frac{1}{V} \sum_{i=1}^{N} P_i(\mathbf{x}, t) \tag{3.22}$$

where V is the volume of the diffusion medium and $P_i(\mathbf{x}, t)$ is the probability distribution of the ith Brownian particle which is represented by the diffusion constant D_i Then, the number concentration obeys the diffusion equation:

$$\frac{\partial c}{\partial t} = D \nabla^2 c \tag{3.23}$$

where

$$D = \sum_{i=1}^{N} D_i \tag{3.24}$$

Note that Eq. (3.23) is the diffusion equation for molecules that follows *Fick's diffusion law*.

Equation (3.19) immediately consequences that the MSD follows

$$\left\langle \|\mathbf{x}(t) - \mathbf{x}(0)\|^2 \right\rangle = 6Dt \tag{3.25}$$

Therefore, the Stokes–Einstein equation, Eq. (3.14), holds.

3.3 Liouville Equation

When the phenomena of Brownian motion were found, the size of the Brownian particle is much larger than those of the fluid molecules. The explanation why Brownian motion occurs does not exclude the Brownian motion of a particle whose size is comparative with molecular size. Extension to such molecular entity, we need to know the origin of the random force.

Individual system of an ensemble is represented by a single point in $6N$-dimensional phase space. The point moves in phase space according to the law of mechanics. We know the law of mechanics which is represented by a set of differential equations, called the equations of motion. The equations of motion in the Newtonian mechanics are the second-order ordinary differential equations. Any second-order ordinary differential equation can be split into two first-order ordinary differential equations. As for the Hamiltonian of Eq. (1.2), the equations of motion can be expressed as

$$\frac{\partial H}{\partial \mathbf{p}_\alpha} = \frac{\mathrm{d}\mathbf{r}_\alpha}{\mathrm{d}t}; \quad \frac{\partial H}{\partial \mathbf{r}_\alpha} = -\frac{\mathrm{d}\mathbf{p}_\alpha}{\mathrm{d}t} \tag{3.26}$$

We are interested in finding an evolution equation (kinetic equation) of the probability distribution function of an ensemble from Eq. (3.26).

Consider a system which belongs to an ensemble at time t. Is it possible that the microstate of the system will not be in the ensemble at $t + \mathrm{d}t$? As for microcanonical ensemble, representative point of the system is still in 6 N-dimensional phase space and the positions of molecules are still in V, the volume of the system. It is not difficult to show that the Hamiltonian of Eq. (1.2) conserves the total mechanical energy. Hence, if the microstate of the system was in the region of the ensemble, then the microstate always satisfies the conditions of microcanonical ensemble during the motion according to Eq. (3.26). This is true for other ensembles. Therefore, it can be said that any microstate of an ensemble (or any phase point of an ensemble) maintains in the ensemble. Then, the number of microstates of the ensemble is conserved and so is the probability distribution. This gives the analogy between the mass density of continuum mechanics and the probability distribution of ensemble. Such analogy gives the *Liouville equation* (Goldstein et al. 2001):

$$\frac{\partial P}{\partial t} + \sum_{\alpha=1}^{N} \left[\frac{\partial}{\partial \mathbf{r}_\alpha} \cdot \left(\frac{\mathrm{d}\mathbf{r}_\alpha}{\mathrm{d}t} P \right) + \frac{\partial}{\partial \mathbf{p}_\alpha} \cdot \left(\frac{\mathrm{d}\mathbf{p}_\alpha}{\mathrm{d}t} P \right) \right] = 0 \tag{3.27}$$

Use of Eq. (3.26) and arrangement gives

$$\frac{\mathrm{d}P}{\mathrm{d}t} = \frac{\partial P}{\partial t} + \sum_{\alpha=1}^{N} \left(\frac{\partial H}{\partial \mathbf{p}_\alpha} \cdot \frac{\partial P}{\partial \mathbf{r}_\alpha} - \frac{\partial H}{\partial \mathbf{r}_\alpha} \cdot \frac{\partial P}{\partial \mathbf{p}_\alpha} \right) = 0 \tag{3.28}$$

The analogy of the Liouville equation to the mass balance equation of incompressible fluid becomes clearer if we define the flux of probability by

$$\mathbf{j}_{6N} = \mathbf{u}_{6N} P(\Gamma, t) = \left(\frac{\mathrm{d}\mathbf{r}_1}{\mathrm{d}t}, \ldots, \frac{\mathrm{d}\mathbf{r}_N}{\mathrm{d}t}, \frac{\mathrm{d}\mathbf{p}_1}{\mathrm{d}t}, \ldots, \frac{\mathrm{d}\mathbf{p}_N}{\mathrm{d}t} \right) P(\Gamma, t) \tag{3.29}$$

and the gradient of probability distribution by

$$\nabla_{6N} P = \left(\frac{\partial P}{\partial \mathbf{r}_1}, \ldots, \frac{\partial P}{\partial \mathbf{r}_N}, \frac{\partial P}{\partial \mathbf{p}_1}, \ldots, \frac{\partial P}{\partial \mathbf{p}_N} \right) \tag{3.30}$$

The innerproduct of two $6N$-dimensional vectors is defined as

$$\mathbf{a}_{6N} \cdot \mathbf{x}_{6N} = \sum_{\alpha=1}^{N} (\mathbf{a}_\alpha \cdot \mathbf{x}_\alpha + \mathbf{b}_\alpha \cdot \mathbf{y}_\alpha) \tag{3.31}$$

where

$$\mathbf{a}_{6N} = (\mathbf{a}_1, \ldots, \mathbf{a}_N, \mathbf{b}_1, \ldots, \mathbf{b}_N); \quad \mathbf{x}_{6N} = (\mathbf{x}_1, \ldots, \mathbf{x}_N, \mathbf{y}_1, \ldots, \mathbf{y}_N) \tag{3.32}$$

Then, Eq. (3.27) can be rewritten by

$$\frac{\partial P}{\partial t} + \nabla_{6N} \cdot \mathbf{j}_{6N} = \frac{\partial P}{\partial t} + \nabla_{6N} \cdot (\mathbf{u}_{6N} P) = \frac{\partial P}{\partial t} + \mathbf{u}_{6N} \cdot \nabla_{6N} P = 0 \tag{3.33}$$

Here, it is used that $\nabla_{6N} \cdot \mathbf{u}_{6N} = 0$, which can be easily proved by the equation of motion, Eq. (3.26). It is noteworthy that the steady-state solution of the Liouville equation is the probability distribution function in equilibrium.

The Liouville equation provides a clue to calculate nonequilibrium probability distribution and a belief for the existence of the nonequilibrium ensemble average of Eq. (2.118). However, it is known that solving the Liouville equation is equivalent to solving the whole set of equations of motion which consists of $3N$ ordinary differential equations of second order. Unfortunately, no irreversibility is found in the evolution equation of $\langle \log P \rangle$ derived from the Liouville equation. Although both classical and quantum mechanics are time-reversal, macroscopic phenomena are observed irreversible. This discrepancy is one of the most important mysteries in statistical mechanics and irreversible thermodynamics (Zuvarev 1974).

From Eq. (3.28), we can define the *Liouville operator* as follows:

$$\mathsf{L} = \sum_{\alpha=1}^{N} \left(\frac{\partial H}{\partial \mathbf{p}_\alpha} \cdot \frac{\partial}{\partial \mathbf{r}_\alpha} - \frac{\partial H}{\partial \mathbf{r}_\alpha} \cdot \frac{\partial}{\partial \mathbf{p}_\alpha} \right) \tag{3.34}$$

Then, Eq. (3.28) can be expressed in a simpler way:

$$\frac{\partial P}{\partial t} = -\mathsf{L}P \tag{3.35}$$

Equation (3.35) is the first-order differential equation for time. Just as the exponential function of tensor was defined in Sect. 5 in Chap. 1, we can define

$$e^{t\mathsf{L}} = \sum_{n=0}^{\infty} \frac{t^n}{n!}\mathsf{L}^n \tag{3.36}$$

Note that $\mathsf{L}^0 = \mathsf{I}$ is the identity operator such that for any function f, $\mathsf{I}f = f$. Then, it is obvious that

$$P(\Gamma, t) = e^{-t\mathsf{L}}P(\Gamma, 0) \tag{3.37}$$

Note that Eq. (3.37) is a formal solution, which means that Eq. (3.37) does not give the mathematical structure of $P(\Gamma, t)$ although it satisfies the Liouville equation. To obtain the general solution of the Liouville equation is to solve $3N$ second-order differential equations which are equations of motion.

The Liouville operator is also found in the total time derivative of a dynamic function $A(\Gamma, t)$:

$$\begin{aligned}\frac{\mathrm{d}A}{\mathrm{d}t} &= \frac{\partial A}{\partial t} + \sum_{\alpha=1}^{N}\left(\frac{\partial A}{\partial \mathbf{r}_\alpha}\frac{\mathrm{d}\mathbf{r}_\alpha}{\mathrm{d}t} + \frac{\partial A}{\partial \mathbf{p}_\alpha}\frac{\mathrm{d}\mathbf{p}_\alpha}{\mathrm{d}t}\right) \\ &= \frac{\partial A}{\partial t} + \sum_{\alpha=1}^{N}\left(\frac{\partial H}{\partial \mathbf{p}_\alpha}\cdot\frac{\partial A}{\partial \mathbf{r}_\alpha} - \frac{\partial H}{\partial \mathbf{r}_\alpha}\cdot\frac{\partial A}{\partial \mathbf{p}_\alpha}\right) \\ &= \frac{\partial A}{\partial t} + \mathsf{L}A\end{aligned} \tag{3.38}$$

With the help of Eq. (3.33), use of divergence theorem for $6N$-dimensional space gives the following identities:

$$\int \mathsf{L}B\,\mathrm{d}\Gamma = 0 \tag{3.39a}$$

$$\int P\mathsf{L}A\mathrm{d}\Gamma = -\int A\mathsf{L}P\mathrm{d}\Gamma \tag{3.39b}$$

where A and B are dynamic variables and

$$\lim_{\|\mathbf{r}_\alpha\|\to\infty} B(\Gamma) = \lim_{\|\mathbf{p}_\alpha\|\to\infty} B(\Gamma) = 0 \quad \text{for any } \alpha \tag{3.40}$$

Note that the probability distribution $P(\Gamma, t)$ satisfies Eq. (3.40).

3.4 Generalized Langevin Equation

Consider a Brownian particle imbedded in a heat bath which consists of N molecules. Then, for the $N+1$ molecules, the Hamiltonian is given by

$$H = H_B + H_{\mathrm{o}} \tag{3.41}$$

where

$$H_B = \frac{\mathbf{p}^2}{2m} \tag{3.42}$$

and

$$H_{\mathrm{o}} = \sum_{\alpha=1}^{N} \frac{\mathbf{p}_\alpha^2}{2m_\alpha} + V(\mathbf{r}, \mathbf{r}_1, \ldots, \mathbf{r}_N) \tag{3.43}$$

Here, $\mathbf{r}$, $\mathbf{p}$, and m without subscript indicate position, momentum, and mass of the Brownian particle while quantities with subscript are those of the molecules of the heat bath. Then, it is clear that

$$\frac{\mathrm{d}\mathbf{r}}{\mathrm{d}t} = \frac{\mathbf{p}}{m}; \quad \frac{\mathrm{d}\mathbf{p}}{\mathrm{d}t} = \mathbf{f} \tag{3.44}$$

where the force exerted on the Brownian particle is given from the gradient of the coupling potential U_{c} as follows:

$$\mathbf{f} = -\frac{\partial V}{\partial \mathbf{r}} \tag{3.45}$$

On the other hand, the equations of motion for the molecules of the heat bath are given by

$$\frac{\mathrm{d}\mathbf{r}_\alpha}{\mathrm{d}t} = \frac{\mathbf{p}_\alpha}{m_\alpha}; \quad \frac{\mathrm{d}\mathbf{p}_\alpha}{\mathrm{d}t} = -\frac{\partial V}{\partial \mathbf{r}_\alpha} \tag{3.46}$$

Equation (3.46) cannot be solved analytically in general because of the complexity of potentials V. To simplify the problem, assume that

$$\frac{\partial V}{\partial \mathbf{r}_\alpha} = \mathbf{0} \text{ at } \mathbf{r}_\alpha = \bar{\mathbf{r}}_\alpha; \quad \frac{\partial V}{\partial \mathbf{r}} = \mathbf{0} \text{ at } \mathbf{r} = \bar{\mathbf{r}} \tag{3.47}$$

Then, the Taylor expansion of the potentials is given by

$$\begin{aligned} V(\mathbf{r}, \mathbf{r}_1, \ldots, \mathbf{r}_N) = V(\mathbf{r}, \mathbf{r}_1, \ldots, \mathbf{r}_N) + \frac{1}{2}(\mathbf{r} - \bar{\mathbf{r}}) \cdot \mathbf{G}_{00} \cdot (\mathbf{r} - \bar{\mathbf{r}}) \\ + \left[\sum_{\alpha=1}^{N} (\mathbf{r}_\alpha - \bar{\mathbf{r}}_\alpha) \cdot \mathbf{G}_{\alpha 0} \right] \cdot (\mathbf{r} - \bar{\mathbf{r}}) \\ + \frac{1}{2} \sum_{\alpha=1}^{N} \sum_{\beta=1}^{N} (\mathbf{r}_\alpha - \bar{\mathbf{r}}_\alpha) \cdot \mathbf{G}_{\alpha\beta} \cdot \left(\mathbf{r}_\beta - \bar{\mathbf{r}}_\beta\right) \end{aligned} \tag{3.48}$$

where

$$\mathbf{G}_{\alpha\beta} = \left(\frac{\partial^2 V}{\partial \mathbf{r}_\alpha \partial \mathbf{r}_\beta} \right)_{\{\mathbf{r}, \mathbf{r}_\alpha\} = \{\bar{\mathbf{r}}, \bar{\mathbf{r}}_\alpha\}} = \mathbf{G}_{\beta\alpha} \quad \text{with} \quad \alpha, \beta = 0, 1, \ldots, N \tag{3.49}$$

In Eq. (3.49), we consider $\mathbf{r} = \mathbf{r}_0$. The symmetric second-order tensors $\mathbf{G}_{\alpha\beta}$ are constant tensors. Now we can simplify the equations of motion, Eqs. (3.44) and (3.46), as follows:

$$m \frac{\mathrm{d}^2 \mathbf{x}}{\mathrm{d}t^2} = -\mathbf{G}_{00} \cdot \mathbf{x} - \sum_{\alpha=1}^{N} \mathbf{G}_{\alpha 0} \cdot \mathbf{x}_\alpha \tag{3.50}$$

$$m_\alpha \frac{\mathrm{d}^2 \mathbf{x}_\alpha}{\mathrm{d}t^2} = -\mathbf{G}_{\alpha 0} \cdot \mathbf{x} - \sum_{\beta=1}^{N} \mathbf{G}_{\alpha\beta} \cdot \mathbf{x}_\beta \tag{3.51}$$

Since $\bar{\mathbf{r}}$ and $\bar{\mathbf{r}}_\alpha$ are constant vectors, we defined $\mathbf{x} = \mathbf{r} - \bar{\mathbf{r}}$ and $\mathbf{x}_\alpha = \mathbf{r}_\alpha - \bar{\mathbf{r}}_\alpha$.

To solve Eq. (3.51), we need to express Eq. (3.51) in components. Let us use following notations:

$$\mathbf{G}_{\alpha\beta} = m_\alpha G^{ik}_{\alpha\beta} \mathbf{e}_i \mathbf{e}_k; \quad \mathbf{x}_\alpha = x^k_\alpha \mathbf{e}_k; \quad \mathbf{x} = x^k \mathbf{e}_k \tag{3.52}$$

Here we use summation convention for i and k which represent the components of the vector and tensor under consideration. Then, Eq. (3.51) becomes

$$\frac{\mathrm{d}^2 x^i_\alpha}{\mathrm{d}t^2} = -G^{ik}_{\alpha 0} x^k - \sum_{\beta=1}^{N} G^{ik}_{\alpha\beta} x^k_\beta \tag{3.53}$$

To make it simpler, we introduce

$$\xi_{3(\alpha-1)+k} = x^k_\alpha; \quad \Gamma^{3(\alpha-1)+i}_{3(\beta-1)+k} = G^{ik}_{\alpha\beta}; \quad \Gamma^{k}_{3(\alpha-1)+i} = G^{ik}_{\alpha 0} \quad \text{for} \quad 1 \le \alpha, \beta \le N \tag{3.54}$$

Then, Eq. (3.53) becomes

$$\frac{\mathrm{d}^2\xi_A}{\mathrm{d}t^2} = -\Gamma_A^k x^k - \sum_{B=1}^{3N} \Gamma_A^B \xi_B \tag{3.55}$$

Since $\mathbf{G}_{\alpha\beta} = \mathbf{G}_{\alpha\beta}^T = \mathbf{G}_{\beta a}$, it is obvious that $\Gamma_A^B = \Gamma_B^A$. Then, the $3N \times 3N$ symmetric matrix $\Gamma = \left[\Gamma_A^B\right]$ can be diagonalized by

$$\mathbf{\Gamma} = \mathbf{Q}^{-1} \cdot \mathbf{W} \cdot \mathbf{Q} \tag{3.56}$$

where

$$\mathbf{W} = \begin{bmatrix} \omega_1^2 & 0 & \cdots & 0 \\ 0 & \omega_2^2 & \cdots & 0 \\ \vdots & \vdots & \ddots & \vdots \\ 0 & 0 & \cdots & \omega_{3N}^2 \end{bmatrix} \tag{3.57}$$

We apply the vector notation to Eq. (3.55) again as follows:

$$\frac{\mathrm{d}^2\boldsymbol{\xi}}{\mathrm{d}t^2} = -\boldsymbol{\gamma} - \mathbf{\Gamma} \cdot \xi \tag{3.58}$$

where $\boldsymbol{\gamma} = \left[\Gamma_1^k x^k, \Gamma_2^k x^k, \ldots, \Gamma_{3N}^k x^k\right]^T$. Using Eq. (3.56), we have

$$\frac{\mathrm{d}^2\mathbf{a}}{\mathrm{d}t^2} = -\mathbf{g} - \mathbf{W} \cdot \mathbf{a} \tag{3.59}$$

where

$$\mathbf{a} = \mathbf{Q} \cdot \boldsymbol{\xi}; \quad \mathbf{g} = \mathbf{Q} \cdot \boldsymbol{\gamma} \tag{3.60}$$

Then, taking Laplace transform, we have

$$\tilde{a}_I(s) = \frac{1}{s^2 + \omega_I^2}\dot{a}_I(0) + \frac{s}{s^2 + \omega_I^2}a_I(0) - \frac{1}{s^2 + \omega_I^2}\tilde{g}_I(s) \tag{3.61}$$

Where the summation convention for I is not used. Inversion of the transform gives

$$\begin{aligned} a_I(t) = &-\frac{g_I(t)}{\omega_I^2} + \int_0^t \frac{\sin\omega_I(t-\tau)}{\omega_I^2}\frac{\mathrm{d}g_I}{\mathrm{d}\tau}\mathrm{d}\tau \\ &+ a_I(0)\left(1 + \frac{1}{\omega_I^2}\right)\cos\omega_I t + \frac{\dot{a}_I(0)}{\omega_I}\sin\omega_I t \end{aligned} \tag{3.62}$$

Equation (3.62) gives

$$\begin{aligned}\boldsymbol{\xi}(t) = -\boldsymbol{\Gamma}^{-1}\cdot\boldsymbol{\gamma}(t) + \int_0^t \mathbf{Q}^{-1}\cdot\mathbf{W}^{-1}\cdot\mathbf{S}(t-\tau)\cdot\mathbf{Q}\cdot\frac{\mathrm{d}\boldsymbol{\gamma}}{\mathrm{d}\tau}\mathrm{d}\tau \\ + \mathbf{Q}^{-1}\cdot\mathbf{C}(t)\cdot\mathbf{Q}\cdot\boldsymbol{\xi}(0) + \mathbf{Q}^{-1}\cdot\mathbf{W}^{-1/2}\cdot\mathbf{S}(t)\cdot\dot{\boldsymbol{\xi}}(0)\end{aligned} \tag{3.63}$$

where

$$[\mathbf{C}(t)]_{IK} = \frac{\omega_I^2+1}{\omega_I^2}\cos\omega_I t\delta_{IK}; \quad [\mathbf{S}(t)]_{IK} = \sin\omega_I t\delta_{IK}; \quad [\mathbf{W}^{-n}]_{IK} = \frac{\delta_{IK}}{\omega_I^{2n}} \tag{3.64}$$

Further conversion processes from $\boldsymbol{\xi}(t)$ to $\mathbf{x}_\alpha(t)$ and substitution to Eq. (3.50) gives *generalized Langevin equation* (GLE) such that

$$m\frac{\mathrm{d}\mathbf{v}}{\mathrm{d}t} = -\frac{\partial U}{\partial\mathbf{r}} - \int_0^t \mathbf{Z}(t-\tau)\mathbf{v}(\tau)\mathrm{d}\tau + \mathbf{f}_R(t) \tag{3.65}$$

where $\mathbf{v} = \mathrm{d}\mathbf{r}/\mathrm{d}t$. Note that the random force $\mathbf{f}_R(t)$ is originated from the second and third terms of the right-hand side of Eq. (3.63) and the gradient of U is originated from the first term.

It is very tedious and complicate to derive $U(\mathbf{r})$, $\mathbf{Z}(t)$, and $\mathbf{f}_R(t)$ in terms of the molecules of the heat bath (Tuckerman 2010). When the medium is isotropic the friction tensor $\mathbf{Z}(t)$ becomes $\zeta(t)\mathbf{I}$. It can be derived that the random force $\mathbf{f}_R(t)$ satisfies the following:

$$\langle\mathbf{f}_R(t)\rangle = \mathbf{0}; \quad \langle\mathbf{f}_R(t)\mathbf{f}_R(0)\rangle = 2k_\mathrm{B}\theta\mathbf{Z}(t) \tag{3.66}$$

Note that the average means

$$\langle\mathbf{f}_R(t)\mathbf{f}_R(0)\rangle = \int \mathbf{f}_R(t)\mathbf{f}_R(0)P(\Gamma)\mathrm{d}\Gamma \tag{3.67}$$

where the probability distribution follows the Liouville equation and the domain of the integration is the phase space of the molecules of the heat bath.

Hence, the phenomenological Langevin equation has molecular basis. When the potential $U(\mathbf{r})$ is zero and $\mathbf{Z}(t) = \zeta\delta(t)\mathbf{I}$, the original Langevin equation (Eq. 3.3) is recovered. Furthermore, the above derivation implies that the GLE is effective even if the size of the Brownian particle is comparative with those of the molecules of the liquid medium. More generalized derivation can be done by the use of projection operator formalism (Zwanzig 2001). The GLE can be applied to any function of dynamic variables of n Brownian particles. In Part II, we will study that the GLE is applicable to linear viscoelasticity of the medium liquid through the optical measurement of the MSD of a Brownian particle.

3.5 The Fokker–Planck Equation

The Langevin equation is the equation of motion for the dynamic variables of the Brownian particles. Although the original Langevin equation was given by intuition not based on fundamental theory of physics, we have learned that the theory of GLE renders molecular basis to the original one. Now we become interested in the probability distribution of the Brownian dynamic variables. The Fokker–Planck equation is the time-evolution equation of the probability distribution. Diffusion Eq. (3.20) is one of the simplest forms of the *Fokker–Planck equation*.

In the derivation of the Fokker–Planck equation, there are two approaches: one is to use the transition probability which is not given rather than is desired and the other is to use the Langevin equation. As for the former, see McQuarrie (2000). Here, we shall introduce the latter approach (Zwanzig 2001).

3.5.1 General Case

Consider $\widehat{\mathbf{a}}(t)$ as the n-dimensional vector representing dynamics of Brownian particles. Then, the Langevin equation for $\widehat{\mathbf{a}}(t)$ can be represented by

$$\frac{\mathrm{d}\widehat{\mathbf{a}}}{\mathrm{d}t} = -\mathbf{u}\left(\widehat{\mathbf{a}}\right) + \mathbf{f}_R(t) \tag{3.68}$$

where $\mathbf{u}(\widehat{\mathbf{a}})$ is a mapping from n-dimensional vector to n-dimensional vector and the random force $\mathbf{f}_R(t)$ is also a n-dimensional vector.

Although the random force is considered as a stochastic variable, it is not easy to find its probabilistic characteristics in terms of the ensemble probability distribution which obeys the Liouville equation. As shown in Eq. (3.63), the random force is originated from the contributions of a huge number of the molecules in medium liquid. Hence, reminding the central limit theorem, it is a reasonable approximation to consider the probabilistic characteristics of the random force as the Gaussian:

$$\langle \mathbf{f}_R(t) \rangle = \mathbf{0}; \quad \langle \mathbf{f}_R(t)\mathbf{f}_R(t') \rangle = \mathbf{B}\delta(t - t') \tag{3.69}$$

where $\mathbf{B}$ is a symmetric positive definite matrix.

Since the random force is a stochastic variable, the GLE implies that the dynamic variable $\widehat{\mathbf{a}}$ is also a stochastic variable. Then, we are interested in the probability distribution function of $\widehat{\mathbf{a}}$. The dynamic variable is a function of the momentum and position of Brownian particle. Then, the probability distribution can be defined by

$$\Pi(\mathbf{a}, t) = \left\langle \delta\left(\mathbf{a} - \widehat{\mathbf{a}}(t)\right) \right\rangle_{\mathrm{eq}} \tag{3.70}$$

where

$$\widehat{\mathbf{a}}(t) = \widehat{\mathbf{a}}[\mathbf{p}(t), \mathbf{r}(t)] \tag{3.71}$$

Since the random force depends on Γ, Eq. (3.67) implies that $\widehat{\mathbf{a}}(t)$ also depends on Γ while $\mathbf{a}$ is independent of Γ.

Extension of Eq. (6.50 in Chap. 1) to n-dimension, we have

$$\delta\left(\mathbf{a} - \widehat{\mathbf{a}}(t)\right) = \frac{1}{(2\pi)^n} \int e^{-i\mathbf{q}\cdot\left(\mathbf{a} - \widehat{\mathbf{a}}(t)\right)} d\mathbf{q} \tag{3.72}$$

Differentiation of Eq. (3.71) with respect to time gives

$$\frac{d}{dt}\delta\left(\mathbf{a} - \widehat{\mathbf{a}}(t)\right) = -\frac{d\widehat{\mathbf{a}}}{dt}\cdot\frac{\partial}{\partial \mathbf{a}}\delta\left(\mathbf{a} - \widehat{\mathbf{a}}(t)\right) = -\frac{\partial}{\partial \mathbf{a}}\cdot\left[\frac{d\widehat{\mathbf{a}}}{dt}\delta\left(\mathbf{a} - \widehat{\mathbf{a}}(t)\right)\right] \tag{3.73}$$

Then, differentiation of Eq. (3.70) gives

$$\begin{aligned}
\frac{\partial}{\partial t}\Pi(\mathbf{a}, t) &= -\frac{\partial}{\partial \mathbf{a}}\cdot\left\langle\frac{d\widehat{\mathbf{a}}}{dt}\delta\left(\mathbf{a} - \widehat{\mathbf{a}}(t)\right)\right\rangle_{\text{eq}} \\
&= \frac{\partial}{\partial \mathbf{a}}\cdot\left\langle\mathbf{u}\left(\widehat{\mathbf{a}}\right)\delta\left(\mathbf{a} - \widehat{\mathbf{a}}(t)\right)\right\rangle_{\text{eq}} - \frac{\partial}{\partial \mathbf{a}}\cdot\left\langle\mathbf{f}_R(t)\delta\left(\mathbf{a} - \widehat{\mathbf{a}}(t)\right)\right\rangle_{\text{eq}} \\
&= \frac{\partial}{\partial \mathbf{a}}\cdot\left\langle\mathbf{u}(\mathbf{a})\delta\left(\mathbf{a} - \widehat{\mathbf{a}}(t)\right)\right\rangle_{\text{eq}} - \frac{\partial}{\partial \mathbf{a}}\cdot\left\langle\mathbf{f}_R(t)\delta\left(\mathbf{a} - \widehat{\mathbf{a}}(t)\right)\right\rangle_{\text{eq}} \\
&= \frac{\partial}{\partial \mathbf{a}}\cdot\left[\mathbf{u}(\mathbf{a})\Pi(\mathbf{a}, t)\right] - \frac{\partial}{\partial \mathbf{a}}\cdot\left\langle\mathbf{f}_R(t)\delta\left(\mathbf{a} - \widehat{\mathbf{a}}(t)\right)\right\rangle_{\text{eq}}
\end{aligned} \tag{3.74}$$

Here, we assume that we can replace the average in Eq. (3.74) by the average with respect to the probability distribution of the random force. Since the random force is the result from the chaotic motion of a huge number of molecules in the liquid medium, the probability distribution can be considered as the Gaussian. Then, we can exploit Eq. (1.52) by replacing $\mathbf{x}$ and f by $\mathbf{f}_R(t)$ and $\delta(\mathbf{a} - \widehat{\mathbf{a}}(t))$, respectively. Then, we have

$$\begin{aligned}
\left\langle\mathbf{f}_R(t)\delta\left(\mathbf{a} - \widehat{\mathbf{a}}(t)\right)\right\rangle_{\text{eq}} &= \mathbf{B}\cdot\left\langle\frac{\delta}{\delta\mathbf{f}_R(t)}\delta\left(\mathbf{a} - \widehat{\mathbf{a}}(t)\right)\right\rangle \\
&= -\mathbf{B}\cdot\left\langle\frac{\delta\widehat{\mathbf{a}}(t)}{\delta\mathbf{f}_R(t)}\cdot\frac{\partial}{\partial \mathbf{a}}\delta\left(\mathbf{a} - \widehat{\mathbf{a}}(t)\right)\right\rangle
\end{aligned} \tag{3.75}$$

where we introduced functional derivative which is the derivative of functional with respect to a function (Schwabl 2006). As for functional derivative, see appendix.

Functional is a mapping from function to real number or function. A function can be considered as a special functional. Hence, it is clear that

$$\frac{\delta g(t)}{\delta g(\tau)} = \delta(t-\tau); \quad \frac{\delta \mathbf{f}_R(t)}{\delta \mathbf{f}_R(\tau)} = \delta(t-\tau)\mathbf{I} \tag{3.76}$$

where $\boldsymbol{I}$ is the n-dimensional identity matrix. To calculate the last term of random force, we need the solution of the Langevin equation (3.68). Formally, we know that

$$\widehat{\mathbf{a}}(t) = \widehat{\mathbf{a}}(0) - \int_0^t \mathbf{u}\left(\widehat{\mathbf{a}}(\tau)\right)\mathrm{d}\tau + \int_0^t \mathbf{f}_R(\tau)\mathrm{d}\tau \tag{3.77}$$

This is a linear functional of $\mathbf{f}_R(t)$. Hence, we have

$$\frac{\delta \widehat{\mathbf{a}}(t)}{\delta \mathbf{f}_R(t)} = \int_0^t \frac{\delta \mathbf{f}_R(\tau)}{\delta \mathbf{f}_R(t)}\mathrm{d}\tau = \int_0^t \delta(\tau - t)\mathrm{d}\tau = \frac{1}{2} \tag{3.78}$$

Finally, we have

$$\frac{\partial \Pi(\mathbf{a},t)}{\partial t} = \frac{\partial}{\partial \mathbf{a}} \cdot [\mathbf{u}(\mathbf{a})\Pi(\mathbf{a},t)] + \frac{1}{2}\frac{\partial}{\partial \mathbf{a}} \cdot \mathbf{B} \cdot \frac{\partial}{\partial \mathbf{a}}\Pi(\mathbf{a},t) \tag{3.79}$$

If the flux of the probability distribution $\Pi(\mathbf{a},t)$ is given by $\mathbf{j}_p$, then the conservation of probability implies that

$$\frac{\partial \Pi}{\partial t} = -\frac{\partial}{\partial \mathbf{a}} \cdot \mathbf{j}_p \tag{3.80}$$

The probability flux is given by $\mathbf{j}_p = \mathbf{v}_f \Pi(\mathbf{a},t)$, where $\mathbf{v}_f$ is defined by the flux velocity of probability distribution and then the arrangement of Eq. (3.79) implies that

$$\mathbf{v}_f = -\mathbf{u}(\mathbf{a}) - \frac{1}{2}\mathbf{B} \cdot \frac{\partial \log \Pi}{\partial \mathbf{a}} \tag{3.81}$$

Analogy of Eq. (3.81) to the GLE of Eq. (3.68) reminds us that the gradient of the logarithm of probability distribution is related to the random force.

3.5.2 Free Brownian Particle

Note that Eq. (3.68) is a formal Langevin equation. In practice, we can apply Eq. (3.3) to the derivation of the Fokker–Planck equation. Then, we have

$$\mathbf{a} = \mathbf{v}; \quad \mathbf{u}(\mathbf{a}) = \frac{\zeta}{m}\mathbf{v}; \quad \mathbf{B} = 2\zeta k_{\mathrm{B}} T \mathbf{I} \tag{3.82}$$

and the Fokker–Planck equation is given by

$$\frac{\partial \Pi(\mathbf{v}, t)}{\partial t} = \frac{\zeta}{m}\frac{\partial}{\partial \mathbf{v}} \cdot [\mathbf{v}\Pi(\mathbf{v}, t)] + \frac{\zeta k_{\mathrm{B}} T}{m^2}\frac{\partial}{\partial \mathbf{v}} \cdot \frac{\partial}{\partial \mathbf{v}}\Pi(\mathbf{v}, t) \tag{3.83}$$

The probability flux is given by

$$\mathbf{j}_p = -\frac{\zeta}{m}\Pi(\mathbf{v}, t)\left[\mathbf{v} + \frac{k_{\mathrm{B}} T}{m}\frac{\partial}{\partial \mathbf{v}}\log\Pi(\mathbf{v}, t)\right] \tag{3.84}$$

Equilibrium condition is $\partial\Pi/\partial t = 0$. This immediately means that $\mathbf{j}_p = \mathbf{0}$ and

$$\frac{\partial}{\partial \mathbf{v}}\log \Pi_{\mathrm{eq}}(\mathbf{v}) = -\frac{m}{k_{\mathrm{B}} T}\mathbf{v} \tag{3.85}$$

Integration of Eq. (3.85) gives the *Maxwell distribution*:

$$\Pi_{\mathrm{eq}}(\mathbf{v}) \propto \exp\left(-\frac{m}{2k_{\mathrm{B}} T}\mathbf{v} \cdot \mathbf{v}\right) \tag{3.86}$$

3.5.3 Brownian Particle in a Force Field

Consider a Brownian particle in a force field. Then, the Langevin equation of the Brownian particle is given by

$$m\frac{\mathrm{d}^2\mathbf{r}}{\mathrm{d}t^2} = -\zeta\frac{\mathrm{d}\mathbf{r}}{\mathrm{d}t} + \mathbf{f}_E + \mathbf{f}_R(t) \tag{3.87}$$

where it is assumed that the force field is conservative:

$$\mathbf{f}_E = -\frac{\partial V}{\partial \mathbf{r}} \tag{3.88}$$

Of course, V is a potential on the Brownian particle. Then, we define the probability distribution as

$$\Pi(\mathbf{x},\mathbf{v},t)=\left\langle \delta(\mathbf{x}-\mathbf{r})\delta\left(\mathbf{v}-\frac{\mathrm{d}\mathbf{r}}{\mathrm{d}t}\right)\right\rangle \tag{3.89}$$

Similar procedure gives

$$\frac{\partial\Pi}{\partial t}+\mathbf{v}\cdot\frac{\partial\Pi}{\partial\mathbf{x}}+\frac{1}{m}\mathbf{f}_E\cdot\frac{\partial\Pi}{\partial\mathbf{v}}=\frac{\zeta}{m}\frac{\partial}{\partial\mathbf{v}}\cdot\left(\mathbf{v}\Pi+\frac{k_\mathrm{B}T}{m}\frac{\partial\Pi}{\partial\mathbf{v}}\right) \tag{3.90}$$

This is called the generalized Fokker–Planck equation or the *Chandrasekhar equation* (McQuarrie 2000). Note that $\mathbf{f}_E=-\nabla V$ in Eq. (3.90).

If the inertia force is negligibly small compared with other forces on the Brownian particle, then the Langevin equation can be approximated by

$$\frac{\mathrm{d}\mathbf{r}}{\mathrm{d}t}=-\frac{1}{\zeta}\frac{\partial V}{\partial\mathbf{r}}+\frac{1}{\zeta}\mathbf{f}_R(t) \tag{3.91}$$

From Eq. (3.91), we can derive a special Fokker–Planck equation called the *Smoluchowski equation*:

$$\frac{\partial\Pi(\mathbf{x},t)}{\partial t}=-\frac{\partial}{\partial\mathbf{x}}\cdot\left[\frac{\mathbf{f}_E}{\zeta}\Pi(\mathbf{x},t)-\frac{k_\mathrm{B}T}{\zeta}\frac{\partial\Pi(\mathbf{x},t)}{\partial\mathbf{x}}\right] \tag{3.92}$$

In this case, the probability flux is given by

$$\mathbf{j}_p=-\frac{\Pi(\mathbf{x},t)}{\zeta}\frac{\partial}{\partial\mathbf{x}}[V(\mathbf{x})+k_\mathrm{B}T\log\Pi(\mathbf{x},t)] \tag{3.93}$$

If we consider an analogy of the potential energy to the internal energy per Brownian particle and use the concept of information theory on entropy, then the flux velocity can be said to be given from the gradient of the Helmholtz free energy per Brownian particle:

$$\mathbf{v}_f=\frac{\mathbf{j}_p}{\Pi(\mathbf{x},t)}=-\frac{1}{\zeta}\frac{\partial\widehat{F}}{\partial\mathbf{x}} \tag{3.94}$$

where

$$\widehat{F}=V-TS=V+k_\mathrm{B}T\log\Pi(\mathbf{x},t) \tag{3.95}$$

Here, we used $\widehat{F}$ instead of F because we did not take any ensemble average. When $V = 0$, the Smoluchowski equation becomes the diffusion Eq. (3.20). Furthermore, it is obvious that the equilibrium probability distribution is given by

$$\Pi_{\mathrm{eq}}(\mathbf{x}) \propto \exp\left(-\frac{V(\mathbf{x})}{k_{\mathrm{B}}T}\right) \tag{3.96}$$

Problems 3

[1] As for free Brownian particle, prove that

$$D = \int_0^\infty \langle \mathbf{v}(t) \cdot \mathbf{v}(0) \rangle \mathrm{d}t \tag{3.a}$$

[2] Consider a free Brownian particle in a bath with memory:

$$m\frac{\mathrm{d}\mathbf{v}}{\mathrm{d}t} = -\int_0^t \frac{A}{\lambda} e^{-|t-\tau|/\lambda}\mathbf{v}(\tau)\mathrm{d}\tau + \mathbf{f}_R(t) \tag{3.b}$$

where A and λ are positive constants. Using equipartition theorem, determine the diffusion constant in terms of the parameters in Eq. (3.b).

[3] Show that $\nabla_{6N} \cdot \mathbf{u}_{6N} = 0$.

[4] Consider a Smoluchowski equation for $\Pi(x_1, \ldots, x_n, t)$:

$$\frac{\partial \Pi}{\partial t} = \sum_{\alpha=1}^{n}\sum_{\beta=1}^{n}\frac{\partial}{\partial x_\alpha} L_{\alpha\beta}\left(k_{\mathrm{B}}T\frac{\partial \Pi}{\partial x_\beta} - \frac{\partial U(\{x_k\})}{\partial x_\beta}\Pi\right) \tag{3.c}$$

where $n \times n$ matrix $L_{\alpha\beta}$ is symmetric and positive definite. Show that

$$\frac{\mathrm{d}F}{\mathrm{d}t} \geq 0$$

where F is the functional defined by

$$F[\Pi] = \int_{-\infty}^{\infty} \mathrm{d}x_1 \ldots \int_{-\infty}^{\infty} \mathrm{d}x_n (k_{\mathrm{B}}T \log \Pi + U)\Pi \tag{3.d}$$

See Doi and Edwards (1986)

[5] Consider a Langevin equation such that

$$\frac{\mathrm{d}\mathbf{u}}{\mathrm{d}t} = -\zeta\mathbf{u} + \mathbf{f}_R(t), \tag{3.e}$$

where ζ is a positive constant and $\langle \mathbf{f}_R(t) \rangle = \mathbf{0}$; $\langle \mathbf{f}_R(t)\mathbf{f}_R(\tau) \rangle = \mathbf{B}\delta(t-\tau)$ where $\mathbf{B}$ is a constant second-order tensor. The probability distribution of the Brownian particle is defined by $\Pi(\mathbf{v},t) = \langle \delta(\mathbf{v}-\mathbf{u}(t)) \rangle$. The characteristic function of the probability distribution function is given by

$$\hat{\Pi}(\mathbf{q},t) = \left\langle e^{i\mathbf{q}\cdot\mathbf{u}(t)} \right\rangle \tag{3.f}$$

Derive the Fokker–Planck equation by using

$$\frac{\partial \hat{\Pi}(\mathbf{q},t)}{\partial t}\Delta t = \left\langle e^{i\mathbf{q}\cdot[\mathbf{u}(t)+\Delta\mathbf{u}]} \right\rangle - \left\langle e^{i\mathbf{q}\cdot\mathbf{u}(t)} \right\rangle = \left\langle \left(e^{i\mathbf{q}\cdot\Delta\mathbf{u}} - 1\right) e^{i\mathbf{q}\cdot\mathbf{u}(t)} \right\rangle \tag{3.g}$$

$$\Delta\mathbf{u} = \int_t^{t+\Delta t} \frac{\mathrm{d}\mathbf{u}}{\mathrm{d}t'}\mathrm{d}t' = -\zeta\mathbf{u}\Delta t + \mathbf{w}(t,\Delta t) \tag{3.h}$$

$$\mathbf{w}(t,\Delta t) = \int_t^{t+\Delta t} \mathbf{f}_R(\tau)\mathrm{d}\tau \tag{3.i}$$

See Onuki (2004).

References

G.B. Arfken, H.J. Weber, *Mathematical Methods for Physicists* (Harcourt Sci. & Tech, Nigeria, 2001)

M.N. Berberan-Santos, Expressing a probability density function in terms of another PDF: a generalized Gram-Charler expansion. J. Math. Chem. **42**, 585–594 (2007)

D. Chandler, *Introduction to Modern Statistical Mechanics* (Oxford University Press, Oxford, 1987)

M. Doi, S.F. Edwards, *The Theory of Polymer Dynamics* (Oxford University Press, Oxford, 1986)

T.F. Edgar, D.M. Himmelblau, *Optimization of Chemical Processes* (McGraw-Hill, New York, 1989)

H. Goldstein, C.P. Poole, J.L. Safko, *Classical Mechanics*, 3rd edn. (Addison Wesley, Boston, 2001)

K. Huang, *Statistical Mechanics* (Wiley, New York, 1963)

J.H. Irving, J.G. Kirkwood, The statistical mechanical theory of transport processes. IV. The equation of hydrodynamics. J. Chem. Phys. **18**, 817–829 (1950)

E.T. Jaynes, Information theory and statistical mechanics. Phys. Rev. **106**, 620–630 (1957a)

E.T. Jaynes, Information theory and statistical mechanics. II. Phys. Rev. **108**, 171–190 (1957b)

L.D. Landau, E.M. Lifshitz, *Mechanics*, 3rd edn. (Pergamon Press, Oxford, 1976)

D.A. McQuarrie, *Statistical Mechanics* (University Science Books, Sausalito, 2000)

J.E. Marsden, A.J. Tromba, *Vector Calculus*, 5th edn. (W. H. Freeman and Company, New York, 2003)

A. Onuki, *Phase Transition Dynamics* (Cambridge University Press, Cambridge, 2004)
M. Pourahmadi, Taylor expansion of $\exp\left(\sum_{k=0}^{\infty} a_k z^k\right)$ and some applications. *Am. Math Monthly*, **91**, 303–307 (1984)
C.E. Shannon, A note on the concept of entropy. Bell Syst. Tech. J. **27**, 379–423 (1948)
F. Schwabl, *Statistical Mechanics*, 2nd edn. (Springer, Berlin, 2006)
R.J. Swenson, Comments on virial theorem for bounded systems. Am. J. Phys. **51**, 940–942 (1983)
S.T. Thornton, J.B. Marion, *Classical Dynamics of Particles and Systems*, 5th edn. (Thomson Brooks/Cole, Belmont, 2004)
M.E. Tuckerman, *Statistical Mechanics: Theory and Molecular Simulation* (Oxford University Press, Oxford, 2010)
D.N. Zuvarev, *Nonequilibrium statistical thermodynamics* (Consultants Bureau, New York, 1974)
R. Zwanzig, *Nonequilibrium Statistical Mechanics* (Oxford University Press, Oxford, 2001)

Chapter 4
Polymer Physics

Abstract This chapter is focused on the brief review of general aspects of polymer science and some important molecular theories related with polymer rheology. This chapter must be necessary for the readers who have weak basis of polymer science, while it can be omitted by polymer scientists and engineers. The first three sections describe polymer structure and the basics of polymer identification. The last section addresses molecular and phenomenological theory of rubber elasticity. The last section demands the knowledge of Chaps. 2 and 3. Further study is available in Strobl (The Physics of Polymers, 2nd edn. Springer, Berlin, 1997), Ward and Sweeney (An Introduction to Mechanical Properties of Solid Polymers, 2nd edn. Wiley, New York, 2004), Sperling (Introduction to Physical Polymer Science, 4th edn. Wiley Interscience, New York, 2006), and Rubinstein and Colby (Polymer Physics, Oxford University Press, Oxford, 2003).

1 Polymer Structure

1.1 Definition of Polymer

Polymer is a molecule which consists of a number of monomeric units which are connected by covalent bonds in a manner of chain. The connection of monomeric units can be linear or nonlinear. Monomeric units of linear polymer are connected in analogy to a line or chain, while nonlinear polymer has at least one junction point at which more than two linear polymers are covalently bonded.

Most man-made polymers consist of repeating units which are groups of atoms. Usually the repeating units are originated from one or more chemical species called monomer. As for polyethylene (PE), it is a successive linkage of chemical groups, $-CH_2-$. However, it is conventional that the repeating unit of PE is considered as $-CH_2CH_2-$ because it is polymerized from ethylene, $CH_2{=}CH_2$. Ethylene is the monomer of PE, and styrene is the monomer of polystyrene (PS). The constituent of polymer is called repeating unit or monomeric unit or segment. Although the three

K.S. Cho, *Viscoelasticity of Polymers*, Springer Series
in Materials Science 241, DOI 10.1007/978-94-017-7564-9_4

terminologies have subtly different meanings, these differences are often neglected by polymer researchers with weak basis of chemistry. For simplicity, polymer is understood as a high molecular weight molecule which has a chain-like shape.

Natural polymers are protein, DNA, cellulose, and so on. Some natural polymers such as protein and DNA have no repeating units but sequence of several monomers, while other natural polymers have repeating units. Cellulose has repeating unit called glucose unit.

The number of the constituents, exactly saying the monomeric units, is the degree of polymerization. Note that degree of polymerization is proportional to molecular weight of polymer.

As increase of degree of polymerization N, most physical properties of linear polymers increase and become saturated as shown in Fig. 1. Because of this feature of polymer, linearly connected ethylene units with different molecular weight share the same name, polyethylene. However, there is still ambiguity because it is not obvious which molecular weight is the minimum for the definition of polymer.

One of the important features of polymers is very high molecular weight, usually higher than thousands grams per mole. Such high molecular weight results in no vaporization in moderate conditions: Degradation occurs at temperatures lower than boiling point. Polymer is a representing material showing viscoelasticity.

Polymer is synthesized under the influence of various factors which usually give rise to the distribution of molecular weight. Hence, polymer is a mixture of homologous molecules. Some physical properties of polymer are sensitive to molecular weight distribution (MWD) even though an average molecular weight is identical. Other physical properties are relatively insensitive to MWD.

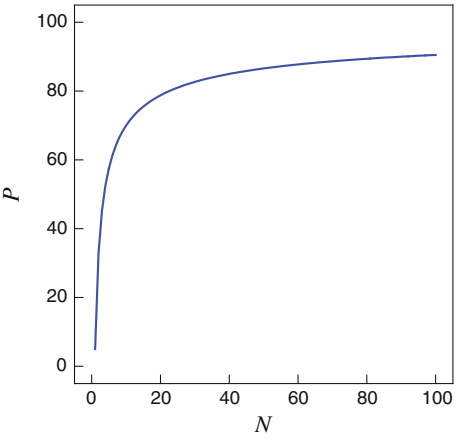

Fig. 1 Schematic illustration of molecular weight dependence of most physical properties of polymer. N, the degree of polymerization is used instead of molecular weight. It must be noted that every physical property follows this tendency. Zero-shear viscosity increases monotonically as molecular weight

1.2 Structure of a Single Polymer Chain

A group of polymers has the structure of monomer $–CH_2CHR–$ where R is a group of atoms. R is called pendent group. The pendent group of PE is hydrogen, while the pendent group of PS is phenyl group. Carbon atom has four single covalent bonds. If the four bonds are represented by segments of straight lines, the angle between adjacent two line segments is about 109°. The second carbon of $–CH_2CHR–$ has two C–C bonds, one C–H bond and one C–R bond. There are three types of arrangements of pendent group as shown in Fig. 2. These types are called tacticity. If all pendent groups are positioned in the same side, the tacticity is called isotactic. Alternative arrangement is called syndiotactic, and random arrangement is called atactic. Tacticity is determined by the polymerization conditions, especially by the catalyst.

In solid state, some polymers can form crystalline phase, while the others cannot. Even crystalline polymer cannot achieve 100 % crystallinity. Hence, the word "semicrystalline" is used. Every polymer has amorphous phase which can be considered as supercooled liquid structure. PE, PP, PET, and Nylon are representative crystalline polymers, while PS and PMMA are known as amorphous polymer because they cannot form crystalline phase. However, there is an exception. Although atactic PS cannot form crystalline phase, syndiotactic PS can form crystalline phase because of its stereoregularity. Hence, in solid state, mechanical properties of syndiotactic PS is superior to those of atactic PS. Note that commercialized PS is atactic. The effect of tacticity on rheological properties of polymer melt is usually weak.

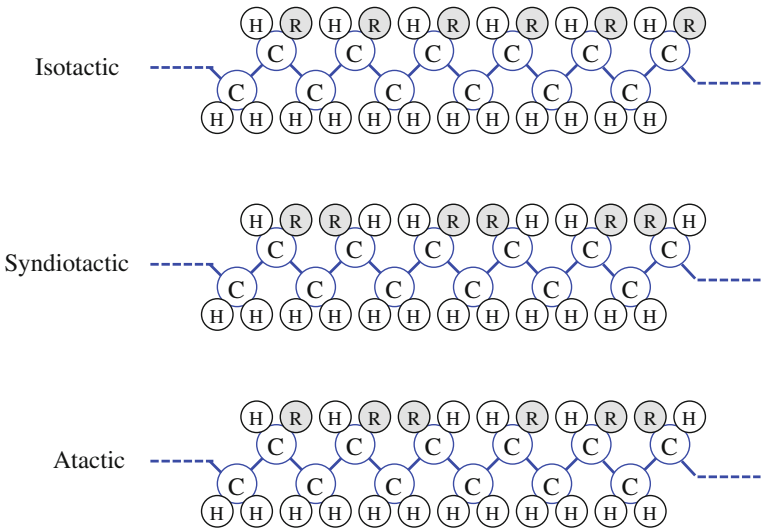

Fig. 2 Tacticity of polymer chain. All the perdent groups R of isotactic chain are located at the same side of the backbone while those of syndiotactic chain are located alternatively. There is not any regularity in the position of the pendent groups of atactic chain

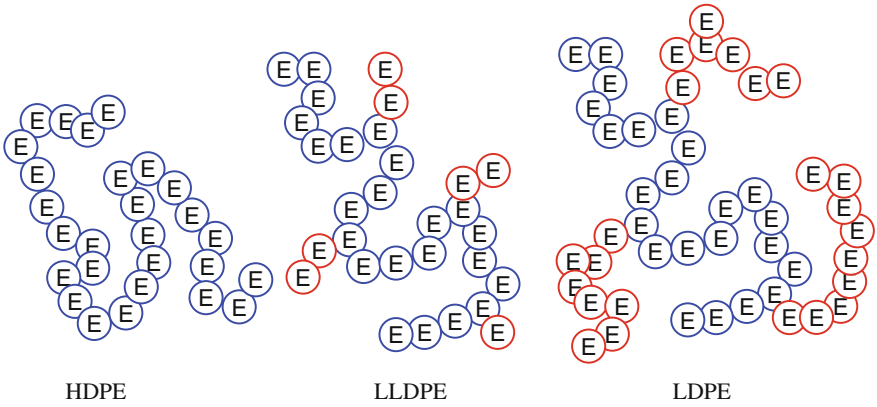

Fig. 3 Chain architecture of polyethylene

Polyethylene is one of the most widely used polymers. High-density polyethylene (HDPE) has linear structure, while linear low-density polyethylene (LLDPE) and low-density polyethylene (LDPE) have nonlinear structures as shown in Fig. 3. Since HDPE is a linear chain, it has high crystallinity (weight fraction of crystalline). However, both LLDPE and LDPE have branch chain, their crystallinities are lower than that of HDPE because the branches prevent crystallization. The length of branch chain of LLDPE is shorter than that of LDPE. LDPE has long-chain branch which affects strongly on viscoelasticity. Polymer cannot have 100 % crystallinity. Note that the higher the crystallinity, the higher the density.

Polymer can be synthesized by two kinds of monomers in various ways. Copolymers are polymers polymerized by two or more kinds of monomers. Consider a copolymer consisting of two monomers A and B. The sequence of A and B is random, and the copolymer is called random copolymer. If the sequence is alternative, $\cdots$ABABAB$\cdots$, then the copolymer is called alternating copolymer. If the sequence is a combination of blocks of single monomers such as $\cdots$AAAAA$\cdots$BBBBBB$\cdots$, then the copolymer is called block copolymer. Compared with copolymer, homopolymer is a polymer consisting of a single kind of monomer.

Since most polymers consist of single covalent C–C bonds (σ bonds) which can rotate due to thermal energy, polymer chains can have a huge number of conformations. Consider pentane chains as shown in Fig. 4. Pentane is a linear hydrocarbon with 5 carbons. Hence, it can be considered as a small scale version of PE. Pentane has 4 C–C σ bonds. Figure 4a is the all-trans conformation which is the maximum extended conformation. The numbers running from 0 to 4 in Fig. 4a indicate the carbons in the all-trans conformation. The first bond is the one connecting 0-carbon with 1-carbon. The second bond rotates about the first bond as shown in Fig. 4b. The third bond rotates about the second bond, and the fourth bond rotates about the third bond. The twisting angle of ith bond is defined as the angle denoted by ϕ_i in Fig. 4b. The conformation of Fig. 4c can be obtained by the rotation indicated by the torsion angle of Fig. 4b.

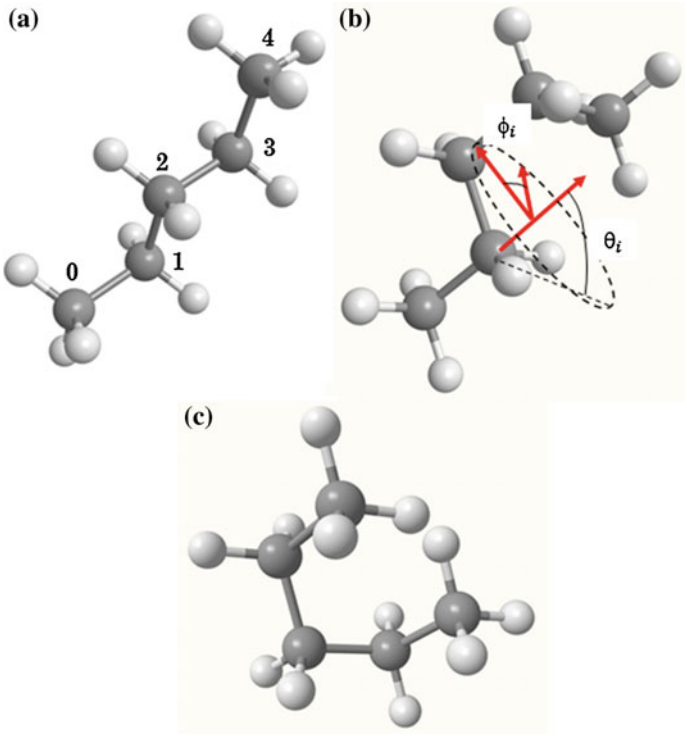

Fig. 4 Conformation

Let the positions of carbons be denoted by $\mathbf{r}_i$ with $i = 0, 1, 2, 3, 4$. Then, we can define bond vectors as follows:

$$\mathbf{b}_i = \mathbf{r}_i - \mathbf{r}_{i-1} \tag{1.1}$$

Assume that bond length is constant, say b. When the orientation of the first bond vector is fixed, the conformation of pentane depends on three twisting angles ϕ_2, ϕ_3 and ϕ_4. Extending this notation to PE with degree of polymerization of N, the conformation of the PE depends on $N - 1$ twisting angles.

Because of steric hindrance, three values of each twist angle are preferred and they are called trans, gauchy+ and gauchy−. Then, the number of frequently observed conformations of PE (or PP or PS) with N bond vectors is given by $N_{\text{conf}} = 3^{N-1}$. Commercially produced PS has usually degree of polymerization of $N \approx 2000$, which is the number of C–C bonds. Then, the number of favorable conformations is about $N_{\text{conf}} \approx 10^{954}$. This means that the longest conformation of such polymer is hard to be observed. Then, new quantities are necessary in order to characterize the size of a single polymer chain of high molecular weight. This will be discussed in Sect. 2 in detail.

1.3 Structure of Assembly of Polymer Chains

As mentioned earlier, some polymers are crystalline polymers, while others are amorphous polymers. It is nearly impossible that crystalline polymer becomes 100 % crystalline material just as metallic materials. It is because the constituents of polymer crystalline are part of polymer chains (partial chains), while those of metallic crystalline are atoms which is much smaller than partial chains. Hence, crystalline polymers in solid state have two distinct phases: crystalline and amorphous phases. It is natural to think of the amount of crystalline phase and the size of crystalline in order to characterize the structure of the assembly of crystalline polymers.

Crystallinity or degree of crystallization is the ratio of the amount of crystalline phase to the total amount of the polymer assembly. Crystallinity can be measured by mass or by volume. X-ray analysis such as WAXS (wide angle X-ray scattering) may give how many partial chains are in a repeating cell of the polymer crystallite and geometric information of the crystallite. Then, the density of crystalline phase can be calculated from the data of WAXS. When the masses of crystalline and amorphous phases are denoted by W_C and W_A, respectively, the mass-based crystallinity, X_M, is given by

$$X_M = \frac{W_C}{W_C + W_A} = \frac{\rho_C}{\rho} \frac{\rho - \rho_A}{\rho_C - \rho_A} \tag{1.2}$$

where ρ is the mass density of the polymeric material, ρ_C is the mass density of the crystalline phase, and ρ_A is the mass density of the amorphous phase. When the volume of crystalline and amorphous phases are denoted by V_C and V_A, respectively, the volume-based crystallinity, X_V, is given by

$$X_V = \frac{V_C}{V_C + V_A} = \frac{\rho - \rho_A}{\rho_C - \rho_A} \tag{1.3}$$

Hence, crystallinity can be obtained from volumetric data which can be measured by dilatometer. Only crystalline phase issues heat of fusion at melting point, and calorimetric data can provide crystallinity. Conventional method is to use differential scanning calorimetry (DSC). Analysis of peaks of X-ray diffraction can also provide the data for crystallinity.

The size of crystallite depends on crystallization conditions such as temperature and pressure as functions of time. The existence of impurity is also important because impurity plays the role of nucleation agency.

Crystallite is anisotropic. Since there are a number of crystallites in crystalline polymer, the orientation of crystallites plays affects the physical properties of crystalline polymers.

Amorphous phase of polymer is similar to supercooled liquid phase of polymer melts. Although crystalline phase has orderliness in structure, it is difficult to find

any regularity in the amorphous structure. Even mass density of amorphous phase depends on the route of formation such as temperature and pressure profile for the treatment of the sample. Amorphous phase of polymeric material has a mysterious transition which is similar to the second-order transition in equilibrium thermodynamics. The transition of amorphous polymer is called glass transition. The glass transition temperature, T_g, depends on both the measurement conditions and the history of the sample preparation. Phenomenologically, thermal expansion coefficient of the amorphous phase changes near glass transition temperature as shown in Fig. 5a.

Figure 5 shows schematic illustration for features of glass transition temperature. When volumetric data are used, the glass transition is considered as the transition point of the thermal expansion coefficient:

$$\alpha = \frac{1}{V}\left(\frac{\partial V}{\partial T}\right)_{\mathrm{p}} \tag{1.4}$$

Note that thermal expansion coefficient is the second-order partial derivative of free energy. Figure 5a implies that there is a temperature at which the second derivative of free energy becomes discontinuous. However, glass transition is not the second-order transition because the transition point varies according to both the conditions of sample treatment and measurement.

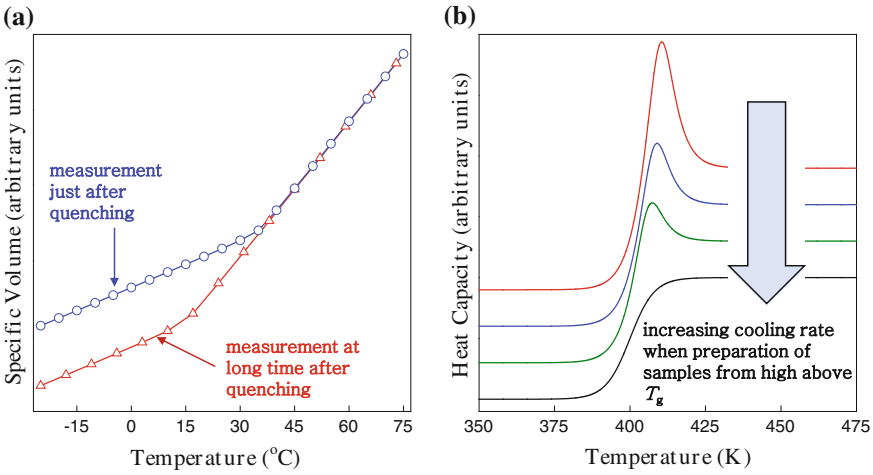

Fig. 5 Schematic illustration of glass transition: **a** Specific volume as a temperature; **b** heat capacity as a function of temperature. The slope of specific volume with respect to temperature changes at glass transition temperature. However, the glass transition temperature determined by the volumetric data varies according to sample treatment. Similar phenomena are observed for different methods for glass transition. In DSC test for heat capacity, cooling rate for sample preparation gives different behavior of heat capacity

Figure 5b illustrates how heat capacity of polymer changes as temperature. The profiles of heat capacity shown in Fig. 5b represent those of the samples prepared from different cooling rates. As cooling rate decreases, the overshoot disappears. Glass transition temperature is considered as the midpoint of the transition of heat capacity. Such glass transition temperature varies even for the cooling rates without overshoot.

Such variation related with glass transition temperature may be explained by the structure of amorphous phase of polymers. Since amorphous phase of polymer is analogous to supercooled liquid, the distribution of atoms of polymers in amorphous phase is not in thermodynamic equilibrium. It is not in the minimum of energy (or free energy). Such nonequilibrium distribution of atoms consequently implies that the mass density of amorphous phase is less than hypothetical equilibrium density because minimization of energy means dense packing of atoms.

Kinetic behaviors of volume and heat capacity are deeply related with glass transition. It is the problem of irreversible thermodynamics. The studies of the themes are called volume relaxation and enthalpy relaxation, respectively. Further information is in Donth (1992), Strobl (1997), Chow (2000) and Gedde (2001).

Problem 1

[1] A certain polymer is known to show molecular weight dependences of some physical properties as follows:

$$\text{Zero-shear viscosity} \quad \eta_o = KM^{\alpha} \tag{1.a}$$

$$\text{Yield stress} \quad \sigma_Y = \sigma_Y^{\infty} - \frac{k}{M^{\beta}} \tag{1.b}$$

where K, α, σ_Y^{∞}, k, and β are positive constants and M is molecular weight. Determine the optimum molecular weight.

[2] Crystallinity of a polymer can be controlled by cooling conditions because the crystallization rate of polymer is very slow. DSC measurements gave the following data of the crystallinity of the polymer in weight.

Density (g/cm^3)	1.349	1.374	1.398	1.426
X_M	0.116	0.322	0.529	0.736

Estimate the densities of the crystalline and amorphous phases.

[3] Derive Eqs. (1.2) and (1.3). Describe the assumptions needed to do that.

[4] Derive the following equations

$$\alpha = \frac{1}{V}\left(\frac{\partial}{\partial T}\left(\frac{\partial G}{\partial p}\right)_T\right)_p \tag{1.c}$$

$$c_{\mathrm{p}} = -T\left(\frac{\partial^2 G}{\partial T^2}\right)_{\mathrm{p}} \tag{1.d}$$

2 Chain Conformation and Size of Polymer Chain

2.1 Size of Polymer Chain

2.1.1 End-to-End Distance

As mentioned before, polymer chains in molten state or in solution are hard to be in fully extended conformation because of ceaseless rotation of σ bonds. The shape of polymer chain is often called coil. The size of polymer chain may be quantified by the end-to-end distance. Numbering the segments in a polymer chain from zero to N, the *end-to-end vector* is given by

$$\mathbf{h} = \mathbf{r}_N - \mathbf{r}_0 \tag{2.1}$$

Bond vector is defined as

$$\mathbf{b}_i = \mathbf{r}_i - \mathbf{r}_{i-1} \text{ with } i = 1, 2, \ldots, N \tag{2.2}$$

Then, it is obvious that

$$\mathbf{h} = \sum_{i=1}^{N} \mathbf{b}_i \tag{2.3}$$

Since the total number of conformation of the chain with $N+1$ segments is extremely high, we use the notation such that $\langle \cdots \rangle$ represents the average over the whole conformations. Under the assumption that bond vectors have the same length, it is clear that

$$\left\langle \|\mathbf{b}_i\|^2 \right\rangle = b^2 \quad \text{for all } i \tag{2.4}$$

where b is the length of bond. Ceaseless rotation of bond vectors allows us to assume that

$$\langle \mathbf{b}_i \rangle = \mathbf{0} \quad \text{for all } i \tag{2.5}$$

However, it does not mean $\langle \mathbf{b}_i \cdot \mathbf{b}_k \rangle = 0$ for any pair of i and k. Because of local structure of polymer chain, it is a reasonable assumption that

$$\langle \mathbf{b}_i \cdot \mathbf{b}_k \rangle = b^2 C(|i-k|) \tag{2.6}$$

where the function $C(x)$ must be a decreasing function and

$$\lim_{n\to\infty} C(n) = 0; \quad C(0) = 1 \tag{2.7}$$

The meaning of the function $C(x)$ is the correlation of the orientation of bond vectors. Hence, we call the function *bond correlation function*. It is straightforward that the correlation between two bond vectors becomes smaller and smaller as the two bond vectors are separated further and further along the contour of the polymer chain. The correlation function depends on valance angles between monomeric units and steric hindrance. Such local interactions between adjacent monomeric units are called *short-range interactions*. The word "short" implies short distance along the contour of the polymer chain rather than the real distance between a pair of monomeric units. It may happen that a monomer unit become close to other monomer which is separated far along the chain contour. Such interaction is called *long-range interaction*. Here, again, long means long distance along the chain contour. The long-range interaction prohibits the overlap of any pair of two monomeric units in the polymer chain. Hence, the result from long-range interaction is called excluded volume effect. When short-range interactions are only considered, the chain model is called *ideal chain*. Meanwhile, long-range interaction is considered, and the chain model is called *real chain*. We consider only ideal chain for a while.

From Eq. (2.5), it is obvious that $\langle \mathbf{h} \rangle = \mathbf{0}$ because of Eq. (2.3). However, we have

$$\langle \mathbf{h} \cdot \mathbf{h} \rangle = \sum_{i=1}^{N} \sum_{k=1}^{N} \langle \mathbf{b}_i \cdot \mathbf{b}_k \rangle = b^2 \sum_{i=1}^{N} \sum_{k=1}^{N} C(|i-k|) \tag{2.8}$$

One of the simplest cases of Eq. (2.7) is

$$C(|i-k|) = \delta_{ik} \tag{2.9}$$

Equation (2.9) implies the orientations of bond vectors are not correlated. We shall show later that Eq. (2.9) corresponds to freely jointed chain model.

Then, Eq. (2.8) gives the end-to-end distance:

$$R \equiv \sqrt{\langle \mathbf{h} \cdot \mathbf{h} \rangle} = b\sqrt{N} \tag{2.10}$$

Although use of Eq. (2.9) looks like unrealistic, the relation $R \sim \sqrt{N}$ is also found for more realistic models of polymer chain. The origin of such universal relation is the central limit theorem (Sect. 1) in Chap. 3. Thus, we recognize that the probability distribution of $\mathbf{h}$ can be approximated by the Gaussian distribution whose mean and standard deviation are given, respectively, by $\mathbf{0}$ and $b\sqrt{N}$.

2.1.2 Radius of Gyration

When polymer is not a linear chain, end-to-end distance cannot be calculated because the polymer has more than two end segments. See Fig. 3 where the LDPE has five end segments. To define the size of chain conformation irrespective of chain topology, consider the center of mass of a polymer such that

$$\mathbf{r}_C \equiv \frac{1}{N+1}\sum_{k=0}^{N}\mathbf{r}_k \tag{2.11}$$

Then, we can define the *radius of gyration* as follows:

$$R_G^2 \equiv \frac{1}{N+1}\left\langle \sum_{k=0}^{N} \|\mathbf{r}_k - \mathbf{r}_C\|^2 \right\rangle \tag{2.12}$$

From Eq. (2.12), we know that the radius of gyration is the average distance from the center of mass to segments.

Using the definition of bond vectors, we obtain the following:

$$\mathbf{r}_n = \mathbf{r}_0 + \sum_{k=1}^{n}\mathbf{b}_k; \tag{2.13}$$

$$\mathbf{r}_C = \mathbf{r}_0 + \frac{1}{N+1}\sum_{n=1}^{N}\sum_{k=1}^{n}\mathbf{b}_k \tag{2.14}$$

Then, Eqs. (2.13) and (2.14) immediately give

$$\left\langle \|\mathbf{r}_n - \mathbf{r}_C\|^2 \right\rangle = b^2 n - \frac{2b^2}{N+1}\left[nN - \frac{n(n+1)}{2}\right] + \frac{b^2 N(2N+1)}{6(N+1)} \tag{2.15}$$

where $\langle \mathbf{b}_i \cdot \mathbf{b}_k \rangle = \delta_{ik}$ was used. Substitution of Eq. (2.15) into Eq. (2.12) yields

$$R_G^2 = \frac{b^2 N}{6}\left[3 - 6\frac{N}{N+1} + 2\frac{N+\frac{1}{2}}{N+1} + \frac{1}{N+1} + 2\frac{N(N+\frac{1}{2})}{(N+1)^2}\right] \tag{2.16}$$

If N is much larger than unity, then Eq. (2.16) becomes

$$R_G^2 \approx \frac{b^2 N}{6} = \frac{1}{6}R^2 \tag{2.17}$$

As for linear chain, the end-to-end distance is equivalent to the radius of gyration. However, the end-to-end distance cannot be defined for nonlinear chain.

For branched polymer, branching parameter is a useful measure for the characterization of nonlinear chain (Teraoka 2002). The *branching parameter* is defined by

$$g = \frac{R_{\mathrm{Gb}}^2}{R_{\mathrm{Gl}}^2} \tag{2.18}$$

where R_{Gb} is the radius of gyration for branched chain and R_{Gl} is the radius of gyration for the linear chain whose molecular weight equals to that of the branched chain.

2.2 Chain Models and Universality

In this section, we shall introduce some chain models which are simplification of polymer chain. The *freely jointed chain model (FJC)* is assumed that all bond vectors can have any orientation. The *freely rotating chain model (FRC)* is the one that all torsion angles are independent and take any value in the interval of $0 \leq \phi_i < 2\pi$. The *hindered-rotation chain model (HRC)* is the one that torsion angle has statistical weight, which represents the steric hindrance. After comparison of the three models for ideal chain, we shall introduce Gaussian chain which is an abstract generalization of ideal chain.

2.2.1 Freely Jointed Chain

In Sect. 2.1, the size of polymer chains depends on the distribution of bond vectors. Because the bond length is fixed, kth bond vector can be described by two angles as follows:

$$\mathbf{b}_k = b(\cos\phi_k \sin\theta_k \mathbf{e}_1 + \sin\phi_k \sin\theta_k \mathbf{e}_2 + \cos\theta_k \mathbf{e}_3) \tag{2.19}$$

where ϕ_k corresponds to torsion angle, while θ_k corresponds to valance angle. Hence, the freely joint chain (FJC) model does not consider the restriction on valance angle, and the two angles can take the intervals such that

$$0 \leq \phi_k < 2\pi; \quad 0 \leq \theta_k < \pi \tag{2.20}$$

Since all values of ϕ_k and θ_k in the ranges of Eq. (2.20) are equally possible, the probability distribution of kth bond vector is given by

$$p(\mathbf{b}_k) = \frac{1}{4\pi} \tag{2.21}$$

And the probability distribution is identical to any bond vector. Assumption of statistical independent of bond vectors results in that the probability distribution for

all bond vectors is the product of the probability distributions of individual bond vector:

$$P_{\text{bond}}(\mathbf{b}_1, \mathbf{b}_2, \ldots, \mathbf{b}_N) = \prod_{i=1}^{N} p(\mathbf{b}_i) = \frac{1}{(4\pi)^N} \tag{2.22}$$

Since the length of bond vector is fixed by b, the average of an arbitrary function of bond vectors $g(\mathbf{b}_1, \mathbf{b}_2, \ldots, \mathbf{b}_N)$ is given by

$$\langle g(\mathbf{b}_1, \mathbf{b}_2, \ldots, \mathbf{b}_N) \rangle = \frac{1}{(4\pi)^N} \oint_{\Omega_1} \mathrm{d}\Omega_1 \oint_{\Omega_2} \mathrm{d}\Omega_2 \ldots \oint_{\Omega_N} \mathrm{d}\Omega_N g(\mathbf{b}_1, \mathbf{b}_2, \ldots, \mathbf{b}_N) \tag{2.23}$$

where the differential solid angle is given by

$$\mathrm{d}\Omega_k = \sin\theta_k \mathrm{d}\theta_k \mathrm{d}\phi_k \tag{2.24}$$

Note that

$$\oint_{\Omega} \mathrm{d}\Omega = \int_0^{2\pi} \int_0^{\pi} \sin\theta \mathrm{d}\theta \mathrm{d}\phi = 4\pi \tag{2.25}$$

It is not difficult to obtain

$$\langle \mathbf{b}_i \cdot \mathbf{b}_k \rangle = b^2 \delta_{ik} \tag{2.26}$$

and $\langle \mathbf{b}_k \rangle = 0$ for any k. Then, it is obvious that

$$R = b\sqrt{N} \tag{2.27}$$

2.2.2 Freely Rotating Chain

Consider a chain which consists of $N+1$ segments as before. Freely rotation chain (FRC) can be obtained by giving some constraints to FJC. The constraints are $\|\mathbf{b}_k\| = b$ and $\mathbf{b}_k \cdot \mathbf{b}_{k+1} = b^2 \cos\theta$. The constraints mean that N bond vectors have the same magnitude of b and $N-1$ adjacent bond vectors maintain constant valance angle θ. The number of constraint equations is, therefore, given by

$$N_{\text{constraint}} = 2N - 1 \tag{2.28}$$

Since positions of $N+1$ segments can be described by $3(N+1)$ real numbers (coordinates), the degree of freedom of the freely rotating chain is given by

$$N_f = 3(N+1) - (2N-1) = N+4 \tag{2.29}$$

The position of the first segment can describe the translational motion of the chain, and the orientation of the first bond is freely given. The orientation of the first bond vector represents the rotation of the whole chain. Hence, 5 is given to the external degree of freedom which is assigned to rigid body motion of the whole chain, while $N_{\text{conf}} \equiv N-1$ is given to the internal degree of freedom which represents the conformation of freely rotating chain. The internal degree of freedom can be assigned to torsion angles $\{\phi_k\}$ of $N-1$ bond vectors except the first bond vector.

Consider coordinate systems assigned to every bond vector. The coordinate system for the ith bond vector is defined by orthonormal basis such as

$$\mathbf{e}_1^{(i)} = \frac{1}{b}\mathbf{b}_i \tag{2.30}$$

The other two base vectors $\mathbf{e}_2^{(i)}$ and $\mathbf{e}_3^{(i)}$ are chosen in order to make the ith coordinate system be a right-handed one.

Figure 6 shows the geometry of the rotation of bond vectors. The $i+1$th bond vector rotates by torsion angle ϕ_{i+1} about the ith bond vector. Rotation about a unit vector $\mathbf{u}$ can be represented by an orthogonal tensor such as

$$\begin{aligned}\mathbf{R}(\phi) &= (1-\cos\phi)\mathbf{uu} + \cos\phi\mathbf{I} + \sin\phi(\mathbf{wv} - \mathbf{vw}) \\ &= \mathbf{uu} + \cos\phi(\mathbf{vv} + \mathbf{ww}) + \sin\phi(\mathbf{wv} - \mathbf{vw})\end{aligned} \tag{2.31}$$

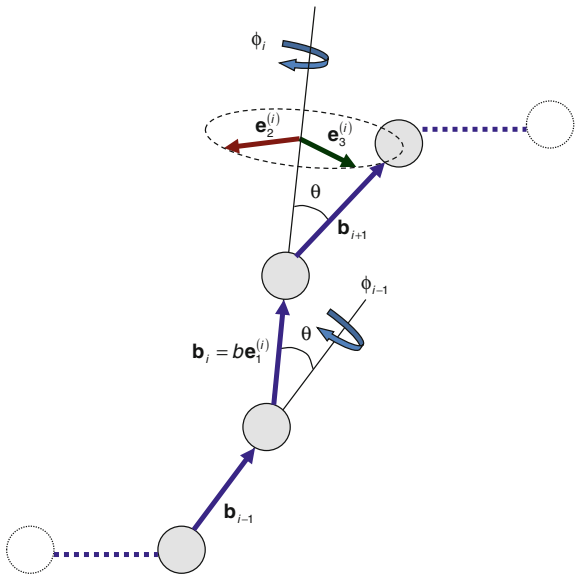

Fig. 6 Geometry of the rotation of bond vectors

where **u**, **v,** and **w** form an orthonormal basis and ϕ is the rotation angle. The right-handed coordinate system implies that $\mathbf{u} \times \mathbf{v} = \mathbf{w}$. Then, we can consider the following two orthogonal tensors such that

$$\mathbf{Q}_i = \mathbf{e}_3^{(i)}\mathbf{e}_3^{(i)} + \cos\theta\left(\mathbf{e}_1^{(i)}\mathbf{e}_1^{(i)} + \mathbf{e}_2^{(i)}\mathbf{e}_2^{(i)}\right) + \sin\theta\left(\mathbf{e}_2^{(i)}\mathbf{e}_1^{(i)} - \mathbf{e}_1^{(i)}\mathbf{e}_2^{(i)}\right) \tag{2.32}$$

and

$$\mathbf{R}_i = \mathbf{e}_1^{(i)}\mathbf{e}_1^{(i)} + \cos\tau_i\left(\mathbf{e}_2^{(i)}\mathbf{e}_2^{(i)} + \mathbf{e}_3^{(i)}\mathbf{e}_3^{(i)}\right) + \sin\tau_i\left(\mathbf{e}_3^{(i)}\mathbf{e}_2^{(i)} - \mathbf{e}_2^{(i)}\mathbf{e}_3^{(i)}\right) \tag{2.33}$$

Use of Eqs. (2.32) and (2.33) allows us to take

$$\mathbf{b}_{i+1} = \mathbf{T}_i \cdot \mathbf{b}_i \tag{2.34}$$

where

$$\begin{aligned}\mathbf{T}_i &= \mathbf{R}_i \cdot \mathbf{Q}_i = T_i^{\alpha\beta}\mathbf{e}_\alpha^{(i)}\mathbf{e}_\beta^{(i)} \\ &= \cos\theta\mathbf{e}_1^{(i)}\mathbf{e}_1^{(i)} + \cos\phi_i\cos\theta\mathbf{e}_2^{(i)}\mathbf{e}_2^{(i)} + \cos\phi_i\mathbf{e}_3^{(i)}\mathbf{e}_3^{(i)} \\ &\quad - \sin\theta\mathbf{e}_1^{(i)}\mathbf{e}_2^{(i)} + \cos\phi_i\sin\theta\mathbf{e}_2^{(i)}\mathbf{e}_1^{(i)} - \sin\phi_i\mathbf{e}_2^{(i)}\mathbf{e}_3^{(i)} \\ &\quad + \sin\phi_i\sin\theta\mathbf{e}_3^{(i)}\mathbf{e}_1^{(i)} + \sin\phi_i\cos\theta\mathbf{e}_3^{(i)}\mathbf{e}_2^{(i)}\end{aligned} \tag{2.35}$$

In Eq. (2.35), summation convention is effective only on Greek indices. Hereafter, we keep using such summation convention. Equation (2.34) implies that

$$\mathbf{b}_{n+1} = \mathbf{T}_n \cdot \mathbf{T}_{n-1} \ldots \mathbf{T}_2 \cdot \mathbf{T}_1 \cdot \mathbf{b}_1 \tag{2.36}$$

From Eqs. (2.30) and (2.34), we can set

$$\mathbf{e}_1^{(i+1)} = \mathbf{T}_i \cdot \mathbf{e}_1^{(i)} = \frac{1}{b}\mathbf{b}_{i+1} \tag{2.37}$$

Similarly, we can define

$$\mathbf{e}_\alpha^{(i+1)} = \mathbf{T}_i \cdot \mathbf{e}_\alpha^{(i)} \quad \text{for } \alpha = 1, 2, 3 \tag{2.38}$$

And we know that

$$\mathbf{e}_\alpha^{(i+1)} \cdot \mathbf{e}_\beta^{(i+1)} = \mathbf{e}_\alpha^{(i)} \cdot \mathbf{e}_\beta^{(i)} = \delta_{\alpha\beta} \tag{2.39}$$

Equation (2.39) is valid because $\mathbf{T}_i$ is an orthogonal tensor.
From Eqs. (2.35) and (2.39), it is clear that

$$T_i^{\alpha\beta} = \mathbf{e}_\alpha^{(i)} \cdot \mathbf{e}_\beta^{(i+1)} \tag{2.40}$$

Then orthogonality of $\mathbf{T}_i$ gives

$$\begin{aligned} \mathbf{T}_n \cdot \mathbf{T}_{n-1} &= \left(T_n^{\alpha\beta}\mathbf{e}_\alpha^{(n)}\mathbf{e}_\beta^{(n)}\right) \cdot \left(T_{n-1}^{\chi\varepsilon}\mathbf{e}_\chi^{(n-1)}\mathbf{e}_\varepsilon^{(n-1)}\right) \\ &= T_n^{\alpha\beta}T_{n-1}^{\chi\varepsilon}\left(\mathbf{e}_\chi^{(n-1)} \cdot \mathbf{e}_\beta^{(n)}\right)\mathbf{e}_\alpha^{(n)}\mathbf{e}_\varepsilon^{(n-1)} \\ &= T_n^{\alpha\varepsilon}\mathbf{e}_\alpha^{(n)}\mathbf{e}_\varepsilon^{(n-1)} \end{aligned} \tag{2.41}$$

Note that

$$\mathbf{e}_\alpha^{(n)} = \mathbf{T}_{n-1} \cdot \mathbf{e}_\alpha^{(n-1)} = \left(T_{n-1}^{\xi\psi}\mathbf{e}_\xi^{(n-1)}\mathbf{e}_\psi^{(n-1)}\right) \cdot \mathbf{e}_\alpha^{(n-1)} = T_{n-1}^{\xi\alpha}\mathbf{e}_\xi^{(n-1)} \tag{2.42}$$

Applying Eq. (2.40) into Eq. (2.41) gives

$$\mathbf{T}_n \cdot \mathbf{T}_{n-1} = T_{n-1}^{\xi\alpha}T_n^{\alpha\varepsilon}\mathbf{e}_\xi^{(n-1)}\mathbf{e}_\varepsilon^{(n-1)} = T_{n-1}^{\alpha\gamma}T_n^{\gamma\beta}\mathbf{e}_\alpha^{(n-1)}\mathbf{e}_\beta^{(n-1)} \tag{2.43}$$

Repetition of similar procedure gives

$$\mathbf{T}_n \cdot \mathbf{T}_{n-1} \ldots \mathbf{T}_m = T_m^{\alpha\gamma}T_{m+1}^{\gamma\varepsilon} \ldots T_{n-1}^{\eta\sigma}T_n^{\sigma\beta}\mathbf{e}_\alpha^{(m)}\mathbf{e}_\beta^{(m)} \tag{2.44}$$

Substitution of Eq. (2.44) into Eq. (2.36) with $m = 1$ yields

$$\mathbf{b}_{n+1} = bT_1^{\alpha\gamma}T_2^{\gamma\varepsilon} \ldots T_{n-1}^{\eta\sigma}T_n^{\sigma 1}\mathbf{e}_\alpha^{(1)} \tag{2.45}$$

Furthermore, it is not difficult to derive

$$\mathbf{b}_{n+1} = bT_m^{\alpha\gamma}T_{m+1}^{\gamma\varepsilon} \ldots T_{n-1}^{\eta\sigma}T_n^{\sigma 1}\mathbf{e}_\alpha^{(m)} \tag{2.46}$$

Then, Eq. (2.46) allows us to have

$$\mathbf{b}_i \cdot \mathbf{b}_{i+n} = b^2\mathbf{e}_1 \cdot \mathbf{T}(\phi_i) \cdot \mathbf{T}\left(\phi_{i+1}\right) \ldots \mathbf{T}\left(\phi_{i+n-1}\right) \cdot \mathbf{e}_1 \tag{2.47}$$

where

$$\begin{aligned} \mathbf{T}(\phi) = &\cos\theta\mathbf{e}_1\mathbf{e}_1 + \cos\phi\cos\theta\mathbf{e}_2\mathbf{e}_2 + \cos\phi\mathbf{e}_3\mathbf{e}_3 \\ &- \sin\theta\mathbf{e}_1\mathbf{e}_2 + \cos\phi\sin\theta\mathbf{e}_2\mathbf{e}_1 - \sin\phi\mathbf{e}_2\mathbf{e}_3 \\ &+ \sin\phi\sin\theta\mathbf{e}_3\mathbf{e}_1 + \sin\phi\cos\theta\mathbf{e}_3\mathbf{e}_2 \end{aligned} \tag{2.48}$$

Since all torsion angles are statistically independent and torsion angle can have any value of the interval of $0 \leq \phi_i < 2\pi$ with the same probability, it is obvious that

$$\langle \mathbf{b}_i \cdot \mathbf{b}_{i+n} \rangle = \frac{b^2}{(2)^n} \mathbf{e}_1 \cdot \left\{ \int_0^{2\pi} \mathrm{d}\phi_{i+1} \ldots \int_0^{2\pi} \mathrm{d}\phi_{i+n} \mathbf{T}(\phi_i) \times \mathbf{T}(\phi_{i+1}) \ldots \mathbf{T}(\phi_{i+n-1}) \right\} \cdot \mathbf{e}_1 \tag{2.49}$$

Note that

$$\frac{1}{2\pi} \int_0^{2\pi} \mathbf{T}(\phi) \mathrm{d}\phi = \cos\theta \mathbf{e}_1 \mathbf{e}_1 - \sin\theta \mathbf{e}_1 \mathbf{e}_2 \equiv \bar{\mathbf{T}} \tag{2.50}$$

It is because

$$\langle \cos\phi \rangle = \frac{1}{2\pi} \int_0^{2\pi} \cos\phi \mathrm{d}\phi = 0; \quad \langle \sin\phi \rangle = \frac{1}{2\pi} \int_0^{2\pi} \sin\phi \mathrm{d}\phi = 0 \tag{2.51}$$

Applying Eq. (2.50) gives

$$\langle \mathbf{b}_i \cdot \mathbf{b}_{i+n} \rangle = b^2 \mathbf{e}_1 \cdot \bar{\mathbf{T}}^n \cdot \mathbf{e}_1 \tag{2.52}$$

Note that

$$\bar{\mathbf{T}}^2 = \cos\theta \bar{\mathbf{T}} \tag{2.53}$$

Then, it is not difficult to derive

$$\langle \mathbf{b}_i \cdot \mathbf{b}_{i+n} \rangle = b^2 \cos^n \theta \tag{2.54}$$

The assumption of $N \gg 1$ gives

$$R \approx b \sqrt{\frac{1+\cos\theta}{1-\cos\theta}} \sqrt{N} \tag{2.55}$$

Equation (2.55) can be obtained by the substitution of Eq. (2.54) into Eq. (2.8). Just as Eq. (2.27), we have the relation $R \propto \sqrt{N}$ again. We can define the effective segment length of FRC as follows:

$$b_{\mathrm{FRC}} = b \sqrt{\frac{1+\cos\theta}{1-\cos\theta}} \tag{2.56}$$

2.2.3 Hindered-Rotation Chain

Rotation of bond vector is hindered by the existence of atomic groups of adjacent segments. This gives rise to nonuniform probability distribution of torsion angle. Hence, the hindered-rotation chain model (HRC) has nonzero averages of $\cos\phi$ and $\sin\phi$, because it includes the interaction between adjacent segments. Then for any n, we can introduce

$$\langle \cos\phi_n \rangle = \chi; \quad \langle \sin\phi_n \rangle = \sigma \tag{2.57}$$

Then, Eq. (2.57) gives

$$\begin{aligned} \bar{\mathbf{T}} = & \cos\theta \mathbf{e}_1\mathbf{e}_1 + \chi\cos\theta \mathbf{e}_2\mathbf{e}_2 + \chi \mathbf{e}_3\mathbf{e}_3 \\ & - \sin\theta \mathbf{e}_1\mathbf{e}_2 + \chi\sin\theta \mathbf{e}_2\mathbf{e}_1 - \sigma \mathbf{e}_2\mathbf{e}_3 \\ & + \sigma\sin\theta \mathbf{e}_3\mathbf{e}_1 + \sigma\cos\theta \mathbf{e}_3\mathbf{e}_2 \end{aligned} \tag{2.58}$$

Long calculation gives

$$R = b\sqrt{\frac{1+\cos\theta}{1-\cos\theta}}\sqrt{\frac{1+\chi}{1-\chi}}\sqrt{N} \tag{2.59}$$

Once more, we obtain the relation $R \propto \sqrt{N}$. The effective segment length of HRC is given as

$$b_{\mathrm{HRC}} = b\sqrt{\frac{1+\cos\theta}{1-\cos\theta}}\sqrt{\frac{1+\chi}{1-\chi}} \tag{2.60}$$

2.2.4 Real Chain

For $|n-m| \gg 1$, the nth and mth segments in the same chain can meet each other in space. In other words, it happens that $\|\mathbf{r}_n - \mathbf{r}_m\| < b$. This case is not excluded in the ideal chain model. However, this case must be excluded in the conformations of real chain. Complicate theory (Doi and Edwards 1986) gives the end-to-end distance of real chain such that

$$R = bN^{\nu} (\nu \approx 0.588) \tag{2.61}$$

It is obvious that $\nu > \frac{1}{2}$, since the exclusion of the case $\|\mathbf{r}_n - \mathbf{r}_m\| < b$ expands the size of chain. The segment length in Eq. (2.61) can be considered as an effective length of segment.

The value of exponent $\nu \approx 0.588$ is observed for the polymers in good solvent, while $\nu = \frac{1}{2}$ is also observed when certain conditions for solvent and polymer are

satisfied. A polymer solution may show the exponent of ideal chain at a temperature called Θ-temperature which depends on kinds of solvent and polymers. It is interesting that polymer chains in molten state obey $\nu = \frac{1}{2}$ (see Rubinstein and Colby (2003) for further information). In summary, we can measure the polymer size which follows the relation of ideal chain. Such size is called unperturbed size and denoted by R_Θ.

2.2.5 Equivalent Chain

From the chemical structure of polymer, we can calculate the maximum length of polymer chain which corresponds to all-trans conformation. When the length is denoted by L, it is obvious that

$$L = b_o N_o \tag{2.62}$$

where b_o is the segment length determined from the chemical structure and N_o is the number of the segment. From the learning from the three models of ideal chain, it can be said that

$$R_\Theta^2 = C_\infty b_o^2 N_o \tag{2.63}$$

where C_∞ is a number called the *characteristic ratio* which depends on chemical structure of the segment.

We can consider successive λ segments as an equivalent segment called Kuhn's segment; then, the orientation of the effective segment is almost random. Let the average length of the Kuhn's segment be denoted by b. Then, we can imagine that the new chain consisting $N = N_o/\lambda$ Kuhn's segments behaves as a FJC in the Θ-condition. Then, we have

$$L = bN; \quad R_\Theta^2 = b^2 N \tag{2.64}$$

Since we can determine L and R_Θ^2 from the chemical structure and experiment, respectively, we can determine b and N as follows:

$$b = \frac{R_\Theta^2}{L}; \quad N = \frac{L^2}{R_\Theta^2} \tag{2.65}$$

Since we know N_o from the chemical structure, we also determine λ by

$$\lambda = \frac{N_o}{N} \tag{2.66}$$

Then, polymer chain can be considered as a freely jointed chain in molten state or in Θ-solution.

2.3 Size Distribution

2.3.1 Size Distribution of Ideal Chain

From the notion of equivalent chain, we can calculate the distribution function of end-to-end vector easily from freely jointed chain model. When the probability distribution of all bond vectors is known, all possible events that end-to-end vector is a certain vector can be extracted by the integration of the product of the Dirac delta function as shown in Eq. (2.67) and bond probability distribution over the whole space of bond vectors. Since the end-to-end vector **h** is a function of bond vectors as shown in Eq. (2.3), the probability distribution of **h** is given by

$$P(\mathbf{h}, N) = \left\langle \delta\left(\mathbf{h} - \sum_{k=1}^{N} \mathbf{b}_k\right)\right\rangle \tag{2.67}$$

To make the mathematics simpler, we replace Eq. (2.21) by

$$p(\mathbf{b}) = \frac{1}{4\pi b^2}\delta(\|\mathbf{b}\| - b) \tag{2.68}$$

and replace Eq. (2.23) by

$$\langle g(\{\mathbf{b}_n\})\rangle = \int \mathrm{d}\mathbf{b}_1 \int \mathrm{d}\mathbf{b}_2 \ldots \int \mathrm{d}\mathbf{b}_N g(\{\mathbf{b}_n\}) P_{\text{bond}}(\{\mathbf{b}_n\}) \tag{2.69}$$

Use of the Dirac delta function made the replacement of the integration over solid angle by easier integration over the whole space of bond vectors.

Using Fourier transform, the Dirac delta function can be expressed by

$$\delta\left(\mathbf{h} - \sum_{k=1}^{N} \mathbf{b}_k\right) = \frac{1}{(2\pi)^3}\int \exp\left[\mathrm{i}\mathbf{q}\cdot\left(\mathbf{h} - \sum_{k=1}^{N} \mathbf{b}_k\right)\right]\mathrm{d}\mathbf{q} \tag{2.70}$$

Substitution of Eq. (2.70) into Eq. (2.67) gives

$$P(\mathbf{h}, N) = \frac{1}{(2\pi)^3}\int e^{\mathrm{i}\mathbf{q}\cdot\mathbf{h}}[\hat{p}(\mathbf{q})]^N \mathrm{d}\mathbf{q} \tag{2.71}$$

where

$$\hat{p}(\mathbf{q}) = \int p(\mathbf{b}) e^{-i\mathbf{q}\cdot\mathbf{b}} d\mathbf{b} = \frac{1}{4\pi b^2} \int_0^{2\pi} d\phi \int_0^{2\pi} \sin\theta d\theta \int_0^{\infty} db\delta(\|\mathbf{b}\| - b) e^{-iqb\cos\theta}$$
$$= \frac{\sin qb}{qb} \tag{2.72}$$

where $q = \|\mathbf{q}\|$. For sufficiently large N, we can use the following approximation:

$$[\hat{p}(\mathbf{q})]^N = \left(\frac{\sin qb}{qb}\right)^N \approx \exp\left(-N\frac{q^2b^2}{6}\right) \tag{2.73}$$

This approximation can be understood easily by looking at Fig. 7.

Substitution of Eq. (2.73) into Eq. (2.71) becomes the Gauss integral, it can be easily calculated, and we have

$$P(\mathbf{h}; N) \approx \left(\frac{3}{2\pi N b^2}\right)^{3/2} \exp\left(-\frac{3\mathbf{h}\cdot\mathbf{h}}{2Nb^2}\right) \tag{2.74}$$

Use of Eq. (2.27) gives

$$P(\mathbf{h}; N) = \left(\frac{3}{2\pi R^2}\right)^{3/2} \exp\left(-\frac{3\mathbf{h}\cdot\mathbf{h}}{2R^2}\right) \tag{2.75}$$

Note that the approximation is valid when N is large and $\|\mathbf{h}\| \ll bN$. Although Eq. (2.75) describes the case of $\|\mathbf{h}\| > bN$, it is impossible because bN is the maximum length of chain. Exact distribution is found in Yamakawa (1971):

$$P(\mathbf{h}; N) = \frac{1}{(2\pi N b^2)^{3/2}} \left\{\frac{\sinh \mathrm{L}^{-1}(\tilde{h})}{\mathrm{L}^{-1}(\tilde{h}) \exp\left[\tilde{h}\mathrm{L}^{-1}(\tilde{h})\right]}\right\}^N$$
$$\times \frac{\left[\mathrm{L}^{-1}(\tilde{h})\right]^2}{\tilde{h}\sqrt{1 - \left[\mathrm{L}^{-1}(\tilde{h})\mathrm{cosech}\ \mathrm{L}^{-1}(\tilde{h})\right]^2}} \tag{2.76}$$

where

$$\tilde{h} \equiv \frac{\|\mathbf{h}\|}{Nb} \tag{2.77}$$

and $\mathrm{L}^{-1}(\tilde{h})$ is the inverse Langevin function. The Langevin function is given by

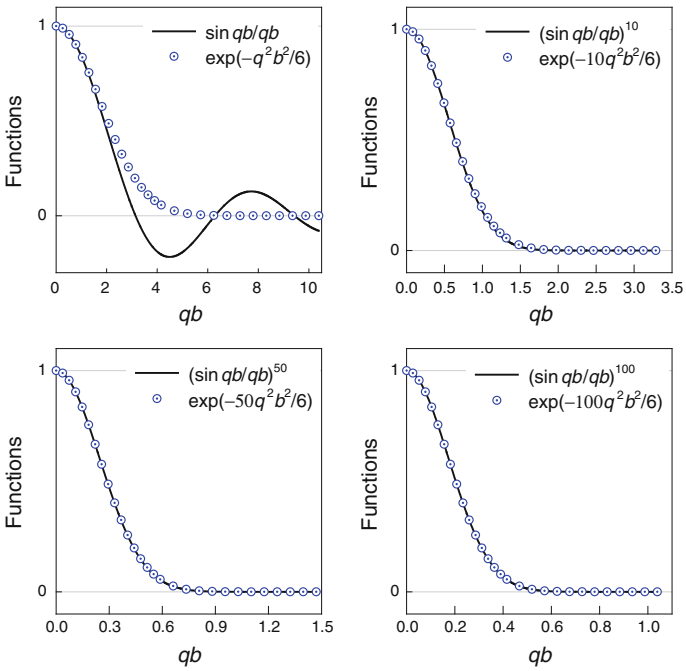

Fig. 7 Illustration of the approximation of Eq. (2.73)

$$\mathsf{L}(\tilde{h}) = \coth \tilde{h} - \frac{1}{\tilde{h}} \tag{2.78}$$

As for other chain models, it is extremely difficult to calculate the distribution function of end-to-end vector analytically. However, computer simulation makes it easy to be implemented. Random generation of N bond vectors according to the chain model gives a single sample of polymer chain. From the data of the bond vectors, end-to-end vector and radius of gyration can be calculated. Repeating these procedure M times, we can obtain distribution of end-to-end distance if M is sufficiently large. Figure 8 shows the distribution of the end-to-end distance for FJC and FRC.

Note that Eq. (2.74) is the distribution of end-to-end vector. Since end-to-end distance is independent of the orientation of end-to-end vector, all the vectors corresponding to the points on the surface of the sphere with radius of h have the same value of end-to-end distance. Hence, the distribution of end-to-end distance h is the product of the surface area of the sphere and the distribution of end-to-end vector:

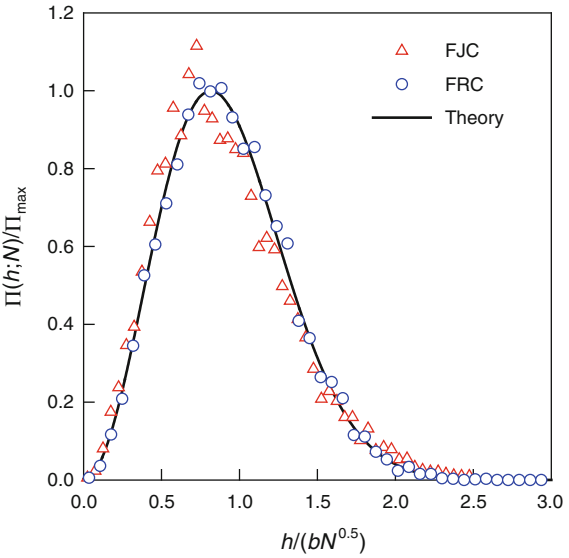

Fig. 8 Superposition of the distribution of end-to-end distance

$$\Pi(h;N) = 4\pi h^2 P(\mathbf{h};N) \tag{2.79}$$

The notion of equivalent chain illustrate that the plot of Π/Π_{max} against $h/(b\sqrt{N})$ must be independent of chain model whenever N is sufficiently large. Of course, b must be the length of Kuhn's segment.

2.3.2 Gauss Chain

When the number of segments N is large enough, the probability distribution of end-to-end distance vector is approximately Gaussian. Since the Kuhn segment contains several monomers, it is convenient in theoretical study of polymer physics to use the Gaussian chain model whose bond vector follows a Gaussian distribution:

$$p(\mathbf{r}) = \left(\frac{3}{2\pi b^2}\right)^{3/2} \exp\left(-\frac{3\mathbf{r}\cdot\mathbf{r}}{2b^2}\right) \tag{2.80}$$

where b is the length of the Kuhn segment. Because of the properties of Gaussian distribution, it is obvious that the probability distribution of the set of position vectors $\{\mathbf{r}_n\} = (\mathbf{r}_0, \mathbf{r}_1, \ldots, \mathbf{r}_N)$ is given by

$$P(\{\mathbf{r}_n\}) = \left(\frac{3}{2\pi b^2}\right)^{3N/2} \exp\left(-\frac{3}{2b^2}\sum_{n=1}^{N}\|\mathbf{r}_n - \mathbf{r}_{n-1}\|^2\right) \tag{2.81}$$

This is the Gaussian chain model. This model has an important property that the probability distribution of the vector $\mathbf{r}_m - \mathbf{r}_n$ is also Gaussian:

$$P(\mathbf{r}_m - \mathbf{r}_n, m-n) = \left(\frac{3}{2\pi b^2|m-n|}\right)^{3/2} \exp\left(-\frac{3\|\mathbf{r}_m - \mathbf{r}_n\|^2}{2|m-n|b^2}\right) \tag{2.82}$$

Although the Gaussian chain model is oversimplified, it satisfies the conditions of equivalent chain and has very convenient mathematical properties which allow us to calculate easily various features of long linear polymers. Hence, this model provides the platform for more advanced problems of polymer physics such as self-avoiding chain, the dynamics of flexible linear chain, and molecular theories of polymer viscoelasticity. It is noteworthy that Eq. (2.82) is the solution of diffusion equation.

2.4 Molecular Weight and Molecular Weight Distribution

2.4.1 Average Molecular Weight

Polymer chain is synthesized by the chemical reaction of monomers. The chemical reaction forming polymer is called polymerization. There are several reaction mechanisms in polymerization. Representative polymerizations are addition polymerization and condensation polymerization. PE, PP, PS, and PMMA are polymerized by the addition polymerization, while PET and Nylon66 are polymerized by the condensation polymerization. The overall polymerization consists of a number of elementary reactions which are coupled with each other. Since such elementary reactions have different rates and various factors influence polymerization, all the polymer chains in the reactor do not have the same number of monomers. Therefore, polymer has MWD and several kinds of average molecular weight are considered in polymer chemistry.

When monomer has the molecular weight of M_o, a polymer chain formed by N_i monomers has the molecular weight of $M_i = M_o N_i$. Suppose that there are n_i moles of polymer chains whose molecular weight is M_i and the total number of polymer chains is n_T in mole. Then, the mole fraction of polymers with M_i is given by $f_i = n_i/n_T$. If there are $N_{\max}$ of n_i's, then we know that

$$n_T = \sum_{i=1}^{N_{\max}} n_i \tag{2.83}$$

Then, the number-average molecular weight $\bar{M}_n$ is defined as

$$\bar{M}_n = \sum_{i=1}^{N_{\max}} M_i f_i \tag{2.84}$$

Since the weight fraction of polymer chains with M_i is given by

$$w_i = \frac{n_i M_i}{\sum_{k=1}^{N_{\max}} n_k M_k} \tag{2.85}$$

the weight-average molecular weight $\bar{M}_w$ is defined as

$$\bar{M}_w = \sum_{i=1}^{N_{\max}} M_i w_i \tag{2.86}$$

Most measurement devices for molecular weight provide weight fraction rather than mole fraction, and the relation between f_i and w_i is useful:

$$f_i = \frac{\bar{M}_n}{M_i} w_i \tag{2.87}$$

From the definition of mole fraction, it is clear that

$$\frac{1}{\bar{M}_n} = \sum_{i=1}^{N_{\max}} \frac{w_i}{M_i} \tag{2.88}$$

Hence, the number-average molecular weight is the harmonic mean with respect to weight fraction.

Since polymer has MWD, we need a representative value for wideness of MWD. Most widely used one is the polydispersity index (PI) which is defined as

$$\mathrm{PI} = \frac{\bar{M}_w}{\bar{M}_n} \tag{2.89}$$

Consider the identity such that

$$\frac{1}{\bar{M}_n} \sum_{i=1}^{N_{\max}} (M_i - \bar{M}_n)^2 f_i \geq 0 \tag{2.90}$$

The equality holds whenever every chain has the same molecular weight. Equation (2.90) immediately gives

$$\mathrm{PI} \geq 1 \tag{2.91}$$

2.4.2 Molecular Weight Distribution

If a polymer sample has PI = 1, then the sample is called monodisperse polymer. Otherwise, the sample is called polydisperse polymer. It is extremely difficult to polymerize monodisperse polymer. Anionic polymerization, which is a kind of addition polymerization, produces polymer samples which have PI very close to unity. Conventional polymer with PI < 1.1 is called monodisperse polymer. Monodisperse polymer, in conventional sense, is very important in studying viscoelasticity of polymers because most molecular theories are based on the assumption of monodispersity and because viscoelasticity of polydisperse polymer can be understood easily from that of monodisperse polymers. Monodisperse polymer is also used for the standard material for the calibration of various measuring devices. However, commercially produced polymers are polydisperse ones whose PI ranges from 2 to 10, usually. The wideness of MWD is an important factor controlling rheological properties of polymers. Even polymers with the same average molecular weight may show different viscoelastic behaviors depending on MWD.

MWD depends largely on types and conditions of polymerization. As for condensation polymerization, analysis of chemical kinetics gives the following MWD (Rubinstein and Colby 2003):

$$w(M) = \frac{M}{\bar{M}_n^2} \exp\left(-\frac{M}{\bar{M}_n}\right) \tag{2.92}$$

Since range of molecular weight is wide, continuous distribution $w(M)$ is preferred to discrete one such as w_i. Note that $w(M)$ is the continuous counterpart of discrete weight fraction. Hence, it is obvious that

$$\int_0^\infty w(M)\mathrm{d}M = 1 \tag{2.93}$$

Addition polymerization is a kind of chain reaction (Silbey et al. 2005). Chain reaction consists of several elementary reactions such as initiation, propagation, branching, and termination. If the probability of termination is very low and the rate of propagation is faster than that of initiation, anionic polymerization usually satisfies this condition, and then PI of the polymer follows

$$\mathrm{PI} = 1 + \frac{M_\mathrm{o}}{\bar{M}_n} \tag{2.94}$$

However, such ideal conditions are not available for most addition polymerization because of considerably high rate of termination. Including the effect of termination, the Shultz MWD is known valid for addition polymerization (Rubinstein and Colby 2003):

$$w(M) = \frac{M_o}{\bar{M}_n \Gamma(s)} \left(\frac{M}{\bar{M}_n} s \right)^s \exp\left(-\frac{M}{\bar{M}_n} s \right) \tag{2.95}$$

where s is a model parameter and $\Gamma(s)$ is the Gamma function which is defined as

$$\Gamma(s) = \int_0^\infty e^{-x} x^{s-1} \mathrm{d}x \tag{2.96}$$

Logarithmic normal distribution is usually used for any type of polymers:

$$w(M) = \frac{1}{\sqrt{2\pi}\sigma} \exp\left[-\frac{1}{2\sigma^2} \left(\log \frac{M}{M_{\max}} \right)^2 \right] \tag{2.97}$$

where $M_{\max}$ is the molecular weight at which $w(M)$ becomes the maximum and

$$\sigma^2 = \log \mathrm{PI} \tag{2.98}$$

2.4.3 Measurement of Molecular Weight

Methods of measuring molecular weight are classified into two kinds: absolute and relative methods. Absolute method can measure molecular weight without the help of any auxiliary samples, while relative method demands standard sample for calibration. End-group analysis, osmometry, cryoscopy, and light scattering belong to the absolute method, while gel permeation chromatography (GPC) and intrinsic viscosity belong to relative method.

Light scattering measures weight-average molecular weight as well as the radius of gyration. Although GPC is a relative method, it is very convenient and provides MWD.

2.4.4 Intrinsic Viscosity and Hydrodynamic Radius

Isolation of a molecule is carried out by vaporization. However, polymer cannot be vaporized since polymer has very high molecular weight. Before vaporization, it becomes decomposed to small molecules which can be gas. Dissolution of polymer in a solvent at very low concentration can isolate individual polymer chain. Hence, dilute solution is frequently used in analysis of polymers. GPC also use dilute polymer solution.

A polymer chain exists as a coil in dilute solution. The coil shape can be considered as a small sphere whose radius is close to R_G. Hence, dilute solution can be considered as a suspension of spheres. The radius of the hypothetical sphere is

called hydrodynamic radius R_H. The viscosity of a dilute suspension is known by Einstein equation such that

$$\eta = \eta_s\left(1 + \frac{5}{2}\phi\right) \tag{2.99}$$

where solvent is considered as a Newtonian fluid of viscosity η_s and ϕ is the volume fraction of the sphere.

The mass concentration of the suspension c is related with the volume fraction as follows:

$$\phi = \frac{c}{\rho} \tag{2.100}$$

where ρ is the density of the sphere. The density ρ can be estimated in terms of monomer characteristics. Usually, the monomer of conventional polymer is in liquid state in moderate temperature. When molar volume of the monomer liquid is known as v_o, then the density can be estimated by M_o/v_o. Then, Eq. (2.100) can be rewritten as follows:

$$\phi = \frac{v_o}{M_o}c \tag{2.101}$$

When the number of sphere is given by N_s, the volume fraction can be expressed by

$$\phi = \frac{4\pi}{3}\frac{N_s R_H^3}{V} \tag{2.102}$$

where V is the volume of the solution. Note that the number of the spheres is the number of polymer chains in the dilute solution. Hence, we have

$$N_s = \frac{w_P}{M} \tag{2.103}$$

where w_P is the mass of the polymer in the dilute solution and M is the molecular weight of the polymer under the assumption of monodisperse polymer. From the definition of mass concentration, it is clear that

$$c = \frac{w_P}{V} \tag{2.104}$$

Finally, the volume fraction can be expressed in terms of polymer characteristics:

$$\phi = \frac{4\pi}{3}\frac{R_H^3}{M}c \tag{2.105}$$

It is noteworthy that mass concentration is more convenient and available than the volume fraction although most theories are based on the volume fraction.

Intrinsic viscosity is defined as

$$[\eta] \equiv \lim_{c\to 0}\frac{\eta - \eta_s}{\eta_s c} \tag{2.106}$$

Applying Eqs. (2.99) and (2.105) gives

$$[\eta] = \frac{10\pi}{3M}R_H^3 \tag{2.107}$$

or

$$R_H = \left(\frac{3}{10\pi}[\eta]M\right)^{\frac{1}{3}} \tag{2.108}$$

If the radius of gyration is considered as the hydrodynamic radius, then Eq. (2.17) allows us to use

$$R_H = kM^{\nu} \tag{2.109}$$

where $\nu = \frac{1}{2}$ for Θ-solvent and $\nu \approx 0.588$ for good solvent. The constant k is a material constant. Substitution of Eq. (2.109) into Eq. (2.107) gives

$$[\eta] = KM^{\alpha} \tag{2.110}$$

where $\alpha = 3\nu - 1$ and $K = \frac{10\pi}{3}k^3$. Equation (2.110) is called the *Mark–Houwink equation.* The constants α and K depend on polymer, solvent, temperature, and pressure. Hence, if samples of several molecular weights are available, then measurement of intrinsic viscosity at the same conditions determines the constants α and K. With the help of the standard samples, we can determine the molecular weight of arbitrary sample. Hence, measurement of intrinsic viscosity is a relative method for molecular weight.

Problem 2

[1] Derive Eqs. (2.15) and (2.16).
[2] Show that the tensor $\mathbf{T}_i$ of Eq. (2.35) is an orthogonal tensor.
[3] Derive Eqs. (2.54) and (2.55).
[4] Derive Eq. (2.59).

[5] Derive Eq. (2.74) using Eq. (2.73).
[6] Derive Eq. (2.74) using $\tilde{h} \ll 1$ from Eq. (2.76).

3 Polymer Solution

This book is focused on viscoelasticity of polymers. Although viscoelasticity of mixtures of polymers depends on phase separation dynamics, we will not deal with thermodynamics of polymer blends and polymer solutions. It is because this book does not contain the viscoelasticity of polymer systems with phase separation. However, it is important to know how configuration of polymer chains changes according to the polymer concentration because such changes influence viscoelasticity of polymer solution without phase separation.

3.1 Polymer Concentration

One of the most important differences between polymer melts and solutions is existence of solvent molecules. As a polymer concentration, volume fraction of polymer is convenient in theoretical studies, while it is not convenient for experiment. Volume fraction of polymer is defined by

$$\phi = \frac{V_\mathrm{p}}{V} \tag{3.1}$$

where V_p is the volume of the polymer and V is the volume of the polymer solution. Exactly saying, V_p must be the partial molar volume of the polymer which can be determined by the consideration of solution thermodynamics. If the Flory–Huggins theory of polymer solution is valid for the polymer solution under the consideration, the partial molar volume can be replaced by the molar volume of the pure polymer because the Flory–Huggins theory does not consider the volume change in mixing. However, it is difficult to measure the molar volume of the pure polymer in liquid state at the temperature of the polymer solution because the polymer is usually in solid state at the solution temperature.

If the polymer is glassy one which cannot form any crystallite in solid state and if its monomer is in liquid state at the solution temperature, then we can replace the polymer volume in the solution by the molar volume of the liquid monomer. As for polyethylene (PE), the polymer is crystalline polymer which consists of both amorphous and crystalline parts. Furthermore, as the monomer of polyethylene, ethane is a gas at most temperatures. In this case, we have to find the oligomer of PE which is in liquid state at the solution temperature.

In this section, it is assumed that there is a substitute for the polymer which is suitable for estimation of the density of the polymer in the solution. Then, the volume of the polymer can be estimated by

$$V_{\mathrm{p}} = \frac{w_{\mathrm{p}}}{\rho_{\mathrm{m}}} \tag{3.2}$$

where w_{p} is the weight of the polymer and ρ_{m} is the density of the substitute such as the liquid monomer. When change of volume in mixing is not significant, we have

$$\phi = \frac{w_{\mathrm{p}}}{w_{\mathrm{p}} + r w_{\mathrm{s}}} \tag{3.3}$$

where w_{s} is the weight of solvent and r is the ratio of density:

$$r = \frac{\rho_{\mathrm{m}}}{\rho_{\mathrm{s}}} \tag{3.4}$$

where ρ_{s} is the density of the solvent.

In experiment, weight concentration is more convenient than volume fraction. The weight concentration is defined by

$$c = \frac{w_{\mathrm{p}}}{V} \tag{3.5}$$

It is obvious that

$$c = \rho_{\mathrm{m}} \phi \tag{3.6}$$

Note that weight concentration c can be easily determined experimentally, and we can calculate volume fraction ϕ from c, if we are equipped with appropriate ρ_{m}.

3.2 Concentration Regimes

When concentration is extremely low, it is obvious that individual polymer chain is separated from each other. Because of the thermal motion, polymer chains have coil conformations. Hence, we can imagine a sphere that envelops a single chain whose radius is close to the radius of gyration of the chain. As discussed in Sect. 2.4, the viscosity of the solution in this concentration regime is proportional to the concentration. This concentration regime is called the dilute regime.

As concentration increases, the blobs of polymer chains become to contact. The *overlap concentration* is the concentration at which the blobs become to contact. Since the blobs of polymer chains pervade the whole space of the polymer solution,

the polymer concentration almost equals to that of the blob. The volume of the blob is approximately given by

$$V_{\text{blob}} \approx \frac{4\pi}{3} R_G^3 = \frac{4\pi}{3} \left(\frac{N^{2\nu} b^2}{6} \right)^{3/2} \propto b^3 N^{3\nu} \tag{3.7}$$

where exponent ν is 1/2 for θ-solution and about 0.6 for good solution. Since a single blob contains a single chain, the overlap concentration in volume fraction is given by

$$\phi^* = \frac{N v_{\text{m}}}{V_{\text{blob}}} \propto N^{1-3\nu} \tag{3.8}$$

where v_{m} is the volume of the Kuhn segment. It is obvious that the volume of the Kuhn segment is proportional to b^3. Hence, N is large, the overlap occurs at very low concentration which corresponds to the concentration of the dilute solution of a solute of low molecular weight. Because of such low value of the overlap concentration, the concentration regime higher than the overlap concentration is called semi-dilute regime. This reasoning is visualized in Fig. 9.

In the semi-dilute regime, the viscosity of polymer solution increases steeply as concentration increases. As for θ-solution, it is known that

$$\eta - \eta_s \propto \phi^2 \tag{3.9}$$

Hence, the overlap concentration can be determined by measuring viscosity as a function of concentration. For wide range of concentration, it is observed that

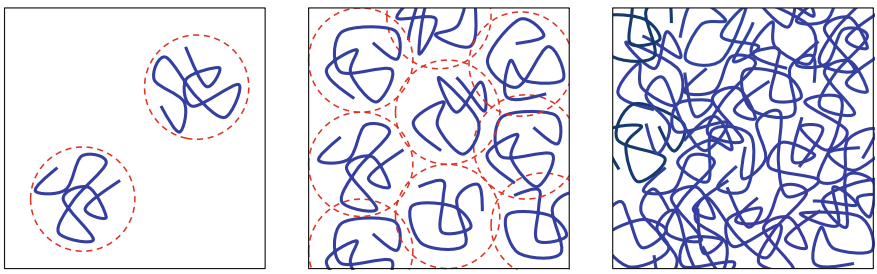

Fig. 9 Graphical illustration of chain distributions depending on concentration. The *left* represents a dilute solution, the *middle* a solution at the overlap concentration c^*, and the *right* a semi-dilute or concentrated solution

$$\eta - \eta_s \approx \begin{cases} \frac{5\eta_s}{2}\phi & \phi < \phi^* \\ \frac{5\eta_s\phi^*}{2}\left(\frac{\phi}{\phi^*}\right)^{\alpha} & \phi^* < \phi < \phi_e \\ \frac{5\eta_s\phi^*}{2}\left(\frac{\phi_e}{\phi^*}\right)^{\alpha}\left(\frac{\phi}{\phi_e}\right)^{\beta} & \phi_e < \phi \end{cases} \tag{3.10}$$

where the exponents α and β depend on solution characteristics. It is known that $\alpha = 2$ and $\beta = 14/3 \approx 4.7$ for θ-solution. Figure 10 shows a schematic illustration of Eq. (2.10) for θ-solution.

The concentration ϕ_e in Eq. (2.10) is found from experiments if N is sufficiently large. It is called *entanglement concentration* at which motion of a chain is influenced largely by neighbor chains. The problem of interaction between chains was solved using tube concept (Rubinstein and Colby 2003). The diameter of the hypothetical tube is known to be proportional to $b\sqrt{N_e(1)}$ in molten state where $N_e(1)$ is interpreted as the number of Kuhn's segments in an entanglement subchain in molten state. It is a material constant of polymer. Here, $N_e(1)$ is the notation which emphasizes that melt can be considered as $\phi = 1$.

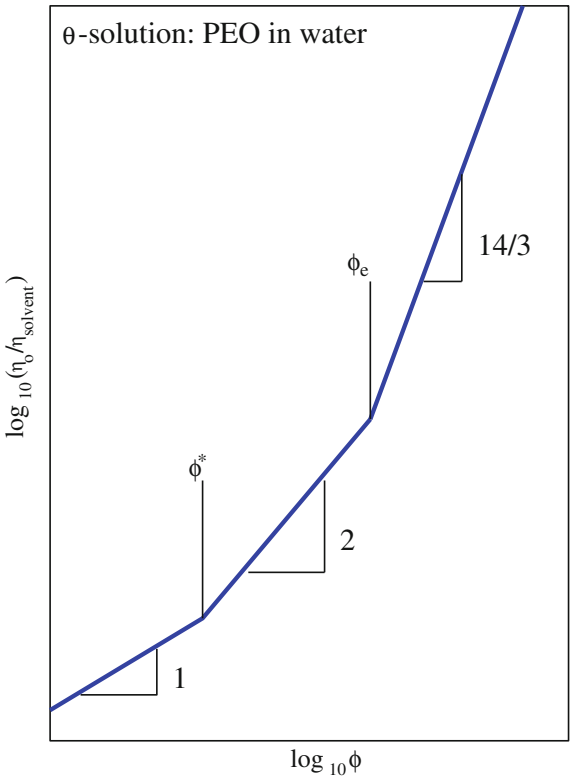

Fig. 10 Schematic illustration of Eq. (3.10) for θ-solution

An example of θ-solution is an aqueous solution of polyethylene oxide (PEO) at the room temperature. If molecular weight is not extremely high, for example, $M \sim 5000$ kg/mol for PEO, it is difficult to expect a sharp transition as shown in Fig. 10. Readers can find experimental data corresponding to Fig. 10 in Rubinstein and Colby (2003). As shown in Fig. 10, both overlap and entanglement concentrations can be determined experimentally as the concentrations at which the slope $d \log \eta_o / d \log \phi$ changes abruptly. However, the two characteristic concentrations can be estimated by molecular theory. As for overlap concentration, although molecular theory provides an equation more detail than Eq. (2.8), such equation requires material information such as radius of gyration which can be measured by light scattering. Radius of gyration depends on polymer and solvent as well as temperature.

3.3 Entanglement

Entanglement in linear polymer is the notion originated from various experimental results and geometric features of flexible polymer chain. Since viscoelastic behavior of polymer dramatically changes at a certain molecular weight, polymer scientists have tried to explain the transition in viscoelastic behavior by the concept of entanglement which is inspired from network structure of rubber. Entanglement has been considered as a result from temporary network compared with rubber structure which is a permanent network. This analogy was made because viscoelastic behaviors of high polymer look like those of rubber. This viewpoint produces entanglement molecular weight $M_e(1)$ which is the molecular weight of the subchain between adjacent junction points of the temporary network. If the molar mass of Kuhn segment is denoted by M_o, then we know that $M_e(1) = M_o N_e(1)$. From this crude definition of entanglement molecular weight, it can be said that polymer chains with $M > 2M_e(1)$ can form entanglement.

It might be impossible to express rigorously multi-chain interactions in a closed form. To make it simpler, a mean field approach was invented by de Gennes. He suggested a hypothetical tube envelop a chain. The tube represents the mean interaction of the tagged chain with environmental chains because repulsive interaction is dominant between chains in melt and solution. Introduction of tube makes the multi-chain problem simpler single-chain problem. Advocates of tube theory assume that the diameter of the tube a is about the end-to-end distance of entangled subchain:

$$a = b\sqrt{N_e} \tag{3.11}$$

From this viewpoint, entanglement is a geometric metaphor of mean interaction between chains.

One of the important problems on entanglement is how to measure the entanglement molecular weight. Statistical mechanical theory of rubber elasticity

provides an equation which relates the initial modulus of rubber with the molecular weight between permanent junction points (see Sect. 4). Although polymer melts do not have permanent junction bonds, their viscoelastic behaviors in certain range of time (or frequency) look like those of rubber. In this range, the plateau modulus can be defined and considered as the rubber modulus. Then, the equation provides the entanglement molecular weight as the molecular weight of subchains between temporal junction points. This method for the determination of entanglement is based on the first viewpoint on entanglement: temporal network. However, tube theories based on Eq. (2.11) give consistency with the first viewpoint.

Solvent molecules between polymer chains give wider spacing between junction points. Hence, addition of solvent molecules increases the entanglement molecular weight. In molten state, polymers with $N < 2N_e(1)$ cannot form entanglement. Hence, such short polymer chain cannot form entanglement in solution at any concentration. Scaling theory (Rubinstein and Colby 2003) gives the following equation under the assumption that $N \gg 2N_e(1)$:

$$\phi_e \approx \begin{cases} \left[\frac{N_e(1)}{N}\right]^{(3\nu-1)} \approx \left[\frac{N_e(1)}{N}\right]^{0.76} & \text{for an athermal solution} \\ \left[\frac{N_e(1)}{N}\right]^{3/4} & \text{for } \theta\text{-solution} \end{cases} \tag{3.12}$$

According to Heo and Larson (2008), viscoelasticity of polymer solution of $\phi \gg \phi_e$ is nearly identical to that of molten polymer if relaxation times and modulus are scaled in a suitable manner.

It is noteworthy that Fetters et al. (1994) suggested a method to determine entanglement molecular weight in terms of the characteristic ratio, the length and the mass of monomer and melt density. This calculation is not based on the concept of temporal network. They showed that their calculation is equivalent to the results from temporal network.

To understand the viscoelasticity of high-mass polymer chains, entanglement concept is very important and we need to study the rubber elasticity to understand entanglement. Reversely, viscoelasticity plays the main role in understanding entanglement. In Chap. 9, we shall revisit the entanglement concept.

Equation (3.12) is very useful because only molecular weight and entanglement molecular weight are necessary. Furthermore, the exponent $3\nu - 1$ indeed becomes close to that of θ-solution ($0.76 \approx 3/4$). Although the calculation of overlap concentration needs consideration of solvent effects, that of entanglement concentration does not. We can use Eqs. (3.6) and (3.12) in the calculation of c_e.

Figure 11 shows zero-shear viscosities of polystyrene solutions as functions of normalized concentration c/c_e where c_e was calculated (Kim 2007). Note that compared with solvent viscosity, the zero-shear viscosity of polymer solution is much higher. Hence, the experimental data of Fig. 11 look like Fig. 10. The two red dotted lines indicate that the calculated entanglement concentration is lower than the experimentally determined one, the cross point at which the two regression lines meet. However, the two concentrations are very close. Different from monodisperse

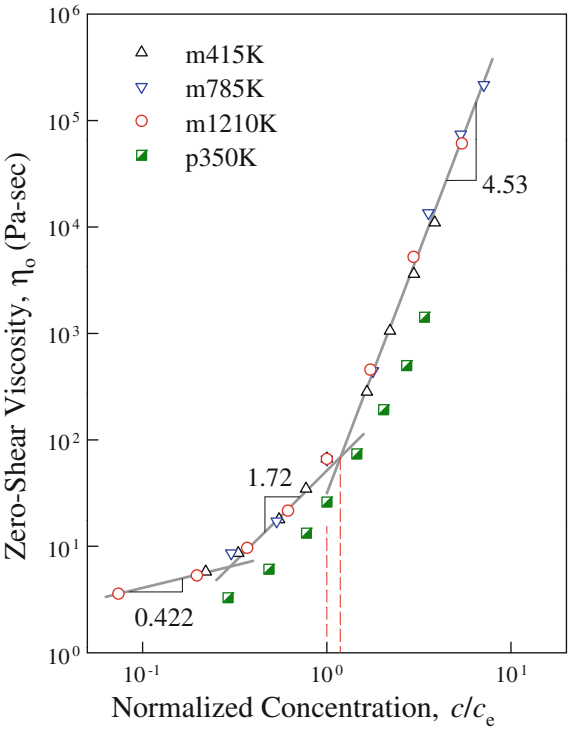

Fig. 11 Zero-shear viscosity of solution of PS in ethylbenzene as a function of normalized concentration. Indicator m implies monodisperse and p implies polydisperse. Molecular weights are 415 kg/mol for m415 K, 785 kg/mol for m785 K, 1210 kg/mol for m1210, and 350 kg/mol ($\bar{M}_w$) for p350 K. The data are from Kim (2007)

PS, polydisperse PS does not show any sharp transition of slope. Furthermore, the zero-shear viscosity of polydisperse PS is lower than that of monodisperse polymer.

Problem 3

[1] Derive

$$c^* \approx \frac{1}{[\eta]} \tag{3.a}$$

[2] It is a reasonable assumption that solution properties are dependent on the number and size of Kuhn monomer as follows:

$$\tilde{P} \equiv \frac{P}{P^*} = \tilde{f}(N, b, \varphi) \tag{3.b}$$

Here, P is a physical property of solution, P^* is the characteristic quantity having the same dimension of P, and φ is the number of Kuhn monomer per unit volume. Dimensional analysis (Barenblatt 1996) results in

$$\tilde{P} = \tilde{g}\left(N, b^3\varphi\right) = \tilde{f}(N, b, \varphi) \tag{3.c}$$

It is well known that physical properties depending on chain conformation obey the self-similarity which means that Eq. (3.c) is invariant with respect to the following transformation:

$$N \to \frac{N}{s}; \quad b \to bs^{\nu}; \quad \varphi \to \frac{\varphi}{s} \tag{3.d}$$

where s is any real number and ν is the exponent of Eq. (2.61). Show that the osmotic pressure Π of solution obeys

$$\Pi = \frac{\varphi}{N} k_B T \tilde{h}\left(\frac{c}{c^*}\right) \tag{3.e}$$

where $\tilde{h}(\cdot)$ is a dimensional function.

[3] When $c > c^*$, it is a reasonable assumption that osmotic pressure is independent of N. Assume that $\tilde{h}(x) = x^z$. Then derive that

$$\Pi \propto c^{9/4} \tag{3.f}$$

[4] Aqueous PEO solution at the room temperature is known as a θ-solution. It is also known that $M_o = 137$ g/mol and $M_e = 2000$ g/mol. Calculate ϕ_e of PEO with $M = 1000$ kg/mol.

4 Rubber Elasticity

Rubber is a polymer network that polymer chains are covalently connected in a three-dimensional manner. The constituent polymer chains called subchains have glass transition temperature much lower than room temperature. Hence, the subchains move like those of polymer melts. However, difference from the melt of linear polymer, the subchains cannot flow because of the three-dimensional network structure. These special features of rubber structure allow it to behave like elastic solid. Different from most elastic material such as metal and plastics, rubber shows much wider strain range of elasticity. After loading rubber up to several times of the original length, unloading gives immediate recover of the original length without any permanent deformation. Although this behavior makes rubber called elastomer, exactly saying, rubber is also viscoelastic material. Loading and unloading shows a very narrow loop. Such small hysteresis might be neglected and rubber is approximately considered as finite elastic material.

In this section, we shall study thermodynamic aspect of rubber elasticity and then introduce rubber elastic models: molecular and phenomenological models. As

for the general aspects of rubber elasticity, Treloar (1975) is recommendable for reading. Ogden's book (Ogden 1984) is recommendable for nonlinear mechanics of elasticity as well as his review paper (Ogden 1986).

4.1 Thermodynamics of Rubber

Here, we shall discuss the origin of rubber elasticity through thermodynamic considerations. For simplification, we consider one-dimensional deformation. Suppose that force f gives rise to extension of length by dL. One of the most important features of rubber is volume preservation during any deformation because shear modulus is much smaller than bulk modulus. Then, the differential of the Helmholtz free energy is given by

$$\mathrm{d}F = -S\mathrm{d}T + f\mathrm{d}L \tag{4.1}$$

The Maxwell relation gives

$$\left(\frac{\partial f}{\partial T}\right)_L = -\left(\frac{\partial S}{\partial L}\right)_T \tag{4.2}$$

Since $f = (\partial F/\partial L)_T$, the force can be decomposed to

$$f = \left(\frac{\partial U}{\partial L}\right)_T - T\left(\frac{\partial S}{\partial L}\right)_T \tag{4.3}$$

Here, $(\partial U/\partial L)_T$ is the force due to change of internal energy, while the second term is the force due to change of entropy. Substitution of Eq. (4.2) into Eq. (4.3) gives

$$f = f_E + T\left(\frac{\partial f}{\partial T}\right)_L \tag{4.4}$$

where $f_E = (\partial U/\partial L)_T$. Rearrangement of Eq. (4.4) gives

$$\frac{f_E}{f} = 1 - \left(\frac{\partial \log f}{\partial \log T}\right)_L \tag{4.5}$$

Although the measurement of $(\partial S/\partial L)_T$ is not easy, it is easy to measure the force change due to temperature change at constant length. Experimental results show that f_E/f is very low for wide range of temperature. Then, it can be concluded that the force of rubber is mainly originated from change of entropy. Since glass transition temperature of rubber is much lower than the room temperature, polymer chains in rubber take coil conformation. However, deformation on rubber restricts

the variety of the conformations of the polymer chains. Then, the reduction of entropy appears and the resistance of rubber results in force. Since glass transition temperature is very low, interactions between segments of subchains render negligible effects on the rotation of bonds. Hence, the force from energy change is negligible compared to that from entropy change (Treloar 1975).

4.2 Statistical Mechanical Theory

4.2.1 Force on a Single Chain

From thermodynamic experiment, we assume that the stress of rubber is generated by only entropy. Before the derivation of the stress equation of rubber, we need to study the force exerted on a single chain. From Eq. (4.3), we know that

$$\mathbf{f} = -T\left(\frac{\partial S}{\partial \mathbf{h}}\right)_T = \left(\frac{\partial F}{\partial \mathbf{h}}\right)_T \tag{4.6}$$

where $\mathbf{h}$ is the end-to-end vector. Since the internal energy is independent of conformation change, the second equality holds. The entropy of a single chain can be calculated by the Boltzmann equation for entropy, Eq. (2.4). The phase volume of Ω can be interpreted by the number of all possible conformations at a given end-to-end vector. If we denote Ω_{total} as the total number of all possible conformations of a chain with N segments, then we have

$$\Omega(\mathbf{h}, N) = \Omega_{\text{total}} P(\mathbf{h}; N) \tag{4.7}$$

where $P(\mathbf{h}; N)$ is the Gaussian distribution of Eq. (2.74). Then, the conformation entropy is given by

$$S = k_{\text{B}} \log \Omega(\mathbf{h}, N) = -\frac{3k_{\text{B}}}{2Nb^2}\mathbf{h} \cdot \mathbf{h} + S_{\text{o}} \tag{4.8}$$

where S_{o} is the term independent of $\mathbf{h}$. Substitution of Eq. (4.8) into Eq. (4.6) gives

$$\mathbf{f} = \frac{3k_{\text{B}}T}{Nb^2}\mathbf{h} \tag{4.9}$$

Gaussian distribution cannot reflect the limitation of extension because of finite contour length of polymer. Although the exact distribution function is Eq. (2.76) (Yamakawa 1971), it is too complicate to calculate the force. Alternative approximation is to use the canonical ensemble. According to Rubinstein (2003), the relation between the magnitudes of force and the end-to-end vector is given by

$$f = \frac{k_B T}{b} \mathsf{L}^{-1}\left(\frac{h}{Nb}\right) \tag{4.10}$$

The inverse Langevin function is so complicate as shown in Eq. (2.78). The Maclaurin series of the inverse Langevin function is known as

$$\mathsf{L}^{-1}(x) = 3x + \frac{9}{5}x^3 + \frac{297}{175}x^5 + \frac{1539}{875}x^7 + \frac{126117}{67375}x^9 + \cdots \tag{4.11}$$

Comparison of Eq. (4.9) with Eq. (4.11) implies that the force from Gaussian distribution is the first-order approximation of more advanced theory.

The force on a single chain is important because it can be applied to the development of nonlinear viscoelastic constitutive equation of polymers. Hence, approximations of the inverse Langevin function have been suggested. One of them is the *FENE (finitely extensible nonlinear elastic) model* (Bird et al. 1987):

$$\mathsf{L}^{-1}(x) = \frac{3x}{1 - x^2} \tag{4.12}$$

4.2.2 Ideal Network

One of the simplest theories for the free energy of rubber is based on the following assumptions:

[1] All subchains are statistically independent.
[2] All subchains are identical—the same number of segments.
[3] Free energy of the rubber is the sum of those of subchains.
[4] In the reference configuration, the orientation of subchain is isotropic.
[5] Deformation of rubber does not alter the volume.
[6] Deformation is affine.

From the assumptions, the end-to-end vector after deformation is given by

$$\mathbf{h} = \mathbf{F} \cdot \tilde{\mathbf{h}} \tag{4.13}$$

where $\mathbf{F}$ is the given deformation gradient and $\tilde{\mathbf{h}}$ is the end-to-end vector in the reference configuration. Furthermore, F, the free energy per unit volume is given by

$$F = \rho_c \int \frac{3k_B T}{2Nb^2} \mathbf{C} : \mathbf{h}\mathbf{h} P\left(\tilde{\mathbf{h}}; N\right) \mathrm{d}\tilde{\mathbf{h}} \tag{4.14}$$

where ρ_c is the number of subchains per unit volume and $\mathbf{C} = \mathbf{F}^T \cdot \mathbf{F}$ is the right Cauchy–Green tensor (Eq. 1.17b in Chap. 2). Note that the free energy of a single chain is given by

$$F_{\text{single}} = \frac{3k_{\text{B}}T}{2Nb^2}\left(\mathbf{F}\cdot\tilde{\mathbf{h}}\right)\cdot\left(\mathbf{F}\cdot\tilde{\mathbf{h}}\right) = \frac{3k_{\text{B}}T}{2Nb^2}\tilde{\mathbf{h}}\cdot\mathbf{F}^T\cdot\mathbf{F}\cdot\tilde{\mathbf{h}} \tag{4.15}$$

To evaluate the integration, we use the change of variable such that $\tilde{\mathbf{h}} = \mathbf{F}^{-1}\cdot\mathbf{h}$. Then, we have

$$F = \rho_c\frac{3k_{\text{B}}T}{2Nb^2}\left(\frac{3}{2\pi Nb^2}\right)^{3/2}\int \mathbf{h}\cdot\mathbf{h}\exp\left(-\frac{3}{2Nb^2}\mathbf{h}\cdot\mathbf{B}^{-1}\cdot\mathbf{h}\right)\left|\det\left(\mathbf{F}^{-1}\right)\right|\mathrm{d}\mathbf{h} \tag{4.16}$$

where $\mathbf{B} = \mathbf{F}\cdot\mathbf{F}^T$ is the left Cauchy–Green tensor (Eq. 1.17a in Chap. 2). Using the property of the Gaussian distribution gives

$$F = \rho_c\frac{3k_{\text{B}}T}{2Nb^2}\mathrm{tr}\left(\frac{Nb^2}{3}\mathbf{B}\right) = \frac{\rho_c k_{\text{B}}T}{2}\mathrm{tr}(\mathbf{B}) \tag{4.17}$$

Here, we used the assumption (Blatz et al. 1974) which means that $\det(\mathbf{F}^{-1}) = \det(\mathbf{B}) = 1$ and omitted irrelevant terms.

Since Eq. (4.17) implies incompressible hyperelasticity, we can calculate stress using Eq. (3.39) in Chap. 2:

$$\mathbf{T} = -p\mathbf{I} + \rho_c k_{\text{B}}T\mathbf{B} \tag{4.18}$$

For uniaxial elongation, we know that

$$\mathbf{F} = \lambda\mathbf{e}_1\mathbf{e}_1 + \frac{1}{\sqrt{\lambda}}(\mathbf{e}_2\mathbf{e}_2 + \mathbf{e}_3\mathbf{e}_3); \quad \mathbf{B} = \lambda^2\mathbf{e}_1\mathbf{e}_1 + \frac{1}{\lambda}(\mathbf{e}_2\mathbf{e}_2 + \mathbf{e}_3\mathbf{e}_3) \tag{4.19}$$

where λ is the draw ratio. Since nonzero stress component of uniaxial elongation is only T_{11}, we know that

$$T_{22} = T_{33} = -p + \frac{\rho_c k_{\text{B}}T}{\lambda} = 0 \tag{4.20}$$

and

$$T_{11} = \rho_c k_{\text{B}}T\left(\lambda^2 - \frac{1}{\lambda}\right) \tag{4.21}$$

The Young's modulus is given by the differentiation of T_{11} with respect to λ:

$$E = \rho_c k_{\text{B}}T\left(2\lambda + \frac{1}{\lambda^2}\right)_{\lambda=1} = 3\rho_c k_{\text{B}}T \tag{4.22}$$

Because of no change in volume, it is obvious that the Poisson ratio of rubber ν is approximately 1/2. Then, Eq. (3.16) in Chap. 2 gives shear modulus of rubber:

$$G = \frac{1}{3}E = \rho_c k_B T \tag{4.23}$$

The number density of subchain is related with mass density of rubber ρ and molecular weight of subchain M_x:

$$\rho_c = \frac{\rho}{M_x / N_A} \tag{4.24}$$

where N_A is the Avogadro's number. Then, Eq. (4.23) becomes

$$G = \frac{\rho RT}{M_x} \tag{4.25}$$

where R is the gas constant. Equation (4.25) means that measurement of initial shear modulus and density gives the average molecular weight of the subchain between adjacent junction points.

4.3 Phenomenological Models

Although statistical mechanical theory achieved successful results at moderate range of strain, most molecular constitutive equations fail in description in high strain range. Even if a molecular constitutive equation has a success in simple elongation, it is usual that the constitutive equation cannot fit simple shear or other experimental data with the parameters determined from the simple elongation. Hence, there have been a number of efforts to develop phenomenological model which can fit almost deformation data by a single set of material parameters. One of the successful phenomenological models is the Ogden model (Treloar 1975).

4.3.1 Mooney–Rivlin Model

Most phenomenological models are to develop strain potential of Eq. (3.36) in Chap. 2. Mooney and Rivlin used the Taylor expansion of the strain potential with respect to the principal invariants of **B** Mooney (1940), Rivlin (1948). Then, the strain potential is given by

$$\begin{aligned}\Phi(I_{\mathbf{B}}, II_{\mathbf{B}}) = {} & G_1^0(I_{\mathbf{B}} - 3) + G_0^1(II_{\mathbf{C}} - 3) \\ & + G_2^0(I_{\mathbf{B}} - 3)^2 + G_0^2(II_{\mathbf{C}} - 3) + G_1^1(I_{\mathbf{B}} - 3)(II_{\mathbf{B}} - 3) + \cdots\end{aligned} \tag{4.26}$$

Here, $III_{\mathbf{B}}$ is not considered because $III_{\mathbf{B}} = \det(\mathbf{B}) = 1$ is usually assumed in rubber elasticity.

When truncating the series up to the first order, the stress is given by

$$\mathbf{T} = -p\mathbf{I} + 2G_1^0\mathbf{B} - 2G_0^1\mathbf{B}^{-1} \tag{4.27}$$

This is the *Mooney–Rivlin model* or the *neo-Hookean model*. Applying Eq. (4.27) to uniaxial elongation, the axial stress T_{11} is given by

$$T_{11} = 2G_1^0\left(\lambda^2 - \frac{1}{\lambda}\right) - 2G_0^1\left(\frac{1}{\lambda^2} - \lambda\right) \tag{4.28}$$

Because rubber is incompressible, the ratio of cross-sectional area is λ^{-1}. Then, the engineering stress $\sigma_E = f/A_o$ is calculated from Eq. (4.28) as follows:

$$\sigma_E = \frac{T_{11}}{\lambda} = 2\left(G_1^0 + \frac{G_0^1}{\lambda}\right)\left(\lambda - \frac{1}{\lambda^2}\right) \tag{4.29}$$

Equation (4.29) implies that the plot of $\sigma_E/(\lambda - \lambda^{-2})$ against λ^{-1} allows us to determine the moduli because the plot for experimental data is a straight line such that the intersection is $2G_1^0$ and the slope is $2G_0^1$. Such plot is called the *Mooney–Rivlin plot*. It is found in Dossin and Graessley (1979) that the Mooney–Rivlin plot is valid for $1 < \lambda < 1.4$.

Compared with metallic material, $1 < \lambda < 1.4$ is very wide range of elastic deformation, and the Mooney–Rivlin model is not a good constitutive equation if wide range of elastic deformation such as $1 < \lambda < 7$ is considered. Hence, we need more advanced models.

4.3.2 Valanis–Landel Hypothesis

Since we consider rubber as incompressible hyperelastic material, the strain potential can be considered as a function of the eigenvalues of $\mathbf{B}$ instead of principal invariants. Note that $\det(\mathbf{B}) = 1$ implies that $\lambda_1^2\lambda_2^2\lambda_3^2 = 1$ where λ_k^2 are the eigenvalues of $\mathbf{B}$. Then, we know that

$$I_\mathbf{B} = \lambda_1^2 + \lambda_2^2 + \frac{1}{\lambda_1^2\lambda_2^2}; \quad II_\mathbf{B} = \frac{1}{\lambda_1^2} + \frac{1}{\lambda_2^2} + \lambda_1^2\lambda_2^2 \tag{4.30}$$

Then, the strain potential of the Mooney–Rivlin model can be rewritten as

$$\Phi = G_1^0(I_\mathbf{B} - 3) + G_0^1(II_\mathbf{B} - 3) = \sum_{k=1}^{3} w(\lambda_k) \tag{4.31}$$

where

$$w(x) = G_1^0(x^2 - 1) + G_0^1\left(\frac{1}{x^2} - 1\right) \tag{4.32}$$

The *Valanis–Landel hypothesis* (Valanis and Landel 1967) is the generalization of Eq. (4.31) that strain potential can be expressed by the sum of identical function of extension ratio. All analytical functions $\Phi(I_\mathbf{B}, II_\mathbf{B})$ cannot be expressed by a function $w(x)$ such that

$$\Phi(I_\mathbf{B}, II_\mathbf{B}) = \sum_{k=1}^{3} w(\lambda_k) \tag{4.33}$$

Rivlin and Sawyer (1976) derived a necessary and sufficient condition for Eq. (4.33):

$$\frac{\partial}{\partial I_\mathbf{B}}\left(\frac{\partial^2\Phi}{\partial I_\mathbf{B}^2} + I_\mathbf{B}\frac{\partial^2\Phi}{\partial I_\mathbf{B}\partial II_\mathbf{B}}\right) = -\frac{\partial}{\partial II_\mathbf{B}}\left(\frac{\partial^2\Phi}{\partial II_\mathbf{B}^2} + II_\mathbf{B}\frac{\partial^2\Phi}{\partial I_\mathbf{B}\partial II_\mathbf{B}}\right) \tag{4.34}$$

Valanis and Landel (1967) also suggested the form of $w(x)$ from the analysis of experimental data:

$$\frac{\mathrm{d}w}{\mathrm{d}x} \equiv w'(x) = 2G\log x \tag{4.35}$$

where G is the initial shear modulus.

Assume that strain potential satisfies Eq. (4.33). Note that chain rule for differentiation gives

$$\frac{\partial\Phi}{\partial\lambda_1} = \frac{\partial I_\mathbf{B}}{\partial\lambda_1}\frac{\partial\Phi}{\partial I_\mathbf{B}} + \frac{\partial II_\mathbf{B}}{\partial\lambda_1}\frac{\partial\Phi}{\partial II_\mathbf{B}}; \quad \frac{\partial\Phi}{\partial\lambda_2} = \frac{\partial I_\mathbf{B}}{\partial\lambda_2}\frac{\partial\Phi}{\partial I_\mathbf{B}} + \frac{\partial II_\mathbf{B}}{\partial\lambda_2}\frac{\partial\Phi}{\partial II_\mathbf{B}} \tag{4.36}$$

Solving Eq. (4.36), we can express $\partial\Phi/\partial I_\mathbf{B}$ and $\partial\Phi/\partial II_\mathbf{B}$ in terms of $\partial\Phi/\partial\lambda_1$. and $\partial\Phi/\partial\lambda_2$ as follows:

$$\frac{\partial\Phi}{\partial I_\mathbf{B}} = \frac{1}{D}\left(\frac{\partial II_\mathbf{B}}{\partial\lambda_2}\frac{\partial\Phi}{\partial\lambda_1} - \frac{\partial II_\mathbf{B}}{\partial\lambda_1}\frac{\partial\Phi}{\partial\lambda_2}\right); \quad \frac{\partial\Phi}{\partial II_\mathbf{B}} = -\frac{1}{D}\left(\frac{\partial I_\mathbf{B}}{\partial\lambda_2}\frac{\partial\Phi}{\partial\lambda_1} - \frac{\partial I_\mathbf{B}}{\partial\lambda_1}\frac{\partial\Phi}{\partial\lambda_2}\right) \tag{4.37}$$

where

$$D = \frac{\partial I_\mathbf{B}}{\partial\lambda_1}\frac{\partial II_\mathbf{B}}{\partial\lambda_2} - \frac{\partial I_\mathbf{B}}{\partial\lambda_2}\frac{\partial II_\mathbf{B}}{\partial\lambda_1} \tag{4.38}$$

Because of Eq. (3.40), substitution of Eq. (4.37) into Eq. (3.39) gives

$$\mathbf{T} = -p\mathbf{I} + \frac{2}{D}\left(\frac{\partial II_{\mathbf{B}}}{\partial \lambda_2}\frac{\partial \Phi}{\partial \lambda_1} - \frac{\partial II_{\mathbf{B}}}{\partial \lambda_1}\frac{\partial \Phi}{\partial \lambda_2}\right)\mathbf{B} + \frac{2}{D}\left(\frac{\partial I_{\mathbf{B}}}{\partial \lambda_2}\frac{\partial \Phi}{\partial \lambda_1} - \frac{\partial I_{\mathbf{B}}}{\partial \lambda_1}\frac{\partial \Phi}{\partial \lambda_2}\right)\mathbf{B}^{-1} \quad (4.39)$$

Note that the eigenvalues of $\mathbf{B}$ are λ_1^2, λ_2^2 and $\lambda_1^{-2}\lambda_2^{-2}$, those of $\mathbf{B}^{-1}$ are $\lambda_1^{-2}, \lambda_2^{-2}$ and $\lambda_1^2\lambda_2^2$ and

$$\frac{\partial \Phi}{\partial \lambda_1} = w'(\lambda_1) - \frac{\lambda_2}{\lambda_3^2}w'(\lambda_3); \quad \frac{\partial \Phi}{\partial \lambda_2} = w'(\lambda_2) - \frac{\lambda_1}{\lambda_3^2}w'(\lambda_3) \quad (4.40)$$

Since $\mathbf{B}$ and $\mathbf{B}^{-1}$ are coaxial, the eigenvalues of the stress are given by

$$\sigma_k = -p + \lambda_k \frac{\partial \Phi}{\partial \lambda_k} = -p + \lambda_k w'(\lambda_k) \ (k = 1, 2, \text{ and } 3, \text{no sum on } k) \quad (4.41)$$

where $\lambda_3 = \lambda_1^{-1}\lambda_2^{-1}$. This calculation requires tedious arithmetic manipulations. See Valanis and Landel (1967) and Rivlin and Sawyer (1976) for the details of the derivation. See problem (Dossin and Graessley 1979).

As for the uniaxial elongation along $\mathbf{e}_1$, the principal axes of $\mathbf{B}$ are $\mathbf{e}_1, \mathbf{e}_2$, and $\mathbf{e}_3$. As before, we know that $\sigma_2 = \sigma_3 = 0$ and $\lambda_2 = \lambda_3 = \lambda_1^{-1/2}$. Hence, we have

$$\sigma_1 = \lambda w'(\lambda) - \frac{1}{\sqrt{\lambda}}w'\left(\frac{1}{\sqrt{\lambda}}\right) \quad \text{with} \quad \lambda_1 = \lambda \quad (4.42)$$

The analogy of Eq. (4.29) gives

$$\sigma_E = w'(\lambda) - \frac{1}{\lambda\sqrt{\lambda}}w'\left(\frac{1}{\sqrt{\lambda}}\right) \quad (4.43)$$

Note that clarification of the mathematical form of $w'(\lambda)$ is the identification of the model based on the Valanis–Landel hypothesis. Hence, it can be said that the Valanis–Landel hypothesis is more convenient to determine strain potential from experimental data than the use of $\Phi(I_{\mathbf{B}}, II_{\mathbf{B}})$. One the other hand, the strain potential of the Valanis–Landel hypothesis is not more convenient than that of principal invariants in solving boundary problems of hyperelasticity because we need to know the change of principal axis of general deformation at every step of calculation.

4.3.3 Phenomenological Models of Hyperelasticity

Phenomenological models of hyperelasticity are the ones whose strain potentials are determined from experimental data with minimized number of material parameters. Since the Valanis–Landel hypothesis is very useful in the identification the strain potential from experiment, several authors have used the hypothesis to develop a

new strain potential. One of the most successful models is the *Ogden model* (Ogden 1972) which has the strain potential such that

$$\Phi = \sum_{k=1}^{n} \frac{\mu_k}{\alpha_k} \left(\lambda_1^{\alpha_k} + \lambda_2^{\alpha_k} + \lambda_3^{\alpha_k} - 3 \right) \quad \text{with} \quad \lambda_1 \lambda_2 \lambda_3 = 1 \tag{4.44}$$

It is usual that any set of experimental data can be fitted very accurately with $n \leq 3$. Ogden applied Eq. (4.44) to Treloar's data (1944) with $n = 3$, and the Ogden model fits three kinds of experimental data (uniaxial extension, pure shear, and equibiaxial tension) with a single set of parameters:

$$\begin{array}{lll} \alpha_1 = 1.3; & \alpha_2 = 5.0; & \alpha_3 = -2.0; \\ \mu_1 = 6.3\,\mathrm{kg/cm^2}; & \mu_1 = 0.012\,\mathrm{kg/cm^2}; & \mu_1 = -0.1\,\mathrm{kg/cm^2} \end{array} \tag{4.45}$$

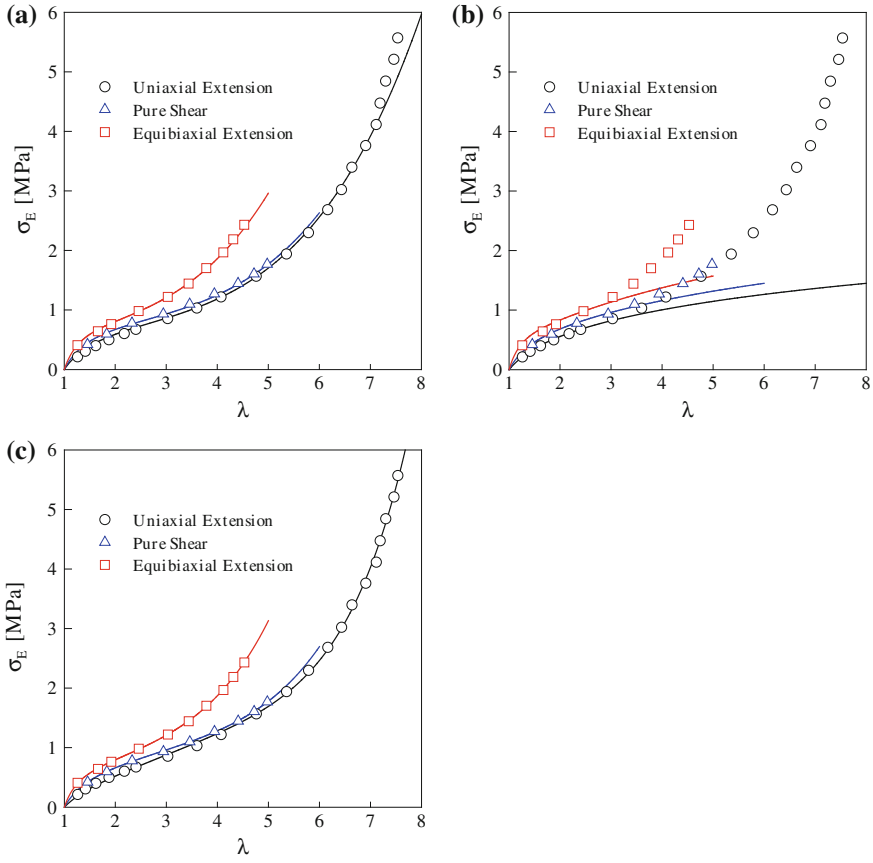

Fig. 12 Comparison of three hyperelastic models. The data were measured by Treloar (1944) and obtained by the digitalization of Fig. 4 of Ogden (1972). **a** Ogden model, **b** VL model, **c** BST model

The Ogden model needs 6 material parameters to fit Treloar's data (Fig. 12a), while the *Valanis–Landel model*, Eq. (4.35) of a single parameter cannot fit high extension regime. Blatz et al. (1974) proposed a four-parameter model which is based on generalized strain such that

$$\Phi = \frac{2G}{n} I_{\mathbf{E}} + B I_{\mathbf{E}}^{m} \tag{4.46}$$

where

$$I_{\mathbf{E}} = \mathrm{tr}(\mathbf{E}); \quad \mathbf{E} = \frac{1}{n}(\mathbf{B}^{n} - \mathbf{I}) \tag{4.47}$$

Note that when $\mathbf{b}_k$ are the normalized eigenvectors of $\mathbf{B}$, the generalized strain $\mathbf{E}$ is given by

$$\mathbf{E} = \frac{\lambda_1^{2n}}{n}\mathbf{b}_1\mathbf{b}_1 + \frac{\lambda_2^{2n}}{n}\mathbf{b}_2\mathbf{b}_2 + \frac{\lambda_3^{2n}}{n}\mathbf{b}_3\mathbf{b}_3 - \frac{1}{n}\mathbf{I} \tag{4.48}$$

Connecting with the single-chain statistics of finite chain length, Arruda and Boyce (1993) proposed the 8-chain model. Although the strain potential of the 8-chain model needs only two parameters, the model cannot fit the three homogeneous deformations by a single set of parameter values. It may be guessed the discrepancy is originated from that the strain potential is a function of only $I_{\mathbf{B}}$:

$$\Phi = \frac{G}{2}\left[(I_{\mathbf{B}} - 3) + \frac{1}{10N}\left(I_{\mathbf{B}}^2 - 3^2\right) + \frac{11}{525N^2}\left(I_{\mathbf{B}}^3 - 3^3\right) + \frac{19}{3500N^3}\left(I_{\mathbf{B}}^4 - 3^4\right) + \cdots\right] \tag{4.49}$$

We shall compare the Ogden, the Valanis–Landel (VL), and the Blatz, Sharda, and Tschoegl (BST) by use of Treloar's data (1944). In order to do that, we need the following:

[1] Uniaxial Extension

$$\lambda_1 = \lambda; \quad \lambda_2 = \lambda_3 = \frac{1}{\sqrt{\lambda}}; \tag{4.50a}$$

$$\sigma_E = \frac{\sigma_1}{\lambda}; \quad \sigma_2 = \sigma_3 = 0 \tag{4.50b}$$

The Ogden model

$$\sigma_E = \sum_{k=1}^{3} \mu_k \left(\lambda^{\alpha_k - 1} - \lambda^{-\frac{1}{2}\alpha_k - 1}\right) \tag{4.50c}$$

The VL model

$$\sigma_E = 2G\left(1 + \frac{1}{2\lambda\sqrt{\lambda}}\right)\log\lambda \tag{4.50d}$$

The BST model

$$\sigma_E = \left(\lambda^{n-1} - \lambda^{-\frac{1}{2}n-1}\right)\left(\frac{2G}{n} + mBI_{\mathbf{E}}^{m-1}\right) \tag{4.50e}$$

where

$$I_{\mathbf{E}} = \frac{\lambda^n + 2\lambda^{-\frac{1}{2}n} - 3}{n} \tag{4.50f}$$

[2] Pure Shear

$$\lambda_1 = \lambda; \quad \lambda_2 = 1; \quad \lambda_3 = \frac{1}{\lambda}; \tag{4.51a}$$

$$\sigma_E = \frac{\sigma_1}{\lambda}; \quad \sigma_3 = 0 \tag{4.51b}$$

The Ogden model

$$\sigma_E = \sum_{k=1}^{3} \mu_k\left(\lambda^{\alpha_k - 1} - \lambda^{-\alpha_k - 1}\right) \tag{4.51c}$$

The VL model

$$\sigma_E = 2G\left(1 + \frac{1}{\lambda^2}\right)\log\lambda \tag{4.51d}$$

The BST model

$$\sigma_E = \left(\lambda^{n-1} - \lambda^{-n-1}\right)\left(\frac{2G}{n} + mBI_{\mathbf{E}}^{m-1}\right) \tag{4.51e}$$

where

$$I_{\mathbf{E}} = \frac{\lambda^n + \lambda^{-n} - 2}{n} \tag{4.51f}$$

[3] Equibiaxial Extension

$$\lambda_1 = \lambda_2 = \lambda; \quad \lambda_3 = \frac{1}{\lambda^2}; \tag{4.52a}$$

$$\sigma_E = \frac{\sigma_1}{\lambda}; \quad \sigma_1 = \sigma_2; \quad \sigma_3 = 0 \tag{4.52b}$$

The Ogden model

$$\sigma_E = \sum_{k=1}^{3} \mu_k \left(\lambda^{\alpha_k - 1} - \lambda^{-2\alpha_k - 1}\right) \tag{4.52c}$$

The VL model

$$\sigma_E = 2G\left(1 + \frac{2}{\lambda^3}\right) \log \lambda \tag{4.52d}$$

The BST model

$$\sigma_E = \left(\lambda^{n-1} - \lambda^{-2n-1}\right)\left(\frac{2G}{n} + mBI_{\mathbf{E}}^{m-1}\right) \tag{4.52e}$$

where

$$I_{\mathbf{E}} = \frac{2\lambda^n + \lambda^{-2n} - 3}{n} \tag{4.52f}$$

Here, it is noteworthy that pure shear is different from simple shear because simple shear is the composition of rotation and pure shear which is extension in one direction and compression in the direction perpendicular to the direction of the extension.

As shown in Fig. 12, both the Ogden and the BST models fit experimental data very well, while the VL model has the limitation ($\lambda < 3$). Such limitation of the VL model seems to be originated from smaller number of material parameters compared to other models. The BST model is better than the Ogden model because it has smaller number of parameters and better quality of fitting. However, it is noteworthy that the mathematical form of the Ogden model is simpler than that of the BST model.

As for solving a boundary value problem, these three models require the calculation of principal axis at every calculation step because these models are based on principal axis. Strain potential of principal invariants is more convenient than the three models. However, it is rare to find such strain potential which can fit experimental data over wide range of extension.

Problems 4

[1] As for FENE model, the force vector on a single chain can be written as

$$\mathbf{f} = -\frac{\partial \phi(\mathbf{h}; N, b)}{\partial \mathbf{h}} \tag{4.a}$$

Find the potential $\phi(\mathbf{h}; N, b)$

[2] Derive the free energy of Eq. (4.17) by replacing the single-chain free energy of Eq. (4.15) by $\phi(\mathbf{h}; N, b)$ of the problem [1].

[3] Apply a simple shear $\mathbf{F} = \mathbf{I} + \gamma \mathbf{e}_1 \mathbf{e}_2$ to Eq. (4.18) and calculate the stress in terms of shear strain γ.

[4] Derive Eqs. (4.27), (4.28), and (4.29).

[5] Derive Eq. (4.41).

[6] As for strain potential of principal invariants, derive the principal stress components in terms of the derivatives of the strain potential with respect to $I_{\mathbf{B}}$ and $II_{\mathbf{B}}$ and extension ratios.

[7] Variational method for the determination of principal stress components
For incompressible elastic material, strain potential should satisfy

$$\left(\frac{\partial \Phi}{\partial \lambda_i} - f_i\right) \delta \lambda_i = 0 \tag{4.b}$$

subject to the incompressible condition $\delta(\lambda_1 \lambda_2 \lambda_3) = 0$. Then, the hydrostatic pressure p can be used as a Lagrangian multiplier. Here, the force f_i is related with principal components of stress by

$$f_i = \sigma_i \lambda_m \lambda_n \quad \text{with } i \neq m \neq n \tag{4.c}$$

Derive the following by using Lagrangian multiplier method:

$$\sigma_i = -p + \lambda_i \frac{\partial \Phi}{\partial \lambda_i} (\text{no sum on } i) \tag{4.d}$$

References

E.M. Arruda, M.C. Boyce, A three-dimensional constitutive model for the large stretch behavior of rubber elastic materials. J. Mech. Phys. Solids **41**, 389–412 (1993)

G.I. Barenblatt, Scaling, *Self-Similarity, and Intermediate Asymptotics: Dimensional Analysis and Intermediate Asymptotics* (Cambridge University Press, Cambridge, 1996)

R.B. Bird, C.F. Curtiss, R.C. Armstrong, O. Hassager, *Dynamics of Polymeric Liquids Vol. 2. Kinetic Theory* (Wiley, New York, 1987)

P.J. Blatz, S.C. Sharda, N.W. Tschoegl, Strain energy function for rubberlike materials based on a generalized measure of strain. Trans. Soc. Rheol. **18**, 145–161 (1974)

T.S. Chow, *Mesoscopic Physics of Complex Materials* (Springer, Berlin, 2000)

M. Doi, S.F. Edwards, *The Theory of Polymer Dynamics* (Oxford University Press, Oxford, 1986)
L.M. Dossin, W.W. Graessley, Rubber elasticity of well-characterized polybutadiene networks. Macromolecules **12**, 123–130 (1979)
E.-J. Donth, *Relaxation and Thermodynamics in Polymers* (Akademie Verlag, Berlin, 1992)
L.J. Fetters, D.J. Lohse, D. Richter, T.A. Witten, A. Zirkel, Connection between polymer molecular weight, density, chain dimensions, and melt viscoelastic properties. Macromolecules **27**, 4639–4647 (1994)
U.W. Gedde, *Polymer Physics* (Kluwer Academic Publishers, Berlin, 2001)
Y. Heo, R.G. Larson, Universal scaling of linear and nonlinear rheological properties of semidilute and concentrated polymer solutions. Macromolecules **41**, 8903–8915 (2008)
D.-J Kim, Study on rheological behavior of ABS and SAN under large amplitude oscillatory shear flow," MS thesis supervised by Prof. K. S. Cho, Kyungpook National University, 2007
M. Mooney, A theory of large elastic deformation. J. Appl. Phys. **11**, 582–592 (1940)
R.W. Ogden, Large deformation isotropic elasticity—on the correlation of theory and experiment for incompressible rubberlike solids. Proc. Roy. Soc. Lond. A. **326**, 565–584 (1972)
R.W. Ogden, *Non-linear Elastic Deformations* (Dover, Mineola, 1984)
R.W. Ogden, Recent advances in the phenomenological theory of rubber elasticity. Rubber Chem. Tech. **59**, 361–383 (1986)
R.S. Rivlin, Large elastic deformations of isotropic materials. I. Fundamental concepts. Phil. Trans. Roy. Soc. Lond. A **240**, 459–490 (1948)
R.S. Rivlin, K.N. Sawyer, The strain-energy function for elastomers. Trans. Soc. Rheol. **20**, 545–557 (1976)
M. Rubinstein, R.H. Colby, *Polymer Physics* (Oxford University Press, Oxford, 2003)
R.J. Silbey, R.A. Alberty, M.G. Bawendi, *Physical Chemistry*, 4th edn. (Wiley, New York, 2005)
L.H. Sperling, *Introduction to Physical Polymer Science*, 4th edn. (Wiley Interscience, New York, 2006)
G. Strobl, *The Physics of Polymers*, 2nd edn. (Springer, Berlin, 1997)
I. Teraoka, *Polymer Solutions* (Wiley-Interscience, New York, 2002)
L.T.G. Treloar, Stress-strain data for vulcanised rubber under various types of deformation. Trans. Faraday Soc. **40**, 59–70 (1944)
L.R.G. Treloar, *The Physics of Rubber Elasticity*, 3rd edn. (Clarendon Press, Oxford, 1975)
K.C. Valanis, R.F. Landel, The strain-energy function of a hyperelastic material in terms of the extension ratios. J. Appl. Phys. **38**, 2997–3002 (1967)
H. Yamakawa, *Modern Theory of Polymer Solutions* (Harper and Row, New York, 1971)
I.M. Ward, J. Sweeney, *An Introduction to Mechanical Properties of Solid Polymers,* 2nd edn. (Wiley, New York, 2004)

Part II
Linear Viscoelasticity

Chapter 5
Theory of Linear Viscoelasticity

Abstract This chapter mainly introduces theories of one-dimensional linear viscoelasticity based on Boltzmann superposition and the concept of linear response. The second section deals with measurement of linear viscoelasticity (experimental aspects), and the third section deals with phenomenological models such as spring–dashpot and parsimonious models. The last section is devoted to molecular theories of polymer viscoelasticity in linear regime.

For mathematical simplicity, we consider mainly one-dimensional case such as simple shear. If necessary, we shall provide three-dimensional extension. This chapter consists of phenomenological theory, linear viscoelastic measurements and data processing, phenomenological models, and molecular theories.

1 Fundamental Theory

Phenomenological theory, here, is the one that expresses mathematically the experimental observation without molecular considerations. Hence, the parameters of phenomenological theory of linear viscoelasticity cannot tell us their relations to molecular structure of polymers by the theory itself. However, experimental results for well-designed samples may give the relations. Although phenomenological theory cannot give detail information, it is more general and exact in some aspects that molecular theory because almost molecular theories are approximations derived from fundamental equations. Here, we shall study phenomenological theory of linear viscoelasticity that must be obeyed.

1.1 The Origin of Viscoelasticity

As mentioned in the head of Sect. 3 in Chap. 2, viscoelastic material can be defined as the one whose stress depends on deformation history: both deformation path and

K.S. Cho, *Viscoelasticity of Polymers*, Springer Series
in Materials Science 241, DOI 10.1007/978-94-017-7564-9_5

deformation rate. Hence, this definition allows the set of viscoelastic materials to include elastic bodies, viscous fluids, and elastoplastic materials as special subsets. Consider only materials which do not belong to such special subsets.

It is found that polymeric materials show time-dependent stress when a given strain is given as $\gamma(t) = \gamma_o \Theta(t)$ where $\Theta(t)$ is the unit step function defined in Eq. (3.79) in Chap. 2 and γ_o is a constant. From experience, we know that stress is a monotonically decreasing function of time for any value of γ_o. What is the origin of this phenomenon?

We have seen that stress is a functional of the configuration of molecules in Sect. 2.3 in Chap. 3 (see Eq. 2.118 in Chap. 3). As for constant strain of $\gamma_o \Theta(t)$, it is expected that the material goes to an equilibrium state complying the constant strain. This implies the configuration of molecules changes to the equilibrium configuration. If the characteristic time needed for the new equilibrium, λ, is much shorter than the observation time, t_{obs}, then the stress looks like a constant. If the characteristic time is sufficiently longer than the observation time, then time-dependent stress is observed. We define the *Deborah number* such that

$$\mathrm{De} = \frac{\lambda}{t_{obs}} \tag{1.1}$$

It is the ratio of material-dependent time to the minimum time for detecting a rheological phenomenon. The extreme case that $\mathrm{De} \to 0$ corresponds to elastic and viscous materials because elastic material shows nonzero constant stress, while viscous fluid shows zero stress. Then, it can be said that both elastic and viscous materials are the limiting cases of viscoelastic materials.

For the strain of $\gamma(t) = \gamma_o \Theta(t)$, stress response of viscoelastic material $\sigma(t)$ is a decreasing function of time and experimental results let us know that

$$\lim_{t \to \infty} \sigma(t, \gamma_o) = \begin{cases} \sigma_\infty(\gamma_o) = 0 & \text{for fluid} \\ \sigma_\infty(\gamma_o) > 0 & \text{for solid} \end{cases} \tag{1.2}$$

Equation (1.2) is a classification of solid and fluid. Then, we can express the stress formally as follows:

$$\sigma(t,\ \gamma_o) = [\sigma_o(\gamma_o)\, \phi_\lambda(t) + \sigma_\infty(\gamma_o)]\, \Theta(t) \tag{1.3}$$

where

$$\frac{d\phi_\lambda}{dt} \le 0\,; \quad \phi_\lambda(0) = 1\,; \quad \lim_{t \to \infty} \phi_\lambda(t) = 0\,; \quad \sigma(0, \gamma_o) = \sigma_o(\gamma_o) + \sigma_\infty(\gamma_o) \tag{1.4}$$

The subscript λ indicates that whenever $t \gg \lambda$, $\phi_\lambda(t) \approx 0$. Equation (1.3) includes the stress behavior of elastic, viscous, and narrow-meaning viscoelastic materials when strain is given by $\gamma(t) = \gamma_o \Theta(t)$. A representative example of $\phi_\lambda(t)$ may be $\exp(-t/\lambda)$. From this viewpoint, viscous fluid is the limiting case that $\lambda \to 0$ and $\sigma_\infty(\gamma_o) = 0$ and elastic solid is the limiting case that $\lambda \to \infty$ and $\sigma_\infty(\gamma_o) > 0$. This

picture means that De $\to 0$ makes viscoelastic material look like viscous fluid and De $\to \infty$ makes viscoelastic material look like elastic solid. This is the key point of the *Pipkin diagram* (Pipkin 1972). The Pipkin picture looks like contradiction to the aforementioned statement that De $\to 0$ gives both viscous and elastic materials. The characteristic time λ of the Pipkin picture is called relaxation time.

A concrete example of elastic solids is crystalline of atoms. Only nearest neighbor atoms interact through harmonic potential. As a toy model, consider one-dimensional array of atoms connected with harmonic potential. Long-wavelength approximation of this discrete system gives linear elastic materials (Kardar 2007). In this model, $\gamma(t) = \gamma_o \Theta(t)$ gives rise to wave of displacement of atoms from the original equilibrium positions. The propagation speed of the wave can be estimated by the sonic speed c. Then, the characteristic time for new equilibrium can be estimated by $\lambda = L/c$ where L is the linear dimension of elastic solid. When $t < L/c$, the wave propagation makes stress fluctuate, and when $t > L/c$, the kinetic energy and potential energy of each atom become equal (equipartition of energy), and neglecting fast oscillation around new equilibrium positions of atoms, we observe that macroscopic stress field is uniform over the whole specimen (Toda 1988). Although equipartition of energy is not found in one-dimensional crystal with harmonic potential, it is believed that equipartition of energy appears in three-dimensional harmonic lattice (Toda 1988). Then, we can modify the function $\phi_\lambda(t)$ as the one that behaves like a bounded wave packet when $0 < t \ll \lambda$ and $\phi_\lambda(t) \approx 0$ for $t > \lambda$. Then, observed equilibrium stress becomes $\sigma_\infty(\gamma_o)$. Here, we need to distinguish the characteristic time $\lambda = L/c$ from the relaxation time. In this picture, $\sigma_o(\gamma_o)$ cannot be defined clearly because it includes fluctuating nature of microstate (see Chap. 3). Since rheology is a macroscopic theory of physics, we will follow mainly the Pipkin picture.

In summary, most materials are viscoelastic and limiting cases are elastic and viscous materials.

1.2 The Boltzmann Superposition Principle

We can give a stimulus to a system in order to understand the structure of the system through the analysis of the response of the system. Here, we consider only linear systems which have a linear relation between the stimulus and the response of the system.

Both strain $\gamma(t)$ and stress $\sigma(t)$ can be used as stimulation for a rheological system. Both quantities are considered as functions of time t. When strain is given as a stimulus, stress is measured as the response and vice versa. The relation between stress and strain can be expressed formally by

$$\sigma(t) = \top[\gamma(t)] \tag{1.5}$$

where $\top[\gamma(t)]$ represents a suitable functional because both stress and strain are functions of time. Since we consider only linear rheological systems, the functional must satisfy the following for any real numbers and functions of time:

$$\top[\alpha\gamma_1(t)+\beta\gamma_2(t)] = \alpha\top[\gamma_1(t)]+\beta\top[\gamma_2(t)] \tag{1.6}$$

To identify the linear viscoelastic system, we need to express any strain function as

$$\gamma(t) = \int_{-\infty}^{t} \frac{\mathrm{d}\gamma(\tau)}{\mathrm{d}\tau}\Theta(t-\tau)\,\mathrm{d}\tau \tag{1.7}$$

where it is assumed that $\gamma(-\infty)=0$. Since integration is a summation over infinitely many terms indexed by the dummy variable of the integration, substitution of Eq. (1.7) into Eq. (1.5) gives

$$\sigma(t) = \int_{-\infty}^{t} G(t-\tau)\frac{\mathrm{d}\gamma}{\mathrm{d}\tau}\mathrm{d}\tau \tag{1.8}$$

where

$$G(t) = \top[\Theta(t)] \tag{1.9}$$

Note that the functional $\top[\bullet]$ maps a function of τ to a function of t as shown in Eq. (1.8). The linearity of the functional results in Eq. (1.8). Equation (1.8) is the *Boltzmann superposition principle*.

The function $G(t)$ represents the response of the rheological system, which can be determined by the measurement of the response driven by the stimulation of the unit step function. Since strain is used as the stimulation, the dimension of the response function $G(t)$ is that of modulus. Hence, we call $G(t)$ *relaxation modulus*. Relaxation modulus can be determined experimentally by the use of strain of $\gamma(t)=\gamma_o\Theta(t)$. This experiment is called *stress relaxation test.* However, it must be noticed that Eq. (1.8) is valid for any strain although relaxation modulus is determined by the strain of the unit step function.

It must be recognized that the response function $G(t)$ is a monotonic decreasing function of time such that

$$\frac{\mathrm{d}G}{\mathrm{d}t} \le 0 \quad \text{for any } t \tag{1.10}$$

Consider the case that $\gamma(t)=\gamma_o\Theta(t)$ where γ_o is a constant. Substitution of this function of time into Eq. (1.5) gives

$$\sigma(t) = \gamma_o G(t) \tag{1.11}$$

If $dG/dt > 0$ for any time, even an infinitesimally small strain makes the material break because at constant strain stress increases infinitely. Thus, the function $G(t)$ must be bounded:

$$0 \leq G(t) \leq G_{\max} \tag{1.12}$$

The lower bound of zero is needed because it cannot be imagined that the direction of stress is reverse to that of strain. If $G(0^+) < G_{\max}$, then there must exist an interval of time. Assume that the material breaks at $\sigma > \sigma_B$. Then, we can adjust strain amplitude γ_o to make $\gamma_o G_{\max}$ be larger than the breaking stress σ_B. This allows an impossible situation that at constant strain, the material breaks after the time $t_{\max}$ at which $G(t_{\max}) = G_{\max}$. Hence, we can conclude that

$$\frac{dG}{dt} \leq 0\,; \quad G(t) \geq 0 \quad \text{for any } t > 0 \tag{1.13}$$

Since elastic material has stress as a function of current strain, constant strain implies constant stress. Then, it is obvious that the relaxation modulus of elastic material is a positive constant. Since the stress of Newtonian fluid is linearly proportional to strain rate, Eq. (1.8) implies that the relaxation modulus is proportional to the Dirac delta function. Definition of solid and fluid in Eq. (1.2) gives

$$\lim_{t \to \infty} G(t) \geq 0 \tag{1.14}$$

Since relaxation modulus is a monotonic decreasing function of time, Eq. (1.8) implies that the strain given at far past gives smaller effect on current stress than that given at near past. Because of the *principle of causality*, we can say that strain to be given at future cannot influence current stress. Then, we can impose additional condition on the mathematical form of relaxation modulus:

$$G(t) = \begin{cases} G(t) \geq 0 & t \geq 0 \\ 0 & t < 0 \end{cases} \tag{1.15}$$

Then formally, relaxation modulus can be expressed formally as follows:

$$G(t) = [G_\infty + (G_o - G_\infty)\,\phi(t)]\,\Theta(t) \tag{1.16}$$

where

$$\phi(t) \geq 0\,; \quad \phi(0) = 1\,; \quad \lim_{t \to \infty} \phi(t) = 0\,; \quad \frac{d\phi}{dt} \leq 0 \tag{1.17}$$

and $G_o > G_\infty \geq 0$ and $G_\infty = 0$ for fluid and $G_\infty > 0$ for solid, respectively. Note that $\phi(t)$ is a dimensionless function.

Similarly, we can apply the same reasoning to the case that stress is given and strain is measured. Then, the Boltzmann superposition is expressed by

$$\gamma(t) = \int_{-\infty}^{t} J(t-\tau)\frac{\mathrm{d}\sigma}{\mathrm{d}\tau}\mathrm{d}\tau \tag{1.18}$$

where the response function $J(t)$ is called *creep compliance* and

$$J(t) = \top^{-1}[\Theta(t)] \tag{1.19}$$

Creep compliance can be determined by the experiment which uses stress input of $\sigma(t) = \sigma_o\Theta(t)$. Such experiment is called *creep test*.

Experimental observation tells us that creep compliance is a monotonically increasing function of time. Then, we know that

$$J(t) = \begin{cases} J(t) \geq 0 & t \geq 0 \\ 0 & t < 0 \end{cases}; \quad \frac{\mathrm{d}J}{\mathrm{d}t} \geq 0 \text{ for } t > 0 \tag{1.20}$$

Equation (1.20) includes the principle of causality, too.

Note that the functional $\top^{-1}[\bullet]$ is the mapping from stress to strain and it is the inverse of $\top[\bullet]$. Then, it can be said that when strain is given by $\gamma(t) = J(t)\,\Theta(t)$, stress must be the unit step function:

$$\Theta(t) = \int_{-\infty}^{t} G(t-\tau)\frac{\mathrm{d}J(\tau)}{\mathrm{d}\tau}\mathrm{d}\tau \tag{1.21}$$

Because of the principle of causality, $\mathrm{d}J/\mathrm{d}\tau = 0$ for $\tau < 0$. Then, Eq. (1.21) can be rewritten by

$$\Theta(t) = \int_{0}^{t} G(t-\tau)\frac{\mathrm{d}J}{\mathrm{d}\tau}\mathrm{d}\tau \tag{1.22}$$

The right-hand side is the convolution of relaxation modulus and the derivative of creep compliance. Application of Laplace transform gives

$$\widetilde{G}(s)\,\widetilde{J}(s) = \frac{1}{s^2} \tag{1.23}$$

and

$$\int_{0}^{t} G(t-\tau)\,J(\tau)\,\mathrm{d}\tau = \int_{0}^{t} G(\tau)\,J(t-\tau)\,\mathrm{d}\tau = t \tag{1.24}$$

We now can derive mathematical form of creep compliance from the formal expression of relaxation modulus. Application of Eq. (1.16)–(1.23) gives

$$s\widetilde{J}(s) = \frac{1}{G_\infty + (G_\mathrm{o} - G_\infty)\, s\, \widetilde{\phi}(s)} \tag{1.25}$$

The initial value theorem of Laplace transform (see Problem 6, Baumgärtel et al. 1990) gives

$$J(0^+) = \lim_{s\to\infty} \frac{1}{G_\infty + (G_\mathrm{o} - G_\infty)\, s\, \widetilde{\phi}(s)} = \frac{1}{G_\mathrm{o}} \tag{1.26}$$

Here, we used

$$\phi(0^+) = \lim_{s\to\infty} s\, \widetilde{\phi}(s) = 1 \tag{1.27}$$

The *final value theorem of Laplace transform* (see Problem 6, Baumgärtel et al. 1990) gives

$$\lim_{t\to\infty} J(t) = \lim_{s\to 0} \frac{1}{G_\infty + (G_\mathrm{o} - G_\infty)\, s\, \widetilde{\phi}(s)} = \frac{1}{G_\infty} \tag{1.28}$$

Here, we used

$$\lim_{t\to\infty} \phi(t) = \lim_{s\to 0} s\, \widetilde{\phi}(s) = 0 \tag{1.29}$$

Equation (1.28) implies that the creep compliance of fluid becomes infinite because fully relaxed modulus of fluid is zero: $G_\infty = 0$. Hence, we are interested in the asymptotic behavior of $\mathrm{d}J/\mathrm{d}t$. Applying the final value theorem of Laplace transform to the Laplace transform of $\mathrm{d}J/\mathrm{d}t$, we have

$$\lim_{t\to\infty} \frac{\mathrm{d}J}{\mathrm{d}t} = \lim_{s\to 0} s\left[s\widetilde{J}(s) - J(0^+)\right] = \begin{cases} \frac{1}{G_\mathrm{o}\widetilde{\phi}(0)} & \text{for fluid} \\ 0 & \text{for solid} \end{cases} \tag{1.30}$$

Note that

$$\widetilde{\phi}(0) = \int_0^\infty \phi(t)\, \mathrm{d}t = \frac{1}{G_\mathrm{o} - G_\infty} \int_0^\infty [G(t) - G_\infty]\, \mathrm{d}t > 0 \tag{1.31}$$

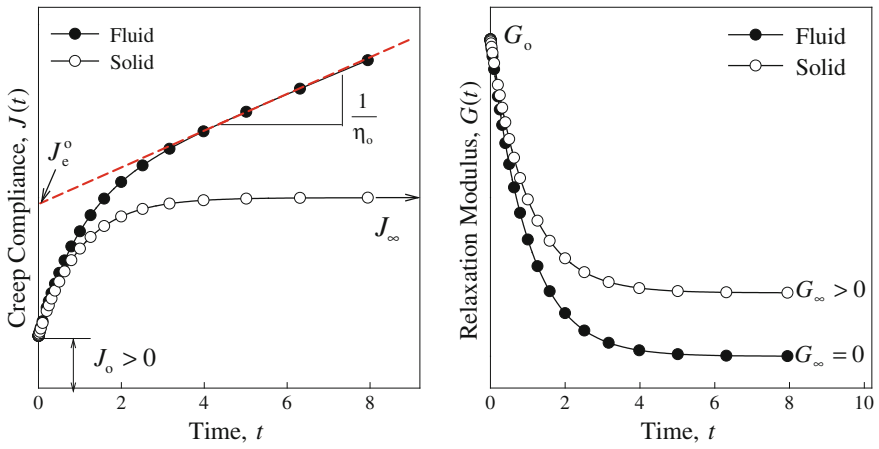

Fig. 1 Schematic illustration of viscoelastic fluid and solid

Since $\widetilde{\phi}(0)$ is a positive constant, it can be said that for viscoelastic fluid, we know that

$$J(t) \propto t \quad \text{for large } t \tag{1.32}$$

Figure 1 shows a schematic illustration of viscoelastic fluid and solid in terms of creep compliance and relaxation modulus.

Since creep compliance is an increasing function of time, we can formally express the creep compliance as follows:

$$J(t) = \begin{cases} \left[\frac{1}{G_o} + J_r\Psi(t) + \frac{t}{\eta_o}\right]\Theta(t) & \text{for fluid} \\ \left[\frac{1}{G_o} + J_r\Psi(t)\right]\Theta(t) & \text{for solid} \end{cases} \tag{1.33}$$

where dimensionless function $\Psi(t)$ satisfies

$$\Psi(0) = 0\,; \quad \lim_{t\to\infty}\Psi(t) = 1\,; \quad \frac{d\Psi}{dt} \geq 0 \tag{1.34}$$

As for solid, it is obvious that

$$\frac{1}{G_\infty} = \frac{1}{G_o} + J_r \tag{1.35}$$

As for fluid, asymptotic equation for creep compliance is given by

$$J(t) = J_e^o + \frac{t}{\eta_o} \quad \text{for large } t \tag{1.36}$$

The *steady-state compliance* J_e^o is related to J_r by

$$J_e^o = \frac{1}{G_o} + J_r \tag{1.37}$$

In Eq. (1.33), we introduced a new quantity called the *zero-shear viscosity*:

$$\eta_o = G_o \int_0^\infty \phi(t)\,dt \tag{1.38}$$

Since the zero-shear viscosity appears in viscoelastic fluid, Eq. (1.38) can be rewritten by

$$\eta_o = \int_0^\infty G(t)\,dt \tag{1.39}$$

1.3 Dynamic Experiment

Both stress relaxation and creep tests are called static experiment because stimulation is constant for $t > 0$. Static experiments are not easy to implement because we cannot generate the unit step function perfectly. On the other hand, it is experimentally easy to generate sinusoidal stimulation. Such experiment is called dynamic experiment. If we can generate sinusoidal stimulation without any limitation of frequency, then the response function from dynamic test is more accurate than that from static experiment. It is because the response functions from static experiments are not reliable at short-time regime in which implementation of the unit step function is not exact.

For simplicity, we consider only the case of $G_\infty = 0$. The case of $G_\infty > 0$ can be easily recovered if replacing $G(t)$ by $G(t) - G_\infty$ in the following equations. See Problems 1.

Consider strain can be generated by $\gamma(t) = \gamma_o \sin \omega t$ where γ_o is the strain amplitude and ω is the angular frequency. Then, the Boltzmann superposition principle gives

$$\sigma(t) = \gamma_o \omega \int_{-\infty}^{t} G(t-\tau)\cos \omega\tau\,d\tau \tag{1.40}$$

Changing variable by $\xi = t - \tau$ and using formula of trigonometric functions, we have

$$\sigma(t) = G'(\omega)\,\gamma(t) + \eta'(\omega)\,\dot{\gamma}(t) \tag{1.41}$$

where $\gamma(t) = \gamma_o \sin \omega t$, $\dot{\gamma}(t) = d\gamma/dt$, and

$$G'(\omega) \equiv \omega \int_0^\infty G(t) \sin \omega t \, dt; \quad \eta'(\omega) \equiv \int_0^\infty G(t) \cos \omega t \, dt \tag{1.42}$$

If $G'(\omega) = 0$, then Eq. (1.41) is analogous to the constitutive equation of viscous fluid because $\sigma(t) = \eta'(\omega)\,\dot{\gamma}(t)$. If $\eta'(\omega) = 0$, then Eq. (1.41) is analogous to the constitutive equation of elastic solid because $\sigma(t) = G'(\omega)\,\gamma(t)$. Elastic solid stores energy, while viscous fluid dissipates mechanical energy. Hence, $G'(\omega)$ is called *storage modulus*, and *loss modulus* is defined by

$$G''(\omega) = \omega\eta'(\omega) = \omega \int_0^\infty G(t) \cos \omega t \, dt \tag{1.43}$$

Both storage and loss moduli are called *dynamic moduli*. Note that Eq. (1.41) holds for strain of $\gamma(t) = \gamma_o \sin(\omega t + \phi)$ for any real number ϕ:

$$\sigma(t) = G'(\omega)\,\gamma(t) + \frac{G''(\omega)}{\omega}\frac{d\gamma}{dt} \tag{1.44}$$

In summary, storage modulus represents elastic characteristics of viscoelastic material, while loss modulus represents viscous characteristics.

1.3.1 Complex Notation

Every measurable quantity is real number. However, the use of complex numbers is very convenient in the description of the results of dynamic tests. Adopting complex strain such as $\gamma^*(t) = \gamma_o \exp(i\omega t)$, Eq. (1.8) can be rewritten by

$$\sigma^*(t) = i\omega\gamma_o \int_{-\infty}^{t} G(t-\tau)\, e^{i\omega\tau} d\tau = G^*(\omega)\,\gamma^*(t) \tag{1.45}$$

where complex modulus $G^*(\omega)$ is defined as

$$G^*(\omega) \equiv i\omega \int_0^\infty G(t)\, e^{-i\omega t} dt \tag{1.46}$$

Applying Euler's formula such as $e^{i\theta} = \cos\theta + i\sin\theta$, Eq. (1.46) can be rewritten by

$$G^*(\omega) = G'(\omega) + iG''(\omega) \tag{1.47}$$

Since $d\gamma^*/dt = i\omega\gamma^*(t)$, Eq. (1.45) can be rewritten by

$$\sigma^*(\omega) = \eta^*(\omega)\frac{d\gamma^*(t)}{dt} \tag{1.48}$$

where complex viscosity is defined by

$$\eta^*(\omega) = \frac{G^*(\omega)}{i\omega} \tag{1.49}$$

The immediate consequences of Eq. (1.49) are

$$\eta'(\omega) \equiv \frac{G''(\omega)}{\omega}; \quad \eta''(\omega) \equiv \frac{G'(\omega)}{\omega} \tag{1.50}$$

If we replace $i\omega$ by s, then Eq. (1.46) can be rewritten in terms of Laplace transform:

$$G^*(\omega) = \left[s\widetilde{G}(s)\right]_{s=i\omega} \tag{1.51}$$

As for Eq. (1.49), we have

$$\eta^*(\omega) = \widetilde{G}(i\omega) \tag{1.52}$$

From the properties of relaxation modulus, we know that there exists the Fourier transform of relaxation modulus. The principle of causality gives

$$\hat{G}(\omega) = \int_{-\infty}^{\infty} G(t)\, e^{-i\omega t} dt = \int_{0}^{\infty} G(t)\, e^{-i\omega t} dt = \widetilde{G}(i\omega) = \eta^*(\omega) \tag{1.53}$$

Then, replacement of $\chi'(\omega)$ and $\chi''(\omega)$ of Eq. (6.44) in Chap. 1 by $\eta'(\omega)$ and $\eta''(\omega)$, respectively, gives

$$G(t) = \frac{2}{\pi}\int_{0}^{\infty} \eta'(\omega)\, \cos\omega t\, d\omega = \frac{2}{\pi}\int_{0}^{\infty} \eta''(\omega)\, \sin\omega t\, d\omega \tag{1.54}$$

This is the consequence from the inverse Fourier transform of complex viscosity. See Sect. 6 in Chap. 1.

Equation (1.54) says that relaxation modulus can be determined by the measurement of dynamic moduli. On the other hand, Eqs. (1.42) and (1.43) imply that the measurement of relaxation modulus allows us to determine dynamic moduli. Therefore, these equations show that dynamic experiment is equivalent to static experiments. However, the use of Eqs. (1.42), (1.43), and (1.54) is not effective because experimental data are obtained in a finite range of time or frequency.

If we apply $\sigma^*(t) = \sigma_o \exp(i\omega t)$ to Eq. (1.18), then we can define complex compliances such that

$$J^*(\omega) = i\omega \int_0^\infty J(t)\, e^{-i\omega t} dt \tag{1.55}$$

Since $J(t)$ is an increasing function of time, it is difficult to complex compliance by the use of Eq. (1.55) directly. Analogy to Laplace transform is easier:

$$J^*(\omega) = \left\lfloor s\widetilde{J}(s) \right\rfloor_{s=i\omega} \tag{1.56}$$

With the help of Eq. (1.23), it is easy to derive

$$J^*(\omega) = \frac{1}{G^*(\omega)} \tag{1.57}$$

Analogous to dynamic moduli, we define storage and loss compliances as the real and imaginary parts of complex compliance:

$$J^*(\omega) = J'(\omega) - iJ''(\omega) \tag{1.58}$$

Then, we have the relations:

$$J'(\omega) = \frac{G'(\omega)}{[G'(\omega)]^2 + [G''(\omega)]^2}; \quad J''(\omega) = \frac{G''(\omega)}{[G'(\omega)]^2 + [G''(\omega)]^2} \tag{1.59}$$

1.3.2 Terminal Behavior

When frequency is extremely low, we can use the approximations such that

$$\sin \omega t \approx \omega t; \quad \cos \omega t \approx 1 \tag{1.60}$$

Then, dynamic moduli are approximated at extremely low frequencies as follows:

$$G'(\omega) \approx \omega^2 \int_0^t tG(t)\, dt; \quad G''(\omega) \approx \eta_o \omega \tag{1.61}$$

Here, we used Eq. (1.39). Equation (1.61) implies

$$\int_0^t tG(t)\,\mathrm{d}t = \lim_{\omega\to 0}\frac{G'(\omega)}{\omega^2};\quad \int_0^t G(t)\,\mathrm{d}t = \lim_{\omega\to 0}\frac{G''(\omega)}{\omega} \tag{1.62}$$

As for dynamic compliances, we have

$$\lim_{\omega\to 0} J'(\omega) = \frac{1}{\eta_o^2}\int_0^\infty tG(t)\,\mathrm{d}t;\quad \lim_{\omega\to 0}\frac{1}{\omega J''(\omega)} = \eta_o \tag{1.63}$$

As for dynamic viscosities, we have

$$\lim_{\omega\to 0}\eta'(\omega) = \eta_o;\quad \lim_{\omega\to 0}\frac{\eta''(\omega)}{\omega} = \int_0^t tG(t)\,\mathrm{d}t \tag{1.64}$$

Note that all these equations hold when $G_\infty = 0$.

Asymptotic behavior (Eq. 1.36) gives the Laplace transforms of creep compliance and relaxation modulus as follows:

$$s\widetilde{J}(s) = J_e^o + \frac{1}{\eta_o s};\quad s\widetilde{G}(s) = \frac{\eta_o s}{1 + J_e^o\eta_o s} \tag{1.65}$$

Then, we have asymptotic dynamic moduli:

$$G'(\omega) = \frac{J_e^o\eta_o^2\omega^2}{1 + \left(J_e^o\eta_o\omega\right)^2};\quad G'(\omega) = \frac{\eta_o\omega}{1 + \left(J_e^o\eta_o\omega\right)^2} \tag{1.66}$$

It is interesting that dynamic moduli of Eq. (1.66) are those of the Maxwell model such that $G_o = 1/J_e^o$ and $\lambda_o = J_e^o\eta_o$. Dynamic moduli of Eq. (1.66) give the following terminal behavior:

$$\int_0^t tG(t)\,\mathrm{d}t = J_e^o\eta_o^2;\quad \int_0^t G(t)\,\mathrm{d}t = \eta_o \tag{1.67}$$

Note that the asymptotic behavior is the result from neglecting detailed behavior at low-frequency regime.

Equation (1.67) allows us to define *mean relaxation time* $\overline{\lambda}$ as follows:

$$\overline{\lambda} = J_e^o\eta_o = \frac{\int_0^t tG(t)\,\mathrm{d}t}{\int_0^t G(t)\,\mathrm{d}t} \tag{1.68}$$

Equation (1.68) illustrates the reason why we call $J_e^o \eta_o$ mean relaxation time. This is the characteristic time scale of stress relaxation.

1.4 The Kramers–Kronig Relations

Storage and loss moduli can be calculated from relaxation modulus as shown in Eqs. (1.42) and (1.43). Therefore, storage modulus is not independent of loss modulus. The *Kramers–Kronig relations* allow us to calculate storage modulus from loss modulus and vice versa. The relations were originally derived by the use of Cauchy's residue theorem for complex integration. However, we shall use Laplace transform in order to minimize the knowledge of complex analysis.

We start from Eq. (1.54). Taking Laplace transform on both sides of Eq. (1.54), we have

$$s\widetilde{G}(s) = \frac{2}{\pi}\int_0^\infty G'(w)\frac{s}{s^2+w^2}\mathrm{d}w \tag{1.69}$$

and

$$s\widetilde{G}(s) = \frac{2}{\pi}\int_0^\infty \frac{G''(w)}{w}\frac{s^2}{s^2+w^2}\mathrm{d}w \tag{1.70}$$

Note that complex notation for dynamic moduli gives

$$G'(\omega) = \mathrm{Re}\left\{\mathrm{i}\omega\widetilde{G}(\mathrm{i}\omega)\right\}; \quad G''(\omega) = \mathrm{Im}\left\{\mathrm{i}\omega\widetilde{G}(\mathrm{i}\omega)\right\} \tag{1.71}$$

Then, we replace s by $\mathrm{i}\omega$ and obtain

$$G'(\omega) = \frac{2\omega^2}{\pi}\int_0^\infty \frac{G''(w)/w}{\omega^2-w^2}\mathrm{d}w; \quad G''(w) = \frac{2\omega}{\pi}\int_0^\infty \frac{G'(\omega)}{w^2-\omega^2}\mathrm{d}w \tag{1.72}$$

or

$$\eta'(\omega) = \frac{2}{\pi}\int_0^\infty \frac{w\eta''(w)}{w^2-\omega^2}\mathrm{d}w; \quad \eta''(\omega) = \frac{2\omega}{\pi}\int_0^\infty \frac{\eta'(w)}{\omega^2-w^2}\mathrm{d}w \tag{1.73}$$

Since both storage and loss moduli are simultaneously measured in dynamic experiment, the Kramers–Kronig relations are not frequently used. Hence, in usual case, it is not necessary to determine one dynamic modulus from the data of the other dynamic modulus. However, as for reactive systems such as polymer under curing reaction, one of the dynamic moduli is not precisely measured because the

material undergoes transition from fluid to solid. If solid-like feature is stronger than fluid-like feature, then storage modulus is more precisely measured than loss modulus and vice versa. However, since the frequency range of such experiment is very narrow, direct use of Eq. (1.72) is not effective. Booij and Thoone (1982) invented an effective approximation of the Kramers–Kronig relations.

1.5 Thermodynamic Analysis

As for elastic solid, thermodynamic state can be described by strain. Since stress is determined by the current strain, the work is a function of strain. As shown in Eqs. (4.65) and (4.72) in Chap. 2, no heat flux gives no entropy production in elastic solid. On the other hand, Eqs. (4.58) and (4.71) in Chap. 2 imply that viscous fluid can generate entropy production without heat flux. Without heat flux, the temperature Eq. (4.104) in Chap. 2 becomes

$$\rho c_V \frac{\mathrm{d}T}{\mathrm{d}t} = \mathbf{T} : \mathbf{D} + \rho T^2 \frac{\partial}{\partial T}\left[\frac{1}{T}\left(\frac{\mathrm{d}f}{\mathrm{d}t}\right)_T\right] \tag{1.75}$$

As for elastic body, the right-hand side is canceled. Hence, no temperature rise occurs in elastic body without heat transfer. As for viscous fluid, $f = f(\rho,\ T)$ and

$$\left(\frac{\mathrm{d}f}{\mathrm{d}t}\right)_T = \left(\frac{\partial f}{\partial \rho}\right)_T \frac{\mathrm{d}\rho}{\mathrm{d}t} = \frac{\nabla \cdot \mathbf{v}}{\rho}\left(\frac{\partial f}{\partial v}\right)_T = -\frac{p\,(\nabla \cdot \mathbf{v})}{\rho} \tag{1.76}$$

Substitution of Eq. (1.76) to Eq. (1.75) gives

$$\rho c_V \frac{\mathrm{d}T}{\mathrm{d}t} = 2\eta_s \mathbf{D}' : \mathbf{D}' + \eta_b (\nabla \cdot \mathbf{v})^2 - \rho T \frac{\partial}{\partial T}\left(\frac{p}{\rho}\right) \tag{1.77}$$

where the constitutive equation of Newtonian fluid, Eq. (3.43), in Chap. 2 was used. Thus, flow induces temperature rise of the viscous fluid. In summary, it can be said that the work given to elastic body cannot be transformed to heat without heat flux, while the work given to viscous fluid is transformed to heat without heat flux.

Then, we can guess that if we can decompose the work given to viscoelastic material to elastic and viscous parts, then the partial work due to viscous stress is transformed to heat. It is practically impossible to do such decomposition for general deformation processes. However, in linear viscoelasticity, the use of Eq. (1.44) gives

$$W = \int_0^t \sigma(t')\frac{\mathrm{d}\gamma}{\mathrm{d}t'}\mathrm{d}t' = \frac{G'(\omega)}{2}\left[\gamma^2(t) - \gamma^2(0)\right] + \frac{G''(\omega)}{\omega}\int_0^t \left(\frac{\mathrm{d}\gamma}{\mathrm{d}t'}\right)^2 \mathrm{d}t' \tag{1.78}$$

The first term can be considered as the strain energy potential whose modulus is storage modulus, and the second term is not negative for any time. If t is the period of strain $t = 2\pi/\omega$, then the elastic term disappears and the viscous term is given by

$$W\left(\frac{2\pi}{\omega}\right) = \pi G''(\omega)\,\gamma_o^2 \tag{1.79}$$

The above analysis tells us that elastic energy stored in the material can be represented by $G'(\omega)$ and energy dissipation by $G''(\omega)$. Then, we can define the ratio of loss of energy to stored energy by

$$\tan\delta(\omega) = \frac{G''(\omega)}{G'(\omega)} \tag{1.80}$$

It is called *loss tangent*. The meaning of *phase angle* $\delta(\omega)$ can be easily understood if we take strain as $\gamma(t) = \gamma_o \sin\omega t$. Then, Eq. (1.44) can be rewritten by

$$\sigma(t) = |G^*(\omega)|\,\gamma_o \sin[\omega t + \delta(\omega)] \tag{1.81}$$

where

$$|G^*(\omega)| = \sqrt{[G'(\omega)]^2 + [G''(\omega)]^2} \tag{1.82}$$

Problem 1

[1] When relaxation modulus is given by

$$G(t) = \sqrt{\frac{\lambda_o}{t}}\exp\left(-\frac{t}{\lambda_R}\right)\Theta(t) \tag{1.a}$$

Find $J(t)$, $G'(\omega)$, and $G''(\omega)$.

[2] For an analytic function $H(\lambda) \geq 0$, suppose a material whose relaxation modulus is given by

$$G(t) = \int_0^\infty \frac{H(\lambda)}{\lambda}\exp\left(-\frac{t}{\lambda}\right)d\lambda \tag{1.b}$$

Find dynamic moduli.

[3] Derive Eq. (1.41) for $\gamma(t) = \gamma_o \sin(\omega t + \phi)$ by the use of the Boltzmann superposition principle.

[4] When the Fourier transform of shear stress is denoted by $\hat{\sigma}(\omega)$, derive

$$\hat{\sigma}(\omega) = i\omega\hat{G}(\omega)\,\hat{\gamma}(\omega) \tag{1.c}$$

where $\hat{G}(\omega)$ and $\hat{\gamma}(\omega)$ are, respectively, Fourier transforms of relaxation modulus and strain.

[5] Derive Eq. (1.63).

[6] Using Eq. (1.8), calculate the stress from the strain of $\gamma(t) = \dot{\gamma}_o t$ where $\dot{\gamma}_o$ is a constant.

[7] Calculate steady-state compliance and mean relaxation time by using the following data:

ω (rad/s)	0.100	0.200	0.398	0.794	1.58	3.16	6.31
G'(Pa)	0.0360	0.142	0.543	1.86	4.79	8.00	9.98
G''(Pa)	0.633	1.25	2.40	4.16	5.54	5.20	4.48

[8] Consider a viscoelastic material whose creep compliance is given by

$$J(t) = \left[J_g + J_r\left(1 - e^{-t/\tau}\right) + \frac{t}{\eta_N}\right]\Theta(t) \tag{1.d}$$

Impose the stress of $\sigma_o[\Theta(t) - \Theta(t - t_R)]$ on the material and calculate the strain. Note that all parameters are positive constants.

[9] Calculate the zero-shear viscosity and steady-state compliance of the material which can be described by Eq. (1.d).

[10] Calculate dynamic moduli of the material such that

$$s\tilde{J}(s) = J_g + \frac{J_r}{1 + \sqrt{\tau s}} + \frac{1}{\eta_N s} \tag{1.e}$$

[11] When $G_\infty > 0$, show that

$$\begin{aligned} G'(\omega) &= G_\infty + \omega \int_0^\infty [G(t) - G_\infty] \sin \omega t \, dt; \\ G''(\omega) &= \omega \int_0^\infty [G(t) - G_\infty] \cos \omega t \, dt; \end{aligned} \tag{1.f}$$

$$\begin{aligned} G(t) &= G_\infty + \frac{2}{\pi} \int_0^\infty \frac{G'(\omega) - G_\infty}{\omega} \sin \omega t \, d\omega; \\ G(t) &= G_\infty + \frac{2}{\pi} \int_0^\infty \frac{G''(\omega)}{\omega} \cos \omega t \, d\omega; \end{aligned} \tag{1.g}$$

[12] When $G_\infty > 0$, how can we define the characteristic time scale for stress relaxation?

[13] Show that for $G_\infty = 0$

$$\overline{G} \equiv \frac{1}{J_e^o} \approx \frac{2}{\pi} \int_0^\infty \eta'(\omega)\, d\omega \tag{1.h}$$

[14] Show that the following are valid in the terminal region:

$$\log G'(\omega) \approx 2 \log G''(\omega) + \log J_e^o \tag{1.i}$$

2 Measurement of Linear Viscoelasticity

We shall study experimental aspects of linear viscoelasticity of polymer by focusing on rotational rheometer and data processing in this section.

2.1 Devices and Instruments

Rheometer is an instrument designed to measure viscoelastic properties of materials. Commercialized rheometers can measure not only linear viscoelastic properties but also nonlinear ones. Rheometer consists of units for controlling stimulation and measuring material responses.

Rotational rheometer is classified into two types: *stress-controlled and strain-controlled rheometers*. The former controls stress as stimulation and measures strain as the response of the material, while the latter controls strain and measures stress. As for stress-controlled rheometer, strain is measured by an optical device which is firmly fixed in the machine. Hence, it is not often to make some damage on the measuring device when the specimen is loaded in the rheometer. On the other hand, the sensor for stress measuring in strain-controlled rheometer can be damaged often during sample loading. In principle, stress-controlled rheometer cannot be used for stress relaxation experiment, while strain-controlled rheometer cannot be used for creep experiment. Both types of rheometers can be applied to dynamic test. Although strain-controlled rheometer is free from inertia problem, stress-controlled rheometer suffers from inertia problem because the torque applied by the rheometer gives rise to both the stress due to material and the acceleration of the fixture which has nonzero moment of inertia. Although the inertia effect of the fixture can be removed in dynamic test of linear viscoelasticity, it could not be removed in creep test until Kim et al. (2015) developed a method using Laplace transform. The inertia effect remains still unsolved in large-amplitude oscillatory shear (LAOS), a nonlinear dynamic test. Hence, we have to make a caution on types of rotational rheometers.

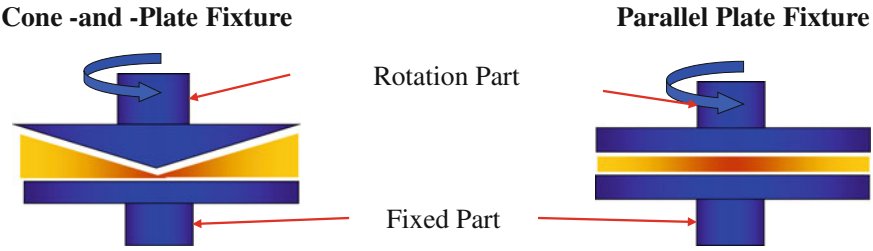

Fig. 2 Fixtures of rotational rheometers

There are several fixtures used in both types of rotational rheometers. As for polymer melts and polymer solutions with high viscosity, cone-and-plate and parallel plate fixtures of various sizes are popularly used. Figure 2 shows the two representative fixtures. Cup-and-bowl or other fixtures may be adopted for low-viscosity samples.

In *parallel plate fixture*, strain rate varies along the distance from the rotational axis, while strain is almost constant everywhere in *cone-and-plate fixture*. Detailed kinematic analysis is found in Macosko (1994). Although cone-and-plate fixture looks like better than parallel plate fixture because of homogeneity of strain, it is difficult to load high elastic material in cone-and-plate fixture. Parallel plate fixture gives acceptable results in linear viscoelastic tests with easy sample loading.

2.2 *Preliminary Tests*

In order to measure linear viscoelastic response functions, the linearity conditions must be checked. Even if linearity is valid, there are a number of things to be taught to reduce errors in measurements. Examples are sample preparation, temperature calibration, thermal expansion of fixture, alignment of rotating axis of fixture, thermal stability of materials, and so on. There is a review paper recommendable for the readers interested in error sources in rotational rheometer (Stadler 2014). This paper is focused on practical aspects in linear viscoelastic experiments. This subsection mainly deals with preliminary test methods and related mathematical principles.

2.2.1 Linearity Experiments

Consider the case of stress relaxation first. To check the linearity of material, one has to choose several strain amplitudes. For n strain amplitudes of $\gamma_1 < \gamma_2 < \cdots < \gamma_n$, the set n stress functions $\sigma_1(t)$, $\sigma_2(t), \ldots, \sigma_n(t)$ would be measured. If all strain amplitudes satisfy the linearity conditions, then we would

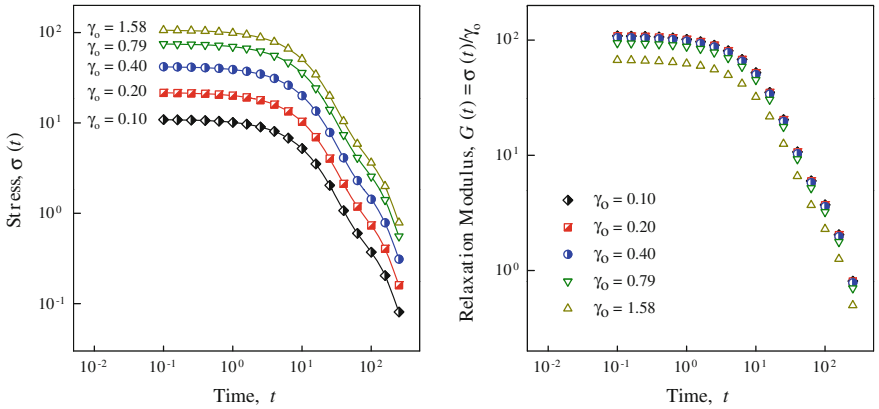

Fig. 3 Schematic illustration for linearity check in stress relaxation

have $G_1(t) = G_2(t) = \cdots = G_n(t)$ where $G_k(t) = \sigma_k(t)/\gamma_k$. There is upper bound of strain amplitude such that linearity holds if and if $\gamma_k < \gamma_{\max}$. Assume that

$$\gamma_1 < \cdots < \gamma_k < \gamma_{\max} < \gamma_{k+1} < \cdots < \gamma_n \tag{2.1}$$

Then, for k strain amplitudes, identical relaxation modulus is obtained, while different relaxation moduli are obtained for $i > k$. If strain amplitude is too small, then stress signal is apt to be lower than the lower bound of the torque sensor of strain-controlled rheometer. Thus, it is usual to choose strain amplitude as γ_k or γ_{k-1}. Figure 3 illustrates schematically how strain amplitude is chosen. The figure shows that strain amplitudes higher than 0.4 give nonlinear results.

Similar test must be done for creep and dynamic tests. By varying the amplitude of stimulation, we have to found the region of stimulation amplitude where superposition of the response functions as shown on the right graph in Fig. 3. As for dynamic test, linearity checking can be done by amplitude sweep test which is the test at a fixed frequency with varying stimulation amplitude. Here, stimulation amplitude is strain amplitude for strain-controlled rheometer and stress amplitude for stress-controlled rheometer.

If a strain amplitude belongs to linear regime, then dynamic moduli at the same frequency must be identical. As shown in Fig. 4, as strain amplitude increases, storage modulus becomes to show bigger deviation from a constant value. The upper bound of strain amplitude for linearity depends on frequency as shown in Fig. 4. Hence, if one wants to frequency sweep test for $\omega_{\min} \leq \omega \leq \omega_{\max}$ with strain-controlled rheometer, then strain amplitude sweep test must be done, at least, two times for the two frequencies $\omega_{\min}$ and $\omega_{\max}$. We select the optimum amplitude for frequency sweep test as the minimum of the two upper bounds.

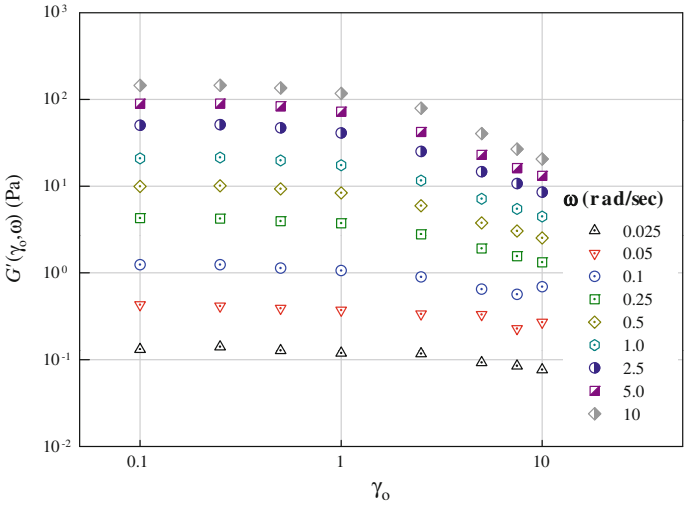

Fig. 4 Strain sweep test for PEO solution (Cho et al. 2010)

2.2.2 Waiting Time for Dynamic Test

Consider a dynamic test by strain-controlled rheometer. When strain is given by $\gamma(t) = \gamma_o \sin \omega t$, transient response of stress is observed in short-time region as shown in Fig. 5. After a certain time is passed, stress amplitude is nearly independent of time. This is the stationary response. From the signal of stress as a function of time, the rheometer can determine the stress amplitude $\sigma_o = |G^*(\omega)|\,\gamma_o$ and phase difference $\delta(\omega)$. Then, storage and loss moduli are calculated by

$$G'(\gamma_o,\omega) = \frac{\sigma_o(\gamma_o,\omega)}{\gamma_o}\cos\delta(\gamma_o,\omega); \quad G''(\gamma_o,\omega) = \frac{\sigma_o(\gamma_o,\omega)}{\gamma_o}\sin\delta(\gamma_o,\omega) \tag{2.2}$$

Assume that linearity check was done. If measurement is not taken for sufficiently long time, that is, stationary response is not obtained, then the use of Eq. (2.2) is erroneous.

Equation (1.44) can be interpreted geometrically. Consider the three-dimensional space of $(\sigma,\ \gamma,\ \omega^{-1}\dot{\gamma})$. Then, Eq. (1.44) is the equation for a plane passing the origin of the space. The orientation of the plane is represented by the vector $(G',\ G'',\ \pm 1)$. Since $\gamma^2 + (\omega^{-1}\dot{\gamma})^2 = \gamma_o^2$, an ellipse on the plane is formed by the data of dynamic test at a fixed frequency and a fixed strain amplitude. The ellipse is the projection of the circle in the plane of $\sigma = 0$ on the incline plane of Eq. (1.44). Then, the Lissajou curve on the left of Fig. 6 is the projection of the ellipse to the plane $\omega^{-1}\dot{\gamma} =$ constant and that on the right is the projection to the plane $\gamma =$ constant. This geometric interpretation was developed first by Cho et al. (Cho et al. 2005). Storage modulus is the slope of the longest axis of the slope in the

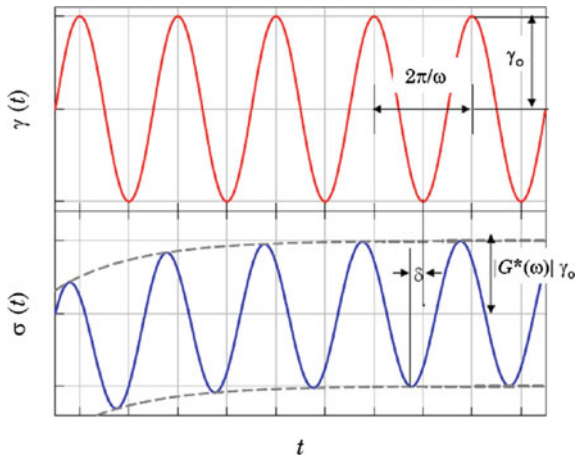

Fig. 5 Schematic illustration of dynamic test

Lissajou plot of stress against strain and loss modulus can be identified in the same way for the Lissajou plot of stress as a function of strain rate/ω. As shown in Fig. 6, stationary response forms an elliptical loop in linear viscoelastic regime. Hence, Lissajou plot lets us recognize transient and stationary responses explicitly.

The waiting time necessary for stationary state can be estimated by the use the Maxwell model. When strain is given by $\gamma(t) = \gamma_o \sin \omega t$, the stress is given by

$$\sigma(t) = \left[\sigma(t_o) - G'(\omega)\,\gamma(t_o) - \frac{G''(\omega)}{\omega}\dot{\gamma}(t_o)\right] e^{-(t-t_o)/\lambda} + G'(\omega)\,\gamma(t) + \frac{G''(\omega)}{\omega}\dot{\gamma}(t) \tag{2.3}$$

The first term is the transient response, and the last two terms are stationary response. We are interested in frequency sweep test. Let $\sigma(t_o)$ be the stress in

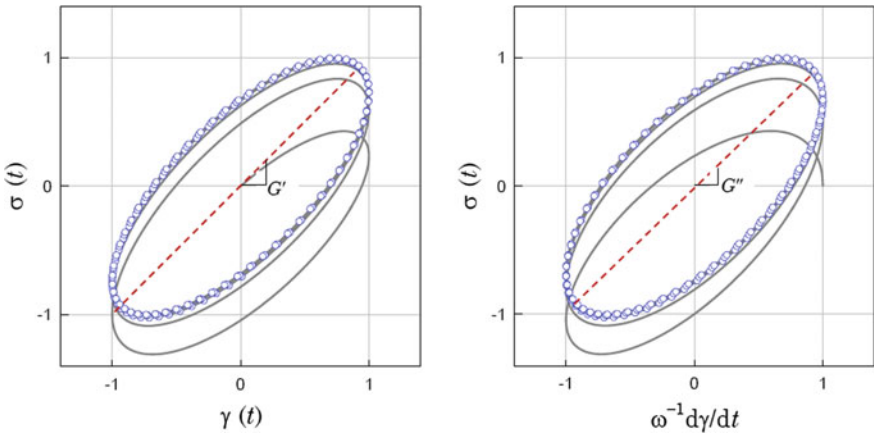

Fig. 6 Lissajou plots of linear viscoelasticity

stationary state at the frequency ω_o. This means that frequency is changed from ω_o to ω at time of t_o. Then, the initial stress is given

$$\sigma(t_o) \approx G'(\omega_o)\,\gamma(t_o) + \frac{G''(\omega_o)}{\omega_o}\dot{\gamma}(t_o) \tag{2.4}$$

and Eq. (2.3) can be rewritten by

$$\begin{aligned}\sigma(t) = {} & \{[G'(\omega_o) - G'(\omega)]\,\gamma(t_o) + [\eta'(\omega_o) - \eta'(\omega)]\,\dot{\gamma}(t_o)\}\, e^{-(t-t_o)/\lambda} \\ & + G'(\omega)\,\gamma(t) + \frac{G''(\omega)}{\omega}\dot{\gamma}(t)\end{aligned} \tag{2.5}$$

If $t - t_o = 3\lambda$, then the transient stress is reduced to 0.05 of the value at t_o. Thus, data sampling must be done by waiting for a time longer than several times of relaxation time λ after changing frequency. Since we cannot know the mean relaxation time of the sample before measurement, we need a preliminary test for determination of waiting time.

2.2.3 Time Sweep Test

Consider a material whose mean relaxation time is λ. We are interested in frequency sweep test which consists of n frequencies, $\omega_1 < \omega_2 < \cdots < \omega_n$. Assume that $m\lambda$ is chosen as the waiting time and stationary stress of a single cycle is necessary for accurate determination of stress amplitude and phase angle. Then, the total time for experiment is given by

$$t_{ex} = \sum_{k=1}^{n} \frac{2\pi}{\omega_k} + (n-1)\,m\lambda \tag{2.6}$$

Polymer is very weak at high temperature if oxygen is diffused in the sample. Degradation of polymer can be prevented by the use of small amount of antioxidant or the use of inert gas such as nitrogen. If material starts degradation after a certain time t_d when it is loaded in an experimental condition, then reliable data can be obtained whenever $t_{ex} < t_d$. Hence, both calculation of t_{ex} and determination of t_d. Time sweep test is necessary to determine degradation time, t_d.

Time sweep test is the dynamic test at a fixed frequency and a fixed amplitude. If material is stable, the dynamic modulus does not vary for long time. If dynamic modulus starts to increase or decrease at a time, the time is the degradation time.

2.2.4 Creep Recovery Test

In stress relaxation test, relaxation modulus at long time is not reliable when stress becomes outside of the lower bound of torque sensor. Because of the imperfection

of the unit step function in experiment, relaxation modulus at short time is not reliable, neither. This limitation of stress relaxation test can be overcome when time–temperature superposition is available. When time–temperature superposition is not available, long-time viscoelasticity can be measured by creep test. It is because the strain of creep test increases as time. However, stress-controlled rheometer has mainly two problems: residual torque and inertia effect. The inertia problem shall be discussed in separate subsections.

We shall use the first equation of Eq. (1.33). It is usual that $G_o^{-1} \sim 10^{-9}\,\mathrm{Pa}^{-1}$ for most polymers because G_o corresponding to the modulus of the polymer at a temperature much below the glass transition temperature. Hence, it is usually called glassy modulus and neglected in creep experiment at temperatures higher than the glass transition temperature. Creep recovery test is necessary to determine exactly J_r and the creep function $\Psi(t)$. Extrapolation of long-time data is not accurate because of the effect of residual torque which is originated from the bearing system of the stress-controlled rheometer.

Creep recovery test is done by the use of stress profile such that

$$\sigma(t) = \sigma_o[\Theta(t) - \Theta(t - t_o)] \tag{2.7}$$

where $t_o > 0$ is called creep time. Then, the response from the stress is given by

$$\frac{\gamma(t)}{\sigma_o} = J(t) - J(t - t_o) \tag{2.8}$$

Substitution of Eq. (1.33) into Eq. (2.8) yields

$$\begin{aligned}\frac{\gamma(t)}{\sigma_o} = {} & \frac{t_o}{\eta_o}\Theta(t - t_o) + J_r[\Psi(t)\,\Theta(t) - \Psi(t - t_o)\,\Theta(t - t_o)] \\ & + \left(\frac{1}{G_o} + \frac{t}{\eta_o}\right)[\Theta(t) - \Theta(t - t_o)]\end{aligned} \tag{2.9}$$

For $t > t_o$, Eq. (2.9) becomes simpler as follows:

$$\frac{\gamma(t)}{\sigma_o} = J_r[\Psi(t) - \Psi(t - t_o)] + \frac{t_o}{\eta_o} \tag{2.10}$$

Note that when $t = t_o$, we have

$$\frac{\gamma(t_o)}{\sigma_o} = J_r\Psi(t_o) + \frac{t_o}{\eta_o} \tag{2.11}$$

because $\Psi(0) = 0$ from the definition of the creep function.

We define creep recovery compliance (shortly recovery compliance) by

$$J_R(t) = \frac{\gamma(t_o) - \gamma(t)}{\sigma_o} \tag{2.12}$$

Note that for $t \geq t_o$, $J_R(t) \geq 0$. From the definition of recovery compliance, we have

$$J_R(t_R) = J_r[\Psi(t_o) - \Psi(t_o + t_R)] + J_r\Psi(t_R) \tag{2.13}$$

where we defined recovery time as $t_R = t - t_o$. If creep time t_o is sufficiently large, then $\Psi(t_o) \approx \Psi(t_o + t_R) \approx 1$. Remind the properties of the creep function. Then, the recovery compliance is given by

$$J_R(t_R) \approx J_r\Psi(t_R) \tag{2.14}$$

To help understanding, model calculation was done with

$$J(t) = \frac{1}{G_o} + J_r\left(1 - e^{-t/\tau}\right) + \frac{t}{\eta_o} \tag{2.15}$$

where $\tau = 10^2$ s, $G_o = 10^8$ Pa, $J_r = 10^{-5}\,\text{Pa}^{-1}$, and $\eta_o = 10^7$ Pa s. Figure 7 shows $J(t) - J(t - t_o)$ with various creep time and recovery compliance as functions of time. As creep time increases, recovery compliance converges to $J_r\psi(t_R) = J_r\left(1 - e^{-t_R/\tau}\right)$.

Note that the recovery compliance on the right graph looks different from the broken lines of the left graph because the graphs are double logarithmic plots. Figure 7 indicates that creep time must be sufficiently larger than the retardation time.

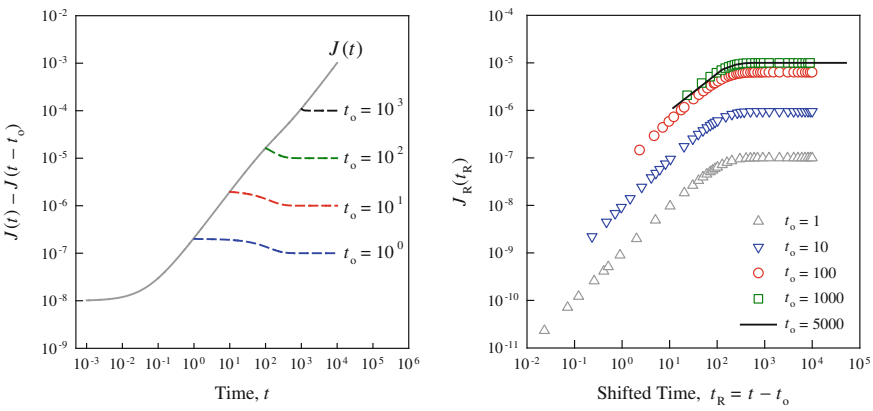

Fig. 7 Simulation of creep recovery experiment

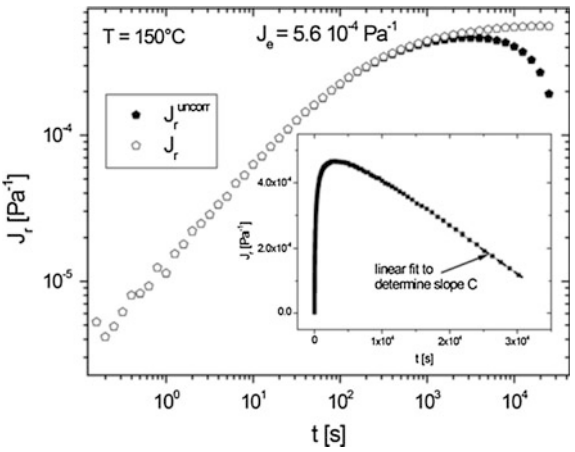

Fig. 8 Example of a correction for residual torque. *Filled symbols* are uncorrected $J_R^{\text{uncorr}}(t)$, and *open symbols* are corrected recovery compliance (Stadler 2014)

Residual torque deteriorates the horizontal region where $t_R > \tau$ in real experiment. The effect of residual torque can be corrected by

$$J_R(t) = J_R^{\text{uncorr}}(t) - Ct \tag{2.16}$$

where C is the correction constant which can be determined by the constant slope of J_R^{uncorr} at long-time regime (see inset of Fig. 8). Note that t in Eq. (2.16) is the recovery time. Figure 8 shows the recovery compliance of LLDPE with long-chain branch and it is Fig. 6 of (Stadler 2014).

2.3 Inertia Effect in Stress-Controlled Rheometer

Stress-controlled rheometer applies torque (machine torque) to the fixture, the fixture transfers stress to specimen, and specimen generates material torque. However, the mass of the fixture generates additional torque called inertia torque. Then, the torque balance equation affects the relation between stimulation and material response. If the torque balance equation is translated to stress balance form (Baravian and Quemada 1998), then we have

$$\mu \frac{d^2\gamma}{dt^2} + \sigma(t) = \sigma_m(t) \tag{2.17}$$

where μ is the constant depending on the geometry of the fixture, called the inertia coefficient, σ is the material stress, and σ_m is the machine stress which is applied by the rheometer. Hence, the stimulation is σ_m rather than σ. When the inertia term is negligible, machine stress equals to material stress. However, inertia effect exists always because fixture has mass. When the inertia effect is significant, strain is no

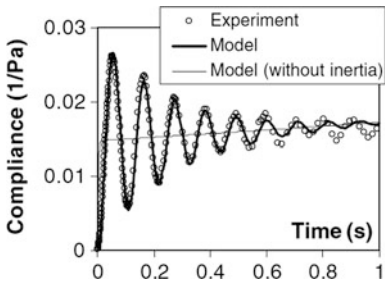

Fig. 9 Creep ringing of 0.075 wt% Carbopol 940. The model is the Jeffreys model. Adopted from Baravian et al. (2007)

longer a monotonic function of time and oscillates with decreasing amplitude as shown in Fig. 9. This phenomenon is called *creep ringing*. Figure 9 is adopted from (Baravian et al. 2007).

Here, we will study how to extract material response functions by the use of Eq. (2.17). Note that the value of μ is given by the makers of rheometers. The machine stress is assumed to be given by $\sigma_m = \sigma_0 f(t)\,\Theta(t)$. The function $f(t)$ is unity for creep experiment and $\sin \omega t$ for dynamic experiment. Then, it is obvious that $\gamma(t) = 0$ for $t < 0$. Then, the Boltzmann superposition principle can be rewritten by

$$\sigma(t) = \int_0^t G(t-t')\frac{\mathrm{d}\gamma}{\mathrm{d}t'}\mathrm{d}t' \tag{2.18a}$$

$$\gamma(t) = \int_0^t J(t-t')\frac{\mathrm{d}\sigma}{\mathrm{d}t'}\mathrm{d}t' \tag{2.18b}$$

It is the convolution of relaxation modulus and strain rate. Hence, applying Laplace transform to Eq. (2.17) gives

$$\mu s^2\widetilde{\gamma}(s) - \mu s\gamma(0) - \dot{\gamma}(0) + s\widetilde{G}(s)\widetilde{\gamma}(s) - \widetilde{G}(s)\gamma(0) = \widetilde{\sigma}_m(s) \tag{2.19}$$

Kim et al. (2015) derived the initial condition

$$\gamma(0) = \dot{\gamma}(0) = 0 \tag{2.20}$$

by the use of Eq. (2.18b). Then, Eq. (2.19) becomes simpler:

$$\widetilde{\gamma}(s) = \frac{\widetilde{\sigma}_m(s)}{\mu s^2 + s\widetilde{G}(s)} \tag{2.21}$$

or

$$s\widetilde{G}(s) = \frac{\widetilde{\sigma}_m(s) - \mu s^2 \widetilde{\gamma}(s)}{\widetilde{\gamma}(s)} \tag{2.22}$$

We know $\widetilde{\sigma}_m(s)$ and $\widetilde{\gamma}(s)$ can be calculated numerically from the measured data $\gamma(t)$. Then, we need numerical method for inverse Laplace transform. As for numerical inversion of Laplace transform, there have been hundreds of papers published (Cohen 2007). Finally, we can obtain relaxation modulus from the numerical inversion of Laplace transform.

As for dynamic test, we are interested in stationary response. After sufficiently long time, we can assume that strain and material stress are sinusoidal functions like machine stress. Then, we can use the following complex notation:

$$\gamma^*(t) = \gamma_o(\omega)\, e^{i(\omega t - \phi(\omega))}; \quad \sigma^*(t) = G^*(\omega)\,\gamma^*(\omega); \quad \sigma_m^*(t) = \sigma_o e^{i\omega t} \tag{2.23}$$

Substitution of Eq. (2.23) to Eq. (2.17) gives

$$G^*(\omega) = \frac{\sigma_o}{\gamma_o(\omega)} e^{i\phi(\omega)} + \mu\omega^2 \tag{2.24}$$

Since both strain amplitude $\gamma_o(\omega)$ and phase difference $\phi(\omega)$ can be determined from the measured data of strain, Eq. (2.24) gives dynamic moduli as follows:

$$G'(\omega) = \frac{\sigma_o}{\gamma_o(\omega)} \cos\phi(\omega) + \mu\omega^2; \quad G''(\omega) = \frac{\sigma_o}{\gamma_o(\omega)} \sin\phi(\omega) \tag{2.25}$$

Occurrence of creep ringing can be understood by the equation of motion Eq. (2.17) similar to the equation of vibration. As for the Voigt model, Eq. (2.17) becomes

$$\mu \frac{d^2\gamma}{dt^2} + \eta_o \frac{d\gamma}{dt} + G_o\gamma = \sigma_m(t) \tag{2.26}$$

This is analogous to forced oscillation of the mass μ supported by spring and damper. There have been studies on creep ringing by the use of spring–dashpot models (Baravian and Quemada 1998; Jaishankar et al. 2011).

Baravian and Quemada (1998) derived ringing criteria for the Maxwell–Jeffreys and the Voigt models. On the other hand, Kim et al. (2015) developed numerical methods to extract viscoelastic response functions such as dynamic moduli and continuous relaxation spectrum. It will be studied what is relaxation spectrum and how relaxation spectrum is used in the calculation of various viscoelastic response functions in Chap. 7. The approach of Kim et al. requires numerical method to calculate the Laplace transform of strain data. The numerical method is also important in diffusion wave spectroscopy (DWS).

It is still an important research theme to derive ringing criteria from viscoelastic response function such as relaxation modulus or creep compliance without depending on spring–dashpot models. From Eq. (2.26), we can guess that if viscous stress (represented by η_o) is weaker than elastic stress (represented by G_o), then creep ringing occurs.

2.4 Diffusion Wave Spectroscopy

Mason and Weitz developed a new method to measure linear viscoelasticity (Mason and Weitz 1995). It is called DWS and is to measure the mean square distance of Brownian particle which moves in viscoelastic medium. Using the generalized Langevin equation, the mean square distance can be related to the Laplace transform of the relaxation modulus of the viscoelastic medium.

Since the viscoelastic medium has memory, the generalized Langevin equation is given by

$$m\frac{\mathrm{d}\mathbf{v}}{\mathrm{d}t} = \mathbf{f}_R(t) - \int_0^t \zeta(t-\tau)\,\mathbf{v}(\tau)\,\mathrm{d}\tau \tag{2.27}$$

where m is the mass of the Brownian particle, v is the velocity, $f_R(t)$ is the random force, and $\zeta(t)$ is the friction function which represents the memory effect of the viscoelastic medium. As learned in Sect. 3.4 in Chap. 4, we know that

$$\langle \mathbf{f}_R(t)\rangle = \mathbf{0}\,; \quad \langle \mathbf{f}_R(t)\cdot\mathbf{f}_R(0)\rangle = 3k_\mathrm{B}T\zeta(t) \tag{2.28}$$

In order to connect $\zeta(t)$ with the viscoelastic response function of the medium, Mason and Weitz generalized the Stokes equation, Eq. (3.2), in Chap. 3 as follows:

$$\widetilde{\eta}(s) = \frac{\widetilde{\zeta}(s)}{6\pi a} \tag{2.29}$$

Here, Laplace transform is applied in order to make complicate time dependence simpler. A question occurs on the definition of $\widetilde{\eta}(s)$. The answer may be Eqs. (1.49) and (1.51). Then, we have

$$\widetilde{\eta}(s) = \widetilde{G}(s) \tag{2.30}$$

Note that the dimension of the Laplace transform equals that of viscosity.

Mason and Weitz (1995) applied Eqs. (2.29) and (2.30) to the generalization of the Stokes–Einstein equation, Eq. (3.14) in Chap. 3, and the relation between diffusion constant and the mean square distance, Eq. (3.13) in Chap. 3:

$$s\widetilde{G}(s) = \frac{k_B T}{\pi a} \frac{1}{s\left\langle \Delta \widetilde{r}^2(s) \right\rangle} - \frac{m}{6\pi a} s^2 \tag{2.31}$$

where $\left\langle \Delta \widetilde{r}^2(s) \right\rangle$ is the Laplace transform of the mean square distance

$$\left\langle \Delta r^2(t) \right\rangle \equiv \left\langle \left\| \mathbf{x}(t) - \mathbf{x}(0) \right\|^2 \right\rangle \tag{2.32}$$

The second term represents inertia effect and can be neglected except at high s. Then, Eq. (2.31) becomes

$$s\widetilde{G}(s) = \frac{k_B T}{\pi a} \frac{1}{s\left\langle \Delta \widetilde{r}^2(s) \right\rangle} \tag{2.33}$$

If Eq. (1.23) is applied to Eq. (2.33), we get

$$\widetilde{J}(s) = \frac{\pi a}{k_B T} \left\langle \Delta \widetilde{r}^2(s) \right\rangle \tag{2.34}$$

This implies that the mean square distance is proportional to creep compliance. From Eq. (2.33), the use of Fourier transform or Laplace transform gives

$$G^*(\omega) = \frac{k_B T}{\pi a} \frac{1}{\mathrm{i}\omega \hat{F}\left[\left\langle \Delta r^2(t) \right\rangle\right]} = \frac{k_B T}{\pi a} \frac{1}{\mathrm{i}\omega \left\langle \Delta \widetilde{r}^2(\mathrm{i}\omega) \right\rangle} \tag{2.35}$$

According to Mason (2000), dynamic modulus can be calculated by *fast Fourier transform* (FFT) or Laplace transform through numerical integration. Evans et al. (2009) used discrete Fourier transform in order to convert creep compliance data to dynamic moduli. Although the conversion is plausible compared with measured dynamic moduli, it was nosy and needs a smoothing process. Hence, Mason used power law approximation for Laplace transform because both integral transforms suffer from the finite range of data (Mason 2000). His method fitted effectively the data of storage modulus which was measured by rotational rheometer. The method underestimated loss modulus. Hence, further research is demanded on better numerical method to convert the mean square distance to dynamic moduli.

Mason and Weitz opened a new field called *microrheology*: measurement of mean square distance and its conversion to linear viscoelasticity. From the working principle of DWS, the inertia effect of DWS seems to be smaller than that of creep experiment. Hence, DWS is better than creep experiment, especially when the material shows creep ringing. As for creep-ringing materials, strain data from creep test should be processed by a suitable method such as (Kim et al. 2015) in order to eliminate inertia effect. Creep ringing is often found in biopolymer solutions because of higher elasticity than viscosity. Further information on microrheology is available in some review papers such as Waigh (2005) and Squires and Mason (2010).

Problem 2

[1] Derive Eq. (2.3).
[2] Derive Eq. (2.13).
[3] Derive the initial condition $\gamma(0) = \dot{\gamma}(0) = 0$, Eq. (2.20), by the use of Eq. (2.18b) (Kim et al. 2015).
[4] Derive Eq. (2.24).
[5] Derive ringing condition for Eq. (2.26) (Baravian and Quemada 1998).
[6] If the scale factor $\pi a/(k_B\theta)$ in Eq. (2.34) is not acceptable, then how can you determine an appropriate scale factor? (Mason 2000).
[7] A quarter cycle of stationary state in dynamic test is given in the table below. Calculate dynamic moduli by the use of multilinear regression with respect to Eq. (1.44).

t/ s	0.5984	1.1968	1.7952	2.3936	2.9920	3.5904
$\gamma(t)$	0.0782	0.0975	0.0434	−0.0434	−0.0975	−0.0782
$\sigma(t)$/Pa	0.7799	−0.0275	−0.8142	−0.9877	−0.4175	0.4671

[8] Consider the Jeffreys model such that

$$\eta_0 G_1 \frac{d\gamma}{dt} + \eta_1 \eta_0 \frac{d^2\gamma}{dt^2} = (\eta_1 + \eta_0)\frac{d\sigma}{dt} + G_1\sigma \tag{2.a}$$

Derive that the ringing compliance is given by

$$J(t) = \frac{\gamma(t)}{\sigma_o} = \frac{t}{\eta_0} - A + e^{-t/\tau}\left[A\cos\omega t + \left(A - \frac{\tau}{\eta_0}\right)\frac{\sin\omega t}{\tau\omega}\right] \tag{2.b}$$

where

$$A = \frac{\mu(\eta_0 + \eta_1)}{\eta_0 G_1}\left(\frac{2}{\tau\eta_0} - \frac{1}{\mu}\right) \tag{2.c}$$

$$\tau = \frac{2\mu(\eta_0 + \eta_1)}{\mu G_1 + \eta_0\eta_1} \tag{2.d}$$

and

$$\omega = \sqrt{\frac{\eta_0 G_1}{\mu(\eta_0 + \eta_1)} - \frac{1}{\tau^2}} \tag{2.e}$$

See Baravian et al. (2007).

3 Phenomenological Models

3.1 Spring–Dashpot Models Revisited

We have studied spring–dashpot models in 3.4 in Chap. 2. Although the Maxwell model and the Voigt model give qualitatively correct description of linear viscoelasticity, they cannot fit experimental data of linear viscoelasticity of polymers. There have been efforts to develop a realistic model of spring and dashpot (Tschoegl 1989). For simplicity, we consider only fluid models. One of the most representative models is the generalized Maxwell model which is a parallel connection of N Maxwell elements with different relaxation times and moduli. Then, it is easy to calculate the relaxation modulus of the model:

$$G(t) = \sum_{k=1}^{N} G_k e^{-t/\lambda_k} \tag{3.1}$$

Here, we omitted the unit step function for simplicity. Without loss of generality, we choose $0 < \lambda_1 < \lambda_2 < \cdots < \lambda_N$. The model can be characterized a set of parameters $\{G_n,\ \lambda_n\,;\, N\}$. The plot of G_n against λ_n gives us an insight that relaxation times are distributed. Hence, the set is called *discrete relaxation time spectrum* or discrete relaxation time distribution. Shortly, we call it discrete relaxation spectrum. Increasing imagination, one may invent continuous relaxation spectrum $H(\lambda)$ such that

$$G(t) = \int_{-\infty}^{\infty} H(\lambda) e^{-t/\lambda} \mathrm{d} \log \lambda \tag{3.2}$$

Note that integration in logarithmic scale is introduced in order to make the dimension of $H(\lambda)$ equal to that of relaxation intensities G_k of discrete relaxation spectrum.

Another generalized spring–dashpot model is the series connection of $N-1$ Voigt models with different retardation times and compliances and a single Maxwell model of viscosity η_M and modulus $G_M = 1/J_M$. This model has creep compliance such as

$$J(t) = J_M + \frac{t}{\eta_M} + \sum_{k=1}^{N-1} J_k \left(1 - e^{-t/\tau_k}\right) \tag{3.3}$$

The set $\{J_k,\ \tau_k,\ N-1\}$ is called *discrete retardation time spectrum* or shortly discrete retardation spectrum. Without loss of generality, we assume that

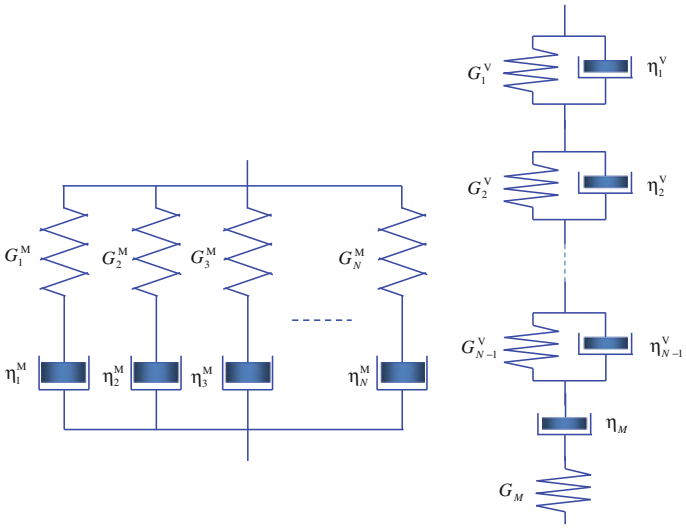

Fig. 10 Spring–dashpot models for viscoelastic fluids: Eqs. (3.1) and (3.3). Note that $\lambda_k = \eta_k^M/G_k^M$, $G_k = G_k^M$, $\tau_k^V = \eta_k^V/G_k^V$, and $J_k = 1/G_k^V$

$\tau_1 < \tau_2 < \cdots < \tau_{N-1}$. Similar to Eq. (3.2), we can define *continuous retardation spectrum* $L(\tau)$ as follows:

$$J(t) = J_M + \frac{t}{\eta_M} + \int_{-\infty}^{\infty} L(\tau)\left(1 - e^{-t/\tau}\right) \mathrm{d}\log\tau \tag{3.4}$$

Both Eqs. (3.1) and (3.3) are a kind of one-dimensional constitutive equation. A good constitutive equation is the one that can fit experimental data as well as the one whose parameters can be easily determined from experimental data. How to determine relaxation spectrum will be learned in Chap. 6. Here, we shall introduce the concept of relaxation and retardation time spectra and conditions that the two models are identical. The two models are depicted in Fig. 10.

Taking Laplace transform on both sides of Eq. (3.1), we have

$$s\widetilde{G}(s) = \sum_{k=1}^{N} G_k \frac{\lambda_k s}{1+\lambda_k} = \frac{Q_N(s)}{P_N(s)} \tag{3.5}$$

Since we can obtain $s\widetilde{G}(s)$ from experiment such as DWS (see Sect. 2.4), regression of experimental data by Eq. (3.3) is a way to identify the discrete model. However, it is questionable whether the regression gives positive coefficients of

$P_N(s)$ and $Q_N(s)$. Hence, it is necessary to analyze the coefficients of the polynomials. The polynomials of Nth order are given by

$$P_N(s) = \prod_{n=1}^{N} (1 + \lambda_n s) = 1 + \left(\sum_{k=1}^{N} \lambda_k \right) s + \cdots + \left(\prod_{k=1}^{N} \lambda_k \right) s^N \tag{3.6}$$

and

$$\begin{aligned} Q_N(s) &= \sum_{n=1}^{N} G_n \lambda_n s \frac{P_N(s)}{1 + \lambda_n s} \\ &= \eta_o \, s + \eta_o \left(\sum_{k=1}^{N} \lambda_k - \eta_o J_e^o \right) s^2 + \cdots + G_o \left(\prod_{k=1}^{N} \lambda_k \right) s^N \end{aligned} \tag{3.7}$$

where

$$G_o = G(0) = \sum_{n=1}^{N} G_n \tag{3.8}$$

The zero-shear viscosity η_o and the steady-state compliance J_e^o can be expressed in terms of the model parameters. The terminal behavior of the model gives

$$\eta_o = \lim_{\omega \to 0} \frac{\mathrm{Im}\left\{ \mathrm{i}\omega \widetilde{G}(\mathrm{i}\omega) \right\}}{\omega} = \sum_{k=1}^{N} G_k \lambda_k \tag{3.9}$$

and

$$\eta_o^2 J_e^o = \lim_{\omega \to 0} \frac{\mathrm{Re}\left\{ \mathrm{i}\omega \widetilde{G}(\mathrm{i}\omega) \right\}}{\omega^2} = \sum_{k=1}^{N} G_k \lambda_k^2 \tag{3.10}$$

Then, the polynomial $Q_N(s)$ can be factorized as follows:

$$Q_N(s) = \eta_o s \, \Theta_{N-1}(s) \tag{3.11}$$

where

$$\Theta_{N-1}(s) = 1 + \left(\sum_{k=1}^{N} \lambda_k - \eta_o J_e^o \right) s + \cdots + \frac{G_o}{\eta_o} \left(\prod_{k=1}^{N} \lambda_k \right) s^{N-1} \tag{3.12}$$

From Eqs. (3.9) to (3.10), we know that

$$\sum_{k=1}^{N} \lambda_k - \eta_o J_e^o = \sum_{k=1}^{N} \lambda_k (1 - p_k) > 0 \tag{3.13}$$

where

$$0 < p_k = \frac{G_k \lambda_k}{\eta_o} < 1\,; \quad \sum_{k=1}^{N} p_k = 1 \tag{3.14}$$

Returning to Eq. (3.3), we take Laplace transform and have

$$s\widetilde{J}(s) = J_M + \frac{1}{\eta_M s} + \sum_{k=1}^{N-1} \frac{J_k}{1 + \tau_k s} \tag{3.15}$$

It can be rewritten as a rational function of s as follows:

$$s\widetilde{J}(s) = \frac{R_N(s)}{\eta_M s\, \Psi_{N-1}(s)} \tag{3.16}$$

where

$$R_N(s) = (1 + J_M \eta_M s)\, \Psi_{N-1}(s) + \sum_{k=1}^{N-1} J_k \frac{\Psi_{N-1}(s)}{1 + \tau_k s} \tag{3.17}$$

and

$$\Psi_{N-1}(s) = \prod_{k=1}^{N-1} (1 + \tau_k s) \tag{3.18}$$

The zero-shear viscosity and the steady-state compliance of the model (3) are, respectively, given by

$$\eta_o = \lim_{\omega \to 0} \frac{1}{\omega \mathrm{Im}\{\, \mathrm{i}\omega \widetilde{J}(\mathrm{i}\omega)\}} = \eta_M \tag{3.19}$$

and

$$J_e^o = \lim_{\omega \to 0} \mathrm{Re}\{\, \mathrm{i}\omega \widetilde{J}(\mathrm{i}\omega)\} = J_M + \sum_{k=1}^{N-1} J_k \tag{3.20}$$

We know that both Eqs. (3.1) and (3.3) represent viscoelastic fluid. Then, it is natural to investigate the conditions that the two models become identical. If the two models are identical, then it is obvious that $s\widetilde{G}(s)\,s\widetilde{J}(s) = 1$. This immediately results in that

$$\Theta_{N-1}(s) = \prod_{n=1}^{N-1}(1+\tau_n s) = \Psi_{N-1}(s) \tag{3.21}$$

Determination of τ_n is to find the zeros of $N-1$th-order polynomial $\Theta_{N-1}(s)$.

From the convolution, Eq. (1.23), the Laplace transform of the creep compliance of the model, Eq. (3.1), is given by

$$s\widetilde{J}(s) = \frac{P_N(s)}{Q_N(s)} = \frac{1}{\eta_o s\Theta_{N-1}(s)}\prod_{n=1}^{N}(1+\lambda_n s) \tag{3.22}$$

Partial fraction gives

$$s\widetilde{J}(s) = J_g + \frac{1}{\eta_o s} + \sum_{n=1}^{N-1}\frac{J_n}{1+\tau_n s} \tag{3.23}$$

where J_g is determined by the initial value theorem of Laplace transform:

$$J_g = J(0^+) = \lim_{s\to\infty} s\widetilde{J}(s) = \frac{1}{G_o} \tag{3.24}$$

Comparison of Eq. (3.23) with Eq. (3.15) gives $J_g = J_M = G_o^{-1} = G_M^{-1}$. The identification of the two models also gives

$$J_n = \lim_{s\to-\tau_n^{-1}}(1+\tau_n s)\,s\widetilde{J}(s) = -\frac{\tau_n}{\eta_o}\frac{\prod_{k=1}^{N}\left(1-\frac{\lambda_k}{\tau_n}\right)}{\prod_{k\neq n}^{N-1}\left(1-\frac{\tau_k}{\tau_n}\right)} > 0 \tag{3.25}$$

This is the result of partial fraction, and the inequality must hold for realistic model.

Now, we will prove the following inequality by the use of the inequality of Eq. (3.25):

$$\lambda_1 < \tau_1 < \lambda_2 < \tau_2 < \cdots < \tau_{N-2} < \lambda_{N-1} < \tau_{N-1} < \lambda_N \tag{3.26}$$

To prove the inequality, assume the existence of $\lambda_m < \tau_n < \lambda_{m+1}$. Then, we know that

$$\prod_{k=1}^{N}\left(1-\frac{\lambda_k}{\tau_n}\right) = (-1)^{N-m}\prod_{k=1}^{N}\left|1-\frac{\lambda_k}{\tau_n}\right| \tag{3.27}$$

and

$$\prod_{k\neq n}^{N-1}\left(1-\frac{\tau_k}{\tau_n}\right) = (-1)^{N-n-1}\prod_{k\neq n}^{N-1}\left|1-\frac{\tau_k}{\tau_n}\right| \tag{3.28}$$

The positive J_n implies that $n-m$ must be an even integer. The simplest case is $n=m$. The cases of $\lambda_N < \tau_n$ and $\tau_n < \lambda_1$ imply that the sign of J_n equals $(-1)^{N-n}$ and $(-1)^n$, respectively. Since $J_n > 0$ must hold irrespective of n and N, we have to exclude the cases of $\lambda_N < \tau_n$ and $\tau_n < \lambda_1$. If $\lambda_m < \tau_n < \tau_{n+1} < \lambda_{m+1}$, then $J_n J_{n+1} < 0$. Therefore, the inequality of Eq. (3.26) must hold.

Direct regression of $s\widetilde{G}(s)$ by the use of the rational approximation is not reliable because the condition of Eq. (3.21) may not be valid. Although it happens to give acceptable results, it is apt to give undesirable results if the range of s is wide. Simhambhatla and Leonov developed the extended Padé–Laplace method which determines the Taylor coefficients of $\widetilde{G}(s)$ systematically and obtains the rational approximation from the Taylor coefficients Simhambhatla and Leonov (1993). However, the method suffers from high-frequency data and needs determination of poles. Malkin and Masalova found negative results for the uniqueness of discrete relaxation spectrum (Malkin and Masalova 2001). In this respect, modeling by spring and dashpot model is not fundamental, but it is sometimes convenient because of reduction of computation time. On the other hand, it was proven by Fuoss and Kirkwood that continuous spectra can be determined uniquely, at least, in principle (Fuoss and Kirkwood 1941). We shall deal with both mathematical and numerical aspects of relaxation and retardation spectra in Chap. 6 in detail.

3.2 Parsimonious Models

To fit data of wide range of time or frequency, Eq. (3.1) [or (3)] needs a number of relaxation (or retardation) times. Hereafter, we shall deal with linear viscoelastic models with a few numbers of parameters. It is interesting that most parsimonious models in this section are originated from dielectric relaxation of organic materials (Riande and Díaz-Calleja 2004). We changed terminologies of dielectrics to those of rheology. There are a number of analogies between viscoelasticity and dielectrics. It is easy to implement high frequencies of the order of MHz at a fixed temperature in dielectrics experiments, while such high frequency is practically

impossible in rheology. This may be the reason why a number of parsimonious models were developed in dielectrics. Note that the analogy to dielectrics gives direct correspondence of dielectric permittivity to recovery compliance rather than relaxation modulus.

3.2.1 The Cole–Cole Model and Modifications

We start from the dynamic response functions of the Maxwell and the Voigt models:

The Maxwell model

$$\begin{aligned} G^*(\omega) &= G_M \frac{i\lambda_M \omega}{1 + i\lambda_M \omega} \\ G'(\omega) &= G_M \frac{\lambda_M^2 \omega^2}{1 + \lambda_M^2 \omega^2}; \quad G''(\omega) = G_M \frac{\lambda_M \omega}{1 + \lambda_M^2 \omega^2} \end{aligned} \tag{3.29a}$$

The Voigt model

$$\begin{aligned} J^*(\omega) &= \frac{J_V}{1 + i\tau_V \omega} \\ J'(\omega) &= \frac{J_V}{1 + \tau_V^2 \omega^2}; \quad J''(\omega) = J_V \frac{\tau_V \omega}{1 + \tau_V^2 \omega^2} \end{aligned} \tag{3.29b}$$

Elimination of frequency in Eqs. (3.29a) and (3.29b) gives the equations for circles:

The Maxwell model

$$\left[G'(\omega) - \frac{G_M}{2}\right]^2 + [G''(\omega)]^2 = \left(\frac{G_M}{2}\right)^2 \tag{3.30a}$$

The Voigt model

$$\left[J'(\omega) - \frac{J_V}{2}\right]^2 + [J''(\omega)]^2 = \left(\frac{J_V}{2}\right)^2 \tag{3.30b}$$

Figure 11 shows the plots of loss components versus storage components: Eqs. (3.30a) and (3.30b). This plot is called the *Cole–Cole plot*.

Although the simple models show semicircle in the Cole–Cole plot, experimental data show distorted and rotated ellipse. Hence, Cole and Cole suggested

$$J^*(\omega) = J_g + \frac{1}{i\eta_o \omega} + \frac{J_r}{1 + (i\tau\omega)^\alpha} \tag{3.31}$$

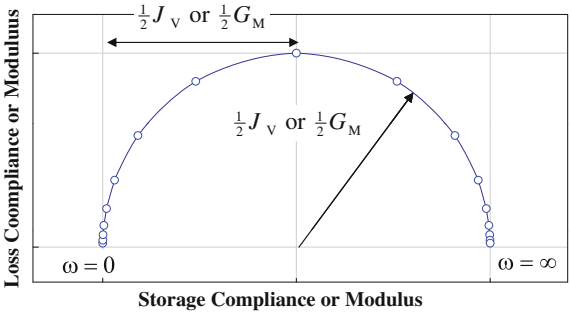

Fig. 11 Cole–Cole plots of the Maxwell and the Voigt models

This is called the *Cole–Cole model* (Cole and Cole 1941). Note that Cole and Cole originally considered dielectric relaxation rather than linear viscoelasticity. After the Cole–Cole, there have been developed the following modifications:

The Davidson–Cole model (Davidson and Cole 1951)

$$J^*(\omega) = J_g + \frac{1}{i\eta_o\omega} + \frac{J_r}{(1+i\tau\omega)^{\beta}} \tag{3.32}$$

The Havriliak–Negami model (1967)

$$J^*(\omega) = J_g + \frac{1}{i\eta_o\omega} + \frac{J_r}{[1+(i\tau\omega)^{\alpha}]^{\beta}} \tag{3.32}$$

The equations for complex compliance can be rewritten by the Laplace transform as follows:

The Cole–Cole model

$$s\widetilde{J}(s) = J_g + \frac{1}{\eta_o s} + \frac{J_r}{1+(\tau s)^{\alpha}} \tag{3.33}$$

The Davidson–Cole model

$$s\widetilde{J}(s) = J_g + \frac{1}{\eta_o s} + \frac{J_r}{(1+\tau s)^{\beta}} \tag{3.34}$$

The Havriliak–Negami model

$$s\widetilde{J}(s) = J_g + \frac{1}{\eta_o s} + \frac{J_r}{[1+(\tau s)^{\alpha}]^{\beta}} \tag{3.35}$$

where $0<\alpha,\ \beta<1$.

Although there is an analytic method to convert Laplace transform to the original function, it is not easy to find $J(t)$ as a closed analytical form from Eqs. (3.33) to (3.35). The use of Euler's formula $e^{i\theta} = \cos\theta + i\sin\theta$ can give real and imaginary parts of the complex compliances. Here, we shall show such decomposition for the Cole–Cole model. Note that $i = \exp(i\pi/2)$. Then, we know that

$$(i\omega\tau)^{\alpha} = \left(e^{\frac{1}{2}\pi i}\omega\tau\right)^{\alpha} = \omega^{\alpha}\tau^{\alpha}e^{i\phi} \tag{3.36}$$

where $\phi = \frac{1}{2}\pi\alpha$. Substitution of Eq. (3.36) to Eq. (3.31) gives

$$J'(\omega) = J_g + J_r\frac{1+z\cos\phi}{1+2z\cos\phi+z^2}; \quad J''(\omega) = \frac{1}{\eta_o\omega} + J_r\frac{z\sin\phi}{1+2z\cos\phi+z^2} \tag{3.37}$$

where $z = \tau^{\alpha}\omega^{\alpha}$. Dynamic moduli are calculated by

$$G'(\omega) = \frac{J'(\omega)}{[J'(\omega)]^2 + [J''(\omega)]^2}; \quad G''(\omega) = \frac{J''(\omega)}{[J'(\omega)]^2 + [J''(\omega)]^2} \tag{3.38}$$

Marin and Graessley (1977) found that linear viscoelasticity of monodisperse polymer melts can be described quite accurately by the extended Cole–Cole model such that

$$J^*(\omega) = J_g + \frac{1}{i\eta_o\omega} + \frac{J_1}{1+(i\tau_1\omega)^{\alpha_1}} + \frac{J_2}{1+(i\tau_2\omega)^{\alpha_2}} \tag{3.39}$$

Without loss of generality, we set $\tau_1 < \tau_2$. Figure 12 show the application of Eq. (3.39) to the dynamic data of polybutadiene (PBD) which was measured by Stadler and Ruymbeke. The molecular weight of PBD is 430 kg/mole. Detailed information is available in Stadler and van Ruymbeke (2010). The data were obtained from time–temperature superposition which will be given in Chap. 7.

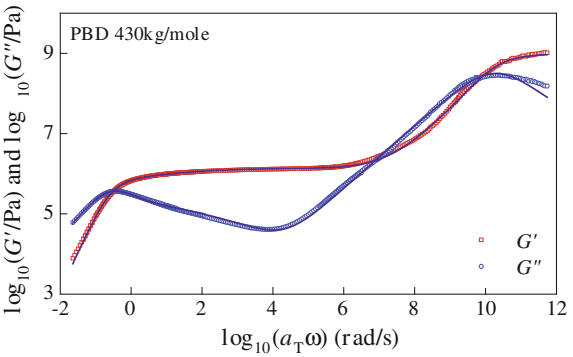

Fig. 12 Application of the extended Cole–Cole model to nearly monodisperse polybutadiene melt. Values of parameters are in Eq. (3.40). Note that $a_T\omega$ is the equivalent frequency from time–temperature superposition (see Chap. 7)

The parameters are determined from the Laplace transform $s\widetilde{J}(s)$ which can be obtained from loss modulus data (Chap. 8). The numerical method will be introduced in Chap. 8. The values are

$$\begin{array}{ll} \eta_o = 2.658 \times 10^6\,\text{Pa s}, & J_1 = 1.162 \times 10^{-6}\,\text{Pa}^{-1} \\ J_2 = 7.274 \times 10^{-7}\,\text{Pa}^{-1}, & J_g = 1.004 \times 10^{-9}\,\text{Pa}^{-1} \\ \tau_1 = 2.136\,\text{s}, & \tau_2 = 2.482 \times 10^{-7}\,\text{s} \\ \alpha_1 = 0.3605, & \alpha_2 = 0.7835 \end{array} \tag{3.40}$$

It is amazing that only 8 parameters fit the dynamic data whose frequency range is about 14 decades. Note that the maximum value of parameter is the order of 10^6, while the minimum value of parameter is the order of 10^{-9}.

3.2.2 Model for Relaxation Spectrum

If we know relaxation spectrum, then relaxation modulus can be calculated by Eq. (3.2) easily. Application of Laplace transform to Eq. (3.2) gives

$$s\widetilde{G}(s) = \int_{-\infty}^{\infty} \frac{\lambda s}{1+\lambda s} H(\lambda)\,\mathrm{d}\log\lambda \tag{3.41}$$

Replacing s by $\mathrm{i}\omega$, we have

$$G'(\omega) = \int_{-\infty}^{\infty} \frac{\lambda^2\omega^2}{1+\lambda^2\omega^2} H(\lambda)\,\mathrm{d}\log\lambda\,; \quad G''(\omega) = \int_{-\infty}^{\infty} \frac{\lambda\omega}{1+\lambda^2\omega^2} H(\lambda)\,\mathrm{d}\log\lambda \tag{3.42}$$

Application of Eq. (3.42) to Eq. (1.59) yields dynamic compliances. It is known that Eq. (3.42) is better than Eqs. (1.42) and (1.43) when data range is finite. If one wants to convert dynamic modulus to relaxation modulus, then it is known that Eq. (3.2) is better than Eq. (1.54). Relaxation spectrum is the most versatile viscoelastic function in linear viscoelasticity. Hence, it is natural to model relaxation spectrum.

Baumgärtel et al. (1990) suggested a model for the relaxation time spectrum of nearly monodisperse polymer melt such that

$$H(\lambda) = \begin{cases} H_e\lambda^{n_e} + \frac{H_g}{\lambda^{n_g}} & \lambda_1 < \lambda < \lambda_{\max} \\ 0 & \text{otherwise} \end{cases} \tag{3.43}$$

This is called the BSW spectrum which was invented from the discrete spectra that were calculated by the algorithm of (Baumgärtel and Winter 1989). This model of relaxation spectrum fits dynamic data very accurately (Baumgärtel et al. 1992).

However, the spectrum of (3.43) is not the correct spectrum of monodisperse polymer melt because more advanced algorithms of continuous relaxation spectrum calculate more complicate but nearly identical spectra from the dynamic data of monodisperse polymer melts (Honerkamp and Weese 1993; Cho and Park 2013; Cho 2013; Bae and Cho 2015). Hence, it can be said that Eq. (3.43) is a simple but effective approximation of realistic spectrum. The ill-posedness of spectrum problem is the reason why such simple approximation gives accurate dynamic modulus (Davies and Anderssen 1997).

Baumgärtel and Winter (1992) extended the BSW spectrum by introducing a stretched exponential cutoff at a characteristic relaxation time λ_{max} as follows:

$$H(\lambda) = \left[n_e G_N^o \left(\frac{\lambda}{\lambda_e} \right)^{n_e} + H_g \left(\frac{\lambda_e}{\lambda} \right)^{n_g} \right] \exp\left[-\left(\frac{\lambda}{\lambda_{max}} \right)^{\beta} \right] \quad \text{for} \quad \overline{M}_W \gg M_e \tag{3.44}$$

This model can be applied to polydisperse polymer melt whose weight-average molecular weight is much higher than entanglement molecular weight M_e.

3.2.3 The KWW Model

In Sect. 3.3 in Chap. 2, various parsimonious models for linear viscoelasticity were introduced. The Kohlrausch–Williams–Watts (KWW) Eq. (3.102) in Chap. 2 is a stretched exponential function whose Fourier transform must be calculated by a numerical method or series approximation. Hence, its applicability is restricted to only relaxation modulus or recovery compliance. Equation (3.102) in Chap. 2 is effective in the description of the relaxation modulus of polymers at near glass transition temperature (Riande et al. 2000).

Originally, KWW equation is analogous to recovery compliance. Hence, we can model creep compliance of viscoelastic fluid as follows:

$$J(t) = \left\{ J_g + \frac{t}{\eta_o} + J_r \left[1 - e^{-(t/\tau)^{\beta}} \right] \right\} \Theta(t) \tag{3.45}$$

Then, the series expansion of complex compliance is given by

$$J^*(\omega) = J_g - \frac{i}{\eta_o \omega} + J_r \sum_{k=1}^{\infty} \frac{(-1)^{k-1}}{(\tau\omega)^{\beta k}} \frac{\Gamma(\beta k + 1)}{\Gamma(k+1)} \exp\left(i \frac{\pi}{2} \beta k \right) \tag{3.46}$$

where $\Gamma(x)$ is the gamma function.

3.3 Models Based on Fractional Derivatives

Some viscoelastic materials show power law–like behavior in dynamic moduli. Representative examples are rubber-like materials. However, even polymer melts show such behavior in some intervals of frequency as shown in Fig. 12 (see the interval of $8 < \log_{10} a_T\omega < 10$). A number of elements of spring and dashpot are necessary if one wishes to fit such viscoelastic behaviors by conventional viscoelastic models based on ordinary springs and dashpots. Hence, various parsimonious models have been developed. Models based on fractional derivatives are the ones replacing ordinary time derivatives of spring–dashpot models by fractional derivatives. One may call the models based on fractional derivatives the fractional spring–dashpot models or the generalized spring–dashpot models. Since there are infinitely many ways to construct spring and dashpot elements, it can be said that the use of fractional spring and dashpot elements is easier to develop a new constitutive equation than the modification of the complex plane model such as the Cole–Cole model.

3.3.1 Fractional Derivatives

In this section, we study how fractional derivatives are defined and mathematical consequences from the definition. At first, consider integration operator defined as

$$\widetilde{I}[f(t)] = \int_0^t f(\tau)\,\mathrm{d}\tau \tag{3.47}$$

Repetition of this operator on a continuous function gives

$$\widetilde{I}^2[f(t)] \equiv \widetilde{I}\left[\widetilde{I}[f(t)]\right] = \int_0^t \left[\int_0^\tau f(\xi)\,\mathrm{d}\xi\right]\mathrm{d}\tau = \int_0^t (t-\tau) f(\tau)\,\mathrm{d}\tau \tag{3.48}$$

Then, for arbitrary positive integer n, we have the Cauchy formula for repeated integration:

$$\widetilde{I}^n[f(t)] = \frac{1}{(n-1)!}\int_0^t (t-\tau)^{n-1} f(\tau)\,\mathrm{d}\tau \tag{3.49}$$

If we are interested in the replacement of n by a noninteger α, then the factorial in Eq. (3.49) can be replaced by the gamma function. Then, we have a generalized operator of repeated integration as follows:

$$\widetilde{I}^{\alpha}[f(t)] = \frac{1}{\Gamma(\alpha)} \int_0^t (t-\tau)^{\alpha-1} f(\tau)\, \mathrm{d}\tau \tag{3.50}$$

where α is a positive real number. This definition results in that for $\alpha > 0$ and $\beta > 0$

$$\widetilde{I}^{\alpha}\left[\widetilde{I}^{\beta}[f(t)]\right] = \widetilde{I}^{\beta}\left[\widetilde{I}^{\alpha}[f(t)]\right] = \widetilde{I}^{\alpha+\beta}[f(t)] = \frac{1}{\Gamma(\alpha+\beta)} \int_0^t (t-\tau)^{\alpha+\beta-1} f(\tau)\, \mathrm{d}\tau \tag{3.51}$$

Here, we used a mathematical identity such that

$$\int_0^1 (1-x)^{\alpha-1} x^{\beta-1} \mathrm{d}x = \frac{\Gamma(\alpha)\Gamma(\beta)}{\Gamma(\alpha+\beta)} \tag{3.52}$$

Hereafter, we consider only the function which is vanishing for $t<0$ whenever fractional calculus such as Eq. (3.50) is considered.

The notion of fractional integration, Eq. (3.50), is apt to be extended to that of fractional derivative of order $\alpha > 0$ by the replacement of α in Eq. (3.50) by $-\alpha$. However, this generalization may give rise to a problem of integral convergence as well as problems of preserving properties of ordinary derivative of integer order. Note that the gamma function has poles at 0, -1, -2, and so on. We denote the operator of fractional derivative by $\widetilde{D}^{\alpha} = \mathrm{d}^{\alpha}/\mathrm{d}t^{\alpha}$. If $m-1<\alpha\leq m$ for a natural number m, then we define

$$\widetilde{D}^{\alpha} = \frac{\mathrm{d}^m}{\mathrm{d}t^m} \widetilde{I}^{m-\alpha}[f(t)] = \frac{1}{\Gamma(m-\alpha)} \frac{\mathrm{d}^m}{\mathrm{d}t^m} \int_0^t \frac{f(\tau)}{(t-\tau)^{\alpha+1-m}} \mathrm{d}\tau \tag{3.53}$$

When $0<\alpha\leq 1$, Eq. (3.53) becomes Eq. (3.103) in Chap. 2. This definition of fractional derivative is called the *Riemann and Liouville derivative*. This fractional derivative for $0<\alpha<1$ has been popularly used in rheology (Bagley and Torvik 1983, 1986; Palade et al. 1996; Song and Jiang 1998; Wharmby and Bagley 2013). On the other hand, some researchers (Jaishankar and McKinley 2013) have used the *Caputo derivative* which is defined by

$$\widetilde{D}_{*}^{\alpha} = \widetilde{I}^{m-\alpha}\left[\frac{\mathrm{d}^m}{\mathrm{d}t^m}f(t)\right] = \frac{1}{\Gamma(m-\alpha)}\int_0^t \frac{1}{(t-\tau)^{\alpha+1-m}}\frac{\mathrm{d}^m f(\tau)}{\mathrm{d}\tau^m}\mathrm{d}\tau \tag{3.54}$$

where $m-1<\alpha\leq m$ and m is a positive integer. This definition requires the integrability of the mth-order derivative. The relation between the two fractional derivatives is found as

$$\widetilde{D}^{\alpha}f(t) = \widetilde{D}_{*}^{\alpha}f(t) + \sum_{k=0}^{m-1}\frac{t^{k-\alpha}}{\Gamma(k-\alpha+1)}f^{(k)}(0^+) \tag{3.55}$$

where $f^{(k)}(t) = \mathrm{d}^k f/\mathrm{d}t^k$. Hereafter, it is assumed that $m-1<\alpha\leq m$ whenever a positive integer m appears in fractional derivative. A number of definitions of fractional derivative found are found in Dalir and Bashour (2010).

Laplace transform of fractional derivative is important in linear viscoelasticity. Note that

$$\widetilde{L}\left[\widetilde{D}^{\alpha}f(t)\right] = s^{\alpha}\widetilde{f}(s) - \sum_{k=0}^{m-1}\left\{\frac{\mathrm{d}^k}{\mathrm{d}t^k}\widetilde{I}^{m-\alpha}[f(t)]\right\}_{t=0^+} s^{m-1-k} \tag{3.56}$$

As for the Caputo derivative

$$\widetilde{L}\left[\widetilde{D}_{*}^{\alpha}f(t)\right] = s^{\alpha}\widetilde{f}(s) - \sum_{k=0}^{m-1}f^{(k)}(0^+)\,s^{\alpha-1-k} \tag{3.57}$$

3.3.2 The Fractional Models

Before considering fractional models, it is necessary to describe their original counterparts. Here, we consider the Maxwell, the Voigt, the Zener (standard solid model), and the Jeffreys models. The Zener model is the parallel connection of Hookean spring and the Maxwell model, and the Jeffreys model is the series connection of the Voigt model and Newtonian dashpot.

The Maxwell model

$$\sigma + \lambda_M\frac{\mathrm{d}\sigma}{\mathrm{d}t} = \eta_M\frac{\mathrm{d}\gamma}{\mathrm{d}t} \quad \text{with} \quad \eta_M = \lambda_M G_M \tag{3.58a}$$

$$G(t) = G_M\exp\left(-\frac{t}{\lambda_M}\right) \tag{3.58b}$$

$$J(t) = \frac{1}{G_M} + \frac{t}{\eta_M} \tag{3.58c}$$

The Voigt model

$$\sigma(t) = G_V\gamma(t) + \eta_V\frac{\mathrm{d}\gamma}{\mathrm{d}t} \quad \text{with} \quad \eta_V = \tau_V G_V \tag{3.59a}$$

$$G(t) = G_V + \eta_V\delta(t) \tag{3.59b}$$

$$J(t) = \frac{1}{G_V}\left[1 - \exp\left(-\frac{t}{\tau_V}\right)\right] \tag{3.59c}$$

The Zener model

$$\sigma + \lambda_M\frac{\mathrm{d}\sigma}{\mathrm{d}t} = G_H\gamma + \lambda_M(G_M + G_H)\frac{\mathrm{d}\gamma}{\mathrm{d}t} \tag{3.60a}$$

$$G(t) = G_H + G_M\exp\left(-\frac{t}{\lambda_M}\right) \tag{3.60b}$$

$$J(t) = \frac{1}{G_M + G_H} + \frac{1}{G_H}\left[1 - \exp\left(-\frac{t}{\tau_Z}\right)\right] \tag{3.60c}$$

$$\tau_Z = \lambda_M\left(1 + \frac{G_M}{G_H}\right) \tag{3.60d}$$

The Jeffreys model

$$\sigma + \lambda_J\frac{\mathrm{d}\sigma}{\mathrm{d}t} = \eta_N\frac{\mathrm{d}\gamma}{\mathrm{d}t} + \eta_N\tau_V\frac{\mathrm{d}^2\gamma}{\mathrm{d}t^2} \tag{3.61a}$$

$$G(t) = \eta_N\frac{\tau_V}{\lambda_J}\delta(t) + \frac{\eta_N}{\lambda_J}\exp\left(-\frac{t}{\lambda_J}\right) \tag{3.61b}$$

$$J(t) = \frac{t}{\eta_N} + \frac{\lambda_J - \tau_V}{\eta_N}\left[1 - \exp\left(-\frac{t}{\tau_V}\right)\right] \tag{3.61c}$$

$$\lambda_J = \frac{\eta_N}{G_V}\left(1 + \frac{\eta_V}{\eta_N}\right) \tag{3.61d}$$

Note that G_H, G_M, and G_V are moduli of the Hookean solid, the Maxwell fluid, and the Voigt solid, respectively; η_N is the viscosity of Newtonian fluid; λ_M is the relaxation time of the Maxwell fluid; and τ_V is the retardation time of the Voigt solid. The constitutive Eqs. (3.58a), (3.59a), (3.60a), and (3.61a) are expressed in a unified manner:

$$\sigma + \sum_{k=1}^{n}(\lambda_k)^k\frac{\mathrm{d}^k\sigma}{\mathrm{d}t^k} = G_1\gamma + \sum_{k=1}^{m}G_k(\tau_k)^k\frac{\mathrm{d}^k\gamma}{\mathrm{d}t^k} \tag{3.62}$$

where λ_k are relaxation times; τ_k are retardation times; and G_k are moduli. We followed the framework of Mainardi and Spada (2011) by emphasizing the physical meaning of parameters.

The fractional counterparts of the four models are the ones to be obtained by the replacement of the ordinary time derivatives by fractional ones. Mainardi and Spada suggested fractional version of Eq. (3.62) as follows:

$$\sigma + \sum_{k=1}^{n} \left(\overline{\lambda}_k\right)^{\alpha_k} \widetilde{D}^{\alpha_k} \sigma = \overline{G}_1 \gamma + \sum_{k=1}^{m} \overline{G}_k (\overline{\tau}_k)^{\alpha_k} \widetilde{D}^{\alpha_k} \gamma \tag{3.63}$$

where $\alpha_k = \alpha + k - 1$ with $0 < \alpha < 1$. Then, the relaxation modulus and creep compliance of the model are calculated as

$$G(t) = G_\infty + \sum_{k=1} G_k E_\alpha \left[-\left(\frac{t}{\lambda_k}\right)^\alpha \right] + \frac{G_N}{\Gamma(1-\alpha)} \left(\frac{t}{\lambda_N}\right)^{-\alpha} \tag{3.64}$$

and

$$J(t) = J_g + \sum_{k=1} J_k \left\{ 1 - E_\alpha \left[-\left(\frac{t}{\tau_k}\right)^\alpha \right] \right\} + \frac{J_P}{\Gamma(1+\alpha)} \left(\frac{t}{\tau_P}\right)^\alpha \tag{3.65}$$

where $E_\alpha(x)$ is the Mittag–Leffler function which is defined by

$$E_\alpha(x) = \sum_{k=0}^{\infty} \frac{x^k}{\Gamma(\alpha k + 1)} \tag{3.66}$$

Note that in general $\overline{\lambda}_k \neq \lambda_k$; $\overline{\tau}_k \neq \tau_k$ and the parameters of Eqs. (3.64) and (3.65) can be expressed in terms of those of Eq. (3.63).

We know that the original Maxwell and Jeffreys models are viscoelastic fluids and the original Voigt and Zener models are viscoelastic solids. As for viscoelastic fluid, it is known that at long-time regime, $J(t) \propto t$. However, the fractional models cannot describe such long-term behavior. Similar trends are found in dynamic moduli. Jaishankar and McKinley (2013) summarized the asymptotic behavior of the dynamic moduli of the fractional Maxwell model.

A strong point of fractional models is to predict the power law behavior of complex materials (Bagley and Torvik 1983; Friedrich 1991; Song and Jiang 1998; Jaishankar and McKinley 2013; Wharmby and Bagley 2013). Unfortunately, these papers deal with experimental data measured over three decades or more. As shown in Fig. 12, power law behavior appears locally in the viscoelastic data of even a monodisperse polymer melt whenever the measurement is sufficiently extended. As for network-like materials such as gel, such power law behavior is usual and the measurement is restricted in comparatively small interval of frequency or time. Hence, in order to fit wide experimental data over ten decades, hybrid-type model might be required. An example is the work of Palade, Verney, and Attane, which fit

wide viscoelastic data of polybutadiene by adopting fractional model only for high-frequency region (Palade et al. 1996). In this respect, the author prefers the Cole–Cole-type models to fractional models because of easy mathematics.

Problem 3

[1] Derive Eq. (3.30) as for complex viscosity.
[2] Derive storage and loss compliances of the Davidson–Cole model, Eq. (3.34).
[3] Derive relaxation modulus, creep compliance, and dynamic moduli of Eq. (3.62).
[4] Derive storage and loss compliances of the Havriliak–Negami model, Eq. (3.35).
[5] As for viscoelastic fluid, the Cole–Cole plot is the plot of $J''(\omega) - (\eta_o \omega)^{-1}$ versus $J'(\omega) - J_g$. Draw the Cole–Cole plots for the Cole–Cole, the Davidson–Cole, and the Havriliak–Negami models with various values of parameters.

4 Molecular Theories

4.1 Dynamic Equation

Here, we consider the situation where every single polymer chain is separated far from other chain by the distance much longer than the size of polymer chain. A dilute polymer solution is a representative example. When molecular weight is lower than the critical molecular weight, polymer chains in molten state behave approximately as an isolated chain. A simple criterion for dilute polymer solution is that mass concentration of polymer (polymer weight per volume of polymer solution) is smaller than the intrinsic viscosity (Larson 2005).

In a dilute solution, motion of a segment is influenced by various interactions such as the interaction with adjacent segments of the same chain, the interaction with segments other than adjacent segments, and the interaction with solvent molecules. The former interaction can be simplified by the introduction of Kuhn monomer which is a collection of a few real monomers. A hypothetical chain consisting of Kuhn monomers, called equivalent chain, behaves like the Gaussian chain. Then, the interaction between adjacent Kuhn monomers in the same chain can be modeled by the entropic spring of Eq. (4.9) in Chap. 4. Then, the potential is given by

$$U_C(\mathbf{r}_1, \cdots, \mathbf{r}_N) = \frac{3k_B T}{2b^2} \sum_{\gamma=1}^{N-1} (\mathbf{r}_{\gamma+1} - \mathbf{r}_\gamma) \cdot (\mathbf{r}_{\gamma+1} - \mathbf{r}_\gamma) = \frac{3k_B T}{2b^2} \sum_{\beta=1}^{N} \sum_{\gamma=1}^{N} A_{\beta\gamma} \mathbf{r}_\beta \cdot \mathbf{r}_\gamma \tag{4.1}$$

where

$$A_{\alpha\beta} = 2\delta_{\alpha\beta}\left(1 - \frac{\delta_{1,\beta} + \delta_{N,\beta}}{2}\right) - \delta_{\alpha+1,\beta} - \delta_{\alpha-1,\beta}$$

$$\left[A_{\alpha\beta}\right] = \begin{bmatrix} 1 & -1 & 0 & 0 & 0 & \cdots & 0 \\ -1 & 2 & -1 & 0 & 0 & \cdots & 0 \\ 0 & -1 & 2 & -1 & 0 & \ddots & 0 \\ 0 & 0 & -1 & 2 & -1 & \ddots & \vdots \\ 0 & \vdots & \ddots & \ddots & \ddots & \ddots & 0 \\ \vdots & 0 & \cdots & 0 & -1 & 2 & -1 \\ 0 & 0 & \cdots & 0 & 0 & -1 & 1 \end{bmatrix} \tag{4.2}$$

From this potential, we know the force acting on the αth Kuhn segment is given by

$$\mathbf{f}_{\alpha}^{(C)} = -\frac{\partial U_C}{\partial \mathbf{r}_{\alpha}} = -\frac{3k_{\mathrm{B}}T}{b^2}\sum_{\gamma=1}^{N} A_{\alpha\gamma}\mathbf{r}_{\gamma} = -\frac{3k_{\mathrm{B}}T}{b^2}\left(2\mathbf{r}_{\alpha} - \mathbf{r}_{\alpha+1} - \mathbf{r}_{\alpha-1}\right) \tag{4.3}$$

The second interaction is called exclusive volume interaction. Any two Kuhn monomers far from each other along the chain connection can be close to each other spatially. Since the exclusive volume interaction prevents the overlap of two different Kuhn monomers, the potential of exclusive volume is approximated by Doi and Edwards (1986)

$$U_{EV} = k_{\mathrm{B}}Tv_{\mathrm{e}}\sum_{\alpha=1}^{N}\sum_{\beta=1}^{N}\delta\left(\mathbf{r}_{\alpha} - \mathbf{r}_{\beta}\right) \tag{4.4}$$

where v_{e} is the exclusive volume of Kuhn monomer and modeled by

$$v_e = v_e^{(0)}\left(1 - \frac{T_{\Theta}}{T}\right) \tag{4.5}$$

where T_{Θ} is the theta temperature of the solution which depends on the chi parameter of the solution (Rubinstein and Colby 2003). Since Eq. (4.4) includes the Dirac delta function, it is difficult to express the force due to exclusive volume effect. Hence, it may be replaced by (Doi and Edwards 1986)

$$U_{EV} = k_{\mathrm{B}}Tv_{\mathrm{e}}\sum_{\alpha=1}^{N} c^2(\mathbf{r}_{\alpha}) \tag{4.6}$$

where $c(\mathbf{r})$ is the local concentration of Kuhn monomer.

The effects of solvent molecules are modeled by two contributions: stochastic force and dissipative force. The stochastic force is the random force acting on Kuhn

monomer and is the key point of the Langevin equation. We denote the random force by $\mathbf{f}_\alpha^{(R)}$. The dissipative force is the friction force due to difference between velocities of the Kuhn monomer and ambient solvent molecules. Then, the use of Stokes Eq. (3.2) in Chap. 3 gives the friction force acting on the αth Kuhn monomer:

$$\mathbf{f}_\alpha^{(F)} = -\zeta\left(\frac{\mathrm{d}\mathbf{r}_\alpha}{\mathrm{d}t} - \mathbf{v}(\mathbf{r}_\alpha)\right) \quad \text{with} \quad \zeta = 6\pi\eta_s b \tag{4.7}$$

where η_s is the viscosity of the pure solvent liquid and $\mathbf{v}(\mathbf{r}_\alpha)$ is the solvent velocity near the αth Kuhn monomer. The velocity of the solvent is usually modeled by

$$\mathbf{v}(\mathbf{r}_\alpha) = \mathbf{L}\cdot\mathbf{r}_\alpha - \sum_{\beta=1}^{N}\mathbf{H}_{\alpha\beta}\cdot\mathbf{f}_\beta^{(F)} \tag{4.8}$$

where $\mathbf{L}$ is the velocity gradient defined in continuum mechanics and $\mathbf{H}_{\alpha\beta}$ is the mobility tensor. The mobility tensor gives the velocity perturbation due to the motion of other Kuhn monomer (Doi and Edwards 1986). This interaction is called the *hydrodynamic interaction*. The tensor $\mathbf{H}_{\alpha\beta}$ can be calculated by solving the Stokes equation with Fourier transform (Doi and Edwards 1986; Deen 1998):

$$\mathbf{H}_{\alpha\beta} = \frac{1}{8\pi\eta_s r_{\alpha\beta}}\left(\mathbf{I} + \frac{\mathbf{r}_{\alpha\beta}\mathbf{r}_{\alpha\beta}}{r_{\alpha\beta}^2}\right) \tag{4.9}$$

where

$$r_{\alpha\beta} = \left\|\mathbf{r}_\alpha - \mathbf{r}_\beta\right\|; \quad \mathbf{r}_{\alpha\beta} = \mathbf{r}_\alpha - \mathbf{r}_\beta \tag{4.10}$$

Note that since the motion of a Kuhn monomer cannot influence that of the Kuhn monomer itself through the perturbation of solvent motion, it is obvious to define $\mathbf{H}_{\alpha\beta} = \mathbf{0}$ whenever $\alpha = \beta$.

Arrangement of Eq. (4.7) gives

$$\sum_{\gamma=1}^{N}\mathbf{M}_{\beta\gamma}\cdot\mathbf{f}_\gamma^{(F)} = -\zeta\left(\frac{\mathrm{d}\mathbf{r}_\beta}{\mathrm{d}t} - \mathbf{L}\cdot\mathbf{r}_\beta\right) \tag{4.11}$$

where

$$\mathbf{M}_{\beta\gamma} = \delta_{\beta\gamma}\mathbf{I} + \zeta\,\mathbf{H}_{\beta\gamma} \tag{4.12}$$

Let the inverse of $\mathbf{M}_{\alpha\beta}$ be denoted by $\mathbf{M}_{\alpha\beta}^{-1}$ then Eq. (4.11) becomes

$$\mathbf{f}_\alpha^{(F)} = -\zeta\sum_{\beta=1}^{N}\mathbf{M}_{\alpha\beta}^{-1}\cdot\left(\frac{\mathrm{d}\mathbf{r}_\beta}{\mathrm{d}t} - \mathbf{L}\cdot\mathbf{r}_\beta\right) \tag{4.13}$$

It is difficult to calculate the inverse of $\mathbf{M}_{\alpha\beta}$ exactly. For two-particle chain (dumbbell model), the exact equation is found in Pokrovskii (2000).

As for polymer melts with molecular weight less than the critical molecular weight, it is known that chain conformation is equivalent to that in theta solution. It is the *Flory theorem* that conformation of polymer chains in molten state is equivalent to that of ideal chain (De Gennes 1979). Hence, in such polymer melts, it is not necessary to consider the interaction of exclusive volume effect. Since there is no solvent in molten polymer with short chain, it is not necessary to consider hydrodynamic interaction, neither. Then, Eq. (4.13) becomes for melt of short chains:

$$\mathbf{f}_{\alpha}^{(F)} = -\zeta\left(\frac{\mathrm{d}\mathbf{r}_{\alpha}}{\mathrm{d}t} - \mathbf{L}\cdot\mathbf{r}_{\alpha}\right) \tag{4.14}$$

Although there are no solvent molecules in such melt with short chains, contact of the pervade volumes of different chains might result in stochastic random force.

In semi-dilute solution without entanglement, it is known that the hydrodynamic interaction is strong within the length scale called the *hydrodynamic screening length* ξ_h which approximately equals the static correlation length ξ (Rubinstein and Colby 2003). Since $\xi \approx b\phi^{-\nu/(3\nu-1)}$, both exclusive volume and hydrodynamic interactions in melt disappear because $\phi = 1$ and $\xi \approx b$ (Rubinstein and Colby 2003).

In polymer melt with entanglement, interactions with other segments become important. We shall express the force due to surrounding segments by $\mathbf{f}_{\alpha}^{(s)}$. Since the force $\mathbf{f}_{\alpha}^{(s)}$ depends on the conformation changes of surrounding chains, modeling $\mathbf{f}_{\alpha}^{(s)}$ is really difficult. The tube model is to replace $\mathbf{f}_{\alpha}^{(s)}$ by the reptation of chain in a hypothetical tube. Then, the many-chain problem due to $\mathbf{f}_{\alpha}^{(s)}$ can be reduced to a single-chain problem.

In summary, the dynamic equation of Kuhn monomer can be expressed formally by the Langevin equation:

$$\mu\frac{\mathrm{d}^2\mathbf{r}_{\alpha}}{\mathrm{d}t^2} = \mathbf{f}_{\alpha}^{(C)} + \mathbf{f}_{\alpha}^{(EV)} + \mathbf{f}_{\alpha}^{(s)} + \mathbf{f}_{\alpha}^{(F)} + \mathbf{f}_{\alpha}^{(R)}(t) \tag{4.15}$$

where μ is the mass of Kuhn monomer and $\mathbf{f}_{\alpha}^{(EV)}$ is the force due to the exclusive volume effect. Because hydrodynamic interaction covers the exclusive volume effect (Rubinstein and Colby 2003), Eq. (4.15) can be rewritten by

$$\mu\frac{\mathrm{d}^2\mathbf{r}_{\alpha}}{\mathrm{d}t^2} = \mathbf{f}_{\alpha}^{(C)} + \mathbf{f}_{\alpha}^{(s)} + \mathbf{f}_{\alpha}^{(F)} + \mathbf{f}_{\alpha}^{(R)}(t) \tag{4.16}$$

where the friction force $\mathbf{f}_{\alpha}^{(F)}$ includes the hydrodynamic interaction through Eq. (4.13).

In dilute solution, Eq. (4.15) becomes

$$\mu \frac{\mathrm{d}^2 \mathbf{r}_\alpha}{\mathrm{d}t^2} = -\frac{3k_\mathrm{B}T}{b^2} \sum_{\gamma=1}^{N} A_{\alpha\gamma} \mathbf{r}_\gamma - \zeta \left(\frac{\mathrm{d}\mathbf{r}_\alpha}{\mathrm{d}t} - \mathbf{L} \cdot \mathbf{r}_\alpha \right) + \mathbf{f}_\alpha^{(R)}(t) \tag{4.17}$$

and

$$\mu \frac{\mathrm{d}^2 \mathbf{r}_\alpha}{\mathrm{d}t^2} = -\frac{3k_\mathrm{B}T}{b^2} \sum_{\gamma=1}^{N} A_{\alpha\gamma} \mathbf{r}_\gamma - \zeta \sum_{\beta=1}^{N} \mathbf{M}_{\alpha\beta}^{-1} \cdot \left(\frac{\mathrm{d}\mathbf{r}_\beta}{\mathrm{d}t} - \mathbf{L} \cdot \mathbf{r}_\beta \right) + \mathbf{f}_\alpha^{(R)}(t) \tag{4.18}$$

Equation (4.17) is the one without hydrodynamic interaction, while Eq. (4.18) is the one with hydrodynamic interaction.

Most solvents for polymer have the viscosity whose order of magnitude is about 10^{-3} Pa s, the size of Kuhn monomers of most polymers have the order of magnitude of 10^{-9} m, and the mass of Kuhn monomers is of the order of 10^{-24} kg. Hence, using the Stokes Eq. (3.2) in Chap. 3, the order of ζ is about 10^{-11} Nm^{-1} s. If the room temperature is assumed, then we know that the inertia term is negligible because

$$\frac{\mu}{\zeta} \sim 10^{-13}; \quad \frac{k_\mathrm{B}T}{\zeta b^2} \sim 10^{8} \tag{4.19}$$

Then, Eqs. (4.17) and (4.18) can be approximated by

$$\frac{\mathrm{d}\mathbf{r}_\alpha}{\mathrm{d}t} = \mathbf{L} \cdot \mathbf{r}_\alpha - \frac{k}{\zeta} \sum_{\gamma=1}^{N} A_{\alpha\gamma} \mathbf{r}_\gamma + \mathbf{g}_\alpha(t) \tag{4.20}$$

and

$$\frac{\mathrm{d}\mathbf{r}_\alpha}{\mathrm{d}t} = \mathbf{L} \cdot \mathbf{r}_\alpha - \frac{k}{\zeta} \sum_{\beta=1}^{N} \sum_{\gamma=1}^{N} A_{\beta\gamma} \mathbf{M}_{\alpha\beta} \cdot \mathbf{r}_\gamma + \sum_{\beta=1}^{N} \mathbf{M}_{\alpha\beta} \cdot \mathbf{g}_\beta(t) \tag{4.21}$$

where

$$k = \frac{3k_\mathrm{B}T}{b^2}; \quad \mathbf{g}_\alpha = \frac{1}{\zeta} \mathbf{f}_\alpha \tag{4.22}$$

Note that

$$\langle \mathbf{g}_\alpha(t) \rangle = \mathbf{0}; \quad \langle \mathbf{g}_\alpha(t) \mathbf{g}_\beta(t') \rangle = \frac{2k_\mathrm{B}T}{\zeta} \delta_{\alpha\beta} \delta(t - t') \mathbf{I} \tag{4.23}$$

The dynamic equation of entangled system must be different from Eqs. (4.20) to (4.21) because the surrounding effect $\mathbf{f}_\alpha^{(s)}$ will be replaced by the tube. Dynamic equation of entangled system will be discussed separately later.

4.2 The Stress of Polymeric Fluid

Stress of simple fluid has been derived in Eq. (2.118) in Chap. 3 where the first term can be reduced isotropic pressure, while the second term represents the effect of molecular interaction. Similar equation can be obtained from the Chandrasekhar Eq. (3.90) in Chap. 3 by deriving momentum balance equation. Similar approach for polymeric fluid is found in Pokrovskii (2000). Simpler derivation of polymer stress is found in Doi and Edwards (1986) and Doi (1996). The Doi's approach is to consider only chain connecting force $\mathbf{f}_\alpha^{(C)}$. This is the most dominant contribution to the stress of polymeric fluid. Hence, we will follow the approximation because it is simple as well as because it agrees well with experimental data.

From the analysis in Sect. 2.3 in Chap. 3, we know the polymer stress is the ensemble average of the internal virial tensor $\hat{\mathbf{V}}_{\text{in}}$:

$$\hat{\mathbf{V}}_{\text{in}} = \frac{1}{2}\sum_{\alpha=1}^{L}\sum_{\gamma\neq\alpha}^{L}\mathbf{f}_{\alpha\gamma}\mathbf{r}_{\alpha\gamma} \tag{4.24}$$

In Eq. (4.24), particles are Kuhn monomers of various chains and solvent molecules. Hence, a rigorous approach needs to use new notations for particle identification. However, we will follow Doi's approach such that only a single chain is considered and only nonzero forces among $\mathbf{f}_{\alpha\gamma}$ are

$$\mathbf{f}_{\alpha,\alpha+1} = -k\left(\mathbf{r}_\alpha - \mathbf{r}_{\alpha+1}\right) \quad \text{and} \quad \mathbf{f}_{\alpha,\alpha-1} = -k\left(\mathbf{r}_\alpha - \mathbf{r}_{\alpha-1}\right) \tag{4.25}$$

Then, Eq. (4.24) is given by

$$\hat{\mathbf{V}}_{\text{in}} = -k\sum_{\alpha=1}^{N-1}(\mathbf{r}_\alpha - \mathbf{r}_{\alpha+1})(\mathbf{r}_\alpha - \mathbf{r}_{\alpha+1}) \tag{4.26}$$

With the help of Eq. (2.90) in Chap. 3, we have the stress of a single polymer chain:

$$\mathbf{T} = -p\mathbf{I} - \frac{1}{\Omega}\left\langle\hat{\mathbf{V}}_{\text{in}}\right\rangle = -p\mathbf{I} + \frac{k}{\Omega}\sum_{\alpha=1}^{N-1}\left\langle(\mathbf{r}_{\alpha+1} - \mathbf{r}_\alpha)(\mathbf{r}_{\alpha+1} - \mathbf{r}_\alpha)\right\rangle \tag{4.27}$$

where the momentum term of Eq. (2.110) in Chap. 3 is replaced by the hydrostatic pressure. If all chains are assumed to contribute to stress independently, then Eq. (4.27) becomes

$$\mathbf{T} = -p\mathbf{I} + \frac{\rho_{\text{num}}}{N} k \sum_{\alpha=1}^{N-1} \langle (\mathbf{r}_{\alpha+1} - \mathbf{r}_{\alpha})(\mathbf{r}_{\alpha+1} - \mathbf{r}_{\alpha}) \rangle \tag{4.28}$$

where ρ_{num} is the number density of Kuhn monomers and N is the number of Kuhn monomers in a single chain. Equation (4.28) is the stress equation derived by Doi (1996). Note that the total number of chains in the volume Ω is $\rho_{\text{num}}\Omega/N$.

It must be noted that Eq. (4.28) does not consider any effect of neighbor chains. Hence, nematic effect is neglected in Eq. (4.28). The validity of Eq. (4.28) is discussed in Doi and Edwards (1986), Doi (1996), and Watanabe (1999).

4.3 The Rouse Model

The Rouse model is the first molecular theory which describes experimental data quite successfully when hydrodynamic interaction is negligible (Rouse 1953). The Rouse model is given by Eq. (4.20). We need to integrate Eq. (4.20) in order to derive the linear viscoelastic functions of the Rouse model. This is a system of linear ordinary differential equations. To solve this, we have to use the normal coordinate which makes the second term of the right-hand side of Eq. (4.20) diagonalized. This approach needs a long algebraic calculation. This approach is found in Pokrovskii (2000), Lin (2003), and Teraoka (2002). Since Eq. (4.28) is a rough approximation, it is convenient to use continuous monomer index instead of discrete index α. Then, we adopt the transform such that $\mathbf{r}_{\alpha}(t) \to \mathbf{r}(n,t)$ and $\mathbf{g}_{\alpha} \to \mathbf{g}(n,t)$. The dynamic equation of the Rouse model becomes

$$\frac{\partial \mathbf{r}}{\partial t} = \frac{k}{\zeta}\frac{\partial^2 \mathbf{r}}{\partial n^2} + \mathbf{L}\cdot\mathbf{r} + \mathbf{g}(n,\ t) \tag{4.29}$$

Note that we used

$$\sum_{\gamma=1}^{N} A_{\alpha\gamma}\mathbf{r}_{\gamma} = 2\mathbf{r}_{\alpha} - \mathbf{r}_{\alpha+1} - \mathbf{r}_{\alpha-1} \to \frac{\partial^2 \mathbf{r}}{\partial n^2} \tag{4.30}$$

The continuous index runs from 0 to N. For $n = 0$ and $n = N$, we know that

$$\begin{aligned} \frac{\mathrm{d}\mathbf{r}_0}{\mathrm{d}t} &= \frac{k}{\zeta}(\mathbf{r}_1 - \mathbf{r}_0) + \mathbf{L}\cdot\mathbf{r}_0 + \mathbf{g}_0 \\ \frac{\mathrm{d}\mathbf{r}_N}{\mathrm{d}t} &= \frac{k}{\zeta}(\mathbf{r}_{N-1} - \mathbf{r}_N) + \mathbf{L}\cdot\mathbf{r}_N + \mathbf{g}_N \end{aligned} \tag{4.31}$$

Adding hypothetical Kuhn monomers such as

$$\mathbf{r}_{-1} = \mathbf{r}_0; \quad \mathbf{r}_{N+1} = \mathbf{r}_N \tag{4.32}$$

Equation (4.31) can be transformed to Eq. (4.29). The boundary condition of Eq. (4.32) is transformed to

$$\frac{\partial \mathbf{r}}{\partial n} = \mathbf{0} \quad \text{at} \quad n = 0 \quad \text{and} \quad n = N \tag{4.33}$$

Note that the continuous transform for monomer index transforms, Eq. (4.28), as follows:

$$\mathbf{T} = -p\mathbf{I} + \frac{\rho_{\text{num}} k}{N} \sum_n^N \left\langle \frac{\partial \mathbf{r}}{\partial n} \frac{\partial \mathbf{r}}{\partial n} \right\rangle \tag{4.34}$$

The use of continuous monomer index is to see a flexible chain as a continuous curve with the parameter of n. This is called the continuous chain model. Just as the discrete Rouse model, the continuous Rouse model can be solved by the use of a normal coordinate which is a finite Fourier transform. The normal coordinate is defined as

$$\mathbf{x}_p(t) = \frac{1}{N} \int_0^N \cos \frac{\pi p n}{N} \mathbf{r}(n,\ t)\, \mathrm{d}n \tag{4.35}$$

This technique for solving linear partial differential equation is explained in detail in Deen (1998). Note that

$$\frac{1}{N} \int_0^N \cos \frac{\pi p n}{N} \frac{\partial^2 \mathbf{r}}{\partial n^2} \mathrm{d}n = -\left(\frac{\pi p}{N}\right)^2 \mathbf{x}_p(t) \tag{4.36}$$

where we used integration by parts twice and the boundary condition, Eq. (4.33). The boundary condition indicates why we used $\cos(\pi pn/N)$ instead of $\sin(\pi pn/N)$. Application of the finite Fourier transform to Eq. (4.29) gives

$$\frac{\mathrm{d}\mathbf{x}_p}{\mathrm{d}t} = -\frac{k_p}{\zeta_p} \mathbf{x}_p + \mathbf{L} \cdot \mathbf{x}_p + \hat{\mathbf{g}}_p \tag{4.37}$$

where

$$\zeta_0 = N\zeta; \quad \zeta_p = 2N\zeta; \quad k_p = \frac{2\pi^2 p^2 k}{N} = \frac{6\pi^2 k_{\text{B}} \theta}{Nb^2} p^2 \tag{4.38}$$

and

$$\hat{\mathbf{g}}_p = \frac{1}{N}\int_0^N \cos\frac{\pi p n}{N}\mathbf{g}(n,\ t)\,\mathrm{d}n \tag{4.39}$$

From Eq. (4.23), we have

$$\left\langle \hat{\mathbf{g}}_p(t)\right\rangle = \mathbf{0}\,;\quad \left\langle \hat{\mathbf{g}}_p(t)\hat{\mathbf{g}}_q(t')\right\rangle = 2\frac{k_\mathrm{B}T}{\zeta_p}\delta_{pq}\mathbf{I}\delta(t-t') \tag{4.40}$$

With the help of the finite Fourier transform, Eq. (4.34) can be rewritten by

$$\mathbf{T} = -p\mathbf{I} + \frac{c}{N}\sum_p k_p\left\langle \mathbf{x}_p(t)\mathbf{x}_p(t)\right\rangle \tag{4.41}$$

Consider simple shear $\mathbf{L} = \dot{\gamma}(t)\,\mathbf{e}_1\mathbf{e}_2$ in order to calculate the linear viscoelastic function of the Rouse model. Then, Eq. (4.37) can be rewritten in a component-wise manner:

$$\frac{\mathrm{d}x_{p1}}{\mathrm{d}t} = -\frac{k_p}{\zeta_p}x_{p1} + \dot{\gamma}x_{p2} + \hat{g}_{p1}; \tag{4.42a}$$

$$\frac{\mathrm{d}x_{p2}}{\mathrm{d}t} = -\frac{k_p}{\zeta_p}x_{p2} + \hat{g}_{p2}; \tag{4.42b}$$

$$\frac{\mathrm{d}x_{p3}}{\mathrm{d}t} = -\frac{k_p}{\zeta_p}x_{p3} + \hat{g}_{p3} \tag{4.42c}$$

Integrating Eqs. (4.42a, b) and taking the ensemble average, we have

$$T_{12}(t) = \int_{-\infty}^{t} G(t-t')\,\dot{\gamma}(t')\,\mathrm{d}t' \tag{4.43}$$

where

$$G(t) = \frac{\rho_\mathrm{num}}{N}k_\mathrm{B}T\sum_{p=1}^{\infty}\exp\left(-\frac{2t}{\lambda_p}\right) \tag{4.44}$$

Note that

$$\lambda_p = \frac{\lambda_R}{p^2} \tag{4.45}$$

where

$$\lambda_R = \frac{1}{\pi^2}\frac{\zeta N^2}{k} = \frac{\zeta b^2 N^2}{3\pi^2 k_B T} \tag{4.46}$$

Since $\lambda_R = \lambda_1 > \lambda_2 > \cdots$, we have

$$\begin{aligned}\sum_{p=1}^{\infty} e^{-t/\lambda_p} &= e^{-t/\lambda_R}\sum_{p=1}^{\infty}\exp\left(-\frac{2p^2-1}{\lambda_R}t\right) \approx Ne^{-t/\lambda_R}\int_0^{\infty}\exp\left(-\frac{2t}{\lambda_o}x^2\right)\mathrm{d}x \\ &= \frac{N}{2}\sqrt{\frac{\pi\lambda_o}{2t}}e^{-t/\lambda_R}\end{aligned} \tag{4.47}$$

where $\lambda_o = \lambda_R N^{-2}$, $\mathrm{d}x = N^{-1}$, $x = p/N$ and $1/N^2 \approx 0$ was used. Then, we can replace the infinite series by a closed expression:

$$G(t) \approx \phi\frac{k_B T}{b^3}\sqrt{\frac{\lambda_o}{t}}\exp\left(-\frac{t}{\lambda_R}\right) \quad \text{for } t > \lambda_o \tag{4.48}$$

where ϕ is the volume fraction of polymer, which can be calculated by $b^3\rho_{num} = \phi$ under the assumption that the volume of Kuhn monomer is approximately b^3. Equation (4.48) is the approximation obtained by Rubinstein and Colby using similarity (Rubinstein and Colby 2003).

In order to calculate dynamic moduli, we rewrite Eq. (4.48) as follows:

$$G(t) = \phi\frac{k_B T}{b^3 N}\sqrt{\frac{\lambda_R}{t}}\exp\left(-\frac{t}{\lambda_R}\right) \tag{4.49}$$

where we used $\lambda_o = \lambda_R N^{-2}$. The Laplace transform of the relaxation modulus is calculated

$$s\widetilde{G}(s) = \phi\frac{k_B T}{b^3 N}s\int_0^{\infty}\sqrt{\frac{\lambda_R}{t}}\exp\left(-\frac{t}{\lambda_R}-st\right)\mathrm{d}t = \sqrt{\pi}\phi\frac{k_B T}{b^3 N}\frac{\lambda_R s}{\sqrt{1+\lambda_R s}} \tag{4.50}$$

Here, we used variable transforms such as $t = \lambda_R\tau$ and $x = \sqrt{\tau}$. Substitution of $s = \mathrm{i}\omega$ gives

$$G^*(\omega) = \sqrt{\pi}\phi\frac{k_B T}{b^3 N}\frac{\mathrm{i}\lambda_R\omega}{\sqrt{1+\mathrm{i}\lambda_R\omega}} = \sqrt{\pi}\phi\frac{k_B T}{b^3 N}\lambda_R\omega\frac{\sin\left(\frac{1}{2}\theta\right)+\mathrm{i}\cos\left(\frac{1}{2}\theta\right)}{\left(1+\lambda_R^2\omega^2\right)^{1/4}} \tag{4.51}$$

where $\theta = \arctan \lambda_R \omega$. Note that

$$\sin\frac{\theta}{2} = \sqrt{\frac{\sqrt{1+\lambda_R^2\omega^2}-1}{2\sqrt{1+\lambda_R^2\omega^2}}}; \quad \cos\frac{\theta}{2} = \sqrt{\frac{\sqrt{1+\lambda_R^2\omega^2}+1}{2\sqrt{1+\lambda_R^2\omega^2}}} \tag{4.52}$$

The use of Eq. (4.52) gives the dynamic moduli of the Rouse model as follows:

$$\begin{aligned} G'(\omega) &\approx \sqrt{\frac{\pi}{2}}\phi\frac{k_B T}{b^3 N}\frac{\lambda_R^2\omega^2}{\sqrt{\sqrt{1+\lambda_R^2\omega^2}\left(1+\sqrt{1+\lambda_R^2\omega^2}\right)}}; \\ G''(\omega) &\approx \sqrt{\frac{\pi}{2}}\phi\frac{k_B T}{b^3 N}\lambda_R\omega\sqrt{\frac{1+\sqrt{1+\lambda_R^2\omega^2}}{1+\lambda_R^2\omega^2}} \end{aligned} \tag{4.53}$$

for $\omega < \lambda_o^{-1}$.

The zero-shear viscosity can be calculated by the use of (1.64):

$$\eta_o = \lim_{\omega\to 0}\frac{G''(\omega)}{\omega} = \sqrt{\frac{\pi}{2}}\phi\frac{k_B T}{b^3 N}\lambda_R = \sqrt{\frac{\pi}{2}}\phi\frac{k_B T}{b^3}\lambda_o N \tag{4.54}$$

The steady-state compliance can be calculated by

$$J_e^o = \frac{1}{\eta_o^2}\lim_{\omega\to 0}\frac{G'(\omega)}{\omega^2} = \sqrt{\frac{2}{\pi}}\frac{b^3}{\phi k_B T}N \tag{4.55}$$

The Rouse model predicts that both zero-shear viscosity and steady-state compliance are proportional to molecular weight. Equations (4.54) and (4.55) imply that the mean relaxation time is $\overline{\lambda} = \lambda_R \propto N^2$.

Figure 10 shows the comparison of Eq. (4.53) with experimental data which were measured for cellulose solutions whose concentrations are slightly higher than the overlap concentration. The data were obtained from Fig. 6 of Lu et al. (2013). Figure 10 shows that both $G'(\omega)$ and $G''(\omega)$ are proportional to ω^2 in high-frequency regime.

Equation (4.50) does not give the conventional form of the Laplace transform of the creep compliance of viscoelastic liquid such that

$$s\widetilde{J}(s) = J_g + \frac{1}{\eta_o s} + J_r s\widetilde{\Psi}(s) \tag{4.56}$$

It is because Eq. (4.49) shows that relaxation modulus goes to infinite as time goes to zero. Hence, we modify Eq. (4.49) as follows:

$$G(t) = \begin{cases} G_{\mathrm{o}} \exp\left(-\frac{\lambda_{\mathrm{o}}}{\lambda_R}\right) & 0 < t < \lambda_{\mathrm{o}} \\ G_{\mathrm{o}} \sqrt{\frac{\lambda_{\mathrm{o}}}{t}} \exp\left(-\frac{t}{\lambda_R}\right) & \lambda_{\mathrm{o}} < t \end{cases} \tag{4.57}$$

where

$$G_{\mathrm{o}} = \phi \frac{k_{\mathrm{B}} T}{b^3 N} \tag{4.58}$$

Then, we have

$$s\widetilde{G}(s) = \frac{G_{\mathrm{o}}}{s} e^{-\lambda_{\mathrm{o}}/\lambda_R} \left(1 - e^{-\lambda_{\mathrm{o}} s}\right) + \sqrt{\pi} G_{\mathrm{o}} \lambda_{\mathrm{o}} s \frac{\mathrm{Erfc}\left(\sqrt{\lambda_{\mathrm{o}} s + \lambda_R^{-1}}\right)}{\sqrt{\lambda_{\mathrm{o}} s + \lambda_R^{-1}}} \tag{4.59}$$

The reciprocal of Eq. (4.59) obeys Eq. (4.56). However, Eq. (4.59) is too complicate, while the Rouse model itself is a rough approximation. One may calculate J_g, J_r, and η_{o} from Eq. (4.59) with the help of theorem of the initial and final values for Laplace transform. Most theories of viscoelastic constitutive equations have the common features:

[1] Stress is derived from given deformation field.
[2] The models deal with a finite range of frequency (or time) and are not valid for the whole frequency (or time).

We will learn the Doi–Edwards theory later, which is valid in lower-frequency range and cannot be applied to the frequency range of the Rouse model. On the other hand, the Rouse model is not valid for lower-frequency range. Each model describes local behaviors rather than the global behaviors. Most papers on molecular simulation of polymer viscoelasticity are based on the assumption that the whole viscoelasticity might be the sum of the modulus of the two models (Benallal et al. 1993; Pattamaprom et al. 2000; Pattamaprom and Larson 2001): additivity of stresses of the two regimes. A question arises: What is the foundation of such assumption? One may think that when a constant stress is given, fast mode of molecular motion gives rise to deformation first in short-time regime and then slow mode adds further deformation. This picture of viscoelasticity of polymeric fluid might be represented by the modified Cole–Cole model, Eq. (3.39), if the third term is considered as the slow mode and the fourth term as the fast mode. Further research is necessary for this argument.

4.4 The Zimm Model

Although the Rouse model predicts $\overline{\lambda} \sim \lambda_R \propto N^2$, experimental data reveal that $\overline{\lambda} \propto N^{3\nu}$ where $\nu \approx 3/5$ for good solvent and $\nu = 1/2$ for Θ-solvent. The origin of the deviation was thought as the absence of hydrodynamic interaction. Hence, Zimm introduced the hydrodynamic interaction and tried to calculate Eq. (4.21). However, it is very difficult to solve the equation without any approximation. If preaverage was applied, then the relaxation modulus of the Zimm model is given by

$$G(t) \approx \phi \frac{k_B T}{b^3} \left(\frac{\lambda_o}{t}\right)^{\frac{1}{3\nu}} \exp\left(-\frac{t}{\lambda_Z}\right) \quad \text{for} \quad t > \lambda_o \tag{4.60}$$

where

$$\lambda_Z = \lambda_o N^{3\nu} \tag{4.61}$$

Then, counterpart of Eq. (4.53) is given by

$$\begin{aligned} G'(\omega) &\approx \phi \frac{k_B T}{b^3 N} \frac{\lambda_Z \omega \sin\left[\left(1-(3\nu)^{-1}\right)\arctan(\lambda_Z\omega)\right]}{\left[1+(\lambda_Z\omega)^2\right]^{\frac{1}{2}\left(1-(3\nu)^{-1}\right)}}; \\ G''(\omega) &\approx \phi \frac{k_B T}{b^3 N} \frac{\lambda_Z \omega \cos\left[\left(1-(3\nu)^{-1}\right)\arctan(\lambda_Z\omega)\right]}{\left[1+(\lambda_Z\omega)^2\right]^{\frac{1}{2}\left(1-(3\nu)^{-1}\right)}} \end{aligned} \tag{4.62}$$

for $\omega < \lambda_o^{-1}$.

Readers interested in more detailed calculation are recommended to refer to Doi and Edwards (1986), Doi (1996), and Lin (2003). If interested in physical interstation, refer to Rubinstein and Colby (2003).

4.5 The Doi–Edwards Model

Linear viscoelasticity of polymeric fluid consisting of linear polymers changes dramatically if entanglement occurs. As for polymer melts, zero-shear viscosity increases as $M^{3.5\pm0.1}$ when molecular weight M is higher than the critical molecular weight M_C as mentioned in Eq. (3.68) in Chap. 2. This phenomenon has been a mystery for a long time until the Doi–Edwards model was developed (Doi and Edwards 1986).

4.5.1 Basic Concepts

When temperature is sufficiently high, dominant molecular interaction is repulsive one rather than attractive one. The repulsive interaction is mediated by the collision of molecules. When a small molecule collides with one another, the collision makes them apart faraway. On the other hand, collision between two segments of polymeric chains cannot separate the two segments to a far distance because the segments are connected with the segments of their chains. A single collision cannot alter the conformation of the whole chain to which the segments belong. Hence, the two adjacent chains contact persistently during the time whose order is approximately equivalent to L^2/D where L is the characteristic size of the chain and D is the diffusion constant for the motion of polymer chain. Hence, the influence of neighbor chains on a chain's motion can be approximated as that of fixed obstacles. The tube model is to consider the obstacles as a tube enveloping the tagged chain. The Doi–Edwards model is a mean field theory which replaces multichain problem by the single-chain problem that the interaction of neighbor chains is modeled by the tube.

If the diameter of the tube is ξ, then the tagged chain in the tube can be divided as the series of blobs whose size is ξ as shown in Fig. 13. Let the number of Kuhn segments in the blob be denoted by N_e. Then, the blob size ξ can be expressed by

$$\xi = b\sqrt{N_e} \tag{4.64}$$

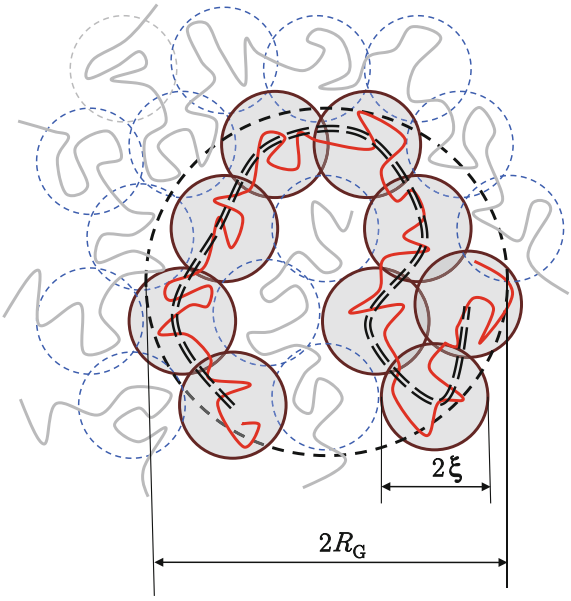

Fig. 13 Illustration of the tube model. The envelop of the series of blobs is the tube. The blobs can be considered as a newly scaled segments whose diameter is ξ. The motion of the subchain in the blob can be considered as a Rouse chain because the subchain is free from neighbor chains. The primitive chain is the line passing the centers of the blobs

If the chain of the blobs is considered as an equivalent chain discussed in Sect. 2.2 in Chap. 4, then the contour length of the tube L should satisfy

$$L = \xi \frac{N}{N_\mathrm{e}} = b \frac{N}{\sqrt{N_\mathrm{e}}} \tag{4.65}$$

Here, the number of blobs is obviously $N_b = N/N_\mathrm{e}$ where N is the number of Kuhn segments in the tagged chain.

The positions of the blobs can be considered to be on the centeroidal curve passing the tube. This curve is called the *primitive chain*. That is, the blob is indicated by a continuous variable s which is the parameter representing the curve. This coarse graining is based on the assumption that the time scale of the observation is sufficiently longer than that of the motion of segments in the blobs. Hence, the detailed mechanics in the blobs appears as averaged.

4.5.2 Dynamics and Stress

Then, the position vector is a function of s and time t: $\mathbf{r}(s,\ t)$. The range of s should be $0 \leq s \leq L$. Since the chain moves along the tube, the dynamics is simply given by

$$\mathbf{r}(s,\ t + \Delta t) = \mathbf{r}(s + \nu(t),\ t) \tag{4.66}$$

where $\nu(t)$ is assumed as a stochastic variable following the Gaussian process such that

$$\langle \nu(t) \rangle = 0\,; \quad \left\langle \nu^2(t) \right\rangle = 2D_\mathrm{c}\Delta t \tag{4.67}$$

and the probability distribution is given by

$$P(\nu) = \frac{1}{\sqrt{4\pi D_\mathrm{c}\Delta t}} \exp\left(-\frac{\nu^2}{4D_c\Delta t} \right) \tag{4.68}$$

The curvilinear diffusion constant D_c should be determined in an appropriate manner.

Since Eq. (4.65) implies $\partial s/\partial n = L/N$, the stress of Eq. (4.34) can be rescaled:

$$\mathbf{T} = -p\mathbf{I} + \frac{\rho_\mathrm{num} k}{N} \frac{L}{N} \int_0^L \left\langle \frac{\partial \mathbf{r}}{\partial s} \frac{\partial \mathbf{r}}{\partial s} \right\rangle \mathrm{d}s \tag{4.69}$$

Since polymeric liquid can be considered an incompressible fluid, the integrand can be replaced by the equivalent traceless tensor such that

$$\mathbf{T} = -p\mathbf{I} + \frac{\rho_{\text{num}} k}{N}\frac{L}{N}\int_0^L \mathbf{Y}(s,\ t)\,\mathrm{d}s \tag{4.70}$$

where

$$\mathbf{Y}(s,t) \equiv \langle \mathbf{u}(s,t)\mathbf{u}(s,t)\rangle - \frac{1}{3}\mathbf{I} \tag{4.71}$$

and

$$\mathbf{u} = \frac{\partial \mathbf{r}}{\partial s} \tag{4.72}$$

It is noteworthy that the second-order tensor $\mathbf{Y}$ is proportional to optical anisotropy tensor (Watanabe 1999). The proportionality between stress and optical anisotropy is called the *stress-optical rule*. The experimental conformity of the stress-optical rule supports the validity of Eq. (4.69). Since we take s as the arc length of the tube, it is obvious that the tangent vector $\mathbf{u}$ is a unit vector (O'Neill 2006).

4.5.3 Solution of Stress Relaxation

Consider stress relaxation test where deformation field is given by

$$\mathbf{F}(t, \widetilde{\mathbf{x}}) = \overline{\mathbf{F}}\Theta(t) \tag{4.73}$$

where $\overline{\mathbf{F}}$ is a constant second-order tensor. It is one of the simplest assumptions that the tangent vector at $t = 0^+$ is given by

$$\mathbf{u}(t = 0^+) = \frac{\overline{\mathbf{F}} \cdot \widetilde{\mathbf{u}}}{\left\|\overline{\mathbf{F}} \cdot \widetilde{\mathbf{u}}\right\|} \tag{4.74}$$

where $\widetilde{\mathbf{u}}$ is the tangent vector at the reference configuration. Then, deformed $\mathbf{Y}$ at $t = 0^+$ is given by

$$\mathbf{Y}(t = 0^+) = \left\langle \frac{\left(\overline{\mathbf{F}} \cdot \widetilde{\mathbf{u}}\right)\left(\overline{\mathbf{F}} \cdot \widetilde{\mathbf{u}}\right)}{\overline{\mathbf{C}} : \widetilde{\mathbf{u}}\widetilde{\mathbf{u}}} \right\rangle_0 - \frac{1}{3}\mathbf{I} \equiv \mathbf{Z}\left(\overline{\mathbf{F}}\right) \tag{4.75}$$

where $\overline{\mathbf{C}}$ is the *right Cauchy–Green tensor*: $\overline{\mathbf{C}} = \overline{\mathbf{F}}^T \cdot \overline{\mathbf{F}}$ (see Sect. 7 in Chap. 1). The average of Eq. (4.75) can be obtained by the assumption that the orientation of $\widetilde{\mathbf{u}}$ is isotropic:

$$\left\langle \frac{\left(\overline{\mathbf{F}} \cdot \widetilde{\mathbf{u}}\right)\left(\overline{\mathbf{F}} \cdot \widetilde{\mathbf{u}}\right)}{\overline{\mathbf{C}} : \widetilde{\mathbf{u}}\widetilde{\mathbf{u}}} \right\rangle_0 = \frac{1}{4\pi} \int_0^{2\pi} \int_0^{\pi} \frac{\left(\overline{\mathbf{F}} \cdot \widetilde{\mathbf{u}}\right)\left(\overline{\mathbf{F}} \cdot \widetilde{\mathbf{u}}\right)}{\overline{\mathbf{C}} : \widetilde{\mathbf{u}}\widetilde{u}} \sin\widetilde{\theta} \mathrm{d}\widetilde{\theta}\mathrm{d}\widetilde{\phi} \tag{4.76}$$

where

$$\widetilde{\mathbf{u}} = \cos\widetilde{\phi}\sin\widetilde{\theta}\,\mathbf{e}_1 + \sin\widetilde{\phi}\sin\widetilde{\theta}\,\mathbf{e}_2 + \cos\widetilde{\theta}\,\mathbf{e}_3 \tag{4.77}$$

is considered.

Since the chain moves along the tube, the dynamics of the unit tangent vector obeys

$$\mathbf{u}(s,\, t+\Delta t) = \mathbf{u}(s+\mathrm{v}(t),\, t) \tag{4.78}$$

Application of the Taylor expansion gives

$$\frac{\partial \mathbf{u}}{\partial t}\Delta t = \frac{\partial \mathbf{u}}{\partial s}\mathrm{v} + \frac{1}{2}\frac{\partial^2 \mathbf{u}}{\partial s^2}\mathrm{v}^2 \tag{4.79}$$

And Eq. (4.71) gives

$$\frac{\partial \mathbf{Y}}{\partial t} = D_\mathrm{c}\frac{\partial^2 \mathbf{Y}}{\partial s^2} \tag{4.80}$$

Note that all directions are equivalent at the both ends of the primitive chain, and the following boundary conditions are available

$$\mathbf{Y}(0,\ t) = \mathbf{Y}(L,\ t) = \mathbf{0} \tag{4.81}$$

The solution of Eq. (4.80) subject to the boundary conditions of Eq. (4.81) can be obtained by the finite Fourier transform (Deen 1998). Consider base functions such as

$$\Psi_m(s) = \sin\frac{m\pi s}{L} \quad \text{with} \quad m = 1, 2, \ldots \tag{4.82}$$

Note that the base functions satisfy

$$\Psi_m(0) = \Psi_m(L) = 0 \tag{4.83}$$

and

$$\frac{2}{L}\int_0^L \Psi_m(s)\,\Psi_n(s)\,\mathrm{d}s = \delta_{mn} \tag{4.84}$$

Assume that the solution is given by

$$\mathbf{Y}(s,\ t) = \sum_{m=1}^{\infty} \mathbf{T}_m(t)\,\Psi_m(s) \tag{4.85}$$

Substitution of Eq. (4.85) into Eq. (4.80) gives

$$\sum_{m=1}^{\infty} \frac{\mathrm{d}\mathbf{T}_m}{\mathrm{d}t}\,\Psi_m(s) = -D_{\mathrm{c}} \sum_{m=1}^{\infty} \left(\frac{m\pi}{L}\right)^2 \mathbf{T}_m(t)\,\Psi_m(s) \tag{4.86}$$

Application of the orthogonal properties of the base function gives

$$\frac{\mathrm{d}\mathbf{T}_m}{\mathrm{d}t} = -D_c \left(\frac{m\pi}{L}\right)^2 \mathbf{T}_m(t) \tag{4.87}$$

The general solution of Eq. (4.87) is given by

$$\mathbf{T}_m(t) = \mathbf{T}_m(0)\,\exp\left(-\frac{t}{\lambda_m}\right) \tag{4.88}$$

where

$$\lambda_m = \frac{\lambda_{\max}}{m^2} \quad \text{with} \quad \lambda_{\max} = \frac{L^2}{\pi^2 D_{\mathrm{c}}} \tag{4.89}$$

Finally, we have

$$\mathbf{Y}(s,\ t) = \sum_{m=1}^{\infty} \mathbf{T}_m(0)\,e^{-t/\lambda_m} \sin\frac{m\pi s}{L} \tag{4.90}$$

Equation (4.75) implies that

$$\mathbf{Z}(\overline{\mathbf{F}}) = \sum_{m=1}^{\infty} \mathbf{T}_m(0)\,\sin\frac{m\pi s}{L} \tag{4.91}$$

Since the left-hand side of Eq. (4.91) is independent of s, it is obvious that

$$\mathbf{T}_m(0) = \begin{cases} \dfrac{4}{\pi m}\mathbf{Z}(\overline{\mathbf{F}}) & \text{for odd } m \\ \mathbf{0} & \text{for even } m \end{cases} \tag{4.92}$$

Then, we have

$$\mathbf{Y}(s,\ t) = \mathbf{Z}(\overline{\mathbf{F}}) \sum_{m=\text{odd}}^{\infty} \frac{4}{\pi m} e^{-t/\lambda_m} \sin\frac{m\pi s}{L} \tag{4.90}$$

and Eq. (4.70) becomes

$$\mathbf{T} = -p\mathbf{I} + \rho_{\text{num}} k \left(\frac{L}{N}\right)^2 \mathbf{Z}(\overline{\mathbf{F}})\ \phi(t) \tag{4.91}$$

where

$$\phi(t) = \sum_{m=\text{odd}}^{\infty} \frac{8}{\pi^2 m^2} e^{-t/\lambda_m} \tag{4.92}$$

We are interested in simple shear flow which can be represented by

$$\overline{\mathbf{F}} = \gamma \mathbf{e}_1\mathbf{e}_2 + \mathbf{I} \tag{4.93}$$

Substitution of Eq. (4.93) into Eq. (4.74) gives

$$\mathbf{u}(t = 0^+) = \frac{\widetilde{\mathbf{u}} + \gamma\widetilde{u}_2\mathbf{e}_1}{\sqrt{(\widetilde{u}_1 + \gamma\widetilde{u}_2)^2 + \widetilde{u}_2^2 + \widetilde{u}_3^2}} \tag{4.94}$$

where $\widetilde{u}_k$ is the kth component of $\widetilde{\mathbf{u}}$. Then, we have

$$\mathbf{Z}(\overline{\mathbf{F}}) = \left\langle \frac{\widetilde{\mathbf{u}}\widetilde{\mathbf{u}} + \gamma\widetilde{u}_2(\mathbf{e}_1\widetilde{\mathbf{u}} + \widetilde{\mathbf{u}}e_1) + \gamma^2\widetilde{u}_2^2\mathbf{e}_1\mathbf{e}_1}{1 + 2\gamma\widetilde{u}_1\widetilde{u}_2 + \gamma^2\widetilde{u}_2^2} \right\rangle_0 - \frac{1}{3}\mathbf{I} \tag{4.95}$$

When $\gamma \ll 1$, we have

$$Z_{12} = \frac{\gamma}{5} \tag{4.96}$$

Then, shear stress is given by

$$T_{12}(t) = \frac{3\rho_{\text{num}} k_{\text{B}} T}{5N_{\text{e}}} \gamma\phi(t)\ \Theta(t) \tag{4.97}$$

Remind Eq. (4.22) for k.

4.5.4 Linear Viscoelasticity

Equation (4.97) gives relaxation modulus:

$$G(t) = \frac{3\rho_{\text{num}} k_{\text{B}} T}{5N_{\text{e}}} \phi(t)\, \Theta(t) \tag{4.98}$$

Now, we return to the curvilinear diffusion constant D_c. Since the chain moves in the tube like the Rouse chain, D_c can be modeled by

$$D_c = \frac{k_{\text{B}} T}{N\zeta} \tag{4.99}$$

The use of Eq. (4.99) gives the zero-shear viscosity:

$$\eta_{\text{o}} = \int_0^\infty G(t)\, \mathrm{d}t = \frac{\pi^2}{20} \frac{\rho_{\text{num}} k_{\text{B}} T}{N_{\text{e}}} \lambda_{\text{d}} \tag{4.100}$$

where disentanglement time λ_{d} is defined as

$$\lambda_{\text{d}} = \frac{1}{\pi^2} \frac{\zeta N^3 b^2}{N_{\text{e}} k_{\text{B}} T} = \lambda_{\text{max}} \tag{4.101}$$

On the other hand, we have

$$J_{\text{e}}^{\text{o}} \eta_{\text{o}}^2 = \int_0^\infty t G(t)\, \mathrm{d}t = \frac{\pi^4}{200} \frac{\rho_{\text{num}} k_{\text{B}} T}{N_{\text{e}}} \lambda_{\text{d}}^2 \tag{4.102}$$

and

$$\overline{\lambda} = J_{\text{e}}^{\text{o}} \eta_{\text{o}} = \frac{\int_0^\infty t G(t)\, \mathrm{d}t}{\int_0^\infty G(t)\, \mathrm{d}t} = \frac{\pi^2}{10} \lambda_{\text{d}} \approx 0.987\, \lambda_{\text{d}} \tag{4.103}$$

For these calculations, we need to solve Problem 22 (Baumgärtel et al. 1992).

Dynamic modulus can be calculated from Eq. (4.98) by the use of Eqs. (1.42) and (1.43):

$$G'(\omega) = \frac{8\, G_{\text{e}}}{\pi^2} \sum_{m=\text{odd}}^{\infty} \frac{1}{m^2} \frac{\lambda_m^2 \omega^2}{1 + \lambda_m^2 \omega^2}; \quad G''(\omega) = \frac{8\, G_{\text{e}}}{\pi^2} \sum_{m=\text{odd}}^{\infty} \frac{1}{m^2} \frac{\lambda_m \omega}{1 + \lambda_m^2 \omega^2} \tag{4.104}$$

where

$$G_e \equiv \frac{3\rho_{num} k_B T}{5N_e} \tag{4.105}$$

It is well known that as for the Maxwell model (see Eq. 3.29a), the following identity holds:

$$G_M = \frac{2}{\pi}\int_0^\infty \frac{G''(\omega)}{\omega} d\omega \tag{4.106}$$

The plateau modulus G_N^o can be defined by analogy with Eq. (4.106):

$$G_N^o \equiv \frac{2}{\pi}\int_0^\infty \frac{G''(\omega)}{\omega} d\omega \tag{4.107}$$

Then, Eq. (4.107) gives the plateau modulus of the Doi–Edwards model given by

$$G_N^o = G_e = \frac{3\rho RT}{5M_e} \tag{4.108}$$

Here, we used that $R = k_B N_A$ and $M_e = N_A m_{Kuhn} N_e$ where R is the gas constant, ρ is the mass density, N_A is the Avogadro's number, and m_{Kuhn} is the mass of the Kuhn monomer. Statistical theory of rubber elasticity reads that the shear modulus of polymer network is given by

$$G = \frac{\rho RT}{M_x} \tag{4.109}$$

This is Eq. (4.25) in Chap. 4, and M_x is the average molecular weight of the subchains between adjacent junction points. By analogy with Eq. (4.109), M_e can be considered as the average molecular weight between physical junction points if entangled chains are considered as a temporary network.

Equation (1.16) is the general form of relaxation modulus. If $G_\infty = 0$, Eq. (1.16) is the model for viscoelastic fluid. As mentioned in Problem 19 (Cole and Cole 1941), the inverse of steady-state compliance is almost same with the plateau modulus defined by Eq. (4.107). However, the Doi–Edwards model gives $2J_e^o = G_e^{-1}$.

Equation (4.101) implies that the zero-shear viscosity is proportional to N^3. This result is slightly different from experimental observation Eq. (3.68) in Chap. 2. Doi and Edwards (1986) explain this deviation due to the fluctuation of the tube length L. Including contour length fluctuation (CLF), Doi and Edwards showed that

$$\lambda_d \approx \frac{1}{\pi^2}\frac{\zeta N^3 b^2}{N_e k_B T}\left(1 - 1.3\sqrt{\frac{N_e}{N}}\right)^2 \tag{4.110}$$

Equation (4.110) behaves like $\lambda_d \propto N^{3.5\pm0.1}$ for $10N_e < N < 100N_e$, while λ_d becomes proportional to N^3 as N goes infinite. Experimental verification of the Doi–Edwards fluctuation model is found in Fig. 9.21 and 9.24 of Rubinstein and Colby (2003).

4.6 Modification of the Doi–Edwards Model

Although the original Doi–Edwards theory unveils the mystery of entanglement, the linear viscoelasticity from the model shows nontrivial deviation from experimental data. To remove the deviation, a number of modifications have been developed. CLF and constraint release (CR) are some of the ramification. Detailed comparison of these efforts for improvement of the original theory is found in Benallal et al. (1993), Watanabe (1999), Pattamaprom et al. (2000), Pattamaprom and Larson (2001), and Leygue et al. (2006).

Contour length fluctuation is to render variation to tube length, while constraint release is the effects of the relaxation of the surrounding chains. Double reptation is considered as a simplification of constraint release. In order to introduce these modifications of tube models, it is necessary to mention mathematical formalism of relaxation modulus of the tube-based theories. The tube-based theories consider that the relaxation modulus is proportional to the average tube survival probability along the chain:

$$G(t) = \frac{G_N^o}{2}\int_{-1}^{1} P(\tilde{s},\ t)\,d\tilde{s} \tag{4.111}$$

where the plateau modulus is used as the scale factor for the relaxation modulus, $\tilde{s}$ is the dimensionless position of the segment of the primitive chain, and $P(\tilde{s},\ t)$ is the probability for a segment of the primitive chain at $\tilde{s}$ to survive between the initial time 0 and time t. The probability $P(\tilde{s},\ t)$ obeys

$$\frac{\partial P}{\partial t} = \frac{\partial}{\partial \widetilde{s}}\left[\widetilde{D}_{\mathrm{CLF}}(\widetilde{s})\frac{\partial P}{\partial \widetilde{s}}\right] + BP \tag{4.112}$$

$$P(t, \pm 1) = 0 \quad \text{for} \quad t > 0 \tag{4.113}$$

and

$$P(0,\ s) = 1 \quad \text{for} \quad -1 < s < 1 \tag{4.114}$$

where $\widetilde{s}$-dependent diffusion constant $\widetilde{D}_{\mathrm{CLF}}(\widetilde{s})$ represents the contour length fluctuation and B is a functional of $P(\widetilde{s},\ t)$, which can represent constraint release as well as contour length fluctuation depending on its mathematical form (Bae and Cho 2015). As for the original Doi–Edwards theory, it is obvious that $\widetilde{D}_{\mathrm{CLF}}$ is constant and $B = 0$. Since Eq. (4.112) is a nonlinear diffusion equation, it is hard to expect analytical solution. Hence, improved versions of the Doi–Edwards model need numerical method.

This approach is effective only for low-frequency region such as $a_T\omega < 10^2$ for the case of monodisperse polybutadiene in Fig. 12. In order to extend the effective range of frequency, fast mode of relaxation such as the Rouse model should be included:

$$G_{\mathrm{Rouse}}(t) = G_{\mathrm{N}}^{\mathrm{o}}\left[\sum_{n=Z+1}^{\infty}\frac{1}{Z}\exp\left(-\frac{n^2}{\lambda_R}t\right) + \frac{1}{3}\sum_{n=1}^{Z}\frac{1}{Z}\exp\left(-\frac{n^2}{\lambda_R}t\right)\right] \tag{4.115}$$

where Z is the closest integer to $M/M_{\mathrm{e}} = N/N_{\mathrm{e}}$ and λ_R is the Rouse time of Eq. (4.46). Equation (4.115) is called fragmented Rouse model which was suggested by Milner and McLeigh (1998).

Even though several relaxation mechanisms other than pure reptation have been introduced, the frequency regions of $a_T\omega > 10^8$ in Fig. 12 cannot be predicted. This region of frequency may be called glassy region. Benallal et al. (1993) added a phenomenological model such as the Davidson–Cole model for the glassy region.

Although the original Doi–Edwards theory deals with only monodisperse linear polymer, great progression in the tube-based theory opened ways to predict linear viscoelasticity of polydisperse polymers. Effect of molecular weight distribution can be described by the quadratic mixing rule (des Cloizeaux 1988; Tsenoglou 1991). When relaxation modulus of monodisperse polymer melt of M_k is denoted by $G_{\mathrm{m}}(t,\ M_k)$, the mixing rule addresses that the relaxation modulus of the polydisperse polymer melt with molecular weight distribution of w_k is given by

$$\sqrt{G(t)} = \sum_{k=1}^{N_{\text{chain}}} w_k \sqrt{G_{\text{m}}(t,\ M_k)} \tag{4.116}$$

This mixing rule is known to hold whenever $M_k \gg M_{\text{e}}$ for all k.

Recent progression in molecular theory makes it possible to predict viscoelasticity of nonlinear polymers which have divergent branch chains.

Problem 4

[1] Consider Eq. (4.20). Assume that $\mathbf{L} = \mathbf{0}$. When bond vector $\mathbf{b}_\alpha$ is defined as

$$\mathbf{b}_\alpha = \mathbf{r}_{\alpha+1} - \mathbf{r}_\alpha \quad \text{for} \quad \alpha = 1, 2, \ldots, N-1 \tag{4.a}$$

Show that Eq. (4.20) can be rewritten in terms of bond vectors as follows:

$$\frac{\mathrm{d}\mathbf{b}_\alpha}{\mathrm{d}t} = -\frac{3k_{\text{B}}T}{\zeta b^2} \sum_{\beta=1}^{N-1} A'_{\alpha\beta}\mathbf{b}_\beta + \mathbf{g}_{\alpha+1}(t) - \mathbf{g}_\alpha(t) \tag{4.b}$$

where the Rouse matrix $A'_{\alpha\beta}$ is defined as

$$A'_{\alpha\beta} = 2\delta_{\alpha\beta} - \delta_{\alpha+1,\beta} - \delta_{\alpha-1,\beta} \tag{4.c}$$

[2] Show that the eigenvalues of the Rouse matrix are given by

$$a_\beta = 4\sin^2\frac{\beta\pi}{2N} \quad \text{for} \quad \beta = 1, 2, \ldots, N-1 \tag{4.d}$$

See Lin (2003).

[3] Consider Stokes equation

$$\eta\nabla^2\mathbf{v} + \nabla p = -\mathbf{g} \tag{4.e}$$

where $\mathbf{g}(\mathbf{x})$ is a vector field. Assume the fluid is incompressible:

$$\nabla \cdot \mathbf{v} = 0 \tag{4.f}$$

The boundary condition of velocity field is given by

$$\lim_{\|\mathbf{x}\|\to\infty} \mathbf{v}(\mathbf{x}) = \mathbf{0} \tag{4.g}$$

When the Fourier transform is defined as

$$\hat{\mathbf{v}}(\mathbf{k}) = \int \mathbf{v}(\mathbf{x})\, e^{\mathrm{i}\mathbf{k}\,\mathbf{x}} \mathrm{d}\mathbf{x} \tag{4.h}$$

Show that Eqs. (4.e) and (4.f) are rewritten by

$$\eta\,(\mathbf{k}\cdot\mathbf{k})\,\hat{\mathbf{v}} + \mathrm{i}\mathbf{k}\hat{p} = \hat{\mathbf{g}}; \quad \mathbf{k}\cdot\hat{\mathbf{v}} = 0 \tag{4.i}$$

[4] Show that the solution of Eq. (4.e) is given by

$$\mathbf{v}(\mathbf{x}) = \int \mathbf{H}(\mathbf{x}-\mathbf{r})\cdot\mathbf{g}(\mathbf{r})\,\mathrm{d}\mathbf{r} \tag{4.j}$$

where $\mathbf{H}(\mathbf{r})$ is the Oseen tensor defined as

$$\mathbf{H}(\mathbf{r}) = \frac{1}{8\pi\eta\|\mathbf{r}\|}(\mathbf{I}+\mathbf{r}\mathbf{r}) \tag{4.k}$$

See Doi and Edwards (1986) or Deen (1998).

[5] For the purpose of calculation of Eqs. (4.100), (4.102), and (4.103), it is necessary to be familiar with some properties of the Riemann zeta function which is defined as

$$\zeta(x) = \sum_{n=1}^{\infty} \frac{1}{n^x}$$

We are interested in integer values of x larger than unity. As for the interval of $-\pi < x < \pi$, the Fourier series of x^2 is known as

$$x^2 = \frac{\pi^2}{3} + 4\sum_{k=1}^{\infty} (-1)^k \frac{\cos kx}{k^2}$$

If we set $x = \pi$, then we have

$$\zeta(2) = \frac{\pi^2}{6}$$

Prove that

$$\zeta(4) = \frac{\pi^4}{90}; \quad \zeta(6) = \frac{\pi^6}{945}$$

See the Chap. 5 of Arfken and Weber (2001).

[6] It is obvious that

$$\sum_{n=\mathrm{odd}}^{\infty} \frac{1}{n^x} = \sum_{n=1}^{\infty} \frac{1}{n^x} - \sum_{n=\mathrm{even}}^{\infty} \frac{1}{n^x} = \left(1 - \frac{1}{2^x}\right)\zeta(x)$$

Calculate the following infinite series:

$$\sum_{m=\text{odd}}^{\infty} \frac{1}{n^k} \quad \text{for} \quad k = 2,\ 4,\ \text{and}\ 6$$

References

G.B. Arfken, H.J. Weber, *Mathematical methods for physicists* (Harcourt Sci. & Tech, Port Harcourt, 2001)

J.-E. Bae, K.S. Cho, Logarithmic method for continuous relaxation spectrum and comparison with previous methods. J. Rheol. **59**, 1081–1112 (2015)

R.L. Bagley, P.J. Torvik, A theoretical basis for the application of fractional calculus to viscoelasticity. J. Rheol. **27**, 201–210 (1983)

R.L. Bagley, P.J. Torvik, On the fractional calculus model of viscoelastic behavior. J. Rheol. **30**, 133–155 (1986)

C. Baravian, D. Quemada, Using instrumental inertia in controlled stress rheometry. Rheol. Acta **37**, 223–233 (1998)

C. Baravian, G. Benbelkacem, F. Caton, Unsteady rheometry: can we characterize weak gels with a controlled stress rheometer. Rheol. Acta **46**, 577–581 (2007)

M. Baumgärtel, H.H. Winter, Determination of discrete relaxation and retardation time spectra form dynamic mechanical data. Rheol. Acta **28**, 511–519 (1989)

M. Baumgärtel, H.H. Winter, Interrelation between continuous and discrete relaxation time spectra. J. Non-Newtonian Fluid Mech. **44**, 15–36 (1992)

M. Baumgärtel, A. Schausberger, H.H. Winter, The relaxation of polymers with linear flexible chains of uniform length. Rheol. Acta **29**, 400–408 (1990)

M. Baumgärtel, M.E. De Rosa, J. Machado, M. Masse, H.H. Winter, The relaxation time spectrum of nearly monodisperse polybutadiene melts. Rheol. Acta **31**, 75–82 (1992)

A. Benallal, G. Marin, J.P. Montfort, C. Derail, Linear viscoelasticity revisted: the relaxation function of monodisperse polymer melts. Macromolecules **26**, 7229–7235 (1993)

H.C. Booij, G.P.J.M. Thoone, Generalization of Kramers-Kronig transforms and some approximations of relations between viscoelastic quantities. Rheol. Acta **21**, 15–24 (1982)

K.S. Cho, Power series approximations of dynamic moduli and relaxation spectrum. J. Rheol. **57**, 679–697 (2013)

K.S. Cho, G.W. Park, Fixed-point iteration for relaxation spectrum from dynamic mechanical data. J. Rheol. **57**, 647–678 (2013)

K.S. Cho, K. Hyun, K.H. Ahn, S.J. Lee, A geometrical interpretation of large amplitude oscillatory shear response. J. Rheol. **49**, 747–758 (2005)

K.S. Cho, K.-W. Song, G.-S. Chang, Scaling relations in nonlinear viscoelastic behavior of aqueous PEO solutions under large amplitude oscillatory shear flow. J. Rheol. **54**, 27–63 (2010)

A.M. Cohen, *Numerical Methods for Laplace Transform Inversion* (Springer, Berlin, 2007)

K.S. Cole, R.H. Cole, Dispersion and absorption in dielectrics I. Alternating current characteristics. J. Chem. Phys. **9**, 341–351 (1941)

M. Dalir, M. Bashour, Applications of fractional calculus. Appl. Math. Sci. **4**, 1021–1032 (2010)

D.W. Davidson, R.H. Cole, Dielectric relaxation in glycerol, propylene glycol, and n-propanol. J. Chem. Phys. **19**, 1484–1490 (1951)

A.R. Davies, R.S. Anderssen, Sampling localization in determining the relaxation spectrum. J. Non-Newtonian Fluid Mech. **73**, 163–179 (1997)

P.-G. De Gennes, *Scaling Concepts in Polymer Physics* (Cornell University Press, Ithaca, 1979)

W.E. Deen, *Analysis of Transport Phenomena* (Oxford University Press, Oxford, 1998)
J. des Cloizeaux, Double reptation vs. simple reptation in polymer melts. Europhys. Lett. **5**, 437–442 (1988)
M. Doi, *Introduction to Polymer Physics* (Clarendon Press, Oxford, 1996)
M. Doi, S.F. Edwards, *The Theory of Polymer Dynamics* (Oxford University Press, Oxford, 1986)
R.M.L. Evans, M. Tassieri, D. Auhl, T.A. Waigh, Direct conversion of rheological compliance measurements into storage and loss moduli. Phys. Rev. E **80**, 012501 (2009)
C. Friedrich, Relaxation and retardation functions of the maxwell model with fractional derivatives. Rheol. Acta **30**, 151–158 (1991)
R.M. Fuoss, J.G. Kirkwood, Electrical properties of solids. VIII. Dipole moments in polyvinyl chloride-diphenyl systems. J. Am. Chem. Soc. **63**, 385–394 (1941)
S. Havriliak, S. Negami, A complex plane representation of dielectric and mechanical relaxation processes in some polymers. Polymer **8**, 161–210 (1967)
J. Honerkamp, J. Weese, A nonlinear regularization method for the calculation of relaxation spectra. Rheol. Acta **32**, 65–73 (1993)
A. Jaishankar, G.H. McKinley, Power-law rheology in the bulk and at the interface: quasi-properties and fractional constitutive equations. Proc. Roy. Soc. A **469**, 1–18 (2013)
A. Jaishankar, V. Sharma, G.H. McKinley, Interfacial viscoelasticity, yielding and creep ringing of globular protein-surfactant mixtures. Soft Matter **7**, 7623–7634 (2011)
M. Kardar, *Statistical Physics of Fields* (Cambridge University Press, Cambridge, 2007)
M.K. Kim, J.-E. Bae, N. Kang, K.S. Cho, Extraction of viscoelastic functions from creep data with ringing. J. Rheol. **59**, 237–252 (2015)
R.G. Larson, The rheology of dilute solutions of flexible polymers: progress and problems. J. Rheol. **49**, 1–70 (2005)
A. Leygue, C. Bailly, R. Keunings, A differential tub-based model for predicting the linear viscoelastic moduli of polydisperse entangled linear polymers. J. Non-Newtonian Fluid Mech. **133**, 28–34 (2006)
Y.-H. Lin, *Polymer Viscoelasticity* (World Scientific, Singapore, 2003)
F. Lu, J. Song, B.-W. Cheng, X.-J. Ji, L.-J. Wang, Viscoelasticity and rheology in the regimes from dilute to concentrated in cellulose 1-ethyl-3-methylimidazolium acetate solutions. Cellulose **20**, 1343–1352 (2013)
C.W. Macosko, *Rheology: Principles, Measurements and Applications* (VCH Publisher, New York, 1994)
F. Mainardi, G. Spada, Creep, relaxation and viscosity properties for basic fractional models in rheology. Eur. Phys. J. Special Topics **193**, 133–160 (2011)
A.Y. Malkin, I. Masalova, From dynamic modulus via different relaxation spectra to relaxation and creep functions. Rheol. Acta **40**, 261–271 (2001)
G. Marin, W.W. Graessley, Viscoelastic properties of high molecular weight polymers in the molten state I. Study of narrow molecular weight distribution samples. Rheol. Acta **16**, 527–533 (1977)
T.G. Mason, Estimating the viscoelastic moduli of complex fluids using the generalized Stokes-Einstein equation. Rheol. Acta **39**, 371–378 (2000)
T.G. Mason, D.A. Weitz, Optical measurements of frequency-dependent linear viscoelastic moduli of complex fluids. Phys. Rev. Lett. **74**, 1250–1253 (1995)
S.T. Milner, T.C.B. McLeish, Reptation and contour-length fluctuations in melts of linear polymers. Phys. Rev. Lett. **81**, 725–728 (1998)
B. O'Neill, *Elementary Differential Geometry*, 2nd edn. (Academic Press, Cambridge, 2006)
L.-I. Palade, V. Verney, P. Attané, A modified fractional model to describe the entire viscoelastic behavior of polybutadienes from flow to glassy regime. Rheol. Acta **35**, 265–273 (1996)
C. Pattamaprom, R.G. Larson, Predicting the linear viscoelastic properties of monodisperse and polydisperse polystyrenes and polyethylenes. Rheol. Acta **40**, 516–532 (2001)
C. Pattamaprom, R.G. Larson, T.J. Van Dyke, Quantitative predictions of linear viscoelastic rheological properties of entangled polymers. Rheol. Acta **39**, 517–531 (2000)
A.C. Pipkin, *Lectures on Viscoelasticity Theory* (Springer, Berlin, 1972)

V.N. Pokrovskii, *The Mesoscopic Theory of Polymer Dynamics* (Kluwer Academic Publishers, Berlin, 2000)
E. Riande, R. Díaz-Calleja, *Electrical Properties of Polymers* (Marcel Dekker, New York, 2004)
E. Riande, R. Díaz-Calleja, M.G. Prolongo, R.M. Masegosa, C. Salom, *Polymer Viscoelasticity, Stress and Strain in Practice* (Marcel Dekker, New York, 2000)
P.E. Rouse, A theory of the linear viscoelastic properties of dilute solutions of coiling polymers. J. Chem. Phys. **21**, 1272 (1953)
M. Rubinstein, R.H. Colby, *Polymer Physics* (Oxford University Press, Oxford, 2003)
M. Simhambhatla, A.I. Leonov, The extended Padé-Laplace method for efficient discretization of linear viscoelastic spectra. Rheol. Acta **32**, 589–600 (1993)
D.Y. Song, T.Q. Jiang, Study on the constitutive equation with fractional derivative for the viscoelastic fluids—modified Jeffreys model and its application. Rheol. Acta **37**, 512–517 (1998)
T.M. Squires, T.G. Mason, Fluid mechanics of microrheology. Ann. Rev. Fluid Mech. **42**, 413–438 (2010)
F.J. Stadler, What are typical sources of error in rotational rheometry of polymer melts? Korea-Aust. Rheol. J. **26**, 277–291 (2014)
F.J. Stadler, E. van Ruymbeke, An improved method to obtain direct rheological evidence of monomer density reequilibration for entangled polymer melts. Macromolecules **43**, 9209–9250 (2010)
I. Teraoka, *Polymer Solutions* (Wiley-Interscience, Hoboken, 2002)
M. Toda, *Theory of Nonlinear Lattices* (Springer, Berlin, 1988)
N.W. Tschoegl, *The Phenomenological Theory of Linear Viscoelastic Behavior* (Springer, Berlin, 1989)
C. Tsenoglou, Molecular weight polydispersity effects on the viscoelasticity of entangled linear polymers. Macromolecules **24**, 1762–1767 (1991)
T.A. Waigh, Microrheology of complex fluids. Rep. Prog. Phys. **68**, 685–742 (2005)
H. Watanabe, Viscoelasticity and dynamics of entangled polymers. Prog. Polym. Sci. **24**, 1253–1403 (1999)
A.W. Wharmby, R.L. Bagley, Generalization of a theoretical basis for the application of fractional calculus to viscoelasticity. J. Rheol. **57**, 1429–1440 (2013)

Chapter 6
Numerical Methods

Abstract One of the important features of the book is the numerical algorithms for the viscoelastic identification of polymeric materials. Hence, this chapter introduces the numerical methods which are necessary for the algorithms. Different from conventional text books of numerical methods, this chapter deals with some numerical methods for experimental data which inevitably contain errors. The first three sections are devoted to regressions. The other sections deal with numerical methods which is necessary for the conversion of viscoelastic data of a viscoelastic function to those of another viscoelastic function: numerical integration and differentiation and Fourier transform.

We need to analyze viscoelastic data through various numerical methods in order to characterize and identify arbitrary polymeric systems. Representative examples are relaxation time spectrum and time temperature superposition. In this section, we shall introduce regression methods, numerical integration and differentiation, and *discrete Fourier transform (DFT)*. Regression for polynomial and general nonlinear functions is important in both model fitting and the calculation of continuous spectrum. Since the polynomial regression by the Chebyshev polynomial is a key to facilitate the quantitative analysis of large amplitude oscillator shear (LAOS), it will be treated again in the part III. Numerical integration and differentiation are helpful for interconversion of linear viscoelastic functions. Different from ordinary textbooks on numerical analysis, this chapter is focused on the integration and differentiation of experimental data which always contain statistical errors. Discrete Fourier transform is applicable to the conversion of static viscoelastic functions such as relaxation modulus and creep compliance to dynamic moduli and compliances. Furthermore, it is more important in quantitative analysis of LAOS such as FT-rheology. This chapter is mainly related to Chaps. 7–9 and 11.

K.S. Cho, *Viscoelasticity of Polymers*, Springer Series
in Materials Science 241, DOI 10.1007/978-94-017-7564-9_6

1 Polynomial Regression

1.1 Basics

According to the Weierstrass theorem (Atkinson and Han 2000), a continuous function defined on a closed interval can be expressed by an infinite series such that

$$f(x) = \sum_{n=0}^{\infty} a_n x^n \tag{1.1}$$

If the convergence rate of the infinite series is fast enough, then one can obtain an acceptable approximation for a finite positive integer N, as follows

$$f(x) \approx \sum_{n=0}^{N} a_n x^n \equiv \Pi_N(x) \tag{1.2}$$

We have used this for approximation of a mathematically defined function in Sect. 2.4 in Chap. 1.

Since any measurable quantity is experimentally obtained in a finite closed interval of the controllable variable on which the measurable quantity depends, Eq. (1.2) is applicable to most experimental data under the assumption that the measurable quantity is continuously dependent on its independent variable. Suppose that measured data can be expressed by

$$y_\alpha = f(x_\alpha) + \varepsilon_\alpha \tag{1.3}$$

for every pair of (x_α, y_α). Here, ε_α is the experimental error imposed on the αth data point. The errors are usually regarded as statistical entities such that

$$\langle \varepsilon_\alpha \rangle = 0; \quad \langle \varepsilon_\alpha \varepsilon_\beta \rangle = \sigma^2 \delta_{\alpha\beta} \tag{1.4}$$

These characteristics of errors mean statistical independence.

For M data, the sum of square errors can be obtained as follows

$$\sum_{\alpha=1}^{M} \varepsilon_\alpha^2 = \sum_{\alpha=1}^{M} [y_\alpha - f(x_\alpha)]^2 \tag{1.5}$$

Taking expectation on both sides of Eq. (1.5), Eq. (1.4) gives

$$\sigma = \sqrt{\frac{1}{M} \sum_{\alpha=1}^{M} \left\langle [y_\alpha - f(x_\alpha)]^2 \right\rangle} \approx \sqrt{\frac{1}{M} \sum_{\alpha=1}^{M} [y_\alpha - f(x_\alpha)]^2} \tag{1.6}$$

Hence, the *root-mean-square error* (RMSE) estimates the expectation of the amplitude of experimental error. It is obvious that the better approximation Eq. (1.2) is, the smaller RMSE is expected. However, any approximation cannot make it smaller than σ. The best choice of the coefficients a_n is to minimize

$$\chi^2 \equiv \sum_{\alpha=1}^{M} [y_\alpha - \Pi_N(x_\alpha)]^2 \tag{1.7}$$

This is the reason why regression is usually called the *least square method*.

Note that χ^2 is a quadratic function of $\{a_n\}$. Hence, χ^2 has the unique minimum at the values of the coefficients which satisfy

$$\frac{\partial \chi^2}{\partial a_n} = 0 \tag{1.8}$$

These are $N+1$ linear equations for the coefficients. This system of linear equations is called the *normal equations*:

$$\mathbf{S} \cdot \mathbf{a} = \mathbf{b} \tag{1.9}$$

Here, vector notation was used and we know that

$$S_{nk} = \sum_{\alpha=1}^{M} x_\alpha^{n+k} = S_{kn} \tag{1.10}$$

and

$$b_n = \sum_{\alpha=1}^{M} x_\alpha^n y_\alpha \tag{1.11}$$

Of course, a_n is the nth component of the vector **a**. It should be noted that the matrix **S** might be singular when the number of coefficients is larger than the number of data. If $N+1=M$, then the problem becomes that of interpolation. Since the matrix **S** is not a diagonal-dominant one, it is apt to be singular or ill-conditioned if N is large. If more information is necessary, refer to Lawson and Hanson (1995).

1.2 Use of Orthogonal Polynomials

Although the matrix **S** is symmetric and invertible, it is apt to be an ill-conditioned matrix when N is sufficiently large. Hence, when higher-order polynomial is necessary, an alternative is needed. We have seen that orthogonal polynomials make the matrix **S** diagonal when a mathematical function is considered instead of

experimental data (see Sect. 2.4 in Chap. 1). Since Nth order polynomial can be replaced by orthogonal polynomials as follows

$$\Pi_N(x) = \sum_{n=0}^{N} a'_n \phi_n(x) \tag{1.12}$$

Then, the normal equation becomes $\mathbf{S}' \cdot \mathbf{a}' = \mathbf{b}'$ where

$$S'_{nk} = \sum_{\alpha=1}^{M} \phi_n(x_\alpha)\phi_k(x_\alpha); \quad b'_n = \sum_{\alpha=1}^{M} \phi_n(x_\alpha) y_\alpha \tag{1.13}$$

It must be noted that although $S'_{nk} \neq 0$ for $n \neq k$, the matrix is a diagonal-dominant one:

$$\left|S'_{nn}\right| \ll \left|S'_{pq}\right| \quad \text{with} \quad p \neq q \tag{1.14}$$

Although there are a number of orthogonal polynomials, one of the most popular orthogonal polynomials is the Chebyshev polynomial of the first kind, $T_n(x)$. Since $T_n(x)$ is defined on $[-1, 1]$, for the data given for the interval of $[x_{\min}, x_{\max}]$, the transform is required such as

$$\xi = \frac{2x - (x_{\max} + x_{\min})}{x_{\max} - x_{\min}} \tag{1.15}$$

The same transform is also used for the Legendre polynomial $P_n(x)$. Thus, we will use

$$\Pi_N(x) = \sum_{n=0}^{N} c_n T_n(\xi) \tag{1.16}$$

or

$$\Pi_N(x) = \sum_{n=0}^{N} c'_n P_n(\xi) \tag{1.17}$$

As for the Legendre polynomial, its orthogonality explains Eq. (1.14) because

$$\sum_{\alpha=1}^{M} P_n(\xi_\alpha) P_k(\xi_\alpha) \approx \int_{-1}^{1} P_n(\xi) P_k(\xi) \mathrm{d}\xi \tag{1.18}$$

However, the weight function of the Chebyshev polynomial is not unity. Because of Eq. (2.34 in Chap. 1),

$$\sum_{\alpha=1}^{M} T_n(\xi_\alpha)T_k(\xi_\alpha) = \sum_{\alpha=1}^{M} T_n(\cos\theta_\alpha)T_k(\cos\theta_\alpha) = \sum_{\alpha=1}^{M} \cos(n\theta_\alpha)\cos(k\theta_\alpha)$$
$$\approx \int_{-\pi}^{\pi} \cos n\theta \cos k\theta \, \mathrm{d}\theta \tag{1.19}$$

Here, we considered $\xi_\alpha = \cos\theta_\alpha$ because $-1 \le \xi_\alpha \le 1$. The orthogonality of cosine functions explains the reason why Eq. (1.14) is valid.

The Chebyshev polynomials $T_n(\xi)$ are known to satisfy a discrete orthogonality such that if ξ_α ($\alpha = 1, \ldots, M$) are the M zeros of $T_M(\xi)$, then for any $m, n < M$ (Press et al. 2002)

$$\sum_{\alpha=1}^{M} T_m(\xi_\alpha)T_n(\xi_\alpha) = \begin{cases} 0 & \text{for } m \neq n \\ \frac{1}{2}M & \text{for } m = n = 0 \\ M & \text{for } m = n \neq 0 \end{cases} \tag{1.20}$$

The M zeros of $T_M(\xi)$ are called the *Chebyshev nodes* and are given by

$$\xi_\alpha = \cos\frac{\pi(\alpha - \frac{1}{2})}{M} \quad \text{with} \quad \alpha = 1, \ldots, M \tag{1.21}$$

When c_n is determined by solving the normal equation, it is not guaranteed that a_n of Eq. (1.2) can be determined robustly from c_n for any N. The problem of ill-conditioned matrix remains because the conversion from ξ to x may give rise to another problem when N is large.

Figure 1 shows the reason why orthogonal polynomials are used in polynomial regression. The data are $y = e^{-x/5}\sin 3x$ with statistical error of 2 %. As for simple polynomial, RMSE becomes minimum at $N = 11$. On the other hand, RMSE decreases monotonically as N when the Chebyshev polynomial is used. Hence, it can be said that simple polynomial regression cannot fit the data, while the use of the Chebyshev polynomial can do.

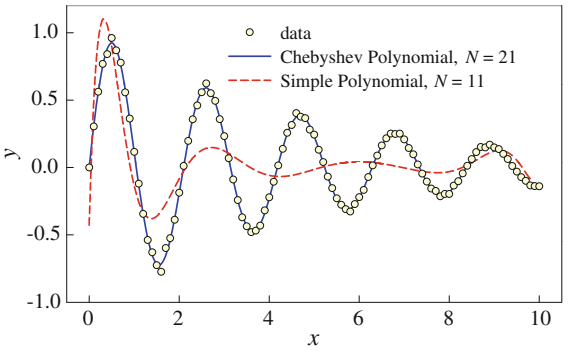

Fig. 1 Comparison of the methods of polynomial regression

1.3 B-Spline Regression

It must be noted that although polynomial regression is very powerful, sometimes it gives rise to the *Runge phenomenon* that further increase of the degree of the polynomial deteriorates the regression result, especially near the boundary of the interval (Süli and Mayers 2003). To prevent such oscillatory failures, piecewise polynomials are recommended. The whole interval of the independent variable is divided into L subintervals, and then, each of the partitioned data is fitted by a polynomial of low degree. Since the whole interval is divided, we have to impose constraints that polynomials of adjacent subintervals are smoothly connected. Smooth connection of adjacent polynomials implies that

$$\Pi_N^{(n+1)}(x_n) = \Pi_N^{(n)}(x_n); \quad \frac{\mathrm{d}\Pi_N^{(n+1)}(x_n)}{\mathrm{d}x} = \frac{\mathrm{d}\Pi_N^{(n)}(x_n)}{\mathrm{d}x} \tag{1.22}$$

where $\Pi_N^{(n+1)}(x)$ and $\Pi_N^{(n)}(x)$ are, respectively, the Nth order polynomials on the subintervals $I_{n+1} = \{x | x_n \le x < x_{n+1}\}$ and $I_n = \{x | x_{n-1} \le x < x_n\}$. Here, $L+1$ x_n $(n = 0, 1, \ldots, L)$ are called node points that define the partitioning of the interval. Since each polynomial has $N+1$ coefficients and the constraints of Eq. (1.22) are $2(L-1)$ equations, the degree of freedom of this regression problem, F, is $(N-1)L+2$. Hence, it is usual to choose N as 2 or 3. When the number of data is given by M, $M = F$ means interpolation. Hence, we are interested in the case of $M > F$.

As for interpolation, *cubic Hermite polynomial* is commonly used because the polynomial of third degree for each subinterval is formulated in terms of the values of the function and the derivative at both ends of the subinterval. However, if cubic Hermite polynomial is used for regression, then the normal equations are apt to be ill-conditioned. Hence, we prefer cubic B-splines which are nearly identical peak-like functions consisting of four cubic polynomials. The letter "B" stands for basis because the base functions $B_m(x)$ are designed to satisfy $B_m(x)B_n(x) = 0$ whenever $|m-n| > 3$ (decoupling property). Furthermore, every base function $B_m(x)$ is also designed as piecewisely continuous cubic polynomial whose derivatives are continuous at any order. Hence, a function $f(x)$ can be approximated by

$$f(x) \approx \sum_{k=-1}^{L+1} c_k B_k(x) \tag{1.23}$$

The index k runs from -1 to $L+1$ because the base functions are constructed over four subintervals:

$$B_k(x) = \begin{cases} t^3 & t \equiv \dfrac{x - \xi_{k-2}}{\xi_{k-1} - \xi_{k-2}} \quad \text{and} \quad \xi_{k-2} \le x \le \xi_{k-1} \\ 1 + 3t + 3t^2 - 3t^3 & t \equiv \dfrac{x - \xi_{k-1}}{\xi_k - \xi_{k-1}} \quad \text{and} \quad \xi_{k-1} \le x \le \xi_k \\ 1 - 3t + 3t^2 + 3t^3 & t \equiv \dfrac{x - \xi_{k+1}}{\xi_{k+1} - \xi_k} \quad \text{and} \quad \xi_k \le x \le \xi_{k+1} \\ -t^3 & t \equiv \dfrac{x - \xi_{k+2}}{\xi_{k+2} - \xi_{k+1}} \quad \text{for} \quad \xi_{k+1} \le x \le \xi_{k+2} \\ 0 & \text{otherwise} \end{cases} \tag{1.24}$$

where ξ_k $(k = 0, 1, \ldots, L)$ are node points which define subintervals

$$I_n = \left\{ x \middle| \xi_{n-1} \le x \le \xi_{n+1} \right\} \tag{1.25}$$

Note that nonzero values of $B_{-1}(x)$ are defined only over the interval I_L as

$$B_{-1}(x) = -\left(\frac{x - \xi_1}{\xi_1 - \xi_0} \right)^3 \tag{1.26}$$

and $B_{-1}(x) = 0$ otherwise. Figure 2 illustrates the base functions. It can be recognized that $B_0(x)$ is not zero only in the interval of $I_1 \cup I_2$. For $0 \le k \le L$, $B_k(x)$ are peak functions that have their maxima at $x = \xi_k$.

Decoupling property of the base functions makes it easier to solve normal equation because the matrix of the normal equation is very similar to a diagonal one. Hence, the regression by cubic B-spline is as accurate as that by orthogonal polynomials. Furthermore, since the regression results are equivalent to locally polynomial of third order, it is nearly free from the Runge phenomenon. This merit of B-spline allows the applications to numerical differentiation of experimental data and inferring continuous relaxation spectrum by

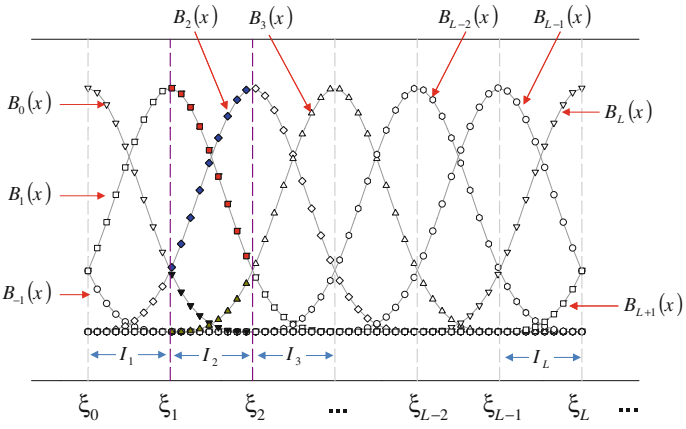

Fig. 2 Illustration of the base functions of cubic B-spline

$$H(\lambda) = \exp\left[\sum_{k=-1}^{L} c_k B_k(\log\ \lambda)\right] \tag{1.27}$$

Bae and Cho (2015) applied cubic B-spline of Eq. (1.27) to the calculation of continuous relaxation spectrum.

Problem 1

[1] Precision of regression can be indicated by the coefficient of determination which is defined by

$$R^2 = 1 - \frac{\text{SSE}}{\text{SST}} \tag{1.a}$$

where

$$\text{SSE} = \sum_{\alpha=1}^{M} [y_\alpha - f(x_\alpha)]^2; \quad \text{SST} = \sum_{\alpha=1}^{M} \left(y_\alpha - \frac{1}{M}\sum_{\beta=1}^{M} y_\beta\right)^2 \tag{1.b}$$

SSE is called sum of square error and SST is called the total sum of squares. Show that $0 < R^2 \leq 1$.

[2] Derive the base functions $B_k(x)$ for quadratic B-spline.

[3] Denote kth base function of nth order by $B_k^{(n)}(x)$. Show that if

$$B_k^{(1)}(x) = \begin{cases} 1 & \text{for } \xi_k \leq x < \xi_{k+1} \\ 0 & \text{otherwise} \end{cases} \tag{1.c}$$

then

$$B_k^{(n)}(x) = \frac{x - \xi_k}{\xi_{k+n+1} - \xi_k} B_k^{(n-1)}(x) + \frac{\xi_{k+n} - x}{\xi_{k+n} - \xi_{k+1}} B_{k+1}^{(n-1)}(x) \tag{1.d}$$

[4] Show that any Nth order polynomial $\Pi_N(x)$ on the interval of [0, 1] can be represented by a linear combination of the *Bernstein basis polynomials* of degree N which are defined by

$$b_k^{(N)}(x) = \binom{N}{k} x^k (1-x)^{N-k}, \quad k = 0, 1, \ldots, N \tag{1.e}$$

[5] For a given continuous function f on the interval of [0, 1], the Bernstein polynomial of the function f is defined by

$$B_f^{(N)}(x) = \sum_{k=0}^{N} f\left(\frac{k}{N}\right) b_k^{(N)}(x) \tag{1.f}$$

When $f(x) = \Pi_N(x)$, show that $B_{\Pi_N}^{(N)}(x) = \Pi_N(x)$.

2 Nonlinear Regression

2.1 Basics

Consider a case that polynomial approximation of Eq. (1.2) can be replaced by a function, $f_L(x)$, which contains small number of parameters, $p_1, \ldots, p_L$. For a good model, the number of parameters L should be much smaller than the order of polynomial approximation N if $\|f(x) - f_L(x)\| = \|f(x) - \Pi_N(x)\|$ where $\|\cdot\|$ is a norm defined on the function space under consideration. In order to determine the parameters $\{p_k\}$, we need to minimize the sum of square error

$$\chi^2 = \sum_{\alpha=1}^{M} [y_\alpha - f_L(x_\alpha)]^2 \tag{2.1}$$

Of course, χ^2 is usually a nonlinear function of the parameters $\{p_k\}$. Different from polynomial regression, the nonlinear function may have several minima. Existence of several local minima makes the determination of the parameters difficult. Most algorithms for minimization are to use the gradient of the objective function (χ^2). In this case, regression results are largely dependent on the initial values of the parameters. If an initial guess of the parameters is not appropriate, then the algorithm gives undesirable results such as no convergence in even a high iteration number and ridiculous values of the parameters. We shall introduce some methods based on gradient.

The parameters to be determined are one of the points in parameter space which satisfy $\partial\chi^2/\partial p_k = 0$. These nonlinear normal equations can be rewritten in detail by

$$\sum_{\alpha=1}^{M} f_L(x_\alpha) \frac{\partial f_L}{\partial p_i} = \sum_{\alpha=1}^{M} y_\alpha \frac{\partial f_L}{\partial p_i} \quad \text{for } i = 1, 2, \ldots, L \tag{2.2}$$

Since $\partial f_L/\partial p_i$ involves not only x_α but also $\{p_k\}$, Eq. (2.2) must be solved by a numerical method in most cases. There are several algorithms for simultaneous nonlinear equations: the gradient descent method, the conjugate gradient method, the Newton method, and so on. However, it is known that the *Levenberg–Marquardt method* (LM) is one of the most stable and reliable methods for most

cases of nonlinear regression. Most commercial programs for scientific graph such as SigmaPlot™ adopt the Levenberg–Marquardt method as the algorithm of nonlinear regression.

2.2 The Levenberg–Marquardt Algorithm

In vector notation, Eq. (2.1) can be rewritten as $\chi^2 = \|\mathbf{y} - \mathbf{f}_L(\mathbf{p})\|^2$ where

$$\mathbf{y} = \begin{bmatrix} y_1 \\ y_2 \\ \vdots \\ y_M \end{bmatrix}; \quad \mathbf{f}_L = \begin{bmatrix} f_L(x_1, \mathbf{p}) \\ f_L(x_2, \mathbf{p}) \\ \vdots \\ f_L(x_M, \mathbf{p}) \end{bmatrix}; \quad \mathbf{p} = \begin{bmatrix} p_1 \\ p_2 \\ \vdots \\ p_L \end{bmatrix} \tag{2.3}$$

Note that both $\mathbf{y}$ and $\mathbf{f}_L$ are M-dimensional vectors, while $\mathbf{p}$ is an L-dimensional vector. We are interested in an iterative equation for the parameter vector $\mathbf{p}_r$ where r is the iterative number. We want $\mathbf{y} - \mathbf{f}_L(\mathbf{p}_r) = \mathbf{0}$ for $r > N$. One of the simplest iterative equations may be given by

$$\mathbf{p}_{r+1} = \mathbf{p}_r + \mathbf{B} \cdot [\mathbf{y} - \mathbf{f}_L(\mathbf{p}_r)] \tag{2.4}$$

where $\mathbf{B}$ is an $L \times M$ matrix which must be chosen to make the iterative equation result in the desirable solution. Various algorithms might be suggested depending on how to choose the matrix $\mathbf{B}$. See a textbook of numerical method if the condition of $\mathbf{B}$ is interesting. Here, it is sufficient to say that if $\mathbf{y} - \mathbf{f}_L(\mathbf{p}_r) = \mathbf{0}$, then $\mathbf{p}_N = \mathbf{p}_r$ for any N larger than r.

The Levenberg–Marquardt algorithm starts from

$$\mathbf{f}_L(\mathbf{p} + \delta\mathbf{p}) = \mathbf{f}_L(\mathbf{p}) + \mathbf{J} \cdot \delta\mathbf{p} \tag{2.5}$$

where $\mathbf{J}$ is the Jacobian matrix of $\mathbf{f}_L$: $\mathbf{J} = \partial\mathbf{f}_L(\mathbf{p})/\partial\mathbf{p}$. The iterative equation of the Levenberg–Marquardt algorithm is obtained from $\partial\|\mathbf{y} - \mathbf{f}_L(\mathbf{p} + \delta\mathbf{p})\|^2/\partial\delta\mathbf{p} = \mathbf{0}$. This gives

$$\mathbf{J}^T \cdot \mathbf{J} \cdot \delta\mathbf{p} = \mathbf{J}^T \cdot [\mathbf{y} - \mathbf{f}_L(\mathbf{p})] \tag{2.6}$$

Introduction of $\delta\mathbf{p} = \mathbf{p}_{r+1} - \mathbf{p}_r$ with $\mathbf{p} = \mathbf{p}_r$ gives

$$\mathbf{p}_{r+1} = \mathbf{p}_r + \left(\mathbf{J}^T \cdot \mathbf{J}\right)^{-1} \cdot \mathbf{J}^T \cdot [\mathbf{y} - \mathbf{f}_L(\mathbf{p}_r)] \tag{2.7}$$

This iterative equation implies that if $\|\mathbf{y} - \mathbf{f}_L(\mathbf{p}_r)\| \to 0$ as iteration number r increases, then $\mathbf{p}_r$ converges to a certain vector as $r \to \infty$. We expect that the further iteration makes the parameter vector closer to the optimum at which $\|\mathbf{y} - \mathbf{f}_L(\mathbf{p}_r)\|^2$

is minimized. If the sum of square error has the global minimum, then the sequence of $\mathbf{p}_r$ goes to the optimum vector irrespective of the initial guess. However, if $\|\mathbf{y} - \mathbf{f}_L(\mathbf{p})\|^2$ has multiple minima, then the iterative equation gives the correct answer whenever the initial guess is close to the global minimum. Equation (2.7) breaks down if the square matrix $\mathbf{J}^T \cdot \mathbf{J}$ is singular. To prevent such a bad case, the Levenberg–Marquardt algorithm uses

$$\mathbf{p}_{r+1} = \mathbf{p}_r + \left(\mathbf{J}^T \cdot \mathbf{J} + \kappa_r \mathbf{I}\right)^{-1} \cdot \mathbf{J}^T \cdot [\mathbf{y} - \mathbf{f}_L(\mathbf{p}_r)] \tag{2.8}$$

where $\kappa_r > 0$. It is well known that $\mathbf{J}^T \cdot \mathbf{J} + \kappa_r \mathbf{I}$ is not singular. It is an example of *Tikhonov regularization* (Kirsch 2010). The choice of κ_r is somewhat heuristic. See a textbook of numerical analysis (Press et al. 2002).

2.3 Example I

It is well known that shear viscosity of polymer melt is a function of both shear rate and temperature. One of the most popular models for shear viscosity is the Carreau–Yasuda model (Bird et al. 1987) such that

$$\eta(\dot{\gamma}, T) = \frac{\eta_o(T)}{\{1 + [\eta_o(T)\dot{\gamma}/\sigma_o]^a\}^b} \tag{2.9}$$

where

$$\eta_o(T) = K \exp\left(\frac{T_A}{T}\right) \tag{2.10}$$

Note that a, b, σ_o, K, and T_A are positive real numbers to be determined by nonlinear regression. Experimental data may consist of three columns of numbers such as $[\dot{\gamma}_1, \dot{\gamma}_2, \ldots, \dot{\gamma}_M]^T$, $[T_1, T_2, \ldots, T_M]^T$ and $[\eta_1, \eta_2, \ldots, \eta_M]^T$. The regression based on least square is to minimize

$$\chi^2 = \sum_{\alpha=1}^{M} [\eta_\alpha - \eta(\dot{\gamma}_\alpha, T_\alpha)]^2 \tag{2.11}$$

Since commercial softwares such as SigmaPlot™ are equipped with the LM algorithm, it seems trivial to determine the parameters. However, it is not trivial because viscosity and shear rate vary in logarithmic scale and the order of magnitude of parameters varies very widely. Parameters a and b are in (0, 1), while T_A varies from hundreds to thousands in Kelvin and K and σ_o vary in logarithmic scale depending on materials. Since most algorithms of nonlinear regression largely depend on initial guess of parameters, most novices of regression often give up the

regression after hundreds of trial and errors in guessing initial values of parameters. An expert may guess appropriate initial values if experimental data are sufficiently large for recognizing the outline shape of Eq. (2.9) for all temperatures under consideration. In this fortunate case, the expert determines the zero-shear viscosities first at a few temperatures, say $\{T_1, T_2, \ldots, T_n\}$. Then, we can extract a data set consisting two column vectors $[T_1, T_2, \ldots, T_n]^T$ and $[\eta_o(T_1), \eta_o(T_2), \ldots, \eta_o(T_n)]^T$ from the original data set. This reduced set of data can be applied to Eq. (2.10) by changing variables as follows

$$\log \eta_o = \log K + \frac{T_A}{T} \tag{2.12}$$

A linear regression gives the values of $\log K$ and T_A. Then, the number of parameters to be determined is reduced from 5 to 3. The initial value of σ_o can be guessed by the shear rate at which viscosity changes from Newtonian to power law types. As for a and b, the value of ab can be guessed by the slope of the plot of $\log \eta$ with respect to $\log \dot{\gamma}$ in the power law region of shear rate. Then, the LM method immediately gives the optimum values of all parameters.

Unfortunately, no rheometer allows us to measure the viscosity data for sufficiently wide range of shear rate. Figure 3 represents simulated data. Note that only 270 °C data show Newtonian region. Since there is a limit of shear rate for any rheometer, Fig. 3 can be considered to represent one of usual cases. To make the order of magnitudes of parameters normalized, we use

$$\begin{aligned} &\widetilde{a} = a; \quad \widetilde{b} = b; \quad \widetilde{T}_A = \log T_A; \quad \widetilde{K} = \log K; \quad \widetilde{\sigma}_o = \log \sigma_o; \\ &\widetilde{T} = \log T; \quad g = \log \dot{\gamma} \end{aligned} \tag{2.13}$$

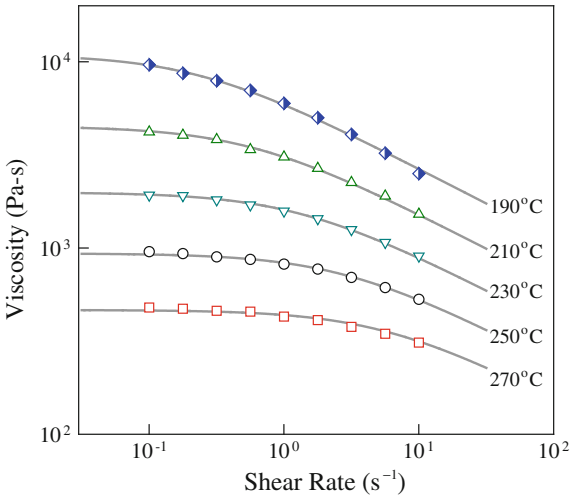

Fig. 3 Simulated data of shear viscosity and regression results

Then, Eq. (2.9) becomes

$$\log \eta = \widetilde{K} + e^{\widetilde{T}_A - \widetilde{T}} + b \log\left\{1 + \exp\left[a\left(\widetilde{K} + e^{\widetilde{T}_A - \widetilde{T}} - \widetilde{\sigma}_o + g\right)\right]\right\} \tag{2.14}$$

As the first guess, set $a = 1$, $b = 0.5$, $\widetilde{T}_A = 10$, $\widetilde{K} = -10$, and $\widetilde{\sigma}_o = 10$. Then, regression for Eq. (2.14) gives

$$\begin{aligned} &a = 1; \quad b = 0.3747; \quad T_A = 9928\,\mathrm{K}; \\ &K = 5.323 \times 10^{-6}\,\mathrm{Pa\ s}; \quad \sigma_o = 2553\,\mathrm{Pa} \end{aligned} \tag{2.15}$$

with the coefficient of determination $R^2 = 0.9996$. The lines in Fig. 3 represent the results of the regression. Note that $a = 1$ is fixed, while other parameters are determined by the minimization of Eq. (2.11). If one of a and b is not fixed by 1, then it is usual that unrealistic exponents are obtained. Since $R^2 = 0.9996$ is very close to unity, it is sufficient to use $a = 1$.

Another method to fit the data of Fig. 3 is to use superposition. Since σ_o is independent of temperature, Eq. (2.9) can be rewritten as

$$\widetilde{\eta} \equiv \frac{\eta(\gamma, T)}{\eta_o(T)} = \frac{1}{[1 + (\widetilde{g}/\sigma_o)^a]^b} \leq 1 \tag{2.16}$$

where $\widetilde{g} \equiv \eta_o(T)\dot{\gamma}$. This equation implies that a temperature function $B_T \propto \eta_o(T)$ makes a master curve such that

$$\frac{\eta(\dot{\gamma}, T)}{B_T} = \frac{h_o}{[1 + c(B_T\dot{\gamma})^a]^b} \tag{2.17}$$

It is possible to determine shift factor B_T without the knowledge of η_o by the procedure similar to those of time–temperature superposition. Set the reference temperature, for example, $T_{\mathrm{ref}} = 270\,^\circ\mathrm{C}$ as for the data of Fig. 3. In the double logarithmic plot of viscosity against shear rate, seek B_{250} which makes the plot of $\eta(\dot{\gamma}, 250)/B_{250}$ against $B_{250}\dot{\gamma}$ superposed on the plot of $\eta(\dot{\gamma}, 270)$ against $\dot{\gamma}$. Repetition of this procedure for other temperatures gives a master curve as shown in Fig. 4. Then, we can form a data set such as $[190, 210, 230, 250, 270]^T$ and $[B_{190}, B_{210}, B_{230}, B_{250}, B_{270} = 1]^T$. Then, it follows that

$$B_T = \exp\left(\frac{T_A}{T} - \frac{T_A}{T_{\mathrm{ref}}}\right) \tag{2.18}$$

Regression of Eq. (2.18) gives T_A. Regression of Eq. (2.17) for the master curve gives

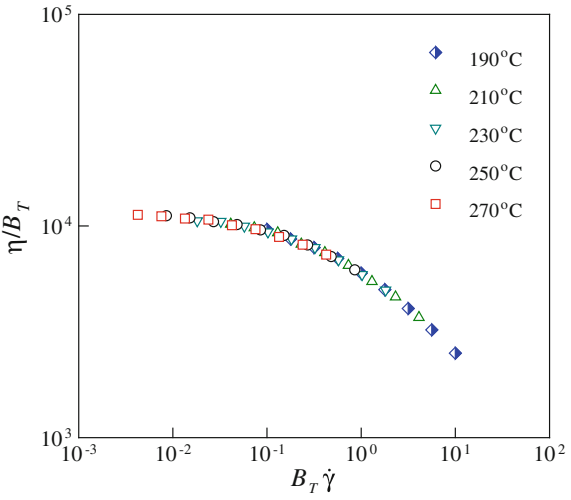

Fig. 4 Master curve from the data of Fig. 3

$$h_o = K\exp\left(\frac{T_A}{T_{ref}}\right); \quad c = \left[\frac{K}{\sigma_o}\exp\left(\frac{T_A}{T_{ref}}\right)\right]^a \tag{2.19}$$

The problem is how to make such superposition. We shall deal with numerical methods for superposition by vertical and horizontal shifting in the section for time–temperature superposition.

2.4 Example II

Another example of model fitting is the determination of the parameters of linear viscoelastic model. Marin and Graessley (1977) showed that dynamic moduli of monodisperse polymer melts are described well by the modified Cole–Cole model such as

$$J^*(\omega) = \frac{1}{i\eta_o\omega} + J_g + \frac{J_1}{1+(it_1\omega)^{\alpha_1}} + \frac{J_2}{1+(it_2\omega)^{\alpha_2}} \tag{2.20}$$

where $i = \sqrt{-1}$ is the imaginary unit, η_o is the zero-shear viscosity, J_g is the compliance of the glassy region, J_1, J_2, t_1, t_2, α_1, and α_2 are positive constants, and $J^*(\omega) = J'(\omega) - iJ''(\omega)$ is the complex compliance. Without loss of generality, we choose $t_1 > t_2$, which corresponds to the retardation times for the relaxations in molten and glassy states, respectively. Note that the terms of longer time t_1 includes reptation and the Rouse mode. Then, J_1 and J_2 are corresponding compliances. The exponents, α_1 and α_2, characterize the retardation spectrum.

However, fitting experimental data with respect to Eq. (2.20) is too complicate because Eq. (2.20) is the equation of complex variables. Tediously, long manipulation of algebra gives

$$J'(\omega) = J_g + \sum_{k=1}^{2} J_k \frac{1 + z_k \cos\theta_k}{1 + 2z_k \cos\theta_k + z_k^2} \tag{2.21a}$$

$$J''(\omega) = \frac{1}{\eta_o \omega} + \sum_{k=1}^{2} J_k \frac{z_k \sin\theta_k}{1 + 2z_k \cos\theta_k + z_k^2} \tag{2.21b}$$

where

$$\theta_k = \frac{\pi\alpha_k}{2}, \quad z_k = (t_k\omega)^{\alpha_k}, \quad k = 1 \text{ or } 2 \tag{2.22}$$

Here, we used $ix = x\exp(\frac{1}{2}\pi i)$ and $\left(ae^{i\phi}\right)^m = a^m e^{im\phi} = a^m(\cos m\phi + i\sin m\phi)$. Although $0 \le a_k < 1$, other parameters vary in logarithmic scale. Hence, we have to adopt the technique used for shear viscosity again. However, Eqs. (2.21a, b) are more complicate than Eq. (2.9). To simplify the problem, we exploit

$$J^*(\omega) = \left[s\widetilde{J}(s)\right]_{s=i\omega} \Rightarrow s\widetilde{J}(s) = \frac{1}{\eta_o s} + J_g + \frac{J_1}{1 + (t_1 s)^{\alpha_1}} + \frac{J_2}{1 + (t_2 s)^{\alpha_2}} \tag{2.23}$$

where $\widetilde{J}(s)$ is the Laplace transform of creep compliance. If we can convert dynamic data to the Laplace transform of creep compliance, we can use

$$\log \Pi(\sigma) = \log\left\{ e^{-\sigma - h_o} + \frac{e^{j_1}}{\left[1 + e^{\alpha_1\left(\sigma + \widetilde{t}_1\right)}\right]^{\beta_1}} + \frac{e^{j_2}}{\left[1 + e^{\alpha_2\left(\sigma + \widetilde{t}_2\right)}\right]^{\beta_2}} + e^{j_g} \right\} \tag{2.24}$$

where $\Pi(\sigma) = s\widetilde{J}(s)$ with $\sigma = \log s$ and

$$h_o = \log \eta_o, \quad j_k = \log J_k, \quad \widetilde{t}_k = \log t_k, \quad k = 1, 2 \text{ or } g \tag{2.25}$$

Then, the problem to be solved is how to obtain the Laplace transform $s\widetilde{J}(s)$ from the data of $G'(\omega)$ and $G''(\omega)$. Numerical Laplace transform of experimental data usually faces the problem of finite window. Experimental data are essentially measured in a finite range of test conditions. We shall deal with how to obtain reliable Laplace transform from experimental data later. For a while, it is assumed that such Laplace transform is available. We shall show how to do it later.

Remind Fig. 12 in Chap. 5 which is the dynamic modulus of monodisperse polybutadiene measured by Stadler (Stadler and van Ruymbeke 2010). Figure 5 is obtained by the application of the method of numerical Laplace transform to the data of Fig. 12 in Chap. 5. The lines in Figs. 12 in Chap. 5 and 5 are calculated by the values of the parameters as follows

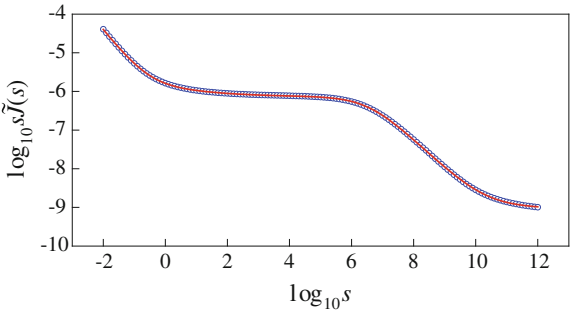

Fig. 5 The Laplace transform of creep compliance $s\tilde{J}(s)$. Symbols are calculated from loss modulus of Fig. 12 in Chap. 5 and line is the curve fitting by Eq. (2.24)

$$\begin{aligned} \eta_o &= 2.658 \times 10^6 \text{ Pa s}, \quad J_1 = 1.162 \times 10^{-6} \text{ Pa}^{-1} \\ J_2 &= 7.274 \times 10^{-7} \text{ Pa}^{-1}, \quad J_g = 1.004 \times 10^{-9} \text{ Pa}^{-1} \\ t_1 &= 2.136 \text{ s}, \quad t_2 = 2.482 \times 10^{-7} \text{ s} \\ \alpha_1 &= 0.3605, \quad \alpha_2 = 0.7835 \end{aligned} \tag{2.26}$$

It must be mentioned that the use of Eq. (2.24) gives more precise values of the parameters than those of Eqs. (2.21a, b) and (2.23).

In summary, logarithmic scaling of parameters of viscoelastic model makes initial guess of parameters much easier. Without such scaling, a number of trail and errors are necessary to have an acceptable fitting.

Problem 2

[1] Fixed-point iteration is a method to compute the solution of nonlinear equations in an iterative manner. Fixed-point iteration can be written formally

$$\mathbf{x}_{r+1} = \mathbf{T}(\mathbf{x}_r) \tag{2.a}$$

where $\mathbf{x}_r$ is an N-dimensional vector and $\mathbf{T}(\mathbf{x})$ is a mapping from N-dimensional vector space V to the same vector space. The vector space V is assumed to be the complete metric space. Suppose that for any two vectors $\mathbf{x}$ and $\mathbf{y}$, there exists a positive constant $0 \leq L < 1$ such that

$$\|\mathbf{T}(\mathbf{x}) - \mathbf{T}(\mathbf{y})\| \leq L\|\mathbf{x} - \mathbf{y}\| \tag{2.b}$$

Then, the mapping $\mathbf{T}$ is called *contraction map*. Show that the contraction map $\mathbf{T}$ admits a unique fixed point $\mathbf{x}^*$ in V (Atkinson and Han 2000).

[2] If $y = f_L(x) > 0$ for a given interval and we are interested in nonlinear regression for the same interval, then instead of Eq. (2.1), one may be interested in the minimization of

$$\chi^2_{\mathrm{Rel}} = \sum_{\alpha=1}^{M} \left[1 - \frac{f_L(x_\alpha)}{y_\alpha} \right]^2 \tag{2.c}$$

What would be the merit of the use of Eq. (2.c)?

[3] Derive Eqs. (2.21a) and (2.21b).

[4] Some nonlinear function can be linearized by transform of variables. One of the simplest examples is $y = A\exp(kx)$. If taking $\widetilde{y} = \log y$ and $\widetilde{x} = x$, then we have $\widetilde{y} = a\widetilde{x} + b$ where $a = k$ and $b = \log A$. Then, find the transforms for the following relations:

$$y = \exp\left(\frac{c_1 x}{c_2 + x}\right); \tag{2.d}$$

$$y = \frac{1}{1 + e^{-\beta_1 - \beta_2 x}}. \tag{2.e}$$

3 Padé Approximation

3.1 Basics

We know that $\pi \approx 3.141592$. The three-digit approximation by decimal notation is 3.14, while three-digit approximation by rational number is 22/7. It is interesting to compare $|1 - 3.14/\pi| \approx 5.07 \times 10^{-4}$ with $|1 - 22/(7\pi)| \approx 4.03 \times 10^{-4}$. The rational approximation is better than decimal approximation!

Then, one must be interested in which is better among the two following approximations:

$$f(x) \approx \sum_{n=0}^{M+N} c_n x^n \tag{3.1}$$

and

$$f(x) \approx \frac{\sum_{k=0}^{M} a_k x^k}{1 + \sum_{n=1}^{N} b_n x^n} \equiv R_{M/N}(x) \tag{3.2}$$

Note that both approximations have the same number of coefficients to be determined, $M + N + 1$. Under the assumption of $b_0 \neq 0$, Eq. (3.2) is obtained by dividing both numerator and denominator by b_0. The rational approximation,

Eq. (3.2), is called *Padé approximation*. Although the authors have found no mathematical proof, there are a number of examples that Padé approximation is better than polynomial ones. One of demerits of the Padé approximation is that the denominator happens to be zero at some values of x. There is no systematic way to prevent such a bad case.

Suppose that the coefficients a_n of Eq. (3.1) are given. Then, comparing Eq. (3.1) with Eq. (3.2), we obtain

$$\left(c_0 + c_1 x + \cdots + c_{N+M} x^{N+M}\right)\left(1 + b_1 x + \cdots + b_N x^N\right) = a_0 + a_1 x + \cdots a_N x^N \tag{3.3}$$

The left hand side of Eq. (3.3) can be expanded by

$$c_0 + (c_0 b_1 + c_1)\, x + (c_0 b_2 + c_1 b_1 + c_2)\, x^2 + \cdots + c_{N+M} b_M x^{N+2M} \tag{3.4}$$

Comparison of Eq. (3.4) with the right-hand side of Eq. (3.3) gives a system of linear equations which assume coefficients $\{a_n\}$ and $\{b_m\}$ as unknowns. The system of linear equations can be constructed in a systematic manner (Press et al. 2002). As for $M = N$, the system of linear equations is given by

$$\sum_{m=1}^{N} b_m c_{N-m+k} = -c_{N+k}, \quad k = 1, 2, \ldots, N \tag{3.5a}$$

$$\sum_{m=0}^{k} b_m c_{k-m} = a_k, \quad k = 1, 2, \ldots, N \tag{3.5b}$$

After b_k is obtained from Eq. (3.5a), a_k can be determined from b_k through Eq. (3.5b).

These identity equations hold even if we replace the simple polynomials of Eq. (3.3) by orthogonal polynomials. Instead of Eq. (3.1), we can fit experimental data by

$$f(x) \approx \sum_{k=0}^{M+N} c_k T_k(\xi) \tag{3.6}$$

where ξ is the normalized variable of Eq. (1.15). Such polynomial regression gives $\{c_k\}$ for even high $M + N$. Solving Eqs. (3.5a) and (3.5b) gives

$$f(x) \approx \frac{\sum_{k=0}^{M} a_k T_k(\xi)}{1 + \sum_{n=1}^{N} b_n T_n(\xi)} \tag{3.7}$$

3.2 Application to the FENE Model

Statistical mechanical theory gives the magnitude of force exerted on a single polymer chain as follows

$$f = \frac{k_B T}{b} \mathsf{L}^{-1}\left(\frac{r}{Nb}\right) \tag{3.8}$$

where f is the magnitude of the force, k_B is the Boltzmann constant, T is absolute temperature, r is the root mean square of end-to-end distance, N is the number of the Kuhn's segments (Rubinstein and Colby 2003), b is the length of the Kuhn's segment, and $\mathsf{L}^{-1}(x)$ is the inverse Langevin function such that

$$\mathsf{L}(x) = \coth x - \frac{1}{x} \tag{3.9}$$

It is known that the inverse Langevin function becomes infinite as x approaches to unity. The Maclaurin series of $\mathsf{L}^{-1}(x)$ is known as

$$\mathsf{L}^{-1}(x) = 3x + \frac{9}{5}x^3 + \frac{297}{175}x^5 + \frac{1539}{875}x^7 + \frac{126{,}117}{67{,}375}x^9 + \cdots \tag{3.10}$$

Finitely extensible nonlinear elastic (FENE) model (Bird et al. 1987) is the approximation such that

$$\mathsf{L}^{-1}(x) = \frac{3x}{1 - x^2} \tag{3.11}$$

Equation (3.11) is called the *Warner's approximation* which seems to be based on the following features of the inverse Langevin function:

$$\mathsf{L}^{-1}(-x) = -\mathsf{L}^{-1}(x); \tag{3.12a}$$

$$\mathsf{L}^{-1}(x) \approx 3x \quad \text{for} \quad |x| \gg 1; \tag{3.12b}$$

$$\lim_{x \to 1} \mathsf{L}^{-1}(x) = \infty \tag{3.12c}$$

However, applications of Eq. (3.10) to $R_{2/2}(x)$ and $R_{3/3}(x)$ give, respectively

$$\mathsf{L}^{-1}(x) \approx \frac{3x}{1 - \frac{3}{5}x^2} \tag{3.13}$$

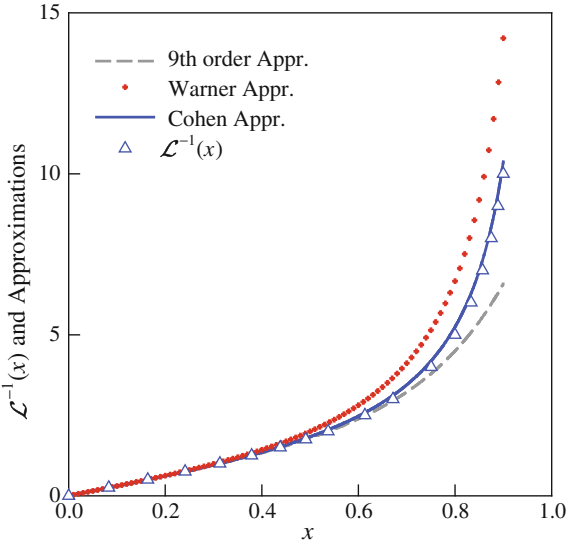

Fig. 6 Comparison of various approximations of the inverse Langevin function

and

$$\mathsf{L}^{-1}(x) \approx \frac{3x - \frac{36}{35}x^3}{1 - \frac{33}{35}x^2} \tag{3.14}$$

For simplicity, Cohen (1991) adopted

$$\mathsf{L}^{-1}(x) \approx \frac{3x - x^3}{1 - x^2} \tag{3.15}$$

Figure 6 compares the ninth order Taylor series (Eq. 3.10), the Warner approximation (Eq. 3.11), and the Cohen approximation (Eq. 3.15) with the inverse Langevin function. It is obvious that Eq. (3.15) is the best among the three approximations.

3.3 Application to Discrete Spectrum

We have learned that the Laplace transforms of spring–dashpot models are expressed by rational functions. So do both dynamic moduli and compliances. If we know the Taylor expansion coefficients of $s\widetilde{G}(s)$, then the use of Eq. (3.1) gives the coefficients of numerator and denominator. We shall learn how to determine the Taylor expansion coefficients of $s\widetilde{G}(s)$ in Chap. 7 (Padé–Laplace method). Nonlinear regression by the Levenberg–Marquardt algorithm can also determine all the coefficients of the Padé approximation.

It is necessary to mention some characteristics of the problem to infer discrete spectrum. The multimode Maxwell model reads

$$\widetilde{G}(s) = \sum_{k=1}^{N} \frac{G_k}{s + \lambda_k^{-1}} = \frac{Q_0 + Q_1 s + \cdots + Q_{N-1} s^{N-1}}{1 + P_1 s + \cdots + P_N s^N} \tag{3.16}$$

Since all G_k and λ_k are positive, it is obvious that all coefficients P_k and Q_k must be positive too. Hence, nonlinear regression should be done under the constraints of $P_k > 0$ and $Q_k > 0$. To avoid the use of auxiliary constraints, reformulation of Eq. (3.16) is needed:

$$\widetilde{G}(s) = \frac{e^{q_0} + e^{q_1} s + \cdots + e^{q_{N-1}} s^{N-1}}{1 + e^{p_1} s + \cdots + e^{p_N} s^N} \tag{3.17}$$

where $p_k = \log P_k$ and $q_k = \log Q_k$. However, this approach is not successful even if the range of s is not too wide.

Even if all the coefficients of the rational approximation of $\widetilde{G}(s)$ are determined, inferring the discrete spectrum can be completed by the determination of G_k and λ_k from the coefficients of the Padé approximation. Relaxation times λ_k can be determined by the algorithms for roots of polynomial (Press et al. 2002). If λ_k is determined, then the relaxation intensities G_k are determined by

$$G_k = \left[\left(s + \lambda_k^{-1} \right) \frac{Q_0 + Q_1 s + \cdots + Q_{N-1} s^{N-1}}{1 + P_1 s + \cdots + P_N s^N} \right]_{s = -\lambda_k^{-1}} \tag{3.18}$$

Problem 3

[1] Derive

$$e^{-x} \approx \frac{840 - 360x + 60x^2 - x^3}{840 + 480x + 120x^2 + 16x^3 + x^4} \tag{3.a}$$

[2] Derive

$$\arctan x \approx \frac{x + \frac{7}{9}x^3 + \frac{64}{945}x^5}{1 + \frac{10}{9}x^2 + \frac{5}{21}x^4} \tag{3.b}$$

[3] When a function $f(x)$ can be expressed by

$$f(x) = \sum_{k=0}^{\infty} a_k T_k(x) \quad \text{with} \quad -1 \le x \le 1 \tag{3.c}$$

one may think the Chebyshev–Padé approximation such as

$$f(x) \approx \frac{\sum_{k=1}^{N} b_k T_k(x)}{\sum_{k=0}^{M} c_k T_k(x)} \tag{3.d}$$

Consider the identity such that

$$T_m(x)T_n(x) = \frac{T_{m+n}(x) + T_{|m-n|}(x)}{2} \tag{3.e}$$

Then, you can determine the coefficients $\{b_k\}$ and $\{c_k\}$ from $\{a_k\}$ by using

$$\left[\sum_{k=0}^{\infty} a_k T_k(x)\right]\left[\sum_{k=0}^{M} c_k T_k(x)\right] - \sum_{k=0}^{N} b_k T_k(x) = 0 \tag{3.f}$$

Find $\{b_k\}$ and $\{c_k\}$ of $f(x) = e^{-x}$ with $M = 2$ and $N = 3$.

4 Numerical Integration and Differentiation

Most readers of this book are assumed to be familiar with numerical integration and differentiation of sophomore course in engineering college:

Numerical Integration (Trapezoidal Rule)

$$\int_a^b f(x)\,\mathrm{d}x \approx \frac{b-a}{N}\left[\frac{f(a)}{2} + \sum_{k=1}^{N-1} f\left(a + k\frac{b-a}{N}\right) + \frac{f(b)}{2}\right] \tag{4.1}$$

Numerical Differentiation

$$f(x_k) \approx \frac{f(x_{k+1}) - f(x_k)}{x_{k+1} - x_k} \approx \frac{f(x_k) - f(x_{k-1})}{x_k - x_{k-1}} \approx \frac{f(x_{k+1}) - f(x_{k-1})}{x_{k+1} - x_{k-1}} \tag{4.2}$$

However, this section is devoted to the numerical integration and differentiation of experimental data. Since any experimental data are contaminated by experimental error, some cautions must be necessary.

4.1 Error Analysis of Integration of Experimental Data

We are interested in numerical integration and differentiation of experimental data rather than given functions. The basic assumption is that the αth data, x_α and y_α, satisfy

$$y_\alpha = f(x_\alpha) + \varepsilon_\alpha \tag{4.3}$$

where ε_α is the error involved in the αth data, whose expectations satisfy

$$\langle \varepsilon_\alpha \rangle = 0; \quad \langle \varepsilon_\alpha \varepsilon_\beta \rangle = \sigma^2 \delta_{\alpha\beta} \tag{4.4}$$

The second condition implies that errors are statistically independent. For numerical integration and differentiation, it is usually assumed that $|x_{\alpha+1} - x_\alpha|$ is sufficiently small. For simplicity, assume equally spaced x_α such that irrespective of α, $x_{\alpha+1} - x_\alpha \equiv h > 0$, and $h \ll 1$.

When trapezoidal method is applied to the data, the numerical integration is given by

$$I = \frac{h}{2} \sum_{\alpha=1}^{M-1} (y_{\alpha+1} + y_\alpha) = \frac{h}{2} \sum_{\alpha=1}^{M-1} [(f_{\alpha+1} + f_\alpha) + (\varepsilon_\alpha + \varepsilon_{\alpha+1})] \tag{4.5}$$

where $f_\alpha = f(x_\alpha)$. Then the expectation of the numerical integration is given by

$$\langle I \rangle = \frac{h}{2} \sum_{\alpha=1}^{M-1} (f_\alpha + f_{\alpha+1}) \tag{4.6}$$

On the other hand, the variance of the integral is given by

$$\langle I^2 \rangle - \langle I \rangle^2 = \frac{h^2}{4} \left\langle \sum_{\alpha=1}^{M-1} \sum_{\beta=1}^{M-1} (\varepsilon_\alpha + \varepsilon_{\alpha+1})(\varepsilon_{\beta+1} + \varepsilon_\beta) \right\rangle = \frac{\sigma^2 h^2}{4} \left(M - \frac{3}{2} \right) \tag{4.7}$$

The ratio of standard deviation to mean is called *coefficient of variation* (CV), which is an important measure of precision. Equation (4.7) gives the coefficient of variation:

$$CV[I] = \frac{\sqrt{\langle I^2 \rangle - \langle I \rangle^2}}{\langle I \rangle} \approx \frac{\sigma \sqrt{M}}{\sum_{\alpha=1}^{M-1} (f_\alpha + f_{\alpha+1})} \approx \frac{\sigma}{2\bar{y}\sqrt{M}} = \frac{CV[y]}{2\sqrt{M}} \tag{4.8}$$

where we used

$$\overline{y} = \frac{1}{M}\sum_{\alpha=1}^{M} f_\alpha \approx \langle y \rangle \approx \frac{1}{2M}\sum_{\alpha=1}^{M-1} (f_\alpha + f_{\alpha+1}) \tag{4.9}$$

Equation (4.8) implies that the CV of integration is much smaller than that of experimental data. Hence, the numerical integration of experimental data becomes more stable for the errors in the data as the number of data, M increases. x_α is sufficiently narrow.

For sufficiently small h, it is known that

$$\frac{\mathrm{d}f(x_\alpha)}{\mathrm{d}x} \approx \frac{f_{\alpha+1} - f_\alpha}{h} \tag{4.10}$$

This is the forward numerical differentiation of function $f(x)$. Application of the numerical differentiation to the data of Eq. (4.3) gives

$$y'_\alpha \equiv \frac{y_{\alpha+1} - y_\alpha}{h} = \frac{f_{\alpha+1} - f_\alpha}{h} + \frac{\varepsilon_{\alpha+1} - \varepsilon_\alpha}{h} \tag{4.11}$$

Taking expectation on both sides of Eq. (4.11), we have

$$\langle y'_\alpha \rangle = \frac{f_{\alpha+1} - f_\alpha}{h} \tag{4.12}$$

Similar to the variance of the numerical integration, we have

$$\left\langle \left(y'_\alpha\right)^2 \right\rangle - \langle y'_\alpha \rangle^2 = \langle y'_\alpha \rangle^2 + \frac{2\sigma^2}{h^2} \tag{4.13}$$

Then, the CV of numerical differentiation is given by

$$\mathrm{CV}\left[\langle y'_\alpha \rangle\right] = \sqrt{1 + \frac{2}{h^2}\{\mathrm{CV}[y]\}^2} > \mathrm{CV}[y] \tag{4.14}$$

Equation (4.14) implies that the smaller the h is, the larger the variation occurs in the numerical differentiation of Eq. (4.11). On the other hand, the smaller the h *is*, the higher the precision is achieved for the numerical differentiation of the exact function: Eq. (4.2). It can be said that errors in raw data are magnified by numerical differentiation. Therefore, it is usual that numerical differentiation of experimental data, Eq. (4.11), gives undesirable result. It is the ill-posedness of the numerical differentiation of experimental data.

Figure 7 shows stability of numerical integration of experimental data. Here, $\mathrm{d}Y/\mathrm{d}x = y = (1+x^2)^{-1}$ and $Y = \arctan x$. We add Gaussian error ε whose mean is zero and standard deviation σ is unity, that is, $y = (1+x^2)^{-1}(1+0.1\varepsilon)$. Hence, it can be said that $\mathrm{CV}[y] = 0.1$. This contaminated data are used to calculate Y by

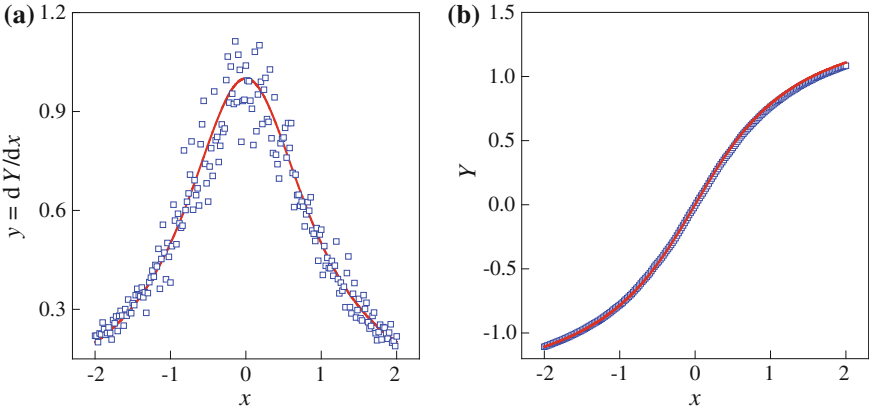

Fig. 7 Stability of numerical integration. Symbols represent hypothetical experimental data and their numerical integration of them and lines are exact ones

$$Y(x_n) = \arctan(-2) + \frac{h}{2}\sum_{\alpha=2}^{n}(y_{\alpha-1} + y_\alpha) \tag{4.15}$$

Figure 7 illustrates that numerical integration gives a reliable result because of mutual canceling of statistical errors, while numerical differentiation is a kind of ill-posed problem.

4.2 *Numerical Differentiation with Regularization*

We have learned that numerical differentiation is very unstable for experimental error, while numerical integration is very stable. Since numerical integration is stable, we shall show an approach that considers numerical differentiation as the inverse problem of numerical integration (Cullum 1971).

4.2.1 The IIR Algorithm

Without loss of generality, we consider two functions such that

$$\frac{df}{dx} = g(x); \quad f(0) = 0 \tag{4.16}$$

Here, we consider that data are $y_\alpha = f(x_\alpha) + \varepsilon_\alpha$ and $y'_\alpha = g(x_\alpha)$. Using the trapezoidal rule for numerical integration, we have

$$y_\alpha \approx \sum_{\beta=0}^{\alpha-1} h_\beta \left(y'_\alpha + y'_{\alpha+1}\right) \tag{4.17}$$

where $h_\alpha = \frac{1}{2}(x_\alpha - x_{\alpha-1})$. Then, Eq. (4.17) can be rewritten as

$$y_\alpha = \sum_{\beta=0}^{N} A_{\alpha\beta} y'_\beta \quad 0 < \alpha \leq N, \;\; f_0 = 0 \tag{4.18}$$

where

$$A_{\alpha\beta} = \begin{cases} h_1 & \text{for} \quad \beta = 0 \\ h_\beta + h_{\beta+1} & \text{for} \;\; 0 < \beta < \alpha \\ h_\alpha & \text{for} \;\; \beta = \alpha \\ 0 & \text{otherwise} \end{cases} \tag{4.19}$$

As an example, we know that

$$\begin{bmatrix} y_1 \\ y_2 \\ y_3 \\ y_4 \end{bmatrix} = \begin{bmatrix} h_1 & h_1 & 0 & 0 & 0 \\ h_1 & h_1 + h_2 & h_2 & 0 & 0 \\ h_1 & h_1 + h_2 & h_2 + h_3 & h_3 & 0 \\ h_1 & h_1 + h_2 & h_2 + h_3 & h_3 + h_4 & h_4 \end{bmatrix} \begin{bmatrix} y'_0 \\ y'_1 \\ y'_2 \\ y'_3 \\ y'_4 \end{bmatrix} \tag{4.20}$$

Since we are interested in an algorithm stable for experimental error, the introduction of the *Tikhonov regularization* (Kirsch 2010) is to minimize

$$\chi^2 = \sum_{\alpha=1}^{N} \left(y_\alpha - \sum_{\beta=1}^{N} A_{\alpha\beta} y'_\beta \right)^2 + \rho \sum_{\alpha=1}^{N} y'^2_\alpha \tag{4.21}$$

This is very similar to the linear regularization algorithm for continuous relaxation spectrum (Honerkamp and Weese 1989). Numerical differentiation is obtained by

$$\mathbf{y}' = \left(\mathbf{A}^T \cdot \mathbf{A} + \rho \mathbf{I}\right)^{-1} \cdot \mathbf{A}^T \cdot \mathbf{y} \tag{4.22}$$

For convenience, we call this method the *inverse integration with regularization* (IIR) to compare with cubic B-spline method which will be introduced later. The matrix **A** can be changed if we adopt other integration algorithms different from the trapezoidal rule.

Now, it is necessary to explain the reason why the regularization parameter ρ is introduced. When the regularization parameter is not used: $\rho = 0$, Eq. (4.22) can be rewritten as

$$\mathbf{y}' = \left(\mathbf{A}^T \cdot \mathbf{A}\right)^{-1} \cdot \mathbf{A}^T \cdot \mathbf{y} \tag{4.23}$$

If an $M \times N$ matrix $\mathbf{A}$ is given, then the theorem of *singular value decomposition* (Lawson and Hanson 1995) reads that

$$\mathbf{A} = \mathbf{U} \cdot \mathbf{E} \cdot \mathbf{V} \tag{4.24}$$

where $\mathbf{U}$ is an $M \times M$ orthogonal matrix, $\mathbf{E}$ is an $M \times N$ diagonal matrix whose diagonal components are nonnegative real numbers, and $\mathbf{V}$ is an $N \times N$ orthogonal matrix. Substitution of Eq. (4.24) into Eq. (4.23) gives

$$\mathbf{y}' = \left(\mathbf{V}^T \cdot \mathbf{E}^T \cdot \mathbf{E} \cdot \mathbf{V}\right)^{-1} \cdot \mathbf{V}^T \cdot \mathbf{E}^T \cdot \mathbf{U}^T \cdot \mathbf{y} \tag{4.25}$$

Since Eq. (4.20) implies that $M < N$, $\mathbf{E}$ should have M nonnegative diagonal components, $\sigma_i \geq 0$ and the $N \times N$ diagonal matrix $\mathbf{D} \equiv \mathbf{E}^T \cdot \mathbf{E}$ has M nonnegative diagonal components

$$D_{ik} = \begin{cases} \sigma_i^2 & \text{for } i = k \leq M \\ 0 & \text{for } i = k > M \\ 0 & \text{for } i \neq k \end{cases} \tag{4.26}$$

where σ_i are called *singular value* of the matrix $\mathbf{A}$, which is very similar to the eigenvalue of a square matrix. Hence, $\mathbf{D}$ is singular, and $\mathbf{V}^T \cdot \mathbf{E}^T \cdot \mathbf{E} \cdot \mathbf{V} = \mathbf{A}^T \cdot \mathbf{A}$ is also singular. It is impossible to obtain numerical differentiation with $\rho = 0$ as the inverse of integration. On the other hand, with $\rho > 0$, it is clear that

$$\mathbf{A}^T \cdot \mathbf{A} + \rho \mathbf{I}_N = \mathbf{V}^T \cdot (\mathbf{D} + \rho \mathbf{I}_N) \cdot \mathbf{V} \tag{4.27}$$

is not singular because

$$\left[(\mathbf{D} + \rho \mathbf{I}_N)^{-1}\right]_{ik} = \begin{cases} \left(\sigma_i^2 + \rho\right)^{-1} > 0 & \text{for } i = k \leq M \\ \rho^{-1} > 0 & \text{for } i = k > M \\ 0 & \text{for } i \neq k \end{cases} \tag{4.28}$$

Note that $\mathbf{I}_N$ is the $N \times N$ identity matrix. Furthermore, the inverse matrix of Eq. (4.27) is given by

$$\left(\mathbf{A}^T \cdot \mathbf{A} + \rho \mathbf{I}_N\right)^{-1} = \mathbf{V}^T \cdot (\mathbf{D} + \rho \mathbf{I}_N)^{-1} \cdot \mathbf{V} \tag{4.29}$$

This is called *pseudo-inverse matrix* of $\mathbf{A}^T \cdot \mathbf{A}$.

If we denote the numerical differentiation of Eq. (4.22) by $\mathbf{y}'_r(\rho)$, then Eq. (4.18) gives $\mathbf{y}_r(\rho) = \mathbf{A} \cdot \mathbf{y}'_r(\rho)$. Then, the norm $\|\mathbf{y} - \mathbf{y}_r(\rho)\|$ should be very small for the validity of $\mathbf{y}'_r(\rho)$ as a good approximation of differentiation. It is usual that if ρ is sufficiently small, then so is $\|\mathbf{y} - \mathbf{y}_r(\rho)\|$ but calculated differentiation becomes

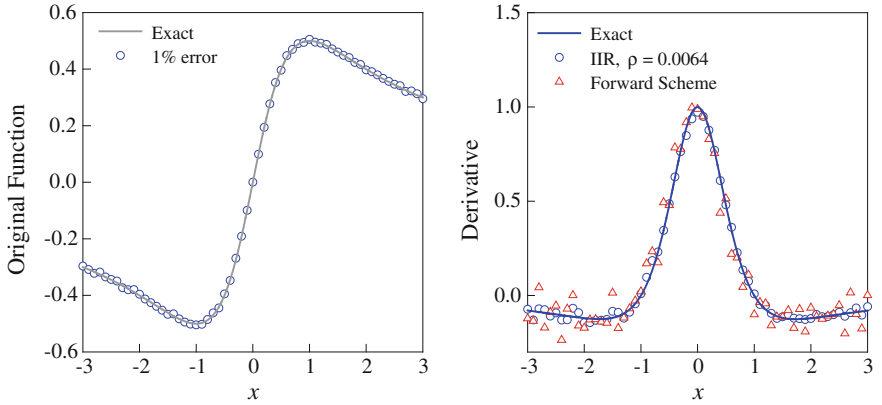

Fig. 8 Comparison of algorithms of numerical differentiation: the inverse integration with regularization and conventional forward scheme

noisy. On the other hand, the calculated differentiation becomes smoother as ρ increases. Hence, it is of importance to determine the optimum value of ρ. However, determination of the optimum ρ is heuristic.

Figure 8 shows the comparison of conventional numerical differentiation (forward scheme) with the inverse integration with regularization. The regularization parameter is chosen as $\rho = 6.4 \times 10^{-3}$. The original data are $y = x/(1+x^2)$ with 1 % errors. The errors are generated from the normal distribution with mean of 0 and standard deviation of 1. As shown in Fig. 8, the IIR algorithm is superior to the conventional one (forward scheme) because conventional ones are not equipped with suppression of error effect. As for error-contaminated data, higher-order derivatives are not reliable even if any error-suppression algorithm is applied. It is noteworthy that the recovered function from the numerical derivative of IIR is nearly indistinguishable from the exact function $y = x/(1+x^2)$.

4.2.2 The Error-Suppression Mechanism of Regularization

The error-suppression mechanism of the inverse integration with regularization can be understood by the use of the theorem of singular value decomposition. The experimental data $\mathbf{y}$ can be decomposed into the exact and error parts: $\mathbf{y} = \hat{\mathbf{y}} + \mathbf{e}$. Then, Eq. (4.22) can be rewritten as

$$\mathbf{y}' = \mathbf{V}^T \cdot (\mathbf{D} + \rho \mathbf{I}_N)^{-1} \cdot \mathbf{E}^T \cdot \mathbf{U}^T \cdot (\hat{\mathbf{y}} + \mathbf{e}) \tag{4.30}$$

where $\hat{\mathbf{y}}'$ is the derivative from exact function $\hat{\mathbf{y}}$:

$$\hat{\mathbf{y}}' = \mathbf{V}^T \cdot (\mathbf{D} + \rho \mathbf{I}_N)^{-1} \cdot \mathbf{E}^T \cdot \mathbf{U}^T \cdot \hat{\mathbf{y}} \tag{4.31}$$

and $\mathbf{y}'_e$ is the error originated from $\mathbf{e}$:

$$\mathbf{y}'_e = \mathbf{V}^T \cdot (\mathbf{D} + \rho \mathbf{I}_N)^{-1} \cdot \mathbf{E}^T \cdot \mathbf{U}^T \cdot \mathbf{e} \tag{4.32}$$

Because the expectation of $\mathbf{e}$ is zero, we know that

$$\langle \mathbf{y}' \cdot \mathbf{y}' \rangle = \langle \hat{\mathbf{y}}' \cdot \hat{\mathbf{y}}' \rangle + \langle \mathbf{y}'_e \cdot \mathbf{y}'_e \rangle \tag{4.33}$$

Note that

$$\langle \hat{\mathbf{y}}' \cdot \hat{\mathbf{y}}' \rangle = \sum_{k=1}^{M} \frac{\sigma_k^2}{(\sigma_k^2 + \rho)^2} \hat{y}_k'^2 \tag{4.34a}$$

and

$$\langle \mathbf{y}'_e \cdot \mathbf{y}'_e \rangle = \sum_{k=1}^{M} \frac{\sigma_k^2}{(\sigma_k^2 + \rho)^2} \langle \overline{\varepsilon}_k^2 \rangle \tag{4.34b}$$

where $\overline{\varepsilon}_k$ is the kth component of the M-dimensional vector $\overline{\mathbf{e}} = \mathbf{U}^T \cdot \mathbf{e}$. Since $\mathbf{U}$ is an $M \times M$ orthogonal matrix, it is obvious that if $\langle \varepsilon_i \varepsilon_k \rangle = \sigma^2 \delta_{ik}$, then $\langle \overline{\varepsilon}_i \overline{\varepsilon}_k \rangle = \sigma^2 \delta_{ik}$ where ε_k is the kth component of the M-dimensional error vector $\mathbf{e}$. Then, we have

$$\langle \mathbf{y}'_e \cdot \mathbf{y}'_e \rangle = \sigma^2 \sum_{k=1}^{M} \left(\frac{\sigma_k}{\sigma_k^2 + \rho} \right)^2 \tag{4.35}$$

Note that

$$\Sigma_k \equiv \left(\frac{\sigma_k}{\sigma_k^2 + \rho} \right)^2 \leq \frac{1}{4\rho} \tag{4.36}$$

Then,

$$\langle \mathbf{y}'_e \cdot \mathbf{y}'_e \rangle \leq \frac{M\sigma^2}{4\rho} \tag{4.37}$$

Furthermore, note that the maximum value of Σ_k occurs at $\rho = \sigma_k^2$ and it decreases steeply as $\left| \log(\sigma_k^2/\rho) \right|$ increases. Since all singular values cannot be the same, it can be said that

$$\left\langle \mathbf{y}'_e \cdot \mathbf{y}'_e \right\rangle \sim \frac{\sigma^2}{4\rho} \tag{4.38}$$

Hence, the errors in the numerical derivative are in the same order of the raw data. This is the error-suppressing effect of the Tikhonov regularization.

4.2.3 Numerical Differentiation by Cubic B-Spline

Although the inverse integration method is effective, it still gives rise to a noisy shape for $|x| > 1$. Smoother derivative is expected if appropriate regression is combined with numerical differentiation. One of the most versatile regressions is polynomial regression. As the shape of a function becomes more complicate, higher-order polynomial is required. Since the Runge phenomenon appears usually in derivative, cubic B-spline is better than higher-order polynomial. To enhance smoothness of the derivative, coefficients of B-spline may be determined by the minimization of

$$\chi^2 = \sum_{\alpha=1}^{M} \left[y_\alpha - \sum_{k=-1}^{L+1} c_k B_k(x_\alpha) \right]^2 + \rho \sum_{\alpha=1}^{M} \left[\sum_{k=-1}^{L+1} c_k B''_k(x_\alpha) \right]^2 \tag{4.39}$$

where $B''_k(x) = \mathrm{d}^2 B_k / \mathrm{d}x^2$. If the coefficients c_k are determined by the minimization of χ^2, then it is obvious that

$$y'_\alpha = \sum_{k=-1}^{L+1} c_k \left(\frac{\mathrm{d}B_k}{\mathrm{d}x} \right)_{x=x_\alpha} \tag{4.40}$$

Figure 9 shows the result from the application of cubic B-spline ($\rho = 10^{-3}$ and $L = 9$) to the data of Fig. 8. Partitioning of data was done by the same length of subintervals. Comparison with the inverse integration method (IIR) reveals that cub B-spline is superior. Regression by cubic B-spline depends on both the number of subintervals and how to partition the whole interval. Determination of them seems to be heuristic.

A reliable algorithm for numerical differentiation is important for showing the validity of time–temperature superposition, which will be discussed in Chap. 8. Another application of numerical differentiation is to calculate probability density function from the cumulative distribution function obtained from experiment.

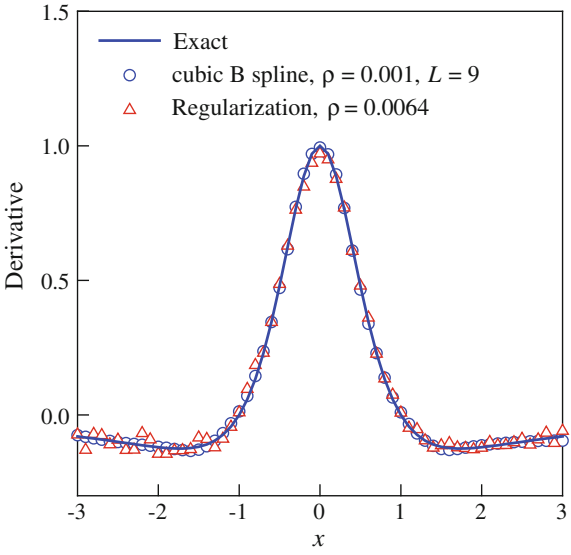

Fig. 9 Numerical differentiation by cubic B-spline ($\rho = 10^{-3}$, $L = 9$). Regularization (*triangle*) is the derivative obtained from inverse integration with $\rho = 6.4 \times 10^{-3}$

Problem 4

[1] Derive that the error of the trapezoidal rule for exact function is given by

$$\int_{x_{\min}}^{x_{\max}} f(x)\,\mathrm{d}x - h\left[\frac{f(x_{\max})+f(x_{\min})}{2} + \sum_{k=1}^{N-1} f(x_{\min}+kh)\right] = -\frac{(x_{\max}-x_{\min})^3}{12N^2} f''(\xi) \tag{4.a}$$

where $h = (x_{\max} - x_{\min})/N$ and $x_{\min} \le \xi \le x_{\max}$.

[2] A set of experimental data $\{(t_\alpha, G_\alpha)\}$ is given with $t_{\min} \le t_\alpha \le t_{\max}$. We are interested in the numerical Laplace transform of the experimental data. Assume that $G_\alpha = G(t_\alpha) + \varepsilon_\alpha$ and $G(t)$ have the asymptotic behavior such that

$$G(t) \sim \exp\left(-\frac{t}{\lambda}\right) \quad \text{with } t_{\min} < \lambda < t_{\max} \tag{4.b}$$

What are the conditions for s and $G(t)$ in order that the following is an acceptable approximation:

$$\widetilde{G}(s) \approx \sum_{\alpha=1}^{N-1} \frac{t_{\alpha+1} - t_\alpha}{2} \left(e^{-st_\alpha} G_\alpha + e^{-st_{\alpha+1}} G_{\alpha+1}\right) \tag{4.c}$$

[3] Calculate the singular values of the matrix **A** of Eq. (4.20) under the assumption that $h_k = h$ for all k.

[4] What is the reason why the numerical differentiation by cubic B-spline is superior to the inverse integration with regularization?
[5] Derive

$$\frac{\mathrm{d}B_k^{(n)}(x)}{\mathrm{d}x} = (n-1)\left(\frac{B_k^{(n-1)}(x)}{\xi_{k+n-1}-\xi_k} - \frac{B_{k+1}^{(n-1)}(x)}{\xi_{k+n}-\xi_{k+1}}\right) \tag{4.d}$$

where $B_k^{(n)}(x)$ is the nth order basis function of B-spline.

5 Discrete Fourier Transform

5.1 Fourier Series

Fourier series of a periodic function defined in the interval of $(-L, L)$ is given by

$$f(x) = \frac{a_0}{2} + \sum_{n=1}^{\infty}\left(a_n \cos\frac{n\pi x}{L} + b_n \sin\frac{n\pi x}{L}\right) \tag{5.1}$$

where the Fourier coefficients a_n and b_n are

$$a_n = \frac{1}{L}\int_{-L}^{L} f(x)\,\cos\frac{n\pi x}{L}\mathrm{d}x; \quad b_n = \frac{1}{L}\int_{-L}^{L} f(x)\,\sin\frac{n\pi x}{L}\mathrm{d}x \tag{5.2}$$

Using Euler's formula, Eq. (5.1) can be rewritten in complex notation as follows

$$f(x) = \sum_{n=-\infty}^{\infty} \hat{c}_n e^{\mathrm{i}n\pi x/L} \tag{5.3}$$

where

$$\hat{c}_n = \frac{1}{2L}\int_{-L}^{L} f(x)\, e^{-\mathrm{i}n\pi x/L} \tag{5.4}$$

with

$$\hat{c}_n = \frac{a_n - \mathrm{i}b_n}{2}; \quad \hat{c}_{-n} = \frac{a_n + \mathrm{i}b_n}{2} \quad \text{for } n > 0 \tag{5.5}$$

and

$$c_0 = \frac{a_0}{2} \tag{5.6}$$

This is an approximation method for a function in terms of trigonometric functions which satisfy orthogonality

$$\frac{1}{2L}\int_{-L}^{L} e^{im\pi x/L} e^{in\pi x/L} \mathrm{d}x = \begin{cases} 0 & \text{for } m \neq -n \\ 1 & \text{for } m = -n \end{cases} \tag{5.7}$$

Hence, Fourier series is equivalent to series approximation by orthogonal polynomials. When it is necessary to find an approximate equation for experimental data, Eq. (5.1) implies that trigonometric functions are used for base function just as Eq. (1.23). Then, a better choice of base function type depends on the number of base functions is needed for the description of the experimental data when truncated series is considered. In other words, the better choice depends on how fast the series converges.

5.2 Discrete Fourier Transform

Nowadays, most measuring instruments are equipped with computer, and the analogy signal from sensor is converted to the digital signal and the digital signal is stored in the memory system of the computer. For simplicity assume that the measured quantity is a function of time. Taking creep experiment as an example, rheometer measures strain as a function of time. When rheometer measures strain from $t = 0$ to $t = T$, data storage is carried at

$$t_k = \frac{T}{2N}k, \quad k = 0, 1, 2, \ldots, 2N-1 \tag{5.8}$$

Hence, the sampling interval is given by $\Delta t = \frac{1}{2}T/N$. The rheometer also stores compliance data J_k which is measured at $t = t_k$.

To define discrete Fourier transform (DFT), we define frequencies as follows

$$\omega_n = \frac{2\pi n}{T}, \quad n = 0, 1, 2, \ldots, 2N-1 \tag{5.9}$$

Analogous to continuous Fourier transform, we define discrete Fourier transform of $f_k = f(t_k)$ as follows

$$\hat{f}_n = \hat{f}(\omega_n) = \frac{1}{2N}\sum_{k=0}^{2N-1} f_k e^{-i\omega_n t_k} \tag{5.10}$$

In vector notation, Eq. (5.10) can be rewritten as

$$\hat{\mathbf{f}} = \frac{1}{2N}\mathbf{F}\cdot\mathbf{f} \tag{5.11}$$

where $F_{nk} = \exp(-\mathrm{i}\omega_n t_k)$. It is not difficult to prove discrete orthogonality relation (Arfken and Weber 2001):

$$\frac{1}{2N}\sum_{n=0}^{2N-1} e^{-\mathrm{i}\omega_n t_k} e^{\mathrm{i}\omega_n t_m} = \delta_{km} \tag{5.12}$$

The use of Eq. (5.12) gives

$$f_k = \sum_{n=0}^{2N-1} \hat{f}_n e^{\mathrm{i}\omega_n t_k} \tag{5.13}$$

In vector notation, Eq. (5.13) is rewritten as

$$\mathbf{f} = \overline{\mathbf{F}}\cdot\hat{\mathbf{f}} \tag{5.14}$$

where $\overline{F}_{kn} = \exp(\mathrm{i}\omega_n t_k)$. Hence, it is obvious that

$$\overline{\mathbf{F}}\cdot\mathbf{F} = \mathbf{F}\cdot\overline{\mathbf{F}} = 2N\,\mathbf{I} \tag{5.15}$$

Equations (5.10) and (5.13) are discrete Fourier transform pair, which is analogous to Eq. (6.33 in Chap. 1).

It must be noted that although the discrete Fourier transform pair is exact, when N is not sufficiently large, aliasing becomes a significant problem. When

$$t_k = 0,\ \frac{\pi}{2},\ \pi,\ \frac{3\pi}{2} \tag{5.16}$$

$\cos t_k = \frac{1}{2}(\cos t_k + \cos 3t_k)$ holds for the four times.

Computation of Eq. (5.14) demands about N^2 multiplications. Hence, if $N = 2^{10} = 1024$, the number of multiplications becomes about $2^{20} \approx 10^6$. The *fast Fourier transform (FFT)* algorithm reduces the number of multiplications to $N\log_2 N \approx 10^4$. The FFT algorithm is to exploiting factoring and rearrangement of the terms in Eq. (5.11).

Dynamic moduli (dynamic compliances) can be calculated from relaxation modulus (or creep compliance) by Fourier transform instead of Laplace transform and substitution of $s = \mathrm{i}\omega$. Evans et al. (2009) applied DFT to creep compliance

data in order to obtain dynamic moduli. However, their method suffers from high-frequency noises because of finite data and experimental error. On the other hand, Kim et al. (2015) used fitting of the Laplace transform of creep compliance by a suitable model and converted it to dynamic moduli analytically. Their results were very smooth. However, the use of a model is not a direct method which should be influenced by the model used. Hence, for smooth dynamic moduli, it is recommendable to use relaxation spectrum.

Problem 5

[1] Prove Eq. (5.15).

[2] A physical quantity P is expected to be a periodic function of time such that

$$P(t) = \sum_{k=0}^{5} \frac{1}{(2k+1)^2} \sin[(2k+1)\omega t] \tag{5.a}$$

where the period is known as $T = 2\pi/\omega$. Assume that the quantity is measured with the sampling times:

$$t_\alpha = \frac{T}{100}\alpha \quad \text{with} \quad \alpha = 0, 1, \ldots, 99 \tag{5.b}$$

Apply the DFT to the data generated by Eq. (5.b) in order to identify $P_k = (2k+1)^{-2}$ and calculate the error.

[3] Instead of DFT, apply regression to the Problem [2].

References

G.B. Arfken, H.J. Weber, *Mathematical Methods for Physicists* (Harcourt Sci. & Tech., 2001)

K. Atkinson, W. Han, *Theoretical Numerical Analysis*, 3rd edn. (Springer, New York, 2000)

J.-E. Bae, K.S. Cho, Logarithmic method for continuous relaxation spectrum and comparison with previous methods. J. Rheol. **59**, 1081–1112 (2015)

R.B. Bird, R.C. Armstrong, O. Hassager, *Dynamics of Polymeric Liquids. Fluid Mechanics*, vol. 1 (Wiley, New York, 1987a)

R.B. Bird, C.F. Curtiss, R.C. Armstrong, O. Hassager, *Dynamics of Polymeric Liquids, Kinetic Theory*, vol. 2 (Wiley, New York, 1987b)

A. Cohen, A Padé approximant to the inverse Langevin function. Rheol. Acta **30**, 270–273 (1991)

J. Cullum, Numerical differentiation and regularization. SIAM J. Numer. Anal. **8**, 254–265 (1971)

R.M.L. Evans, M. Tassieri, D. Auhl, T.A. Waigh, Direct conversion of rheological compliance measurements into storage and loss moduli. Phys. Rev. E **80**, 012501 (2009)

J. Honerkamp, J. Weese, Determination of the relaxation spectrum by a regularization method. Macromolecules **22**, 4327–4377 (1989)

M.K. Kim, J.-E. Bae, N. Kang, K.S. Cho, Extraction of viscoelastic functions from creep data with ringing. J. Rheol. **59**, 237–252 (2015)

A. Kirsch, *An Introduction to the Mathematical Theory of Inverse Problems*, 2nd edn. (Springer, New York, 2010)

C.L. Lawson, R.J. Hanson, *Solving Least Squares Problems* (SIAM, Philadelphia, 1995)
G. Marin, W.W. Graessley, Viscoelastic properties of high molecular weight polymer in the molten state. I. Study of narrow molecular weight distribution samples. Rheol. Acta **16**, 527–533 (1977)
W.H. Press, S.A. Teukolsky, W.T. Vetterling, B.P. Flannery, *Numerical Recipes in C++*, 2nd edn. (Cambridge University Press, Cambridge, 2002)
M. Rubinstein, R.H. Colby, *Polymer Physics* (Oxford University Press, Oxford, 2003)
F.J. Stadler, E. van Ruymbeke, An improved method to obtain direct rheological evidence of monomer density reequilibration for entangled polymer melts. Macromolecules **43**, 9205–9209 (2010)
E. Süli, D.F. Mayers, *An Introduction to Numerical Analysis* (Cambridge University Press, Cambridge, 2003)

Chapter 7
Viscoelastic Spectrum

Abstract This chapter deals with the mathematical fundamentals and numerical algorithms of relaxation and retardation spectra. The first section consists of the importance of spectrum, the Fuoss–Kirkwood relations, the ill-posedness in inferring viscoelastic spectra and some mathematical formulas related with the spectra. The second and third sections are the introduction to the algorithms of continuous and discrete spectra, respectively.

1 Fundamentals

1.1 Importance of Spectrum

We have introduced relaxation and retardation spectra in Sect. 3 in Chap. 5 where we studied the multimode Maxwell model. Hence, the origin of the spectra is hypothetical, which means that spectra cannot be measured directly. However, both relaxation and retardation spectra are important because they provide a very powerful tool to convert a viscoelastic response function to another if they are determined. Furthermore, spectrum gives a new insight on molecular processes in rheology. Somebody may think that studies on spectrum are already old and are not useful because of brightly developing molecular theories. However, all molecular theories are not so rigorous because almost all of them are based on Brownian motion and rough approximations. Theories based on Brownian motion (the Langevin or Fokker–Planck equation) are seen as phenomenological ones compared with more rigorous ones based on atomic scales. They also contain phenomenological parameters such as friction coefficient ζ. Nevertheless, molecular theories are superior to phenomenological ones because they allow us to relate independent experimental results through molecular structure. If spectrum can be determined uniquely from experimental data, then it must be a severe method to check the validity of a molecular theory.

For a long time, a number of researchers tried to calculate spectrum from measured data of viscoelasticity (Ferry 1980; Tschoegl 1989). In the author's

K.S. Cho, *Viscoelasticity of Polymers*, Springer Series
in Materials Science 241, DOI 10.1007/978-94-017-7564-9_7

opinion, remarkable achievements in this field appear since 1978: Wiff (1978), Honerkamp and Weese (1989), Baumgärtel and Winter (1989) and Honerkamp and Weese (1989) recognized that calculation of continuous relaxation spectrum is an ill-posed problem and suggested regularization as a breakthrough. Because of the ill-posedness, some of the researchers have doubted the uniqueness of spectrum. However, the uniqueness of continuous spectrum had been proved already by Fuoss and Kirkwood in 1941. They focused on the relaxation spectrum of dielectrics rather than viscoelasticity. Fourier transform was used to derive the relation between dielectric permittivity and dielectric relaxation function. Note that Fourier transform is uniquely determined. However, the uniqueness of discrete spectrum is still doubted (Malkin and Masalova 2001) and the authors do not believe the uniqueness of discrete spectrum. Since discrete spectrum is an approximation of continuous one, it is not a significant problem to prove the uniqueness of discrete spectrum. In summary, continuous spectrum is unique, but it is necessary to develop an appropriate method to calculate the spectrum from experimental data which inevitably contain experimental errors.

This chapter is devoted mainly to algorithms for relaxation and retardation spectra. In this section, we will study fundamental aspects of spectrum such as the relations between spectrum and other viscoelastic functions.

1.2 The Fuoss–Kirkwood Relations

Although Fuoss and Kirkwood derived the *Fuoss–Kirkwood relation* (FK relation) long time ago, a number of literatures in rheology have not recognized their achievements. Here, we shall derive the FK relations and their consequences.

1.2.1 Derivation of the FK Relations

The definition of continuous relaxation spectrum is given in Eq. (3.2) in Chap. 5. Since the FK relation is the one between relaxation spectrum and dynamic moduli, we take Laplace transform on both sides of Eq. (3.2) in Chap. 5; then, we have

$$s\tilde{G}(s) = \int_{-\infty}^{\infty} H(\lambda)\frac{\lambda s}{1+\lambda s}\mathrm{d}\log\lambda \tag{1.1}$$

Substitution of $s = \mathrm{i}\omega$ gives

$$G'(\omega) = \int_{-\infty}^{\infty} H(\lambda)\frac{\lambda^2\omega^2}{1+\lambda^2\omega^2}\mathrm{d}\log\lambda; \quad G''(\omega) = \int_{-\infty}^{\infty} H(\lambda)\frac{\lambda\omega}{1+\lambda^2\omega^2}\mathrm{d}\log\lambda \tag{1.2}$$

Since both frequency and relaxation time vary in logarithmic scale, we introduce the notation such that

$$\nu = \log \omega; \quad \mu = -\log \lambda \tag{1.3}$$

The notation allows us to use

$$H(\lambda) = H(e^{-\mu}) = h(\mu); \quad G(\omega) = G(e^{\nu}) = g(\nu) \tag{1.4}$$

where $G(x)$ means $G'(x)$ or $G''(x)$ depending on the context. Then, Eq. (1.2) can be rewritten by

$$g'(\nu) = \int_{-\infty}^{\infty} K'(\nu - \mu) h(\mu) \mathrm{d}\mu; \quad g''(\nu) = \int_{-\infty}^{\infty} K''(\nu - \mu) h(\mu) \mathrm{d}\mu \tag{1.5}$$

where

$$K'(\xi) = \frac{1 + \tanh\xi}{2} = \frac{x^2}{1 + x^2}; \quad K''(\xi) = \frac{1}{2}\operatorname{sech}\xi = \frac{x}{1 + x^2} \tag{1.6}$$

Here, we used $\xi = \log x$. Note that the kernel function $K'(\xi)$ is a monotonic increasing function converging to unity as its argument increases, while the kernel function $K''(\xi)$ is a peaklike function that has the maximum value of $1/2$ at $\xi = 0$.

Since Eq. (1.5) is the convolution of Fourier transform, it is obvious that

$$\hat{g}''(q) = \int_{-\infty}^{\infty} g''(\nu) e^{-\mathrm{i}q\nu} \mathrm{d}\nu = \hat{K}''(q) \hat{h}(q) \tag{1.7}$$

and

$$\hat{K}''(q) = \frac{\pi}{2} \operatorname{sech}\left(\frac{\pi}{2} q\right) \tag{1.8}$$

Equation (1.7) gives

$$\hat{h}(q) = \frac{e^{\pi q/2} + e^{-\pi q/2}}{\pi} \hat{g}''(q) \tag{1.9}$$

and inversion of the Fourier transform gives

$$h(\nu) = \frac{1}{\pi} \left[g''\left(\nu + \mathrm{i}\frac{\pi}{2}\right) + g''\left(\nu - \mathrm{i}\frac{\pi}{2}\right) \right] \tag{1.10}$$

To obtain (1.10), we need

$$g''\left(\nu \pm \frac{\pi}{2}\mathrm{i}\right) = \frac{1}{2\pi}\int_{-\infty}^{\infty} \hat{g}''(q)\exp\left[\mathrm{i}\left(\nu \pm \frac{\pi}{2}\mathrm{i}\right)q\right]\mathrm{d}q \tag{1.11}$$

and

$$\log(\pm\mathrm{i}\omega) = \log\omega \pm \frac{\pi}{2}\mathrm{i} = \nu \pm \frac{\pi}{2}\mathrm{i} \tag{1.12}$$

With the help of (1.4), we recover continuous spectrum as follows:

$$H\left(\frac{1}{\omega}\right) = \frac{G''(\mathrm{i}\omega) + G''(-\mathrm{i}\omega)}{\pi} \tag{1.13}$$

If a physical quantity is measurable as a function of other controllable variable, it is really rare to find a reason to object to the analyticity of the function. Hence, we assume that dynamic moduli are analytic functions. Then, we can write

$$G''(z) = \sum_{n=0}^{\infty} c_n z^n \tag{1.14}$$

where z is a complex variable, but all coefficients c_n are real because loss modulus is real whenever z is real. Then, it is obvious that

$$\mathrm{Re}\{G''(\mathrm{i}\omega)\} = \frac{G''(\mathrm{i}\omega) + G''(-\mathrm{i}\omega)}{2}; \quad \mathrm{Im}\{G''(\mathrm{i}\omega)\} = \frac{G''(\mathrm{i}\omega) - G''(-\mathrm{i}\omega)}{2\mathrm{i}} \tag{1.15}$$

Finally, we have

$$H\left(\frac{1}{\omega}\right) = \frac{2}{\pi}\mathrm{Re}\{G''(\mathrm{i}\omega)\} \tag{1.16}$$

This is the FK relation for loss modulus.

We can apply these calculations to storage modulus, too. The success of (1.16) is originated from the feature of the kernel function $K''(x)$. Hence, we modify the equation for storage modulus of (1.5) as follows:

$$\eta(\nu) = \int_{-\infty}^{\infty} K''(\nu - \mu)W(\mu)\mathrm{d}\mu \tag{1.17}$$

where

$$\eta(\nu) = \frac{G'(\omega)}{\omega}; \quad W(\mu) = \lambda H(\lambda) \tag{1.18}$$

Since (1.17) is also the convolution equation, we have

$$e^{-\nu} H(e^{-\nu}) = \frac{1}{\omega} H\left(\frac{1}{\omega}\right) = \frac{1}{\pi}\left[\frac{G'(\mathrm{i}\omega)}{\mathrm{i}\omega} - \frac{G'(-\mathrm{i}\omega)}{\mathrm{i}\omega}\right] \tag{1.19}$$

Then, we have

$$H\left(\frac{1}{\omega}\right) = \frac{2}{\pi}\mathrm{Im}\{G'(\mathrm{i}\omega)\} \tag{1.20}$$

The Laplace transform is one of the useful viscoelastic functions even though DWS is not considered. We shall introduce how the Laplace transform is used in viscoelastic characterization of polymeric materials in Chap. 8. Here, we shall derive the FK relation of $\tilde{G}(s)$. Dividing both sides of (1.1) by $\sqrt{s}$, we have

$$\sqrt{s}\tilde{G}(s) = \int_{-\infty}^{\infty} \frac{\sqrt{\lambda s}}{1+\lambda s} \sqrt{\lambda} H(\lambda) \mathrm{d}\log\lambda \tag{1.21}$$

To exploit the feature of $K''(x)$, we introduce

$$2\sigma = \log s; \quad 2\theta = -\log\lambda \tag{1.22}$$

Then, we can deal with the following functions:

$$\sqrt{s}\tilde{G}(s) = e^{\sigma}\tilde{g}(e^{\sigma}) = \Phi(\sigma); \quad \sqrt{\lambda}H(\lambda) = \frac{1}{e^{\theta}}\tilde{h}\left(\frac{1}{e^{\theta}}\right) = Q(\theta) \tag{1.23}$$

The use of (1.23) gives

$$\Phi(\sigma) = 2\int_{-\infty}^{\infty} K''(\sigma-\theta)Q(\theta)\mathrm{d}\theta \tag{1.24}$$

and similar procedures used before give

$$Q(\sigma) = \frac{4}{\pi}\mathrm{Re}\left\{\mathrm{i}\sqrt{s}\tilde{g}\left(\mathrm{i}\sqrt{s}\right)\right\} \tag{1.25}$$

and

$$H\left(\frac{1}{s}\right) = \frac{4}{\pi}\sqrt{s}\mathrm{Re}\left\{\mathrm{i}\sqrt{s}\tilde{g}\left(\mathrm{i}\sqrt{s}\right)\right\} = -\frac{4}{\pi}s\mathrm{Im}\left\{\tilde{g}\left(\mathrm{i}\sqrt{s}\right)\right\} \tag{1.26}$$

Note that $\tilde{G}(s) = \tilde{g}(\sqrt{s})$ and $H(s) = \tilde{h}(\sqrt{s})$.

When available data are in compliance, then we can apply the FK relation for retardation spectrum. The definition of the retardation spectrum is shown in Eq. (3.4) in Chap. 5 which implies that the spectrum is related to recovery compliance:

$$J_r(t) = J(t) - J_g - \frac{t}{\eta_o} = \int_{-\infty}^{\infty} L(\tau)\left(1 - e^{-t/\tau}\right) \mathrm{d}\log\tau \tag{1.27}$$

Taking the Laplace transform, we have

$$s\tilde{J}_r(s) = s\tilde{J}(s) - J_g - \frac{1}{\eta_o s} = \int_{-\infty}^{\infty} \frac{L(\tau)}{1+\tau s} \mathrm{d}\log\tau \tag{1.28}$$

Equation (1.28) implies that for viscoelastic fluids,

$$J'(\omega) - J_g = \int_{-\infty}^{\infty} \frac{L(\tau)}{1+\tau^2\omega^2} \mathrm{d}\log\tau; \quad J''(\omega) - \frac{1}{\eta_o\omega} = \int_{-\infty}^{\infty} L(\tau)\frac{\tau\omega}{1+\tau^2\omega^2} \mathrm{d}\log\tau \tag{1.29}$$

Since viscoelastic solid is the case of infinite zero-shear viscosity, it is not difficult to imagine the corresponding Eq. (1.29). Here, we consider only the case of viscoelastic fluid. Since the kernel function for loss compliance is identical to that of Eq. (1.2) for loss modulus, we have the FK relation such that

$$L\left(\frac{1}{\omega}\right) = \frac{2}{\pi}\mathrm{Re}\left\{J''(\mathrm{i}\omega) - \frac{1}{\mathrm{i}\eta_o\omega}\right\} = \frac{2}{\pi}\mathrm{Re}\{J''(\mathrm{i}\omega)\} \tag{1.31}$$

If we define $R(\tau) = \tau^{-1}L(\tau)$, then modification of the first equation of (1.39) gives

$$\omega\left[J'(\omega) - J_g\right] \equiv \int_{-\infty}^{\infty} R(\tau)\frac{\tau\omega}{1+\tau^2\omega^2} \mathrm{d}\log\tau \tag{1.32}$$

The FK relation from Eq. (1.32) is given by

$$L\left(\frac{1}{\omega}\right) = -\frac{2}{\pi}\mathrm{Im}\{J'(\mathrm{i}\omega)\} \tag{1.33}$$

Although the FK relations are exact, it must be recognized that if we do not know the exact functions of measurable quantities such as dynamic moduli and the Laplace transform of the relaxation modulus, we cannot determine relaxation spectrum. If someone wants to develop an algorithm for relaxation spectrum by the use of the FK relation, an effective approximation can describe the experimental data of corresponding measurable viscoelastic functions. Cho and coworkers (2015) used the Chebyshev polynomials as follows:

$$G(\nu) \approx \exp\left[\sum_{n=0}^{N} g_n T_n(\tilde{\nu})\right] \quad \text{with} \quad \tilde{\nu} = \frac{2\nu - (\nu_{\max} + \nu_{\min})}{\nu_{\max} - \nu_{\min}} \tag{1.34}$$

Detailed numerical methods will be given in Sect. 2.3 in Chap. 7.

1.2.2 Cautions for the Use of the FK Relations

It must be mentioned that the derivation of Eqs. (1.16), (1.20), (1.26), (1.31), and (1.32) omitted to check the convergence of the integration of Fourier transforms. Hence, the five equations are not mathematically exact. Although all viscoelastic functions can be assumed to be analytic on the linear line of their arguments, the analyticity cannot guarantee the analyticity on imaginary axis. First of all, since storage modulus is an increasing function of frequency and is expected to have a constant value at infinite frequency, the existence of the Fourier transform of storage modulus is questionable. Note that Eq. (6.21) in Chap. 1 is one of the conditions for ordinary Fourier transform, while storage modulus does not satisfy this condition. Thus, the Fourier transforms used above are not the Fourier transforms of ordinary functions but those of distributions (Zemanian 1987). The exact equations for the generalized FK relations are given by

$$H\left(\frac{1}{\omega}\right) = \lim_{\varepsilon\to 0}\frac{2}{\pi}\mathrm{Im}\{G'(\mathrm{i}\omega+\varepsilon)\} = \lim_{\varepsilon\to 0}\frac{2}{\pi}\mathrm{Re}\{G''(\mathrm{i}\omega+\varepsilon)\} \tag{1.35}$$

$$H\left(\frac{1}{s}\right) = -\lim_{\varepsilon\to 0}\frac{4}{\pi}s\mathrm{Im}\left\{\tilde{g}\left(\mathrm{i}\sqrt{s}+\varepsilon\right)\right\} \tag{1.36}$$

and

$$L\left(\frac{1}{\omega}\right) = \lim_{\varepsilon\to 0}\frac{2}{\pi}\mathrm{Re}\{J''(\mathrm{i}\omega+\varepsilon)\} = -\lim_{\varepsilon\to 0}\frac{2}{\pi}\mathrm{Im}\{J'(\mathrm{i}\omega+\varepsilon)\} \tag{1.37}$$

As an example, consider the Maxwell model of a single relaxation time λ_M. The dynamic moduli are given by

$$G'(\omega) = G_M \frac{\lambda_M^2 \omega^2}{1+\lambda_M^2 \omega^2}; \quad G''(\omega) = G_M \frac{\lambda_M \omega}{1+\lambda_M^2 \omega^2} \tag{1.38}$$

Hence, it is obvious that the relaxation spectrum is $H(\lambda) = G_M \delta(\lambda - \lambda_M)$. If the simple substitution of $\omega \to i\omega$ is done, then we have useless results such that

$$\begin{aligned} \mathrm{Im}\{G'(i\omega)\} &= \mathrm{Im}\left\{ G_M \frac{\lambda_M^2 \omega^2}{\lambda_M^2 \omega^2 - 1} \right\} = 0 \\ \mathrm{Re}\{G''(i\omega)\} &= \mathrm{Re}\left\{ G_M \frac{i\lambda_M \omega}{1-\lambda_M^2 \omega^2} \right\} = 0 \end{aligned} \tag{1.39}$$

On the other hand, the use of Eq. (1.35) gives

$$\begin{aligned} \lim_{\varepsilon \to 0} \frac{2}{\pi} \mathrm{Re}\{G''(i\omega)\} &= \lim_{\varepsilon \to 0} \frac{2}{\pi} G_M \mathrm{Re}\left\{ \frac{\lambda_M \varepsilon + i\lambda_M \omega}{1 + (\lambda_M \varepsilon + i\lambda_M \omega)^2} \right\} \\ &= \lim_{\varepsilon \to 0} \frac{2}{\pi} G_M \frac{\lambda_M \varepsilon}{(\lambda_M \varepsilon)^2 + (\lambda_M \omega - 1)^2} \frac{(\lambda_M \varepsilon)^2 + (\lambda_M \omega)^2 + 1}{(\lambda_M \varepsilon)^2 + (\lambda_M \omega + 1)^2} \end{aligned} \tag{1.40}$$

Note that the Dirac delta function can be defined by

$$\delta(x) = \frac{1}{\pi} \lim_{\varepsilon \to 0} \frac{\varepsilon}{\varepsilon^2 + x^2} \tag{1.41}$$

Furthermore, it is obvious that for any continuous function $f(x)$

$$f(x)\, \delta(x - x_o) = f(x_o)\, \delta(x - x_o) \tag{1.42}$$

Application of both Eqs. (1.41) and (1.42) gives

$$\lim_{\varepsilon \to 0} \frac{2}{\pi} \mathrm{Re}\{G''(i\omega + \varepsilon)\} = G_M \delta\left(\frac{1}{\omega} - \lambda_M \right) \tag{1.43}$$

The simple substitution of ω by $i\omega$ as shown Eq. (1.16) often happen to give the same results which can be obtained from the limit process shown in Eqs. (1.35)–(1.37). However, the simple substitution sometimes gives useless results. Hence, Eqs. (1.35)–(1.37) are recommendable in general. However, we will use the notation of simple substitution because of simplicity.

1.2.3 The Relation Between Relaxation and Retardation Spectra

We shall derive the relation between relaxation and retardation spectra by the use of the FK relations. We start from Eq. (1.33). Substitute Eq. (1.59) in Chap. 1 to Eq. (1.33) with the replacement of frequency by iω. Long algebraic manipulation gives

$$L\left(\omega^{-1}\right) = \frac{H(\omega^{-1})}{\left[\mathrm{Re}\{G'(\mathrm{i}\omega)\} - \mathrm{Im}\{G''(\mathrm{i}\omega)\}\right]^2 + \pi^2 H^2(\omega^{-1})} \tag{1.44a}$$

or

$$L(\tau) = \frac{H(\tau)}{\left[\mathrm{Re}\{G'(\mathrm{i}\tau^{-1})\} - \mathrm{Im}\{G''(\mathrm{i}\tau^{-1})\}\right]^2 + \pi^2 H^2(\tau)} \tag{1.44b}$$

Similar equation is found in (Ferry 1980):

$$L(\tau) = \frac{H(\tau)}{\Pi^2(\tau) + \pi^2 H^2(\tau)} \tag{1.45}$$

where

$$\Pi(\tau) = \int_{-\infty}^{\infty} \frac{\lambda H(\lambda)}{\lambda - \tau} \mathrm{d}\log\lambda \tag{1.46}$$

With the help of Eq. (1.2), it is easy to show that

$$\Pi^2(\tau) = \left[\mathrm{Re}\left\{G'\left(\mathrm{i}\tau^{-1}\right)\right\} - \mathrm{Im}\left\{G''\left(\mathrm{i}\tau^{-1}\right)\right\}\right]^2 \tag{1.47}$$

Equation (1.59) in Chap. 1 is equivalent to

$$G'(\omega) = \frac{J'(\omega)}{\left[J'(\omega)\right]^2 + \left[J''(\omega)\right]^2}; \quad G''(\omega) = \frac{J''(\omega)}{\left[J'(\omega)\right]^2 + \left[J''(\omega)\right]^2} \tag{1.48}$$

Hence, substitution of Eq. (1.48) to the corresponding FK relation gives

$$H\left(\omega^{-1}\right) = \frac{L(\omega^{-1})}{\left[\mathrm{Re}\{J'(\mathrm{i}\omega)\} + \mathrm{Im}\{J''(\mathrm{i}\omega)\}\right]^2 + \pi^2 L^2(\omega^{-1})} \tag{1.49a}$$

or

$$H(\lambda) = \frac{L(\lambda)}{\left[\mathrm{Re}\left\{J'\left(\mathrm{i}\lambda^{-1}\right)\right\} + \mathrm{Im}\left\{J''\left(\mathrm{i}\lambda^{-1}\right)\right\}\right]^2 + \pi^2 L^2(\lambda)} \tag{1.49b}$$

Similar equation is found in Ferry (1980), too:

$$H(\lambda) = \frac{L(\lambda)}{\Omega^2(\lambda) + \pi^2 L^2(\lambda)} \tag{1.50}$$

where

$$\Omega(\lambda) = J_g + \int_{-\infty}^{\infty} \frac{\lambda L(\tau)}{\lambda - \tau} \mathrm{d}\log\tau - \frac{\lambda}{\eta_o} \tag{1.51}$$

It is not difficult to show that

$$\Omega^2(\lambda) = \left[\mathrm{Re}\left\{J'\left(\mathrm{i}\lambda^{-1}\right)\right\} + \mathrm{Im}\left\{J''\left(\mathrm{i}\lambda^{-1}\right)\right\}\right]^2 \tag{1.52}$$

Use of Eqs. (1.44a) and (1.44b) require to learn how to calculate real functions such as $\mathrm{Re}\{G'(\mathrm{i}\omega)\}$ and $\mathrm{Im}\{G''(\mathrm{i}\omega)\}$. Since we can consider dynamic moduli as analytical functions, we can express them as follows:

$$G'(\omega) = e^{P'(\omega)}; \quad G''(\omega) = e^{P''(\omega)} \tag{1.53}$$

where

$$P'(\omega) = \sum_{n=0}^{\infty} \gamma'_n (\log\omega)^n; \quad P''(\omega) = \sum_{n=0}^{\infty} \gamma''_n (\log\omega)^n \tag{1.54}$$

Then, we know that

$$\begin{aligned} \mathrm{Re}\{G'(\mathrm{i}\omega)\} &= \exp[\mathrm{Re}\{P'(\mathrm{i}\omega)\}]\cos[\mathrm{Im}\{P'(\mathrm{i}\omega)\}] \\ \mathrm{Im}\{G''(\mathrm{i}\omega)\} &= \exp[\mathrm{Re}\{P''(\mathrm{i}\omega)\}]\sin[\mathrm{Im}\{P''(\mathrm{i}\omega)\}] \end{aligned} \tag{1.55}$$

We shall illustrate how to implement Eq. (1.55) effectively in Sect. 2.4 in this chapter. Note that the pole of the kernel function in Eq. (1.46) makes the evaluation of the integral difficult. On the other hand, regression of experimental data by Eq. (1.53) is easier.

1.3 Ill-Posedness of Spectrum

Consider the second of Eq. (1.5). This is an integral equation called the *Fredholm integral equation of the 1st kind*. Linear operator theory of inverse problem refers to the ill-posed problem of the integral equation as the discontinuity of the inverse operator (Kirsch 2010). This theory is based on the functional analysis, and most

rheologist and engineers are not familiar with the mathematical theory. Hence, the effect of ill-posedness is explained by using the FK relation.

Addition of small perturbation in a relaxation spectrum $h(\tau) = h^*(\tau) + \delta h(\tau)$ results in $g''(\nu) = g''^*(\nu) + \delta g''(\nu)$, and we know that when $\delta h(\tau) = \varepsilon \sin k\tau$ with $k > 0$ and $\varepsilon > 0$, the perturbation in modulus is given by

$$\delta g'' = \frac{\pi}{2} \operatorname{sech} \frac{\pi k}{2} \varepsilon \sin k\nu \tag{1.56}$$

Equation (1.56) implies that the perturbation of modulus is negligible for large k, while it is comparative to that of the spectrum. Even if the amplitude of the perturbation is considerably high, the error in modulus $\delta g''$ seems to be negligible if $\frac{1}{2}\pi k \gg 1$. In this case, it is interesting that $h(\tau)$ looks very different from $h^*(\tau)$, while $g''(\nu) \approx g''^*(\nu)$.

To show this effect, consider the two spectra, the original and perturbed spectra:

$$H_o(\lambda) = \exp\left[-\frac{(\log \lambda)^2}{10}\right]; \quad H_E(\lambda) = H_o(\lambda) + \varepsilon \sin(k \log \lambda) \tag{1.57}$$

Figure 1 shows the two spectra and dynamic moduli calculated from them. Here, we used $\varepsilon = 0.1$ and $k = 2$. We used linear scale for dynamic moduli to emphasize that the two calculation results are nearly identical.

On the other hand, if $\delta g''(\nu)$ is given by $\delta g''(\nu) = \varepsilon \sin k\nu$, the FK relation gives

$$\delta h = \frac{2}{\pi} \cosh \frac{\pi k}{2} \varepsilon \sin k\nu \tag{1.58}$$

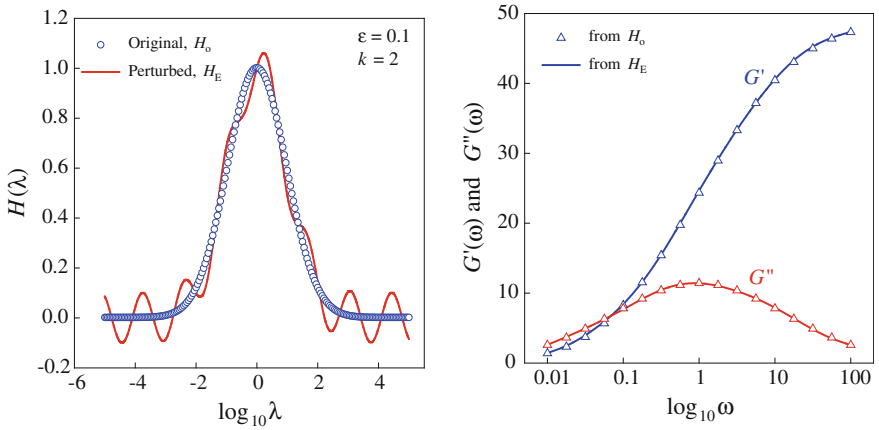

Fig. 1 A model spectrum and its perturbed spectrum [Eq. (1.57)] give nearly identical moduli. Here, the amplitude of the perturbation ε is 0.1, and the wave number k is 2.0

Hence, if the wave number k is large, a small error in modulus data results in a huge error in the spectrum. Since an experimental error can be considered as a linear combination of sinusoidal waves with various wave numbers, a component of high k could magnify the error of the spectrum enormously. Because of this, the problem of relaxation spectrum is called ill-posed problem. On the other hand, calculation of modulus for a given spectrum does not suffer from this problem. Therefore, it is difficult to infer an acceptable spectrum from experimental data.

There is another problem in spectrum calculation. Some algorithms result in negative value of spectrum (Wiff 1978; Honerkamp and Weese 1989), which is unrealistic because of the definition of continuous spectrum.

Therefore, a good algorithm for continuous spectrum should satisfy the following conditions:

1. The effect of experimental errors in the data must be suppressed.
2. The calculated spectrum must not be negative at any relaxation time (or retardation time).
3. The shorter the computation time, the better the algorithm.

1.4 Some Important Equations and Inequalities

The use of relaxation spectrum or retardation spectrum allows us to know some important inequalities among viscoelastic functions. A look at experimental data of $G'(\omega)$ and $G(t)$ in double logarithmic plots gives an insight that if relaxation modulus is plotted by ω^{-1} instead of t, then the shapes of the two plots of $G'(\omega)$ and $G(\omega^{-1})$ look similar. Using relaxation spectrum, we have

$$G'(\omega) - G\left(\frac{1}{\omega}\right) = \int_{-\infty}^{\infty} H(\lambda)\left[\frac{\lambda^2\omega^2}{1+\lambda^2\omega^2} - e^{-(\lambda\omega)^{-1}}\right] \mathrm{d}\log\lambda \tag{1.59}$$

Note that for $x > 0$

$$\frac{x^2}{1+x^2} - e^{-1/x} > 0 \tag{1.60}$$

Since $H(\lambda) \geq 0$ for any $\lambda > 0$, it is obvious that

$$G'(\omega) > G\left(\frac{1}{\omega}\right); \quad G'\left(\frac{1}{t}\right) > G(t) \tag{1.61}$$

Similarly, we can have

$$J'(\omega) > J\left(\frac{1}{\omega}\right) - \frac{1}{\eta_o \omega}; \quad J'\left(\frac{1}{t}\right) > J(t) - \frac{t}{\eta_o} \tag{1.62}$$

Combination of Eqs. (1.61) and (1.62) gives

$$J'(\omega) < \frac{1}{G'(\omega)}; \quad G'\left(\frac{1}{t}\right) < \frac{1}{J'(t^{-1})} \tag{1.63}$$

The viscoelastic constants in the terminal regime can be calculated from relaxation spectrum. Using Eqs. (1.67), (1.68) and (3.2) in Chap. 5, we can express the zero-shear viscosity, the steady state compliance and the mean relaxation time in terms of relaxation spectrum as follows

$$\eta_o = \int_{-\infty}^{\infty} \lambda H(\lambda) \mathrm{d} \log \lambda = \int_0^{\infty} H(\lambda) \mathrm{d}\lambda \tag{1.64}$$

$$J_e^o = \frac{1}{\eta_o^2} \int_{-\infty}^{\infty} \lambda^2 H(\lambda) \mathrm{d} \log \lambda = \frac{1}{\eta_o^2} \int_0^{\infty} \lambda H(\lambda) \mathrm{d}\lambda \tag{1.65}$$

$$\bar{\lambda} = \frac{\int_{-\infty}^{\infty} \lambda^2 H(\lambda) \mathrm{d} \log \lambda}{\int_{-\infty}^{\infty} \lambda H(\lambda) \mathrm{d} \log \lambda} = \frac{\int_0^{\infty} \lambda H(\lambda) \mathrm{d}\lambda}{\int_0^{\infty} H(\lambda) \mathrm{d}\lambda} \tag{1.66}$$

Problem 1

[1] Derive Eqs. (1.1), (1.2), and (1.3).

[2] Show that the Havriliak–Negami equation has the retardation spectrum such that

$$s\tilde{J}_r(s) = \frac{1}{[1 + (\tau_o s)^{\alpha}]^{\beta}} \Rightarrow L(\tau) = \frac{1}{\pi} \frac{(\tau/\tau_o)^{\alpha\beta} \sin \beta\theta}{\left[(\tau/\tau_o)^{2\alpha} + 2(\tau/\tau_o)^{\alpha} \cos \pi\alpha + 1\right]^{\beta/2}} \tag{1.a}$$

where

$$\theta = \begin{cases} \arctan \Omega(\tau) & \text{if} \quad \Omega(\tau) > 0 \\ \pi + \arctan \Omega(\tau) & \text{if} \quad \Omega(\tau) \leq 0 \end{cases}; \quad \Omega(\tau) = \frac{\sin \pi\alpha}{(\tau/\tau_o)^{\alpha} + \cos \pi\alpha} \tag{1.b}$$

[3] Derive Eqs. (1.31) and (1.33).
[4] Derive

$$\lim_{\varepsilon\to 0}\frac{2}{\pi}\left\{\frac{\lambda^2(\mathrm{i}\omega+\varepsilon)^2}{1+\lambda^2(\mathrm{i}\omega+\varepsilon)^2}\right\}=\delta\left(\frac{1}{\omega}-\lambda\right) \tag{1.c}$$

[5] Derive Eqs. (1.44a, b) and (1.49a, b).
[6] Derive Eqs. (1.56) and (1.57).
[7] Prove Eq. (1.59).
[8] Derive Eqs. (1.63), (1.64), and (1.65).
[9] Derive

$$\frac{\mathrm{d}g}{\mathrm{d}\nu}=\int_{-\infty}^{\infty}K(\nu-\mu)\frac{\mathrm{d}h}{\mathrm{d}\mu}\mathrm{d}\mu \tag{1.d}$$

[10] From the FK relation, derive the following (Anderssen et al. 2014):

$$h(-\nu)=\frac{2}{\pi}\sum_{n=0}^{\infty}\frac{(-1)^n}{(2n+1)!}\frac{\mathrm{d}^{2n+1}g'(\nu)}{\mathrm{d}\nu^{2n+1}}\left(\frac{\pi}{2}\right)^{2n+1}=\frac{2}{\pi}\sum_{n=0}^{\infty}\frac{(-1)^n}{(2n)!}\frac{\mathrm{d}^{2n}g''(\nu)}{\mathrm{d}\nu^{2n}}\left(\frac{\pi}{2}\right)^{2n} \tag{1.e}$$

[11] Prove that storage modulus is an increasing function of frequency.
[12] As for most monodisperse polymer melts, loss modulus increases as $G''\propto\omega$ in the terminal regime and then decreases as $G''\propto\omega^{-1/4}$ (Liu et al. 2006). Then, one may approximate this behavior as

$$G''(\omega)=G_{\mathrm{N}}^{\mathrm{o}}\frac{\lambda_{\max}\omega}{1+(\lambda_{\max}\omega)^{5/4}} \tag{1.f}$$

Show that Eq. (1.f) gives

$$H(\lambda)=\frac{2G_N^{\mathrm{o}}}{\pi}\frac{(\lambda_{\max}/\lambda)^{9/4}\sin\frac{\pi}{8}}{1+\left(1+\cos\frac{\pi}{8}\right)(\lambda_{\max}/\lambda)^{5/4}} \tag{1.g}$$

2 Algorithms for Continuous Spectrum

Before the appearance of the regularization method, most researchers of relaxation spectrum may have been unaware of ill-posedness of the problem. Since Eq. (3.2) in Chap. 5 looks like a Laplace transform between spectrum and relaxation modulus, early works of this field seem to be focused on the inversion of Laplace transform. Most classical methods in (Tschoegl 1989) applied the *Post–Widder formula* (Cohen 2007):

$$f(t) = \lim_{k\to\infty} \frac{(-1)^k}{k!} \left[s^{k+1} \frac{\mathrm{d}^k \tilde{f}(s)}{\mathrm{d}s^k} \right]_{s=k/t} \tag{2.1}$$

Since higher-order numerical differentiation of experimental data is very unstable because of another ill-posedness, we shall not introduce the classical works. As for the readers interested in the classical works on relaxation spectrum, (Tschoegl 1989) and (Ferry 1980) are recommendable.

2.1 Regularization Method

Wiff (1978) and Honerkamp and Weese (1989) adopted the regularization method in inferring continuous relaxation spectrum. Although most monographs on regularization exploit functional analysis, we shall explain the method from the viewpoint of linear regression for the case where the number of parameters is larger than the number of data. It is noteworthy that we already explained regularization method by the use of singular value decomposition when we deal with numerical differentiation as an inverse problem in Sect. 4.2 in Chap. 6. Although this approach is well explained in Honerkamp and Weese (1989), further detailed information is found in Lawson and Hanson (1995).

Although we are interested in continuous spectrum, we have to start from discrete spectrum in order to make the explanation of regularization easier. Consider the case that dynamic moduli are measured at M frequencies $\{\omega_\alpha\}$. Then, the dynamic moduli at ω_α must follow

$$G'(\omega_\alpha) = \sum_{k=1}^{N} K'(\lambda_k \omega_\alpha) h_k; \quad G''(\omega_\alpha) = \sum_{k=1}^{N} K''(\lambda_k \omega_\alpha) h_k \tag{2.2}$$

where

$$K'(x) = \frac{x^2}{1+x^2}; \quad K''(x) = \frac{x}{1+x^2} \tag{2.3}$$

For simplicity, it is assumed that for any k, $\log(\lambda_{k+1}/\lambda_k) = 2\Delta\mu$. Since the number of relaxation times N is sufficiently large, small $\Delta\mu$ guarantees

$$h_k \approx \frac{H(\lambda_k)}{2\Delta\mu} \approx \int_{\log\lambda_k - \Delta\mu}^{\log\lambda_k + \Delta\mu} H(\lambda)\mathrm{d}\log\lambda \tag{2.4}$$

This is the consequence from the mean value theorem. Hence, if h_k are determined from dynamic moduli data, then the continuous spectrum can be constructed if N is sufficiently large and $\Delta\mu$ is sufficiently small.

Note that all experimental data have errors. Hence, to determine h_k, the least squares should be used. The relative sum of square is popularly used because moduli are positive and vary in logarithmic scale:

$$\chi^2 = \sum_{\alpha=1}^{M}\left(G'_\alpha - \sum_{k=1}^{N} K'_{\alpha k}h_k\right)^2 + \sum_{\alpha=1}^{M}\left(G''_\alpha - \sum_{k=1}^{N} K''_{\alpha k}h_k\right)^2 \tag{2.5}$$

where G_α is the modulus data at frequency ω_α and $K_{\alpha k} = K'(\lambda_k\omega_\alpha)$ or $K_{\alpha k} = K''(\lambda_k\omega_\alpha)$. Since Eq. (2.5) is a quadratic function of $\{h_k\}$, the minimization of χ^2 is to solve the following set of linear equations:

$$\sum_{i=1}^{N} S_{ik}h_k = \bar{g}_i \text{ or } \mathbf{S}\cdot\mathbf{h} = \bar{\mathbf{g}} \tag{2.6}$$

where

$$S_{ik} = \sum_{\alpha=1}^{M}\left(K'_{i\alpha}K'_{k\alpha} + K''_{i\alpha}K''_{k\alpha}\right) \quad \text{or} \quad \mathbf{S} = \mathbf{K}\cdot\mathbf{K}^T \tag{2.7}$$

$$\bar{g}_i = \sum_{\alpha=1}^{M}\left(K'_{i\alpha}G'_\alpha + K''_{i\alpha}G''_\alpha\right) \quad \text{or} \quad \bar{\mathbf{g}} = \mathbf{K}\cdot\mathbf{g} \tag{2.8}$$

$$\mathbf{K} = \begin{bmatrix} K'(\lambda_1\omega_1) & \cdots & K'(\lambda_1\omega_M) & K''(\lambda_1\omega_1) & \cdots & K''(\lambda_1\omega_M) \\ \vdots & \ddots & \vdots & \vdots & \ddots & \vdots \\ K'(\lambda_N\omega_1) & \cdots & K'(\lambda_N\omega_M) & K''(\lambda_N\omega_1) & \cdots & K''(\lambda_N\omega_M) \end{bmatrix} \tag{2.9}$$

and

$$\mathbf{h} = [h_1\, h_2\, \cdots\, h_N]^T; \quad \mathbf{g} = \left[G'_1\, G'_2\, \cdots\, G'_M\, G''_1\, G''_2\, \cdots\, G''_M\right]^T \tag{2.10}$$

Note that the matrix $\mathbf{S}$ is $N \times N$ symmetric and $\mathbf{K}$ is an $N \times 2M$ matrix. The column vector $\mathbf{h}$ can be determined uniquely if $\mathbf{S}$ is nonsingular. However,

nonsingularity of $\mathbf{S}$ may not guarantee in general and especially when $N > 2M$. Thus, we need an alternative method to determine $\mathbf{h}$.

For any $N \times 2M$ matrix $\mathbf{K}$, the theorem of *singular value decomposition* (Lawson and Hanson 1995) reads that

$$\mathbf{K} = \mathbf{U} \cdot \mathbf{E} \cdot \mathbf{V} \tag{2.11}$$

where $\mathbf{U}$ is a $N \times N$ orthogonal matrix, $\mathbf{E}$ is a $N \times 2M$ rectangular diagonal matrix, and $\mathbf{V}$ is a $2M \times 2M$ orthogonal matrix. As examples, if $\mathbf{E}$ is a 3×4 matrix, then

$$\mathbf{E} = \begin{bmatrix} \sigma_1 & 0 & 0 & 0 \\ 0 & \sigma_2 & 0 & 0 \\ 0 & 0 & \sigma_3 & 0 \end{bmatrix} \tag{2.12}$$

and if $\mathbf{E}$ is a 3×2 matrix, then

$$\mathbf{E} = \begin{bmatrix} \sigma_1 & 0 \\ 0 & \sigma_2 \\ 0 & 0 \end{bmatrix} \tag{2.13}$$

Here, σ_k are singular values of $\mathbf{K}$. Then, from the definition of $\mathbf{S}$, we have

$$\mathbf{S} = \mathbf{U} \cdot \mathbf{E} \cdot \mathbf{E}^T \cdot \mathbf{U}^T \tag{2.14}$$

If $\mathbf{D} = \mathbf{E} \cdot \mathbf{E}^T$ is invertible, then

$$\mathbf{S}^{-1} = \mathbf{U} \cdot \mathbf{D}^{-1} \cdot \mathbf{U}^T \tag{2.15}$$

Then, we can determine $\mathbf{h}$ without any problem:

$$\mathbf{h} = \mathbf{U} \cdot \mathbf{D}^{-1} \cdot \mathbf{E} \cdot \mathbf{V} \cdot \mathbf{g} \tag{2.16}$$

This is a fortunate case. However, $N > 2M$ is usual for the purpose of Eq. (2.2) and the matrix $\mathbf{S}$ is singular.

The regularization method is to replace $\mathbf{S} = \mathbf{K} \cdot \mathbf{K}^T$ by $\mathbf{S} = \rho\mathbf{I} + \mathbf{K} \cdot \mathbf{K}^T$. Here, I is the $N \times N$ identity matrix. The parameter ρ is called the regularization parameter which is usually small positive real number. It is clear that as ρ goes to zero, the original matrix $\mathbf{S}$ is recovered. It is interesting that $\rho\mathbf{I} + \mathbf{K} \cdot \mathbf{K}^T$ is non-singular even if $\mathbf{K} \cdot \mathbf{K}^T$ is singular. Hence, $\left(\rho\mathbf{I} + \mathbf{K} \cdot \mathbf{K}^T\right)^{-1}$ is called *pseudo-inverse*. It is also interesting that the minimization of

$$\chi_\rho^2 = \chi^2 + \rho \sum_{k=1}^{N} h_k^2 \tag{2.17}$$

is reduced to

$$\left(\rho\mathbf{I}+\mathbf{K}\cdot\mathbf{K}^{T}\right)\cdot\mathbf{h}=\mathbf{K}\cdot\mathbf{g} \tag{2.18}$$

It is usual to determine the regularization parameter ρ as the one which makes χ^2 minimized. This is the *Tikhonov regularization* used in inverse integration with regularization (Sect. 4.2) in Chap. 6. This algorithm works well even if $N > M$. Hence, we can increase the number of relaxation times of the discrete spectrum at will in order to increase the accuracy of the conversion from the discrete spectrum to the continuous one by the mean value theorem (Eq. 2.4). Honerkamp and Weese (1989) showed that the continuous spectrum is nearly independent of the number of relaxation times N.

Error suppression of the regularization method is easily understood by the analysis done in Sect. 4.2 in Chap. 6. We will not repeat it. However, the regularization algorithm cannot prevent the occurrence of negative $H(\lambda_k)$ in principle. Therefore, Honerkamp and Weese (1993) developed a modified version of regularization method called *nonlinear regularization* (NLREG). This is the minimization of

$$\begin{aligned}\chi^2(\rho)=&\sum_{\alpha=1}^{M}\left[G'_\alpha-\int_{-\infty}^{\infty}K'(\lambda\omega_\alpha)e^{h(\lambda)}\mathrm{d}\log\lambda\right]^2\\&+\sum_{\alpha=1}^{M}\left[G'_\alpha-\int_{-\infty}^{\infty}K'(\lambda\omega_\alpha)e^{h(\lambda)}\mathrm{d}\log\lambda\right]^2+\rho\int_{-\infty}^{\infty}\left[\frac{\mathrm{d}^2h(\lambda)}{\mathrm{d}\lambda^2}\right]^2\mathrm{d}\log\lambda\end{aligned} \tag{2.19}$$

Even if $h(\lambda)<0$, the spectrum remains as positive, $H(\lambda)=e^{h(\lambda)}>0$.

2.2 Fixed-Point Iteration

Cho and Park (2013) developed a simple algorithm based on fixed-point iteration. If we know the variation of spectrum, $\delta H(\lambda)$ in terms of modulus data, then we have

$$\delta H(\lambda)=H^{(r+1)}(\lambda)-H^{(r)}(\lambda)=\Gamma\left[G(\omega),H^{(r)}(\lambda)\right] \tag{2.20}$$

where r denotes the iteration step. However, it is difficult to find a functional $\Gamma[\bullet]$. Cho and Park noticed that the kernel function of loss modulus $K''(\lambda\omega)$ is a peaklike one. The kernel may be considered as a broadened delta function. They replaced the functional $\Gamma[\bullet]$ by the difference of modulus data and calculated modulus from the inferred spectrum:

$$H^{(r+1)}(\lambda) = H^{(r)}(\lambda) + G''\left(\frac{1}{\lambda}\right) - \int_{-\infty}^{\infty} H^{(r)}(\mu) K''\left(\frac{\mu}{\lambda}\right) \mathrm{d}\log\mu \tag{2.21}$$

Discretized version of Eq. (2.21) is

$$\mathbf{h}^{(r+1)} = \mathbf{h}^{(r)} + \mathbf{g} - \mathbf{S}\cdot\mathbf{h}^{(r)} \tag{2.22}$$

where **h**, **g**, and **S** are those defined in the previous subsection. This linear iteration scheme cannot prevent the occurrence of negative components of **h**. Hence, they replace Eq. (2.22) by

$$\log h_n^{(r+1)} = \log h_n^{(r)} + \log g_n - \log\left(\sum_{k=1}^{N} S_{nk} h_k^{(r)}\right) \tag{2.23}$$

where

$$S_{nk} = \sum_{\alpha=1}^{M} K''_{n\alpha} K''_{k\alpha}; \quad g_n = \sum_{\alpha=1}^{M} K''_{n\alpha} G'_{\alpha} \tag{2.24}$$

This is equivalent to

$$h_n^{(r+1)} = h_n^{(r)} \frac{g_n}{\sum_{k=1}^{N} S_{nk} h_k^{(r)}} \tag{2.25}$$

This is the iteration equation of the *fixed-point iteration* (FPI).

If the initial spectrum is positive, $h_k^{(0)} > 0$ for any k, then $h_k^{(r)} > 0$ at any step because all components of g_n and S_{nk} are positive. Since every singular values of **K** are in the denominator of the right-hand side, error can be stabilized by the similar mechanism in the regularization method. If $h_k^{(r)}$ is the exact spectrum, then the denominator equals the numerator and $h_k^{(r+1)} = h_k^{(r)}$.

For better spectrum, Cho and Park considered the minimization of

$$\chi^2 = \sum_{\alpha=1}^{M} \left(1 - \frac{1}{G''_{\alpha}} \sum_{k=1}^{N} K''_{k\alpha} h_k\right)^2 \tag{2.26}$$

This gives the normal equation $\mathbf{S}\cdot\mathbf{h} = \mathbf{g}$, but

$$S_{nk} = \sum_{\alpha=1}^{M} \frac{K''_{n\alpha}}{G''_{\alpha}} \frac{K''_{k\alpha}}{G''_{\alpha}}; \quad g_n = \sum_{\alpha=1}^{M} \frac{K''_{n\alpha}}{G''_{\alpha}} \tag{2.27}$$

This modification gives the better spectrum. Note that the singular values of $K''_{n\alpha}/G''_{\alpha}$ appears in the numerator of Eq. (2.25) and the linear combination of the squares of the singular variables is also in the denominator. This feature of the modified FPI enhances the stabilization of error more compared to the original FPI.

One of the demerits of FPI is that application of FPI to storage modulus data gives poor results because the kernel of storage modulus is not a peak. However, we can use storage modulus effectively if we modify Eq. (1.2) as follows:

$$\frac{G'(\omega)}{\omega} = \eta''(\omega) = \int_{-\infty}^{\infty} K''(\lambda\omega) W(\lambda) \mathrm{d}\log\lambda \tag{2.28}$$

where $W(\lambda) = \lambda H(\lambda)$ is called the weighted relaxation spectrum. Then, the same iterative equation can be applied to elastic viscosity $\eta''(\omega)$, and we can obtain the relaxation spectrum from the calculated $W(\lambda)$. Kwon (2012) applied this modification of FPI to immiscible polymer blends because the relaxation of interface is mainly related to storage modulus rather than loss modulus.

Kim et al. (2015) modified FPI to calculate relaxation spectrum from the Laplace transform of relaxation modulus, $s\tilde{G}(s)$, which requires numerical differentiation of $s\tilde{G}(s)$ with respect to s. As we have seen in Chap. 6, numerical differentiation is apt to be unstable for any error in the data.

One of the most important merits of FPI is fast convergence to an acceptable spectrum which is very similar to that of the nonlinear regularization of Honerkamp and Weese. Of course, FPI is independent of both initially guessed spectra and the number of relaxation times N.

2.3 Power Series Approximation

2.3.1 Algorithm

There is no reason why we deny that viscoelastic functions are not analytical. It is usual to draw viscoelastic data in double logarithmic scale. Therefore, we can write formally

$$G'(\omega) = \exp\left(\sum_{k=0}^{\infty} \gamma'_k \nu^k\right); \quad G''(\omega) = \exp\left(\sum_{k=0}^{\infty} \gamma''_k \nu^k\right) \tag{2.29}$$

where $\nu = \log \omega$. From experience, most data of dynamic moduli can be described accurately by

$$G'(\omega) = \exp\left(\sum_{k=0}^{N} \gamma'_k \nu^k\right); \quad G''(\omega) = \exp\left(\sum_{k=0}^{N} \gamma''_k \nu^k\right) \tag{2.30}$$

Since dynamic moduli are analytic, for $\theta = \pi/2$, we have

$$G(\nu + i\theta) = \sum_{n=0}^{\infty} g_n (\nu + i\theta)^n = \sum_{n=0}^{\infty} \left[\sum_{k=n}^{\infty} \binom{k}{n} g_k \nu^{k-n}\right] (i\theta)^n \tag{2.31}$$

It is assumed that the order of summation is interchangeable. Then, we also have

$$\mathrm{Re}\{G(\nu + i\theta)\} = \sum_{n=0}^{\infty} \left[(-1)^n \sum_{k=2n}^{\infty} \binom{k}{2n} g_k \nu^{k-2n}\right] \theta^{2n} \tag{2.32}$$

$$\mathrm{Im}\{G(\nu + i\theta)\} = \sum_{n=0}^{\infty} \left[(-1)^n \sum_{k=2n+1}^{\infty} \binom{k}{2n+1} g_k \nu^{k-2n+1}\right] \theta^{2n+1} \tag{2.33}$$

Note that it is a reasonable assumption that modulus is an infinitely differentiable function of ν, and then, the following series are convergent:

$$\begin{aligned} \frac{1}{(2n)!} \frac{\mathrm{d}^{2n} G(\nu)}{\mathrm{d}\nu^{2n}} &= \sum_{k=2n}^{\infty} \binom{k}{2n} g_k \nu^{k-2n} \\ \frac{1}{(2n+1)!} \frac{\mathrm{d}^{2n+1} G(\nu)}{\mathrm{d}\nu^{2n+1}} &= \sum_{k=2n+1}^{\infty} \binom{k}{2n+1} g_k \nu^{k-2n+1} \end{aligned} \tag{2.34}$$

Then, the FK relation gives

$$H\left(\frac{1}{\omega}\right) = \frac{2}{\pi} \sum_{n=0}^{\infty} \frac{(-1)^n}{(2n+1)!} \frac{\mathrm{d}^{2n+1} G'(\nu)}{\mathrm{d}\nu^{2n+1}} \left(\frac{\pi}{2}\right)^{2n+1} \tag{2.35}$$

and

$$H\left(\frac{1}{\omega}\right) = \frac{2}{\pi} \sum_{n=0}^{\infty} \frac{(-1)^n}{(2n)!} \frac{\mathrm{d}^{2n} G''(\nu)}{\mathrm{d}\nu^{2n}} \left(\frac{\pi}{2}\right)^{2n} \tag{2.36}$$

Although Eqs. (2.35) and (2.36) are exact, it is difficult to implement higher-order numerical differentiation for experimental data. Furthermore, the derivation of them is based on the two assumptions mentioned above, which are equivalent to the assumptions used by Anderssen et al. (2014). They derived Eqs. (2.35) and (2.36) in a standard way and applied them in inferring relaxation

spectrum. They adopted the Gureyev iteration in order to avoid the problem of numerical differentiation of higher order.

On the other hand, it can be assumed that relaxation spectrum is also an analytic function in order to avoid the problem of numerical differentiation:

$$H\left(e^{\xi}\right) = \sum_{n=0}^{\infty} h_n \xi^n \quad \text{with} \quad \xi = \log \lambda \tag{2.37}$$

It is obvious that Eq. (2.30) can be rewritten by

$$G'(\omega) = \sum_{n=0}^{\infty} g'_n \nu^n; \quad G''(\omega) = \sum_{n=0}^{\infty} g''_n \nu^n \tag{2.38}$$

Substitution of Eqs. (2.37) and (2.38) to Eqs. (2.35) and (2.36) gives

$$h_n = \frac{(-1)^n}{n!}\left(\frac{\mathrm{d}^n H}{\mathrm{d}\nu^n}\right)_{\nu=0} = \sum_{p=0}^{\infty} (-1)^{p+n} \binom{2p+1+n}{n} \left(\frac{\pi}{2}\right)^{2p} g'_{2p+1+n} \tag{2.39}$$

and

$$h_n = \sum_{p=0}^{\infty} (-1)^{p+n} \binom{2p+n}{n} \left(\frac{\pi}{2}\right)^{2p-1} g''_{2p+n} \tag{2.40}$$

The problem to be solved is how to calculate g'_n and g''_n from γ'_n and γ''_n of Eq. (2.30). Pourahmadi (1984) developed a simple equation such that

$$g_{n+1} = \sum_{k=0}^{n} \left(1 - \frac{k}{n+1}\right) \gamma_{n+1-k} g_k, \quad n = 0, 1, 2, \ldots \tag{2.41}$$

with $g_0 = \exp(\gamma_0)$. Although the number of γ_n is $N+1$, Eq. (2.41) allows us to calculate g_n for any n, if we set $\gamma_m = 0$ for $m > N$.

When very large N is necessary in order that Eq. (2.30) fits experimental data accurately, orthogonal polynomials such as the Chebyshev polynomial should be used:

$$G(\omega) = \exp\left[\sum_{n=0}^{N} c_n T_n(\tilde{\nu})\right] \tag{2.42}$$

where

$$\tilde{\nu} = \frac{2\nu - (\nu_{\max} + \nu_{\min})}{\nu_{\max} - \nu_{\min}}, \quad \nu_{\min} \le \nu \le \nu_{\max} \tag{2.43}$$

Here, the normalization of $\nu = \log \omega$ is used by Eq. (2.43) because the Chebyshev polynomials should be defined in the interval of [−1, 1]. Therefore, the use of Eq. (2.42) makes it difficult to obtain γ_n from c_n. To solve this problem, regression can be done by the partition of data with a polynomial of low order, which is the regression of partitioned data chosen N_S near $\nu_\alpha = \log \omega_\alpha$ with respect to Eq. (2.30) with $N < 10$. Since the sampled data have considerably narrow range of frequency, lower-order polynomial is sufficient to fit the sampled data precisely. Then, we can use

$$G(\nu) \approx \exp\left[\sum_{k=0}^{N} \gamma_k^{(\alpha)} (\nu - \nu_\alpha)^k\right] \tag{2.44}$$

for the sampled data. Then, Eq. (2.41) gives $g_k^{(\alpha)}$ and Eqs. (2.39) or (2.40) gives $h_k^{(\alpha)}$. Then, finally we can calculate

$$H(-\nu_\alpha) = h_0^{(\alpha)}; \quad H(-\nu_\alpha + \Delta\nu) = \sum_{k=0}^{N} h_k^{(\alpha)} (\Delta\nu)^k \tag{2.45}$$

where $\Delta\nu$ can be chosen arbitrarily, but $|\Delta\nu| \gg 1$ usually gives rise to poor results.

2.3.2 Error Analysis

Here, it is assumed that the effect of experimental errors is sufficiently eliminated by a suitable regression. Because of the analyticity of modulus, we can write

$$G(\omega) = \exp\left[\sum_{n=0}^{\infty} \gamma_n (\nu - \nu_c)^n\right] \tag{2.46}$$

where ν_c can be arbitrarily chosen. The double logarithmic power series of modulus should be valid in the interval of $|\nu - \nu_c| < R_G$. The convergence radius of modulus, R_G, cannot be determined from experimental data because we do not know the exact equation of modulus. However, it is obvious that there exists $0 < R_G < \infty$. Only available information from experimental data is that experimental data can be fitted very accurately by

$$G_N(\omega) = \exp\left[\sum_{n=0}^{N} \gamma_n (\nu - \nu_c)^n\right] \equiv \exp[P_N(\nu)] \tag{2.47}$$

where $P_N(\nu)$ is the Nth-order polynomial. This implies that there exists a small positive number δ such that

$$\left|1 - \frac{G_N(\omega)}{G(\omega)}\right| < \delta \ll 1 \text{ for } \quad |\nu - \nu_c| < R_G \tag{2.48}$$

If experimental data for the regression have the interval of $|\nu_\alpha - \nu_c| < R_E$, then it is a reasonable assumption that $R_E \leq R_G$.

Using the theory of the Taylor series, we can relate Eqs. (2.46) with (2.47) as follows:

$$G(\omega) = G_N(\omega) \exp[R_N(\nu)] \tag{2.49}$$

where $R_N(\nu)$ is the remainder of the Taylor series:

$$R_N(\nu) = \bar{\gamma}_{N+1}(\nu - \nu_c)^{N+1} \tag{2.50}$$

with

$$\bar{\gamma}_{N+1} \equiv \frac{1}{(N+1)!} \frac{\partial^{N+1} \log G}{\partial \nu^{N+1}}\bigg|_{\nu=\xi_N} \tag{2.51}$$

Note that ξ_N is a real number in the interval of $|\nu - \nu_c| < R_G$. Immediate consequences of Eq. (2.48) are

$$|R_N(\nu)| = |\Gamma_{N+1}| \left|\frac{\nu - \nu_c}{R_G}\right|^{N+1} < |\Gamma_{N+1}| < \delta \quad \text{for } |\nu - \nu_c| < R_G \tag{2.52}$$

where

$$\Gamma_{N+1} = \bar{\gamma}_{N+1} R_G^{N+1} \tag{2.53}$$

As an example, we consider the case of loss modulus. Using the FK relation, we have

$$H\left(\frac{1}{\omega}\right) = \frac{2}{\pi} \exp\left[P'_N(\nu) + R'_N(\nu)\right] \cos\left[P''_N(\nu) + R''_N(\nu)\right] \tag{2.54}$$

where

$$\begin{aligned} P'_N(\nu) &= \mathrm{Re}\left\{P_N\left(\nu + \frac{\pi}{2}\mathrm{i}\right)\right\}; \quad P''_N(\nu) = \mathrm{Im}\left\{P_N\left(\nu + \frac{\pi}{2}\mathrm{i}\right)\right\}; \\ R'_N(\nu) &= \mathrm{Re}\left\{R_N\left(\nu + \frac{\pi}{2}\mathrm{i}\right)\right\}; \quad R''_N(\nu) = \mathrm{Im}\left\{R_N\left(\nu + \frac{\pi}{2}\mathrm{i}\right)\right\} \end{aligned} \tag{2.55}$$

Note that the approximate spectrum is given by

$$H_N\left(\frac{1}{\omega}\right) = \frac{2}{\pi}\mathrm{Re}\left\{G_N''(\mathrm{i}\omega)\right\} = \frac{2}{\pi}\exp\left[P_N'(\nu)\right]\cos\left[P_N''(\nu)\right] \tag{2.56}$$

As for the remainder, we can write

$$\begin{aligned} R_N\left(\nu + \frac{\pi}{2}\mathrm{i}\right) &= \Gamma_{N+1}(h + \mathrm{i}\phi)^{N+1} \\ &= \Gamma_{N+1}\rho_N(h)[\cos\theta_N(h) + \mathrm{i}\sin\theta_N(h)] \end{aligned} \tag{2.57}$$

where

$$h = \frac{\nu - \nu_c}{R_G}; \quad \phi = \frac{\pi}{2R_G}; \quad \rho_N = \left(h^2 + \phi^2\right)^{\frac{N+1}{2}}; \quad \theta_N = (N+1)\arctan\frac{\phi}{h} \tag{2.58}$$

Since it is usual that the interval of experimental data is larger than a few decades, we can assume that $\frac{1}{2}\pi < R_E \le R_G$. Then, it is obvious that $\phi < 1$ and $\rho_N < 1$.

Substitution of Eq. (2.57) to (2.54) gives

$$H\left(\frac{1}{\omega}\right) \approx e^{\delta}H_N\left(\frac{1}{\omega}\right) - \frac{2}{\pi}\delta e^{\delta}\mathrm{Im}\left\{G_N''(\mathrm{i}\omega)\right\} \tag{2.59}$$

Note that the last term of Eq. (2.59) is

$$\frac{2}{\pi}\delta e^{\delta}\mathrm{Im}\left\{G_N''(\mathrm{i}\omega)\right\} = \delta e^{\delta}H_N\left(\frac{1}{\omega}\right)\tan P_N''(\nu) \tag{2.60}$$

Up to the first order, we know that $e^{\delta} = 1 + \delta$. Then, we have

$$\left|1 - \frac{H_N(\omega^{-1})}{H(\omega^{-1})}\right| \approx \delta\left|1 + \tan P_N''(\nu)\right| \quad \text{for} \quad \left|\log\frac{\omega}{\omega_c}\right| < R_G \tag{2.61}$$

Equation (2.47) indicates that if $\left|P_N''(\nu)\right|$ is not too large, then $H_N(\lambda)$ is a good approximation of a spectrum.

The limiting behaviors of R_N' and R_N'' are important in error analysis. If the order of polynomial N is even, then

$$\lim_{h\to 0} R_N'(\nu) = 0; \quad \lim_{h\to 0} R_N''(\nu) = (-1)^{[(N+1)/2]}\Gamma_{N+1}\phi^{N+1} \tag{2.62}$$

If N is odd, then

$$\lim_{h\to 0} R_N'(\nu) = (-1)^{[(N+1)/2]}\Gamma_{N+1}\phi^{N+1}; \quad \lim_{h\to 0} R_N''(\nu) = 0 \tag{2.63}$$

This implies that

$$H\left(\frac{1}{\omega_c}\right) \approx \begin{cases} \left[1-\delta\tan P_N''(\nu_c)\right]H_N\left(\frac{1}{\omega_c}\right) & \text{for even } N \\ (1+\delta)H_N\left(\frac{1}{\omega_c}\right) & \text{for odd } N \end{cases} \tag{2.64}$$

where $\nu_c = \log\omega_c$. This error analysis shows that whenever N is odd,

$$\left|1-\frac{H_N\left(\omega_c^{-1}\right)}{H\left(\omega_c^{-1}\right)}\right| \approx \left|\frac{\delta}{1+\delta}\right| \approx \delta \quad \text{for } 0<\delta\ll 1 \tag{2.65}$$

Note that the δ-term for even N of Eq. (2.64) fluctuates depending on the value of $P_N''(\nu_c)$. Hence, it can be said that the use of odd N infers spectrum with the error order of δ.

2.3.3 Comparison with the Original Version of PSA

This approximation of a spectrum is an improved version of the power series approximation (improved PSA) developed by Cho (2013). In the old version of power series approximation, the relation between g_n and h_n is g_n-explicit form, while Eqs. (2.39) and (2.40) are h_n-explicit form. The relation is a system of linear equations which are derived from substitution of the Taylor expansion of the spectrum to

$$G(\nu) = \int_{-\infty}^{\infty} K(\xi)H(\xi-\nu)\mathrm{d}\xi \tag{2.66}$$

Since g_n is determined by the regression of partitioned data with respect to Eq. (2.38), the old version of power series approximation gives the poor spectrum in terminal region. On the other hand, the improved power series approximation gives the better spectrum because Eq. (2.30) is very powerful in fitting any experimental data of dynamic moduli.

2.4 *Other Algorithms*

Remarkable algorithms and mathematical theorems have been developed by Davies and Anderssen (1997, 1998), Anderssen and Davies (2001), Davies and Goulding (2012), and Anderssen et al. (2014). Their algorithms and underlying mathematical theories are based on the FK relation and functional analysis. Here, we shall introduce the wavelet method (Davies and Goulding 2012) and the derivative-based method (Anderssen et al. 2014) briefly.

The wavelet method is to assume that relaxation spectrum is a linear combination of peaklike functions. To avoid the occurrence of negative coefficient, they used sparse approximation. However, it is doubted that such approximation is always valid for fitting arbitrary modulus data. Fitting modulus data by the wavelet functions is equivalent to the calculation of discrete spectrum. The nonlinear regression might give rise to another ill-posed problem. In the author's opinion, this algorithm requires that users have high-level knowledge on spectrum.

The derivative-based method is to exploit Eqs. (2.35) and (2.36). To avoid higher derivatives of modulus, they used the Gureyev iteration which is a successive application of convolution. This algorithm needs 10–50 convolution integrals. Although numerical integral is well posed, fifty integrals are time-consuming procedures compared to the improved power series approximation.

Stadler and Bailly (2009) developed a new algorithm which exploits the cubic Hermite spline (CHS). The algorithm needs a discrete spectrum for the determination of the knots of the CHS. The algorithm adjusts iteratively the knots until the root mean square between data and calculated modulus arrives at a certain value. Hence, this algorithm is like a brutal searching method and very slow, although the algorithm can fit some special spectra whose derivative has discontinuity, for example, a box-shaped spectrum. However, it is believed that experimental data have a smooth spectrum whose derivatives are also continuous.

Since most viscoelastic functions vary in logarithmic scale, it is a very natural attempt to describe viscoelastic functions as a logarithmic power series such as Eq. (2.29). Bae and Cho (2015) applied this mathematical form to relaxation spectrum, too:

$$H(\lambda) = \exp\left(\sum_{k=0}^{N} \hat{h}_n \xi^k\right) \quad \text{with } \xi = \log\lambda \tag{2.67}$$

Then, Eq. (1.2) can be rewritten as

$$\begin{aligned} \exp\left(\sum_{n=0}^{N} \gamma'_n \nu^n\right) &= \frac{1}{2}\int_{-\infty}^{\infty} [1 + \tanh(\nu+\xi)] \exp\left(\sum_{n=0}^{N} \hat{h}_n \xi^n\right) \mathrm{d}\xi \\ \exp\left(\sum_{n=0}^{N} \gamma''_n \nu^n\right) &= \frac{1}{2}\int_{-\infty}^{\infty} \operatorname{sech}(\nu+\xi) \exp\left(\sum_{n=0}^{N} \hat{h}_n \xi^n\right) \mathrm{d}\xi \end{aligned} \tag{2.68}$$

Since the coefficients γ'_n and γ''_n can be determined by the regression of data, Bae and Cho tried to determine $\hat{h}_n$ by the use of the Levenberg–Marquardt method. It is known that simple polynomial regression is not stable when N is large (Sokolnikoff and Redheffer 1958). This problem can be solved by the use of orthogonal polynomials instead of simple polynomial. However, Runge's phenomenon cannot be avoided whenever N is large (Trefethen and Weideman 1991). Hence, Bae and Cho adopted cubic B-spline and obtained successful results. They applied this calculation scheme not only to dynamic modulus but also to the Laplace transform of

relaxation modulus. We call this method *BLM* because the algorithm exploits B-spline and the Levenberg–Marquardt method.

It is noteworthy that Runge's phenomena is not significant when fitting modulus data but is significant when spectrum is calculated from modulus data. Hence, it is difficult to give up using Eq. (1.34). Lee et al. (2015) developed an algorithm exploiting Eq. (1.34) and the FK relation. We shall call the method *CFK* (Chebyshev–Fuoss–Kirkwood).

If the approximation of Eq. (1.34) can fit experimental data in sufficient precision, then the spectrum can be determined by the use of the FK relation. Note that

$$G(\mathrm{i}\omega) = \exp\left[\sum_{k=0}^{N} g_n T_n(\tilde{\nu} + \mathrm{i}\phi)\right] = e^{R(\nu)} \cos\Omega(\nu) + \mathrm{i} e^{R(\nu)} \sin\Omega(\nu) \tag{2.69}$$

where $\tilde{\nu}$ is normalized one so that $-1 \le \tilde{\nu} \le 1$ as shown in Eq. (2.43),

$$\phi = \frac{\pi}{\nu_{\max} - \nu_{\min}} \tag{2.70}$$

and

$$\begin{aligned} R(\nu) &= \mathrm{Re}\left\{\sum_{k=0}^{N} g_n T_n(\tilde{\nu} + \mathrm{i}\phi)\right\} = \sum_{k=0}^{N} g_n \mathrm{Re}\{T_n(\tilde{\nu} + \mathrm{i}\phi)\} \\ \Omega(\nu) &= \mathrm{Im}\left\{\sum_{k=0}^{N} g_n T_n(\tilde{\nu} + \mathrm{i}\phi)\right\} = \sum_{k=0}^{N} g_n \mathrm{Im}\{T_n(\tilde{\nu} + \mathrm{i}\phi)\} \end{aligned} \tag{2.71}$$

Then, the FK relation gives

$$\begin{aligned} H\left(\frac{1}{\omega}\right) &= \frac{2}{\pi} \exp\left[\sum_{k=0}^{N} g'_k \mathrm{Re}\{T_k(\tilde{\nu} + \mathrm{i}\phi)\}\right] \sin\left[\sum_{k=0}^{N} g'_k \mathrm{Im}\{T_k(\tilde{\nu} + \mathrm{i}\phi)\}\right] \\ &= \frac{2}{\pi} \exp\left[\sum_{k=0}^{N} g''_k \mathrm{Re}\{T_k(\tilde{\nu} + \mathrm{i}\phi)\}\right] \cos\left[\sum_{k=0}^{N} g''_k \mathrm{Im}\{T_k(\tilde{\nu} + \mathrm{i}\phi)\}\right] \end{aligned} \tag{2.72}$$

Equation (2.71) becomes available if we find a systematic method to calculate real and imaginary parts of the Chebyshev polynomials $T_k(\tilde{\nu} + \mathrm{i}\phi)$. For convenience, we introduce the notation

$$T'_k(\tilde{\nu}) = \mathrm{Re}\{T_k(\tilde{\nu} + \mathrm{i}\phi)\}; \quad T''_k(\tilde{\nu}) = \mathrm{Im}\{T_k(\tilde{\nu} + \mathrm{i}\phi)\} \tag{2.73}$$

Since $T_0(x) = 1$ and $T_1(x) = x$, it is obvious that

$$T'_0(\tilde{\nu}) = 1; \quad T''_0(\tilde{\nu}) = 0; \quad T'_1(\tilde{\nu}) = \tilde{\nu}; \quad T''_1(\tilde{\nu}) = \phi \tag{2.74}$$

Then, the recursion equation of the Chebyshev polynomial, Eq. (2.32) in Chap. 1, gives

$$\begin{aligned} T'_{n+1}(\tilde{\nu}) &= 2\tilde{\nu}T'_n(\tilde{\nu}) - 2\phi\, T''_n(\tilde{\nu}) - T'_{n-1}(\tilde{\nu}) \\ T''_{n+1}(\tilde{\nu}) &= 2\tilde{\nu}T''_n(\tilde{\nu}) + 2\phi\, T'_n(\tilde{\nu}) - T''_{n-1}(\tilde{\nu}) \end{aligned} \tag{2.75}$$

for $n \geq 1$. The recursive equation allows us to calculate Eq. (2.72). For some experimental data, the second equation of Eq. (2.72) gives fairly a good spectrum, while the first one does not. Even if regression of modulus by Eq. (1.34) may not give rise to Runge's phenomena, Eq. (2.72) is not free from Runge's phenomena. Hence, with low N, partitioned regression gives a good spectrum just as the improved PSA does.

2.5 *Comparison of Algorithms*

2.5.1 How to Test Algorithms

To test how well an algorithm works, it is necessary to generate modulus data from a model spectrum through Eq. (1.2). One of the most popular model spectra is the asymmetric double-peak model which is the sum of two lognormal distributions. An example is given by

$$H(\lambda) = H_1 \exp\left[-\frac{1}{w_1}\left(\log_{10}\frac{\lambda}{\lambda_1}\right)^2\right] + H_2 \exp\left[-\frac{1}{w_2}\left(\log_{10}\frac{\lambda}{\lambda_2}\right)^2\right] \tag{2.76}$$

To enhance the precision of modulus data, the frequency range is taken shorter than that of relaxation time. If simulated modulus data are wished to be generated over $\omega_{\min} < \omega < \omega_{\max}$, then the numerical integration of the modulus should be done over $10^{-n}/\omega_{\max} \leq \lambda \leq 10^{n}/\omega_{\min}$ where $n > 1$.

On the other hand, when modulus data over $\omega_{\min} < \omega < \omega_{\max}$ are used in inferring relaxation spectrum, the calculated spectrum is reliable in a shorter interval of

$$\frac{e^{\pi/2}}{\omega_{\max}} \leq \lambda \leq \frac{e^{-\pi/2}}{\omega_{\min}} \tag{2.77}$$

This inequality was derived by Davies and Anderssen (1997). Equation (2.77) is called the *Davies and Anderssen limit* (DA limit).

2.5.2 Comparison with Simulated Data

It is a difficult work to test a number of algorithms made by several research groups for the same data. From this viewpoint, the work of Dealy and coworkers is

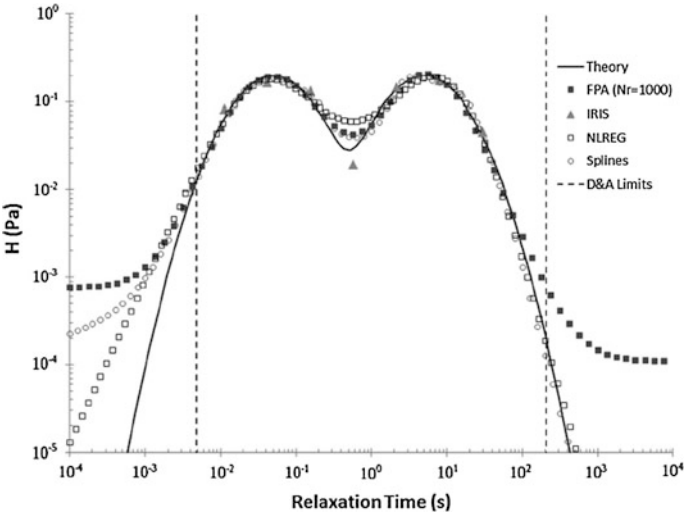

Fig. 2 Comparison of calculated spectra from four algorithms: FPI is the fixed-point iteration (*FPI*), IRIS is the discrete algorithm of Baumgärtel and Winter (1989), NLREG is the nonlinear regularization, and spline is the cubic Hermite spline (*CHS*). This is Fig. 6 of McDougall et al. (2014). It must be noted that the modulus data for this calculation were generated with 4 % random error [see Fig. 2 of McDougall et al. (2014)]

valuable (McDougall et al. 2014). They compared three algorithms of continuous spectrum (FPI, NLREG, and CHS) and an algorithm of discrete spectrum [IRIS (Baumgärtel and Winter 1989)]. To test the three algorithms, they used the model spectrum given as the sum of two logarithmic Gaussian functions with different centers with the same width and height. The model spectrum will be called symmetric double peak (SDP). Dealy and coworkers used $H_1 = H_2 = \left(2\sqrt{2\pi}\right)^{-1}, w_1 = w_2 = 2, \lambda_1 = 0.05$ and $\lambda_2 = 5$.

Within the Davies and Anderssen limit, the three algorithms of continuous spectrum agree well with the model spectrum of SDP when data are generated from the model spectrum. Outside the DA limit, NLREG is the best, CHS is the second, and the FPI is the last. On the other hand, in the Valley region, FPI and CHS are similarly close to the model spectrum, while NLREG overestimates the spectrum (Fig. 2).

2.5.3 Comparison with Experimental Data

Figure 3 shows the relaxation spectrum from the data of PBD 430K (Fig. 12) in Chap. 5 by various algorithms such as FPI, improved PSA with 3rd order polynomial and data partitioning, CFK with 21st order Chebyshev polynomial without data partitioning, BLM with $M = 40$ and CHS. As for CHS, the spectrum was obtained from Fig. 1 of (Stadler and van Ruymbeke 2010) by the use of digitization of the graph.

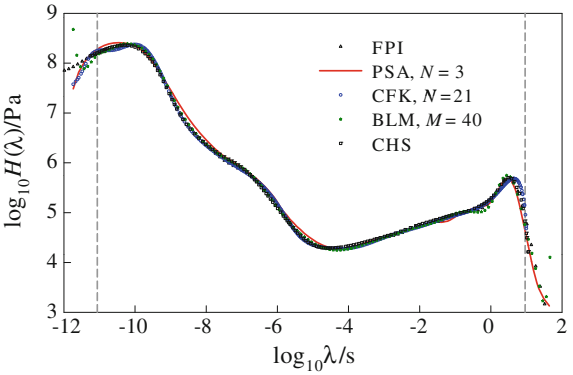

Fig. 3 Comparison of five algorithms for continuous spectrum. Modulus data of Fig. 12 in Chap. 5 are used. The modulus data were kindly provided by Professor Stadler (Stadler and van Ruymbeke 2010)

Although all algorithms give almost same spectra within the Davies–Anderssen limit, both spectra from PSA and BLM are wavier than others in long time regime.

Problem 2

[1] Derive the normal equation $\partial\chi_\rho^2 \Big/ \partial h_k = 0$ from Eq. (2.17).

[2] For $m \times n$ matrix $\mathbf{K}$, the theorem of singular value decomposition reads

$$\mathbf{K} = \mathbf{U} \cdot \mathbf{E} \cdot \mathbf{V}^T \tag{2.a}$$

where $\mathbf{U}$ is an $m \times m$ orthogonal matrix such that $\mathbf{U} \cdot \mathbf{U}^T = \mathbf{I}_m$ and $\mathbf{V}$ is an $n \times n$ orthogonal matrix such that $\mathbf{V} \cdot \mathbf{V}^T = \mathbf{I}_n$. The m-dimensional and n-dimensional orthonormal bases are denoted by $\mathbf{e}_k^{(m)}$ and $\mathbf{e}_i^{(n)}$, respectively. Show that

$$\mathbf{K} \cdot \mathbf{K}^T \cdot \mathbf{u}_k = \sigma_k^2 \mathbf{u}_k; \quad \mathbf{K}^T \cdot \mathbf{K} \cdot \mathbf{v}_i = \sigma_i^2 \mathbf{v}_i \tag{2.b}$$

where $\mathbf{u}_k = \mathbf{U} \cdot \mathbf{e}_k^{(m)}$, $\mathbf{v}_i = \mathbf{V} \cdot \mathbf{e}_i^{(n)}$, and σ_i are singular values of $\mathbf{K}$.

[3] Derive Eq. (2.56).

[4] Derive Eq. (2.59) from Eq. (2.32) in Chap. 1.

3 Algorithms for Discrete Spectrum

3.1 Nonlinear Least Squares

Discrete spectrum is a set of parameters $\{G_k\}$, $\{\lambda_k\}$ and N. From Eq. (3.1) in Chap. 5, we have

$$G'(\omega) = \sum_{k=1}^{N} G_k \frac{\lambda_k^2 \omega^2}{1+\lambda_k^2 \omega^2}; \quad G''(\omega) = \sum_{k=1}^{N} G_k \frac{\lambda_k \omega}{1+\lambda_k^2 \omega^2} \tag{3.1}$$

Thus, determination of discrete spectrum is the minimization of

$$\chi^2 = \sum_{\alpha=1}^{M} \left[G'(\omega_\alpha) - \sum_{k=1}^{N} G_k \frac{\lambda_k^2 \omega_\alpha^2}{1+\lambda_k^2 \omega_\alpha^2} \right]^2 + \sum_{\alpha=1}^{M} \left[G''(\omega_\alpha) - \sum_{k=1}^{N} G_k \frac{\lambda_k^2 \omega_\alpha}{1+\lambda_k^2 \omega_\alpha^2} \right]^2 \tag{3.2}$$

If $\{\lambda_k\}$ are given, then the problem becomes linear regression. Hence, one may choose N relaxation times in the interval $\omega_{\max}^{-1} \le \lambda_k \le \omega_{\min}^{-1}$ with satisfying

$$\log \frac{\lambda_{k+1}}{\lambda_k} = \Delta\mu \quad \text{for } 1 \le k \le N-1 \tag{3.3}$$

Then, the problem can be solved by the linear regularization method (LREG) developed by Honerkamp and Wesse (1989). However, this algorithm does not give a parsimonious spectrum because the algorithm is not equipped with any mathematical device to determine the number of relaxation times and because the locations of relaxation times are not optimized (uniformly distributed relaxation times). If non-uniform spacing of relaxation is introduced to the LREG, then the problem becomes the one of nonlinear regression. Hence, the sum of square error must not have the global minimum. Nonlinear regression cannot guarantee the exclusion of the occurrence of negative relaxation intensities $G_k < 0$.

Baumgärtel and Winter (1989) replaced the sum of squares of Eq. (3.2) by

$$\chi^2 = \sum_{\alpha=1}^{M} \left[1 - \frac{1}{G'(\omega_\alpha)} \sum_{k=1}^{N} G_k \frac{\lambda_k^2 \omega_\alpha^2}{1+\lambda_k^2 \omega_\alpha^2} \right]^2 + \sum_{\alpha=1}^{M} \left[1 - \frac{1}{G''(\omega_\alpha)} \sum_{k=1}^{N} G_k \frac{\lambda_k^2 \omega_\alpha}{1+\lambda_k^2 \omega_\alpha^2} \right]^2 \tag{3.4}$$

and took not only G_k but also λ_k as adjustable parameters to minimize the relative sum of square error, as in Eq. (3.4). When N is large, it is probable to find negative G_k. Therefore, they made a strategy to start from small N. They chose N to make the density of relaxation time be between 1 and 2 relaxation times per decade. As increasing N, they eliminated irrelevant mode which may be suffered from negative relaxation intensity. Since they did not describe the algorithm in detail (Baumgärtel and Winter 1989), it is difficult to analyze why the algorithm is successful. The algorithm was commercialized and is called IRIS. The performance of the algorithm is also found in (McDougall et al. 2014).

Since Eq. (3.4) is so complicated, one may guess that there are so many local minima in the parameter space. Although a brutal searching may be applicable for small N, it takes too long computation time to be applied to the case of large

N. Hence, Jensen applied simulated annealing (SA) to this problem (Jensen 2002). SA is originated in thermodynamics and is a heuristic method. The more information on SA is found in Press and Teukolsky (2002).

3.2 The Padé–Laplace Methods

Both IRIS and SA determine the number of relaxation modes by trial error. The optimum number of relaxation modes is determined as the one at which significant decrease of χ^2 is not shown as increasing the number of the modes further. Hence, there have been efforts to determine N on a mathematical foundation. The Pade–Laplace method has been applied to discrete spectrum (Fulchiron et al. 1993; Simhambhatla and Leonov 1993).

Note that the Laplace transform of relaxation modulus is expressed in terms of discrete spectrum as follows:

$$s\tilde{G}(s) = \sum_{k=1}^{N} \frac{\eta_k s}{1+\lambda_k s} = \frac{P_N(s)}{Q_N(s)} \tag{3.5}$$

where $\eta_k = G_k\lambda_k$. If Eq. (3.5) is expressed by the reduction to common denominator, then it is a rational function such that both denominator and numerator are polynomials of Nth order. Fitting the Laplace transform of relaxation modulus determines the coefficients of the two polynomials. Relaxation times are determined from the poles of the denominator which are the zeroes of the polynomial $QN(s)$. After the determination of relaxation times, relaxation intensity can be determined by

$$G_k = \lim_{s\to -1/\lambda_k} (1+\lambda_k s)\frac{s\tilde{G}(s)}{\lambda_k} \tag{3.6}$$

Even if N increases, the number of poles of the denominator does not increase in principle. Hence, the Padé–Laplace transform method determines the number of relaxation times on the mathematical foundation.

The success of the Padé–Laplace method depends on how precisely all the coefficients of polynomials can be determined. Fulchiron et al. (1993) used stress relaxation data for the Laplace transform, while Simhambhatla and Leonov (1993) used dynamic data. Simhambhatla and Leonov suggested a method to determine the coefficients of the Taylor series of $\tilde{G}(s)$ by the use of the following exact equations:

$$\tilde{G}(s) = \sum_{k=0}^{\infty} c_k (s-s_o)^k \tag{3.7}$$

with

$$
\begin{aligned}
c_k &= \frac{1}{k!}\int_0^\infty (-t)^k G(t) e^{-s_o t}\mathrm{d}t \\
&= \frac{2}{\pi}\int_{-\infty}^{\infty} \frac{(-1)^k G'(\omega)}{\left(s_o^2+\omega^2\right)^{(k+1)/2}} \sin\left[(k+1)\arctan\frac{\omega}{s_o}\right]\mathrm{d}\log\omega \\
&= \frac{2}{\pi}\int_{-\infty}^{\infty} \frac{(-1)^k G''(\omega)}{\left(s_o^2+\omega^2\right)^{(k+1)/2}} \cos\left[(k+1)\arctan\frac{\omega}{s_o}\right]\mathrm{d}\log\omega
\end{aligned}
\tag{3.8}
$$

Since the integrands of Eq. (3.8) decay to zero very fast as $|\log\omega| \to \infty$, the integrations of Eq. (3.8) can be replaced by the ones over the frequency interval of experimental data. However, the center of Taylor expansion, s_o, should be determined empirically. If c_k are determined up to a certain order of polynomial, N, then it is not difficult to determine the polynomials of the denominator and numerator. Details are shown in Sect. 2.3 in Chap. 1.

It is interesting that one may apply Padé approximations to dynamic moduli because of Eq. (3.1). Malkin and Kuznetsov (2000) invented this idea to calculate discrete spectrum. This algorithm seems to be simpler than that of Simhambhatla and Leonov.

Since rational function approximation may not be effective for the viscoelastic data with wide frequency range, both the Padé-Laplace method and the method of Malkin and Kuznetsov must have some weak point for wide-frequency data. It is because viscoelastic functions vary in logarithmic scale. The studies using Padé–Laplace methods deal with the data defined on 4–5 decades of frequency (or time). Simhambhatla and Leonov used the Levenberg–Marquardt algorithm jointly for the supplement to the Padé–Laplace method.

3.3 *Approximation from Continuous Spectrum*

Malkin and Masalova (2001) tested several algorithms of discrete spectrum and concluded that the unique relaxation time spectrum cannot be determined [see Fig. 4 which is Fig. 2 of Malkin and Masalova (2001)]. However, their conclusion is only valid for discrete spectrum. They tested only algorithms of discrete spectrum. Then, a question arises: Why is not discrete spectrum unique? The answer might be that a discrete spectrum is an approximation of the corresponding continuous spectrum.

If a discrete spectrum is an approximation of the unique continuous one, then what is the condition that the discrete spectrum should satisfy? The author thinks that IRIS is one of the most reliable algorithms for discrete spectrum because the

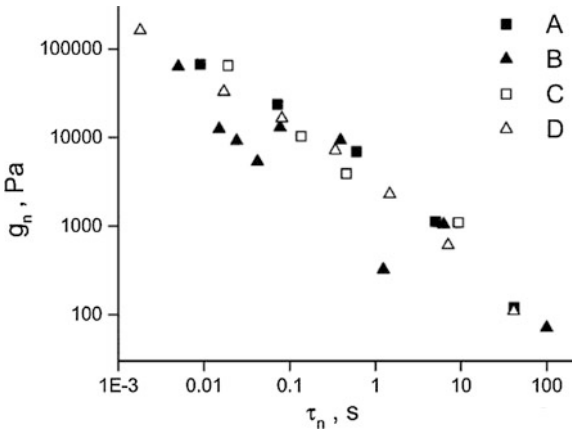

Fig. 4 Discrete relaxation spectra obtained from four different algorithms: *A* is the algorithm using linear regression with relaxation times assigned uniformly along log-frequency range, *B* is the one using linear regression with relaxation times assigned by power law, *C* is the algorithm of Malkin and Kuznetsov (2000), and *D* is IRIS (Baumgärtel and Winter 1989). This is Fig. 2 of (Malkin and Masalova 2001). Note that g_n and τ_n are G_k and λ_k of Eq. (3.1), respectively

discrete spectrum of IRIS agrees with continuous spectrum in shape as shown by Dealy and coworkers (McDougall et al. 2014). Simhambhatla and Leonov (1993) tested their algorithm for modulus data generated from a continuous spectrum and confirm that their discrete spectrum lies on the original continuous one. This implies that relaxation intensities of the discrete spectrum should satisfy

$$G_k = \sigma H(\lambda_k) \tag{3.9}$$

where $H(\lambda)$ is the unique continuous spectrum and σ is the scale factor which must depend on the number of relaxation modes. If the scale factor σ, the number of relaxation modes N, and the continuous spectrum are given, then the determination of discrete spectrum is reduced to the determination of N relaxation times to experimental data.

Equation (3.9) implies that

$$\int_{-\infty}^{\infty} H(\lambda) \mathrm{d} \log \lambda = \sum_{k=1}^{N} G_k = \sigma \sum_{k=1}^{N} H(\lambda_k) \tag{3.10}$$

Since we can obtain the continuous spectrum from various algorithms, we replace Eq. (3.10) by

$$\int_{\log \lambda_{\min}}^{\log \lambda_{\max}} H(\lambda) \mathrm{d} \log \lambda = \sigma \sum_{k=1}^{N} H(\lambda_k) \tag{3.11}$$

Since we can determine the left-hand side of Eq. (3.11), denoting it by g, we have

$$\sigma = g \Big/ \sum_{k=1}^{N} H(\lambda_k) \tag{3.12}$$

Choosing node points by

$$\log_{10} t_k = \frac{k}{N} \log_{10} \frac{\omega_{\min}}{\omega_{\max}} - \log \omega_{\max} \quad \text{with } k = 0, 1, \ldots, N \tag{3.13}$$

Assign N relaxation times to be located as

$$t_{k-1} \le \lambda_k \le t_k \quad \text{with } k = 1, 2, \ldots, N \tag{3.14}$$

We are looking for the optimum relaxation times by varying λ_k in the intervals of Eq. (3.14). The optimum relaxation times are defined as the ones minimizing

$$\chi^2 = \sum_{\alpha=1}^{M} \left[1 - \frac{g}{G'_\alpha} \sum_{k=1}^{N} \tilde{H}(\lambda_k) \frac{\lambda_k^2 \omega_\alpha^2}{1 + \lambda_k^2 \omega_\alpha^2} \right]^2 + \sum_{\alpha=1}^{M} \left[1 - \frac{g}{G''_\alpha} \sum_{k=1}^{N} \tilde{H}(\lambda_k) \frac{\lambda_k \omega_\alpha}{1 + \lambda_k^2 \omega_\alpha^2} \right]^2 \tag{3.15}$$

where

$$\tilde{H}(\lambda_k) = \frac{H(\lambda_k)}{\sum_{n=1}^{N} H(\lambda_n)} \tag{3.16}$$

This is a nonlinear regression problem which may be solved by the Levenberg–Marquardt method. Hence, we shall call this algorithm DLM (discrete algorithm using LM method). Since $H(\lambda)$ can be determined by an algorithm of continuous spectrum, we can express $H(\lambda)$ by a simple equation such as Eq. (2.51).

Bae (2015) tested this method for the extraction of relaxation times. As iteration of the Levenberg–Marquardt algorithm progresses, the sum of square error χ^2 decreases monotonically. The sum of square error also decreases as the number of relaxation modes N for a given iteration number. After the minimum, higher N does not show significant change of χ^2. Hence, the optimum number of relaxation modes N^* can be determined, too. It is interesting that as for $N > N^*$, $\lambda_k \approx \sqrt{t_{k-1} t_k}$: almost equal spacing between adjacent relaxation times in logarithmic scale. This implies that if a continuous spectrum is given and the optimum number of relaxation modes is determined, then the discrete spectrum can be easily determined by

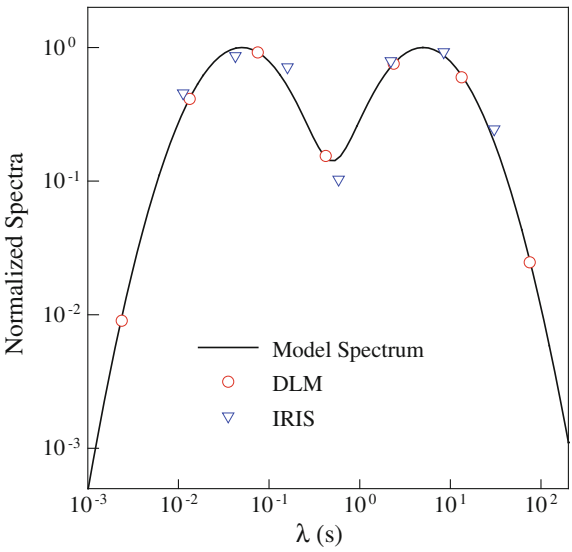

Fig. 5 Comparison of two discrete algorithms: DLM and IRIS. To check the consistency of the model continuous spectrum, all spectra are normalized

$$\log_{10}\lambda_k = \frac{k-\frac{1}{2}}{N}\log_{10}\frac{\omega_{\min}}{\omega_{\max}} - \log\omega_{\max} \quad \text{with } k = 1, 2, \ldots, N \tag{3.17}$$

and

$$G_k = g\tilde{H}(\lambda_k) \tag{3.18}$$

It is interesting that the discrete relaxation spectrum from IRIS shows similar behavior. From this, one may think that allocation of equally spaced relaxation times in logarithm scale and linear regression may give the same result. However, this allocation method happens to give negative relaxation intensities because of the ill-posedness and Eqs. (3.17) and (3.18) show slight deviation of calculated modulus from the data at the boundary of the frequency range. Furthermore, the relation $\lambda_k \approx \sqrt{t_{k-1}t_k}$ is not valid always.

Figure 5 shows the calculated discrete spectra from the dynamic moduli data which is shown in Fig. 2. For easy comparison with the model spectrum of Eq. (2.76), all discrete spectra of Fig. 5 are normalized to be close to the continuous model spectrum which is also normalized by the maximum of the original one. Note that we fixed the number of relaxation times as $N = 7$. As shown in Fig. 5, both DLM and IRIS give discrete spectra consistent with the continuous model spectrum. However, DLM shows higher consistency than IRIS because of the principle of DLM.

Problem 3

[1] Derive Eq. (3.6).
[2] What is the merit of Padé approximation compared to Taylor expansion?
[3] What is the disadvantage of Padé approximation?
[4] For a given polynomial of *N*th order, how can we determine the zeroes of the polynomial numerically?

References

R.S. Anderssen, A.R. Davies, Simple moving-average formulae for the direct recovery of the relaxation spectrum. J. Rheol. **45**, 1–27 (2001)
R.S. Anderssen, A.R. Davies, F.R. de Hoog, R. J. Loy, Derivative based algorithms for continuous relaxation spectrum recovery. J. Non-Newtonian Fluid Mech. (in press, 2014) [Online 24 Oct 2014]
J.-E. Bae, *Numerical studies on viscoelastic characterization of polymeric fluids: relaxation spectrum and LAOS of viscoelastic models*, Ph. D. thesis supervised by Prof. K. S. Cho, Kyungpook National University (2015)
J.-E. Bae, K.S. Cho, Logarithmic method for continuous relaxation spectrum and comparison with previous methods. J. Rheol. **59**, 1081–1112 (2015)
M. Baumgärtel, H.H. Winter, Determination of discrete relaxation and retardation time spectra form dynamic mechanical data. Rheol. Acta. **28**, 511–519 (1989)
K.S. Cho, Power series approximations of dynamic moduli and relaxation spectrum. J. Rheol. **57**, 679–697 (2013)
K.S. Cho, G.W. Park, Fixed-point iteration for relaxation spectrum from dynamic mechanical data. J. Rheol. **57**, 647–678 (2013)
A.M. Cohen, Numerical methods for laplace transform inversion. (Springer, Berlin, 2007)
A.R. Davies, R.S. Anderssen, Sampling localization in determining the relaxation spectrum. J. Non-Newtonian Fluid Mech. **73**, 163–179 (1997)
A.R. Davies, R.S. Anderssen, Sampling localization and duality algorithms in practice. J. Non-Newtonian Fluid Mech. **79**, 235–253 (1998)
A.R. Davies, N.J. Goulding, Wavelet regularization and continuous relaxation spectrum. J. Non-Newtonian Fluid Mech. **189**, 19–30 (2012)
J.D. Ferry, *Viscoelastic properties of polymers*. (Wiley, USA, 1980)
R.M. Fuoss, J.G. Kirkwood, Electrical properties of solids. VIII. Dipole moments in polyvinyl chloride-diphenyl systems. J. Am. Chem. Soc. **63**, 385–394 (1941)
R. Fulchiron, V. Verney, P. Cassagnau, A. Michel, P. Levoir, J. Aubard, Deconvolution of polymer melt stress relaxation by the padé-laplace method. J. Rheol. **37**, 17–34 (1993)
J. Honerkamp, J. Weese, Determination of the relaxation spectrum by a regularization method. Macromolecules **22**, 4327–4377 (1989)
J. Honerkamp, J. Weese, A nonlinear regularization method for the calculation of relaxation spectra. Rheol. Acta. **32**, 65–73 (1993)
E.A. Jensen, Determination of discrete relaxation spectra using simulated annealing. J. Non-Newtonian Fluid Mech. **107**, 1–11 (2002)
M.K. Kim, J.-E. Bae, N. Kang, K.S. Cho, Extraction of viscoelastic functions from creep data with ringing. J. Rheol. **59**, 237–252 (2015)
A. Kirsch, *An introduction to the mathematical theory of inverse problems, 2nd edn*. (Springer, Berlin, 2010)

M. Kwon, *Application of new algorithms for relaxation time spectrum to immiscible polymer blends*, MS thesis supervised by Prof. K. C. Cho. (Kyungpook National University, Korean, 2012)

C.L. Lawson, R.J. Hanson, *Solving least squares problems*, SIAM (1995)

S. Lee, J.-E. Bae, K.S. Cho, Complex decomposition method for relaxation time spectrum. Ann. Eur Rheol. Conf. (Nante, 2015)

C. Liu, J. He, E. van Ruymbeke, R. Keunings, C. Bailly, Evaluation of different methods for the determination of the plateau modulus and the entanglement molecular weight. Polymer **47**, 4461–4479 (2006)

A.Y. Malkin, V.V. Kuznetsov, Linearization as a method for determining parameters of relaxation spectra. Rheol. Acta. **39**, 379–383 (2000)

A.Y. Malkin, I. Masalova, From dynamic modulus via different relaxation spectra to relaxation and creep functions. Rheol. Acta. **40**, 261–271 (2001)

I. McDougall, N. Orbey, J.M. Dealy, Inferring meaningful relaxation spectra from experimental data. J. Rheol. **58**, 779–797 (2014)

M. Pourahmadi, Taylor expansion of exp ($\sum_{k=0}^{\infty} a_k z^k$) and some applications. Am. Math Monthly **91**, 303–307 (1984)

W.H. Press, S.A. Teukolsky, W.T. Vetterling, B.P. Flannery, *Numerical Recipes in C++* 2nd edn. (Cambridge University Press, UK, 2002)

F.J. Stadler, C. Bailly, A new method for the calculation of continuous relaxation spectra from dynamic-mechanical data. Rheol. Acta. **48**, 33–49 (2009)

M. Simhambhatla, A.I. Leonov, The extended padé-laplace method for efficient discretization of linear viscoelastic spectra. Rheol. Acta. **32**, 589–600 (1993)

I.S. Sokolnikoff, R.M. Redheffer, *Mathematics of Physics and Modern Engineering*. (McGraw-Hill, USA, 1958)

F.J. Stadler, E. van Ruymbeke, An improved method to obtain direct rheological evidence of monomer density reequilibration for entangled polymer melt. Macromolecules **43**, 9205–9209 (2010)

L.N. Trefethen, J.A.C. Weideman, Two results on polynomial interpolation in equally spaced points. J. Approx. Theory **65**, 247–260 (1991)

N.W. Tschoegl, *The Phenomenological Theory of Linear Viscoelastic Behavior.* (Springer, Verlag, 1989)

D.R. Wiff, RQP method of inferring a mechanical relaxation spectrum. J. Rheol. **22**, 589–597 (1978)

A.H. Zemanian, *Distribution Theory and Transform Analysis.* (Dover, 1987)

Chapter 8
Time-Temperature Superposition

Abstract This chapter consists of three sections: the fundamentals, the geometric interpretation, and the algorithms of time-temperature superposition. The first section deals with the phenomenology, mathematical formulas, models for horizontal shift factor, and molecular explanation of time-temperature superposition. The second section is devoted to a new insight on time-temperature superposition, the so-called geometric interpretation which provides new methods for the analysis of the viscoelastic data measured at various temperatures. The last section introduces two numerical algorithms for time-temperature superposition.

The time-temperature superposition (TTS) is an empirical principle. This principle is valid for most polymer melts in linear viscoelastic regime as well as in nonlinear regime. The core of the principle is that long-time relaxation at lower temperature is equivalent to short-time relaxation at higher temperature. Hence, this principle opens a way to predict viscoelastic phenomena at very long-time regime (or very short-time regime) by the measurements at various temperatures. Since every rheometer has a finite range of measurement, this principle is also the way to expand our horizons on viscoelasticity of polymer. In this chapter, we shall introduce the phenomenology, mathematical relations, and validity of TTS. These are easily found in other textbooks of rheology or polymer physics, too. However, this chapter deals with a new interpretation and numerical algorithms of TTS.

1 Fundamentals of TTS

1.1 Phenomenology of TTS

Before the publication of the Williams–Landel–Ferry equation (WLF equation) (Williams et al. 1955), there have been a number of reports on the superposition of viscoelastic data (Tobolsky and McLouglin 1952; Ferry 1950; Ferry et al. 1953; Leaderman et al. 1954). When viscoelastic data measured at a temperature different

K.S. Cho, *Viscoelasticity of Polymers*, Springer Series
in Materials Science 241, DOI 10.1007/978-94-017-7564-9_8

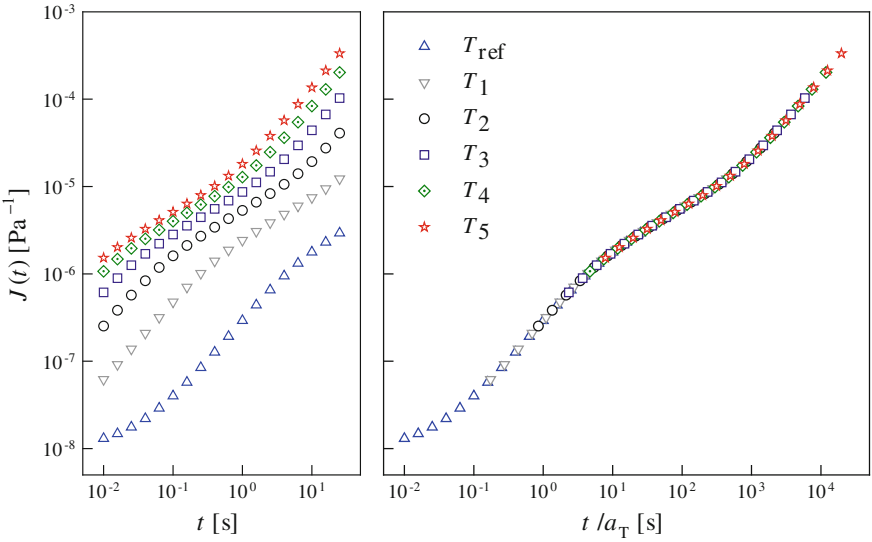

Fig. 1 Schematic illustration of the phenomena of time-temperature superposition. Temperatures have the order: $T_{\mathrm{ref}} < T_1 < \cdots < T_5$

from the reference temperature is plotted as a function of frequency or time in double logarithmic scale, the horizontal and vertical shifts of the data to those at the reference temperature give a single superposed curve called the master curve. This superposition of viscoelastic data is called the principle of *time-temperature superposition* (TTS). Since the distance of the shifting depends on the temperature, the horizontal and vertical shift factors are denoted by a_T and b_T, respectively.

Figure 1 shows a set of hypothetical data of creep compliance which illustrates what is TTS. When data of higher temperature are moved to right, the creep data of six different temperatures form a single smooth curve. This interesting phenomenon has been observed for various viscoelastic materials not only for creep compliance but also for other linear viscoelastic functions (Ferry 1980).

1.1.1 Mathematical Relations

Since the data on the left-hand side graphs can be on a single smooth curve by both horizontal and vertical shifting, the mathematical expression for the creep compliance of Fig. 1 is given by:

$$J(t,T) = \frac{1}{b_T} J\left(\frac{t}{a_T}, T_{\mathrm{ref}}\right) \tag{1.1}$$

where T_{ref} is the reference temperature and a_T and b_T are, respectively, the horizontal and vertical shift factors which are functions of the temperature difference $T - T_{\text{ref}}$. As for homopolymer melts, it is often observed that $b_T \approx 1$.

Similarly, TTS is valid for relaxation modulus, too. It is not difficult to recognize that

$$G(t, T) = b_T G\left(\frac{t}{a_T}, T_{\text{ref}}\right) \tag{1.2}$$

This is consistent with Eq. (1.24) in Chap. 5. Equations (1.42) and (1.43) in Chap. 5 immediately result in:

$$G'(\omega, T) = b_T G'(a_T\omega, T_{\text{ref}}); \quad G''(\omega, T) = b_T G''(a_T\omega, T_{\text{ref}}) \tag{1.3}$$

From Eq. (1.59) in Chap. 5, we also know that

$$J'(\omega, T) = \frac{1}{b_T} J'(a_T\omega, T_{\text{ref}}); \quad J''(\omega, T) = \frac{1}{b_T} J''(a_T\omega, T_{\text{ref}}) \tag{1.4}$$

Further application of TTS gives the following mathematical relations:

$$H(\lambda, T) = b_T H\left(\frac{\lambda}{a_T}, T_{\text{ref}}\right) \tag{1.5}$$

$$L(\tau, T) = \frac{1}{b_T} L\left(\frac{\tau}{a_T}, T_{\text{ref}}\right) \tag{1.6}$$

$$\tan\delta(\omega, T) = \tan\delta(a_T\omega, T) \tag{1.7}$$

$$\eta_{\text{o}}(T) = a_T b_T \eta_{\text{o}}(T_{\text{ref}}) \tag{1.8}$$

$$\bar{\lambda}(T) = a_T \bar{\lambda}(T_{\text{ref}}) \tag{1.9}$$

and

$$J_{\text{e}}^{\text{o}}(T) = \frac{1}{b_T} J_{\text{e}}^{\text{o}}(T_{\text{ref}}) \tag{1.10}$$

1.1.2 Shift Factor

Equations (1.8) and (1.10) imply that if we can measure the zero-shear viscosity and the steady-state compliance at various temperatures, we can determine the temperature dependence of shift factors a_T and b_T:

$$a_T = \frac{\eta_o(T)J_e^o(T)}{\eta_o(T_{ref})J_e^o(T_{ref})} = \frac{\bar{\lambda}(T)}{\bar{\lambda}(T_{ref})} \tag{1.11}$$

and

$$b_T = \frac{J_e^o(T_{ref})}{J_e^o(T)} \tag{1.12}$$

Compared with the molecular theory (Ferry 1980), the vertical shift factor b_T is considered as

$$b_T = \frac{\rho_{ref}T_{ref}}{\rho T} \tag{1.13}$$

When $b_T \approx 1$, Eq. (1.11) becomes simpler as follows:

$$a_T \approx \frac{\eta_o(T)}{\eta_o(T_{ref})} \tag{1.14}$$

It is usually hard to measure zero-shear viscosity at any desired temperature when molecular weight of polymer is high. Hence, one of the most common methods for shifting factor is to choose the optimum shift factor which gives the best superposition. This procedure has been done by eye inspection. However, the eye inspection gives different shift factors depending on the inspectors. For the purpose of objective TTS, several algorithms have been developed. We shall introduce some algorithms in Sect. 3.

1.1.3 Checking the Validity of TTS

Although TTS is valid for most polymeric systems, there are some exceptions. Representative examples of breakdown of TTS are some miscible polymer blends (Colby 1989) and block copolymers (Han and Kim 1993). If a set of data includes the temperature of phase transition or degradation, the failure of TTS is observed. Before seeking shift factor, the validity of TTS for the given data must be checked.

One of the simplest methods is to plot loss modulus as a function of storage modulus. It is not difficult to show that storage modulus is a monotonic increasing function of frequency [Problem 1 in Chap. 6 (Ferry 1950)]. Then, we can invert frequency as a function of storage modulus. Substitution of frequency as a function of storage modulus to loss modulus gives a relation between storage and loss modulus. If $b_T = 1$, the relation is independent of the horizontal shift factor. In other words, the plot of loss modulus as a function of storage modulus is independent of temperature. Analogous to the Cole–Cole plot, the plot of $\log G''$ versus $\log G'$ is called the modified Cole–Cole plot. Figure 2 shows the modified Cole–Cole plots of

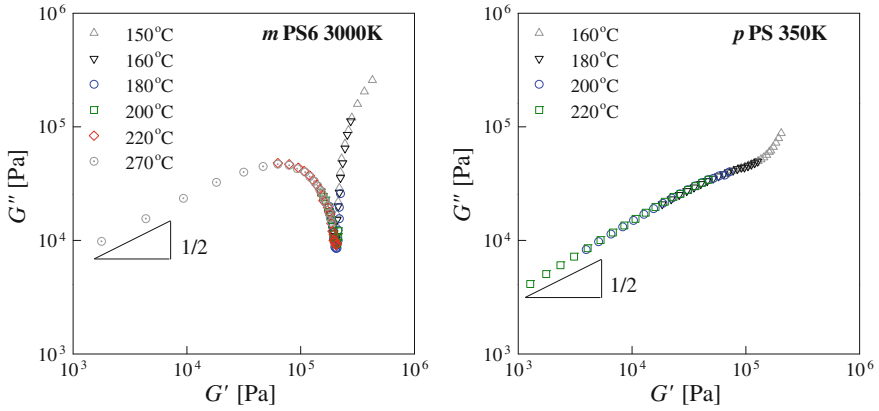

Fig. 2 Modified Cole–Cole plots of monodispersed and polydispersed polystyrene melts (*m*PS6, M = 3000 kg/mol; *p*PS, M = 350 kg/mol). The data of *m*PS6 are that of PS6 measured by Schausberger et al. (1985)

a monodisperse polystyrene melt (mPS6) measured by Schausberger et al. (1985) and a polydisperse polystyrene melt measured by Bae (2010).

Since homopolymer shows $b_T \approx 1$, the modified Cole–Cole plots of different temperatures align on a single curve. The terminal regime is the low-G' region where the curve approaches a straight line with the slope of 1/2. Since monodisperse polymers show a local minimum in the plot of $\log G''$ as a function of $\log \omega$, the modified Cole–Cole plot of monodisperse polystyrene of high molecular weight shows a sharp valley at $G'(\omega) \approx 2 \times 10^5$ Pa. On the other hand, that of polydisperse polystyrene does not show sharp valley because molecular weight distribution screens the local minimum.

As for monodisperse polymers, it is known that the steady-state compliance is nearly independent of molecular weight if the molecular weight is much larger than three times of the critical molecular weight which can be determined from zero-shear viscosity (Cho et al. 2004). When molecular weight is smaller than a certain value, the steady-state compliance of monodisperse polymer is proportional to molecular weight (Doi 1986). The molecular weight at such a transition of steady-state compliance is called the *secondary critical molecular weight* and denoted by M'_C.

The terminal behavior of polymer can be expressed by:

$$\log G'' = \frac{1}{2}\log G' - \frac{1}{2}\log J_e^o \tag{1.15}$$

Figure 3 shows that the terminal regimes of monodisperse polymers of high molecular weight (PS4–PS6) merge to a straight line with the slope of 1/2, whereas those of polymer of low molecular weight (PS1–PS3) are represented by three parallel straight lines with the slope of 1/2.

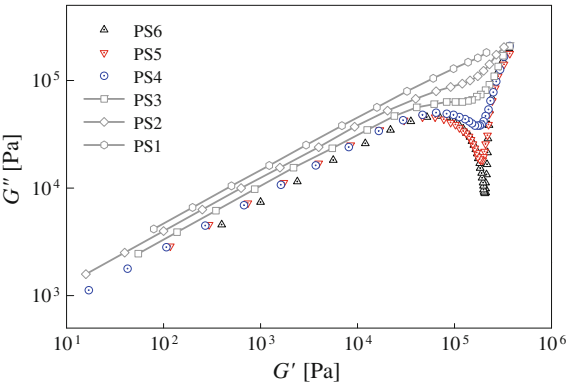

Fig. 3 Modified Cole–Cole plot of monodisperse polystyrene melts. It was drawn by the use of numeric data in (Schausberger et al. 1985). Molecular weights of polymers are PS1 (39 kg/mol), PS2 (70 kg/mol), PS3 (128 kg/mol), PS4 (275 kg/mol), PS5 (770 kg/mol), and PS6 (3000 kg/mol)

1.2 Temperature Dependence of Shift Factor

1.2.1 The WLF Equation

It is important to know the mathematical form of a_T. Williams et al. (1955) adopted the viscosity model of Doolittle (1951) which is a phenomenological model of viscosity.

Doolittle assumed that the logarithm of the viscosity of glassy material is reciprocally proportional to free volume fraction f. Free volume V_f is the difference between the whole volume where molecules occupy, V and the core volume of molecules, V_c. Then, $f = (V - V_c)/V$, and viscosity is given by:

$$\eta = A \exp\left(\frac{B}{f}\right) \tag{1.16}$$

Doolittle further assumed that the free volume fraction has linear dependence on temperature as follows:

$$f = f_g + \alpha_f (T - T_g) \quad \text{for} \quad T > T_g \tag{1.17}$$

where f_g is the free volume fraction at glass transition temperature T_g and α_f is the expansion coefficient. Applying Eq. (1.17) to Eqs. (1.14) and (1.16) gives

$$\log a_T = \frac{B}{f_g + \alpha_f (T - T_g)} - \frac{B}{f_g + \alpha_f (T_{ref} - T_g)} \tag{1.18}$$

The use of the notation such that

$$c_1 = \frac{B}{f_g + \alpha_f (T_{ref} - T_g)}; \; c_2 = \frac{f_g}{\alpha_f} + T_{ref} - T_g \tag{1.19}$$

gives the celebrated WLF equation:

$$\log a_T = \frac{-c_1(T - T_{\text{ref}})}{c_2 + T - T_{\text{ref}}} \tag{1.20}$$

It must be noted that the WLF equation itself cannot explain why TTS is valid for polymer melts. The WLF equation gives just only mathematical expression of the temperature dependence of horizontal shift factor. Furthermore, the equation was derived in a phenomenological way. To the author's knowledge, no body has succeeded in deriving a_T from the fundamental laws of physics.

1.2.2 The Arrhenius Equation

The most popular model for temperature dependence of viscosity might be

$$\eta(T) = A \exp\left(\frac{E}{RT}\right) \tag{1.21}$$

where A is the front factor, E is the activation energy, R is the gas constant, and T is the absolute temperature. To the author's knowledge, Eq. (1.21) was first derived by Eyring (1936) from the notion of the absolute reaction rate. More pedagogic derivation of Eq. (1.21) is found in the textbook of transport phenomena (Bird et al. 2002). From Eq. (1.21), one-parameter model for horizontal shift factor is given by

$$\log a_T = \frac{E}{R}\left(\frac{1}{T} - \frac{1}{T_{\text{ref}}}\right) \tag{1.22}$$

This is called the *Arrhenius equation*. Note that absolute temperature must be used in Eq. (1.22), while temperature in Celsius scale can be used in Eq. (1.20).

To compare the two viscosity models, the Doolittle and the Eyring model, we adopt the Doolittle parameters of polystyrene:

$$\frac{f_{\text{g}}}{B} = 0.033; \quad \frac{\alpha_{\text{f}}}{B} = 6.9 \times 10^{-4}\,\text{K}^{-1}; \quad T_g = 100\,^{\circ}\text{C} \tag{1.23}$$

The Eyring model cannot fit the viscosity data generated from the Doolittle model for a wide range of temperature. However, the Eyring model can fit the data at sufficiently high temperatures. The symbols shown in Fig. 4 represent the viscosity of the Doolittle model and the shift factor of the WLF equation, while the lines are the Eyring viscosity and the shift factor of Arrhenius type. Good agreement of the two models for viscosity and shift factor is found in high temperature regime, while significant deviation is found in low temperature regime. It is known that the WLF equation can describe the horizontal shift factor very well for wide range of temperatures. Hence, it can be said that the Arrhenius equation, Eq. (1.22),

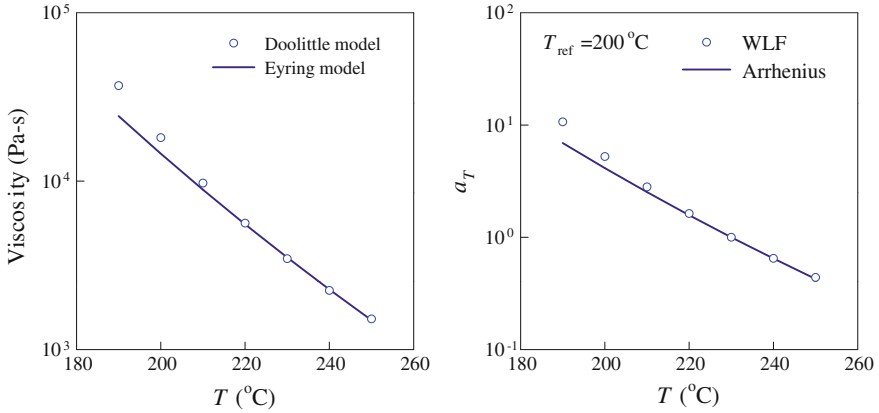

Fig. 4 Comparison of models of viscosity and shift factor

is applicable at temperatures much higher than the glass transition temperature T_g. Figure 4 illustrates these features.

Some relaxation modes in solid polymers are known to obey the shift factor of Arrhenius type rather than the WLF (Ward and Sweeney 2004). As for molten polymers such as polyolefin with long-chain branches, the Arrhenius-type shift factor is often used (Stadler et al. 2008; Kessner et al. 2010).

1.2.3 Determination of Model Parameters of Shift Factor

Before studying how to determine the shift factor, we shall explain how to determine the model parameters of shift factor under the assumption that data of shift factor is determined as a function of temperature for a given reference temperature. One must find out which model is better among the WLF and the Arrhenius. As shown in Fig. 4, the values of shift factor at 220, 230, 240, and 250 °C look like satisfying both the models. The plot of shift factor as a function of temperature is not effective in the selection of the model of shift factor. We need a new plot which is effective in finding better model for a given data.

As for the Arrhenius model of shift factor, the plot of $\log a_T$ as a function of T^{-1} is the best choice to check whether the data of shift factor satisfy the model or not, because a straight line is observed whenever the data follow the Arrhenius model. The WLF model can be rewritten as follows: (Schausberger et al. 1985)

$$\frac{\Delta T}{\log a_T} = -\frac{c_2}{c_1} - \frac{\Delta T}{c_1} \tag{1.24}$$

where $\Delta T = T - T_{\text{ref}}$. Thus, the data appropriate for the WLF equation form a straight line in the plot of $\Delta T / \log a_T$ as a function of ΔT.

Sometimes, one may want to know the shift factors with respect to a new reference temperature when the shift factors are given with respect to the old reference temperature. Let the old reference temperature be denoted by T_{old} and the new one by T_{new}. Similarly, we also use a_T^{old} and a_T^{new}. Using Eq. (1.14), we have

$$a_T^{\text{new}} = \frac{\eta_o(T)}{\eta_o(T_{\text{new}})} = \frac{\eta_o(T)}{\eta_o(T_{\text{old}})}\frac{\eta_o(T_{\text{old}})}{\eta_o(T_{\text{new}})} = \frac{a_T^{\text{old}}}{a_{T_{\text{new}}}^{\text{old}}} \tag{1.25}$$

Applying Eq. (1.25) to the WLF equation gives

$$\log a_T^{\text{new}} = \frac{-c_1^{\text{old}}(T - T_{\text{old}})}{c_2^{\text{old}} + T - T_{\text{old}}} + \frac{c_1^{\text{old}}(T_{\text{new}} - T_{\text{old}})}{c_2^{\text{old}} + T_{\text{new}} - T_{\text{old}}} = \frac{-c_1^{\text{new}}(T - T_{\text{new}})}{c_2^{\text{new}} + T - T_{\text{new}}} \tag{1.26}$$

Equation (1.26) immediately gives

$$c_1^{\text{new}} = \frac{c_1^{\text{old}} c_2^{\text{old}}}{c_2^{\text{old}} + T_{\text{new}} - T_{\text{old}}};\ c_2^{\text{new}} = c_2^{\text{old}} + T_{\text{new}} - T_{\text{old}} \tag{1.27}$$

Since the Arrhenius equation has only a single parameter, E/R, it is obvious that we do not have to consider the relation between old and new parameters.

1.3 Molecular Explanation of TTS

We shall begin with a speculation on stress relaxation from the viewpoint of molecular motion. How can a material reduce the stress when strain is fixed? Although atoms in metallic materials ceaselessly move (vibration), the range of motion of each atom is equal to or less than the order of atomic size. Averaging out the fast vibration, atoms in metal look like fixed in their sites in crystalline lattice. Hence, stress relaxation in metal is hardly observed. On the other hand, even if the segments of polymer chains in molten state move in the range whose linear dimension is order of the segment size, the accumulation of individual segmental motion gives a big change in chain conformation. Since the stress in polymer largely depends on chain conformation, stress relaxation is observed. In summary, stress relaxation takes into account the total effect of motions of individual segments.

The speed of stress relaxation, therefore, depends on how fast segment motion is. As temperature increases, molecular motion becomes rapider. The timescale for the molecular motion is the relaxation times. Then, the higher the temperature is, the shorter the relaxation time is. Since this means that relaxation time is a decreasing function of temperature, TTS implies that viscoelastic quantities measured at higher temperature at a short time (high frequency) correspond to those measured at a

lower temperature at longer time (or low frequency). In mathematical language, we can write

$$T \geq T_{\text{ref}} \Rightarrow a_T \leq 1 \quad \text{and} \quad T < T_{\text{ref}} \Rightarrow a_T > 1 \tag{1.28}$$

The molecular theory of relaxation modulus can be expressed formally as follows:

$$G(t) = \frac{\rho RT}{M^*} \sum_{k=1}^{\infty} h_k \exp\left(-\frac{t}{\lambda_k}\right) \quad \text{with} \quad \lambda_k(T) = \beta_k \lambda_*(T) \tag{1.29}$$

where ρ is density, R is the gas constant, M^* is a characteristic molar mass of the polymeric fluid, both h_k and β_k are dimensionless numbers dependent on index k, and $\lambda_{\max}(T)$ is the maximum relaxation time which is proportional to $T^{-1}\zeta(T)$ (see Sect. 4 in Chap. 5). Since every relaxation time λ_k has the identical temperature dependence of $T^{-1}\zeta(T)$, it is clear that Eq. (1.29) obeys the time-temperature superposition and we have

$$a_T = \frac{T_{\text{ref}}}{T} \frac{\zeta(T)}{\zeta(T_{\text{ref}})} \tag{1.30}$$

Unfortunately, no molecular theory manifests the temperature dependence of the friction coefficient $\zeta(T)$ because it is a phenomenological quantity.

Problem 1

[1] From Eq. (1.2), derive Eqs. (1.3)–(1.10).

[2] As for a polymeric material, the WLF parameters are determined as $c_1 = 10$ and $c_2 = 50$ with respect to $T_{\text{ref}} = 170\,^{\circ}\text{C}$. Calculate the WLF parameters with respect to $T_{\text{ref}} = 200\,^{\circ}\text{C}$.

[3] It is well known that the loss modulus of monodisperse polymer melt shows a local maximum at a certain frequency which is higher than the frequencies which belong to the terminal regime. Let the frequency be denoted by $\omega_{\max}$. Because of TTS, we recognize that $\omega_{\max}$ is a function of temperature at which loss modulus is measured. Show that if $b_T = 1$ then

$$a_T = \frac{\omega_{\max}(T)}{\omega_{\max}(T_{\text{ref}})} \tag{1.a}$$

[4] Consider the following model for linear viscoelastic fluid:

$$s\widetilde{J}(s) = J_g + \frac{1}{\eta_{\text{o}} s} + \frac{J_r}{[1 + (\tau s)^a]^b} \tag{1.b}$$

Express the temperature dependence of parameters J_g, J_r, η_{o}, τ, a, and b under the assumption that the fluid obeys TTS.

[5] If relaxation modulus is given by $G(t,\ T) = G[t/\lambda(T)]$, then show that

$$a_T = \frac{\lambda(T)}{\lambda(T_{\text{ref}})} \tag{1.c}$$

[6] Define

$$g'(\omega, T) \equiv \frac{G'(\omega, T)}{\eta_o^2 J_e^o \omega^2}; \quad g''(\omega, T) \equiv \frac{G'(\omega, T)}{\eta_o \omega} \tag{1.d}$$

Show that

$$g'(\omega, T) = g'(a_T\omega, T_{\text{ref}}); \quad g''(\omega, T) = g''(a_T\omega, T_{\text{ref}}) \tag{1.e}$$

2 Geometric Interpretation

2.1 Geometric Analogy to TTS

In this section, we shall introduce a geometric viewpoint on TTS, which is not new, but an illustration of TTS geometrically. Consider an insect such as ant whose motion becomes faster as temperature increases. Assume that the insect moves on a two-dimensional curve. Suppose that an observer has a weak vision sensor which works during the time interval of $t_{\min} \le t \le t_{\max}$. The hypothetical observer looks at the motion of the insect at temperatures $T_1 < T_2 < \cdots < T_N$. Assume further that the seed of the insect is constant when temperature is fixed and that the observations are repeated for a fixed curve. The record of the motion at a temperature of T_k can be expressed by $x(t, T_k)$ and $y(t, T_k)$. Since the observations are repeated for the same curve, the position of the insect at $t = 0$ is independent of temperature. Let it can be denoted as x_0 and y_0. How can we know the whole path on which the insect moves from the only data measured by the hypothetical observer?

Since the path of the insect is fixed, we know that collecting position data at various temperatures gives the whole path if they are plotted in the x-y plane. Since the speed of the insect decreases as temperature decreases, the starting point of the path is given by

$$x_0 = \lim_{T\to 0} x(t_{\min}, T);\ y_0 = \lim_{T\to 0} y(t_{\min}, T) \tag{2.1}$$

Figure 5 is a graphical illustration of this thought experiment. The left-hand side two graphs are raw data for the position of the insect, while the right-hand side is the contour of the path.

It is not difficult for a believer of TTS to recognize that coordinates $x(t, T_k)$ and $y(t, T_k)$ correspond to dynamic moduli $G'(\omega, T_k)$ and $G''(\omega, T_k)$ and t is analogous to

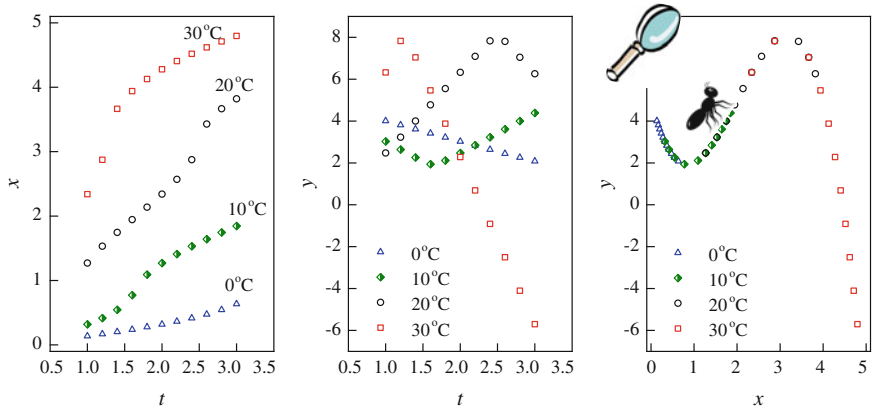

Fig. 5 The locus of the insect motion

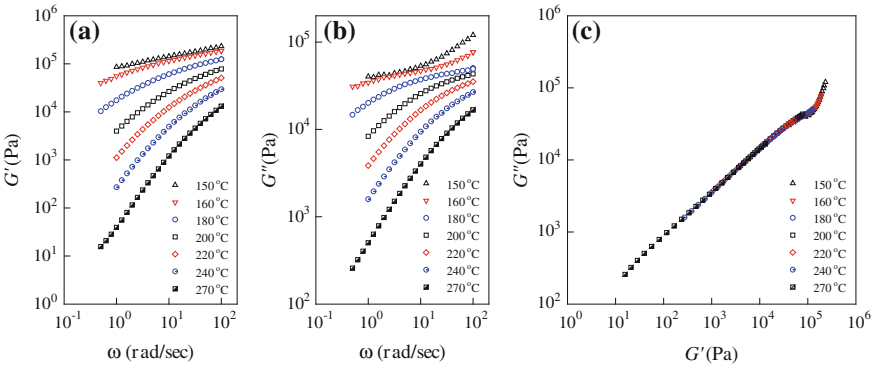

Fig. 6 Viscoelastic version of Fig. 5. The data are that of *p*PS350K of Fig. 2

frequency ω. The plot of y as a function of x is analogous to the modified Cole–Cole plot. As for viscoelastic fluid, it is obvious that the fixed point of (x_0, y_0) corresponds to $(G', G'') = (0, 0)$. We shall proceed the reasoning with the assumption of $b_T = 1$. The modified Cole–Cole plot of Fig. 6 is the direct translation of Fig. 5 to viscoelastic language. Figure 6 is the duplication of *m*PS6 of Fig. 2.

2.2 *New Master Curve*

Any parameterized curve can be reparameterized by its arc length. If two measurable quantities are dependent on two independent variables, say t and T, and they obey the superposition of Fig. 5, then we can write

$$x(t,T) = \xi[l(t,T)]; \quad y(t,T) = \psi[l(t,T)] \tag{2.2}$$

where the arc length l is defined as

$$l(t,T) = \int_0^t v(\tau,T)\mathrm{d}\tau \tag{2.3}$$

with

$$v(\tau,T) = \sqrt{\left[\frac{\partial x(\tau,T)}{\partial \tau}\right]^2 + \left[\frac{\partial y(\tau,T)}{\partial \tau}\right]^2} \tag{2.4}$$

Since the path of the insect is fixed, it is obvious that if $l(t_\alpha, T_i) = l(t_\gamma, T_k)$, then

$$x(t_\alpha, T_i) = x(t_\gamma, T_k);\ y(t_\alpha, T_i) = y(t_\gamma, T_k) \tag{2.5}$$

We can apply the concept of arc length to the data of dynamic moduli. The arc length can be approximated by

$$l - l_{\min} = \int_{\log G'_{\min}}^{\log G'} \sqrt{1 + \left(\frac{\partial \log G''}{\partial \log G'}\right)^2}\, \mathrm{d}\log G' \approx \sum_{\alpha=1}^{N-1} \sqrt{\left(\log \frac{G'_{\alpha+1}}{G'_\alpha}\right)^2 + \left(\log \frac{G''_{\alpha+1}}{G''_\alpha}\right)^2} \tag{2.6}$$

where dynamic moduli at different frequencies and temperatures are sorted in the order of ascending storage modulus because storage modulus is an increasing function of frequency. Here, $G'_{\min}$ is the minimum value among $\{G'_\alpha\}$.

Figure 7 shows that the plots of dynamic moduli as functions of the arc length are independent of temperature.

$$\begin{aligned} G'(\omega,T) &= \Gamma'[l(\omega,T)] = G'(a_T\omega, T_{\mathrm{ref}}) \\ G''(\omega,T) &= \Gamma''[l(\omega,T)] = G''(a_T\omega, T_{\mathrm{ref}}) \end{aligned} \tag{2.7}$$

Note that the conventional TTS by using a_T does not adopt a different function, while the TTS by the use of the arc length $l(\omega,\ T)$ needs to use a different function $\Gamma'(\bullet)$ and $\Gamma''(\bullet)$ (Cho 2009).

Combining the definition of $l(\omega, T)$ with the conventional TTS, we have the following equations for the arc length:

$$l(\omega,T) = l(a_T\omega, T_{\mathrm{ref}}) \tag{2.8}$$

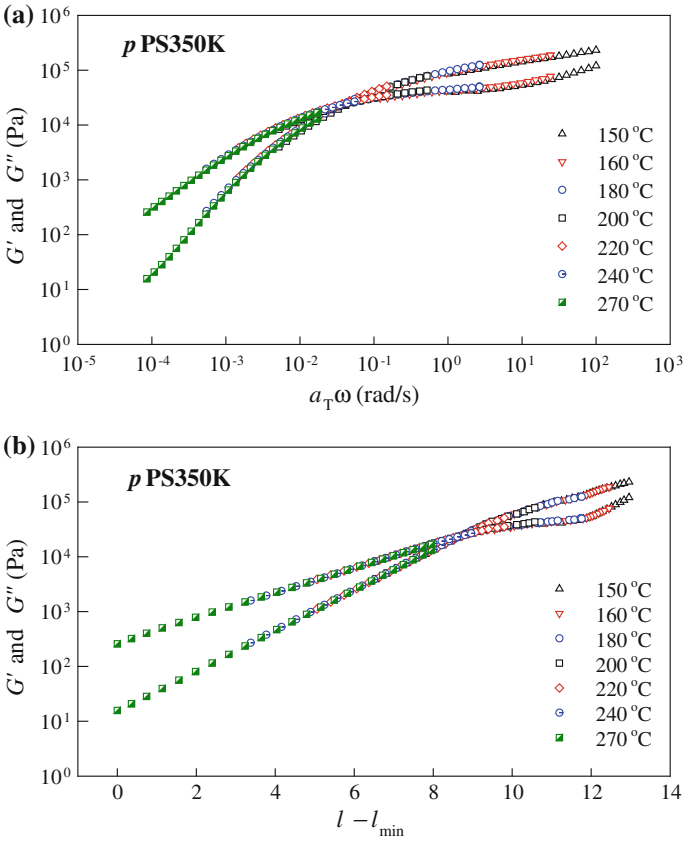

Fig. 7 Comparison of conventional master curve with the master curve with respect to the arc length of Eq. (2.6). The material is polydisperse PS of $\bar{M}_w = 350$ kg/mol

and

$$\frac{\partial l}{\partial \omega} \geq 0 \tag{2.9}$$

These properties are also satisfied by the storage modulus. There are a number of ways to invent a function of frequency and temperature, which satisfy both Eqs. (2.8) and (2.9). As for loss angle $\delta(\omega, T) = \arctan(G''/G')$, the intrinsic phase angle (Cho 2012) can be defined as follows:

$$v(\omega, T) = \int_0^{\omega} \sqrt{\left[\frac{\partial}{\partial w}\sin\delta(w, T)\right]^2 + \left[\frac{\partial}{\partial w}\cos\delta(w, T)\right]^2}\, \mathrm{d}w \tag{2.10}$$

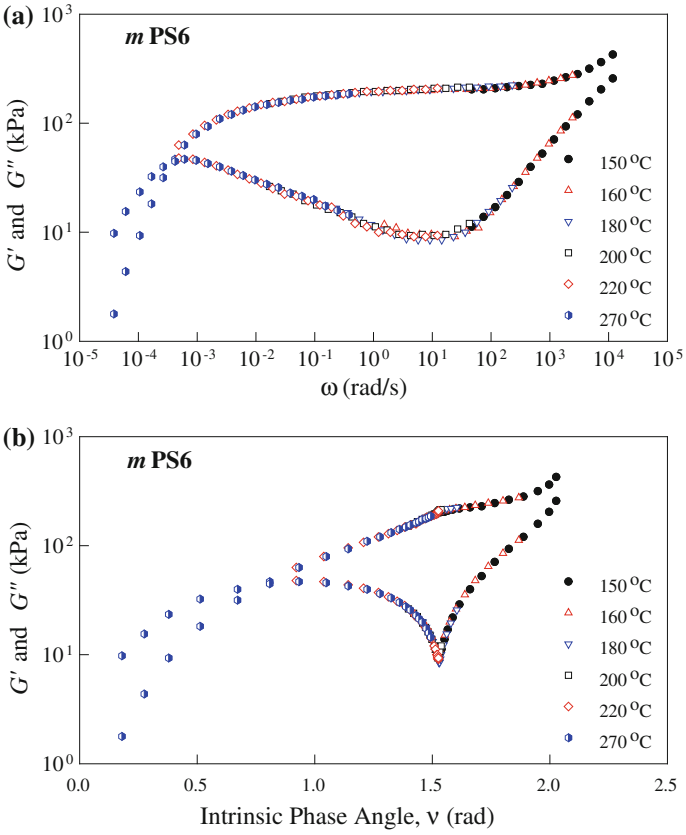

Fig. 8 Comparison of conventional master curve with the master curve with respect to the arc length of Eq. (2.11). The material is monodisperse PS6 of (Schausberger et al. 1985)

This is the arc length of the plot of $\sin\delta(\omega, T)$ as a function of $\cos\delta(\omega, T)$. Since $\sin^2\delta + \cos^2\delta = 1$, it is clear that

$$v(\omega, T) = \int_0^{\omega} \left| \frac{\partial\delta(w, T)}{\partial w} \right| dw \tag{2.11}$$

From problem 26 (Cho 2012), it is obvious that $\delta(\omega, T) = \delta[\lambda(T)\omega]$. As for viscoelastic fluid, it is also obvious that $\delta(0, T) = \pi/2$ and as frequency increases, $\delta(\omega, T)$ decreases. At a frequency $\omega_1(T)$, the first crossover frequency, the phase angle increases as frequency. Hence, we can write

$$\nu = \begin{cases} \frac{1}{2}\pi - \delta(\omega, T) & 0 \le \omega < \omega_1(T) \\ \frac{1}{2}\pi - 2\delta(\omega_1(T), T) + \delta(\omega, T) & \omega_1(T) < \omega \end{cases} \tag{2.12}$$

If there is another crossover frequency, $\omega_2(T) > \omega_1(T)$, then we have

$$\nu = \begin{cases} \frac{1}{2}\pi - \delta(\omega, T) & 0 \le \omega < \omega_1(T) \\ \frac{1}{2}\pi - 2\delta(\omega_1, T) + \delta(\omega, T) & \omega_1(T) \le \omega < \omega_2(T) \\ \frac{1}{2}\pi - 2\delta(\omega_1, T) + 2\delta(\omega_2, T) - \delta(\omega, T) & \omega_2(T) \le \omega \end{cases} \tag{2.13}$$

The intrinsic phase angle is also a kind of arc length and can be calculated more easily than the arc length $l(\omega, T)$ of Eq. (2.6). Note that although the arc length approach does not provide a way to determine the shift factor a_T, the plots of viscoelastic functions with respect to the arc length give a master curve. It should be noted that the new master curve emphasizes the local minimum and maximum of loss modulus as shown in Fig. 8. As for conventional master curve, a small deviation from TTS is not difficult to be found. However, such a tiny discrepancy is amplified in the plot of the new master curve. Hence, the new master curve is comparative to the *plot of van Gurp and Palmen* (Trinkle and Friedrich 2002; Trinkle et al. 2002).

Compared with the phase angle of Eq. (2.11), the arc length of Eq. (2.6) suffers from the arbitrariness of $l_{\min}$ because the logarithms of dynamic moduli become minus infinity as frequency goes to zero.

2.3 Application of Numerical Differentiation

However, the modified Cole–Cole plot allows one to check the validity of TTS for experimental data without the determination of horizontal shift factor a_T, whenever $b_T = 1$. When $b_T \neq 1$, we need a different method for checking TTS. Equation (1.3) can be rewritten as follows:

$$\begin{aligned} \log G'(\omega, T) &= \log G'(\log a_T \omega, T_{\text{ref}}) + \log b_T \\ \log G''(\omega, T) &= \log G''(\log a_T \omega, T_{\text{ref}}) + \log b_T \end{aligned} \tag{2.14}$$

Then it is obvious that

$$\begin{aligned} u_E &\equiv \frac{\partial \log G'(\omega, T)}{\partial \log \omega} = \frac{\partial \log G'(a_T \omega, T_{\text{ref}})}{\partial \log\, a_T \omega}; \\ u_V &\equiv \frac{\partial \log G''(\omega, T)}{\partial \log \omega} = \frac{\partial \log G''(a_T \omega, T_{\text{ref}})}{\partial \log a_T \omega} \end{aligned} \tag{2.15}$$

Since the gradients are independent of temperature, the plot of u_E versus u_V is invariant with respect to temperature.

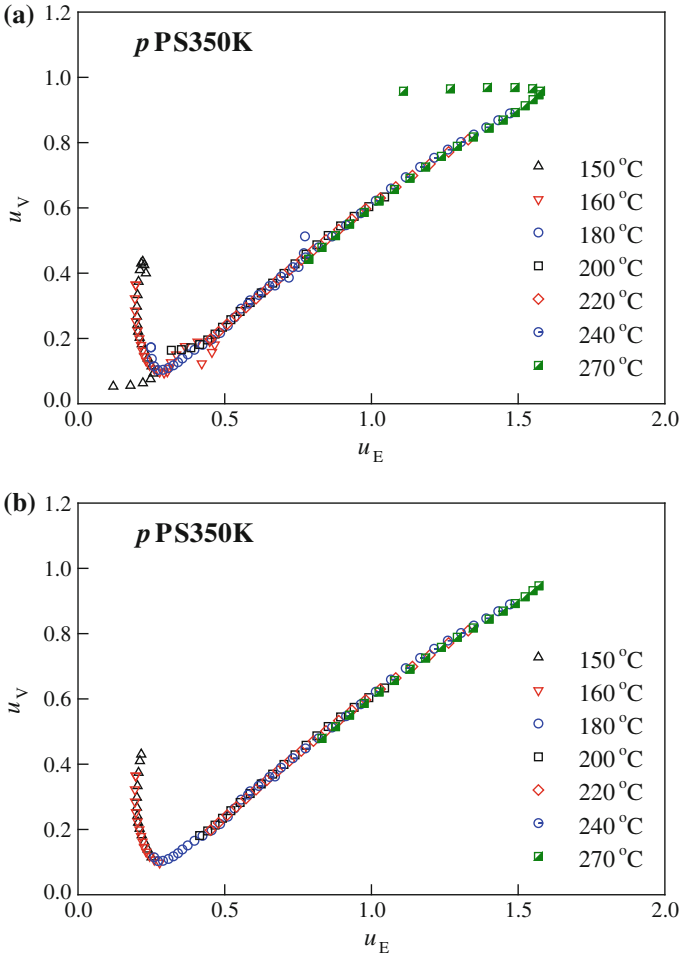

Fig. 9 Locus of gradients of dynamic moduli: **a** the whole data; **b** collection of relevant values

Numerical differentiation of experimental data is largely affected by the experimental error. We have learned the ill-posedness of numerical differentiation in Chap. 6. Figure 9 shows the feature of numerical differentiation. Figure 9a shows the whole result of numerical differentiation by the use of B-spline regression, while Fig. 9b shows the result excluding unrealistic values of differentiation.

Note that the limit point of the plot of u_E versus u_V is the point of (2, 1) which corresponds to zero frequency.

Problem 2

[1] What is the advantage of the new master curve of Fig. 8?
[2] Invent a new arc length from any viscoelastic function.

[3] Assume that $b_T = 1$. If dynamic modulus has a characteristic frequency which corresponds to a frequency intrinsic to the shape of the conventional master, then derive

$$\frac{d\omega_c}{dT} = \frac{d \log a_T}{dT} \tag{2.a}$$

3 Algorithms for TTS

Time-temperature superposition could be implemented by eye inspection. However, this method is apt to give the results depending on the persons who conduct TTS. A reliable numerical method is needed to avoid the obscurity. Here, a few algorithms are addressed.

3.1 Nonlinear Regression Method

Honerkamp and Weese (1993) developed an algorithm for TTS based on nonlinear regression. Consider Eq. (1.2). Since viscoelastic data are nonnegative and vary in logarithmic scale, it is convenient to use the notation such that

$$g = \log G(t, T);\ \tau = \log t;\ A = \log a_T;\ B = \log b_T \tag{3.1}$$

Applying Eq. (3.1) to Eq. (1.2) gives

$$g(\tau, T) = g(\tau + A, T_{\text{ref}}) + B \tag{3.2}$$

Assume that

$$g(\tau, T_{\text{ref}}) \approx \sum_{k=0}^{N} c_k \tau^k \tag{3.3}$$

If the relaxation modulus is measured at M temperatures and at M_α times, then the nonlinear regression method is to minimize the following sum of square:

$$\chi^2 = \sum_{\alpha=1}^{M} \sum_{\beta=1}^{M_\alpha} \left[g_{\alpha\beta} - \sum_{k=1}^{N} c_k (\tau_{\alpha\beta} + A_\alpha)^k - B_\alpha \right]^2 \tag{3.4}$$

Here, index α indicates temperature and β indicates time. Hence, $\tau_{\alpha\beta} = \log t_{\alpha\beta}$ and $g_{\alpha\beta} = \log G(t_{\alpha\beta}, T_\alpha)$.

This method is needed to determine the optimum order of the polynomial, say N^*. It is expected that if N is larger than N^*, then both A_α and B_α are nearly independent of the order of the polynomial. Depending on the size of the whole data, N is apt to be the order of 10.

3.2 *Minimization of Arc Length*

When we consider two sets of data measured at two different temperatures, T_0 and T_1, unacceptable guess of shift factor gives Fig. 10a while proper shift factor gives Fig. 10b. If we calculate the sum of distances between two adjacent data points, then imperfect superposition gives longer distance than the perfect superposition as shown in Fig. 10. The sum of the distances, say arc length, can be calculated by the use of the Pythagoras theorem, and we have

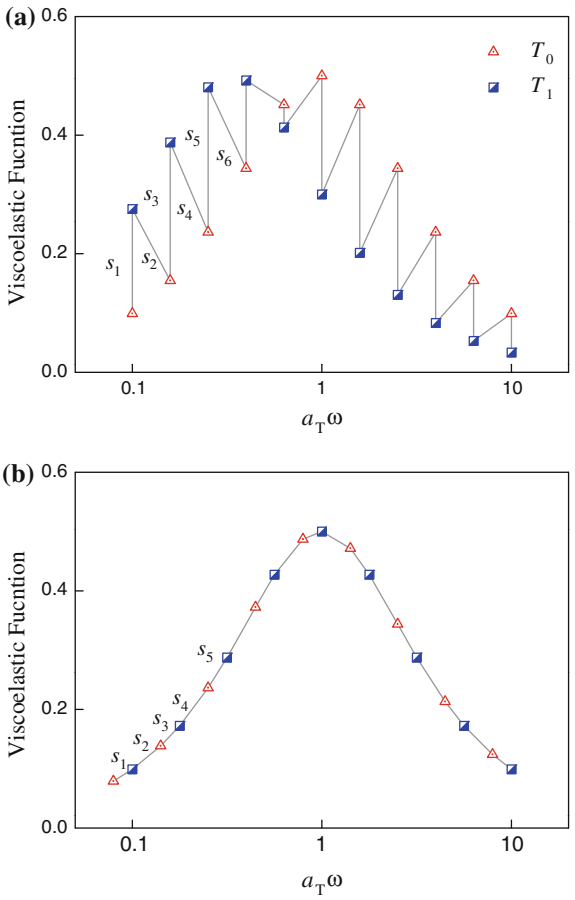

Fig. 10 Illustration of the algorithm of arc length minimization

$$S = \sum_{k=1}^{N-1} s_k = f(a_{T_1}, a_{T_2}, \ldots, a_{T_{M-1}}) \tag{3.5}$$

where N is the total number of data and M is the number of temperatures, and it is assumed that $T_0 < T_1 < \cdots < T_{M-1}$. Of course, T_0 is considered as the reference temperature. Then, it is obvious that

$$a_{T_{M-1}} < a_{T_{M-2}} < \cdots < a_{T_1} < 1 \tag{3.6}$$

Keeping this order, we guess the values of shift factors and calculate the S after sorting the N data in the order of the reduced frequency (for dynamic moduli). Repeating this procedure until the minimum of S, we will have the optimized shift factors. This is the method of arc length minimization (Cho 2009). The algorithm requires sorting of data in the order of $a_T\omega$ at every step of the calculation of the arc length.

Problem 3

[1] Derive the normal equation for Eq. (3.4).
[2] What is the reason why loss tangent is used for the horizontal shift factor rather than storage or loss moduli?

References

J.-E. Bae, Development of the algorithm of time-temperature superposition based on geometric characteristic of linear viscoelastic data and its application. MS thesis supervised by Prof. K. C. Cho, Kyungpook National University (in Korean) (2010)

R.B. Bird, W.E. Stewart, E.N. Lightfoot, *Transport Phenomena,* 2nd edn. (Wiley, London, 2002)

K.S. Cho, Geometric interpretation of time-temperature superposition. Korea-Aust. Rheol. J. **21**, 13–16 (2009)

K.S. Cho, Geometric interpretation of linear viscoelasticity and characterization of chain architecture of polymers. Korea-Aust. Rheol. J. **24**, 323–331 (2012)

K.S. Cho, K.H. Ahn, S.J. Lee, Simple method for determining the critical molecular weight from the loss modulus. J. Polym. Sci. Part B Polym. Phys. Ed. **42**, 2730–2737 (2004)

R.H. Colby, Breakdown of time-temperature superposition in miscible polymer blends. Polymer **30**, 1275–1278 (1989)

M. Doi, S.F. Edwards, *The Theory of Polymer Dynamics* (Oxford, 1986)

A.K. Doolittle, Studies in newtonian flow. II. The dependence of the viscosity of liquids on free-space. J. Chem. Phys. **22**, 1471–1475 (1951)

H. Eyring, Viscosity, plasticity, and diffusion as examples of absolute reaction rates. J. Chem. Phys. **4**, 283–291 (1936)

J.D. Ferry, Mechanical properties of substances of high molecular weight. VI. Dispersion in concentrated polymer solutions and its dependence on temperature and concentration. J. Am. Chem. Soc. **72**, 3746–3752 (1950)

J.D. Ferry, *Viscoelastic Properties of Polymers* (Wiley, London, 1980)

J.D. Ferry, L.D. Grandine Jr, E.R. Fitzgerald, The relaxation distribution function of polystyrene in the transition from rubber-like to glass-like behavior. J. Appl. Phys. **24**, 911–916 (1953)

C.D. Han, J.K. Kim, On the use of time-temperature superposition in multicomponent/multiphase polymer systems. Polymer **34**, 2533–2539 (1993)
J. Honerkamp, J. Weese, A note on estimating mastercurves. Rheol. Acta **32**, 57–64 (1993)
U. Kessner, J. Kaschta, F.J. Stadler, C.S. Le Duff, X. Drooghaag, H. Münstedt, Thermorheological behavior of various short- and long-chain branched polyethylenes and their correlations with the molecular structure. Macromolecules **43**, 7341–7350 (2010)
H. Leaderman, R.G. Smith, R.W. Jones, Rheology of polyisobutylene. II. Low molecular weight polymers. J. Polym. Sci. **14**, 47–80 (1954)
A. Schausberger, G. Schindlauer, H. Janeschitz-Kriegl, Linear elasto-viscous properties of molten standard polystyrenes. I. presentation of complex moduli; role of short range structural parameters. Rheol. Acta **24**, 220–227 (1985)
F.J. Stadler, J. Kaschta, H. Münstedt, Thermorheological behavior of various long-chain branched polyethylene. Macromolecules **41**, 1328–1333 (2008)
A.V. Tobolsky, J.R. McLouglin, Elastoviscous properties of polyisobutylene. V. the transition region. J. Polym. Sci. **8**, 543–553 (1952)
S. Trinkle, C. Friedrich, Van gurp-palmen-plot: a way to characterize polydispersity of linear polymers. Rheol. Acta **40**, 322–328 (2002)
S. Trinkle, P. Walter, C. Friedrich, Van Gurp-Palmen plot II—classification of long chain branched polymers by their topology. Rheol. Acta **41**, 103–113 (2002)
I.M Ward, J. Sweeney, *An Introduction to Mechanical Properties of Solid Polymers*, 2nd edn. (Wiley, London, 2004)
M.L. Williams, R.F. Landel, J.D. Ferry, The temperature dependence of relaxation mechanisms in amorphous polymers and other glass-forming liquids. J. Am. Chem. Soc. **77**, 3701–3707 (1955)

Chapter 9
Applications to Polymer Systems

Abstract The previous chapters of the second part deal with various theories and numerical methods of linear viscoelasticity of polymer system. This chapter is their applications to the characterization of polymer systems such as the interconversion of viscoelastic functions, the rheological characterization of monodisperse polymer melts, the effect of molecular weight distribution on the linear viscoelasticity of polydisperse polymer melts, and the viscoelasticity of polymer solutions and blends.

1 Interconversion of Various Experimental Data

Conversion of linear viscoelastic data is important because every experimental method has its own merits and demerits. This was discussed in Chap. 5 already. To enlarge the range of viscoelasticity, it is necessary to combine various types of viscoelastic measurements. One of the most reliable and versatile methods is to calculate the relaxation time spectrum (or retardation time spectrum). Other methods are mostly based on integral transforms such as Laplace and Fourier transforms.

1.1 Static Data to Dynamic Data

There are two static tests: stress relaxation and creep. Before discussion for the conversion of static data to dynamic ones, it is noteworthy that long-time data of relaxation modulus is less reliable than that of creep compliance. Furthermore, asymptotic behavior of creep compliance is more convenient than that of relaxation modulus. Hence, we shall focus on creep data mainly.

K.S. Cho, *Viscoelasticity of Polymers*, Springer Series
in Materials Science 241, DOI 10.1007/978-94-017-7564-9_9

1.1.1 From Creep Compliance to Dynamic Modulus

The first step for the conversion of creep compliance data to dynamic moduli is to use the Laplace transform of relaxation modulus, $s\widetilde{G}(s) = 1/[s\widetilde{J}(s)]$. One may think that the following steps are the conversion from the Laplace transform to relaxation modulus and use of cosine and sine transform of the relaxation modulus (Eqs. 1.42 and 1.43 in Chap. 5). This scheme demands numerical inversion of Laplace transform. However, we shall introduce simpler scheme which uses the relation between complex modulus and the Laplace transform of relaxation modulus: $G^*(\omega) = i\omega\widetilde{G}(i\omega)$.

Before learning how to calculate $s\widetilde{J}(s)$ from the experimental data of $J(t)$, we have to see the bird's eye photograph of creep compliance. Consider Eq. (1.33) in Chap. 5 for viscoelastic fluid:

$$J(t) = \frac{1}{G_o} + J_r\psi(t) + \frac{t}{\eta_o} \quad \text{for } t > 0 \tag{1.1}$$

The creep function $J_r\psi(t)$ is a monotonically increasing function of time:

$$J_r\psi(t) = \int_{-\infty}^{\infty} L(\tau)\left(1 - e^{-t/\tau}\right) \mathrm{d}\log\tau \tag{1.2}$$

where $L(\tau)$ is the retardation time spectrum. Equation (1.2) immediately gives

$$J_r\dot{\psi}(0) = J_r\left(\frac{\mathrm{d}\psi}{\mathrm{d}t}\right)_{t=0} = \int_{-\infty}^{\infty} \frac{L(\tau)}{\tau}\mathrm{d}\log\tau \equiv \frac{J_r}{\tau_H} > 0 \tag{1.3}$$

and $\psi(0) = 0$. Since $\psi(t) \to 1$ for $t \to \infty$, we know that

$$J_r = \int_{-\infty}^{\infty} L(\tau)\,\mathrm{d}\log\tau \tag{1.4}$$

Hence, the meaning of τ_H appears in the equation of

$$\tau_H = \frac{\int_{-\infty}^{-\infty} L(\tau)\,\mathrm{d}\log\tau}{\int_{-\infty}^{-\infty} \tau^{-1}L(\tau)\,\mathrm{d}\log\tau} \tag{1.5}$$

It is the harmonic mean retardation time. Note that if $L(\tau)$ has finite width, then the harmonic mean is always smaller than the arithmetic mean which is defined as

$$\overline{\tau} = \frac{\int_{-\infty}^{-\infty} \tau L(\tau)\, \mathrm{d}\log\tau}{\int_{-\infty}^{-\infty} L(\tau)\, \mathrm{d}\log\tau} \tag{1.6}$$

From experience, one may find the following inequality

$$\frac{\tau_H}{G_\mathrm{o} J_r} < \tau_H < \overline{\tau} < \overline{\lambda} \tag{1.7}$$

Note that $(G_\mathrm{o} J_r)^{-1} \sim 10^{-4}$ for most polymer melts because $G_\mathrm{o} \sim 10^9\,\mathrm{Pa}$ and $J_r \sim 10^{-5}\,\mathrm{Pa}^{-1}$. A careful look at Eq. (1.1) reveals that

$$J(t) \approx \begin{cases} \frac{1}{G_\mathrm{o}} & t < \frac{\tau_H}{G_\mathrm{o} J_\mathrm{e}^\mathrm{o}} \\ \frac{1}{G_\mathrm{o}} + \frac{J_\mathrm{e}^\mathrm{o}}{\tau_H} t \approx \frac{J_\mathrm{e}^\mathrm{o}}{\tau_H} t & \frac{\tau_H}{G_\mathrm{o} J_\mathrm{e}^\mathrm{o}} < t < \tau_H \\ J_\mathrm{e}^\mathrm{o} & \tau_H < t < \overline{\lambda} \approx J_\mathrm{e}^\mathrm{o} \eta_\mathrm{o} \\ J_\mathrm{e}^\mathrm{o} + \frac{t}{\eta_\mathrm{o}} & \overline{\lambda} = J_\mathrm{e}^\mathrm{o} \eta_\mathrm{o} < t \end{cases} \tag{1.8}$$

Here, we replace J_r by J_e^o because of Eq. (1.37) in Chap. 5.

This schematic equation is important because experimental data of creep compliance is measured always in a finite range of time: $t_\mathrm{min} \le t \le t_\mathrm{max}$, while Laplace transform is the integration over the infinite range of time: $0 < t < \infty$. Most creep experiments have $t_\mathrm{min} \sim 10^{-2}\,\mathrm{s}$ because for $t < 10^{-2}$ the stress is far from step functions. The Laplace transform $s\widetilde{J}(s)$ can be divided into three parts:

$$s\widetilde{J}(s) = s\int_0^{t_\mathrm{min}} J(t)\, e^{-st}\mathrm{d}t + s\int_{t_\mathrm{min}}^{t_\mathrm{max}} J(t)\, e^{-st}\mathrm{d}t + s\int_{t_\mathrm{max}}^{\infty} J(t)\, e^{-st}\mathrm{d}t \tag{1.9}$$

Since the second integral can be replaced by numerical integration, the first and the last integral must be estimated using the approximations of Eq. (1.8). Since $t_\mathrm{min} \sim 10^{-2}\,\mathrm{s}$ and $J(t)$ for the interval of the first integration is smaller than those of other integrations, the contribution of the first integral is relatively small. However, creep compliance is an increasing function of time, and the third integral must be estimated. In order to do that, t_max must be much larger than $\overline{\lambda} = J_\mathrm{e}^\mathrm{o} \eta_\mathrm{o}$.

Assume that there are sufficiently many data available in the interval of $\overline{\lambda} < t < t_\mathrm{max}$. Then, the third integral can be estimated by

$$s\int_{t_\mathrm{max}}^{\infty} J(t)\, e^{-st}\mathrm{d}t \approx \begin{cases} \frac{e^{-st_\mathrm{max}}}{s}\left(\frac{1+st_\mathrm{max}}{\hat{\eta}_\mathrm{o}} + \hat{J}_\mathrm{e}^\mathrm{o} s\right) & \text{for fluid} \\ \hat{J}_\mathrm{e}^\mathrm{o} e^{-st_\mathrm{max}} & \text{for solid} \end{cases} \tag{1.10}$$

where both $\hat{J}_e^o$ and $\hat{\eta}_o$ can be determined by the linear regression of long-time data of $J(t)$ for $\overline{\lambda} < t < t_{max}$. Of course we know that $\hat{J}_e^o \approx J_e^o$ and $\hat{\eta}_o \approx \eta_o$. The trapezoidal rule is sufficient for the calculation of the second integration:

$$s\int_{t_{min}}^{t_{max}} J(t)\, e^{-st} dt \approx \frac{s}{2}\sum_{\alpha=0}^{M-1} (t_{\alpha+1} - t_\alpha)\left(J_{\alpha+1} e^{-st_{\alpha+1}} + J_\alpha e^{-st_\alpha}\right) \tag{1.11}$$

The estimation of the first integral depends on t_{min}. If $t_{min} < \tau_H \left(G_o J_e^o\right)^{-1}$, then

$$s\int_0^{t_{min}} J(t)\, e^{-st} dt \approx \frac{1 - e^{-st_{min}}}{G_o} \tag{1.12}$$

If $\tau_H \left(G_o J_e^o\right)^{-1} < t_{min} < \tau_H$ then

$$s\int_0^{t_{min}} J(t)\, e^{-st} dt \approx \frac{\dot{J}_o}{s}\left[1 - e^{-st_{min}}(1 + st_{min})\right] \tag{1.13}$$

where $\dot{J}_o \approx J_r/\tau_H$ can be determined by the linear regression for the first few data ($t_\alpha > t_{min}$).

Now, we are equipped with algorithm for conversion of creep data to the Laplace transform $s\widetilde{J}(s)$. If a model for $s\widetilde{J}(s)$ is available, then nonlinear regression on $s\widetilde{J}(s)$ gives the values of the parameters and analytical calculation produces dynamic compliance. This was discussed in Sect. 3.2 in Chap. 5 and in Sect. 2.2 in Chap. 7. If no model is not available, then we can use the approximation such that

$$s\widetilde{J}(s) = \exp\left[\sum_{k=0}^{N} j_k T_k(\widetilde{\sigma})\right] = \frac{1}{s\widetilde{G}(s)} \tag{1.14}$$

where

$$\widetilde{\sigma} = \frac{\log s - \log\sqrt{s_{max} s_{min}}}{\log\sqrt{s_{max}/s_{min}}} \tag{1.15}$$

Equation (1.15) guarantees $-1 \le \widetilde{\sigma} \le 1$. We used also the notation $\sigma = \log s$ as before.

After the determination of the Chebyshev coefficients c_k, we will use Eq. (1.56) in Chap. 5. Note that for $s \to i\omega$, we know that $\tilde{\sigma} \to \tilde{\nu} + i\phi$ where

$$\tilde{\nu} = \frac{\log \omega - \log \sqrt{s_{\max} s_{\min}}}{\log \sqrt{s_{\max}/s_{\min}}} \tag{1.16}$$

and

$$\phi = \frac{\pi}{\log(s_{\max}/s_{\min})} \tag{1.17}$$

Then, we can use the calculation method which was used in the calculation of relaxation spectrum through the FK relation. Reminding Eqs. (2.69) and (2.71) in Chap. 7, we have

$$J'(\omega) = \exp\left[\sum_{k=0}^{N} j_k T_k'(\tilde{\nu})\right] \cos\left[\sum_{k=0}^{N} j_k T_k''(\tilde{\nu})\right] \tag{1.18}$$

and

$$J''(\omega) = \exp\left[\sum_{k=0}^{N} j_k T_k'(\tilde{\nu})\right] \sin\left[\sum_{k=0}^{N} j_k T_k''(\tilde{\nu})\right] \tag{1.19}$$

Similarly, use of $s\tilde{G}(s) = 1/\left[s\tilde{J}(s)\right]$ gives

$$G'(\omega) = \exp\left[\sum_{k=0}^{N} g_k T_k'(\tilde{\nu})\right] \cos\left[\sum_{k=0}^{N} g_k T_k''(\tilde{\nu})\right] \tag{1.20}$$

and

$$G''(\omega) = \exp\left[\sum_{k=0}^{N} g_k T_k'(\tilde{\nu})\right] \sin\left[\sum_{k=0}^{N} g_k T_k''(\tilde{\nu})\right] \tag{1.21}$$

where $g_k = -j_k$.

To test this algorithm, we generate creep compliance data by using a simple model such that

$$J(t) = \left[J_g + \frac{t}{\eta_o} + J_r\left(1 - e^{-t/\tau}\right)\right] \Theta(t) \tag{1.22}$$

We adopt parameters as follows:

$$J_g = 10^{-9}\,\mathrm{Pa}^{-1}; \quad J_r = 10^{-5}\,\mathrm{Pa}^{-1}; \\ \eta_o = 5 \times 10^5\,\mathrm{Pa\ s}; \quad \tau = 0.1\,\mathrm{s} \tag{1.23}$$

For this model, we know that

$$s\widetilde{G}(s) = \frac{1}{J_g + (\eta_o s)^{-1} + J_r(1+\tau)^{-1}} \tag{1.24}$$

and

$$J'(\omega) = J_g + \frac{J_r}{1+\tau^2\omega^2}; \quad J''(\omega) = \frac{1}{\eta_o \omega} + J_r \frac{\tau\omega}{1+\tau^2\omega^2} \tag{1.25}$$

Then dynamic moduli can be calculated by using Eq. (1.59) in Chap. 5.

We calculate $s\widetilde{G}(s)$ using the above equations for $s\widetilde{J}(s)$. Figure 1 shows that addition of 2 % statistical error cannot prevent recovery of high accurate $s\widetilde{G}(s)$. This is the error-suppression effect of numerical integration as mentioned in Sect. 2 in Chap. 7. In the generation of compliance data, we adopted $t_{\min} = \Delta t = 0.01\,\mathrm{s}$ and $t_\alpha = t_{\min} + \alpha\Delta t$ with $\alpha = 0, 1, \ldots, M$ and $t_M = t_{\max}$.

Since the simulated creep data shown in Fig. 1 imply $\tau_H \left(G_o J_e^o\right)^{-1} < t_{\min} < \tau_H$, Eq. (1.13) was used for the estimation of the first integral of Eq. (1.9). The parameter $\dot{J}_0$ is determined by the linear regression of the first four data. The simulated creep data have linear region for $\overline{\lambda} < t < t_{\max}$. Hence, we determined $\hat{\eta}_o$ and $\hat{J}_e^o$ by the linear regression for the last 300 data. Because of the error, sufficiently many data are necessary in accurate determination of $\hat{\eta}_o$ and $\hat{J}_e^o$.

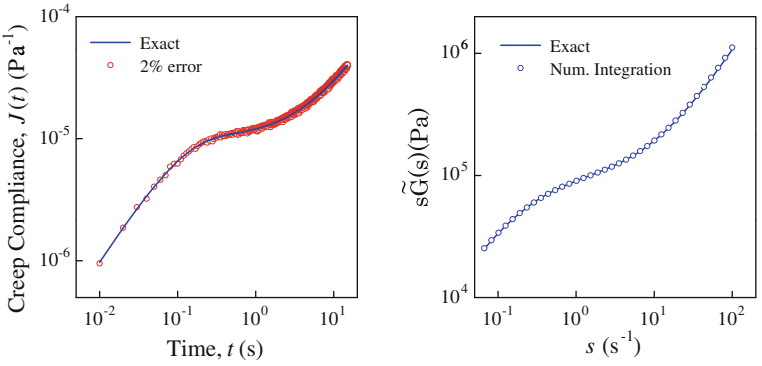

Fig. 1 Simulated data of creep compliance from Eq. (1.22) with 2 % error addition (*left*) and the Laplace transform of relaxation modulus $s\widetilde{G}(s)$ (*right*). Equations (1.9) and (1.24) were used for the symbol (numerically recovered) and line (exact one), respectively

Dynamic moduli are calculated using Eqs. (1.20), (1.21), and (1.59) in Chap. 5. Figure 2 compares calculated moduli of 0 and 2 % errors with exact ones. Loss modulus looks perfect, while storage modulus shows big deviation at high-frequency region. It can be explained by the inaccuracy of the correction term for $t < t_{\min}$ in Eq. (1.9). On the other hand, the extrapolation using $J(t) \to \hat{J}_e^o + t/\hat{\eta}_o$ in long-time region is very stable for error.

A careful look at the high-s region of the left-hand side of Fig. 1 finds that numerically obtained $s\widetilde{G}(s)$ slightly deviates from the exact one at high s which corresponds to high-frequency ω. Figure 2 shows that this negligibly small deviation becomes significant in storage modulus at high frequency. This error in storage modulus becomes more significant as the error in creep compliance increases.

It is of importance to compare the regression of the Laplace transform with the DFT method of Evans et al. (2009). The core of the methods of Evans et al. is as follows:

$$\frac{\mathrm{i}\omega}{G^*(\omega)} = \mathrm{i}\omega J_0 + \left(1 - e^{\mathrm{i}\omega t_{\min}}\right)\frac{J_1 - J_0}{t_{\min}} + \sum_{\alpha=1}^{M}\frac{J_\alpha - J_{\alpha-1}}{t_\alpha - t_{\alpha-1}}\left(e^{-\mathrm{i}\omega t_{\alpha-1}} - e^{-\mathrm{i}\omega t_\alpha}\right) + \frac{e^{-\mathrm{i}\omega t_{\max}}}{\hat{\eta}_o} \tag{1.26}$$

The summation term involves conventional differentiation which is weak for experimental error, while integration can suppress the error effect. Figure 4 of Evans et al. (2009) shows considerable noisy for the frequencies higher than the crossover point. This noisy region of frequency corresponds to the first three terms of Eq. (1.14), while smooth region of frequency is the terminal region which depends largely on the precision of $\hat{\eta}_o$ term. Meanwhile, the regression method is very stable for the experimental error, while it depends on the correction for $t < t_{\min}$.

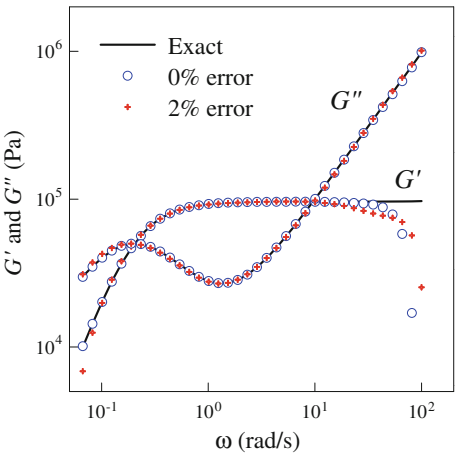

Fig. 2 Effect of error on the conversion to dynamic modulus

The correction for initial stage of creep can be changed depending on the creep data. The creep data used by Evans et al. show $J(t) \to J_0$ instead of $J(t) \to \dot{J}_o t$. It should be recognized that the J_0 of Evans et al. is not J_g. It is because $J_0^{-1} \approx G_N^o$.

If Eq. (1.14) is sufficiently accurate then Eqs. (1.18) and (1.19) are not negative. However, negative value of dynamic modulus happens to appear at the ends of frequency range.

1.1.2 From Relaxation Modulus to Dynamic Modulus

When relaxation modulus is given as an available data, the Laplace transform of relaxation modulus may be obtained by the trapezoidal method as follows:

$$s\widetilde{G}(s) \approx \frac{s}{2}\sum_{\alpha=0}^{M-1}\left(G_{\alpha+1}e^{-st_{\alpha+1}} + G_\alpha e^{-st_\alpha}\right)(t_{\alpha+1} - t_\alpha) + E \tag{1.27}$$

where $G_\alpha = G(t_\alpha)$ and $t_{\min} = t_0 < t_1 < \cdots < t_M = t_{\max}$. Hence the correction term E is given by

$$E = s\int_0^{t_{\min}} G(t)\, e^{-st}\mathrm{d}t + s\int_{t_{\max}}^{\infty} G(t)\, e^{-st}\mathrm{d}t \tag{1.28}$$

As for viscoelastic fluid, it is obvious that in long-time regime

$$G(t) \approx \frac{1}{J_e^o}\exp\left(-\frac{t}{\overline{\lambda}}\right) \tag{1.29}$$

where $\overline{\lambda} = J_e^o \eta_o$ is the mean relaxation time. The last integral of Eq. (1.17) can be estimated by

$$s\int_{t_{\max}}^{\infty} G(t)\, e^{-st}\mathrm{d}t \approx \frac{1}{J_e^o}\frac{\overline{\lambda}s}{1+\overline{\lambda}s}\exp\left[-\frac{t_{\max}}{\overline{\lambda}}\left(1+\overline{\lambda}s\right)\right] \tag{1.30}$$

If $t_{\max} \gg \overline{\lambda}$, then this term should be negligible irrespective of the value of s. On the other hand, the first term can be estimated by

$$G(t_{\min})\left(1 - e^{-st_{\min}}\right) \le s\int_0^{t_{\min}} G(t)\, e^{-st}\mathrm{d}t \le G(0^+)\left(1 - e^{-st_{\min}}\right) \tag{1.31}$$

If $st_{\min} \ll 1$, then this term may be negligible. Hence, finite range of relaxation modulus data restricts the range of s. Once the Laplace transform $s\widetilde{G}(s)$ is obtained,

then the same method used above can be applied for the determination of dynamic moduli.

1.2 Laplace Transform from Dynamic Data

Consider the dynamic modulus data whose frequency range is given by $\omega_{\min} \le \omega \le \omega_{\max}$. Under the assumption that $\eta'(\omega_{\min}) \approx \eta_o$, we can obtain the Laplace transform from dynamic moduli as follows:

$$\widetilde{G}(s) = \int_0^\infty e^{-st}\left[\frac{2}{\pi}\int_0^\infty \frac{G''(\omega)}{\omega}\cos\omega t\,\mathrm{d}\omega\right]\mathrm{d}t = \int_0^\infty e^{-st}\left[\frac{2}{\pi}\int_0^\infty \frac{G'(\omega)}{\omega}\sin\omega t\,\mathrm{d}\omega\right]\mathrm{d}t \tag{1.32}$$

Change in the order of integration gives

$$\widetilde{G}(s) = \frac{2}{\pi}\int_0^\infty \eta''(\omega)\frac{\omega}{s^2+\omega^2}\mathrm{d}\omega = \frac{2}{\pi}\int_0^\infty \eta'(\omega)\frac{s}{s^2+\omega^2}\mathrm{d}\omega \tag{1.33}$$

where $\eta'(\omega) = \omega^{-1}G''(\omega)$ and $\eta''(\omega) = \omega^{-1}G'(\omega)$. To make the numerical integration more effective, consider the following change of variables:

$$\sigma = \log s, \quad \nu = \log\omega \tag{1.34}$$

Then, the second integral of Eq. (1.33) can be rewritten by

$$\widetilde{G}(\sigma) = \frac{1}{\pi}\int_{-\infty}^{\infty} \frac{\eta'(\nu)}{\cosh(\nu-\sigma)}\mathrm{d}\nu \tag{1.35}$$

Since $\mathrm{sech}(x) = 1/\cosh(x)$ shows a peak at $x = 0$ and decays exponentially as $|x| \to \infty$, numerical integration of Eq. (1.35) is very reliable compared with its counterpart using $\eta''(\nu)$. Although experimental data are obtained in a finite range of frequency, the assumption of $\eta_o \approx \eta'(\omega_{\min})$ allows us to write

$$\widetilde{G}(\sigma) \approx \int_{-\infty}^{\nu_{\min}} \frac{\eta_o}{\cosh(\nu-\sigma)}\mathrm{d}\nu + \int_{\nu_{\min}}^{\nu_{\max}} \frac{\eta'(\nu)}{\cosh(\nu-\sigma)}\mathrm{d}\nu \tag{1.36}$$

Note that for $\nu > \sigma$, $\mathrm{sech}(\nu-\sigma)$ is a steeply decreasing function and $\eta'(\nu)$ is also a decreasing function of v. Hence, it is reasonable to assume that

$$\int_{\nu_{max}}^{\infty} \frac{\eta'(\nu)}{\cosh(\nu-\sigma)} d\nu \approx 0 \tag{1.37}$$

Then, Eq. (1.36) becomes

$$\begin{aligned}\widetilde{G}(\sigma) \approx \frac{\eta_o}{\pi}\left[\frac{\pi}{2} + 2\arctan\left(\tanh\frac{\nu_{min}-\sigma}{2}\right)\right] \\ + \frac{1}{2\pi}\sum_{k=0}^{M-1}(\nu_{k+1}-\nu_k)\left[\frac{\eta'(\nu_k)}{\cosh(\nu_k-\sigma)} + \frac{\eta'(\nu_{k+1})}{\cosh(\nu_{k+1}-\sigma)}\right]\end{aligned} \tag{1.38}$$

The summation of Eq. (1.38) is the numerical integration over $\nu_{min} \le \nu \le \nu_{max}$. After obtaining $\widetilde{G}(s)$, the Laplace transform of creep compliance $\widetilde{J}(s)$ can be determined by the relation between them:

$$\widetilde{J}(s)\,\widetilde{G}(s) = \frac{1}{s^2} \tag{1.39}$$

Equation (1.36) was used to calculate $s\widetilde{J}(s)$ of Fig. 5 in Chap. 6.

Problem 1

[1] Generate $s\widetilde{J}(s)$ using the Cole–Cole model of Eq. (2.23) in Chap. 6 and apply Eq. (1.14) and calculate dynamic compliances and compare the exact ones of Eqs. (2.21a, b) in Chap. 6.
[2] Generate dynamic moduli from the Cole–Cole model of Eq. (2.23) in Chap. 6 and convert them to $s\widetilde{J}(s)$.
[3] Derive Eq. (1.24).
[4] You can find numeric data of dynamic moduli of 6 monodisperse PS's in Schausberger et al. (1985). Calculate $s\widetilde{J}(s)$ of PS6.
[5] Using the data of Schausberger et al. (1985), find the parameters of the Cole–Cole model.

2 Polymer Melts and Solutions

2.1 Monodisperse Linear Polymer in Molten State

2.1.1 Characteristic Relaxation Times

Viscoelastic data of monodisperse linear polymers is very important in developing molecular theory of polymer viscoelasticity. When molecular weight is sufficiently high ($M \gg M_e$), one can find three phenomenological times of two local maxima

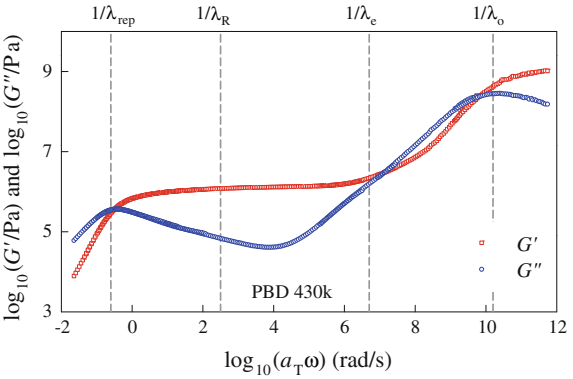

Fig. 3 Characteristic times of linear monodisperse polymer

and one local minimum of loss modulus: $\lambda_{max}^{(1)} > \lambda_{min} > \lambda_{max}^{(2)}$ (Fig. 3). We can assign molecular meaning to the four characteristic times: the reptation time, λ_{rep}; the Rouse time of the whole chain, λ_R; the Rouse time of the subchain between entanglement, λ_e; and relaxation time of monomer, λ_o.

As shown in Fig. 3, $\lambda_{rep} \approx \lambda_{max}^{(1)}$; $\lambda_o \approx \lambda_{max}^{(2)}$; $\lambda_e < \lambda_{min} < \lambda_R$. Molecular theory (Rubinstein and Colby 2003) gives

$$\lambda_e = \lambda_o N_e^2 \tag{2.1}$$

$$\lambda_R = \lambda_o N^2 = \lambda_e \left(\frac{N}{N_e}\right)^2 \tag{2.2}$$

and

$$\lambda_{rep} = 6\lambda_o \frac{N^3}{N_e} = 6\lambda_e \left(\frac{N}{N_e}\right)^3 = 6\lambda_R \frac{N}{N_e} \tag{2.3}$$

where $N = M/M_o$; $N_e = M_e/M_o$; M is the molecular weight; M_e is the entanglement molecular weight; and M_o is the molecular weight of the Kuhn monomer. The exponent 3 of Eq. (2.3) holds when M is extremely large. When M is intermediate but sufficiently higher than the entanglement molecular weight, the exponent value is about 3.4.

2.1.2 Plateau Modulus

Hence, as N becomes larger, both $\lambda_{rep} - \lambda_R$ and $\lambda_R - \lambda_e$ becomes larger. Similarly, $\lambda_{max}^{(1)} - \lambda_{min}$ and $\lambda_{min} - \lambda_{max}^{(2)}$ become larger. Since storage modulus between $\omega = 1/\lambda_{rep}$ and $\omega = 1/\lambda_e$ is nearly constant, this region of frequency is called plateau region. This tendency is clearly shown in Fig. 4. It is known that the

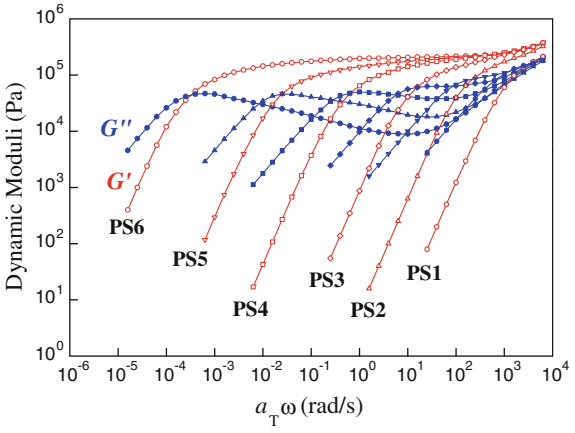

Fig. 4 Linear viscoelasticity of linear monodisperse PS. The data are from Schausberger et al. (1985). Molecular weights of 6 PS's are 34 kg/mol (PS1), 65 kg/mol (PS2), 125 kg/mol (PS3), 292 kg/mol (PS4), 757 kg/mol (PS5), and 3000 kg/mol (PS6). The *lines* are drawn as eye guide

entanglement molecular weight of polystyrene is about 16,000 g/mol and molecular weight of Kuhn monomer is about 720 g/mol. Although PS4, PS5, and PS6 show clear local minimum of loss modulus, PS3, PS2, and PS1 do not. This implies that plateau region appears, at least, when $M > 8M_e$.

Interpretation of entanglement as a temporary network implies the existence of the plateau modulus such that

$$G_N^o = \frac{\rho RT}{M_e} \tag{2.4}$$

However, as shown in Fig. 4, storage modulus slowly increases as frequency in the plateau region. Although experimental data do not show a constant value of storage modulus in this frequency, Fig. 1.3, in Chap. 8, indicates that the value of storage modulus at the local minimum of loss modulus is nearly independent of both temperature and molecular weight. Figure 1.2 in Chap. 8 makes us recognize that the curves of Fig. 1.3 in Chap. 8 consist of data of various temperatures. If the plateau modulus is defined as the storage modulus at the local minimum of loss modulus, then Eq. (2.4) implies that temperature dependences of ρRT and M_e are mutually canceled. Fetters et al. investigated in detailed the determination of plateau modulus and entanglement molecular weight (Fetters et al. 1994).

2.1.3 Zero-Shear Viscosity

It is well known that zero-shear viscosity of linear polymer melt is proportional to 3.4 power of molecular weight when molecular weight is larger than the critical molecular weight which is about two times of the entanglement molecular weight. Figure 5 shows the collection of experimental data from various papers. These experimental data are PS/S from Schausberger et al. (1985); PS/M from Marin and

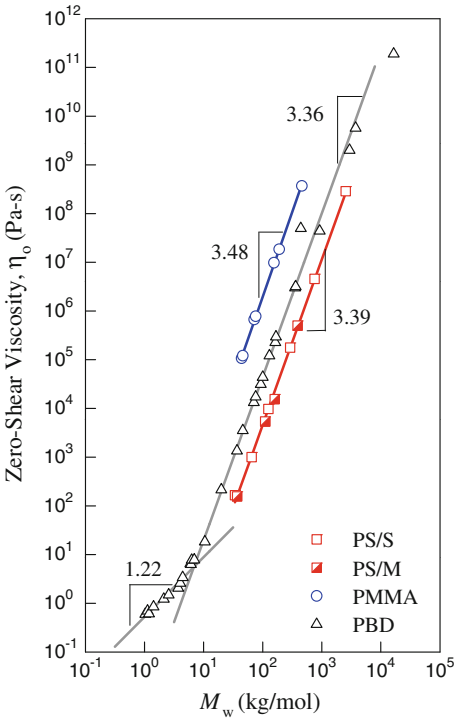

Fig. 5 Zero-shear viscosity as a function of molecular weight. The data of PS/S are adopted from Schausberger et al. (1985); PS/M from Marin and Graessley (1977); PMMA from Fuchs et al. (1996); and PBD from Colby et al. (1987). All polymers are nearly monodisperse

Graessley (1977); PMMA from Fuchs et al. (1996); and PBD from Colby et al. (1987). As shown in Fig. 5, the slopes of the double logarithmic plot of zero-shear viscosity versus weight-average molecular weight is approximately 3.4. The critical molecular weight is defined as the molecular weight at which the slope changes dramatically. One of the successes of the Doi–Edwards theory is the prediction and explanation of the behavior of zero-shear viscosity as shown in Fig. 5.

It is interesting that this molecular weight dependence of zero-shear viscosity holds for polydisperse polymers, too. In industries, melt flow index (MI) is more popular than zero-shear viscosity because of its convenience in measurement. If the weight for the measurement of MI is not too heavy, then the inverse of MI is nearly proportional to zero-shear viscosity.

2.1.4 Characteristic Molecular Weights

There are three characteristic molecular weights of linear monodisperse polymers: entanglement, the first critical, and the second critical molecular weights. The first critical molecular weight M_C is defined in Eq. (3.68) in Chap. 2:

$$\eta_o(M) = \begin{cases} \eta_o(M_C)\frac{M}{M_C} & \text{for } M \le M_C \\ \eta_o(M_C)\left(\frac{M}{M_C}\right)^{3.4} & \text{for } M \ge M_C \end{cases} \tag{2.5}$$

Polybutadiene data of Fig. 5 quantitatively follow Eq. (2.5). While the exponent for $M > M_C$ is approximately 3.4, the exponent for $M < M_C$ deviates from unity. The deviation seems to be originated from the lack or the imprecision of low-viscosity data. The second critical molecular weight is the molecular weight at which the steady-state compliance of monodisperse polymer melts changes its molecular weight dependency as follows:

$$J_e^o(M) \approx \begin{cases} J_e^o(M_C')\left(\frac{M}{M_C'}\right) & \text{for } M \le M_C' \\ J_e^o(M_C') & \text{for } M \ge M_C' \end{cases} \tag{2.6}$$

This relation does not hold for polydisperse polymers.

It is observed that for any polymers, $M_e < M_C < M_C'$. Determination of critical molecular weight using Eq. (2.5) or (2.6) requires a group of monodisperse polymers whose molecular weights should be the one such that $M_{min} < M_C$ and $M_{max} > M_C$. It is usual that low-viscosity samples suffer from imprecision of measurement, while considerably more accurate measurements are performed for moderately high-viscosity samples. As for samples of $M > M_C$, we can observe local maximum and minimum of loss modulus in usual range of frequency. Let the two characteristic times be denoted by $\lambda_{max} = 1/\omega_{max}$ and $\lambda_{min} = 1/\omega_{min}$. Note that we mean $\lambda_{max} = \lambda_{max}^{(1)}$. Similar to Eqs. (2.1)–(2.3), we can assume that

$$\lambda_{min} = \lambda_E\left(\frac{M}{M_C''}\right)^{\alpha}; \quad \lambda_{max} = \lambda_E\left(\frac{M}{M_C''}\right)^{\beta} \tag{2.7}$$

Samples with $M > M_C$ are sufficient to determine the parameters of Eq. (2.7). Cho et al. (2004a) analyzed linear viscoelastic data measured by various researchers and found that Eq. (2.7) gives the determination of the critical molecular weight from loss modulus data. Figure 6 shows the result. It is interesting that $\lambda_E \approx \lambda_e$ and $M_C'' \approx 2M_e$. Some literatures show that the critical molecular weight from zero-shear viscosity deviates from the relation $M_C \approx 2M_e$. Hence, it can be said that use of Eq. (2.7) is more efficient than use of Eq. (2.5) in determining the critical molecular weight.

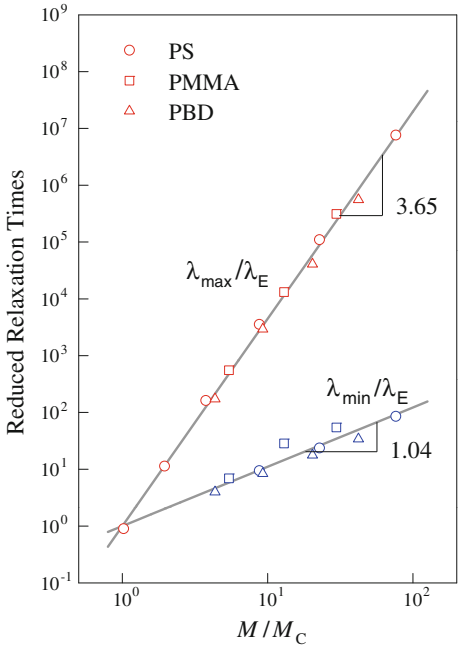

Fig. 6 Reduced phenomenological relaxation times λ_{max}/λ_E and λ_{min}/λ_E as functions of reduced molecular weight M/M_C. PS data are from Schausberger et al. (1985); PMMA data from Fuchs et al. (1996); and PBD from Baumgaertel et al. (1992)

2.2 *Polydisperse Polymer Melts*

2.2.1 Mixing Rule

It is an interesting research theme to formulate viscoelastic functions of polydisperse polymer melt in terms of those of monodisperse polymers and molecular weight distribution. Bright progress in molecular theory makes it possible to fit experimental data of monodisperse polymers only a few number of parameters such as the plateau modulus G_N^o and the relaxation time at which the effect of entanglement starts, λ_e. The molecular theory addresses that the same function is applied to the relaxation modulus of monodisperse linear polymer of any molecular weight M. Then, it is a reasonable assumption that the relaxation modulus of polydisperse linear polymer melt is given by

$$[G(t)]^{1/\mu} = \int_{M_{min}}^{\infty} w(M)\,[G_m(t,\ M)]^{1/\mu} dM \tag{2.8}$$

where $w(M)\,dM$ is the weight fraction of chains with molecular weight ranges from $M - \frac{1}{2}dM$ to $M + \frac{1}{2}dM$ and $G_m(t,\ M)$ is the relaxation modulus of the monodisperse polymer with molecular weight of M.

Des Cloizeaux (1988) derived Eq. (2.8) with $\mu = 2$ using *double reptation*. The same equation was derived by Tsenoglou (1991) by the application of detailed balance to the dynamics of temporary network. These theories seem to be valid whenever $M_{\min} > M_C$. Since $\mu = 2$, Eq. (2.8) can be rewritten by

$$G(t) = \int_{M_{\min}}^{\infty} \int_{M_{\min}}^{\infty} w(M)\, w(M')\, \sqrt{G_m(t,\ M)\, G_m(t,\ M')}\, dM'\, dM \tag{2.9}$$

Equation (2.9) is called quadratic mixing rule. Validity of Eq. (2.9) could be tested if accurate equation of G_{mono} was equipped. Approximate consequences of Eq. (2.9) are as follows:

$$\eta_o \approx 2 \int_{M_{\min}}^{\infty} \int_{M_{\min}}^{\infty} w(M)\, w(M')\, \frac{\eta_o^m(M)\, \eta_o^m(M')}{\eta_o^m(M) + \eta_o^m(M')}\, dM'\, dM \tag{2.10}$$

$$G'(\omega) \approx G_N^o \int_{M_{\min}}^{\infty} \int_{M_{\min}}^{\infty} w(M)\, w(M')\, G_E(\omega,\ M,\ M')\, dM'\, dM \tag{2.11}$$

and

$$G''(\omega) \approx G_N^o \int_{M_{\min}}^{\infty} \int_{M_{\min}}^{\infty} w(M)\, w(M')\, G_V(\omega,\ M,\ M')\, dM'\, dM \tag{2.12}$$

where

$$G_E(\omega,\ M,\ M') = \left[1 + \frac{1}{4}\left(\sqrt{\frac{G_N^o}{G'_m(\omega,\ M)}} + \sqrt{\frac{G_N^o}{G'_m(\omega,\ M')}}\right)^2\right]^{-1} \tag{2.13}$$

and

$$G_V(\omega,\ M,\ M') = \left(\Gamma + \frac{1}{\Gamma}\right)^{-1} \tag{2.14}$$

with

$$\Gamma = \frac{G_N^o - G'_m(\omega,\ M)}{2G''_m(\omega,\ M)} + \frac{G_N^o - G'_m(\omega,\ M')}{2G''_m(\omega,\ M')} \tag{2.15}$$

Note that super- or subscript m denotes monodisperse.

Tsenoglou (1991) showed that the approximate Eqs. (2.10)–(2.12) agree with experimental data. Although direct verification can be done using the data of relaxation modulus, the author has not find any literature which tests the mixing rule in terms of the data of relaxation modulus. It is guessed that technical difficulty in measurement of relaxation modulus prevents such approach. Bae and Cho (2015) converted dynamic modulus to relaxation modulus for various monodisperse polymers and their mixtures and tested the mixing rule of Eq. (2.8). The conversion was done by the BLM method for continuous relaxation spectrum (Fig. 7).

Since the ingredient polystyrenes are monodisperse ones, Bae and Cho (2015) used discrete version of Eq. (2.9) such that

$$G(t) = \sum_{i=1}^{M} \sum_{k=1}^{M} \phi_i \phi_k \sqrt{G_{\mathrm{m}}(t,\ M_i)\, G_{\mathrm{m}}(t,\ M_k)} \tag{2.16}$$

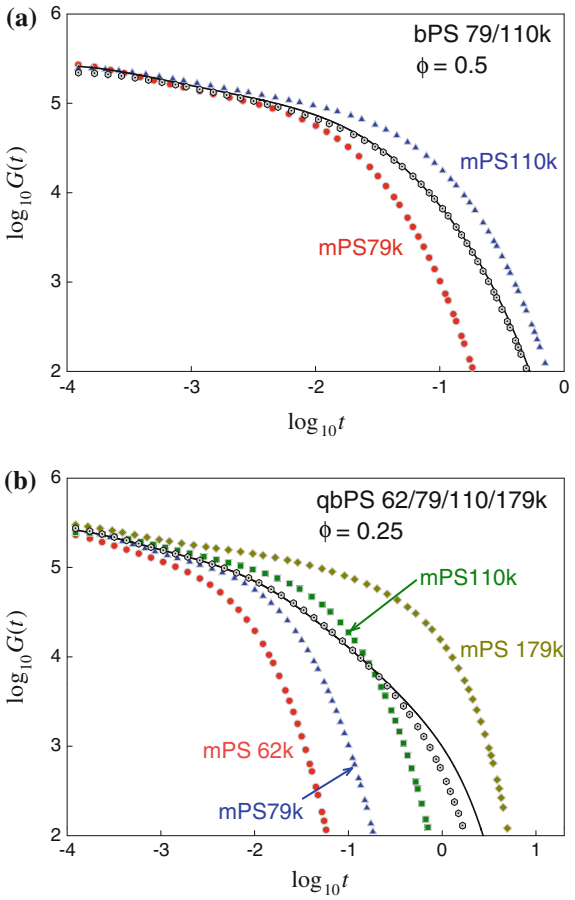

Fig. 7 Relaxation moduli converted from dynamic moduli (*symbols*) and relaxation moduli calculated from the mixing rule of $\mu = 2$ (*line*). mPS 110k denotes monodisperse PS with $M = 110$ kg/mol. The meaning of legends can be understood similarly. Note that ϕ is the volume fraction (=weight fraction w) of ingredients of the mixtures: **a** binary mixture; **b** quartic mixture (Bae and Cho 2015)

where ϕ_i is the volume fraction of the chains of the molecular weight of M_i. Note that as for the mixture of the same kind of polymers, volume fraction is equivalent to weight fraction. As for binary mixture, generalized mixing rule of Eq. (2.8) is rewritten by

$$G(t) = \left[\phi \sqrt[\mu]{G_{\mathrm{m}}(t,\ M_1)} + (1-\phi)\sqrt[\mu]{G_{\mathrm{m}}(t,\ M_2)}\right]^{\mu} \tag{2.17}$$

where $\phi_1 = \phi$ and $\phi_2 = 1 - \phi$. Bae and Cho calculated the optimum exponent μ which minimizes the sum of square of the difference between given data of $G(t)$ and the calculated modulus according to the generalized mixing rule Eq. (2.17). Similar method can be applied to quartic mixture. This calculation gives 2.18 for binary mixture and 2.15 for quartic mixture. These values of μ is very close to the one predicted from molecular theories.

On the other hand, Maier et al. (1998) calculated the optimum exponent $\mu = 3.84$ for binary mixtures of PS with various compositions. Different from Bae and Cho, they used continuous version of generalized mixing rule. They obtained molecular weight distribution of monodisperse ingredients from size exclusion chromatography (SEC). Even a monodisperse sample with PDI = 1.05 shows considerably wide peak of molecular weight distribution. It is because most molecular weight distributions of polymers follow lognormal distribution. Assume that there exists a hypothetical polymer sample with exactly PDI = 1 although there is not such sample in reality. This means the MWD is proportional to the Dirac delta function. SEC measures weight fraction of a molecular weight through refractive index as a function of elution time. Even a perfect monodisperse polymer cannot give a single elution time. Hence, MWD from SEC is an approximation. Hence, this may explain the difference in the optimum exponents from the two research groups. However, it is noteworthy that the calculation of Bae and Cho agrees with the molecular theories.

2.2.2 Calculation of MWD

If the exponent μ is given as a correct one and accurate model of $G_{\mathrm{m}}(t,\ M)$ is available, then Eq. (2.8) implies that we can predict viscoelasticity of polydisperse polymer. Reversely, if we know $G(t)$ and want to find MWD, then it is to solve the Fredholm integral equation of the first kind. It is an inverse problem just as relaxation time spectrum. In this inverse problem, $\sqrt[\mu]{G_{\mathrm{m}}(t,\ M)}$ is the kernel function which should be given by a model, while the kernel of relaxation spectrum is exact. Furthermore, there are other problems in inferring MWD from rheological data except numerical method to solve the integral equation.

After the Doi–Edwards theory, there have been a number of advances in molecular model for linear viscoelasticity of linear monodisperse polymers. Some examples are Benallal et al. (1993), Guzmán et al. (2005), Léonardi et al. (2000), Pattamaprom and Larson (2001), Pattamaprom et al. (2008), and Pattamaprom et al.

(2000). Some of them provide $G_{\mathrm{m}}(t,\ M)$ by solving nonlinear diffusion equation numerically. Others give $G_{\mathrm{m}}(t,\ M)$ including an integration of a given function. Leonardi et al. (2000) decomposed relaxation modulus of monodisperse polymer into five parts: the slowest mode corresponding to λ_{rep} ($G_C(t,\ M)$); the Rouse mode of full chain corresponding to λ_{R} ($G_B(t,\ M)$); the Rouse mode of the subchain between entanglement points, which corresponds to λ_{e} ($G_A(t)$); the high-frequency mode corresponding to λ_{o} ($G_{\mathrm{HF}}(t)$); and the Rouse mode of unentangled chains ($G_R(t,\ M)$). It is assumed that G_C follows the quadratic mixing rule, and G_B and G_R follow the linear mixing rule. On the other hand, G_A and G_{HF} are independent of molecular weight. Note that G_C is effective for the chains whose molecular weight is larger than the critical molecular weight $M_{\mathrm{C}} \approx 2M_{\mathrm{e}}$, while G_R is effective for the chains with $M < M_{\mathrm{C}}$. Then, Leonardi et al. used the following mixing rule:

$$G(t) = \left[\int_{M_{\mathrm{C}}}^{\infty} w(M)\,\sqrt{G_C(t,M)}\,\mathrm{d}M\right]^2 + \int_0^{\infty} w(M)\,G_B(t,M)\,\mathrm{d}M + \int_0^{M_{\mathrm{C}}} w(M)\,G_R(t,M)\,\mathrm{d}M + G_A(t) + G_{HF}(t) \tag{2.18}$$

Equation (2.18) looks plausible, and experimental data agree well with Eq. (2.18). However, it is raised that chains with $M < M_{\mathrm{C}}$ may play the role of solvent which widens the tube size or reduces constraints on long chains. Hence, better mixing rule is still demanded.

2.3 Polymer Solution

Polymer solution has been used in polymer process such as solution spinning and film casting. These polymer processes require solidification after shape forming. Evaporation of solvent thickens the polymer solution and results in solid film. Although low concentration is better for shape forming process, the concentration lower than entanglement concentration gives rise to fracture of film when the polymer solution is solidified. When polymer has very high molecular weight, both overlap and entanglement concentrations are too low [see Eqs. (3.8) and (3.12) in Chap. 4]. As shown in Fig. 3.3 in Chap. 4, the increase of concentration over c_{e} results in explosive increase in viscosity, which makes shape process very difficult. Because of this reason, electronics industries usually use polymer solutions with reactive polymers which become polymer network through curing reaction and evaporation of solvent. Sufficiently low viscosity of the reactive polymer solution helps the shape process, and curing reaction overcomes the fracture due to the lack of entanglement. Since curing reaction increases molecular weight of the polymer

and solvent evaporation increases the concentration of the solution, it is necessary to investigate the relation between the rheology and the concentration of polymer solution.

When concentration is sufficiently high to form entanglement, it is known that N_e, the number of Kuhn monomers in subchain between entanglement points follows (Rubinstein and Colby 2003)

$$\frac{N_e(\phi)}{N_e(1)} = \begin{cases} \phi^{-\frac{1}{3\nu-1}} & \text{for an athermal solution} \\ \phi^{-\frac{4}{3}} & \text{for a } \theta\text{-solution} \end{cases} \tag{2.19}$$

where $N_e(1) = M_e/M_o$ is the entanglement number in molten state. The following relations are also known:

$$\frac{G_N^o(\phi)}{G_N^o(1)} = \begin{cases} \phi^{\frac{3\nu}{3\nu-1}} & \text{for an athermal solution} \\ \phi^{\frac{7}{3}} & \text{for a } \theta\text{-solution} \end{cases} \tag{2.20}$$

$$\frac{\lambda_{rep}(\phi)}{\lambda_o} = \frac{N^3}{N_e(1)} \begin{cases} \phi^{\frac{3(1-\nu)}{3\nu-1}} & \text{for an athermal solution} \\ \phi^{\frac{7}{3}} & \text{for a } \theta\text{-solution} \end{cases} \tag{2.21}$$

$$\frac{\eta_o(\phi)}{\eta_{solvent}} = \frac{N^3}{[N_e(1)]^2} \begin{cases} \phi^{\frac{3}{3\nu-1}} & \text{for an athermal solution} \\ \phi^{\frac{14}{3}} & \text{for a } \theta\text{-solution} \end{cases} \tag{2.22}$$

Note that if $\nu = 0.588$, then $3\nu/(3\nu - 1) \approx 2.3 \approx 7/3$. Hence, the plot of plateau modulus versus concentration cannot detect the difference between a thermal and theta solutions. It is reported that linear viscoelasticity of semi-dilute solutions can be superposed if dynamic moduli are normalized by the plateau modulus and frequency is normalized by appropriate relaxation time irrespective of molecular weight and concentration (Cho et al. 2015; Heo and Larson 2008).

On the other hand, viscoelasticity of dilute polymer solutions follows the Zimm model or the Rouse model if solvent effect is removed (Rubinstein and Colby 2003). When solvent viscosity is denoted by η_s, the following normalization of dynamic moduli is expected to give superposed plots:

$$\widetilde{G'} = \frac{M}{cRT} G'; \quad \widetilde{G''} = \frac{M}{cRT} (G'' - \eta_s \omega) \tag{2.23}$$

Frequency should be normalized by $\lambda_R \omega$ or $\lambda_Z \omega$ where λ_Z is the Zimm relaxation time.

Problem 2

[1] As for monodisperse polymer melts, Cho et al. (2004b) defined

$$g' = \frac{G'}{J_e^o \eta_o^2 \omega}; \quad g'' = \frac{G''}{\eta_o \omega} \tag{2.a}$$

and showed that the plot of g' as a function of g'' can be superposed by the shifting defined by

$$g' \to \frac{g'}{\Lambda^{1.56}}; \quad g'' \to \frac{g'}{\Lambda} \tag{2.b}$$

where

$$\Lambda = \Lambda_0 \left(\frac{M}{M_e}\right)^{-2.91} \tag{2.c}$$

You can find numeric data of dynamic moduli of 6 monodisperse PS's in Schausberger et al. (1985). Determine Λ_0.

[2] Using the data of Schausberger et al. (1985), determine the material parameters λ_E, M_C'', α and β of Eq. (2.7).

[3] Derive Eqs. (2.10)–(2.12).

[4] Dyneema is a super strong fiber made of polyethylene with ultra-high molecular weight. It is known that the entanglement molecular weight of PE is about 1000 g/mol. Calculate the entanglement concentration of PE solution if $M = 6000$ kg/mol. What information is needed?

[5] In dilute regime, intrinsic dynamic moduli is defined as

$$[G'] = \lim_{c \to 0} \frac{M}{cRT} G'; \quad [G''] = \lim_{c \to 0} \frac{M}{cRT} (G'' - \eta_s \omega) \tag{2.d}$$

Explain the reason why the limits of Eq. (2.d) exist.

3 Immiscible Blend of Polymers

When two immiscible fluids are blended, there exists interface. Deformation of the interface is usually accepted as elastic one. Hence, even if two immiscible Newtonian fluids are mixed, then viscoelasticity is found in the mixture because of the existence of the interface. If one of two components has low volume fraction, then the minor component forms a spherical phase surrounded by the major

component in equilibrium. The phase of the minor component is called dispersed phase, while that of major component is called matrix phase.

If the concentration of minor component increases, the morphology of the mixture gets to lose characteristic length because cocontinuous structure becomes developed. Then, the rheological properties of the mixture change dramatically. This section will be focused on the mixture whose minor component forms spherical dispersed phase. Such a system can be called emulsion.

3.1 Mixture of Newtonian Fluids

As for immiscible mixture of two Newtonian fluids, the work of Choi and Schowalter (1975) is remarkable. Since their calculation starts from the Navier–Stokes equation, the theory can be applied to nonlinear flow. Neglecting nonlinear terms, Scholz et al. (1989) calculated dynamic moduli as follows:

$$G'(\omega) = \frac{\eta_o}{\lambda_1}\left(1 - \frac{\lambda_2}{\lambda_1}\right)\frac{\lambda_1^2\omega^2}{1+\lambda_1^2\omega^2}; \quad G''(\omega) = \eta_o\frac{\lambda_2}{\lambda_1}\omega + \frac{\eta_o}{\lambda_1}\left(1 - \frac{\lambda_2}{\lambda_1}\right)\frac{\lambda_1\omega}{1+\lambda_1^2\omega^2} \tag{3.1}$$

where

$$\eta_o = \eta_{matrix}\left[1 + \frac{5k+2}{2(k+1)}\phi + \frac{5(5k+2)^2}{8(k+1)^2}\phi^2\right] \tag{3.2}$$

$$\lambda_1 = \lambda_0\left[1 + \frac{5(19k+16)}{4(k+1)(2k+3)}\phi\right] \tag{3.3}$$

$$\lambda_2 = \lambda_0\left[1 + \frac{3(19k+16)}{4(k+1)(2k+3)}\phi\right] \tag{3.4}$$

$$\lambda_0 = \frac{\eta_{matrix}R}{\alpha}\frac{(19k+16)(2k+3)}{40(k+1)} \tag{3.5}$$

and

$$k = \frac{\eta_{disperse}}{\eta_{matrix}} \tag{3.6}$$

Here, R is the radius of the disperse phase, α is the interfacial tension, and ϕ is the volume fraction of the disperse phase.

Note that Eq. (3.2) is the zero-shear viscosity of the mixture. As for the case of $k \to \infty$ and $\phi \ll 1$, Eq. (3.2) becomes the Einstein equation of suspension:

$$\frac{\eta_o}{\eta_{matrix}} \approx 1 + \frac{5}{2}\phi \tag{3.7}$$

Equation (3.1) is the sum of the Newtonian and the Maxwellian models. Note that the effect of interface (represented by the term of R/α) appears only in the Maxwellian model. Hence, it can be understood that the relaxation of the interface is governed by the timescale of λ_1 which depends on ϕ.

3.2 The Gramespacher and Meissner Model

Gramespacher and Meissner (1992) applied the Choi and Schowalter model (CS model) to the linear viscoelasticity of immiscible blend of polymers:

$$G^*(\omega) = \phi\, G^*_{dis}(\omega) + (1-\phi)\, G^*_{mat}(\omega) + G^*_{int}(\omega) \tag{3.8}$$

where $G^* = G' + iG''$, dis and mat represent disperse and matrix, and G^*_{int} is the Maxwellian model of Eq. (3.1). Equation (3.8) is the sum of the arithmetic mean of the linear viscoelasticity of the matrix and disperse phases and that of interface.

Although the Gramespacher and Meissner model (GM model) is a simple extension of the CS model, it agrees quite well with experimental data. Since Eq. (3.8) is considerably simple, it is easy to estimate R/α by fitting experimental data. Furthermore, since the interfacial modulus is Maxwellian, it is obvious that the relaxation spectrum of G^*_{int} is given by

$$H_{int}(\lambda) = \frac{\eta_o}{\lambda_1}\left(1 - \frac{\lambda_2}{\lambda_1}\right)\delta(\log\lambda - \log\lambda_1) \tag{3.9}$$

Since Eq. (3.8) implies that $H = \phi H_{dis} + (1-\phi)H_{mat} + H_{int}$, Gramespacher and Meissner (1992) also calculated the relaxation time spectrum using the nonlinear regularization developed by Honerkamp and Weese (1993). They found that the plot of $\lambda H(\lambda)$ is better than that of $H(\lambda)$ in recognizing that the spectrum of the mixture consists of three parts. The spectrum $\lambda H(\lambda)$ is called weighted spectrum. It is because the weighted spectrum as function of $\log\lambda$ looks like peaks. This feature of the weighted spectrum was also used by Shaayegan et al. (2012) in the study of linear viscoelasticity of immiscible polymer blends.

Figure 8 shows linear viscoelasticity of PP/PS blends. Loss moduli of mixtures vary between those of pure ingredients, while the blends having interface show storage moduli which are absolutely different from those of pure ingredients. This agrees with the expectation that the relaxation of interface is mainly elastic. Although the storage modulus is better than the loss modulus in detection of the

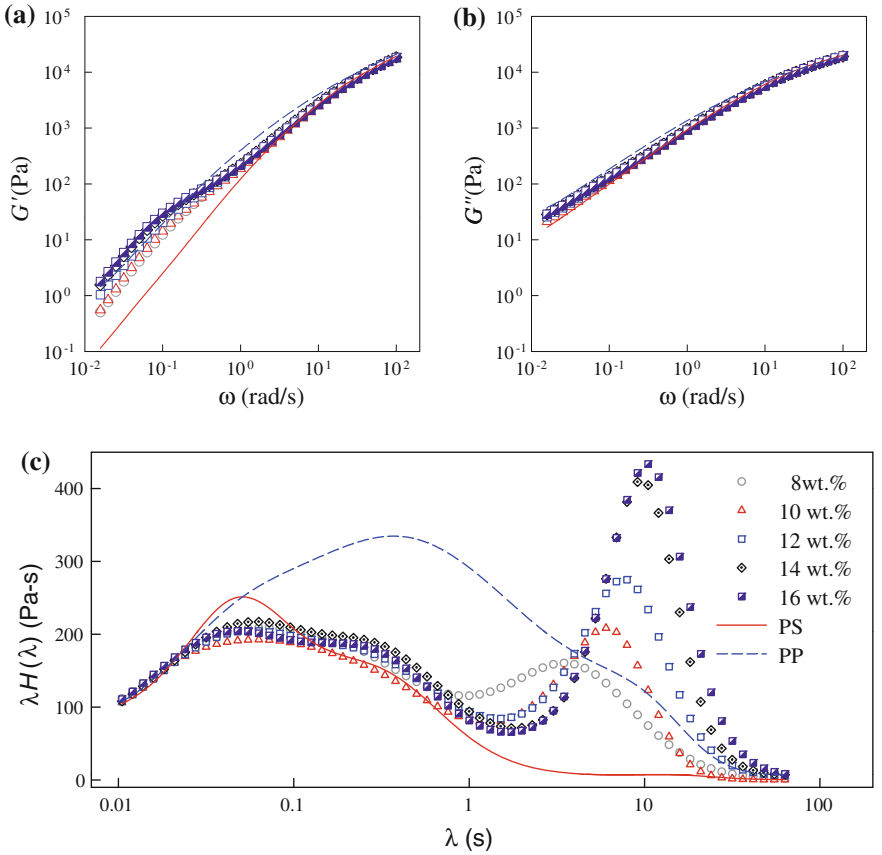

Fig. 8 Dynamic moduli and weighted spectrum of PP/PS blends. Pure PP and PS have weight-average molecular weights of 340 and 350 kg/mol, respectively. The mixtures were blended in an internal mixer at 200 °C and 50 rpm with the addition of 0.15 phr antioxidant (Irganox 1076) for 5 min. The same thermal history was given to neat PS and PP. The weight fractions in the legend are those of PP (disperse phase). The rheological measurement was done at 250 °C in the atmosphere of N_2 (Kwon and Cho 2016)

effect of interface, Fig. 8c shows that additional peak at long-time regime varies according to the amount of disperse phase in a systematic way. Hence, it can be said that the picture of Gramespacher and Meissner, Eq. (3.8) and the use of weighted spectrum, is very effective in characterize immiscible blends of polymers. Note that the spectrum was calculated by a modified version of fixed-point iteration of Cho and Park (2013) [see Eq. (2.28) in Chap. 7].

3.3 The Palierne Model

Although the GM model agrees with experimental data quite well, there is not clear reason why Eq. (3.8) is valid. The formulation of Eq. (3.8) is ad hoc. Two years before the GM model, Palierne (1990) developed a model for the dynamic modulus of the mixture of viscoelastic materials on more rigorous theoretical foundation. The Palierne model is given by

$$G^*(\omega) = G^*_{\text{mat}}(\omega)\frac{1+3\sum_i \phi_i P^*_i(\omega)}{1-2\sum_i \phi_i P^*_i(\omega)} \tag{3.10}$$

where ϕ_i is the volume fraction of disperse phases whose radius is R_i and

$$P^*_i(\omega) = \frac{4\frac{\alpha}{R_i}\left[2G^*_{\text{mat}}(\omega)+5G^*_{\text{dis}}(\omega)\right] - \left[G^*_{\text{mat}}(\omega)-G^*_{\text{dis}}(\omega)\right]\left[16G^*_{\text{mat}}(\omega)+19G^*_{\text{dis}}(\omega)\right]}{40\frac{\alpha}{R_i}\left[G^*_{\text{mat}}(\omega)+G^*_{\text{dis}}(\omega)\right] + \left[3G^*_{\text{mat}}(\omega)+2G^*_{\text{dis}}(\omega)\right]\left[16G^*_{\text{mat}}(\omega)+19G^*_{\text{dis}}(\omega)\right]} \tag{3.11}$$

Although the original Palierne model considers the distribution of the size of disperse phases as shown in Eq. (3.10), it is difficult to infer the distribution from rheological data. Hence, it is more convenient to use the average value of the size of disperse phase:

$$G^*(\omega) = G^*_{\text{mat}}(\omega)\frac{1+3\phi P^*(\omega)}{1-2\phi P^*(\omega)} \tag{3.12}$$

where $P^*(\omega)$ has the same mathematical form of Eq. (3.11) instead of use of R instead of R_i

Compared with the GM model, it is extremely complicate to evaluate the dynamic moduli of the Palierne model. However, the Palierne mode does not need the identification of the zero-shear viscosities of pure ingredients, which requires the data of the terminal region.

3.4 Comparison of the GM and the Palierne Models

Note that the GM model is simple but is not as rigorous as the Palierne model. However, the prediction powers of the two models are almost equivalent. Using the experimental data of pure PP and PS shown in Fig. 8, one may calculate dynamic moduli of PP/PS mixtures with varying both ϕ and α/R. Figure 9 compares the simulated data of storage modulus from the Palierne and the GM models. As shown in Fig. 9, both two models are nearly identical.

Figure 10 shows the comparison of the two models in terms of weighted spectrum with fixing the value of α/R as 1000 Pa. As volume fraction of dispersed

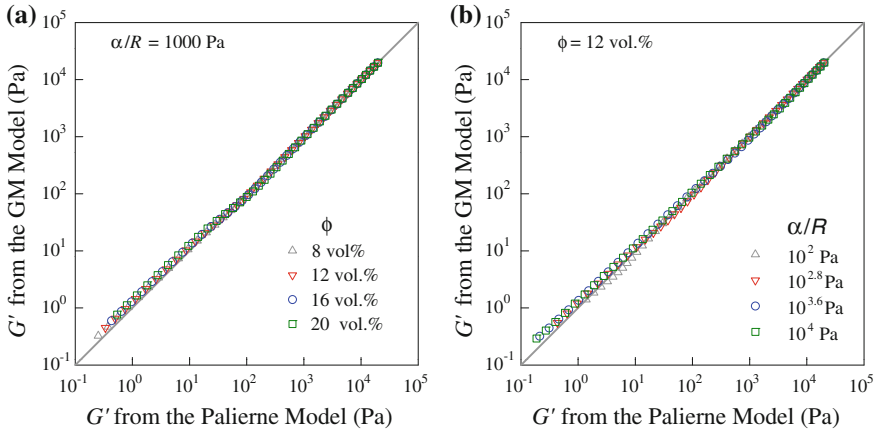

Fig. 9 Comparison of the GM and the Palierne models in terms of storage modulus: **a** various volume fractions of PP at a fixed value of $\alpha/R = 1000\,\text{Pa}$; **b** various values of α/R at a fixed volume fraction of PP, $\phi = 12\,\text{vol.\%}$

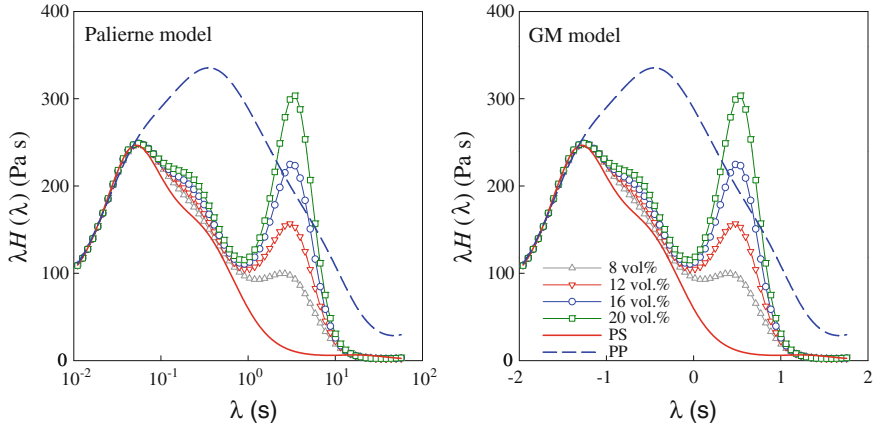

Fig. 10 The effect of the volume fraction of disperse phase. The value of α/R is fixed as 1000 Pa. Both two models behave similarly. The height of interfacial peak increases as the volume fraction and the position moves longer time

phase increases, both models predict that the height of interfacial peak increases. The weighted spectra of two models look same. Hence, it can be said that the two models behave almost equal. Figure 11 compares the two models in terms of weighted spectrum with fixing volume fraction of dispersed phase, $\phi = 12$ vol.%. Here, H_{int} is defined as

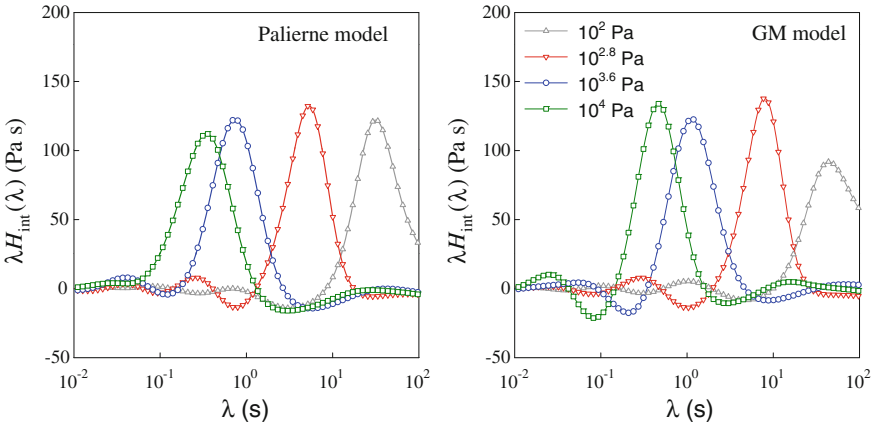

Fig. 11 The effect of α/R on the interfacial peak of weighted spectrum of immiscible PP/PS blends. The volume fraction of disperse phase is 12 vol.%

$$H_{\text{int}}(\lambda) = H(\lambda) - \phi H_{\text{dis}}(\lambda) - (1-\phi) H_{\text{mat}}(\lambda) \tag{3.13}$$

This definition of interfacial spectrum is based on Eq. (3.8) of the GM model. As shown in Fig. 11, both the height and the width of interfacial peak are nearly independent of α/R, while the center of the interfacial peak moves shorter time.

Here, we have found the importance of relaxation spectrum because it gives better and clear understanding than dynamic moduli.

Problem 3

[1] Sketch the plot of the center of interfacial peak as a function of the volume fraction of disperse phase. Assume that $k = 1$.
[2] Explain why weighted relaxation spectrum looks like a peak, while the original spectrum does not.
[3] Explain why the distribution of R cannot be determined by the Palierne model although the model includes the distribution.
[4] What is the condition that the Palierne model can be applied to the suspension of solid particle in a viscoelastic fluid.

References

J.-E. Bae, K.S. Cho, Logarithmic method for continuous relaxation spectrum and comparison with previous methods. J. Rheol. **59**, 1081–1112 (2015)
M. Baumgaertel, M.E. De Rosa, J. Machado, M. Masse, H.H. Winter, The relaxation time spectrum of nearly monodisperse polybutadiene melts. Rheol. Acta **31**, 75–82 (1992)

A. Benallal, G. Marin, J.P. Montfort, C. Derail, Linear viscoelasticity revisted: the relaxation function of monodisperse polymer melts. Macromolecules **26**, 7229–7235 (1993)
K.S. Cho, G.W. Park, Fixed-point iteration for relaxation spectrum from dynamic mechanical data. J. Rheol. **57**, 647–678 (2013)
K.S. Cho, K.H. Ahn, S.J. Lee, Simple method for determining the critical molecular weight from the loss modulus. J. Polym. Sci., Part B: Polym. Phys. Ed. **42**, 2730–2737 (2004a)
K.S. Cho, K.H. Ahn, S.J. Lee, Universality of linear viscoelasticity of monodisperse linear polymers. J. Polym. Sci., Part B: Polym. Phys. Ed. **42**, 2730–2737 (2004b)
K.S. Cho, J.W. Kim, J.-E. Bae, J.H. Youk, H.J. Jeon, K.-W. Song, Effect of temporary network structure on linear and nonlinear viscoelasticity of polymer solutions. Korea-Australia Rheol. J. **27**, 151–161 (2015)
S.J. Choi, W.R. Schowalter, Rheological properties of nondilute suspensions of deformable particles. Phys. Fluids **18**, 420–427 (1975)
R.H. Colby, L.J. Fetters, W.W. Graessley, Melt viscosity-molecular weight relationship for linear polymers. Macromolecules **20**, 2226–2237 (1987)
J. des Cloizeaux, Double reptation vs. simple reptation in polymer melts. Europhys. Lett. **5**, 437–442 (1988)
R.M.L. Evans, M. Tassieri, D. Auhl, T.A. Waigh, Direct conversion of rheological compliance measurements into storage and loss moduli. Phys. Rev. E **80**, 012501 (2009)
L.J. Fetters, D.J. Lohse, D. Richter, T.A. Witten, A. Zirkel, Connection between polymer molecular weight, density, chain dimensions, and melt viscoelastic properties. Macromolecules **27**, 4639–4647 (1994)
K. Fuchs, C. Friedrich, J. Weese, Viscoelastic properties of narrow-distribution poly(methyl methacrylates). Macromolecules **29**, 5893–5901 (1996)
H. Gramespacher, J. Meissner, Interfacial tension between polymer melts measured by shear oscillations of their blends. J. Rheol. **36**, 1127–1141 (1992)
J.D. Guzmán, J.D. Schieber, R. Pollard, A regularization-free method for the calculation of molecular weight distributions from dynamic moduli data. Rheol. Acta **44**, 342–351 (2005)
Y. Heo, R.G. Larson, Universal scaling of linear and nonlinear rheological properties of semidilute and concentrated polymer solutions. Macromolecules **41**, 8903–8915 (2008)
J. Honerkamp, J. Weese, Determination of the relaxation spectrum by a regularization method. Macromolecules **22**, 4327–4377 (1989)
J. Honerkamp, J. Weese, A nonlinear regularization method for the calculation of relaxation spectra. Rheol. Acta **32**, 65–73 (1993)
M.K. Kwon, K.S. Cho, Analysis of the Paliern model by relaxation time spectrum. Korea-Australia Rheol. J. **28**, 1–9 (2016)
F. Léonardi, J.-C. Majesté, A. Allal, G. Marin, Rheological models based on the double reptation mixing rule: the effect of a polydisperse environment. J. Rheol. **44**, 675–692 (2000)
D. Maier, A. Eckstein, Cr Fredrich, J. Honerkamp, Evaluation of models combining rheological data with the molecular weight distribution. J. Rheol. **42**, 1153–1173 (1998)
G. Marin, W.W. Graessley, Viscoelastic properties of high molecular weight polymers in the molten state I. Study of narrow molecular weight distribution samples. Rheol. Acta **16**, 527–533 (1977)
J.F. Palierne, Linear rheology of viscoelastic emulsions with interfacial tension. Rheol. Acta **29**, 204–214 (1990)
C. Pattamaprom, R.G. Larson, Predicting the linear viscoelastic properties of monodisperse and polydisperse polystyrenes and polyethylenes. Rheol. Acta **40**, 516–532 (2001)
C. Pattamaprom, R.G. Larson, T.J. Van Dyke, Quantitative predictions of linear viscoelastic rheological properties of entangled polymers. Rheol. Acta **39**, 517–531 (2000)
C. Pattamaprom, R.G. Larson, A. Sirivat, Determining polymer molecular weight distributions from rheological properties using the dual-constraint model. Rheol. Acta **47**, 689–700 (2008)

M. Rubinstein, H. Colby, *Polymer Physics* (Oxford University Press, Oxford, 2003)
A. Schausberger, G. Schindlauer, H.J. Krigl, Linear elasto-viscous properties of molten standard polystyrenes. I. Presentation of complex moduli; role of short range structural parameters. Rheol. Acta **24**, 220–227 (1985)
P. Scholz, D. Froelich, R. Muller, Viscoelastic properties and morphology of two-phase polypropylene/polyamide 6 blends in the melt. Interpretation of results with an emulsion model. J. Rheol. **33**, 481–499 (1989)
V. Shaayegan, P. Wood-Adams, N.R. Demarquette, Linear viscoelasticity of immiscible blends: the application of creep. J. Rheol. **56**, 1039–1056 (2012)
C. Tsenoglou, Molecular weight polydispersity effects on the viscoelasticity of entangled linear polymers. Macromolecules **24**, 1762–1767 (1991)

Part III
Nonlinear Viscoelasticity

Chapter 10
Nonlinear Constitutive Equations

Abstract This chapter deals with how to measure nonlinear viscoelastic functions and various nonlinear viscoelastic constitutive equations. Since there have been developed a number of constitutive equations which cannot be included in a single chapter, this chapter considers only a few popularly used ones, which are classified to four groups: the models based on mathematical approximations; the models obtained from the generalization of linear viscoelastic models; the models based on the simplification of polymer structure; and the Leonov model which is a class of constitutive equations based on irreversible thermodynamics.

A polymeric fluid shows various flow phenomena which cannot be described by viscous fluid models. Such phenomena are abnormal die swell, nonzero normal stress difference in shear flow, rod climbing, and so on (Bird et al. 1987b; Tanner 2002). We have discussed the problem which appears from the 3D extension of linear viscoelastic models such as the Maxwell or the Jeffreys models [see Sect. 5 in Chap. 2]. Since the birth of the Society of Rheology, development of admissible constitutive equation has been one of the most important themes of rheology. In this chapter, we shall survey formulation of nonlinear viscoelastic constitutive equations.

1 Rheometrics

Rheological measurements are usually based on fluid mechanical calculations which are solving the set of partial differential equations such as balance equations and constitutive equations. It is extremely difficult to find the exact solution of the set of nonlinear partial differential equations. Furthermore, for most cases, we do not know whether the exact solution is unique or not. For some simple problems, the symmetry of the flow geometry allows us to recognize a rough mathematical form of the velocity field. This form is nearly independent of constitutive equation and is very helpful to make the problem simpler. Hence, before studying

K.S. Cho, *Viscoelasticity of Polymers*, Springer Series
in Materials Science 241, DOI 10.1007/978-94-017-7564-9_10

formulation of nonlinear viscoelastic constitutive equations, it is necessary to study kinematics of flow, which is helpful for understanding the physical meanings of the parameters of the constitutive equations as well as identification of the parameters. Rheometrics is the study on how to measure rheological properties of materials with minimizing the information on constitutive equation.

We can form curves which are tangent to the velocity vector of the flow at a given time. A collection of such curves is called *streamlines*. We consider the case that streamlines do not intersect. An example is *laminar flow* in which the space of the flow consists of parallel layers of the same velocity. Then, we can construct a curvilinear coordinate system which has the coordinate line of ξ^1 as the streamlines. We know that the general form of velocity field can be expressed by

$$\mathbf{v}(\mathbf{x}, t) = \nu(\mathbf{x}, t)\mathbf{a} \tag{1.1}$$

Here, we defined the unit vector $\mathbf{a}$ by

$$\mathbf{a} = \frac{\mathbf{g}_1}{\|\mathbf{g}_1\|} \tag{1.2}$$

Note that the unit vector $\mathbf{a}$ represents the flow direction and the base vector $\mathbf{g}_1$ was defined in Eq. (3.15). Then, the scalar function $\nu(\mathbf{x}, t)$ is the magnitude of the velocity field.

If $\nu(\mathbf{x}, t)$ is independent of the coordinate ξ^1, then it can be said that the magnitude of velocity field varies in a direction perpendicular to the flow direction. It is obvious that $\nu(\mathbf{x}, t) = \bar{\nu}\left(\xi^2, \xi^3, t\right)$. Such flow is called *shear flow*. If $\nu(\mathbf{x}, t) = \bar{\nu}\left(\xi^1, t\right)$, then the flow is called *extensional flow*.

Since a polymeric fluid can be approximated as incompressible one, it is basically assumed that velocity field satisfies $\nabla \cdot \mathbf{v} = 0$.

1.1 Shear Flow

1.1.1 Generalized Shear Flow

We are interested in the velocity field such that

$$\mathbf{v} = \nu\left(\xi^2, \xi^3, t\right)\mathbf{a} \tag{1.3}$$

Of course, $\mathbf{a}$ is the unit vector defined by Eq. (1.2). The definition of shear flow and the incompressibility condition gives the following equations:

$$\mathbf{a} \cdot \nabla v = 0 \tag{1.4}$$

and

$$\nabla \cdot \mathbf{a} = 0 \tag{1.5}$$

Equation (1.4) can be understood easily by the consequence of Eq. (1.3):

$$\nabla v = \frac{\partial v}{\partial \xi^2}\mathbf{g}^2 + \frac{\partial v}{\partial \xi^3}\mathbf{g}^3 \tag{1.6}$$

Since $\mathbf{a}$ is a unit vector, it is obvious that

$$\nabla(\mathbf{a} \cdot \mathbf{a}) = 2\mathbf{a} \cdot (\nabla \mathbf{a})^{\mathrm{T}} = \mathbf{0} \tag{1.7}$$

If we define

$$\mathbf{b} = \frac{\nabla v}{\|\nabla v\|}; \quad \mathbf{c} = \mathbf{a} \times \mathbf{b} \tag{1.8}$$

then the three unit vectors form an orthonormal basis. Then, the deformation rate tensor of Eq. (1.3) is given by

$$\mathbf{D} = \frac{\|\nabla v\|}{2}(\mathbf{ab} + \mathbf{ba}) + \frac{\nu}{2}\left[\nabla \mathbf{a} + (\nabla \mathbf{a})^{\mathrm{T}}\right] \tag{1.9}$$

Simple geometry of a shear flow is very helpful for easy measurement of rheological quantities such as shear viscosity and normal stress difference. The simple shear flow may be expressed by

$$\mathbf{v} = \dot{\gamma}(\mathbf{b} \cdot \mathbf{x})\mathbf{a} \tag{1.10}$$

where $\mathbf{a}$ and $\mathbf{b}$ are mutually orthogonal and constant unit vectors and $\dot{\gamma}$ is a positive function of time. In this case, the deformation rate tensor is given by

$$\mathbf{D} = \frac{\dot{\gamma}}{2}(\mathbf{ab} + \mathbf{ba}) \tag{1.11}$$

This agrees with the definition of shear rate Eq. (3.59) in Chap. 2. Tanner (2002) roughly defined *viscometric flow* which has the deformation rate tensor like Eq. (1.11). Several examples are listed in Tanner (2002).

1.1.2 Simple Examples of Viscometric Shear Flows

The parallel flow is the one that has the slip surface $v(x, y, t) =$ constant. Slip surface is the surface on which the same velocity is assigned. If all slip surfaces are parallel to $\mathbf{e}_3$, then the velocity field is given by

$$\mathbf{v} = \mathrm{v}(x, y, t)\mathbf{e}_3 \tag{1.12}$$

In this case, shear rate is given by

$$\dot{\gamma} = \|\nabla v\| \tag{1.13}$$

and the deformation rate tensor is given by Eq. (1.11). Note that $\mathbf{a} = \mathbf{e}_3$, and $\mathbf{b}$ is the unit vector in the direction of ∇v. Note that $\nabla \mathbf{a} = \mathbf{0}$ in this case.

For circular geometry, one may find the following velocity field such that:

$$\mathbf{v} = r\Omega(r, z, t)\mathbf{e}_\phi \tag{1.14}$$

In this case, $\mathbf{a} = \mathbf{e}_\phi$ and we have

$$\nabla \mathbf{e}_\phi + \left(\nabla \mathbf{e}_\phi\right)^T = -\frac{1}{r}\left(\mathbf{e}_\phi \mathbf{e}_r + \mathbf{e}_r \mathbf{e}_\phi\right) \tag{1.15}$$

It is interesting that the deformation rate tensor is given by

$$\mathbf{D} = r\left(\nabla \Omega \mathbf{e}_\phi + \mathbf{e}_\phi \nabla \Omega\right) \tag{1.16}$$

Note that if we set $\mathbf{b} = \nabla\Omega/\|\nabla\Omega\|$ instead of $\mathbf{b} = \nabla v/\|\nabla v\|$, then Eq. (1.16) has the form of Eq. (1.11) with

$$\dot{\gamma} = r\|\nabla\Omega\| \tag{1.17}$$

The Poiseuille flow is the pressure-driven shear flow whose velocity field is given by

$$\mathbf{v} = \mathrm{v}(r, t)\mathbf{e}_3 \quad \text{with } r = \sqrt{x^2 + y^2} \tag{1.18}$$

In this case, we know that $\mathbf{a} = \mathbf{e}_3$ and $\mathbf{b} = \mathbf{e}_r$. Here, we use the cylindrical coordinates. Then, the deformation rate tensor is given by

$$\mathbf{D} = \dot{\gamma}(\mathbf{e}_3 \mathbf{e}_r + \mathbf{e}_r \mathbf{e}_3) \text{ with } \dot{\gamma} = \left|\frac{\partial \mathrm{v}}{\partial r}\right| \tag{1.19}$$

1.1.3 Stresses in Steady Viscometric Flows

In simple shear flow, deformation gradient of the flow is given by $\mathbf{F} = \mathbf{I} + \gamma \mathbf{e}_1 \mathbf{e}_2$ where $\mathbf{I}$ is the identity tensor. Change in the coordinate system does not alter physical phenomena. Consider a physical process that is described by two coordinate systems such that

$$\mathbf{e}_1' = -\mathbf{e}_1, \quad \mathbf{e}_2' = -\mathbf{e}_2, \quad \mathbf{e}_3' = \mathbf{e}_3 \tag{1.20}$$

Because of the symmetry of the simple shear flow, the deformation gradient of the simple shear is invariant over the transform of Eq. (1.20):

$$\mathbf{F} = \mathbf{I} + \gamma \mathbf{e}_1 \mathbf{e}_2 = \mathbf{I} + \gamma' \mathbf{e}'_1 \mathbf{e}'_2; \quad \gamma = \gamma' \tag{1.21}$$

Since the stress of simple shear flow depends on the deformation history, the symmetry of the simple shear flow leads to

$$\begin{aligned} &\mathbf{T} = T_{ik}\mathbf{e}_i\mathbf{e}_k = T'_{ik}\mathbf{e}'_i\mathbf{e}'_k = T_{ik}\mathbf{e}'_i\mathbf{e}'_k \\ &T_{11} = T'_{11}, \quad T_{22} = T'_{22}, \quad T_{33} = T'_{33}, \\ &T_{12} = T'_{12}, \quad T_{23} = -T'_{23}, \quad T_{31} = -T'_{31} \end{aligned} \tag{1.22}$$

Thus, only nonzero components of stress tensor are diagonal components and T_{12}:

$$\mathbf{T} = T_{11}\mathbf{e}_1\mathbf{e}_1 + T_{22}\mathbf{e}_2\mathbf{e}_2 + T_{33}\mathbf{e}_3\mathbf{e}_3 + T_{12}(\mathbf{e}_1\mathbf{e}_2 + \mathbf{e}_2\mathbf{e}_1) \tag{1.23}$$

Equation (1.23) is valid for most shear flows whose deformation rate tensor is given by Eq. (1.11).

Now consider the case of replacement of γ by $-\gamma$. Then, the deformation gradient and the deformation rate are replaced by

$$\mathbf{F} = \mathbf{I} - \gamma \mathbf{e}_1 \mathbf{e}_2; \quad \mathbf{D} = -\frac{\dot{\gamma}}{2}(\mathbf{e}_1\mathbf{e}_2 + \mathbf{e}_2\mathbf{e}_1) \tag{1.24}$$

Equation (1.24) is equivalent to the result from the change of coordinates:

$$\mathbf{e}'_1 = -\mathbf{e}_1; \quad \mathbf{e}'_2 = \mathbf{e}_2; \quad \mathbf{e}'_3 = \mathbf{e}_3 \tag{1.25}$$

Application of the transform of Eq. (1.25) to Eq. (1.23) gives

$$T'_{11} = T_{11}; \quad T'_{22} = T_{22}; \quad T'_{33} = T_{33}; \quad T'_{12} = -T_{12} \tag{1.26}$$

Since the change of the sign of shear strain is equivalent to the change of coordinate, we obtain

$$\begin{aligned} T_{11}(\gamma, \dot{\gamma}) = T_{11}(-\gamma, -\dot{\gamma}); \quad T_{22}(\gamma, \dot{\gamma}) = T_{22}(-\gamma, -\dot{\gamma}); \\ T_{33}(\gamma, \dot{\gamma}) = T_{33}(-\gamma, -\dot{\gamma}); \quad T_{12}(\gamma, \dot{\gamma}) = -T_{12}(-\gamma, -\dot{\gamma}) \end{aligned} \tag{1.27}$$

In steady state, the stress of the shear flow becomes a function of shear rate. Hence, Eq. (1.27) implies that normal stress is an even function of shear rate, while shear stress is an odd function of shear rate.

The definition of the steady shear viscosity is $\eta(\dot{\gamma}) \equiv T_{12}/\dot{\gamma}$. Hence, steady shear viscosity is an even function of shear rate. Furthermore, this symmetry analysis reveals that the response function $\eta(\dot{\gamma})$ must be positive for any shear rate. Since normal stresses are even functions of shear rate, it is obvious that normal stress

differences are also even functions. The first normal stress difference, N_1, is defined as the difference between the normal stresses in the flow direction (**a**) and in the gradient direction (**b**). The second normal stress difference, N_2, is defined as the difference between the normal stresses in the gradient direction (**b**) and in the vorticity direction (**c**). Hence, we know that

$$\begin{aligned} N_1(\dot{\gamma}) &= T_{11}(\dot{\gamma}) - T_{22}(\dot{\gamma}) = N_1(-\dot{\gamma}); \\ N_1(\dot{\gamma}) &= T_{22}(\dot{\gamma}) - T_{33}(\dot{\gamma}) = N_2(-\dot{\gamma}) \end{aligned} \tag{1.28}$$

The symmetric features of normal stresses allow us to define normal stress coefficients such that

$$N_1(\dot{\gamma}) = \dot{\gamma}^2 \psi_1(\dot{\gamma}); \quad N_2(\dot{\gamma}) = \dot{\gamma}^2 \psi_2(\dot{\gamma}) \tag{1.29}$$

This definition results in that normal stress coefficients are even functions of shear rate. Whenever $\dot{\gamma} = 0$, normal stresses become the hydrostatic pressure. Hence, we know that $N_1(0) = N_2(0) = 0$.

Steady shear viscosity and normal stress coefficients are material functions. The stress tensor of steady shear flow can be expressed in terms of the material functions as follows (Tanner 2002)

$$\mathbf{T} = T_{\mathbf{cc}}\mathbf{I} + \dot{\gamma}\eta(\mathbf{ab} + \mathbf{ba}) + (N_1 + N_2)\mathbf{aa} + N_2\mathbf{bb} \tag{1.30}$$

where $T_{\mathbf{cc}} = \mathbf{c} \cdot \mathbf{T} \cdot \mathbf{c}$.

1.2 Measurement of Steady Viscoelastic Functions

Here, we consider only three most popular shear flows in rheology. These are shear flows in parallel plates and cone and plate of rotational rheometer and the Poiseuille flow in capillary rheometer.

1.2.1 Parallel-Plate Rheometer

Parallel-plate fixture [Fig. 2 in Chap. 5] is one of the most popular fixtures of rotational rheometer, because of the convenience in sample loading. When the fixture rotates at the angular velocity of ω_0, the velocity field in the fixture is given by

$$\mathbf{v} = \frac{r\omega_0 z}{h}\mathbf{e}_\phi \tag{1.31}$$

where h is the gap between the two plates. Note that Eq. (1.31) is equivalent to the case of $\Omega = \omega_0 z/h$ when it is compared with Eq. (1.14). In this case, we also know that

$$\mathbf{a} = \mathbf{e}_\phi; \quad \mathbf{b} = \mathbf{e}_z; \quad \dot{\gamma} = \frac{r}{h}\omega_0. \tag{1.32}$$

Assume that the flow is steady, laminar, and isothermal. If the viscosity of the sample is sufficiently high, then body force can be neglected. Furthermore, it does not deteriorate the results significantly to neglect the effect of cylindrical edge. Then, the equations of motion reduce to

$$\frac{\partial T_{\phi z}}{\partial z} = 0; \quad \frac{\partial T_{zz}}{\partial z} = 0; \quad -\frac{\partial p}{\partial r} + \frac{1}{r}\frac{\partial}{\partial r}\left(rT'_{rr}\right) - \frac{T'_{\phi\phi}}{r} = -\rho\frac{v_\phi^2}{r} \tag{1.33}$$

Note that T'_{zz}, T'_{rr} and $T'_{\phi\phi}$ are components of the extra stress, while $T_{zz} = -p + T'_{zz}$. Note that Eq. (1.33) agrees with Eq. (1.30). The first equation of Eq. (1.33) implies that both $T_{\phi z}$ and T_{zz} depend on only r. In the derivation of Eq. (1.33), we used the assumptions that any quantity in the equations of motion is independent of ϕ.

Rotational rheometer measures the torque M and the normal force F_z. These measurable quantities are related with stress components as follows

$$M = \int rT_{\phi z}\mathrm{d}a = 2\pi\int_0^R r^2 T_{\phi z}(r)\mathrm{d}r \tag{1.34}$$

and

$$F_z = -\int T_{zz}\mathrm{d}a = -2\pi\int_0^R T_{zz}r\mathrm{d}r \tag{1.35}$$

where R is the radius of the circular disk.

With the help of Eq. (1.30), Eq. (1.34) can be rewritten as

$$M = 2\pi\int_0^R \eta(\dot{\gamma})\dot{\gamma}r^2\mathrm{d}r \tag{1.36}$$

Since $\dot{\gamma} = r\omega_0/h$, we can replace r by shear rate:

$$m \equiv \frac{M}{2\pi R^3} = \frac{1}{\dot{\gamma}_R^3}\int_0^{\dot{\gamma}_R} \eta(\dot{\gamma})\dot{\gamma}^3\mathrm{d}\dot{\gamma} \tag{1.37}$$

where $\dot{\gamma}_R = R\omega_0/h$. If the torque at steady state is measured as a function of angular velocity ω_0, then we can obtain the plot of m as a function of $\dot{\gamma}_R$. Numerical differentiation of the plot gives the shear viscosity:

$$\eta(\dot{\gamma}_R) = \frac{m}{\dot{\gamma}_R}\left(3 + \frac{\mathrm{d}\log m}{\mathrm{d}\log \dot{\gamma}_R}\right) \tag{1.38}$$

Note that Eq. (1.38) can be obtained by the differentiation of both sides of Eq. (1.37) with respect to $\dot{\gamma}_R$.

Neglecting the inertia term ($\rho v_\varphi^2/r \approx 0$), the third equation of Eq. (1.33) can be rewritten as

$$\frac{\mathrm{d}T_{rr}}{\mathrm{d}r} = \frac{N_1 + N_2}{r} \tag{1.39}$$

Since $T_{rr} = T_{zz} - N_2$, we have

$$\frac{\mathrm{d}T_{zz}}{\mathrm{d}r} = \frac{\mathrm{d}N_2}{\mathrm{d}r} + \frac{N_1 + N_2}{r} \tag{1.40}$$

Using the boundary conditions $T_{zz}(R) = T_{rr}(R) = 0$, integration of Eq. (1.39) gives

$$T_{zz}(r) = N_2(r) - \int_r^R \frac{N_1(\zeta) + N_2(\zeta)}{\zeta}\mathrm{d}\zeta \tag{1.40}$$

Substitution of Eq. (1.40) to Eq. (1.35) gives

$$F_z = -2\pi \int_0^R rN_2\mathrm{d}r + 2\pi \int_0^R r\Phi(r)\mathrm{d}r \tag{1.41}$$

where

$$\Phi(r) \equiv \int_r^R \frac{N_1(\zeta) + N_2(\zeta)}{\zeta}\mathrm{d}\zeta \tag{1.42}$$

Application of integration by parts to Eq. (1.41) gives

$$F_z = -2\pi \int_0^R rN_2\mathrm{d}r + \pi\left[r^2\Phi(r)\right]_{r=0}^{r=R} - \pi \int_0^R r^2 \frac{\mathrm{d}\Phi}{\mathrm{d}r}\mathrm{d}r \tag{1.43}$$

Note that

$$\frac{\mathrm{d}\Phi}{\mathrm{d}r} = -\frac{N_1(r) + N_2(r)}{r} \tag{1.44}$$

Substitution of Eq. (1.44) to Eq. (1.43) gives

$$F_z = \pi \int_0^R [N_1(r) - N_2(r)] r \mathrm{d}r \tag{1.45}$$

Changing the variable from r to $\dot{\gamma}_R$ and differentiating in a suitable way, we have finally

$$N_1(\dot{\gamma}_R) - N_2(\dot{\gamma}_R) = \frac{F_z}{\pi R^2}\left(2 + \frac{\mathrm{d}\log F_z}{\mathrm{d}\log \dot{\gamma}_R}\right) \tag{1.46}$$

1.2.2 Cone-and-Plate Rheometer

The geometry of cone-and-plate fixture is described in Fig. 2 in Chap. 5. Note that we need spherical coordinate system in order to treat the kinematics. Figure 1 is helpful for more easily understanding the kinematics:

$$\mathbf{v} = \mathrm{v}(r, \theta)\mathbf{e}_\phi \tag{1.47}$$

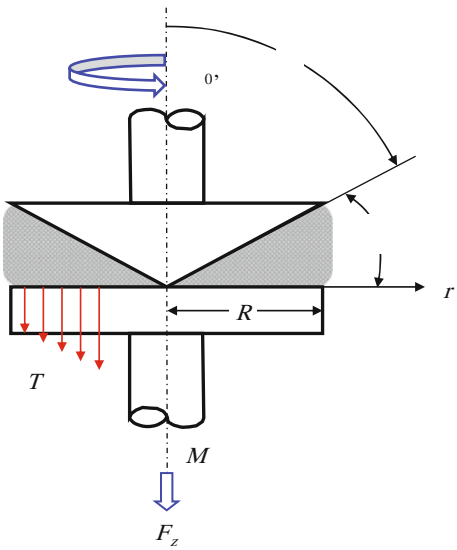

Fig. 1 The geometry of cone-and-plate rheometer

The symmetry of the geometry implies that any quantity in the equations of motion is independent of ϕ. Then, the equations of motion become simpler as follows

$$\begin{aligned}\frac{\rho v^2}{r} &= -\frac{\partial p}{\partial r} + \frac{1}{r^2}\frac{\partial}{\partial r}\left(r^2 T'_{rr}\right) - \frac{T'_{\theta\theta} + T'_{\phi\phi}}{r};\\ 0 &= -\frac{1}{r}\frac{\partial p}{\partial \theta} + \frac{1}{r\sin\theta}\frac{\partial\left(T'_{\theta\theta}\sin\theta\right)}{\partial\theta} - \frac{T'_{\theta\theta}\cot\theta}{r}\\ 0 &= \frac{1}{r}\frac{\partial T'_{\theta\phi}}{\partial\theta} + \frac{2T'_{\theta\phi}\cot\theta}{r}\end{aligned} \tag{1.48}$$

The boundary conditions are given by

$$v\left(r, \frac{\pi}{2}\right) = 0; \quad v\left(r, \frac{\pi}{2} - \beta\right) = r\omega_0 \sin\left(\frac{\pi}{2} - \beta\right) \tag{1.49}$$

Note that the angle β is very small ($\beta < 0.1$ rad). Then, the last equation in Eq. (1.49) can be simplified as

$$v\left(r, \frac{\pi}{2} - \beta\right) = r\omega_0 \tag{1.50}$$

From the geometry, we know that the latitude angle has the range of

$$\frac{\pi}{2} - \beta < \theta < \frac{\pi}{2} \tag{1.51}$$

Since the range of the latitude angle is very small, we can use the following approximation:

$$\cot\theta = \cot\left(\frac{\pi}{2} - \beta + \vartheta\right) \approx \tan(\beta - \vartheta) \approx \beta - \vartheta \tag{1.52}$$

where $0 < \vartheta < \beta$. Use of this approximation allows us to assume that

$$v(r, \theta) \approx \frac{r\omega_0}{\beta}\left(\frac{\pi}{2} - \theta\right) \tag{1.53}$$

Then, we have

$$\dot{\gamma} \approx \frac{\omega_0}{\beta} \tag{1.54}$$

This result is very important because shear rate is nearly constant over the whole region of sample.

It is not difficult to calculate the torque M in terms of shear stress $T_{\phi\theta}$:

$$T_{\phi\theta} = \frac{3M}{2\pi R^3 \sin^2\theta} \approx \frac{3M}{2\pi R^3} \tag{1.55}$$

Hence, the steady shear viscosity is given by

$$\eta = \frac{3\beta}{2\pi R^3}\frac{M}{\omega_0} \tag{1.56}$$

The normal force exerted on the fixture can be calculated by

$$F_z = -2\pi \int_0^R T_{\theta\theta}\left(r, \frac{\pi}{2}\right) r dr \tag{1.57}$$

Hence, we need to integrate the first equation of Eq. (1.48). As before, we neglect the inertia term. Then, we have

$$\frac{\partial T_{rr}}{\partial r} = \frac{N_1 + 2N_2}{r} \tag{1.58}$$

Since $T_{\theta\theta} = N_2 + T_{rr}$, Eq. (1.58) can be rewritten as

$$\frac{\partial T_{\theta\theta}}{\partial r} = \frac{\partial N_2}{\partial r} + \frac{N_1 + 2N_2}{r} \tag{1.59}$$

Note that viscoelastic functions such as η, N_1, and N_2 depend on only shear rate which is independent of r in this case. Hence, we have

$$\frac{\partial T_{\theta\theta}}{\partial r} = \frac{N_1 + 2N_2}{r} \tag{1.60}$$

Application of integration by parts to Eq. (1.57) and use of Eq. (1.60) gives

$$\frac{F_z}{\pi R^2} = \frac{N_1 + 2N_2}{2} - T_{\theta\theta}\left(R, \frac{\pi}{2}\right) \tag{1.61}$$

Since the normal stress on free surface is zero if surface tension is negligible, we know that $T_{rr}(R, \frac{1}{2}\pi) = 0$ and $N_2 = T_{\theta\theta}(R, \frac{1}{2}\pi)$. Then, we finally have

$$N_1 = \frac{2F_z}{\pi R^2} \tag{1.62}$$

Rotational rheometer is apt to suffer from the effects of inertia, secondary flow, and edge effect whenever shear rate is sufficiently high. The correction is discussed in Münstedt and Laun (1981).

1.2.3 Capillary Rheometer

Rotational rheometer is a convenient device for rheological properties because it works for oscillatory shear flow as well as steady shear flow. Furthermore, it can be used for the measurement of extensional viscosity if some special fixture such as SER^{TM} is applied. However, centrifugal problem prevents from the measurement of steady shear viscosity at high shear rate. If steady shear viscosity at high shear rate is necessary, alternative is capillary rheometer. Capillary rheometer consists of reservoir, capillary die, speed controllable piston, and pressure sensor (see Fig. 2).

Capillary rheometer controls the speed of the piston V. Then, the flow rate is given by $Q = VA$ where A is the cross-sectional area of the reservoir containing polymer melt. The pressure sensor located at the bottom of the reservoir measures pressure difference Δp of the polymer melt from ambient pressure. We shall show that Q and Δp are used for the calculation of shear rate and shear stress at the wall of the capillary die, respectively. The dimension of the capillary die is represented by the length and the diameter.

Because of high viscosity of the polymer melt, the flow by only gravitation is hard to occur. Hence, we can neglect the effect of body force. Because of circular symmetry, the velocity field in the capillary die at steady state is given by

$$\mathbf{v} = \nu(r)\mathbf{e}_z \tag{1.63}$$

Note that any quantity in the equations of motion is independent of azimuthal angle ϕ again. Then, we have to consider only a single equation of motion:

$$\frac{\partial p}{\partial z} = \frac{1}{r}\frac{\mathrm{d}}{\mathrm{d}r}\left(rT'_{rz}\right) \tag{1.64}$$

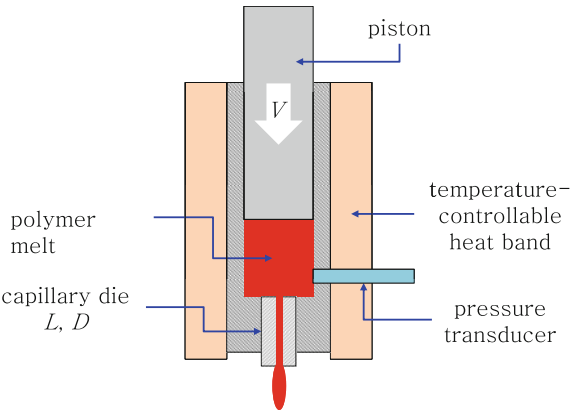

Fig. 2 Schematic description of capillary rheometer

Note that equations of other directions give $\partial p/\partial\phi = \partial p/\partial r = 0$. Since the left-hand side of Eq. (1.64) is a function of z, the right hand is a function of r. This implies that $\partial p/\partial z$ must be a constant:

$$\frac{\partial p}{\partial z} = \frac{\Delta p}{L} \tag{1.65}$$

where L is the length of the capillary die. Integration of Eq. (1.64) gives

$$T'_{rz} = \frac{\Delta p}{2L} r \tag{1.66}$$

It must be noted that Eq. (1.66) is valid for any viscoelastic fluid. Since the shear stress on the wall of the capillary die is

$$T_w \equiv T'_{rz}(R) = \frac{\Delta p}{2L} R \tag{1.67}$$

it is convenient to use

$$T'_{rz} = \frac{T_w}{R} r \tag{1.68}$$

The volume flow rate can be calculated easily:

$$Q = 2\pi \int_0^R \nu(r) r \mathrm{d}r \tag{1.69}$$

Nonslip assumption gives $\nu(R) = 0$. Application of integration by parts gives

$$Q = -\pi \int_0^R r^2 \frac{\mathrm{d}v}{\mathrm{d}r} \mathrm{d}r \tag{1.70}$$

Using Eq. (1.68), we will change the variable from r to T_w. Then, we have

$$\frac{3T_w^2 Q}{\pi R^3} = -\int_0^{T_w} \tau^2 \frac{\mathrm{d}v}{\mathrm{d}r} \mathrm{d}\tau \tag{1.71}$$

Differentiation with respect to T_w gives

$$\frac{3T_w^2 Q}{\pi R^3} + \frac{T_w^3}{\pi R^3} \frac{\mathrm{d}Q}{\mathrm{d}T_w} = T_w^2 \dot{\gamma}_w \tag{1.72}$$

where

$$\dot{\gamma}_w = -\left.\frac{\mathrm{d}v}{\mathrm{d}r}\right|_{T_w} \tag{1.73}$$

Note that the minus sign is introduced to Eq. (1.73) because $\mathrm{d}v/\mathrm{d}r < 0$ and shear rate is defined to be positive. Rearrangement of Eq. (1.72) gives the *Weissenberg–Rabinowitsch equation:*

$$\dot{\gamma}_w = \frac{\dot{\gamma}_\mathrm{A}}{4}\left(3 + \frac{\mathrm{d}\log Q}{\mathrm{d}\log T_w}\right) \tag{1.74}$$

where $\dot{\gamma}_\mathrm{A}$ is the apparent shear rate which is defined as

$$\dot{\gamma}_A = \frac{4Q}{\pi R^3} \tag{1.75}$$

Since Q is controlled by V and T_w is determined by the measurement of pressure difference Δp, numerical differentiation of the data determines $\mathrm{d}\log Q/\mathrm{d}\log T_w$. Finally, shear viscosity is obtained by

$$\eta = \frac{T_w}{\dot{\gamma}_w} = \frac{\pi R^4 \Delta p}{2QL}\frac{n}{3n+1} \tag{1.76}$$

where

$$n \equiv \frac{\mathrm{d}\log \Delta p}{\mathrm{d}\log Q} \tag{1.77}$$

Note that when $n = 1$, Eq. (1.76) becomes the equation for a Newtonian fluid.

Capillary rheometer is powerful when viscosity at high shear rate is necessary. However, the rheometer suffers from several problems. Because of viscoelasticity of polymer melt, the pressure gradient $\partial p/\partial z$ is not constant. Experimental observation shows that Δp at the exit of the capillary die is not zero. Furthermore, there is an abrupt drop of pressure at the entrance of the capillary die. To remove this discrepancy, the *Bagley correction* is necessary. The Bagley correction can be done by the measurement at various L/R. When L/R is sufficiently large, the effect of abnormal drop of pressure becomes negligible. If shear rate exceeds certain value, then the nonslip condition does not hold. Then, flow instability, called melt fracture, occurs. Since polymer melt has high viscosity, viscous heating is also a problem which occurs at high shear rate. Viscous heating breaks the assumption of isothermal condition. Note that steady shear viscosity of polymer melt depends on both shear rate and temperature.

Another demerit of capillary rheometer is the inability to measure shear viscosity at shear rates lower than 0.1 s^{-1}. It is interesting that smooth superposition is usually found between the plots of steady shear viscosity measured by different

rheometers such as rotational and capillary rheometers (Macosko 1994). Furthermore, the plot of complex viscosity as a function of frequency is also superposed on the plot of steady shear viscosity. It is surprising superposition because steady shear viscosity is a nonlinear viscoelastic function, while complex viscosity is a linear viscoelastic function. This superposition of viscosity data is called the *Cox–Merz relation*.

1.3 Simple Elongational Flow

Consider a circular rod made of incompressible material. Simple elongation is a homogeneous deformation such that

$$r = \frac{\tilde{r}}{\sqrt{\lambda}}; \quad \phi = \tilde{\phi}; \quad z = \lambda \tilde{z} \tag{1.78}$$

where λ is a function of time. Deformation gradient is given by

$$\mathbf{F} = \lambda \mathbf{e}_z \mathbf{e}_z + \frac{1}{\sqrt{\lambda}} \left(\mathbf{e}_r \mathbf{e}_r + \mathbf{e}_\phi \mathbf{e}_\phi \right) \tag{1.79}$$

and velocity gradient is given by

$$\mathbf{L} = (\nabla \mathbf{v})^T = \frac{\mathrm{d} \log \lambda}{\mathrm{d}t} \left[\mathbf{e}_z \mathbf{e}_z - \frac{1}{2} \left(\mathbf{e}_r \mathbf{e}_r + \mathbf{e}_\phi \mathbf{e}_\phi \right) \right] = \mathbf{D} \tag{1.80}$$

Because of symmetry, it is obvious that stress is given by

$$\mathbf{T} = T_{zz} \mathbf{e}_z \mathbf{e}_z + T_{rr} \left(\mathbf{e}_r \mathbf{e}_r + \mathbf{e}_\phi \mathbf{e}_\phi \right) \tag{1.81}$$

Since the lateral surface of the rod is free, it is obvious that $\mathbf{e}_r \cdot \mathbf{T} \cdot \mathbf{e}_r = 0$ on the free surface. This means that $T'_{rr} = -p$. Thus, it can be said that

$$T_{zz} - T_{rr} = \frac{f}{A} \tag{1.82}$$

where f is the force on the both ends of the rod and A is the cross-sectional area of the rod. Because the material is incompressible, the area A is related to the initial area by

$$A = \frac{A_\mathrm{o}}{\lambda} \tag{1.83}$$

Extensional viscosity is defined as

$$\eta_E(\dot{\varepsilon}, t) = \frac{T_{zz} - T_{rr}}{\dot{\varepsilon}} \tag{1.84}$$

where

$$\dot{\varepsilon} = \frac{\mathrm{d}\log\lambda}{\mathrm{d}t} \tag{1.85}$$

If we set $\dot{\varepsilon}$ a constant, then the draw ratio is given by integration of Eq. (1.85):

$$\lambda(t) = \exp(\dot{\varepsilon}t) = \frac{L(t)}{L_\mathrm{o}} \tag{1.86}$$

where $L(t)$ is the length of the rod at time t and L_o is the initial length. Since we can measure force f and control L by Eq. (1.86), we can determine extensional viscosity η_E by experiment.

Implementation of the elongational experiment is not easy because the length of the sample should be increased exponentially as shown in Eq. (1.86). Even a tiny inhomogeneity in the radius of the rod is apt to result in significant errors in extensional viscosity. Hence, reproducibility of the experiment is considerably lower than that of any other rheological measurement.

If the rod is not broken, the extensional viscosity may approach to a limit value called steady extensional viscosity $\eta_E(\dot{\varepsilon}, \infty)$. For simplicity, we will denote the steady extensional viscosity as $\eta_E^\infty(\dot{\varepsilon})$. As for a Newtonian fluid, the extensional viscosity is three times of the shear viscosity. This relation is called the *Trouton relation*. It can be extended to viscoelastic fluid by

$$\lim_{\dot{\varepsilon}\to 0} \frac{\eta_E^\infty(\dot{\varepsilon})}{\eta_\mathrm{o}} = 3 \tag{1.87}$$

Laun and Münstedt (1978) compared steady shear viscosity of LDPE with its steady extensional viscosity as shown in Fig. 3. At low $\dot{\varepsilon}$, the zero-extensional viscosity agrees with the Trouton relation.

It is interesting that steady extensional viscosity shows overshot at high extensional rate $\dot{\varepsilon} > 0.001\,\mathrm{s}^{-1}$, while steady shear viscosity shows shear thinning. It can be expected that linear viscoelasticity is valid in the region of deformation rate at which both steady viscosities in shear and extension follow those of Newtonian fluid.

It is well known that extensional viscosity is an indicator of long chain branch. When extensional viscosity is plotted as a function of time, LDPE (having long chain branch) shows strong strain hardening behavior as shown in Fig. 4. Strain hardening means that extensional viscosity increases steeply at a certain time which becomes shorten as extensional rate increases. HDPE has no long chain branch and shows weaker strain hardening.

Problems 1

[1] Show that if velocity field is given by $\mathbf{v} = u(z)\mathbf{e}_1 + \nu(z)\mathbf{e}_2$, then stress tensor is given by

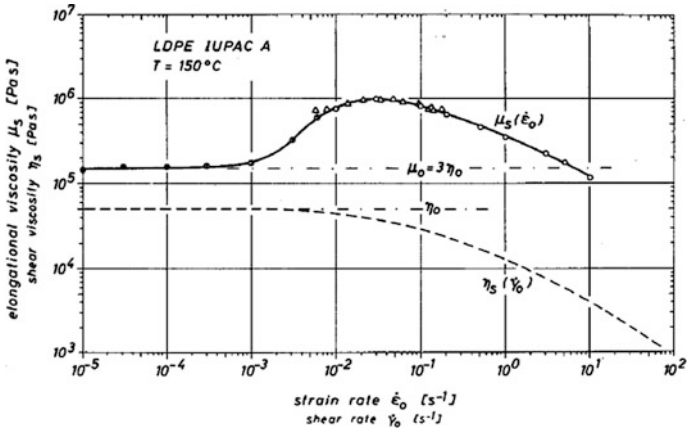

Fig. 3 Comparison of steady extensional viscosity with steady shear viscosity. The graph is the Fig. 5 of Laun and Münstedt (1978)

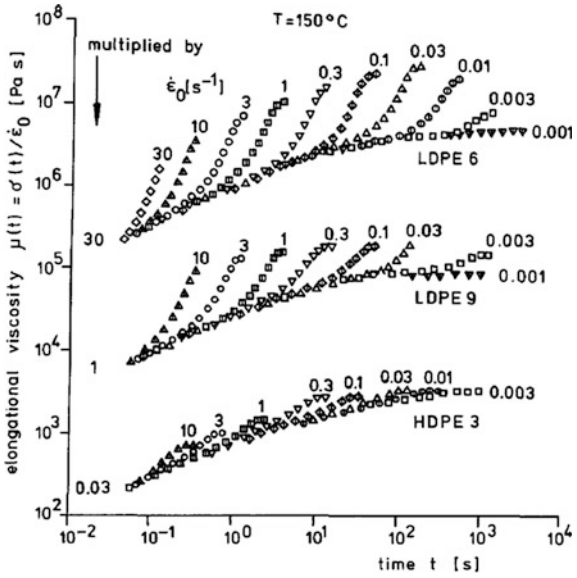

Fig. 4 Typical behavior of extensional viscosity of polyethylene as a function of time. The graph is the Fig. 10 of Münstedt and Laun (1981)

$$\mathbf{T} = -p\mathbf{I} + \eta\left(\frac{\mathrm{d}\mathbf{v}}{\mathrm{d}z}\mathbf{e}_3 + \mathbf{e}_3\frac{\mathrm{d}\mathbf{v}}{\mathrm{d}z}\right) + (\psi_1 + \psi_2)\frac{\mathrm{d}\mathbf{v}}{\mathrm{d}z}\frac{\mathrm{d}\mathbf{v}}{\mathrm{d}z} + \psi_2\left\|\frac{\mathrm{d}\mathbf{v}}{\mathrm{d}z}\right\|^2\mathbf{e}_3\mathbf{e}_3 \qquad (1.a)$$

See Tanner (2002).

[2] Derive Eq. (1.33).

[3] Derive Eq. (1.38).

[4] Derive Eqs. (1.45) and (1.46).

[5] Derive Eq. (1.48).
[6] Consider the Poiseuille flow of a power law fluid such that

$$\mathbf{T} = -p\mathbf{I} + K\dot{\gamma}^m\left[\nabla\mathbf{v} + (\nabla\mathbf{v})^T\right] \tag{1.b}$$

where $0 < m < 1$ and $K > 0$. Calculate $\mathrm{d}\log\Delta p/\mathrm{d}\log Q$.
[7] Derive Eqs. (1.79) and (1.80).
[8] Derive Eq. (1.81) by use of symmetry analysis.

2 Models Based on Expansion

2.1 Rivlin–Ericksen Expansion

The constitutive equation of Newtonian fluid is based on the intuition that the extra stress of the fluid is a linear function of deformation rate tensor. It is one of the most natural ways of developing a constitutive equation to expand a general but formal equation from the well-known previous one. Assume that polymeric fluids are incompressible. Since the stress of a viscoelastic fluid depends on deformation history, the stress can be written formally by

$$\mathbf{T} + p\mathbf{I} = \overset{\tau=t}{\underset{\tau=-\infty}{\mathsf{T}}}[\mathbf{C}_t(\mathbf{x},\tau)] \tag{2.1}$$

where the right-hand side is the extra stress and a tensor-valued functional which involves the effect of deformation at all possible pasts. The effect of past deformation should be smaller if the past time is older. If the observation time is much longer than the material time, low Debora number, then the right-hand side of Eq. (2.1) can be replaced by a proper algebraic function. Assume that the function can be expanded by the Taylor expansion. In Sect. 7 in Chap. 2, we have studied that relative strain measure $\mathbf{C}_t(\mathbf{x},\tau)$ can be expanded by

$$\mathbf{C}_t(\mathbf{x},\tau) = \mathbf{I} + \sum_{n=1}^{\infty}\frac{(\tau - t)^n}{n!}\mathbf{A}_n \tag{2.2}$$

where $\mathbf{A}_n$ is the nth *order Rivlin–Ericksen tensor*.

Before the Taylor expansion, substitution of Eq. (2.2) into Eq. (2.1) gives

$$\mathbf{T} + p\mathbf{I} = \mathbf{G}(\mathbf{A}_1, \mathbf{A}_2, \ldots) \tag{2.3}$$

where $\mathbf{G}(\bullet)$ is an isotropic tensor-valued function. Here, the terms $(\tau - t)^n$ were integrated to material constants. Hence, we want to develop a constitutive equation for slow flow. The series expansion of Eq. (2.3) is given by

$$\mathbf{T} + p\mathbf{I} = \sum_{k=1}^{\infty} b_k \mathbf{A}_k + \sum_{k=1}^{\infty}\sum_{n=1}^{\infty} b_{kn} \mathbf{A}_k \cdot \mathbf{A}_n + \cdots \tag{2.4}$$

Here, b_k, b_{kn}, and so on are called retarded-motion parameters which are functions of the invariants of the Rivlin–Ericksen tensors. Setting all retarded-motion constants zero except b_1, Eq. (2.4) becomes the incompressible Newtonian fluid. *The second-order fluid* is defined by

$$\mathbf{T} = -p\mathbf{I} + b_1 \mathbf{A}_1 + b_{11} \mathbf{A}_1 \cdot \mathbf{A}_1 + b_2 \mathbf{A}_2 \tag{2.5}$$

It should be note that the Rivlin–Ericksen tensors are objective tensors.

For simplicity, consider the simple shear flow of $\mathbf{v} = \dot{\gamma} y \mathbf{e}_1$ where $\dot{\gamma}$ is a constant. As for the shear flow, the Rivlin–Ericksen tensors for the second-order fluid are given by

$$\mathbf{A}_1 = 2\mathbf{D} = \dot{\gamma}(\mathbf{e}_1\mathbf{e}_2 + \mathbf{e}_2\mathbf{e}_1) \tag{2.6}$$

and

$$\mathbf{A}_2 = 2\dot{\gamma}^2 \mathbf{e}_2\mathbf{e}_2 \tag{2.7}$$

Then, Eq. (2.5) gives

$$\mathbf{T} = -p\mathbf{I} + b_{11}\dot{\gamma}^2(\mathbf{I} - \mathbf{e}_3\mathbf{e}_3) + 2b_2\dot{\gamma}^2\mathbf{e}_2\mathbf{e}_2 + b_1\dot{\gamma}(\mathbf{e}_1\mathbf{e}_2 + \mathbf{e}_2\mathbf{e}_1) \tag{2.8}$$

Since the shear viscosity is defined as the shear stress over shear rate, we know that

$$\eta = b_1 \tag{2.9}$$

Although normal stress differences of Newtonian fluid are zero, those of the second-order fluid are given by

$$N_1 \equiv T_{11} - T_{22} = -2b_2\dot{\gamma}^2 \tag{2.10}$$

and

$$N_2 = T_{22} - T_{33} = (b_{11} + 2b_2)\dot{\gamma}^2 \tag{2.11}$$

Then, the constitutive equation of the second-order fluid can be rewritten in terms of material functions as follows:

$$\mathbf{T} = -p\mathbf{I} + \eta\mathbf{A}_1 - \frac{1}{2}\psi_1\mathbf{A}_2 + (\psi_1 + \psi_2)\mathbf{A}_1^2 \tag{2.12}$$

Here, the material functions η, ψ_1, and ψ_2 can be considered as functions of shear rate if the flow under consideration is a viscometric flow. The shear rate can be obtained from

$$\dot{\gamma} = \sqrt{\frac{1}{2}\mathrm{tr}\left(\mathbf{A}_1^2\right)} = \sqrt{\frac{1}{2}\mathrm{tr}(\mathbf{A}_2)} \tag{2.13}$$

Hence, the second-order fluid agrees with experimental data of nonzero normal stress difference. On the other hand, the model for the generalized viscous fluid Eq. (3.41) in Chap. 2 cannot describe nonzero normal stress difference. However, it is known that the second-order fluid is unstable in unsteady flows (Tanner 2002).

2.2 Green–Rivlin Expansion

Green–Rivlin expansion (1957) is another expansion of Eq. (2.1) such that

$$\begin{aligned}\mathbf{T} = -p\mathbf{I} + &\int_{-\infty}^{t} \mu_1(t-t_1)[\mathbf{C}_t(t_1) - \mathbf{I}]\mathrm{d}t_1 \\ &+ \int_{-\infty}^{t}\int_{-\infty}^{t} \mu_2(t-t_1, t-t_2)[\mathbf{C}_t(t_1) - \mathbf{I}]\cdot[\mathbf{C}_t(t_2) - \mathbf{I}]\mathrm{d}t_1\mathrm{d}t_2 + \cdots\end{aligned} \tag{2.14}$$

This is the Taylor expansion of stress functional [see appendix]. For this expansion, the first-order kernel $\mu_1(t)$ corresponds to the derivative of the linear relaxation modulus:

$$\mu_1(t) = -\frac{\mathrm{d}G}{\mathrm{d}t} \tag{2.15}$$

On the other hand, higher-order kernels are difficult to be evaluated from experimental data.

For the simple shear flows of $\mathbf{v} = \dot{\gamma} y \mathbf{e}_1$ with constant shear rate, we know that

$$\mathbf{C}_t(\tau) = \mathbf{I} + \dot{\gamma}(\tau - t)(\mathbf{e}_1\mathbf{e}_2 + \mathbf{e}_2\mathbf{e}_1) + \dot{\gamma}^2(\tau - t)^2\mathbf{e}_2\mathbf{e}_2 \tag{2.16}$$

When the first integral is considered only, the solution of the model for the simple shear flow is given by

$$T_{12} = -\dot{\gamma}\int_0^\infty \tau\mu(\tau)\mathrm{d}\tau = \dot{\gamma}\int_0^\infty G(\tau)\mathrm{d}\tau = \eta_\mathrm{o}\dot{\gamma} \tag{2.17}$$

$$N_1 = -\dot{\gamma}^2\int_0^\infty \tau^2\mu_1(\tau)\mathrm{d}\tau = 2\dot{\gamma}^2\int_0^\infty \tau\, G(\tau)\mathrm{d}\tau = 2J_\mathrm{e}^\mathrm{o}\eta_\mathrm{o}^2\dot{\gamma}^2 \tag{2.18}$$

and

$$N_2 = -N_1 \tag{2.19}$$

Since experimental data usually show $|N_2/N_1| \ll 1$, the consequences from the single integral model are not realistic. This discrepancy seems to be originated from neglecting higher-order integrals.

Consider the first-order Green–Rivlin expansion with

$$\mu_1(t) = \frac{G_o}{\lambda}\exp\left(-\frac{t}{\lambda}\right) \tag{2.20}$$

Then, the material time derivative of the extra stress is given by

$$\frac{d\mathbf{T}'}{dt} = -\frac{\mathbf{T}'}{\lambda} + \int_{-\infty}^{t} \mu_1(t-\tau)\frac{d\mathbf{C}_t(\tau)}{dt}dt \tag{2.21}$$

Note that

$$\frac{d\mathbf{C}_t(\tau)}{dt} = -\mathbf{L}^{\mathrm{T}}(t)\cdot\mathbf{C}_t(\tau) - \mathbf{C}_t(\tau)\cdot\mathbf{L}(t) \tag{2.22}$$

Substitution of Eq. (2.22) to Eq. (2.21) gives

$$\lambda\overset{\Delta}{\mathbf{T}'} + \mathbf{T}' = -2\eta_o\mathbf{D} \tag{2.23}$$

where $\eta_o = G_o\lambda$. Note that the definition of the *lower-convected time derivative* is given by

$$\overset{\Delta}{\mathbf{T}'} \equiv \frac{d\mathbf{T}'}{dt} + \mathbf{L}^{\mathrm{T}}\cdot\mathbf{T}' + \mathbf{T}'\cdot\mathbf{L} \tag{2.24}$$

Lower-convected time derivative is an objective time derivative.

This is the differential constitutive equation of the first-order integral. However, this model gives unrealistic behavior. The *Lodge equation* (Larson 1988) is the first-order integral model with replacement of $\mathbf{C}_t(\tau)$ by the Finger tensor $\mathbf{C}_t^{-1}(\tau)$:

$$\mathbf{T} = -p\mathbf{I} + \int_{-\infty}^{t} \frac{G_o}{\lambda}e^{-(t-\tau)/\lambda}\left[\mathbf{C}_t^{-1}(\tau) - \mathbf{I}\right]d\tau \tag{2.25}$$

Differentiation of the extra stress of Eq. (2.25) gives the *upper-convected Maxwell model* (UCM):

$$\lambda \overset{\nabla}{\mathbf{T}}' + \mathbf{T}' = 2\eta_o \mathbf{D} \tag{2.26}$$

Derivation of Eq. (2.26) from Eq. (2.25) is very similar to that of Eq. (2.23). The Lodge equation is one of the simplest cases of the K-BKZ model which will be given in the next section.

Problems 2

[1] Show that the following tensor-valued function is an isotropic function.

$$\mathbf{G}(\mathbf{A}_1, \mathbf{A}_2) = b_1 \mathbf{A}_1 + b_{11} \mathbf{A}_1 \cdot \mathbf{A}_1 + b_2 \mathbf{A}_2 \tag{2.a}$$

[2] Consider the deformation gradient tensor such that

$$\mathbf{F}(\tilde{\mathbf{x}}, t) = \lambda(t)\mathbf{e}_1\mathbf{e}_1 + \frac{1}{\sqrt{\lambda(t)}}(\mathbf{I} - \mathbf{e}_1\mathbf{e}_1) \tag{2.b}$$

Calculate $\mathbf{A}_1, \mathbf{A}_2, \mathbf{C}_t(\tau)$ and $\mathbf{C}_t^{-1}(\tau)$.

[3] The deformation gradient tensor for equibiaxial extension is given by

$$\mathbf{F}(\tilde{\mathbf{x}}, t) = \lambda(t)(\mathbf{I} - \mathbf{e}_3\mathbf{e}_3) + \frac{1}{\lambda^2(t)}\mathbf{e}_3\mathbf{e}_3 \tag{2.c}$$

Calculate $\mathbf{A}_1, \mathbf{A}_2, \mathbf{C}_t(\tau)$ and $\mathbf{C}_t^{-1}(\tau)$.

[4] The deformation gradient tensor for pure shear is given by

$$\mathbf{F}(\tilde{\mathbf{x}}, t) = \lambda(t)\mathbf{e}_1\mathbf{e}_1 + \mathbf{e}_2\mathbf{e}_2 + \frac{1}{\lambda(t)}\mathbf{e}_3\mathbf{e}_3 \tag{2.d}$$

Calculate $\mathbf{A}_1, \mathbf{A}_2, \mathbf{C}_t(\tau)$ and $\mathbf{C}_t^{-1}(\tau)$.

[5] When stress is given by Eq. (2.25), calculate steady extensional viscosity and steady shear viscosity.

[6] Consider a functional which is a mapping from $\mathbf{C}_t(\tau)$ to extra stress tensor such that

$$\mathbf{T}' = \overset{\tau=t}{\underset{\tau=-\infty}{\mathsf{T}}}[\mathbf{C}_t(\tau)] \tag{2.e}$$

with

$$\overset{\tau=t}{\underset{\tau=-\infty}{\mathsf{T}}}[\mathbf{I}] = \mathbf{0} \tag{2.f}$$

Assume that the tensor-valued functional is isotropic. Then, show that Eq. (2.14) is the Taylor expansion of the functional.

3 Generalization of Linear Viscoelastic Models

3.1 Oldroyd Generalization

Oldroyd revealed that the principle of material frame-indifference does not hold when the stress, the time derivative of stress, and the strain rate of the linear model from the combination of spring and dashpot are replaced by extra stress tensor, the material time derivative of the extra stress tensor, and the deformation rate tensor, respectively. We have discussed this problem in Sect. 5.1 in Chap. 2. In Chap. 11, we focused on objective time derivatives of tensor, which satisfy the principle of material frame-indifference. In addition, when converting various spring–dashpot models, we need a time derivative of deformation rate tensor which satisfies the principle of material frame-indifference, too. Equation (1.81) in Chap. 2 implies that the lower-convected time derivative of deformation rate tensor is the second-order Rivlin–Ericksen tensor:

$$\mathbf{A}_2 = 2\overset{\Delta}{\mathbf{D}} \tag{3.1}$$

Oldroyd generalization is to replace the time derivatives of stress rate and strain rate by an objective time derivative of them.

As an example, consider a parallel combination of a Maxwell model and a viscous element. The linear model of the combination of spring and dashpot is given by

$$\lambda_1 \frac{\mathrm{d}\sigma}{\mathrm{d}t} + \sigma = (\eta_1 + \eta_2)\frac{\mathrm{d}\gamma}{\mathrm{d}t} + \lambda_1\eta_2 \frac{\mathrm{d}^2\gamma}{\mathrm{d}t^2} \tag{3.2}$$

The Oldroyd generalization is the transform such that

$$\frac{\mathrm{d}\sigma}{\mathrm{d}t} \to \overset{\Delta}{\mathbf{T}}' \text{ or } \overset{\nabla}{\mathbf{T}}'; \quad \frac{\mathrm{d}\gamma}{\mathrm{d}t} \to \mathbf{A}_1 = 2\mathbf{D}; \quad \frac{\mathrm{d}^2\gamma}{\mathrm{d}t^2} \to \mathbf{A}_2 = 2\overset{\Delta}{\mathbf{D}} \tag{3.3}$$

and the generalized constitutive equation is

$$\mathbf{T}' + \lambda_1 \overset{\Delta}{\mathbf{T}}' = \eta_\mathrm{o}(\mathbf{A}_1 + \lambda_2\mathbf{A}_2) \tag{3.4a}$$

or

$$\mathbf{T}' + \lambda_1 \overset{\nabla}{\mathbf{T}}' = \eta_\mathrm{o}(\mathbf{A}_1 + \lambda_2\mathbf{A}_2) \tag{3.4b}$$

where $\eta_\mathrm{o} = \eta_1 + \eta_2$ and $\lambda_2 = \lambda_1\eta_2/\eta_\mathrm{o}$.

Use of this reasoning, Oldroyd suggested his *eight-constant model*:

$$\begin{aligned}&\mathbf{T}' + \lambda_1 \overset{\Delta}{\mathbf{T}}' + \frac{\mu_o}{2}\mathrm{tr}(\mathbf{T}')\mathbf{A}_1 - \frac{\mu_1}{2}(\mathbf{T}'\cdot\mathbf{A}_1 + \mathbf{A}_1\cdot\mathbf{T}') + \frac{a_1}{2}\mathrm{tr}(\mathbf{T}'\cdot\mathbf{A}_1)\mathbf{I} \\ &\quad = \eta_o\left[\mathbf{A}_1 + \lambda_2\mathbf{A}_2 - \mu_2\mathbf{A}_1\cdot\mathbf{A}_1 + \frac{a_2}{2}\mathrm{tr}(\mathbf{A}_1\cdot\mathbf{A}_1)\mathbf{I}\right]\end{aligned} \tag{3.5}$$

As for this complicate model, viscometric functions $\eta(\dot\gamma), \psi_1(\dot\gamma)$ and $\psi_2(\dot\gamma)$ are given by

$$\eta(\dot\gamma) = \eta_o\frac{1+k_1\dot\gamma^2}{1+k_2\dot\gamma^2} \tag{3.6}$$

$$\psi_1(\dot\gamma) = 2\eta_o\lambda_1\left[\frac{\eta(\dot\gamma)}{\eta_o} - \frac{\lambda_2}{\lambda_1}\right] \tag{3.7}$$

and

$$\psi_2(\dot\gamma) = (2\lambda_2 - \mu_2)\eta_o - (2\lambda_1 - \mu_1)\eta(\dot\gamma) \tag{3.8}$$

where

$$\begin{aligned}k_1 &= \lambda_1(\mu_1 - a_1) + \mu_o\left(\mu_1 - \lambda_1 - \frac{3a_1}{2}\right) + \mu_1(\lambda_1 + a_1 - \mu_1); \\ k_2 &= \lambda_1(\mu_2 - a_2) + \mu_o\left(\mu_2 - \lambda_2 - \frac{3a_2}{2}\right) + \mu_1(\lambda_2 + a_2 - \mu_2)\end{aligned} \tag{3.9}$$

Since steady shear stress is a monotonic increasing function of shear rate, we have

$$\frac{\mathrm{d}}{\mathrm{d}\dot\gamma\eta}(\dot\gamma) \geq 0 \tag{3.10}$$

Application of Eq. (3.6) to the inequality gives

$$k_2 \geq \frac{k_1}{9} > 0 \tag{3.11}$$

Since the steady shear viscosity at infinite shear rate is $\eta_\infty = k_1/k_2$, the inequality of Eq. (3.11) can be replaced by

$$\frac{\eta_\infty}{\eta_o} \geq \frac{1}{9} \tag{3.12}$$

However, experimental data of a polymeric fluid often show that $\eta_\infty \ll 0.1\eta_o$. Thus, the eight-constant model cannot describe the shear viscosity data of real polymeric fluids.

3.1.1 The Upper-Convected Maxwell Model

When $\mu_o = \mu_2 = \lambda_2 = a_1 = a_2 = 0$ and $\mu_1 = 2\lambda_1$, the eight-constant model becomes the upper-convected Maxwell model:

$$\mathbf{T}' + \lambda \overset{\nabla}{\mathbf{T}}' = 2\eta_o \mathbf{D} \tag{3.13}$$

Under the assumption that stress is homogeneous ($\nabla \mathbf{T}' = \mathbf{0}$), Eq. (3.13) can be rewritten as

$$\frac{\partial \mathbf{T}'}{\partial t} - \left(\mathbf{L} - \frac{1}{2\lambda}\mathbf{I}\right) \cdot \mathbf{T}' - \mathbf{T}' \cdot \left(\mathbf{L} - \frac{1}{2\lambda}\mathbf{I}\right)^{\mathrm{T}} = 2\frac{\eta_o}{\lambda}\mathbf{D} \tag{3.14}$$

If $\mathbf{L}$ is a constant tensor, then Eq. (3.14) corresponds to Eq. (5.83) in Chap. 1 and the general solution is given by

$$\mathbf{T}'(t) = e^{t\mathbf{H}} \cdot \mathbf{T}'(0) \cdot e^{t\mathbf{H}^{\mathrm{T}}} + 2\eta_o \int_0^t e^{-(\tau - t)\mathbf{H}} \cdot \mathbf{D} \cdot e^{-(\tau - t)\mathbf{H}^{\mathrm{T}}} \mathrm{d}\tau \tag{3.15}$$

where $\mathbf{H} = \mathbf{L} - (2\lambda)^{-1}\mathbf{I}$. As for steady simple shear, we know that

$$\mathbf{H} = -\frac{1}{2\lambda}\mathbf{I} + \dot{\gamma}\mathbf{e}_1\mathbf{e}_2 \tag{3.16}$$

and

$$2\mathbf{D} = \dot{\gamma}(\mathbf{e}_1\mathbf{e}_2 + \mathbf{e}_2\mathbf{e}_1) \tag{3.17}$$

Since

$$\mathbf{H}^n = \left(-\frac{1}{2\lambda}\right)^n (\mathbf{I} - 2n\lambda\dot{\gamma}\mathbf{e}_1\mathbf{e}_2) \tag{3.18}$$

we know that

$$e^{x\mathbf{H}} = e^{-x/(2\lambda)}\mathbf{I} + \dot{\gamma}xe^{-x/(2\lambda)}\mathbf{e}_1\mathbf{e}_2; \quad e^{x\mathbf{H}^T} = e^{-x/(2\lambda)}\mathbf{I} + \dot{\gamma}xe^{-x/(2\lambda)}\mathbf{e}_2\mathbf{e}_1 \tag{3.19}$$

Application of Eqs. (3.16)–(3.19) to Eq. (3.15) gives

$$\mathbf{T}'(t) = \eta_o\dot{\gamma}\left(1 - e^{-t/\lambda}\right)(\mathbf{e}_1\mathbf{e}_2 + \mathbf{e}_2\mathbf{e}_1) + 2\frac{\eta_o}{\lambda}(\lambda\dot{\gamma})^2\left(1 - \frac{t+\lambda}{\lambda}e^{-t/\lambda}\right)\mathbf{e}_1\mathbf{e}_1 \quad (3.20)$$

Here, we used the initial condition of $\mathbf{T}'(0) = \mathbf{0}$. Equation (3.20) implies that

$$\begin{aligned}\eta(\dot{\gamma}) &= \lim_{t\to\infty}\frac{\eta_o\dot{\gamma}\left(1 - e^{-t/\lambda}\right)}{\dot{\gamma}} = \eta_o \\ \psi_1(\dot{\gamma}) &= 2\lim_{t\to\infty}\frac{\eta_o}{\lambda}\frac{(\lambda\dot{\gamma})^2}{\dot{\gamma}^2}\left(1 - \frac{t+\lambda}{\lambda}e^{-t/\lambda}\right) = 2\eta_o\lambda \\ \psi_2(\dot{\gamma}) &= 0\end{aligned} \quad (3.21)$$

Hence, steady shear viscosity is a constant. This is clearly unrealistic for polymeric fluids.

As for simple elongational flow, similar calculation can be done for the UCM. The result is

$$\eta_E^{\infty}(\dot{\varepsilon}) = \frac{3\eta_o}{(1+\lambda\dot{\varepsilon})(1-2\lambda\dot{\varepsilon})} \quad (3.22)$$

This result implies that steady extensional viscosity diverges as $\dot{\varepsilon}$ approaches to $(2\lambda)^{-1}$. Hence, this is also unrealistic.

3.2 K-BKZ Model

The Boltzmann superposition principle of Eq. (1.8) in Chap. 5 can be rewritten as

$$\sigma(t) = \int_{-\infty}^{t}\mu(t-\tau)\gamma(\tau)\mathrm{d}\tau \quad (3.23)$$

where $\mu(t) = -\mathrm{d}G/\mathrm{d}t \geq 0$ is the memory function. As for incompressible nonlinear elastic materials, we have learned that stress can be expressed by Eq. (3.39) in Chap. 2:

$$\mathbf{T} = -p\mathbf{I} + 2\left(\frac{\partial\Phi}{\partial I_{\mathbf{B}}}\mathbf{B} - \frac{\partial\Phi}{\partial I_{\mathbf{B}^{-1}}}\mathbf{B}^{-1}\right) \quad (3.24)$$

Equation (3.23) is for linear viscoelastic material, while Eq. (3.24) is for nonlinear elastic material. Kaye (1962) combined the Boltzmann superposition with hyperelastic formalism and suggested

$$\mathbf{T} = -p\mathbf{I} + 2\int_{-\infty}^{t}\left[\frac{\partial\Phi}{\partial I_{\mathbf{C}_t^{-1}(\tau)}}\mathbf{C}_t^{-1}(\tau) - \frac{\partial\Phi}{\partial I_{\mathbf{C}_t(\tau)}}\mathbf{C}_t(\tau)\right]\mathrm{d}\tau \tag{3.25}$$

where the potential Φ is a function such that

$$\Phi = \Phi\left(I_{\mathbf{C}_t^{-1}(\tau)}, I_{\mathbf{C}_t(\tau)}, t-\tau\right) \tag{3.26}$$

Equation (3.25) is called K-BKZ model because Bernstein et al. (1963) developed the model independently. This is an integral-type constitutive equation, while the nonlinear viscoelastic models based on the Oldroyd generalization belong to differential type.

Equation (1.j) in Chap. 2 implies that the upper-convected time derivative of $\mathbf{C}_t^{-1}(\tau)$ is zero tensor, so is that of $\mathbf{B}(t) = \mathbf{F}(t)\cdot\mathbf{F}^{\mathrm{T}}(t)$. This is the reason why $\mathbf{B}$ of Eq. (3.24) is replaced by $\mathbf{C}_t^{-1}(\tau)$ in Eq. (3.25) in order to include deformation history.

Laun (1978) and Osaki et al. (1982) found nonlinear relaxation modulus of polymeric fluids can be factorized to the product of linear relaxation modulus and the damping function which is a function of shear strain:

$$G(\gamma,t) = G(t)h(\gamma) \quad \text{for } t > \lambda_X \tag{3.27}$$

Note that for $t<\lambda_X$, the time–strain separability breaks. This experimental observation suggests the *time–strain separable K-BKZ model* such that

$$\mathbf{T} = -p\mathbf{I} + \int_{-\infty}^{t}\mu(t-\tau)\left[h_1\left(I_{\mathbf{C}_t^{-1}(\tau)}, I_{\mathbf{C}_t(\tau)}\right)\mathbf{C}_t^{-1}(\tau) + h_2\left(I_{\mathbf{C}_t^{-1}(\tau)}, I_{\mathbf{C}_t(\tau)}\right)\mathbf{C}_t(\tau)\right]\mathrm{d}\tau \tag{3.28}$$

The nonlinear viscoelastic constitutive equation of the Doi–Edwards theory (1986) belongs to the time–strain separable K-BKZ model. Although the introduction of time–strain separability gives rise to the instability of the K-BKZ model (Kwon and Cho 2001), the separable K-BKZ model is useful in the interpretation of experiments of nonlinear viscoelasticity. Hence, we shall focus on the separable K-BKZ model.

3.2.1 Simple Shear Flow

In simple shear, the deformation gradient is given by $\mathbf{F}(t) = \mathbf{I} + \gamma(t)\mathbf{e}_1\mathbf{e}_2$. Hence, we have

$$\mathbf{F}_t(\tau) = \mathbf{I} + [\gamma(\tau) - \gamma(t)]\mathbf{e}_1\mathbf{e}_2 \tag{3.29}$$

$$\mathbf{C}_t(\tau) = \mathbf{I} - [\gamma(t) - \gamma(\tau)](\mathbf{e}_1\mathbf{e}_2 + \mathbf{e}_2\mathbf{e}_1) + [\gamma(t) - \gamma(\tau)]^2\mathbf{e}_2\mathbf{e}_2 \tag{3.30}$$

$$\mathbf{C}_t^{-1}(\tau) = \mathbf{I} + [\gamma(t) - \gamma(\tau)](\mathbf{e}_1\mathbf{e}_2 + \mathbf{e}_2\mathbf{e}_1) + [\gamma(\tau) - \gamma(t)]^2\mathbf{e}_1\mathbf{e}_1 \tag{3.31}$$

and

$$I_{\mathbf{C}_t(\tau)} = I_{\mathbf{C}_t^{-1}(\tau)} = 3 + [\gamma(t) - \gamma(\tau)]^2 \tag{3.32}$$

Then we can rewrite Eq. (3.28) as follows

$$\begin{aligned}\mathbf{T} = &\left\{-p + \int_{-\infty}^{t} \mu(t-\tau)\left[\tilde{h}_1\left(\gamma_{t,\tau}^2\right) + \tilde{h}_2\left(\gamma_{t,\tau}^2\right)\right]\mathrm{d}\tau\right\}\mathbf{I} \\ &+ \left\{\int_{-\infty}^{t} \tilde{h}_1\left(\gamma_{t,\tau}^2\right)\gamma_{t,\tau}^2\mathrm{d}\tau\right\}\mathbf{e}_1\mathbf{e}_1 + \left\{\int_{-\infty}^{t} \tilde{h}_2\left(\gamma_{t,\tau}^2\right)\gamma_{t,\tau}^2\mathrm{d}\tau\right\}\mathbf{e}_2\mathbf{e}_2 \\ &+ \left\{\int_{-\infty}^{t} \mu(t-\tau)\left[\tilde{h}_1\left(\gamma_{t,\tau}^2\right) - \tilde{h}_2\left(\gamma_{t,\tau}^2\right)\right]\gamma_{t,\tau}\mathrm{d}\tau\right\}(\mathbf{e}_1\mathbf{e}_2 + \mathbf{e}_2\mathbf{e}_1)\end{aligned} \tag{3.33}$$

where $\gamma_{t,\tau} = \gamma(t) - \gamma(\tau)$ and

$$\tilde{h}_k\left(\gamma_{t,\tau}^2\right) = h_k\left(I_{\mathbf{C}_t^{-1}(\tau)}, I_{\mathbf{C}_t(\tau)}\right) \text{ in simple shear} \tag{3.34}$$

If we use the definition such that

$$h(x) = \tilde{h}_1(x) - \tilde{h}_2(x) \tag{3.35}$$

shear stress and the first normal stress difference can be written, respectively, by

$$T_{12} = \int_{-\infty}^{t} \mu(t-\tau)h\left(\gamma_{t,\tau}^2\right)\gamma_{t,\tau}\mathrm{d}\tau \tag{3.36}$$

and

$$N_1 = \int_{-\infty}^{t} \mu(t-\tau)h\left(\gamma_{t,\tau}^2\right)\gamma_{t,\tau}^2\mathrm{d}\tau \tag{3.37}$$

Of course, the second normal stress difference of the K-BKZ model is zero.

As for stress relaxation test, we know that $\gamma(t) = \gamma_o\Theta(t)$ where γ_o is constant and is called the strain amplitude. Then, it is obvious that $t > 0$ and $\tau \leq t$.

The definition of $\gamma_{t,\tau}$ implies that it is the constant γ_o whenever $\tau<0$ and zero otherwise. Then, the integral of Eq. (3.36) can be rewritten as

$$T_{12} = \gamma_o h\left(\gamma_o^2\right) \int_{-\infty}^{0} \mu(t-\tau)\mathrm{d}\tau \tag{3.38}$$

Since $G(\infty) = 0$ for a viscoelastic fluid, the definition of the memory function gives

$$G(t) = \int_{-\infty}^{0} \mu(t-\tau)\mathrm{d}\tau \tag{3.39}$$

Finally, we recognize that the function $h\left(\gamma_o^2\right)$ is the *damping function* of Eq. (3.27). This implies that nonlinear stress relaxation test identifies the damping function.

Popularly used form of damping functions is

$$h\left(\gamma^2\right) = \frac{1}{1+\left(\gamma/\gamma_C\right)^2} \tag{3.40a}$$

$$h\left(\gamma^2\right) = \exp(-n|\gamma|) \tag{3.40b}$$

and

$$h\left(\gamma^2\right) = \phi\,\exp(-n_1|\gamma|) + (1-\phi)\exp(-n_2|\gamma|) \quad \text{with} \quad 0<\phi<1 \tag{3.40c}$$

The Doi–Edwards theory predicts Eq. (3.40a), while the last two is obtained empirically.

If nonlinear relaxation test confirms the damping function, then the K-BKZ model can calculate shear stress and the first normal stress difference for any function of $\gamma(t)$. It is remarkable that Laun (1978) showed that nonlinear shear behavior of LDPE agrees well with the time–strain separable K-BKZ model. When the damping function of Eq. (3.40b) is chosen, steady shear viscosity and steady normal stress difference are given by Laun (1978)

$$\eta(\dot{\gamma}_o) = \sum_{k=1}^{N} \frac{G_k\lambda_k}{\left(1+n\lambda_k\dot{\gamma}_o\right)^2} \tag{3.41}$$

and

$$\psi_1(\dot{\gamma}_o) = 2\sum_{k=1}^{N} \frac{G_k\lambda_k^2}{\left(1+n\lambda_k\dot{\gamma}_o\right)^3} \tag{3.42}$$

where $\{G_k, \lambda_k\}$ is the discrete relaxation spectrum of the fluid.

3.2.2 Simple Elongational Flow

As for simple elongational flow, the relative deformation gradient is given by

$$\mathbf{F}_t(\tau) = \frac{\lambda(\tau)}{\lambda(t)}\mathbf{e}_3\mathbf{e}_3 + \sqrt{\frac{\lambda(t)}{\lambda(\tau)}}(\mathbf{I} - \mathbf{e}_3\mathbf{e}_3) \tag{3.43}$$

Then, we have

$$\mathbf{C}_t(\tau) = \left[\frac{\lambda(\tau)}{\lambda(t)}\right]^2 \mathbf{e}_3\mathbf{e}_3 + \frac{\lambda(t)}{\lambda(\tau)}(\mathbf{I} - \mathbf{e}_3\mathbf{e}_3) \tag{3.44}$$

$$\mathbf{C}_t^{-1}(\tau) = \left[\frac{\lambda(t)}{\lambda(\tau)}\right]^2 \mathbf{e}_3\mathbf{e}_3 + \frac{\lambda(\tau)}{\lambda(t)}(\mathbf{I} - \mathbf{e}_3\mathbf{e}_3) \tag{3.45}$$

$$I_{\mathbf{C}_t(\tau)} = \left[\frac{\lambda(\tau)}{\lambda(t)}\right]^2 + 2\frac{\lambda(t)}{\lambda(\tau)} \tag{3.46}$$

and

$$I_{\mathbf{C}_t(\tau)} = \left[\frac{\lambda(t)}{\lambda(\tau)}\right]^2 + 2\frac{\lambda(\tau)}{\lambda(t)} \tag{3.47}$$

Substitution of Eqs. (3.44)–(3.47) to Eq. (3.28) gives

$$\begin{aligned}\sigma &= T_{33} - T_{11} \\ &= \int_{-\infty}^{t} \mu(t-\tau)\left[\tilde{h}_1(\lambda_{t,\tau})\left(\lambda_{t,\tau}^2 - \frac{1}{\lambda_{t,\tau}}\right) + \tilde{h}_2(\lambda_{t,\tau})\left(\frac{1}{\lambda_{t,\tau}^2} - \lambda_{t,\tau}\right)\right]\mathrm{d}\tau\end{aligned} \tag{3.48}$$

where

$$\lambda_{t,\tau} = \frac{\lambda(t)}{\lambda(\tau)} \tag{3.49}$$

and

$$\tilde{h}_k(\lambda_{t,\tau}) = h\left(I_{\mathbf{C}_t^{-1}(\tau)}, I_{\mathbf{C}_t(\tau)}\right) \tag{3.50}$$

In this case, the measurement of axial stress (or elongational viscosity) has to determine two functions $\tilde{h}_1(x)$ and $\tilde{h}_2(x)$, while the measurement of shear stress considers only damping function. Hence, it is very difficult to identify the two functions $h_1(I_1, I_2)$ and $h_2(I_1, I_2)$ by only two types of experiments. A better

constitutive equation is the one whose identification is easier if its agreement with experimental data is as precise as the others. In the next two sections, we will meet constitutive equations whose identification is easier than the K-BKZ model.

Problems 3

[1] The Oldroyd B model is the parallel combination of a Maxwell model and a Newtonian fluid. Express the constitutive equation in tensor notation.
[2] Calculate steady shear and extensional viscosities of the Oldroyd B model.
[3] Corotational Maxwell model is given by

$$\mathbf{T}' + \lambda \overset{\mathrm{O}}{\mathbf{T}} = 2\eta_{\mathrm{o}}\mathbf{D} \tag{3.a}$$

Calculate steady shear viscosity and normal stress difference coefficients.
[4] Derive Eqs. (3.6)–(3.8).
[5] Derive Eq. (3.12).
[6] As for the damping function of Eq. (3.40a), calculate $\eta(\dot{\gamma}_{\mathrm{o}})$ and $\psi_1(\dot{\gamma}_{\mathrm{o}})$.
[7] Using Eq. (3.41), discuss whether the time–strain separable K-BKZ model obeys the Cox–Mertz rule.
[8] As for Eq. (3.25), one may consider the following potential

$$\Phi = \mu(t-\tau)\left(I_{\mathbf{C}_t^{-1}(\tau)} - 3\right) \tag{3.b}$$

Calculate viscometric material functions.

4 Models Based on Speculation of Structure

4.1 Spring-Dumbbell Models

This subsection involves a lot of complicate equations which are mainly related with the theory of Brownian motion. Hence, this subsection can be understood easier if the readers remind the contents of Sect. 3 in Chap. 3 Brownian Motion and Sect. 4 in Chap. 5 Molecular Theories.

4.1.1 Langevin Equations

Since a polymer chain is too complicate to develop a constitutive equation from the motion of the segments in the polymer chain, a daring simplification of the chain has been investigated. The simplification is the two mass points connected by a spring (Fig. 5).

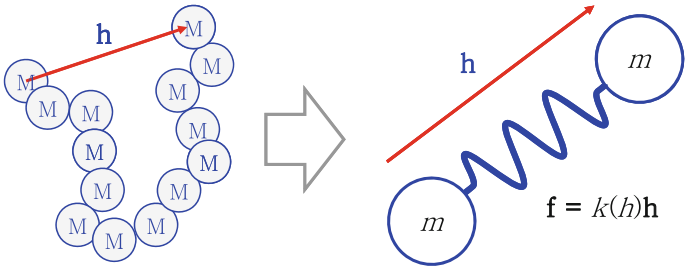

Fig. 5 Schematic illustration of spring-dumbbell

Let the two points have the same mass m and their positions be $\mathbf{r}_1$ and $\mathbf{r}_2$. It is the spring-dumbbell model. Then, the equations of motion for the model are given by

$$\begin{aligned} m\frac{\mathrm{d}^2\mathbf{r}_1}{\mathrm{d}t^2} &= -\zeta\widetilde{\mathbf{M}}^{-1}\cdot\left(\frac{\mathrm{d}\mathbf{r}_1}{\mathrm{d}t}-\mathbf{L}\cdot\mathbf{r}_1\right)-\mathbf{f}_{12}+\mathbf{f}_R^{(1)} \\ m\frac{\mathrm{d}^2\mathbf{r}_2}{\mathrm{d}t^2} &= -\zeta\widetilde{\mathbf{M}}^{-1}\cdot\left(\frac{\mathrm{d}\mathbf{r}_2}{\mathrm{d}t}-\mathbf{L}\cdot\mathbf{r}_2\right)-\mathbf{f}_{21}+\mathbf{f}_R^{(2)} \end{aligned} \tag{4.1}$$

The first terms including friction coefficient ζ represent drag force due to the friction with neighbor molecules. Reminding Eq. (4.13) in Chap. 5, we know that $\widetilde{\mathbf{M}}$ is dimensionless mobility tensor. The force $\mathbf{f}_{12}$ and $\mathbf{f}_{21}$ represents the interaction between the two mass points, and $\mathbf{f}_R^{(k)}$ is the random force exerting on the kth mass point. Because of the third law of Newtonian mechanics, it is obvious that $\mathbf{f}_{12}=-\mathbf{f}_{21}$.

To make the two-body problem easier, it is conventional to use the following variables:

$$\mathbf{r}_c=\frac{1}{2}(\mathbf{r}_1+\mathbf{r}_2);\quad \mathbf{h}=\mathbf{r}_1-\mathbf{r}_2 \tag{4.2}$$

Note that $\mathbf{r}_c$ is the center of mass and $\mathbf{h}$ is the bond vector. Using Eq. (4.2), the equations of motion become

$$\begin{aligned} m\frac{\mathrm{d}^2\mathbf{r}_c}{\mathrm{d}t^2} &= -\zeta\widetilde{\mathbf{M}}^{-1}\cdot\left(\frac{\mathrm{d}\mathbf{r}_c}{\mathrm{d}t}-\mathbf{L}\cdot\mathbf{r}\right)+\mathbf{f}_{\mathrm{R}}^{\mathrm{c}} \\ m\frac{\mathrm{d}^2\mathbf{h}}{\mathrm{d}t^2} &= -\zeta\widetilde{\mathbf{M}}^{-1}\cdot\left(\frac{\mathrm{d}\mathbf{h}}{\mathrm{d}t}-\mathbf{L}\cdot\mathbf{h}\right)-2\mathbf{f}_{12}+\mathbf{f}_{\mathrm{R}}^{\mathrm{h}} \end{aligned} \tag{4.3}$$

It is usually assumed that the interaction force $\mathbf{f}_{12}$ is a central force such that

$$\mathbf{f}_{12} = k(h)\mathbf{h} \tag{4.4}$$

where $h = \|\mathbf{h}\|$.

Dimensional analysis gives neglecting of inertia effect because of high viscosity of a polymeric fluid:

$$\frac{\mathrm{d}\mathbf{r}_c}{\mathrm{d}t} = \mathbf{L}\cdot\mathbf{r}_c + \frac{1}{\zeta}\widetilde{\mathbf{M}}\cdot\mathbf{f}_R^c \tag{4.5}$$

and

$$\frac{\mathrm{d}\mathbf{h}}{\mathrm{d}t} = \mathbf{L}\cdot\mathbf{h} - 2\frac{k(h)}{\zeta}\widetilde{\mathbf{M}}\cdot\mathbf{h} + \frac{1}{\zeta}\widetilde{\mathbf{M}}\cdot\mathbf{f}_R^h \tag{4.6}$$

As for the random forces, the following relations are assumed:

$$\begin{aligned} \left\langle \mathbf{f}_{\mathrm{R}}^{\mathrm{c}}(t)\right\rangle &= \mathbf{0}, \quad \left\langle \mathbf{f}_{\mathrm{R}}^{\mathrm{c}}(t)\mathbf{f}_{\mathrm{R}}^{\mathrm{c}}(t')\right\rangle = \delta(t-t')\mathbf{B}_{\mathrm{c}} \\ \left\langle \mathbf{f}_{\mathrm{R}}^{\mathrm{h}}(t)\right\rangle &= \mathbf{0}, \quad \left\langle \mathbf{f}_{\mathrm{R}}^{\mathrm{h}}(t)\mathbf{f}_{\mathrm{R}}^{\mathrm{h}}(t')\right\rangle = \delta(t-t')\mathbf{B}_{\mathrm{h}} \end{aligned} \tag{4.7}$$

Note that the two second-order tensors $\mathbf{B}_c$ and $\mathbf{B}_h$ are determined by the equipartition theorem (see Chap. 3). Additional assumption on the random forces is that they are mutually independent:

$$\left\langle \mathbf{f}_{\mathrm{R}}^{\mathrm{c}}(t)\mathbf{f}_{\mathrm{R}}^{\mathrm{h}}(t)\right\rangle = \mathbf{0} \tag{4.8}$$

Since the two equations of Eq. (4.3) are decoupled to Eqs. (4.5) and (4.6), we will focus on the evolution of the bond vector $\mathbf{h}$. It is because stress is mainly dependent on $\mathbf{h}$.

4.1.2 Smoluchowski Equation

Since $\mathbf{h}$ is a stochastic variable, it is natural to consider the probability distribution function $P(\mathbf{h}, t)$ which satisfies the normalization condition:

$$\int P(\mathbf{h}, t)\mathrm{d}^3\mathbf{h} = 1 \tag{4.9}$$

Note that the integration covers the whole space of $\mathbf{h}$. The existence of the normal condition immediately implies that

$$\lim_{\|\mathbf{h}\|\to\infty} P(\mathbf{h},t) = 0 \tag{4.10}$$

Since Eq. (4.9) implies the conservation of probability, similarity to mass conservation, we have

$$\frac{\partial P}{\partial t} + \frac{\partial}{\partial \mathbf{h}} \cdot \left(\frac{\mathrm{d}\mathbf{h}}{\mathrm{d}t} P \right) = 0 \tag{4.11}$$

Here, $\partial/\partial\mathbf{h}$ is a short notation such that

$$\frac{\partial}{\partial \mathbf{h}} = \nabla_{\mathbf{h}} = \mathbf{e}_k \frac{\partial}{\partial h_k} \tag{4.12}$$

where h_k is the kth component of $\mathbf{h}$. The notation $\mathrm{d}\mathbf{h}/\mathrm{d}t$ does not imply that $\mathbf{h}$ is a function of the t which is an argument of the probability distribution P. Although Eq. (4.6) is derived from micromechanics, the timescale of P is much longer than the timescale of random fluctuation. Note that the correlation functions of random forces are approximated by the Dirac delta function in Eq. (4.7). Hence, we call the mechanics in terms of P mesoscopic mechanics rather than micromechanics. Mesoscopic is the intermediate scale regime between microscopic and macroscopic.

With the help of Eqs. (4.6) and (4.11), the evolution equation of the probability distribution function is given by

$$\frac{\partial P}{\partial t} = -\frac{\partial}{\partial \mathbf{h}} \cdot \left[\left(\mathbf{L} \cdot \mathbf{h} - \frac{2k}{\zeta} \widetilde{\mathbf{M}} \cdot \mathbf{h} \right) P \right] - \frac{1}{\zeta} \frac{\partial}{\partial \mathbf{h}} \cdot \left(\widetilde{\mathbf{M}} \cdot \mathbf{f}_{\mathrm{R}}^{\mathrm{h}} P \right) \tag{4.13}$$

Since we are interested in mesoscopic mechanics, we have to average out the rapid fluctuation due to the random force. The formal solution of Eq. (4.13) can be expressed in terms of operator:

$$P(\mathbf{h},t) = e^{-t\hat{\mathfrak{R}}} P(\mathbf{h},0) - \int_0^t \mathrm{d}s\, e^{-(t-s)\hat{\mathfrak{R}}} \frac{\partial}{\partial \mathbf{h}} \cdot \left[\widetilde{\mathbf{M}} \cdot \mathbf{f}_{\mathrm{R}}^{\mathrm{h}}(s) P(\mathbf{h},s) \right] \tag{4.14}$$

where the linear operator $\hat{\mathfrak{R}}$ is defined as

$$\hat{\mathfrak{R}} P \equiv -\frac{\partial}{\partial \mathbf{h}} \cdot \left[\left(\mathbf{L} \cdot \mathbf{h} - \frac{2k}{\zeta} \widetilde{\mathbf{M}} \cdot \mathbf{h} \right) P \right] \tag{4.15}$$

Note that if function is considered as a vector of the vector space of the functions which obey certain conditions, then the linear differential (or integral) operators can

be considered as second-order tensors. Then, the notation $\exp\left(x\hat{\Re}\right)$ can be understood [see Eq. (5.76) in Chap. 1]. Further information is found in Zwanzig (2001). Substitution of Eq. (4.14) to Eq. (4.13) gives

$$\begin{aligned}\frac{\partial P}{\partial t} &= \hat{\Re}P - \frac{1}{\zeta}\frac{\partial}{\partial \mathbf{h}}\cdot\left[\widetilde{\mathbf{M}}\cdot\mathbf{f}_{\mathrm{R}}^{\mathrm{h}}(t)e^{-t\hat{\Re}}P\right] \\ &\quad + \frac{1}{\zeta}\frac{\partial}{\partial \mathbf{h}}\cdot\left\{\widetilde{\mathbf{M}}\cdot\mathbf{f}_{\mathrm{R}}^{\mathrm{h}}(t)\int_0^t \mathrm{d}s e^{-(t-s)\hat{\Re}}\cdot\frac{\partial}{\partial \mathbf{h}}\cdot\left[\widetilde{\mathbf{M}}\cdot\mathbf{f}_{\mathrm{z}}^{\mathrm{h}}(s)P\right]\right\}\end{aligned} \tag{4.16}$$

Note that the random force is independent of $\mathbf{h}$. Taking ensemble average, Eq. (4.7) gives

$$\frac{\partial P}{\partial t} = \hat{\Re}P + \frac{2k_{\mathrm{B}}T}{\zeta}\frac{\partial}{\partial \mathbf{h}}\cdot\left\{\widetilde{\mathbf{M}}\cdot\left[\left(\frac{\partial}{\partial \mathbf{h}}\cdot\left(\widetilde{\mathbf{M}}P\right)\right)\right]\right\} \tag{4.17}$$

Here, we used

$$\mathbf{B}_{\mathrm{h}} = 2k_{\mathrm{B}}T\,\mathbf{I} \tag{4.18}$$

Equation (4.17) is the *Smoluchowski equation* of the spring-dumbbell model. This equation can ramify to several branches depending on the modeling of $k(\mathbf{h})$ and $\widetilde{\mathbf{M}}(\mathbf{h})$. If the dimensionless mobility tensor is taken as the identity tensor: $\widetilde{\mathbf{M}} = \mathbf{I}$, then we have

$$\frac{\partial P}{\partial t} = -\frac{\partial}{\partial \mathbf{h}}\cdot\left[\left(\mathbf{L}\cdot\mathbf{h} - \frac{2k(\mathbf{h})}{\zeta}\mathbf{h}\right)P\right] + \frac{2k_{\mathrm{B}}T}{\zeta}\frac{\partial}{\partial \mathbf{h}}\cdot\frac{\partial P}{\partial \mathbf{h}} \tag{4.19}$$

4.1.3 Constitutive Equation

The Smoluchowski equation is not a constitutive equation. To obtain the constitutive equation, we have to relate the vector $\mathbf{h}$ with stress. Molecular theories usually model the stress as follows [see the molecular theory of viscoelasticity, Chaps. 3, 4, and 5]:

$$\mathbf{T} = -p\mathbf{I} + \rho_{\mathrm{N}}k(\langle h\rangle)\left(\langle\mathbf{hh}\rangle - \langle\mathbf{hh}\rangle_{\mathrm{eq}}\right) \tag{4.20}$$

where ρ_{N} is the number density of the spring-dumbbell molecules. Distinguish ρ_{N} from ρ_{num} of Sect. 4 in Chap. 5, which is the number of segments per unit volume. Different from Eqs. (4.28), (4.41), and (4.69) in Chap. 4, the isotropic term $\langle\mathbf{hh}\rangle_{\mathrm{eq}}$ is

introduced in Eq. (4.20) in order to make the extra stress become zero in equilibrium (no flow). This does not give rise to any problem because the hydrostatic pressure p of incompressible fluid is mainly dependent on the boundary condition rather than material property. Equation (4.20) is a preaverage model. In Eq. (4.20), we used

$$\langle h \rangle = \sqrt{\mathrm{tr}(\langle \mathbf{hh} \rangle)} \tag{4.21}$$

Then, it is important to derive the evolution equation of the tensor $\langle \mathbf{hh} \rangle$. We define

$$\langle \mathbf{hh} \rangle = \int \mathbf{hh}\, P(\mathbf{h}, t) \mathrm{d}^3\mathbf{h} \tag{4.22}$$

To obtain the kinetic equation of $\langle \mathbf{hh} \rangle$, it is necessary to investigate the mathematical properties of the last term of Eq. (4.17):

$$\widetilde{\mathbf{M}} \cdot \left[\left(\frac{\partial}{\partial \mathbf{h}} \cdot \left(\widetilde{\mathbf{M}} P \right) \right) \right] = \widetilde{\mathbf{M}} \cdot \left(\frac{\partial}{\partial \mathbf{h}} \cdot \widetilde{\mathbf{M}} + \widetilde{\mathbf{M}} \cdot \frac{\partial \log P}{\partial \mathbf{h}} \right) P \tag{4.23}$$

Here, we used the symmetry of the mobility tensor. Then, the evolution equation of P can be rewritten as

$$\frac{\partial P}{\partial t} = -\frac{\partial}{\partial \mathbf{h}} \cdot (\mathbf{j}_P P) \tag{4.24}$$

where

$$\mathbf{j}_P = \mathbf{L} \cdot \mathbf{h} - \frac{2k}{\zeta} \widetilde{\mathbf{M}} \cdot \mathbf{h} - \frac{2k_\mathrm{B}T}{\zeta} \widetilde{\mathbf{M}} \cdot \left(\frac{\partial}{\partial \mathbf{h}} \cdot \widetilde{\mathbf{M}} \right) - \frac{2k_\mathrm{B}T}{\zeta} \widetilde{\mathbf{M}}^2 \cdot \frac{\partial \log P}{\partial \mathbf{h}} \tag{4.25}$$

The vector $\mathbf{j}_P$ can be interpreted as the flux of probability distribution. The first term of Eq. (4.25) is due to the convection of the flow, the second term due to the connection between the mass points, the third term due to the anisotropy of the mobility tensor, and the last term due to the effect of the random force or diffusional motion of the molecule.

The kinetic equation of $\langle \mathbf{hh} \rangle$ is given by

$$\frac{\mathrm{d}}{\mathrm{d}t} \langle \mathbf{hh} \rangle = \int \mathbf{hh} \frac{\partial P}{\partial t} \mathrm{d}^3\mathbf{h} = -\int \mathbf{hh} \frac{\partial}{\partial \mathbf{h}} \cdot (\mathbf{j}_P P) \mathrm{d}^3\mathbf{h} \tag{4.26}$$

Note that

$$\begin{aligned}\mathbf{hh}\frac{\partial}{\partial \mathbf{h}}\cdot(\mathbf{j}_P P) &= \left[\frac{\partial}{\partial \mathbf{h}}\cdot(\mathbf{j}_P P)\right]\mathbf{hh} \\ &= \frac{\partial}{\partial \mathbf{h}}\cdot(\mathbf{j}_P \mathbf{hh} P) - \left(\mathbf{j}_P \cdot \frac{\partial \mathbf{hh}}{\partial \mathbf{h}}\right)P \\ &= \frac{\partial}{\partial \mathbf{h}}\cdot(\mathbf{j}_P \mathbf{hh} P) - (\mathbf{j}_P \mathbf{h} + \mathbf{h}\mathbf{j}_P)P\end{aligned} \tag{4.27}$$

If taking integral on both sides of Eq. (4.27), then the divergence theorem converts the integral containing divergence to the surface integral. See Problem [4] and [5]. Because of Eq. (4.10), the surface integral vanishes. Then, we finally have

$$\frac{\mathrm{d}}{\mathrm{d}t}\langle \mathbf{hh}\rangle = \langle \mathbf{j}_P \mathbf{h} + \mathbf{h}\mathbf{j}_P\rangle \tag{4.28}$$

Substitution of Eq. (4.25) to Eq. (4.28) gives

$$\begin{aligned}\overset{\nabla}{\langle \mathbf{hh}\rangle} = &-\frac{2}{\zeta}\left\langle k\left(\widetilde{\mathbf{M}}\cdot\mathbf{hh} + \mathbf{hh}\cdot\widetilde{\mathbf{M}}\right)\right\rangle \\ &-\frac{2k_\mathrm{B}T}{\zeta}\left\langle\left[\widetilde{\mathbf{M}}\cdot\left(\frac{\partial}{\partial \mathbf{h}}\cdot\widetilde{\mathbf{M}}\right)\right]\mathbf{h} + \mathbf{h}\left[\widetilde{\mathbf{M}}\cdot\left(\frac{\partial}{\partial \mathbf{h}}\cdot\widetilde{\mathbf{M}}\right)\right]\right\rangle \\ &+\frac{4k_\mathrm{B}T}{\zeta}\left\langle\widetilde{\mathbf{M}}^2\right\rangle + \frac{2k_\mathrm{B}T}{\zeta}\left\langle\left(\frac{\partial}{\partial \mathbf{h}}\cdot\widetilde{\mathbf{M}}^2\right)\mathbf{h} + \mathbf{h}\left(\frac{\partial}{\partial \mathbf{h}}\cdot\widetilde{\mathbf{M}}^2\right)\right\rangle\end{aligned} \tag{4.29}$$

See Problem [6] to understand the treatment of the term of $\partial \log P/\partial \mathbf{h}$. Combining Eq. (4.20) with Eq. (4.29), one can derive the evolution equation of the extra stress which is the constitutive equation.

The symmetric tensor $\langle \mathbf{hh}\rangle$ represents the state of conformation of polymer chain because $\mathbf{h}$ corresponds to the end-to-end vector of a real polymer chain. In equilibrium, it is straightforward that $\langle \mathbf{hh}\rangle$ becomes an isotropic tensor:

$$\langle \mathbf{hh}\rangle_{\mathrm{eq}} = \frac{h_\mathrm{o}^2}{3}\mathbf{I} \quad \text{with} \quad h_\mathrm{o} = \sqrt{\langle \mathbf{h}\cdot\mathbf{h}\rangle_{\mathrm{eq}}} = b\sqrt{N} \tag{4.30}$$

where b and N are, respectively, the size and the number of Kuhn segment. Then, one may invent a symmetric and positive definite tensor which represents the conformation state of polymer as follows

$$\hat{\mathbf{C}} \equiv \frac{3}{h_\mathrm{o}^2}\langle \mathbf{hh}\rangle \tag{4.31}$$

The scale factor $3/h_\mathrm{o}^2$ makes the *conformation tensor* $\hat{\mathbf{C}}$ become the identity tensor in equilibrium state. We will use the notation $\hat{\mathbf{C}}$ for the conformation tensor in order

to distinguish it from the right Cauchy–Green tensor. Then, Eq. (4.20) can be rewritten in terms of the conformation tensor as follows

$$\mathbf{T} = -p\mathbf{I} + \frac{\rho_N h_o^2 k(\langle \mathbf{h} \rangle)}{3}\left(\hat{\mathbf{C}} - \mathbf{I}\right) \tag{4.32}$$

Furthermore, depending on the model of $\widetilde{\mathbf{M}}(\mathbf{h})$, most branches of Eq. (4.29) can be expressed in terms of $\hat{\mathbf{C}}$ in a closed form. Thus, the constitutive equation of the spring-dumbbell model consists of the evolution equation of $\hat{\mathbf{C}}$ with stress equation such as Eq. (4.32). The same formalism is found in various modeling theories of polymer viscoelasticity. Now, we shall move to the discussion on the cases with several models of mobility tensor and spring coefficient.

4.1.4 FENE-P Model

First, we consider the case of isotropic mobility tensor. When $\widetilde{\mathbf{M}} = \mathbf{I}$, Eq. (4.29) becomes dramatically simple:

$$\overset{\nabla}{\langle \mathbf{hh} \rangle} = \frac{4k_B T}{\zeta}\mathbf{I} - \frac{4}{\zeta}\langle k(\mathbf{h})\mathbf{hh} \rangle \tag{4.33}$$

Here, we adopted preaverage decoupling:

$$\langle k(\mathbf{h})\mathbf{hh} \rangle = k(\langle \mathbf{h} \rangle)\langle \mathbf{hh} \rangle \tag{4.34}$$

In equilibrium, the left-hand side of Eq. (4.33) should be zero. Then, we have

$$k\left(\langle h \rangle_{eq}\right)\langle \mathbf{hh} \rangle_{eq} = k_B T\,\mathbf{I} \tag{4.35}$$

Taking trace on both sides of Eq. (4.35), we have

$$k\left(\langle h \rangle_{eq}\right) = \frac{3k_B T}{\langle \mathbf{h} \cdot \mathbf{h} \rangle_{eq}} \equiv k_o \tag{4.36}$$

It is reasonable to assume that

$$\langle \mathbf{h} \cdot \mathbf{h} \rangle_{eq} = Nb^2 \tag{4.37}$$

where N is the number of Kuhn segment in a polymer chain and b is the size of the Kuhn segment. Equation (4.36) agrees with Eq. (4.9) in Chap. 4.

If FENE spring is adopted [see Eq. (4.12) in Chap. 4], then the spring coefficient is given by

$$k(\mathbf{h}) = \frac{k_{\mathrm{o}}}{1 - \mathrm{tr}(\mathbf{hh})/h_{\max}^2} \tag{4.38}$$

Using the nonlinear spring and isotropic mobility tensor, a phenomenological equation can be obtained as follows

$$\overset{\nabla}{\hat{\mathbf{C}}} + \frac{1}{\lambda_{\mathrm{FENE-P}}}\left(z\hat{\mathbf{C}} - \mathbf{I}\right) = \mathbf{0} \tag{4.39}$$

$$z = \frac{\beta}{\beta - \mathrm{tr}\left(\hat{\mathbf{C}}\right)} \tag{4.40}$$

and

$$\mathbf{T} = -p\mathbf{I} + G_{\mathrm{FENE-P}} z\left(\hat{\mathbf{C}} - \mathbf{I}\right) \tag{4.41}$$

where β, $\lambda_{\mathrm{FENE-P}}$, and $G_{\mathrm{FENE-P}}$ are material constants whose physical meanings are understood by the correspondence of $\hat{\mathbf{C}} \propto \langle \mathbf{hh} \rangle$. This constitutive equation is called *FENE-P (finite extensible nonlinear elasticity preaverage)* Bird et al. (1987a)

4.1.5 Upper-Convected Maxwell Model

As the simplest case, consider that the spring coefficient is a constant. This is the Gaussian chain. Then, we do not have to use preaverage process because k is a constant. Equation (4.20) becomes

$$\mathbf{T} = -p\mathbf{I} + 3\frac{\rho_N k_{\mathrm{B}} T}{Nb^2}\left(\langle \mathbf{hh} \rangle - \langle \mathbf{hh} \rangle_{\mathrm{eq}}\right) \tag{4.42}$$

and Eq. (4.33) becomes

$$\overset{\nabla}{\langle \mathbf{hh} \rangle} = \frac{4k_{\mathrm{B}}T}{\zeta}\mathbf{I} - \frac{12k_B T}{\zeta Nb^2}\langle \mathbf{hh} \rangle \tag{4.43}$$

With the help of Eq. (4.35), we have

$$\langle \mathbf{hh} \rangle = \frac{Nb^2}{3\rho_N k_{\mathrm{B}} T}\mathbf{T}' + \frac{Nb^2}{3}\mathbf{I} \tag{4.44}$$

Substitution of Eq. (4.44) to Eq. (4.43) gives

$$\lambda_{\mathrm{M}} \overset{\nabla}{\mathbf{T}}' + \mathbf{T}' = 2\eta_{\mathrm{M}}\mathbf{D} \tag{4.45}$$

where

$$\lambda_{\mathrm{M}} = \frac{\zeta N b^2}{12 k_{\mathrm{B}} T}; \quad \eta_{\mathrm{M}} = \frac{\rho_N \zeta N b^2}{12} \tag{4.46}$$

and we used

$$\overset{\nabla}{\mathbf{I}} = -2\mathbf{D} \tag{4.47}$$

It is interesting that the spring-dumbbell model with linear spring results in the upper-convected Maxwell model. It is also noteworthy that this approach does not consider any interaction between different spring-dumbbell molecules. This means the dilute case. Hence, the FENE-P model seems not to be suitable for polymer melts or concentrated solutions although the model introduces nonlinearity to the chain extension. Extension of chain to the contour length occurs due to the inter-chain interactions such as entanglement. Another interesting feature of this meso-scopic approach is that upper-convected time derivative appears naturally without relying on the principle of material frame-indifference.

4.1.6 Giesekus Model

Giesekus model (1966, 1982) was developed in order to describe the interchain interactions. The idea is that the mobility tensor is not proportional to the identity tensor due to the effect of the environment of the spring-dumbbell molecule. The constitutive equation of the Giesekus model is expressed in terms of extra stress as follows

$$\lambda_{\mathrm{G}} \overset{\nabla}{\mathbf{T}}' + \mathbf{T}' + \frac{\alpha}{G_{\mathrm{G}}} \mathbf{T}'^2 = 2\eta_{\mathrm{G}}\mathbf{D} \tag{4.48}$$

Since $\eta_{\mathrm{G}} = G_{\mathrm{G}}\lambda_{\mathrm{G}}$, the mode has three independent material parameters. The range of dimensionless parameter α is from 0 to 1.

Since the anisotropy arises due to the extra stress, Giesekus used

$$\widetilde{\mathbf{M}} = \mathbf{I} + \frac{\alpha}{\rho_{\mathrm{N}} k_{\mathrm{B}} T} \mathbf{T}' \tag{4.49}$$

Note that the parameter α is a dimensionless one and $\rho_{\mathrm{N}} k_{\mathrm{B}} T$ has the dimension of stress. Since the last term of Eq. (4.49) represents the deviation from isotropic mobility tensor, it is guessed that α is a small positive number. With the help of Eq. (4.20), Eq. (4.48) is equivalent to

$$\widetilde{\mathbf{M}} = \mathbf{I} + \alpha\left(\hat{\mathbf{C}} - \mathbf{I}\right) = (1-\alpha)\mathbf{I} + \alpha\,\hat{\mathbf{C}} \tag{4.50}$$

Hence, Eq. (4.48) is to use preaverage approach. Using this mobility tensor model, Eq. (4.48) can be derived by substitution of Eq. (4.48) to Eq. (4.29).

On the other hand, one might consider the mobility tensor model such as

$$\widetilde{\mathbf{M}} = \mathbf{I} + \frac{3\alpha}{h_o^2}\left(\mathbf{hh} - \frac{h_o^2}{3}\mathbf{I}\right) \tag{4.51}$$

This model looks like more microscopic than its preaverage version. Another candidate of the mobility tensor might be

$$\widetilde{\mathbf{M}} = \alpha\,\mathbf{uu} + \beta(\mathbf{I} - \mathbf{uu}) \tag{4.52}$$

where

$$\mathbf{u} = \frac{\mathbf{h}}{\|\mathbf{h}\|} \tag{4.53}$$

This model implies that if applied force $\mathbf{f}$ is proportional to $\mathbf{h}$, then the velocity is given by $\mathbf{v} = (\alpha/\zeta)\mathbf{f}$, while if applied force is perpendicular to $\mathbf{h}$, then the velocity is given by $\mathbf{v} = (\beta/\zeta)\mathbf{f}$.

It is interesting that the two models of mobility tensor, Eqs. (4.51) and (4.52), cannot result in the term of $\mathbf{T}'^2$ of Eq. (4.48) because of the cancelation of the coefficients of $\langle \mathbf{hh} \cdot \mathbf{hh} \rangle$. Read Bird et al. (1987a) if the consequence of (4.52) in Chap. 1 is interesting.

Substitution of Eq. (4.49) to Eq. (4.29) yields Eq. (4.48) with

$$\lambda_G = \frac{\zeta h_o^2}{12(1-\alpha)k_B T}; \quad G_G = \rho_N k_B T; \quad \eta_G = \lambda_G G_G \tag{4.54}$$

Since relaxation time λ must be positive, it is obvious that $0 \le \alpha < 1$. If $\alpha = 0$, then the Giesekus model becomes the upper-convected Maxwell model.

Consider the simple shear flow of $\mathbf{L} = \dot{\gamma}(t)\mathbf{e}_1\mathbf{e}_2$. Because of the strong nonlinearity of the Giesekus model, it is hard to obtain viscometric material functions analytically. However, as for the stress relaxation ($\mathbf{L} = \gamma_o \delta(t)\mathbf{e}_1\mathbf{e}_2$), Holz et al. (1999) calculated analytically nonlinear relaxation modulus:

$$G(t, \gamma_o) = \frac{G_G}{e^{t/\lambda_G} + 2\alpha^2\gamma_o^2[1 - \cos h(t/\lambda_G)] + \alpha\gamma_o^2(e^{t/\lambda_G} - 1)} \tag{4.55}$$

This equation of relaxation modulus does not show time–strain separability when $t < \lambda_G$. Hence, the Giesekus model may be classified as a non-separable constitutive equation (Larson 1988). However, if $t > \lambda_G$, Eq. (4.55) can be approximated by

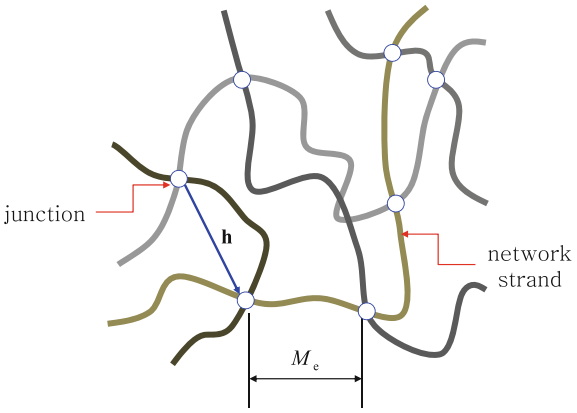

Fig. 6 Schematic illustration of temporary network

$$G(t,\gamma_o) \approx G(t)h_G(\gamma_o) \tag{4.56}$$

where the damping function of the Giesekus model is given by

$$h_G(\gamma_o) = \lim_{t\to\infty} \frac{G(t,\gamma_o)}{G(t,0)} = \frac{1}{1+\alpha(1-\alpha)\gamma_o^2} \tag{4.57}$$

4.2 Temporary Network Approaches

To describe concentrated polymer solutions and melt, concept of temporary network has been used for long time. The concept seems to be originated from molecular theories of rubber which is a network of polymer chains connected by permanent covalent bonds. Temporary network is a metaphor for the permanent network of rubber. Although the permanent network does not allow any relaxation processes, temporary network permits creation and annihilation of substrands between adjacent junctions in order to describe stress relaxation. Figure 6 illustrates the concept of temporary network.

Green and Tobolsky (1946) proposed a constitutive equation based on the simplest model of temporary network:

$$\mathbf{T} = -p\mathbf{I} + \frac{G_{GT}}{\lambda_{GT}} \int_{-\infty}^{t} \exp\left(-\frac{t-\tau}{\lambda_{GT}}\right) \mathbf{C}_t^{-1}(\tau)\mathrm{d}\tau \tag{4.58}$$

This equation is known equivalent to the upper-convected Maxwell model.

Yamamoto (1956) developed the kinetics of creation and annihilation of temporary network in a generalized manner. However, the work of Yamamoto is not constitutive equation. Phan-Thien and Tanner (1977) proposed a nonlinear

viscoelastic constitutive equation which is based on the theory of Yamamoto. The model will be denoted by the *PTT model (Phan-Thien and Tanner model).*

Let the probability distribution function of substrand vector $\mathbf{h}$ be $P(\mathbf{h}, t)$. Then, one may imagine the equation of probability preservation Eq. (4.11). Different from the spring-dumbbell model, the temporary network does not have detailed micromechanics. A formal kinetic equation of $P(\mathbf{h}, t)$ may be given by

$$\frac{\partial P}{\partial t} + \dot{\mathbf{h}} \cdot \frac{\partial P}{\partial \mathbf{h}} = c(\|\mathbf{h}\|) - a(\|\mathbf{h}\|)P \tag{4.59}$$

where $c(\|\mathbf{h}\|)$ is the creation rate and $a(\|\mathbf{h}\|)$ represents annihilation rate. It is not easy to find clear reason why creation rate should be anisotropic function of $\mathbf{h}$. On the other hand, annihilation mechanism should be related to stress which must be anisotropic. Hence, it can be said that $a(\|\mathbf{h}\|)P(\mathbf{h}, t)$ may be one of the simplest forms of annihilation rate. These two functions must be modeled as well as $\dot{\mathbf{h}}$.

As for the time derivative of $\mathbf{h}$, Gordon and Schowalter (1972) suggested non-affine formulation such that

$$\frac{\mathrm{d}\mathbf{h}}{\mathrm{d}t} = \mathbf{L} \cdot \mathbf{h} - \frac{1}{5\lambda_{\mathrm{PTT}}}\mathbf{h} - \xi \mathbf{D} \cdot \mathbf{h} \tag{4.60}$$

where λ_{PTT} and ξ are positive constants. Multiplying $\mathbf{hh}$ on both sides of Eq. (4.59) and integration gives

$$\begin{aligned} &\frac{\mathrm{d}}{\mathrm{d}t}\langle \mathbf{hh} \rangle - (\mathbf{L} - \xi \mathbf{D}) \cdot \langle \mathbf{hh} \rangle - \langle \mathbf{hh} \rangle \cdot (\mathbf{L} - \xi \mathbf{D})^{\mathrm{T}} + \frac{1}{\lambda_{\mathrm{PTT}}}\langle \mathbf{hh} \rangle \\ &\quad = \int c(\|\mathbf{h}\|)\mathbf{hh}\, \mathrm{d}^3\mathbf{h} - \langle a(\|\mathbf{h}\|)\mathbf{hh} \rangle \end{aligned} \tag{4.61}$$

Since the function $c(\|\mathbf{h}\|)$ is an isotropic function of $\mathbf{h}$, it is not difficult to show that the integral of creation rate should be proportional to the identity tensor. Actually, Phan-Thien and Tanner modeled the term as follows

$$\int c(\|\mathbf{h}\|)\mathbf{hh}\, \mathrm{d}^3\mathbf{h} = \frac{\chi_c(\mathrm{tr}\langle \mathbf{hh} \rangle)}{\lambda_{\mathrm{PTT}}}\mathbf{I} \tag{4.62}$$

As for the annihilation term, preaverage approximation can be applied as follows

$$\langle a(\|\mathbf{h}\|)\mathbf{hh} \rangle \approx a(\langle \|\mathbf{h}\| \rangle)\langle \mathbf{hh} \rangle = \frac{\chi_a(\mathrm{tr}\langle \mathbf{hh} \rangle)}{\lambda_{\mathrm{PTT}}}\langle \mathbf{hh} \rangle \tag{4.63}$$

Since this approximation should meet the equilibrium condition, we have

$$\frac{1}{\lambda_{\mathrm{PTT}}}\langle \mathbf{hh}\rangle_{\mathrm{eq}} = \frac{\chi_c\left(\mathrm{tr}\langle \mathbf{hh}\rangle_{\mathrm{eq}}\right)}{\lambda_{\mathrm{PTT}}}\mathbf{I} - \frac{\chi_a\left(\mathrm{tr}\langle \mathbf{hh}\rangle_{\mathrm{eq}}\right)}{\lambda_{\mathrm{PTT}}}\langle \mathbf{hh}\rangle_{\mathrm{eq}} \tag{4.64}$$

If Eq. (4.30) is adopted again and the result is extended to non-equilibrium (flow situation), then we have

$$\frac{3}{h_{\mathrm{o}}^2}\chi_c(\mathrm{tr}\langle \mathbf{hh}\rangle) = 1 + \chi_a(\mathrm{tr}\langle \mathbf{hh}\rangle) \tag{4.65}$$

Just like Eqs. (4.32) and (4.42), the extra stress can be formulated by

$$\mathbf{T}' = G_{\mathrm{PTT}}\left(\hat{\mathbf{C}} - \mathbf{I}\right) \tag{4.66}$$

With the help of Eq. (4.31), (4.61) is transformed to that of extra stress as follows

$$\lambda_{\mathrm{PTT}}\frac{\Delta \mathbf{T}'}{\Delta t} + (1+\chi_a)\mathbf{T}' = 2\eta_{\mathrm{PTT}}(1-\xi)\mathbf{D} \tag{4.67}$$

where $\eta_{\mathrm{PTT}} = G_{\mathrm{PTT}}\lambda_{\mathrm{PTT}}$ and we define a new objective time derivative:

$$\frac{\Delta \mathbf{T}'}{\Delta t} \equiv \frac{\mathrm{d}\mathbf{T}'}{\mathrm{d}t} - (\mathbf{L} - \xi\mathbf{D})\cdot\mathbf{T}' - \mathbf{T}'\cdot(\mathbf{L} - \xi\mathbf{D})^{\mathrm{T}} \tag{4.68}$$

The function $1+\chi_a$ can be replaced by Phan-Thien and Tanner (1977) and Phan–Thien (1978)

$$\phi(\mathrm{tr}\mathbf{T}') = 1 + \frac{\varepsilon}{G}\mathrm{tr}(\mathbf{T}') \quad \text{or} \quad \exp\left[\frac{\varepsilon}{G}\mathrm{tr}(\mathbf{T}')\right] \tag{4.69}$$

4.3 Multimode Versions

Consider $N+1$ mass points of the same mass which are connected by N linear springs of the same spring coefficient. This is the discrete Rouse chain. Similar approaches of Sect. 4.1 in Chap. 10 can be applied to this system. Since detailed calculation is found in Huilgol and Phan-Thien (1997), we write the results here as follows:

$$\mathbf{T} = -p\mathbf{I} + \sum_{k=1}^{N}\mathbf{T}_k' \tag{4.70}$$

and

$$\lambda_k \overset{\nabla}{\mathbf{T}}'_k + \mathbf{T}'_k = 2\eta_k \mathbf{D} \tag{4.71}$$

Note that λ_k and $G_k = \eta_k/\lambda_k$ obey the discrete relaxation time spectrum of the Rouse model (see Sect. 4.3 in Chap. 5).

The constitutive models previously discussed do not contain any distribution of relaxation times. Such models are called a single-mode model. To increase agreement with experimental data, the effect of relaxation spectrum should be included in the nonlinear viscoelastic models. Multimode versions of the Giesekus and the PTT models are, respectively, given by

$$\lambda_k \overset{\nabla}{\mathbf{T}}'_k + \mathbf{T}'_k + \frac{\alpha_k}{G_k}\mathbf{T}'^2_k = 2\eta_k \mathbf{D} \tag{4.72}$$

and

$$\lambda_k \frac{\Delta \mathbf{T}'_k}{\Delta t} + \phi\left(\varepsilon_k \frac{\mathrm{tr}\mathbf{T}'_k}{G_k}\right)\mathbf{T}'_k = 2\eta_k \mathbf{D} \tag{4.73}$$

Of course, we know that $\eta_k = G_k\lambda_k$.

Thus, these nonlinear constitutive equations have two types of material parameters: linear and nonlinear parameters. The linear parameters are discrete relaxation spectrum, and nonlinear ones are α_k, ξ_k and ε_k. We have learned how to determine relaxation time spectrum from linear viscoelastic data. However, it is not easy to determine the distribution of the nonlinear parameters from nonlinear viscoelastic data. Consider the multimode version of the nonlinear relaxation modulus of the Giesekus model:

$$G(t,\gamma_o) = \sum_{k=1}^{N} \frac{G_k}{e^{t/\lambda_k} + 2\alpha_k^2\gamma_o^2[1-\cosh(t/\lambda_k)] + \alpha_k\gamma_o^2(e^{t/\lambda_k}-1)} \tag{4.74}$$

Even if the linear parameters are known, it is doubt that nonlinear regression of Eq. (4.74) could give α_k robustly. It is also curious whether experimental data can be fitted by assigning nonlinear parameters to single value but maintaining distribution of linear parameters. However, there is a report that the nondistributive nonlinear parameter can fit experimental data quite well (Simhambhatla and Leonov 1995; Bae and Cho 2015).

Problems 4

[1] Using the equipartition theorem, derive Eq. (4.18).
[2] Derive Eq. (4.16).
[3] Derive Eq. (4.17).
[4] Consider the divergence theorem

$$\int \frac{\partial}{\partial \mathbf{h}} \cdot \mathbf{v}(\mathbf{h}) \mathrm{d}^3\mathbf{h} = \oint \mathbf{v}(\mathbf{h}) \cdot \mathbf{n} \, \mathrm{d}a_{\mathbf{h}} \tag{4.a}$$

where $\mathbf{n}$ is the outward unit normal vector of the boundary of the domain of $\mathbf{h}$ and $\mathrm{d}a_{\mathbf{h}}$ is the differential element of the boundary surface. Show that for any $\mathbf{h}$-dependent vector $\mathbf{a}$ and tensor $\mathbf{B}$, the followings hold

$$\int \frac{\partial}{\partial \mathbf{h}} \cdot (\mathbf{a}\mathbf{B}P) \mathrm{d}^3\mathbf{h} = \oint (\mathbf{n} \cdot \mathbf{a}) \mathbf{B} P \, \mathrm{d}a_{\mathbf{h}} \tag{4.b}$$

and

$$\int \frac{\partial}{\partial \mathbf{h}} \cdot (\mathbf{B}\mathbf{a}P) \mathrm{d}^3\mathbf{h} = \oint (\mathbf{n} \cdot \mathbf{a}) \mathbf{B} P \, \mathrm{d}a_{\mathbf{h}} \tag{4.c}$$

[5] Show that

$$\mathbf{j}_P \cdot \frac{\partial \mathbf{h}\mathbf{h}}{\partial \mathbf{h}} = \mathbf{j}_P \mathbf{h} + \mathbf{h} \cdot \mathbf{j}_P \tag{4.d}$$

[6] Show that

$$\left\langle \mathbf{h}\mathbf{B} \cdot \frac{\partial \log P}{\partial \mathbf{h}} \right\rangle = -\left\langle \mathbf{h} \left(\frac{\partial}{\partial \mathbf{h}} \cdot \mathbf{B}^{\mathrm{T}} \right) \right\rangle - \langle \mathbf{B}^{\mathrm{T}} \rangle \tag{4.e}$$

and

$$\left\langle \mathbf{B} \cdot \frac{\partial \log P}{\partial \mathbf{h}} \mathbf{h} \right\rangle = -\left\langle \left(\frac{\partial}{\partial \mathbf{h}} \cdot \mathbf{B}^{\mathrm{T}} \right) \mathbf{h} \right\rangle - \langle \mathbf{B} \rangle \tag{4.e}$$

[7] Express the FENE-P model in terms of extra stress.

[8] Derive the evolution equation of the conformation tensor for the linear spring and mobility tensor of Eq. (4.51).

[9] Using Eqs. (4.59) and (4.60), derive Eq. (4.61).

[10] For any function $c(\|\mathbf{h}\|)$ which satisfies

$$\int \|\mathbf{h}\|^2 c(\|\mathbf{h}\|) \mathrm{d}^3\mathbf{h} < \infty \tag{4.f}$$

Show that

$$\int \mathbf{h}\mathbf{h} c(\|\mathbf{h}\|) \mathrm{d}^3\mathbf{h} < \frac{1}{3} \left[\int \|\mathbf{h}\|^2 c(\|\mathbf{h}\|) \mathrm{d}^3\mathbf{h} \right] \mathbf{I} \tag{4.g}$$

[11] Show that the time derivative of Eq. (4.68) is objective.

5 Thermodynamic Theory

Constitutive equation is the relation between macroscopic quantities such as stress, deformation gradient, and time derivatives of deformation gradient. Thermody namics is a macroscopic science on transform of energy and its direction. Hence, it can be said that any proper constitutive equation must satisfy the second law of thermodynamics. However, constitutive equations introduced in previous sections have been developed without the consideration of the second law. Here, we shall introduce a constitutive model which has been developed from the basis of irre-versible thermodynamics of internal variable: the Leonov model. It is interesting that some of constitutive equations in previous sections satisfy the second law, too. After the introduction to the Leonov model, we shall move to the thermodynamic analysis of other models.

5.1 Leonov Model

In theory of metal plasticity, when strain is infinitesimal, it is supposed to be decomposed into elastic and plastic ones. Plastic strain represents permanent deformation when loading exceeds yield condition. However, this infinitesimal plasticity theory cannot be applied to finite deformation. Lee (1969) proposed multiplicative decomposition of deformation. The Leonov model is based on the multiplicative decomposition as well as thermodynamics.

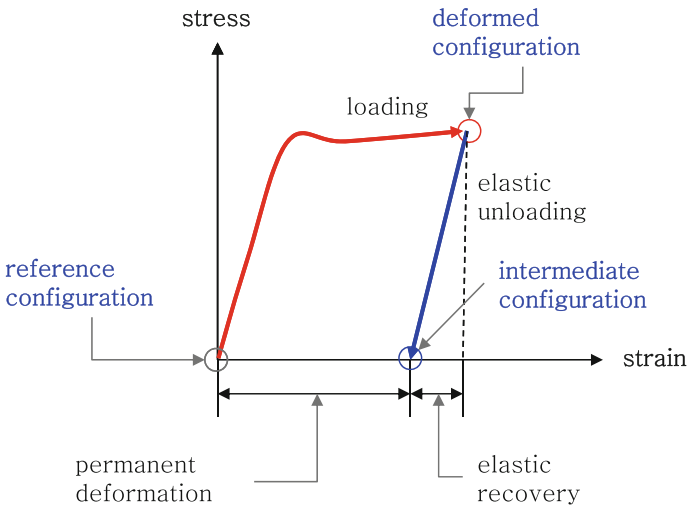

Fig. 7 Schematic illustration of plastic and elastic deformation

The decomposition theory assumes an intermediate configuration which could be observed if elastic unloading is done after the given deformation. Figure 7 illustrates this. If the intermediate configuration be denoted by $\hat{\mathbf{x}}$, then we have relations such that

$$d\mathbf{x} = \mathbf{F} \cdot d\tilde{\mathbf{x}}; \quad d\hat{\mathbf{x}} = \mathbf{F}_e^{-1} \cdot d\mathbf{x} \tag{5.1}$$

This immediately means that

$$\mathbf{F} = \mathbf{F}_\mathrm{e} \cdot \mathbf{F}_\mathrm{p} \tag{5.2}$$

Here, $\mathbf{F}_\mathrm{p}$ represents the deformation gradient for the permanent deformation of Fig. 7.

Using Eq. (1.46) in Chap. 2, the multiplicative decomposition yields

$$\mathbf{L} = \frac{d\mathbf{F}_\mathrm{e}}{dt} \cdot \mathbf{F}_\mathrm{e}^{-1} + \mathbf{F}_\mathrm{e} \cdot \frac{d\mathbf{F}_\mathrm{p}}{dt} \cdot \mathbf{F}_\mathrm{p}^{-1} \cdot \mathbf{F}_\mathrm{e}^{-1} \tag{5.3}$$

Since $\mathbf{L} = \dot{\mathbf{F}} \cdot \mathbf{F}^{-1}$, the first term can be considered as elastic velocity gradient. Then, we can define

$$\mathbf{L}_\mathrm{e} = \frac{d\mathbf{F}_\mathrm{e}}{dt} \cdot \mathbf{F}_\mathrm{e}^{-1}; \quad \mathbf{L}_\mathrm{p} = \mathbf{F}_\mathrm{e} \cdot \frac{d\mathbf{F}_\mathrm{p}}{dt} \cdot \mathbf{F}_\mathrm{p}^{-1} \cdot \mathbf{F}_\mathrm{e}^{-1}; \quad \mathbf{L} = \mathbf{L}_\mathrm{e} + \mathbf{L}_\mathrm{p} \tag{5.4}$$

Analogy to deformation rate and vorticity tensors gives

$$\begin{aligned} 2\mathbf{D}_\mathrm{e} &= \mathbf{L}_\mathrm{e} + \mathbf{L}_\mathrm{e}^\mathrm{T}; \quad 2\mathbf{W}_\mathrm{e} = \mathbf{L}_\mathrm{e} - \mathbf{L}_\mathrm{e}^\mathrm{T}; \\ 2\mathbf{D}_\mathrm{p} &= \mathbf{L}_\mathrm{p} + \mathbf{L}_\mathrm{p}^\mathrm{T}; \quad 2\mathbf{W}_\mathrm{p} = \mathbf{L}_\mathrm{p} - \mathbf{L}_\mathrm{p}^\mathrm{T} \end{aligned} \tag{5.5}$$

Because of Eq. (5.4), we also know that for incompressible fluids,

$$\mathrm{tr}\mathbf{D}_\mathrm{e} + \mathrm{tr}\mathbf{D}_\mathrm{p} = 0 \tag{5.6}$$

From this kinematic analysis, it is obvious that

$$\det \mathbf{F} = \frac{\rho}{\rho_\mathrm{ref}} = 1; \quad \det \mathbf{F}_\mathrm{e} = \frac{\rho_\mathrm{p}}{\rho}; \quad \det \mathbf{F}_\mathrm{p} = \frac{\rho_\mathrm{ref}}{\rho_\mathrm{p}} \tag{5.7}$$

where ρ_ref, ρ_p, and ρ represent, respectively, densities of the reference, intermediate, and current configurations. Further assumption of $\rho = \rho_\mathrm{p}$ gives

$$\det \mathbf{F}_\mathrm{e} = \det \mathbf{F}_\mathrm{p} = 1 \tag{5.8}$$

According to Leonov (1976), $\mathrm{tr}\,\mathbf{D} = 0$ and Eq. (5.8) gives

$$\mathrm{tr}\,\mathbf{D}_\mathrm{p} = \mathrm{tr}\,\mathbf{D}_\mathrm{e} = 0 \tag{5.9}$$

Analogous to the left Cauchy–Green tensor $\mathbf{B}$, we can define conformation tensor as follows

$$\mathbf{B}_\mathrm{e} \equiv \mathbf{F}_\mathrm{e} \cdot \mathbf{F}_\mathrm{e}^\mathrm{T} \equiv \hat{\mathbf{C}} \tag{5.10}$$

The definition of elastic velocity gradient Eq. (5.4) implies that

$$\frac{\mathrm{d}\hat{\mathbf{C}}}{\mathrm{d}t} - \mathbf{L}_\mathrm{e} \cdot \hat{\mathbf{C}} - \hat{\mathbf{C}} \cdot \mathbf{L}_\mathrm{e}^\mathrm{T} = \mathbf{0} \tag{5.11}$$

This form is identical to that of $\mathbf{B}$:

$$\frac{\mathrm{d}\mathbf{B}}{\mathrm{d}t} - \mathbf{L} \cdot \mathbf{B} - \mathbf{B} \cdot \mathbf{L}^\mathrm{T} = \mathbf{0} \tag{5.12}$$

Since incompressible hyperelastic material has the stress such that

$$\mathbf{T} = -p\mathbf{I} + 2\rho\left(\frac{\partial f}{\partial I_\mathbf{B}}\mathbf{B} - \frac{\partial f}{\partial I_{\mathbf{B}^{-1}}}\mathbf{B}^{-1}\right) \tag{5.13}$$

Maxwellian fluid can be defined by the fluid whose stress is given by

$$\mathbf{T} = -p\mathbf{I} + 2\rho\left(\frac{\partial f}{\partial I_{\hat{\mathbf{C}}}}\hat{\mathbf{C}} - \frac{\partial f}{\partial I_{\hat{\mathbf{C}}^{-1}}}\hat{\mathbf{C}}^{-1}\right) \tag{5.14}$$

Thus, the free energy of the Maxwellian fluid depends on only the elastic strain $\hat{\mathbf{C}}$ and temperature:

$$f = f\left(I_{\hat{\mathbf{C}}}, II_{\hat{\mathbf{C}}}, T\right) \tag{5.15}$$

Leonov used the second law of Eq. (4.83) in Chap. 2 in order to make Eq. (5.9) become the closed form. As for isothermal process, Eq. (4.83) in Chap. 2 can be rewritten as

$$\mathbf{T} : \mathbf{D} - \rho\left(\frac{\mathrm{d}f}{\mathrm{d}t}\right)_T \geq 0 \tag{5.16}$$

Here, the conformation tensor is the internal variable and free energy per unit mass is a function of the conformation tensor $\hat{\mathbf{C}}$ and temperature T. Then, we have

$$\begin{aligned}\rho\left(\frac{\mathrm{d}f}{\mathrm{d}t}\right)_T &= \rho\left(\frac{\partial f}{\partial I_{\hat{\mathbf{C}}}}\frac{\partial I_{\hat{\mathbf{C}}}}{\partial \hat{\mathbf{C}}} + \frac{\partial f}{\partial II_{\hat{\mathbf{C}}}}\frac{\partial II_{\hat{\mathbf{C}}}}{\partial \hat{\mathbf{C}}}\right) : \frac{\mathrm{d}\hat{\mathbf{C}}}{\mathrm{d}t} \\ &= 2\rho\mathrm{tr}\left\{\left[\frac{\partial f}{\partial I_{\hat{\mathbf{C}}}}\hat{\mathbf{C}} + \frac{\partial f}{\partial II_{\hat{\mathbf{C}}}}\left(I_{\hat{\mathbf{C}}}\hat{\mathbf{C}} - \hat{\mathbf{C}}^2\right)\right]\cdot \mathbf{D}_\mathrm{e}\right\}\end{aligned} \tag{5.17}$$

With the help of the Cayley–Hamilton theorem, we know that when $\det \mathbf{F}_\mathrm{e} = 1$

$$I_{\hat{\mathbf{C}}} = II_{\hat{\mathbf{C}}^{-1}}; \quad II_{\hat{\mathbf{C}}} = I_{\hat{\mathbf{C}}^{-1}} \tag{5.18}$$

and

$$I_{\hat{\mathbf{C}}}\hat{\mathbf{C}} - \hat{\mathbf{C}}^2 = I_{\hat{\mathbf{C}}}\mathbf{I} - \hat{\mathbf{C}}^{-1} \tag{5.19}$$

Because of Eqs. (5.9), (5.17) can be rewritten as

$$\rho\left(\frac{\mathrm{d}f}{\mathrm{d}t}\right)_T = -2\rho\left(\frac{\partial f}{\partial I_{\hat{\mathbf{C}}}}\hat{\mathbf{C}} - \frac{\partial f}{\partial I_{\hat{\mathbf{C}}^{-1}}}\hat{\mathbf{C}}^{-1}\right) : \mathbf{D}_\mathrm{e} = \mathbf{T}' : \mathbf{D}_\mathrm{e} \tag{5.20}$$

Finally, the Clausius-Duhem inequality becomes simpler

$$\mathbf{T}' : (\mathbf{D} - \mathbf{D}_\mathrm{e}) = \mathbf{T}' : \mathbf{D}_\mathrm{p} = \mathbf{T}' : \mathbf{L}_\mathrm{p} \geq 0 \tag{5.21}$$

Note that we used $\mathrm{tr}\,\mathbf{D} = 0$ for the isotropic part of stress. Equation (5.21) implies that the second law holds irrespective of $\mathbf{W}_\mathrm{p}$. Hence, we can set

$$\mathbf{W}_\mathrm{p} = \mathbf{0} \tag{5.22}$$

If the plastic deformation rate is proportional to the extra stress, then the inequality holds. More general form of the plastic deformation rate tensor may be

$$\mathbf{D}_\mathrm{p} = \mathbf{M} : \mathbf{T}' = \mathbf{L}_\mathrm{p} \tag{5.23}$$

where $\mathbf{M}$ is a positive definite fourth-order tensor. As simpler form, we consider

$$\mathbf{D}_\mathrm{p} = b_1\left(\hat{\mathbf{C}} - \tfrac{1}{3}I_{\hat{\mathbf{C}}}\mathbf{I}\right) - b_2\left(\hat{\mathbf{C}}^{-1} - \tfrac{1}{3}I_{\hat{\mathbf{C}}^{-1}}\mathbf{I}\right) \tag{5.24}$$

where b_1 and b_2 are functions of the principle invariants of the conformation tensor:

$$b_k = b_k\left(I_{\hat{\mathbf{C}}}, I_{\hat{\mathbf{C}}^{-1}}\right) \tag{5.25}$$

The simplest one may be

$$\mathbf{D}_{\mathrm{p}} = \frac{1}{4\lambda_{\mathrm{L}}}\left[\left(\hat{\mathbf{C}} - \frac{1}{3}I_{\hat{\mathbf{C}}}\mathbf{I}\right) - \left(\hat{\mathbf{C}}^{-1} - \frac{1}{3}I_{\hat{\mathbf{C}}^{-1}}\mathbf{I}\right)\right] \tag{5.26}$$

Now, we shall move to the evolution equation of the conformation tensor. Equation (5.11) can be rewritten as

$$\overset{\nabla}{\hat{\mathbf{C}}} + \mathbf{L}_{\mathrm{p}} \cdot \hat{\mathbf{C}} + \hat{\mathbf{C}} \cdot \mathbf{L}_{\mathrm{p}}^{T} = \mathbf{0} \tag{5.27}$$

Here, we used $\mathbf{L}_{\mathrm{e}} = \mathbf{L} - \mathbf{L}_{\mathrm{p}}$. Since $\mathbf{L}_{\mathrm{p}} = \mathbf{D}_{\mathrm{p}}$ and Eq. (5.24) means that $\mathbf{D}_{\mathrm{p}} \cdot \hat{\mathbf{C}} = \hat{\mathbf{C}} \cdot \mathbf{D}_{\mathrm{p}}$, the evolution equation of the conformation tensor can be rewritten as

$$\overset{\nabla}{\hat{\mathbf{C}}} + 2\hat{\mathbf{C}} \cdot \mathbf{D}_{\mathrm{p}} = \mathbf{0} \tag{5.28}$$

The Leonov model is not a single constitutive equation. The model can have various ramifications depending on how plastic deformation rate tensor and stress are modeled.

5.2 *Thermodynamic Analysis of Other Models*

It is interesting that the Leonov, the spring-dumbbell, and the PTT models can with $\xi = 0$ be expressed by the common form such that

$$\overset{\nabla}{\hat{\mathbf{C}}} + \frac{1}{\lambda}\hat{\mathbf{S}}\left(\hat{\mathbf{C}}\right) = \mathbf{0} \tag{5.29}$$

and

$$\mathbf{T} = 2\rho\hat{\mathbf{C}} \cdot \frac{\partial f}{\partial \hat{\mathbf{C}}} \tag{5.30}$$

Here, $\mathbf{S}(\hat{\mathbf{C}})$ is a tensor-valued function of the conformation tensor. Because of Eq. (5.30), these models may be called the Maxwellian fluid models. Equations (5.29) and (5.30) are called the canonical equations. The Leonov model itself was derived in the form of the canonical equation:

$$\frac{1}{\lambda}\hat{\mathbf{S}}\left(\hat{\mathbf{C}}\right) = 2\hat{\mathbf{C}} \cdot \mathbf{D}_{\mathrm{p}} \tag{5.31}$$

We shall find the condition that the Maxwellian fluids satisfy Eq. (5.16). With the help of Eqs. (5.29) and (5.30), we have

$$\mathbf{T} : \mathbf{D} - \rho\left(\frac{\mathrm{d}f}{\mathrm{d}t}\right) = \frac{\rho}{\lambda}\mathrm{tr}\left(\frac{\partial f}{\partial \hat{\mathbf{C}}} \cdot \hat{\mathbf{S}}\right) \geq 0 \tag{5.32}$$

Various models have the free energy of

$$\rho f = \frac{G}{2} I_{\hat{\mathbf{C}}} \tag{5.33}$$

Then, the second law becomes

$$\mathrm{tr}\,(\hat{\mathbf{S}}) \geq 0 \tag{5.34}$$

As for the PTT model with $\xi = 0$, we know that

$$\hat{\mathbf{S}} = \phi\left(\hat{\mathbf{C}} - \mathbf{I}\right) \text{with } \phi\left(I_{\hat{\mathbf{C}}}\right) > 0 \tag{5.35}$$

If $I_{\hat{\mathbf{C}}} \geq 3$, the PTT model with $\xi = 0$ satisfies the second law.

Problems 5

[1] Derive Eq. (5.17).
[2] Find $\hat{\mathbf{S}}(\hat{\mathbf{C}})$ of the Giesekus and the PPT models with $\xi = 0$.
[3] Derive Eq. (5.32)
[4] Consider the nonlinear viscoelastic models: the separable K-BKZ, the Giesekus, the PTT, and the Leonov models. Using these models, explain why experimental data (Laun 1978) show the time–temperature superposition such that

$$\frac{\eta(\dot{\gamma}, T)}{a_T} = f_\eta(a_T\dot{\gamma}); \quad \frac{\psi_1(\dot{\gamma}, T)}{a_T^2} = f_{\psi_1}(a_T\dot{\gamma}) \tag{5.a}$$

Note that Eq. (5.a) assumes $b_T = 1$.

References

J.-E. Bae, K.S. Cho, Semianalytical methods for the determination of the nonlinear parameter of nonlinear viscoelastic constitutive equations from LAOS data. J. Rheol. **59**, 525–555 (2015)
B. Bernstein, E.A. Kearsley, L.J. Zapas, A study of stress relaxation with finite strain. Trans. Soc. Rheol. **7**, 391–410 (1963)
R.B. Bird, C.F. Curtiss, R.C. Armstrong, O. Hassager, *Dynamics of Polymeric Liquids Vol. 2. Kinetic Theory* (Wiley, USA, 1987a)

R.B. Bird, R.C. Armstrong, O. Hassager, *Dynamics of Polymeric Liquids Vol. 1. Fluid Mechanics*, John Wiley and Sons (1987b)
Doi, M., Edwards, S. F., *The Theory of Polymer Dynamics* (Oxford, New York, 1986)
H. Giesekus, Die Elastizität von Flussigkeiten. Rheol. Acata **5**, 29–35 (1966)
H. Giesekus, A simple constitutive equation for polymer fluids based on the concept of deformation-dependent tensorial mobility. J. Non-Newtonian Fluid Mech. **11**, 69–109 (1982)
R.J. Gordon, W.R. Schowalter, Anisotropic fluid theory: a different approach to the dumbell theory of dilute polymer solutions. Trans. Soc. Rheol. **16**, 79–97 (1972)
A.E. Green, R.S. Rivlin, The mechanics of non-linear materials with memory. Archs. Ration. Mech. Anal. **1**, 1–21 (1957)
M.S. Green, A.V. Tobolsky, A new approach to the theory of relaxing polymeric media. J. Chem. Phys. **14**, 80–92 (1946)
T. Holz, P. Fischer, H. Rehage, Shear relaxation in the nonlinear-viscoelastic regime of a Giesekus fluid. J. Non-Newtonian Fluid Mech. **88**, 133–148 (1999)
R.R. Huilgol, N. Phan-Thien, *Fluid Mechanics of Viscoelasticity* (Elsevier, USA, 1997)
A. Kaye, *Non-Newtonian Flow in Incompressible Fluids* (College of Aeronautics, Clanfield, Note No. 134, 1962)
Y. Kwon, K.S. Cho, Time-strain nonseparability in viscoelastic constitutive equations. J. Rheol. **45**, 1441–1452 (2001)
R.G. Larson, *Constitutive Equations for Polymer Melts and Solutions* (Butterworths, UK, 1988)
H.M. Laun, Description of the nonlinear shear behavior of a low density polyethylene melt by means of an experimentally determined strain dependent memory function. Rheol. Acta **17**, 1–15 (1978)
H.M. Laun, H. Münstedt, Elongational behavior of a low density polyethylene melt, I. strain rate and stress dependence of viscosity and recoverable strain in the steady-state. Comparison with shear data. Influence of interfacial tension. Rheol. Acta **17**, 415–425 (1978)
E.H. Lee, Elastic-plastic deformation at finite strains. J. Appl. Mech. **36**, 1–6 (1969)
A.I. Leonov, Nonequilibrium thermodynamics and rheology of viscoelastic polymer media. Rheol. Acta **15**, 85–98 (1976)
C.W. Macosko, *Rheology: Principles Measurements and Applications* (VCH Publisher, Weinheim, 1994)
H. Münstedt, H.M. Laun, Elongational properties and molecular structure of polyethylene melts. Rheol. Acta **20**, 211–221 (1981)
K. Osaki, K. Nishizawa, M. Kurata, Material time constant characterizing the nonlinear viscoelasticity of entangled polymeric systems. Macromolecules **15**, 1068–1071 (1982)
N. Phan-Thien, A nonlinear network viscoelastic model. J. Rheol. **22**, 259–283 (1978)
N. Phan-Thien, R.I. Tanner, A new constitutive equation derived from network theory. J. Non-Newtonian Fluid Mech. **2**, 353–365 (1977)
M. Simhambhatla, A.I. Leonov, On the rheological modeling of viscoelastic polymer liquids with stable constitutive equations. Rheol. Acta **34**, 259–273 (1995)
R. I. Tanner, *Engineering Rheology 2nd Ed.* (Oxford University Press, UK, 2002)
M. Yamamoto, The visco-elastic properties of network structure I. general formalism. J. Phys. Soc. Japan **11**, 413–421 (1956)
R. Zwanzig, *Nonequilibrium Statistical Mechanics* (Oxford University Press, UK, 2001)

Chapter 11
Large Amplitude Oscillatory Shear

Abstract This chapter includes a short review of large amplitude oscillatory shear (LAOS), the details on the analysis methods for LAOS, and the fluid mechanics of LAOS. The first section is the short review of LAOS. The second one deals with analysis methods for the interpretation of LAOS data such as FT-rheology and stress decomposition. The third one introduces how to calculate the analytical solution of LAOS for various constitutive models and the problems involved in the analytical solutions. The last one introduces semi-analytical method for LAOS which is a trial to overcome the limitation of the analytical approaches.

One of the most important themes in polymer rheology is to identify polymeric materials through rheological measurements. For the identification, the measurement must be precise, reproducible, and convenient. Furthermore, the measurement must be able to provide plentiful information of material. *Large amplitude oscillatory shear* (*LAOS*) is one of the most powerful methods of rheological measurement from the viewpoint of these conditions. Although LAOS is very similar to its linear version *small amplitude oscillatory shear* (*SAOS*), it can provide the information of nonlinear viscoelasticity of polymers.

1 Introduction to LAOS

1.1 Phenomenology of LAOS

Consider a usual dynamic experiment of linear viscoelasticity. To determine the linear regime, a strain sweep test is used at a fixed frequency with varying strain amplitude if strain-controlled rheometer is available. As shown in Fig. 4 in Chap. 5, the storage modulus provided from the rheometer software decreases as strain amplitude increases although the storage modulus remains constant in the region of low strain amplitude. The region of low strain amplitude is called SAOS, while LAOS is the region of strain amplitude where linearity does not hold any more.

K.S. Cho, *Viscoelasticity of Polymers*, Springer Series
in Materials Science 241, DOI 10.1007/978-94-017-7564-9_11

Although stress as a function of time is sinusoidal just as the strain given as the input, the stress signal of LAOS is no longer sinusoidal.

One may apply Fourier analysis to the shear stress signal of LAOS and obtain Fig. 1 which implies that

$$\sigma(t) = \sum_{n=0}^{\infty} I_{2n+1}(\gamma_o, \omega_o) \sin[(2n+1)\omega_o t + \delta_{2n+1}(\gamma_o, \omega_o)] \tag{1.1}$$

where γ_o and ω_o are, respectively, the amplitude and the angular frequency of applied strain: $\gamma(t) = \gamma_o \sin \omega_o t$. This phenomenon gives rise to several questions.

[1] Why are only odd harmonics dominant?
[2] What are the mechanical meanings of I_{2n+1} and δ_{2n+1}?
[3] How can we determine these material functions from experimental data?
[4] How can we use the information from LAOS in the identification of polymeric materials?

These questions will be answered in this chapter.

Figure 4 in Chap. 5 is not unique LAOS behavior of polymeric fluids. Hyun et al. (2002) found that dynamic moduli of some materials increase as strain amplitude as shown in Fig. 2. They classified LAOS behaviors of polymeric fluids to four types and specified structural origins. Figure 2 is a representative example which inspired many researchers to find a rheological fingerprint of structures of complex fluids. Such fingerprints may give only qualitative analysis. However, we need quantitative methods for the analysis of LAOS behavior to identify complicate structure of polymeric materials which cannot be unveiled by any linear viscoelastic identification.

1.2 Overview of LAOS Research

1.2.1 Data Acquisition and Rheometers

To the author's knowledge, Payne (1962) might be the first researcher who studied LAOS. From 1960 to 1990s, a lot of experimental researches have done for polymeric materials. Historical survey is well summarized in the review paper of Hyun et al. (2011). When Pilippoff (1966) measured LAOS, stress and strain data were treated in an analog way: use of oscilloscope. He recognized the increase of third harmonic response using of an analog computer which was replaced by a digital computer long time ago. Although an analog instrument gives graphical output such as *Lissajous–Bowditch loop (LB loop)*, quantitative analysis has been done by Matsumoto et al. (1973) in analog age. Even after the birth of a digital computer, digital data acquisition was not popular in early 1990s. Giacomin and Oakley (1993) developed a numerical method to obtain Fourier series from the

Lissajous–Bowditch loop. Before the use of analog-to-digital converter (AD converter) in earnest, Lissajous–Bowditch loop, plot of stress versus strain or plot of stress versus strain rate, has been the major tool of LAOS analysis (Giacomin et al. 1989; Tee and Dealy 1975).

Invent of AD converter made quantitative analysis of LAOS easier. Wilhelm and coworkers (Van Dusschoten et al. 2001; Wilhelm et al. 1998, 1999, 2000) opened a new era of LAOS research by adopting AD converter technology which acquits a long time series of stress data.

In 1960s and 1970s, LAOS of high-viscosity fluids such as molten polymers was very difficult to measure. This problem was firstly tried to break by Giacomin et al. (1989). Progress in rotational rheometer also contributed to the measurement of high-viscosity fluids. Nowadays, LAOS measurements can be conducted easily using of strain-controlled rheometers. Rotational rheometer becomes the main rheometer for LAOS after the work of Wilhelm and coworkers. Recently Läuger and Stettin (2010) showed the possibility of the use of stress-controlled rheometer. This is due to the progress in electric control. However, stress-controlled rheometer suffers from an inertia problem which becomes significant as stress amplitude increases. The work of Cho and coworkers (Bae et al. 2013) may be the support to the work of Läuger and Stettin.

1.2.2 Analysis Methods

As mentioned before, the main analysis method for LAOS data was Lissajous–Bowditch loop before the use of AD converter. Use of AD converter made Fourier analysis become the main tool of LAOS analysis (van Dusschoten et al. 2001; Neidhöfer et al. 2003; Sim et al. 2003; Wilhelm et al. 1998, 1999, 2000). Hence, the word "*Fourier Transform Rheology (FT-Rheology)*" was born.

Although Fourier transform must be an effective method for quantitative analysis of LAOS, it has a distance from mechanics. Mechanistic analysis could be done after the *stress decomposition (SD)* method developed by Cho et al. (2005). Stress decomposition is to decompose the shear stress of LAOS into elastic, and viscous parts just as the shear stress of SAOS can be decomposed to elastic and viscous parts. Cho and coworkers (Kim et al. 2006) showed that SD is mathematically equivalent to FT-rheology. Ewoldt et al. (2008) introduced Chebyshev polynomial to LAOS analysis. Chebyshev polynomial is a natural way to connect SD with FT-rheology. Yu et al. (2009) generalized SD to normal stress of LAOS. Hyun and Wilhelm (2009) invented a nonlinear material function named Q from the experimental observation that I_3/I_1 is proportional to the square of strain amplitude. They applied this material function to identify branched polymers.

Principle of stress decomposition can be applied to stress-controlled rheometer through a little bit modification. Such modification can be called strain decomposition. Application of strain decomposition was studied by Cho and coworkers (Bae et al. 2013) and Ewoldt and coworkers (Dimitriou et al. 2013; Ewoldt and Bharadwaj 2013; Ewoldt 2013).

LAOS measurement is limited in the ranges of both frequency and strain amplitude. Cho et al. (2010) invented an empirical scaling relation which is comparative with time–temperature superposition. The scaling relation is that dimensionless LAOS variables follow *strain-frequency superposition (SFS)*. This scaling is expected to extend the ranges of frequency and strain. Wyss et al. (2007) suggested similar scaling relations called *strain-rate frequency superposition (SRFS)* which plays a similar role.

Rogers et al. (2011) suggested a new qualitative analysis (sequence of physical processes: SPP) which is effective for a yield stress fluid. Rogers (2012) developed this qualitative analysis further by combining differential geometric considerations.

1.2.3 Fluid Mechanics of LAOS

If a constitutive equation is proper, then the calculation of the LAOS behavior of the model should agree with experimental data. Such model calculation must be helpful to understand LAOS behavior of complex fluids. There are two efforts of fluid mechanics of LAOS: numerical simulation and analytical solution.

As for the efforts to find analytical solution of LAOS, Pearson and Rochefort (1982) and Helfand and Pearson (1982) calculated an analytical solution of LAOS for the Doi–Edwards model. Giacomin et al. (2011) calculated analytical solution of LAOS for the co-rotational Maxwell model and Gurnon and Wagner (2012) for the Giesekus model. However, these approaches are limited to 3rd-order harmonics. An exceptional case is the co-rotational Maxwell model. Giacomin and coworkers (2015) succeeded in the calculation of the exact analytic solution for the co-rotational Maxwell model. Hence, the analytical solutions can be applied to middle range of strain amplitude. Such range is called *middle amplitude oscillatory shear (MAOS)*. Furthermore, such an approach is too complicated and requires tedious perturbation calculation. Bae and Cho (2015) developed a semi-analytical method to extend applicable range of strain amplitude. A similar approach was done by Giacomin and coworkers (2015). They derived Pade approximants from the exact analytical solution of the co-rotational Maxwell model. As the low frequency limit, Bharadwaj and Ewoldt (2014) calculate the analytical solution for the fourth-order Rivlin–Ericksen fluid.

Since an analytical solution cannot be obtained for all nonlinear constitutive equations and such calculation is based on the assumption of spatially homogeneous stress, numerical simulation has been investigated for various models (Calin et al. 2010; van Dusschoten et al. 2001; Hyun et al. 2013; Isayev and Wong 1988; Sim et al. 2003; Wagner et al. 2011).

In simple shear flow, normal stress difference is an obvious evidence of nonlinear viscoelasticity. However, it is rare to find literatures on normal stress of LAOS (Nam et al. 2008, 2010).

1.2.4 Applications to Material Characterization

LAOS methodology becomes popular in various fields of material characterizations. Nonlinear architecture of polymer chain or long chain branching is found in Hyun et al. (2006, 2007), Kempf et al. (2013), Vittorias et al. (2007). Applications to yield stress fluid are found in Boisly et al. (2014), Ewoldt et al. (2010). Applications to other materials are found in Gong et al. (2012), Lim et al. (2013), Li et al. (2009), Papon et al. (2012), Park and Song (2010), Senses and Akcora (2013), and Salehiyan et al. (2014). Applications to colloidal systems are found in Renou et al. (2010), Swan et al. (2014).

2 Methods of Analysis

2.1 FT-Rheology

Consider material as a black box. When a sinusoidal strain is given as an input, measured stress is the response of the black box. Since the input is sinusoidal with a period of P, the output becomes a periodic function with constant amplitude and the same period P after sufficiently long time when the transient effect disappears. When transient effect disappears completely, we call the state stationary one. Note that since the material is still excited periodically, the stationary output remains a function of time.

2.1.1 Fourier Series and Fourier Transform

The stress as a function of time does not have to be a sinusoidal function. If the stress is sinusoidal, then the material is linear. If the stress is not sinusoidal, then the material is nonlinear.

If a function $f(t)$ is a periodic function whose period is P, then the following Fourier series converges to the function:

$$f(t) = \frac{a_0}{2} + \sum_{k=1}^{\infty} a_k \cos\frac{2k\pi t}{P} + \sum_{k=1}^{\infty} b_k \sin\frac{2k\pi t}{P} \tag{2.1}$$

where

$$a_k = \frac{2}{P}\int_c^{c+P} f(t)\cos\frac{2k\pi t}{P}\mathrm{d}t; \quad b_k = \frac{2}{P}\int_c^{c+P} f(t)\sin\frac{2k\pi t}{P}\mathrm{d}t \quad k = 0, 1, 2, \ldots \tag{2.2}$$

where c is an arbitrary real number. Note that if the angular frequency of strain input is ω_o, then $P = 2\pi/\omega_o$. Consider the application of this theorem to LAOS, we have

$$\sigma(t) = \frac{\sigma_0'}{2} + \sum_{k=1}^{\infty} \sigma_k' \cos\, k\omega_o t + \sum_{k=1}^{\infty} \sigma_k'' \sin\, k\omega_o t \tag{2.3}$$

or

$$\sigma(t) = \frac{\sigma_0'}{2} + \sum_{k=1}^{\infty} \sigma_k \sin\left(k\omega_o t + \delta_k\right) \tag{2.4}$$

where

$$\sigma_k = \sqrt{\left(\sigma_k'\right)^2 + \left(\sigma_k''\right)^2} \tag{2.5}$$

and

$$\tan \delta_k = \frac{\sigma_k'}{\sigma_k''} \tag{2.6}$$

Application of Fourier transform to Eq. (2.3) gives the train of the Dirac delta functions such as

$$\begin{aligned}\hat{\sigma}(\omega) = {} & \pi\sigma_0'\delta(\omega) + \pi\sum_{k=1}^{\infty} \sigma_k'[\delta(\omega - k\omega_o) + \delta(\omega + k\omega_o)] \\ & - \pi \mathrm{i} \sum_{k=1}^{\infty} \sigma_k''[\delta(\omega - k\omega_o) - \delta(\omega + k\omega_o)]\end{aligned} \tag{2.7}$$

Let the conjugate of $\hat{\sigma}(\omega)$ be denoted by $\overline{\hat{\sigma}(\omega)}$. If we define

$$\hat{I}(\omega) = \sqrt{\hat{\sigma}(\omega)\overline{\hat{\sigma}(\omega)}} \tag{2.8}$$

then we have

$$\frac{\hat{I}(\omega)}{\pi} = \left|\sigma_0'\right|\delta(\omega) + \sum_{k=1}^{\infty} \sigma_k \delta(\omega - k\omega_o) + \sum_{k=1}^{\infty} \sigma_k \delta(\omega + k\omega_o) \tag{2.9}$$

Equation (2.9) implies that the plot of $\hat{I}(\omega)$ in the range of $\omega > 0$ is the train of spikes that have the intensity of $\hat{I}_k \equiv \pi\sigma_k$ at $\omega = k\omega_o$. Hence, Figs. 1b and 2 can be understood mathematically.

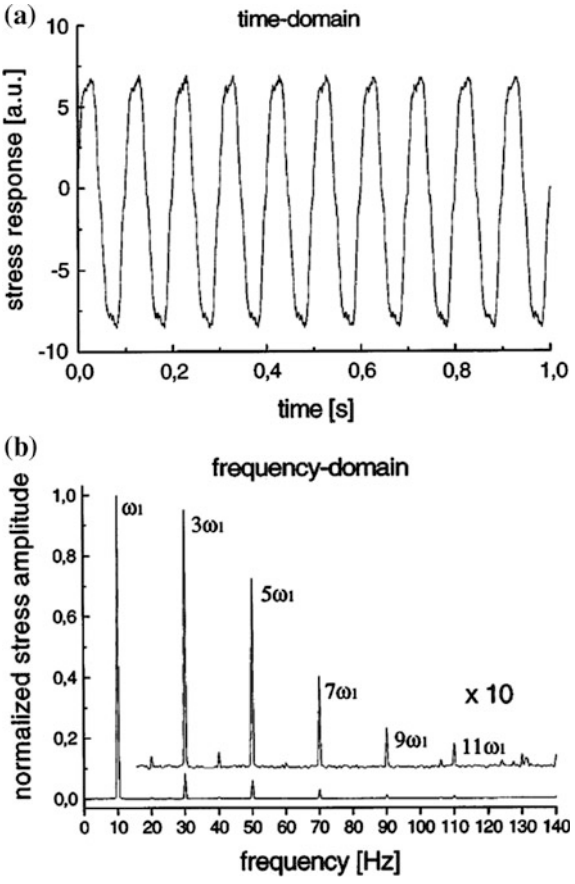

Fig. 1 Measured stress response (**a**) and its normalized amplitude of Fourier transform (**b**). This graph is Fig. 2 of Wilhelm et al. (1998)

We call I_k the Fourier intensity of the kth harmonic. Figure 1b is the Fourier intensity plot which shows only odd harmonics. To explain this, Wilhelm et al. (1998) used a simple relation $\sigma = \eta(\dot{\gamma})\dot{\gamma}$ where viscosity $\eta(\dot{\gamma})$ is an even function of strain rate $\dot{\gamma}$. This simple model implies that only odd harmonics appear in the plot of $\hat{I}(\omega)$. However, it is not general. The reason of disappearance of even harmonics could be proved by the stress decomposition theory (Cho et al. 2005).

AD converter recodes stress as a time series $\sigma_k = \sigma(k\Delta t) + \varepsilon_k$ with $k = 0, 1, \ldots, N_{\text{data}}$. Here, Δt is the interval of sampling time and ε_k is the experimental error at the kth sampling time. Modern instrument technology gives the order of Δt submillisecond. Application of discrete Fourier transform is available to the stress data. Even if no error is assumed, such discrete Fourier transform leaves numerical error. The numerical error decreases as the number of data. The ratio of signal to noise should be maximized by taking long observation time $t_{\max} = N_{\text{data}}\Delta t$. It should be notified that the initial time of data acquisition $t_{\text{o}} = 0$ is the time when the transition effect fades away sufficiently. Although fast Fourier

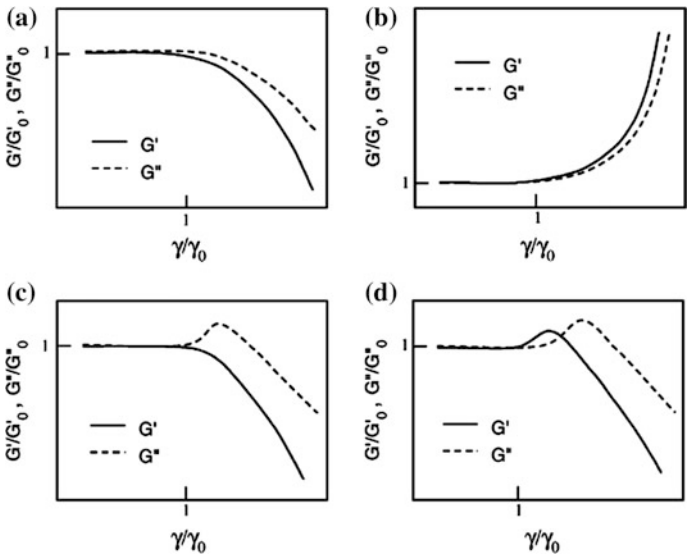

Fig. 2 Four types of LAOS behavior. This figure is Fig. 9 of Hyun et al. (2002). **a** Strain thinning; **b** strain hardening; **c** weak strain overshoot; **d** strong strain overshoot. This is the Fig. 9 of Hyun et al. (2002)

transform (Chap. 6) is very rapid, the LAOS investigation based on the FT-rheology is time-consuming because it takes long experimental time.

2.1.2 *Q*-Variable

The supporters of FT-rheology prefer to use $I_{3/1} \equiv \hat{I}_3/\hat{I}_1$ as an indicator of material nonlinearity. Because $\hat{I}_k$ has the same dimension irrespective of k, $I_{3/1}$ is a dimensionless quantity. Note that $\hat{I}_k(\gamma_o, \omega)$ must be a nonlinear quantity even for $k = 1$ if strain amplitude γ_o is sufficiently high. Hyun and Wilhelm (2009) invented Q-variable which is defined as

$$Q(\gamma_o, \omega) = \frac{I_{3/1}(\gamma_o, \omega)}{\gamma_o^2} \tag{2.10}$$

Note that ω is the angular frequency of strain. This definition originated from the tendency of Fourier intensity such that

$$\hat{I}_k(\gamma_o, \omega) \propto \gamma_o^k \quad \text{for } \gamma_o < \gamma_C \tag{2.11}$$

The critical strain amplitude γ_C depends on materials. Validity of Eq. (2.11) is supported by a lot of experimental and computational results (Bae and Cho 2015;

Cho et al. 2010; Gurnon and Wagner 2012; Hyun and Wilhelm 2009; Pearson and Rochefort 1982).

Since $Q(\gamma_o, \omega)$ becomes a function of only frequency as strain amplitude decreases, Hyun and Wilhelm (2009) defined a material function of frequency such that

$$Q_o(\omega) \equiv \lim_{\gamma_o \to 0} Q(\gamma_o, \omega) \tag{2.12}$$

The definition of Q_o has given rise to a warm debate that Q_o is a linear quantity rather than an indicator of nonlinearity. Stress decomposition and SFS (Cho et al. 2010) implies that

$$Q_o(\omega) = \Theta_o \cos^2 \delta(\omega) \tag{2.13}$$

where $\delta(\omega)$ is the phase angle of linear viscoelasticity:

$$\tan \delta(\omega) = \frac{G''(\omega)}{G'(\omega)} \tag{2.14}$$

However, the proportional coefficient Θ_o cannot be determined by any linear viscoelastic test. Wagner et al. (2011) showed that

$$\Theta_o \propto \alpha - \beta \tag{2.15}$$

where α and β are nonlinear material parameters of the *molecular stress function model (MSF model)* (Wagner et al. 2001). This result clarifies the nonlinearity feature of Q_o.

Wilhelm, Hyun, and their coworkers have published a number of papers using Q_o for material characterization. However, it is questionable how convenient and precise Q_o is. In order to determine $Q_o(\omega)$, one must do a lot of LAOS experiments with varying frequency and strain amplitude. The main objective of the LAOS tests is to determine I_1 and I_3, which takes a long measurement time to reduce the noise effect in FFT. As shown in Eq. (2.13), nonlinear information is concentrated on the proportional constant Θ_o which cannot separately determine α and β. If the frequency dependence of Q_o is tried to characterize material, then Eq. (2.13) implies that linear viscoelasticity can play the same role.

2.2 Stress and Strain Decomposition

2.2.1 Symmetry Analysis

If a material is under stationary state of oscillatory simple shear, then the shear stress must be a function of strain and its time derivatives:

$$\sigma(t) = S\left[\gamma(t), \frac{\mathrm{d}\gamma}{\mathrm{d}t}, \frac{\mathrm{d}^2\gamma}{\mathrm{d}t^2}, \cdots\right] \tag{2.16}$$

Since strain is a sinusoidal function with frequency of ω, it is obvious that

$$\frac{\mathrm{d}^n\gamma}{\mathrm{d}t^n} = \begin{cases} (-1)^k\omega^{2k}\gamma(t) & \text{for} \quad n = 2k \\ (-1)^k\omega^{2k}\dot{\gamma}(t) & \text{for} \quad n = 2k+1 \end{cases} \quad \text{with} \quad k = 0, 1, 2, \ldots \tag{2.17}$$

Since only two functions $\gamma(t)$ and $\dot{\gamma}(t) = \mathrm{d}\gamma/\mathrm{d}t$ are independent, Eq. (2.16) can be rewritten by

$$\sigma(t) = \sigma(\gamma(t), \dot{\gamma}(t)) \tag{2.18}$$

Similar reasoning can be applied to the normal stress of LAOS:

$$N(t) = N(\gamma(t), \dot{\gamma}(t)) \tag{2.19}$$

From the symmetry analysis, we had Eq. (1.27) in Chap. 10. Application of Eq. (1.27) in Chap. 10 gives

$$\sigma(\gamma, \dot{\gamma}) = -\sigma(-\gamma, -\dot{\gamma}) \tag{2.20}$$

and

$$N(\gamma, \dot{\gamma}) = N(-\gamma, -\dot{\gamma}) \tag{2.21}$$

Any function can be decomposed into odd and even parts. Hence, we have

$$\sigma(t) = \sigma_{OE}(t) + \sigma_{EO}(t) \tag{2.22}$$

where

$$\sigma_{OE}(t) = \frac{\sigma(\gamma, \dot{\gamma}) + \sigma(\gamma, -\dot{\gamma})}{2}; \quad \sigma_{EO}(t) = \frac{\sigma(\gamma, \dot{\gamma}) - \sigma(\gamma, -\dot{\gamma})}{2} \tag{2.23}$$

Similarly, we have

$$N(t) = N_{EE}(t) + N_{OO}(t) \tag{2.24}$$

where

$$N_{EE}(t) = \frac{N(\gamma, \dot{\gamma}) + N(\gamma, -\dot{\gamma})}{2}; \quad N_{OO}(t) = \frac{N(\gamma, \dot{\gamma}) - N(\gamma, -\dot{\gamma})}{2} \tag{2.25}$$

The subscript *OE* means that the function is odd for the first argument and even for the second. Subscript *EO*, *EE*, and *OO* can be interpreted similarly.

The symmetry of Eq. (2.20) means that the Lissajous–Bowditch loop for σ and γ has two points for a given γ. These two points correspond to $(\gamma, \dot{\gamma})$ and $(\gamma, -\dot{\gamma})$. Hence, the stress σ_{OE} is the mean of the two stresses at the two deformation states $(\gamma, \dot{\gamma})$ and $(\gamma, -\dot{\gamma})$. If we gather the mean stresses for all strain $-\gamma_o \le \gamma \le \gamma_o$, then the locus implies that σ_{OE} is a single-valued function of γ. Similar discussion can be done for σ_{EO}. Figure 3 shows the meaning of the decomposition of Eq. (2.23) graphically. Since σ_{OE} is a single-valued function of γ and σ_{EO} is a single-valued function of $\dot{\gamma}$, it can be said that σ_{OE} is the elastic component and σ_{EO} is the viscous component.

Stress decomposition can be explained algebraically. Assume that the function of Eq. (2.18) allows the Taylor expansion for the two arguments. Then, we have

$$\sigma(t) = \sum_{m=0}^{\infty} \sum_{n=0}^{\infty} g_{mn}(\omega) \gamma^m(t) \dot{\gamma}^n(t) \tag{2.26}$$

Note that the case of $m = n = 0$ should be excluded.

If the material is linear, then allowed indices are $(m, n) = (1, 0)$ and $(m, n) = (0, 1)$. As for linear viscoelastic material, we have

$$\sigma(t) = G'(\omega)\, \gamma(t) + \frac{G''(\omega)}{\omega} \dot{\gamma}(t) \tag{2.27}$$

Obviously, we know that

$$G'(\omega) = g_{10}(\omega); \quad G''(\omega) = \omega\, g_{01}(\omega) \tag{2.28}$$

Equation (2.27) means that elastic component is a linear odd function of strain and viscous component is a linear function of strain rate.

The symmetrical constraint of Eq. (2.20) implies that the exponents of Eq. (2.26) should satisfy the condition that $m + n$ must be odd. The condition for exponent is

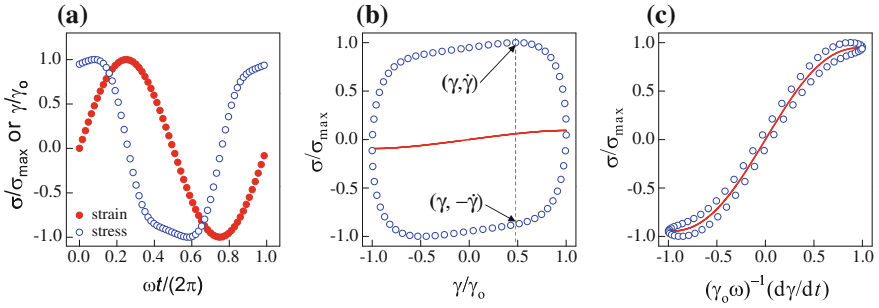

Fig. 3 Schematic illustration of stress decomposition: **a** stress wave; **b** the Lissajous–Bowditch loop of stress and strain; **c** the Lissajous–Bowditch loop of stress and strain rate. All quantities are normalized. The lines of (**b**) and (**c**) are, respectively, σ_{OE} and σ_{EO}

divided to two cases: (Bharadwaj and Ewoldt 2014) m is odd and n is even; (Bae and Cho 2015) m is even and n is odd.

Since strain is sinusoidal, we know that

$$\gamma^2 + \left(\frac{\dot{\gamma}}{\omega}\right)^2 = \gamma_o^2 \tag{2.29}$$

Equation (2.29) allows us to use the following conversions:

$$\dot{\gamma}^{2k}(t) = \omega^{2k}\left[\gamma_o^2 - \gamma^2(t)\right]^k; \quad \gamma^{2k} = \left[\gamma_o^2 - \frac{\dot{\gamma}(t)}{\omega^2}\right]^2 \tag{2.30}$$

Then, Eq. (2.26) can be decomposed to two parts:

$$\sigma(t) = \sum_{k=0}^{\infty} G_{2k+1}^{E}(\gamma_o, \omega)\gamma^{2k+1}(t) + \sum_{k=0}^{\infty} \frac{G_{2k+1}^{V}(\gamma_o, \omega)}{\omega^{2k+1}}\dot{\gamma}^{2k+1}(t) \tag{2.31}$$

Note that G_{2k+1}^{E} and G_{2k+1}^{V} can be determined from $g_{mn}(\omega)$. Since the decomposition of Eq. (2.22) is unique, we know that

$$\sigma_{OE} = \sum_{k=0}^{\infty} G_{2k+1}^{E}(\gamma_o, \omega)\gamma^{2k+1}(t); \quad \sigma_{EO} = \sum_{k=0}^{\infty} \frac{G_{2k+1}^{V}(\gamma_o, \omega)}{\omega^{2k+1}}\dot{\gamma}^{2k+1}(t) \tag{2.32}$$

2.2.2 Numerical Method for SD

Suppose that we have LAOS data measured at fixed frequency and strain amplitude. It is a reasonable assumption that the truncated series of Eq. (2.31) could be a good approximation. Then, the determination of the coefficients G'_{2k+1} and G''_{2k+1} can be done by a polynomial regression. For symmetrical notation, Cho et al. (2005) used notation such that

$$x(t) = \gamma(t); \quad y(t) = \frac{\dot{\gamma}(t)}{\omega}; \quad z(t) = \sigma(t) \tag{2.33}$$

This notation gives

$$\sigma \approx \sum_{k=0}^{N} G_{2k+1}^{E} x^{2k+1} + \sum_{k=0}^{N} G_{2k+1}^{V} y^{2k+1} \tag{2.34}$$

We have learned that when N is not much large, simple polynomial regression is effective. However, if we want to know high harmonics, then orthogonal polynomial should be used:

$$\sigma = \sum_{k=0}^{N} \tau'_{2k+1}(\gamma_o, \omega) T_{2k+1}(\tilde{x}) + \sum_{k=0}^{N} \tau''_{2k+1}(\gamma_o, \omega) T_{2k+1}(\tilde{y}) \tag{2.35}$$

where

$$\tilde{x} = \frac{x(t)}{\gamma_o} = \frac{\gamma(t)}{\gamma_o}; \quad \tilde{y} = \frac{y(t)}{\gamma_o} = \frac{1}{\gamma_o \omega} \frac{d\gamma}{dt} \tag{2.36}$$

Since we have the data set of (x, σ), it is not difficult to extend the data set to $(\tilde{x}, \tilde{y}, \sigma)$. Detained description of the polynomial regression is found in Appendix C of Cho et al. (2010) as well as in Sect. 1 of Chap. 6.

2.2.3 Equivalence to FT-Rheology

If $\gamma(t) = \gamma_o \sin \omega t$, then it is obvious that $\tilde{x} = \sin \omega t$ and $\tilde{y} = \cos \omega t$. As for odd-order Chebyshev polynomial, the following identities hold:

$$T_{2k+1}(\cos \omega t) = \cos[(2k+1)\omega t]; \quad T_{2k+1}(\sin \omega t) = (-1)^k \sin[(2k+1)\omega t] \tag{2.37}$$

Using Eqs. (2.35) and (2.37), we get

$$\begin{aligned} \sigma &= \sum_{k=0}^{N} (-1)^k \tau'_{2k+1} \sin[(2k+1)\omega t] + \sum_{k=0}^{N} \tau''_{2k+1} \cos[(2k+1)\omega t] \\ &= \sum_{k=0}^{N} I_{2k+1} \sin[(2k+1)\omega t + \delta_{2k+1}] \end{aligned} \tag{2.38}$$

where

$$I_{2k+1} = \sqrt{\tau'^2_{2k+1} + \tau''^2_{2k+1}} \tag{2.39}$$

and

$$\tau'_{2k+1} = (-1)^k I_{2k+1} \cos \delta_{2k+1}; \quad \tau''_{2k+1} = I_{2k+1} \sin \delta_{2k+1} \tag{2.40}$$

Chebyshev polynomial proves the equivalence between SD and FT-rheology. Although this equivalence was recognized first by Kim et al. (2006), Ewoldt et al. (2008) introduced Chebyshev polynomial firstly to LAOS analysis.

2.2.4 Geometry of LAOS

The notation of Eq. (2.33) implies that Eq. (2.27) is the equation for the flat plane in the three-dimensional space of (x, y, z). For a fixed frequency, collecting LAOS data with various strain amplitudes forms a curved surface in the three-dimensional space. Equation (2.18) is the surface equation. Cho et al. (2005) invented 3D LAOS plot which is a 3D locus of stress at constant frequency and strain amplitude as shown in Fig. 4.

The 3D LAOS plot explains why the Lissajous–Bowditch loop has such various shapes depending on the frequency and strain amplitude. We call the Lissajous–Bowditch loop for σ–x elastic LB loop and that for σ–y viscous LB loop. As shown in Fig. 4, the elastic Lissajous–Bowditch loop is the projection of 3D LAOS plot on the plane of σ–x and viscous one is the projection of 3D LAOS plot on the plane of σ–y. The projection on the plane of x–y is the circle of radius of γ_o.

It is noteworthy that the viscous LB loop of PEO aqueous solution of Fig. 4 shows secondary loop. The secondary loop implies the existence of self-intersection points. A study on the secondary loop and self-intersection points is found in (Ewoldt and McKinley 2010). Such phenomena are found not only in experimental data but also numerical simulation of nonlinear viscoelastic models. Ewoldt and McKinley derived the condition for the self-intersection points:

$$\begin{aligned} \sigma_{EO}(y) = 0 \text{ and } y \neq 0 \quad & \text{for elastic LB loop} \\ \sigma_{OE}(x) = 0 \text{ and } x \neq 0 \quad & \text{for viscous LB loop} \end{aligned} \tag{2.41}$$

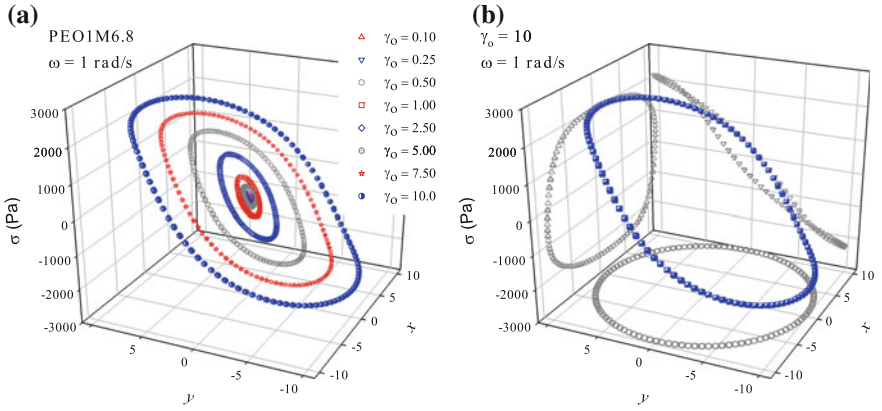

Fig. 4 3D LAOS plot and its geometrical meaning. **a** 3D LAOS plots of various strain amplitude forms the stress surface. **b** The projection of 3D LAOS plot on the plane of σ–x is the elastic Lissajous–Bowditch loop, the projection on the plane of σ–y is the viscous Lissajous–Bowditch loop, and the projection of the plane of x–y is the circle whose radius is the strain amplitude. When strain amplitude belongs to linear regime, the collection of 3D LAOS plots forms a flat plane whose normal vector is proportional to $(G', G'', 1)$. The polymeric fluid of the data is PEO aqueous solution [molecular weight is 1000 kg/mol and concentration is 7 wt% (Cho et al. 2010)]

The existence of secondary loop is thought as the indicator of strong nonlinearity (Ewoldt and McKinley 2010). However, it is forthcoming to unveil the relation between the secondary loop and structural features of complex fluids.

2.2.5 Elastic and Viscous Stresses

Stress decomposition theory decomposes shear stress into σ_{OE} and σ_{EO}. Because σ_{OE} is a single-valued function of strain and σ_{EO} is a single-valued function of strain rate, can we call σ_{OE} elastic stress and σ_{EO} viscous stress? Of course, these are parts of the conditions of elastic and viscous stresses. We shall show more evidence.

In an oscillatory simple shear flow, the stress power is given by

$$\mathrm{tr}(\mathbf{T}\cdot\mathbf{D}) = \mathrm{tr}\left[\frac{\sigma\dot{\gamma}}{2}(\mathbf{e}_1\mathbf{e}_1 + \mathbf{e}_2\mathbf{e}_2)\right] = \sigma\dot{\gamma} \tag{2.42}$$

It is interesting that normal stress does not contribute to stress power. From Eq. (2.53) in Chap. 2, stress power is related to the time derivative of internal energy:

$$\rho\frac{\mathrm{d}u}{\mathrm{d}t} = -\nabla\cdot\mathbf{q} + \rho r + \sigma\dot{\gamma} \tag{2.43}$$

Assumption of spatial homogeneity of internal energy gives

$$\rho\Delta u(t) = HT + u_E[x(t)] - u_E[x(t_\mathrm{o})] + \sum_{k=0}^{\infty}\frac{G^{\mathrm{V}}_{2k+1}(\gamma_\mathrm{o},\omega)}{\omega^{2k+1}}\int_{t_\mathrm{o}}^{t}\left(\frac{\mathrm{d}\gamma}{\mathrm{d}t}\frac{\mathrm{d}\gamma}{\mathrm{d}t}\right)^{k+1}\mathrm{d}t \tag{2.44}$$

where $\Delta u = u(t_\mathrm{o} + 2\pi/\omega) - u(t_\mathrm{o})$, HT is the term due to heat transfer and

$$\frac{\mathrm{d}u_E}{\mathrm{d}x} = \sigma_{OE}[x(t)] \tag{2.45}$$

If $t - t_\mathrm{o} = 2\pi/\omega$, then the term σ_{OE} disappears because of the periodicity of strain and we have

$$\rho\Delta u = \frac{\pi}{2}\sum_{k=0}^{\infty}\frac{(2k+2)!}{2^{2k}(k+1)!(k+1)!}G^{\mathrm{V}}_{2k+1}(\gamma_\mathrm{o},\omega)\gamma_\mathrm{o}^{2(k+1)} + HT \tag{2.46}$$

If there is no change of internal energy, then the first term of the right-hand side of Eq. (2.46) is canceled by the heat transfer term, HT. This means that the work

done by σ_{EO} dissipates through heat transfer. Because of this, one may call σ_{EO} viscous stress.

Cho et al. (2010) calculated σ_{OE} and σ_{EO} for the separable K-BKZ model. The shear stress of the K-BKZ model is given by

$$\sigma(t) = \int_{-\infty}^{t} \mu(t-\tau) h[\Gamma(t,\tau)] \Gamma(t,\tau) \mathrm{d}\tau \tag{2.47}$$

where $\mu(t)$ is the memory function, $h(x)$ is the damping function, and

$$\Gamma(t,\tau) = \gamma(t) - \gamma(\tau) = \gamma_o(\sin\omega t - \sin\omega\tau) \tag{2.48}$$

Since damping function is an even function, we can use

$$h(\gamma) = \sum_{k=0}^{\infty} h_{2k}\gamma^{2k} \tag{2.49}$$

Substitution of Eqs. (2.48) and (2.49) to Eq. (2.47) yields

$$\sigma(t) = \sum_{n=0}^{\infty}\sum_{k=0}^{n} h_{2n}\gamma_o^{2n+1}\left[A_{2k+1}^{2n+1}(\omega)\tilde{x}^{2k+1}(t) + B_{2k+1}^{2n+1}(\omega)\tilde{y}^{2k+1}(t)\right] \tag{2.50}$$

Note that

$$A_{2k+1}^{2n+1}(\omega) = \sum_{m=1}^{2n+1} p_{n,k}^{m} G'(m\omega); \quad B_{2k+1}^{2n+1}(\omega) = \sum_{m=1}^{2n+1} q_{n,k}^{m} G''(m\omega) \tag{2.51}$$

where $p_{n,k}^{m}$ and $q_{n,k}^{m}$ are rational numbers. Some examples of A_{2k+1}^{2n+1} and B_{2k+1}^{2n+1} are

$$A_1^1(\omega) = G'(\omega); \quad B_1^1(\omega) = G''(\omega); \tag{2.52a}$$

$$\begin{aligned} A_1^3(\omega) &= \frac{3}{4}[G'(\omega) + 2G'(2\omega) - G'(3\omega)]; \\ A_3^3(\omega) &= 3G'(\omega) - 3G'(2\omega) + G'(3\omega); \\ B_1^3(\omega) &= \frac{3}{4}[5G''(\omega) - 4G''(2\omega) + G''(3\omega)]; \\ B_3^3(\omega) &= -3G''(\omega) + 3G''(2\omega) - G''(3\omega) \end{aligned} \tag{2.52b}$$

Equation (2.50) implies that σ_{OE} contains only storage modulus, while σ_{EO} contains only loss modulus. This calculation supports that σ_{OE} and σ_{EO} are elastic and viscous stresses, respectively.

A similar approach can be applied to the first normal stress difference. Note that for the K-BKZ model, we know that

$$N_1(t) = \int_{-\infty}^{t} \mu(t-\tau) h[\Gamma(t,\tau)] \Gamma^2(t,\tau) \mathrm{d}\tau \tag{2.53}$$

We can decompose the first normal stress difference as follows

$$\begin{aligned} N_{EE} &= \sum_{k=0}^{\infty} \sum_{p=0}^{k} h_{2k} C_{2p+2}^{2k+2}(\omega) \gamma_{\mathrm{o}}^{2k+2} T_{2p+2}(\tilde{x}); \\ N_{OO} &= \tilde{x}\tilde{y} \sum_{k=0}^{\infty} \sum_{p=0}^{k} h_{2k} D_{2p+2}^{2k+2}(\omega) \gamma_{\mathrm{o}}^{2k+2} T_{2p+2}(\tilde{x}) \end{aligned} \tag{2.54}$$

where

$$\bar{C}_{2n+2}^{2k+2}(\omega) = \sum_{m=1}^{2k+2} c_{k,n}^{m} G'(m\,\omega); \quad \bar{D}_{2n+2}^{2k+2}(\omega) = \sum_{m=1}^{2k+2} d_{k,n}^{m} G''(m\,\omega) \tag{2.55}$$

Note that $c_{k,n}^{m}$ and $d_{k,n}^{m}$ are rational numbers. It is interesting that N_{EE} contains only storage modulus, while N_{OO} contains only loss modulus. Since dissipation analysis seems not to be applied to N_{EE} and N_{OO}, it is difficult to insist that N_{EE} is elastic and N_{OO} is viscous.

2.2.6 Strain Decomposition

For linear viscoelasticity, we know that the shear stress can be expressed by

$$\sigma(t) = G'(\omega)\,\gamma(t) + \frac{G''(\omega)}{\omega}\frac{\mathrm{d}\,\gamma}{\mathrm{d}t} = G'(\omega)\,x(t) + G''(\omega)\,y(t) \equiv \xi(\tau) \tag{2.56}$$

Differentiation gives

$$\psi(t) \equiv \frac{1}{\omega}\frac{\mathrm{d}\sigma}{\mathrm{d}t} = -G''(\omega)\,x(t) + G'(\omega) y(t) \tag{2.57}$$

Solving Eqs. (2.56) and (2.57), we have

$$\gamma(t) = J'(\omega)\xi(t) - J''(\omega)\psi(t); \quad y(t) = J''(\omega)\xi(t) + J'(\omega)\psi(t) \tag{2.58}$$

This agrees with the calculation using the Boltzmann superposition principle. Then, we can assign elastic and viscous strain by

$$\gamma_E(t) = \gamma_{OE}(t) = J''(\omega)\,\sigma(t); \quad \gamma_V(t) = \gamma_{EO}(t) = \frac{J''(\omega)}{\omega}\frac{d\sigma}{dt} \tag{2.59}$$

Just like shear stress, shear strain generated by oscillatory shear stress follows the symmetry:

$$\gamma\left(-\sigma, -\frac{d\sigma}{dt}\right) = -\gamma\left(\sigma, \frac{d\sigma}{dt}\right) \tag{2.60}$$

Then, we can decompose nonlinear shear strain as follows

$$\gamma(t) = \gamma_{OE} - \gamma_{EO} \tag{2.61}$$

where

$$\gamma_{OE} = \frac{\gamma(\sigma, \dot{\sigma}) + \gamma(\sigma, -\dot{\sigma})}{2}; \quad \gamma_{EO} = -\frac{\gamma(\sigma, \dot{\sigma}) - \gamma(\sigma, -\dot{\sigma})}{2} \tag{2.62}$$

Here, we change the sign of γ_{EO} in order to make Eq. (2.61) agree with Eq. (2.58). Then, the analysis done for LAOS data of strain-controlled rheometer can be applied to the LAOS data of stress-controlled rheometer. However, it is not easy to find the inversion from strain to stress or vice versa, which can be done for linear viscoelasticity as shown in Eq. (2.58).

Consider the case that stress is given by $\sigma = \sigma_o \sin \omega t$. Then, we can find that

$$\gamma_{OE} \approx \sum_{k=0}^{N} J'_{2k+1}(\sigma_o, \omega)\sigma^{2k+1}(t); \quad \gamma_{EO} \approx \sum_{k=0}^{N} \frac{J''_{2k+1}(\sigma_o, \omega)}{\omega^{2k+1}}\left(\frac{d\sigma}{dt}\right)^{2k+1} \tag{2.63}$$

If LAOS data are obtained from an ideal stress-controlled rheometer which is free from machine inertia, then we can determine J'_{2k+1} and J''_{2k+1}. Assume that we can generate this strain signal in strain-controlled rheometer. Then can the stress response be $\sigma = \sigma_o \sin \omega t$? Bae et al. (2013) tested this for the third harmonic approximation and found that when inertia effect is negligible (maybe MAOS), the stress measured from strain-controlled rheometer is nearly sinusoidal. It is difficult to extend this experiment to sufficiently high stress amplitude because of both inertia effect and the limitation of the software equipped in commercial strain-controlled rheometer (ARES™). What Bae et al. want to prove is the existence of the functional relation:

$$\gamma_o \sin \omega t = S^{-1}\left[\sigma(t), \frac{d\sigma}{dt}, \frac{d^2\sigma}{dt^2}, \cdots\right] \tag{2.64}$$

where $\sigma(t)$ is a nonsinusoidal periodic function which can be obtained for Eq. (2.16) when $\gamma(t) = \gamma_o \sin \omega t$ is substituted to Eq. (2.16).

It is interesting and concise naming to call the LAOS with strain as input *LAOStrain* and to call the LAOS with stress as input *LAOStress* (Ewoldt and Bharadwaj 2013). We shall use the terminology of Ewoldt and Bharadwaj. Compared with LAOStrain, LAOStress is not still practical because of the inertia problem. We need a theory to extract pure material property from the raw data of LAOStress.

2.3 Scaling Theory of LAOS

2.3.1 Basics

When the input of LAOS is restricted to a sinusoidal function of time, all material functions of the LAOS are functions of frequency and input amplitude. Since we shall consider only LAOStrain, any material function can be expressed by $\Pi(\gamma_o, \omega)$. It is a two-variable function. As for linear viscoelasticity, time–temperature superposition makes the two-variable functions of linear viscoelasticity to single-variable functions. Cho et al. (2010) thought that there may be a scaling rule such that

$$\tilde{\Pi} \equiv \frac{\Pi(\gamma_o, \omega)}{\Pi_{\text{linear}}(\omega)} = \tilde{f}(\zeta) \tag{2.65}$$

where $\Pi(\gamma_o, \omega)$ is a LAOStrain material function, $\Pi_{\text{linear}}(\omega)$ is the linear counter part of $\Pi(\gamma_o, \omega)$ with the same dimension and ζ is a function of both strain amplitude and frequency. Cho et al. (2010) found that the scaling function is the product of strain amplitude and function of frequency such as

$$\zeta = \gamma_o \cos\delta(\omega) = \frac{G'(\omega)}{[G'(\omega)]^2 + [G''(\omega)]^2}\gamma_o \tag{2.66}$$

Cho et al. (2010) thought that ζ must be the product of strain amplitude and a dimensionless function of frequency. They tried to find such dimensionless function of frequency among linear viscoelastic function. Most possible candidates are $\tan\delta$, $\cos\delta$, and $\sin\delta$. They found that only $\cos\delta$ satisfies the superposition. Their scaling rule is found valid for most LAOStrain material functions (Cho et al. 2010, 2015) and for some LAOStress material functions (Bae et al. 2013). We shall call this scaling *strain-frequency superposition (SFS)*.

Similar thought was done by Weitz and coworkers (2007). Their scaling is called *strain-rate frequency superposition (SRSF)*. They measured dynamic moduli at fixed frequency with varying strain amplitude up to LAOS regime. They considered storage and loss modulus as a functions of frequency and strain rate amplitude $\dot{\gamma}_o \equiv \gamma_o\omega$. SRFS is expressed by

$$\frac{G'(\gamma_o,\omega)}{a(\dot{\gamma}_o)} = \Gamma'\left[\frac{\omega}{b(\dot{\gamma}_o)}\right]; \quad \frac{G''(\gamma_o,\ \omega)}{a(\dot{\gamma}_o)} = \Gamma''\left[\frac{\omega}{b(\dot{\gamma}_o)}\right] \tag{2.67}$$

It must be noted that the definition of nonlinear dynamic moduli are not clear. They used the dynamic moduli calculated from the software of commercial rheometer when strain sweep test is assumed. Shift factors $a(\dot{\gamma}_o)$ and $b(\dot{\gamma}_o)$ were determined by the optimized superposition without any underlying theory. It is interesting that they guessed that

$$G'(\omega) \approx \Gamma'(\omega); \quad G''(\omega) \approx \Gamma''(\omega) \tag{2.68}$$

This daring assumption was tested by rheologists. Erwin et al. (2010) found that $\Gamma'(\omega)$ and $\Gamma''(\omega)$ do not satisfy the Kramers–Kronig relation which must be obeyed if the new dynamic moduli are genuine linear dynamic moduli (see Sect. 4). In the author's opinion, the use of SRFS is not positive.

2.3.2 Scaling of Amplitudes of Elastic and Viscous Stresses

Cho et al. (2010) define nonlinear dynamic modulus as the ratio of the amplitudes of elastic and viscous stresses to strain amplitude:

$$G_E(\gamma_o,\omega) \equiv \frac{\sigma_{OE}^{\max}(\gamma_o,\omega)}{\gamma_o}; \quad G_V(\gamma_o,\omega) \equiv \frac{\sigma_{EO}^{\max}(\gamma_o,\omega)}{\gamma_o} \tag{2.69}$$

It must be noted that

$$\lim_{\gamma_o\to 0} G_E(\gamma_o,\omega) = G'(\omega); \quad \lim_{\gamma_o\to 0} G_V(\gamma_o,\omega) = G''(\omega) \tag{2.70}$$

Then, reduced amplitudes for elastic and viscous stresses are defined according to Eq. (2.65) as follows:

$$\tilde{G}_E(\gamma_o,\omega) = \frac{G_E(\gamma_o,\omega)}{G'(\omega)}; \quad \tilde{G}_V(\gamma_o,\ \omega) = \frac{G_V(\gamma_o,\omega)}{G''(\omega)} \tag{2.71}$$

These can be interpreted as dimensionless nonlinear dynamic moduli, too.

Figure 5 supports the assumption of Eq. (2.65) nicely. One may doubt that the dimensionless dynamic moduli may also be superposed when ζ is replaced by $\gamma_o\omega$ or $\gamma_o \sin\delta(\omega)$. However, such candidates failed the superposition. Of course, there is no theoretical foundation for the validity of Eq. (2.66). Although Fig. 5 is the superposition for PEO aqueous solution of 1000 kg/mol and 7 wt%, Cho et al. (2010) found that SFS holds irrespective of concentration and molecular weight.

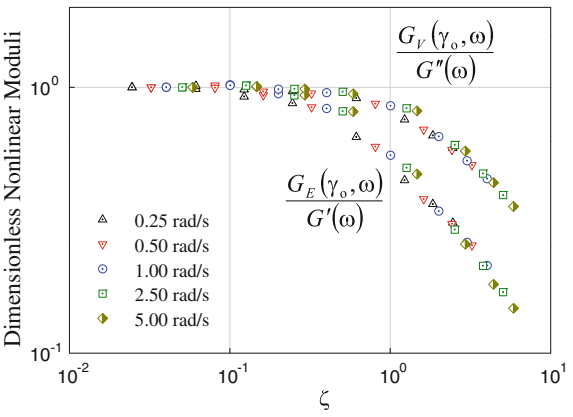

Fig. 5 Dimensionless nonlinear dynamic moduli as functions of ζ show SFS. The sample is PEO aqueous solution (1M6.8). This figure is Fig. 7 of Cho et al. (2010)

They also found that all PEO solutions they used follow the empirical equation:

$$\tilde{G}_E = \exp\left[k\left(\tilde{G}_V - 1\right)\right]; \quad \tilde{G}_V = \exp\left(-\frac{\zeta}{\zeta_C}\right) \tag{2.72}$$

where $k \approx 3$ and $\zeta_C \approx 5$. Note that all PEO solutions are semi-dilute ones such that $c/c_e > 3$. The second equation of Eq. (2.72) implies that $\zeta < \zeta_C$ then nonlinearity is negligible because $\tilde{G}_V \approx 1$. If $\tilde{G}_V \approx 1$, then the first equation also indicates $\tilde{G}_E \approx 1$. Hence, the plot of $\tilde{G}_E$ as a function of $\tilde{G}_V$ maps the whole linear regime to a single point of (1, 1) in the plane of $\left(\tilde{G}_V, \tilde{G}_E\right)$.

Figure 6 shows the validity of Eq. (2.72). The solid lines are Eq. (2.72). Note that 400 K, 600 K, and 1 M denote molecular weights of PEO and the last numbers after the molecular weight in the sample code denote the concentration ratio to entanglement concentration. Hence, the scaling looks valid irrespective of concentration, molecular weight, frequency, and strain amplitude.

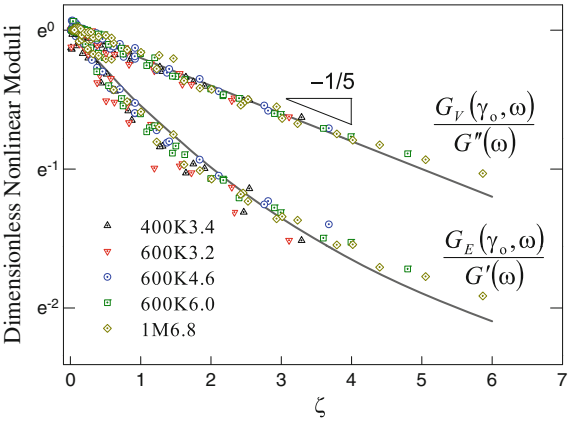

Fig. 6 Dimensionless nonlinear dynamic moduli as functions of ζ. Sample specification is found in Cho et al. (2010). All PEO aqueous solutions are semi-dilute ones such that $c/c_e > 3$. The *lines* are Eq. (2.72). This figure is Fig. 10 of Cho et al. (2010)

2.3.3 Scaling of Fourier Intensities

Cho et al. (2010) found that SFS also holds for Fourier intensities. Since the dimension of I_n is that of stress, we adopt the following normalization:

$$J_n(\gamma_o, \omega) = \frac{I_n(\gamma_o, \omega)}{|G^*(\omega)|\gamma_o} \tag{2.73}$$

As for PEO aqueous solution, J_1 follows the same equation of $N = 3$:

$$J_1(\gamma_o, \omega) = \exp\left(-\frac{\zeta}{\zeta_C}\right) \quad \text{with} \quad \zeta_C = 5 \tag{2.74}$$

Figure 7 shows that SFS holds for J_3 and J_5, too. For these higher harmonics, we observe

$$J_{2k+1}(\gamma_o, \omega) = J^{\infty}_{2k+1} \frac{(\zeta/\zeta_{2k+1})^2}{1 + (\zeta/\zeta_{2k+1})^2} \quad k = 1, 2, \ldots \tag{2.75}$$

It is interesting that the PEO aqueous solution 1M6.8 has $\zeta_3 = \zeta_5 = 1$. The lines in Fig. 7 are Eqs. (2.74) and (2.75).

The supporters of FT-rheology prefer to use $I_{3/1}$ rather than J_3. Using Eqs. (2.74) and (2.75), $I_{3/1}$ can be expressed by

$$I_{3/1} = \frac{J_3}{J_1} = J^{\infty}_3 e^{\zeta/\zeta_C} \frac{(\zeta/\zeta_3)^2}{1 + (\zeta/\zeta_3)^2} \tag{2.76}$$

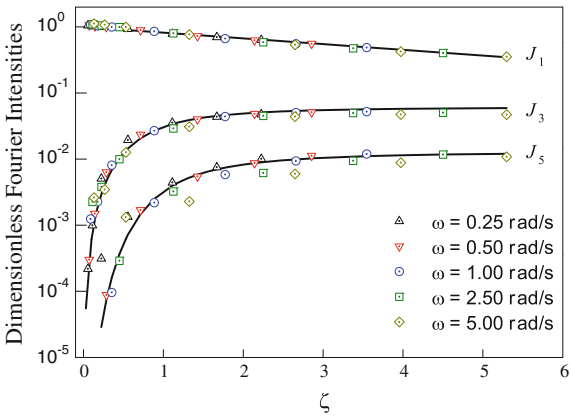

Fig. 7 Dimensionless Fourier intensities as functions of ζ. The *lines* are Eqs. (2.74) and (2.75). The sample is 1M6.8 of Cho et al. (2010). This figure is Fig. 12 of Cho et al. (2010)

If $\zeta < \zeta_3 < \zeta_C$, then Eq. (2.76) becomes

$$I_{3/1} \approx J_3^{\infty} \frac{(\zeta/\zeta_3)^2}{1+(\zeta/\zeta_3)^2} \approx \frac{J_3^{\infty}}{\zeta_3^2} \gamma_o^2 \cos^2 \delta(\omega) \propto \gamma_o^2 \tag{2.77}$$

We can apply Eq. (2.76) to Q_o of Hyun and Wilhelm (2009):

$$Q_o \approx \frac{J_3^{\infty}}{\zeta_3^2} \cos^2 \delta(\omega) = \frac{J_3^{\infty}}{\zeta_3^2} \frac{[G'(\omega)]^2}{[G'(\omega)]^2 + [G''(\omega)]^2} \tag{2.78}$$

This implies that frequency dependency of Q_o is linear viscoelastic, while its scale factor is the genuine nonlinear parameter J_3^{∞}/ζ_3^2.

To check the validity of Eq. (2.76), Cho et al. (2010) used the data of Hyun (2005). Figure 8 compares Eq. (2.76) with the data of Hyun (PP melt, Mw = 240 kg/mol, PDI = 4.8, T = 180 °C) (Fig. 8).

As for Fourier coefficients τ_n' and τ_n'', SFS does not hold except τ_1''. According to Cho et al. (2010), dimensionless τ_1'' of the PEO aqueous solution follows

$$\frac{\tau_1''}{G''(\omega)\gamma_o} = \exp\left(-\frac{\zeta}{\zeta_C}\right) \quad \text{with} \quad \zeta_C = 5 \tag{2.79}$$

Cho and coworkers (2015) tested SFS to other polymeric fluids. They tested polyvinyl alcohol (PVA) dissolved in dimethyl sulfoxide (DMSO), polyvinyl acetate (PVAc) in DMSO and PVA aqueous solution with borax. The molecular weight of PVA in the solution of PVA/DMSO is sufficiently high for entanglement, while that of PVA in the aqueous solution with borax is too low to form any

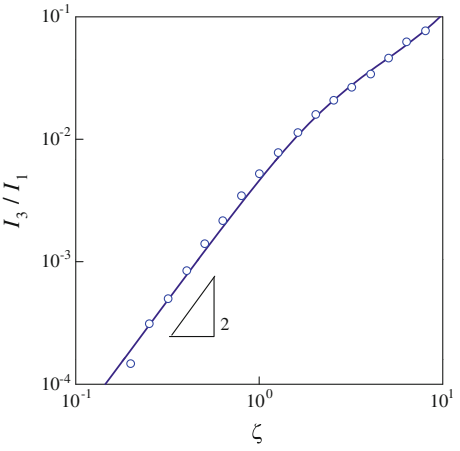

Fig. 8 Validity of Eq. (2.76). The sample is PP melt measured at 180 °C. The regression results are $J_3^{\infty} = 0.029$, $\zeta_C = 7.46$, and $\zeta_3 = 2.49$. This figure is Fig. 13 of Cho et al. (2010)

entanglement. Although PVA/DMSO and PVAc/DMSO behave similarly to PEO aqueous solutions, the PVA aqueous solution with borax behaves in absolutely different manners. According to the classification of Hyun et al. (2002), the former three polymer solutions belong to strain-thinning fluid, while PVA aqueous solution with borax belongs to strain-hardening fluid.

Figure 9 shows that PVAc/DMSO and PVA/DMSO follow Eq. (2.74) quite well, while PVA aqueous solution with borax behaves differently. The slope of the plot of $\log J_1$ versus ζ is positive for the strain-hardening fluid. As for strain-thinning fluids, they look like $J_1 \approx e^{-\zeta/5}$. On the other hand for strain-hardening fluids, we can use $J_1 \approx e^{\zeta/5}$ for small ζ. For the whole data of PVA aqueous solution with borax, we can use

$$J_1 \approx \exp\left[\frac{\zeta}{5} + 4.338\left(\frac{\zeta}{5}\right)^2\right] \tag{2.80}$$

On the other hand, strain-hardening and strain-thinning cannot be distinguished by J_3 as shown in Fig. 10. The third harmonic intensities of both kinds of fluids behave like Eq. (2.75). Then, we can expect that both strain-hardening and strain-thinning fluids give the same behavior of Q_o, Eq. (2.78) in the range of MAOS.

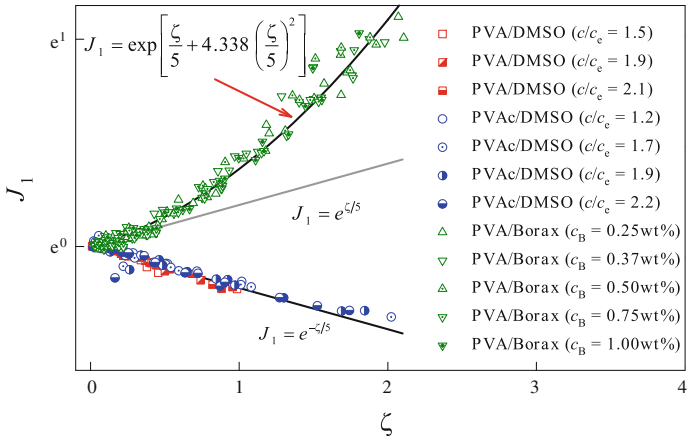

Fig. 9 Comparison of strain-thinning and strain-hardening fluids in terms of dimensionless Fourier intensity of the first harmonic. The dimensionless Fourier intensity of strain-thinning fluid is a decreasing function of ζ while that of strain-hardening fluid is an increasing function. The empirical equations in the figure indicate that $J_1 \approx 1$ for $\zeta \ll 5$. This figure is the summary of Fig. 8 of Cho et al. (2015)

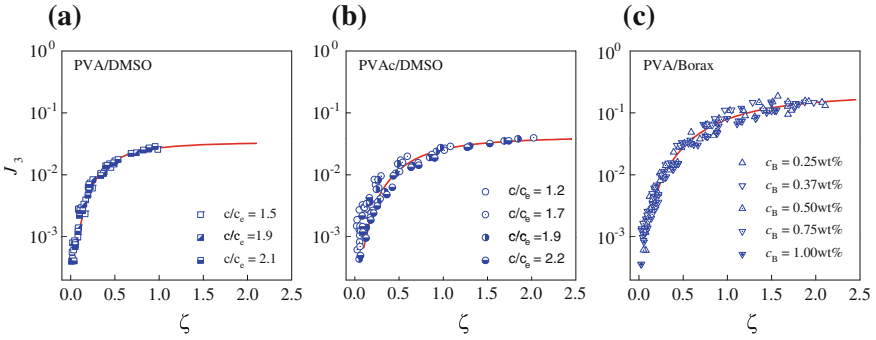

Fig. 10 Comparison of strain-thinning and strain-hardening fluids in terms of dimensionless Fourier intensity of the third harmonic. All fluids follow Eq. (2.75). This figure is redrawn from the data of Fig. 9 of Cho et al. (2015)

2.3.4 SFS for LAOStress

It is questionable whether LAOStress data follow SFS, too. Since $\sigma_o \cos \delta(\omega)$ is not a dimensionless quantity, we have to find dimensional quantity which is proportional to stress amplitude. Note that

$$\sigma_o J'(\omega) = \frac{\sigma_o G'(\omega)}{|G^*(\omega)|^2} = \frac{\sigma_o}{|G^*(\omega)|} \cos \delta(\omega) = \gamma_o \cos \delta(\omega) = \zeta \tag{2.81}$$

Here, we adopted $\sigma_o = |G^*(\omega)|\gamma_o$. See Problem 2 (Ewoldt and Bharadwaj 2013). As for LAOStress, important dimensionless quantities are dimensionless nonlinear compliances and dimensionless Fourier intensity:

$$\tilde{J}_E = \frac{\gamma_E^{\max}(\sigma_o, \omega)}{J'(\omega)\sigma_o}; \quad \tilde{J}_V = \frac{\gamma_V^{\max}(\sigma_o, \omega)}{J''(\omega)\sigma_o} \tag{2.82}$$

and

$$\tilde{H}_n = \frac{I_n(\sigma_o, \omega)}{|J^*(\omega)\sigma_o|} \tag{2.83}$$

Bae et al. (2013) showed that the above dimensionless quantities behave as functions of $\sigma_o J'(\omega)$. However, the quality of superposition is worse compared with LAOStrain.

Problem 1

[1] Show that

$$\begin{aligned}\hat{F}[1] &= 2\pi\delta(\omega)\\ \hat{F}[\cos\omega_o t] &= \pi[\delta(\omega-\omega_o)+\delta(\omega-\omega_o)]\\ \hat{F}[\sin\omega_o t] &= -\pi i[\delta(\omega-\omega_o)-\delta(\omega-\omega_o)]\end{aligned} \tag{2.a}$$

[2] It is obvious that $\delta(\omega-\omega_i)\,\delta(\omega-\omega_k)=\delta_{ik}\delta(\omega-\omega_i)$. Then derive Eq. (2.9).

[3] If oscillatory simple shear flow is considered, then shear stress of a viscoelastic material can be expressed by

$$\sigma=\sigma\left(\gamma,\frac{d\gamma}{dt},\frac{d^2\gamma}{dt^2},\ldots\right) \tag{2.b}$$

If the material is linear, then Eq. (2.b) becomes simpler

$$\sigma(t)=c_0\gamma(t)+\sum_{k=1}^{\infty}c_k\frac{d^k\gamma}{dt^k} \tag{2.c}$$

Show that $G'(\omega)=G'(-\omega)$ and $G''(-\omega)=-G''(\omega)$.

[4] Show that

$$\sigma_{OE}=\frac{\sigma(\gamma,\dot{\gamma})+\sigma(-\gamma,\dot{\gamma})}{2} \tag{2.d}$$

[5] Derive the second equation of Eq. (2.37) from the first equation of Eq. (2.37).

[6] Derive Eq. (2.41).

[7] Show that

$$\int_0^{2\pi}\cos^{2n}t\,dt=\int_0^{2\pi}\sin^{2n}t\,dt=\frac{\pi(2n)!}{2^{2n-1}n!n!} \tag{2.e}$$

[8] Derive Eq. (2.46).

[9] Derive Eq. (2.50). See Cho et al. (2010).

[10] Derive Eq. (2.54). See Cho et al. (2010).

[11] Show that for linear viscoelasticity of stress-controlled rheometer, the amplitude of strain is given by $\gamma_o=\sigma_o|G^*(\omega)|^{-1}$.

[12] Show that stress decomposition results in that decomposed normal stresses can be expressed by

$$N_{\mathrm{EE}}(x,y)=\sum_{k=0}^{\infty}\nu_{2k}^{\mathrm{EX}}(\gamma_{\mathrm{o}},\omega)x^{2k}(t)=\sum_{k=0}^{\infty}\nu_{2k}^{\mathrm{EY}}(\gamma_{\mathrm{o}},\omega)y^{2k}(t) \tag{2.f}$$

and

$$N_{\mathrm{OO}}(x,y)=y(t)\sum_{k=0}^{\infty}\nu_{2k+1}^{\mathrm{OX}}(\gamma_{\mathrm{o}},\omega)x^{2k+1}(t)=x(t)\sum_{k=0}^{\infty}\nu_{2k+1}^{\mathrm{OY}}(\gamma_{\mathrm{o}},\omega)y^{2k+1}(t) \tag{2.g}$$

[13] When LAOStrain gives

$$\begin{aligned}\sigma_{\mathrm{OE}}&=G_1^{\mathrm{E}}(\gamma_{\mathrm{o}},\omega)x(t)+G_3^{\mathrm{E}}(\gamma_{\mathrm{o}},\omega)x^3(t)+G_5^{\mathrm{E}}(\gamma_{\mathrm{o}},\omega)x^5(t)+\cdots;\\ \sigma_{\mathrm{EO}}&=G_1^{\mathrm{V}}(\gamma_{\mathrm{o}},\omega)y(t)+G_3^{\mathrm{V}}(\gamma_{\mathrm{o}},\omega)y^3(t)+G_5^{\mathrm{V}}(\gamma_{\mathrm{o}},\omega)y^5(t)+\cdots\end{aligned} \tag{2.h}$$

one may consider Padé approximants such that

$$\sigma_{OE}\approx\frac{a_0'+a_1'x+a_2'x^2+a_3'x^3}{1+b_1'x+b_2'x^2};\quad \sigma_{EO}\approx\frac{a_0''+a_1''y+a_2''y^2+a_3''y^3}{1+b_0''y+b_2''y^2} \tag{2.i}$$

Find the relation between Padé coefficients of Eq. (2.i) and those of Eq. (2.h).

3 Analytical Solution of LAOS

We shall explain how to calculate analytical solutions of LAOS for various nonlinear constitutive equations. The analytical solution is important in the identification of nonlinear viscoelastic materials.

It seems impossible to obtain the exact solution of LAOS from any nonlinear constitutive equation in a closed form. Only possible analytical solution has the form of power series. Most researchers have obtained power-series approximations for various nonlinear constitutive equations. An exceptional case is the co-rotational Maxwell model for which Saengow et al. (2015) obtained the exact solution as power series. The objectives of this section are introduction to analytical methods for various constitutive equations and to test the conjecture such that decomposed stresses of LAOS have the following forms:

$$\begin{aligned}\sigma_{OE}&=\sum_{k=0}^{\infty}G_{2k+1}^{NE}(\gamma_{\mathrm{o}},\omega)x^{2k+1}(t); &\sigma_{EO}&=\sum_{k=0}^{\infty}G_{2k+1}^{NV}(\gamma_{\mathrm{o}},\omega)y^{2k+1}(t);\\ N_{EE}&=\sum_{k=0}^{\infty}E_{2k}^{NE}(\gamma_{\mathrm{o}},\omega)x^{2k}(t); &N_{OO}&=x(t)\sum_{k=0}^{\infty}E_{2k+1}^{NV}(\gamma_{\mathrm{o}},\omega)y^{2k+1}(t)\end{aligned} \tag{3.1}$$

where

$$\begin{aligned} G'^{NE}_{2n+1}(\gamma_o,\omega) &= f^{ES}_{2n+1}[\gamma_o, G'(\omega), G'(2\omega), G'(3\omega), \ldots]; \\ G''^{NV}_{2n+1}(\gamma_o,\omega) &= f^{VS}_{2n+1}[\gamma_o, G''(\omega), G''(2\omega), G''(3\omega), \ldots]; \\ E'^{NE}_{2n}(\gamma_o,\omega) &= f^{EN}_{2n}[\gamma_o, G'(\omega), G'(2\omega), G'(3\omega), \ldots]; \\ E''^{NV}_{2n}(\gamma_o,\omega) &= f^{VN}_{2n}[\gamma_o, G''(\omega), G''(2\omega), G''(3\omega), \ldots] \end{aligned} \tag{3.2}$$

In other words, frequency dependences of σ_{OE} and N_{EE} are represented by only storage modulus, while those of σ_{EO} and N_{OO} are represented by only loss modulus. We shall show that this conjecture is valid for time–strain separable constitutive equations such as separable K-BKZ model and convected Maxwell models.

Most analytical methods found in previous researches are power-series approximation (Giacomin et al. 2011; Gurnon and Wagner 2012; Helfand and Pearson 1982; Pearson and Rochefort 1982). When power-series solution is considered, of importance are the radius and speed of convergence. However, most papers, except those on co-rotational Maxwell model, deal with lower-order power series which are not available for convergence analysis. Even co-rotational Maxwell model requires order of power series higher than 30 (Saengow et al. 2015). It is usual that third harmonic is the maximum order of most power-series solutions. It is because power-series approaches require tremendously long calculations. Third harmonic approximation is available for the data with $\gamma_o < 2$. This upper bound of strain amplitude corresponds to the MASO regime of most polymeric fluids.

To overcome this limit, Bae and Cho (2015) developed semi-analytical method which extracts closed-form equations for material functions of LAOS from numerical solutions using of the strain-frequency superposition of Cho et al. (2010). Their equations are useful in identification of nonlinear parameters of constitutive equations.

3.1 Convected Maxwell Models

3.1.1 Integrating Factor Approach

There are three kinds of convected Maxwell models: upper-convected, lower-convected, and co-rotational Maxwell models. The three models can be expressed in terms of extra stress as follows:

$$\frac{D_\xi \mathbf{T}'}{Dt} + \frac{1}{\lambda}\mathbf{T}' = 2G\mathbf{D} \tag{3.3}$$

where

$$\frac{\mathrm{D}_{\xi}\mathbf{T}'}{\mathrm{D}t} = \frac{\mathrm{d}\mathbf{T}}{\mathrm{d}t} - (\mathbf{W} + \xi\mathbf{D}) \cdot \mathbf{T}' - \mathbf{T}' \cdot (\mathbf{W} + \xi\mathbf{D})^{\mathrm{T}} \tag{3.4}$$

Note that Eq. (3.3) becomes the upper-convected Maxwell model (UCM) when $\xi = 1$, the lower-convected Maxwell model (LCM) when $\xi = -1$, and the co-rotational Maxwell model (CRM) when $\xi = 0$. For simplicity, we define

$$\mathbf{H} \equiv \mathbf{W} + \xi\mathbf{D} - \frac{1}{2\lambda}\mathbf{I} \tag{3.5}$$

Then, Eq. (3.3) can be rewritten by

$$\frac{\mathrm{d}\mathbf{T}'}{\mathrm{d}t} - \mathbf{H} \cdot \mathbf{T} - \mathbf{T}' \cdot \mathbf{H}^{\mathrm{T}} = 2G\mathbf{D} \tag{3.6}$$

This is very similar to Eq. (5.83) in Chap. 1. Although H is a constant tensor in steady simple shear, we are interested in more general case, LAOS.

LAOS is a simple shear flow, but shear rate is not constant. In this case, the H tensor is given by

$$\mathbf{H} = \frac{1}{2}\frac{\mathrm{d}\gamma}{\mathrm{d}t}[(1+\xi)\mathbf{e}_1\mathbf{e}_2 - (1-\xi)\mathbf{e}_2\mathbf{e}_1] - \frac{1}{2\lambda}\mathbf{I} \tag{3.7}$$

Here, we considered the deformation gradient of $\mathbf{F} = \mathbf{I} + \gamma(t)\mathbf{e}_1\mathbf{e}_2$. In order to use the tensorial integral factor, we define

$$\mathbf{P} = \frac{\gamma}{2}[(\xi+1)\mathbf{e}_1\mathbf{e}_2 + (\xi-1)\mathbf{e}_2\mathbf{e}_1] + \left(1 - \frac{t}{2\lambda}\right)\mathbf{I} \tag{3.8}$$

Then, we know that if $\gamma(0) = 0$, then $\mathbf{P}(0) = \mathbf{I}$ and

$$\frac{\mathrm{d}\mathbf{P}}{\mathrm{d}t} = \mathbf{H} \tag{3.9}$$

and P and H are commutative:

$$\mathbf{P} \cdot \mathbf{H} = \mathbf{H} \cdot \mathbf{P} \tag{3.10}$$

Equations (3.9) and (3.10) give

$$\frac{\mathrm{d}}{\mathrm{d}t}\left(e^{-\mathbf{P}} \cdot \mathbf{T}' \cdot e^{-\mathbf{P}^{\mathrm{T}}}\right) = e^{-\mathbf{P}} \cdot \left(\frac{\mathrm{d}\mathbf{T}'}{\mathrm{d}t} - \mathbf{H} \cdot \mathbf{T}' - \mathbf{T}' \cdot \mathbf{H}^{\mathrm{T}}\right) \cdot e^{-\mathbf{P}^{\mathrm{T}}} \tag{3.11}$$

Then, we know that Eq. (3.6) is equivalent to

$$\frac{\mathrm{d}\mathbf{K}}{\mathrm{d}t} = 2G\, e^{-\mathbf{P}} \cdot \mathbf{D} \cdot e^{-\mathbf{P}^{\mathrm{T}}} \tag{3.12}$$

where

$$\mathbf{K} = e^{-\mathbf{P}} \cdot \mathbf{T}' \cdot e^{-\mathbf{P}^{\mathrm{T}}} \tag{3.13}$$

For simplicity, we assume that $\gamma(0) = 0$. This initial condition can be used for LAOS without loss of generality. Since the initial condition for the extra stress could be $\mathbf{T}'(0) = \mathbf{0}$ if the fluid were in equilibrium before flow, integration of Eq. (3.12) gives

$$\mathbf{T}'(t) = G \int_0^t e^{\mathbf{P}(t)} \cdot e^{-\mathbf{P}(\tau)} \cdot \mathbf{S} \cdot e^{-\mathbf{P}^{\mathrm{T}}(\tau)} \cdot e^{\mathbf{P}^{\mathrm{T}}(t)} \frac{\mathrm{d}\gamma}{\mathrm{d}\tau} \mathrm{d}\tau \tag{3.14}$$

where S is the constant symmetrical tensor defined as

$$\mathbf{S} = \mathbf{e}_1\mathbf{e}_2 + \mathbf{e}_2\mathbf{e}_1 \tag{3.15}$$

If we know the tensor $\exp[\mathbf{P}(t)]$, then Eq. (3.14) immediately gives analytical solution. We introduce the constant tensor defined as

$$\mathbf{J} \equiv \frac{1}{2}[(\xi + 1)\mathbf{e}_1\mathbf{e}_2 + (\xi - 1)\mathbf{e}_2\mathbf{e}_1] \tag{3.16}$$

Then, the tensor P can be expressed in simpler form:

$$\mathbf{P}(t) = \gamma(t)\mathbf{J} + \beta\mathbf{I} \tag{3.17}$$

where

$$\beta = 1 - \frac{t}{2\lambda} \tag{3.18}$$

Note that

$$e^{\mathbf{P}} = e^{\beta\mathbf{I}} \cdot e^{\gamma\mathbf{J}} = e^{\beta}\mathbf{I} \cdot e^{\gamma\mathbf{J}} = e^{\beta}e^{\gamma\mathbf{J}} \tag{3.19}$$

and

$$\begin{aligned} \mathbf{J}^2 &= \frac{\xi^2-1}{2^2}\mathbf{U}; \qquad \mathbf{J}^3 = \frac{\xi^2-1}{2^2}\mathbf{J}; \\ \left(\mathbf{J}^{\mathrm{T}}\right)^2 &= \frac{\xi^2-1}{2^2}\mathbf{U}; \quad \left(\mathbf{J}^{\mathrm{T}}\right)^3 = \frac{\xi^2-1}{2^2}\mathbf{J}^T \end{aligned} \tag{3.20}$$

where

$$\mathbf{U} = \mathbf{e}_1\mathbf{e}_1 + \mathbf{e}_2\mathbf{e}_2 = \mathbf{I} - \mathbf{e}_3\mathbf{e}_3 \tag{3.21}$$

is the two-dimensional identity tensor such that $\mathbf{U}\cdot\mathbf{X} = \mathbf{X}\cdot\mathbf{U} = \mathbf{U}$ for arbitrary two-dimensional tensor

$$\mathbf{X} = X_{11}\mathbf{e}_1\mathbf{e}_1 + X_{22}\mathbf{e}_2\mathbf{e}_2 + X_{12}\mathbf{e}_1\mathbf{e}_2 + X_{21}\mathbf{e}_2\mathbf{e}_1 \tag{3.22}$$

Equation (3.20) implies that for $k = 1, 2, \ldots$

$$\begin{aligned} \mathbf{J}^{2k+1} &= \frac{\left(\xi^2-1\right)^k}{2^{2k}}\mathbf{J}; \qquad \mathbf{J}^{2k} = \frac{\left(\xi^2-1\right)^k}{2^{2k}}\mathbf{U}; \\ \left(\mathbf{J}^{\mathrm{T}}\right)^{2k+1} &= \frac{\left(\xi^2-1\right)^k}{2^{2k}}\mathbf{J}^{\mathrm{T}}; \quad \left(\mathbf{J}^{\mathrm{T}}\right)^{2k} = \frac{\left(\xi^2-1\right)^k}{2^{2k}}\mathbf{U} \end{aligned} \tag{3.23}$$

Then, we have

$$\begin{aligned} e^{\gamma\mathbf{J}} &= \mathbf{I} + 2\left[\sum_{k=0}^{\infty}\frac{\left(\xi^2-1\right)^k}{(2k+1)!}\left(\frac{\gamma}{2}\right)^{2k+1}\right]\mathbf{J} + \left[\sum_{k=1}^{\infty}\frac{\left(\xi^2-1\right)^k}{(2k)!}\left(\frac{\gamma}{2}\right)^{2k}\right]\mathbf{U}; \\ e^{\gamma\mathbf{J}^{\mathrm{T}}} &= \mathbf{I} + 2\left[\sum_{k=0}^{\infty}\frac{\left(\xi^2-1\right)^k}{(2k+1)!}\left(\frac{\gamma}{2}\right)^{2k+1}\right]\mathbf{J}^{\mathrm{T}} + \left[\sum_{k=1}^{\infty}\frac{\left(\xi^2-1\right)^k}{(2k)!}\left(\frac{\gamma}{2}\right)^{2k}\right]\mathbf{U} \end{aligned} \tag{3.24}$$

Now we are equipped with sufficient tools for the calculation of the extra stress of simple shear. Note that when $\xi = \pm 1$, the calculation becomes dramatically simple:

$$e^{\gamma\mathbf{J}} = \mathbf{I} + \gamma\mathbf{J} = \begin{cases} \mathbf{F} = \mathbf{I} + \gamma\mathbf{e}_1\mathbf{e}_2 & \text{for } \xi = 1 \\ \mathbf{F}^{-T} = \mathbf{I} - \gamma\mathbf{e}_2\mathbf{e}_1 & \text{for } \xi = -1 \end{cases} \tag{3.25}$$

On the other hand, for $\xi = 0$, we have

$$e^{\gamma\mathbf{J}} = \sin\frac{\gamma}{2}\mathbf{A} + \cos\frac{\gamma}{2}\mathbf{U} + \mathbf{e}_3\mathbf{e}_3 \tag{3.26}$$

where

$$\mathbf{A} = \mathbf{e}_1\mathbf{e}_2 - \mathbf{e}_2\mathbf{e}_1 \tag{3.27}$$

3.1.2 Upper-Convected Maxwell Model

The stress tensor of the UCM is calculated as follows:

$$\mathbf{T}'(t) = G\int_0^t e^{-(t-\tau)/\lambda}\frac{\mathrm{d}\gamma}{\mathrm{d}\tau}[\mathbf{S} + 2\Gamma(t,\tau)\mathbf{e}_1\mathbf{e}_1]\mathrm{d}\tau \tag{3.28}$$

where

$$\Gamma(t,\tau) = \gamma(t) - \gamma(\tau) \tag{3.29}$$

When strain is given by $\gamma(t) = \dot{\gamma}_o t$ where $\dot{\gamma}_o$ is a constant, shear stress is calculated as follows:

$$\sigma = G\dot{\gamma}_o\int_0^t e^{-(t-\tau)/\lambda}\mathrm{d}\tau = G\lambda\dot{\gamma}_o\left(1 - e^{-t/\lambda}\right) \tag{3.30}$$

Thus, the steady shear viscosity of UCM is a constant $\eta = G\lambda$. Because of Eq. (3.28), it is obvious that only the first normal stress is nonzero:

$$N_1 = 2G\dot{\gamma}_o^2\int_0^t (t-\tau)e^{-(t-\tau)/\lambda}\mathrm{d}\tau = 2G\lambda^2\dot{\gamma}_o^2\left[1 - \left(1 + \frac{t}{\lambda}\right)e^{-t/\lambda}\right] \tag{3.31}$$

Thus, the steady normal stress difference coefficient is a constant:

$$\psi_1 = \frac{N_1}{\dot{\gamma}_o^2} = 2G\lambda^2 \tag{3.32}$$

As mentioned before, UCM cannot describe shear-thinning behavior of polymeric fluids.

As for LAOS, strain is $\gamma(t) = \gamma_o \sin\omega t$. As shown in Eq. (3.28), shear stress depends linearly on shear rate. Hence, shear stress of UCM is linear and cannot agree with LAOS data of most polymeric fluids. Equation (3.28) for LAOS gives

$$\sigma(t) = G'(\omega)\gamma(t) + \frac{G''(\omega)}{\omega}\frac{\mathrm{d}\gamma}{\mathrm{d}t} - G''(\omega)\gamma_o e^{-t/\lambda} \tag{3.33}$$

and

$$N_1 = \left[2G'(\omega) - \frac{G'(2\omega)}{2}\right]x^2(t) + \frac{G'(2\omega)}{2}y^2(t) + [2G''(\omega) - G''(2\omega)]x(t)y(t) - \left[2G''(\omega)\gamma_o\gamma(t) + \frac{G'(2\omega)}{2}\gamma_o^2\right]e^{-t/\lambda} \tag{3.34}$$

where $G'(\omega)$ and $G''(\omega)$ are dynamic moduli of the linear Maxwell model such that

$$G'(\omega) = G\frac{\lambda^2\omega^2}{1+\lambda^2\omega^2}; \quad G''(\omega) = G\frac{\lambda\omega}{1+\lambda^2\omega^2} \tag{3.35}$$

and Eq. (3.33) is the definitions of x and y.

The first two terms of Eq. (3.34) are N_{EE}, the third term is N_{OO}, and the last term is transient one which disappears after a long time. It is interesting that N_{EE} contains only storage modulus, while N_{OO} contains only loss modulus. As for simple shear, it is difficult to assign dissipation to any component of normal stresses because stress power is independent of normal stress. This will be found again in other models.

3.1.3 Lower-Convected Maxwell Model

With the help of Eqs. (3.14) and (3.25), stress of LCM is given by

$$\mathbf{T}'(t) = G\int_0^t e^{-(t-\tau)/\lambda}\frac{d\gamma}{d\tau}[\mathbf{S} - 2\Gamma(t,\tau)\mathbf{e}_2\mathbf{e}_2]d\tau \tag{3.36}$$

The shear stress and the first normal stress difference are not different from those of UCM, while LCM shows nonzero second normal stress difference:

$$N_2 = -N_1 \tag{3.37}$$

These relations hold for both steady and oscillatory shear flows. Note that the normal stress differences of most polymeric fluids satisfy $|N_2/N_1| \ll 1$. Hence, LCM is not adequate for nonlinear viscoelasticity of polymeric fluid, neither.

3.1.4 Co-rotational Maxwell Model

Again, Eqs. (3.14) and (3.26) give stress of CRM as follows:

$$\mathbf{T}'(t) = G\int_0^t e^{-(t-\tau)/\lambda}\frac{\mathrm{d}\gamma}{\mathrm{d}\tau}[\cos\Gamma(t,\tau)\mathbf{S} + \sin\Gamma(t,\tau)(\mathbf{e}_1\mathbf{e}_1 - \mathbf{e}_2\mathbf{e}_2)]\mathrm{d}\tau \tag{3.38}$$

Then, shear stress and normal stress differences are given by

$$\sigma(t) = G\int_0^t e^{-(t-\tau)/\lambda}\cos\Gamma(t,\tau)\frac{\mathrm{d}\gamma}{\mathrm{d}\tau}\mathrm{d}\tau \tag{3.39}$$

$$N_1 = 2G\int_0^t e^{-(t-\tau)/\lambda}\sin\Gamma(t,\tau)\frac{\mathrm{d}\gamma}{\mathrm{d}\tau}\mathrm{d}\tau \tag{3.40}$$

and

$$N_2 = -\frac{1}{2}N_1 \tag{3.41}$$

Equations (3.39) and (3.40) are very similar to Eqs. (3.47) and (3.53) which are shear and the first normal stress difference of K-BKZ model.

For steady shear, we have

$$\sigma(t) = \frac{G\lambda\dot{\gamma}_o}{1+(\lambda\dot{\gamma}_o)^2} + e^{-t/\lambda}\frac{G\lambda\dot{\gamma}_o}{1+(\lambda\dot{\gamma}_o)^2}[\cos(\dot{\gamma}_o t) + \lambda\dot{\gamma}_o\sin(\dot{\gamma}_o t)] \tag{3.42}$$

and

$$N_1(t) = \frac{G(\lambda\dot{\gamma}_o)^2}{1+(\lambda\dot{\gamma}_o)^2} - e^{-t/\lambda}\frac{G\lambda\dot{\gamma}_o}{1+(\lambda\dot{\gamma}_o)^2}[\lambda\dot{\gamma}_o\cos(\dot{\gamma}_o t) + \sin(\dot{\gamma}_o t)] \tag{3.43}$$

It is interesting that both shear viscosity and 1st normal stress coefficient show shear-thinning behavior:

$$\eta(\lambda_o) = \frac{G\lambda}{1+(\lambda\dot{\gamma}_o)^2}; \quad \psi_1(\dot{\gamma}_o) = \frac{G\lambda^2}{1+(\lambda\dot{\gamma}_o)^2} \tag{3.44}$$

As for LAOS, Eqs. (3.39) and (3.40) look like not permitting an exact analytical solution. Series expansions of cosine and sine terms give power-series solutions of shear and normal stress. Giacomin et al. (2011) used this method. We shall show the series expansion of normal stress difference. For shear stress, read Giacomin et al. (2011).

If we take the initial time as $t_o = -\infty$ when integrating Eq. (3.12), then we have

$$\sigma(t) = G \int_{-\infty}^{t} e^{-(t-\tau)/\lambda} \cos \Gamma(t,\tau) \frac{d\gamma}{d\tau} d\tau \tag{3.45}$$

and

$$N_1 = 2G \int_{-\infty}^{t} e^{-(t-\tau)/\lambda} \sin \Gamma(t,\tau) \frac{d\gamma}{d\tau} d\tau \tag{3.46}$$

This removes the transient behavior which is the effect of initial time. The definition of $\Gamma(t,\tau)$ and $\gamma(t) = \gamma_o \sin \omega t$ imply that

$$\frac{\partial}{\partial\tau} \sin \Gamma(t,\tau) = -\frac{d\gamma}{d\tau} \cos \Gamma(t,\tau); \quad \frac{\partial}{\partial\tau} \cos \Gamma(t,\tau) = \frac{d\gamma}{d\tau} \sin \Gamma(t,\tau) \tag{3.47}$$

Substitution of Eq. (3.47) to Eqs. (3.45) and (3.46) and integration by parts yield

$$\sigma = \frac{G}{\lambda} \int_{-\infty}^{t} e^{-(t-\tau)/\lambda} \sin \Gamma(t,\tau) d\tau \tag{3.48}$$

and

$$N_1 = -2\frac{G}{\lambda} \int_{-\infty}^{t} e^{-(t-\tau)/\lambda} \cos \Gamma(t,\tau) d\tau \tag{3.49}$$

Change of variables such as $\zeta = (t-\tau)/\lambda$ gives

$$\sigma = \hat{G}[\sin \Gamma(t, t-\lambda\zeta)] \tag{3.50}$$

and

$$N_1 = -2\hat{G}[\cos \Gamma(t, t-\lambda\zeta)] \tag{3.51}$$

where $\hat{\mathsf{G}}[\cdot]$ is a linear integral transform defined as

$$\hat{\mathsf{G}}[f(\zeta)] \equiv G\int_0^\infty e^{-\zeta} f(\zeta)\mathrm{d}\zeta \tag{3.52}$$

This integral transform is very useful to obtain LAOS solution of Eqs. (3.48) and (3.49) in power-series forms. Hence, it is necessary to know some properties of the integral transform:

$$\hat{\mathsf{G}}[1] = G\int_0^\infty e^{-\zeta}\mathrm{d}\zeta = G = \lim_{\omega\to\infty} G'(\omega) \tag{3.53}$$

$$\hat{\mathsf{G}}[Q_n] = G\int_0^\infty e^{-\zeta}(1-\cos n\lambda\omega\zeta)\mathrm{d}\zeta = G'_n \tag{3.54}$$

$$\hat{\mathsf{G}}[P_n] = G\int_0^\infty e^{-\zeta}\sin n\lambda\omega\zeta\mathrm{d}\zeta = G''_n \tag{3.55}$$

$$\hat{\mathsf{G}}[Q_nP_k] = G''_k - \frac{G''_{k+n}+G''_{k-n}}{2} \tag{3.56}$$

$$\hat{\mathsf{G}}\left[P_n^2\right] = \hat{\mathsf{G}}\left[1-\cos^2 n\lambda\omega\zeta\right] = \hat{\mathsf{G}}\left[1-(1-Q_n)^2\right] = \hat{\mathsf{G}}\left[\frac{Q_{2n}}{2}\right] = \frac{G'_{2n}}{2} \tag{3.57}$$

where

$$Q_n = T_0(\cos\lambda\omega\zeta) - T_n(\cos\lambda\omega\zeta) = 1 - T_n(\cos\lambda\omega\zeta) \tag{3.58}$$

$$P_n = \sin n\lambda\omega\zeta \tag{3.59}$$

and

$$G'_n \equiv G\frac{(n\lambda\omega)^2}{1+(n\lambda\omega)^2};\quad G''_n \equiv G\frac{n\lambda\omega}{1+(n\lambda\omega)^2} \tag{3.60}$$

Application of the Taylor series expansions of trigonometric functions to Eqs. (3.50) and (3.51) gives

$$\sigma_{OE}(x,y) = \sum_{m=0}^{\infty}\sum_{n=0}^{\infty}\frac{(-1)^{m+n}x^{2m+1}y^{2n}}{(2m+1)!(2n)!}\mathrm{G}\left[Q_1^{2m+1}\left(\frac{Q_2}{2}\right)^n\right] \tag{3.61}$$

$$\sigma_{EO}(x,y) = \sum_{m=0}^{\infty}\sum_{n=0}^{\infty}\frac{(-1)^{m+n}x^{2m}y^{2n+1}}{(2m)!(2n+1)!}\mathrm{G}\left[Q_1^{2m}\left(\frac{Q_2}{2}\right)^n P_1\right] \tag{3.62}$$

$$N_{EE}(x,y) = -2\sum_{m=0}^{\infty}\sum_{n=0}^{\infty}\frac{(-1)^{m+n}x^{2m}y^{2n}}{(2m)!(2n)!}\mathrm{G}\left[Q_1^{2m}\left(\frac{Q_2}{2}\right)^n\right] \tag{3.63}$$

and

$$N_{OO}(x,y) = -2\sum_{m=0}^{\infty}\sum_{n=0}^{\infty}\frac{(-1)^{m+n}x^{2m+1}y^{2n+1}}{(2m+1)!(2n+1)!}\mathrm{G}\left[Q_1^{2m+1}\left(\frac{Q_2}{2}\right)^n P_1\right] \tag{3.64}$$

Now, we shall show that the integral transforms of Eqs. (3.61)–(3.63) can be expressed as linear combinations of G'_n and G''_n.

Note that the Chebyshev polynomials of the first kind obey

$$T_m(x)T_n(x) = \frac{T_{m+n}(x) + T_{|m-n|}(x)}{2} \tag{3.65}$$

Then, the definition of Q_n gives

$$Q_m Q_n = Q_m + Q_n - \frac{Q_{m+n} + Q_{|m-n|}}{2} \tag{3.66}$$

This implies that there exists relations such that

$$Q_1^M Q_2^N = \sum_{k=1}^{M+2N} q_k Q_k \tag{3.67}$$

Equations (3.54), (3.56), and (3.67) immediately imply that σ_{OE} and N_{EE} consist of linear combinations of $\{G'_n\}$ and that σ_{EO} and N_{OO} consist of linear combinations of $\{G''_n\}$. These results are consistent with that σ_{OE} is elastic and σ_{EO} is viscous. Along this line of reasoning, one may think that N_{EE} is elastic and N_{OO} is viscous. However, it is difficult to connect normal stresses of shear flow with energy dissipation because of Eq. (3.42) which shows that stress power of shear flow is independent of normal stresses. Similar analysis can be done for time–strain separable K-BKZ model, too.

3.2 Time–Strain Separable K-BKZ Model

LAOS behavior of time–strain separable K-BKZ model can be described easily if a suitable damping function is known. Equations (3.40a, c) in Chap. 10 do not allow power series such as

$$h(\gamma) = \sum_{k=0}^{\infty} h_n \gamma^n \tag{3.68}$$

However, it is easy to show that Eq. (3.40c) in Chap. 10 is equivalent to

$$h(\gamma) = 1 - \frac{2}{\pi}\left[(1-\phi)\arctan\left(\frac{\gamma}{\gamma_{C1}}\right)^2 + \phi\arctan\left(\frac{\gamma}{\gamma_{C2}}\right)^2\right] \tag{3.69}$$

This allows the power-series approximation:

$$h(\gamma) = 1 - \frac{2}{\pi}\sum_{n=0}^{\infty}\frac{(-1)^n}{2n+1}\left[(1-\phi)\left(\frac{\gamma}{\gamma_{C1}}\right)^{4n+2} + \phi\left(\frac{\gamma}{\gamma_{C2}}\right)^{4n+2}\right] \tag{3.70}$$

From Eqs. (3.36) and (3.37) in Chap. 10, we know that

$$\sigma_{OE} = \sum_{n=0}^{\infty}\sum_{k=0}^{n}\binom{2n+1}{2k} h_n x^{2(n-k)+1}\left(\gamma_o^2 - x^2\right)^k \hat{\mathsf{G}}\left[Q_1^{2(n-k)+1}\left(\frac{Q_2}{2}\right)^k\right] \tag{3.71}$$

$$\sigma_{EO} = \sum_{n=0}^{\infty}\sum_{k=0}^{n}\binom{2n+1}{2k+1} h_n\left(\gamma_o^2 - y^2\right)y^{2k+1}\hat{\mathsf{G}}\left[Q_1^{2(n-k)}\left(\frac{Q_2}{2}\right)^k P_1\right] \tag{3.72}$$

$$N_{EE} = \sum_{n=0}^{\infty}\sum_{k=0}^{n}\binom{2n}{2k} h_n x^{2(n-k)}y^{2k}\hat{\mathsf{G}}\left[Q_1^{2(n-k)}\left(\frac{Q_2}{2}\right)^k\right] \tag{3.73}$$

and

$$N_{OO} = \sum_{n=0}^{\infty}\sum_{k=0}^{n}\binom{2n+1}{2k+1} h_n x^{2(n-k)}y^{2k+1}\hat{\mathsf{G}}\left[Q_1^{2(n-k)}\left(\frac{Q_2}{2}\right)^k P_1\right] \tag{3.74}$$

Comparing Eqs. (3.61)–(3.64), it is obvious that separable K-BKZ model also follows the same stress decomposition of convected Maxwell models which are also time–strain separable constitutive equation. The above analysis is also valid multimode versions. Then, it is questionable whether nonseparable constitutive equations (Larson 1988) obeys the conjecture that σ_{OE} and N_{EE} contain only storage moduli of G_n' while σ_{EO} and N_{OO} contain only loss moduli of G_n''.

3.3 Nonseparable Maxwell Models

Equations (3.36) in Chap. 10, (3.28), (3.36), and (3.38) imply that nonlinear relaxation modulus is the product of linear relaxation modulus and the damping function. These constitutive equations are classified to separable constitutive equations. On the other hand, the Leonov, the Giesekus and PTT models do not allow such factorization of relaxation modulus. These nonlinear constitutive equations are classified to nonseparable constitutive equations (Larson 1988). Here, we shall devote an analytical method to the LAOS behavior of the PTT and the Giesekus models.

3.3.1 Perturbation Method

The PTT and the Giesekus models are expressed in terms of extra stress as follows:

$$\overset{\nabla}{\mathbf{T}}' + \frac{1}{\lambda}\exp\left[\frac{\alpha}{G}\mathrm{tr}(\mathbf{T}')\right]\mathbf{T}' = 2G\mathbf{D} \tag{3.75}$$

and

$$\overset{\nabla}{\mathbf{T}}' + \frac{1}{\lambda}\mathbf{T}' + \frac{\alpha}{\lambda G}\mathbf{T}'\cdot\mathbf{T}' = 2G\mathbf{D} \tag{3.76}$$

Here, α is the nonlinear parameter of the two models. Note that these equations are reduced to UCM if $\alpha = 0$. Since α is positive and less than unity, we can take perturbation parameter as

$$\varepsilon = \frac{\alpha}{G} \tag{3.77}$$

Then, it is a reasonable assumption that the extra stress can be expressed as the power series of the perturbation parameter:

$$\mathbf{T}' = \mathbf{T}_0 + \varepsilon\mathbf{T}_1 + \varepsilon^2\mathbf{T}_2 + \cdots \tag{3.78}$$

where $\mathbf{T}_0$ is the solution of UCM.

Substitution of Eq. (3.78) to Eq. (3.75) gives

$$\lambda\overset{\nabla}{\mathbf{T}}_1 + \mathbf{T}_1 = -\mathrm{tr}(\mathbf{T}_0)\mathbf{T}_0 \equiv -\mathbf{R}_1^{\mathrm{PTT}} \tag{3.79a}$$

$$\lambda\overset{\nabla}{\mathbf{T}}_2 + \mathbf{T}_2 = -\mathrm{tr}\left(\mathbf{T}_1 + \tfrac{1}{2}\mathbf{T}_0\right)\mathbf{T}_0 - \mathrm{tr}(\mathbf{T}_0)\mathbf{T}_1 \equiv -\mathbf{R}_2^{\mathrm{PTT}} \tag{3.79b}$$

$$\begin{aligned}\lambda \overset{\nabla}{\mathbf{T}}_3 + \mathbf{T}_3 &= -\operatorname{tr}\left(\mathbf{T}_2 + \frac{1}{2}\mathbf{T}_1 + \frac{1}{6}\mathbf{T}_0\right)\mathbf{T}_0 - \operatorname{tr}\left(\mathbf{T}_1 + \frac{1}{2}\mathbf{T}_0\right)\mathbf{T}_1 - \operatorname{tr}(\mathbf{T}_0)\mathbf{T}_2 \\ &\equiv -\mathbf{R}_3^{\mathrm{PTT}}\end{aligned} \tag{3.79c}$$

and so on. Substitution of Eq. (3.78) to Eq. (3.76) yields

$$\lambda \overset{\nabla}{\mathbf{T}}_1 + \mathbf{T}_1 = -\mathbf{T}_0^2 \equiv -\mathbf{R}_1^{\mathrm{G}} \tag{3.80a}$$

$$\lambda \overset{\nabla}{\mathbf{T}}_2 + \mathbf{T}_2 = -\mathbf{T}_0 \cdot \mathbf{T}_1 - \mathbf{T}_1 \cdot \mathbf{T}_0 \equiv -\mathbf{R}_2^{\mathrm{G}} \tag{3.80b}$$

$$\lambda \overset{\nabla}{\mathbf{T}}_3 + \mathbf{T}_3 = -\mathbf{T}_0 \cdot \mathbf{T}_2 - \mathbf{T}_2 \cdot \mathbf{T}_0 - \mathbf{T}_1^2 \equiv -\mathbf{R}_3^{\mathrm{G}} \tag{3.80c}$$

and so on. We can obtain higher-order equations as we want. Since we know the solution of UCM, it is obvious that the first-order stress $\mathbf{T}_1$ can be calculated analytically using the integrating factor method. The same procedure can be applied to the second-order stress after calculation of the first-order stress. This procedure can be extended to higher-order stresses as we want. However, this calculation is tedious and time-consuming.

Using the integrating factor method to *n*th-order stresses, we have the general solution such that

$$\mathbf{T}_n(t) = -\frac{1}{\lambda}\int_{-\infty}^{t} e^{-(t-\tau)/\lambda} \cdot \mathbf{F}(t) \cdot \mathbf{F}^{-1}(\tau) \cdot \mathbf{R}_n(\tau) \cdot \mathbf{F}^{-\mathrm{T}}(\tau) \cdot \mathbf{F}^{\mathrm{T}}(t)\mathrm{d}\tau \tag{3.81}$$

Note that

$$\mathbf{F}(t) \cdot \mathbf{F}^{-1}(\tau) = \mathbf{I} + \Gamma(t,\tau)\,\mathbf{e}_1\mathbf{e}_2 = \left[\mathbf{F}^{-\mathrm{T}}(\tau) \cdot \mathbf{F}^{\mathrm{T}}(t)\right]^{\mathrm{T}} \tag{3.82}$$

Then, use of Eq. (3.82) gives

$$\begin{aligned}-G\lambda\mathbf{T}_n(t) = \hat{\mathsf{G}}[\mathbf{R}_n(t-\lambda\zeta)] &+ \left\{\mathbf{e}_2 \cdot \hat{\mathsf{G}}\left[\Gamma^2(t,t-\lambda\zeta)\mathbf{R}_n(t-\lambda\zeta)\right] \cdot \mathbf{e}_2\right\}\mathbf{e}_1\mathbf{e}_1 \\ &+ \mathbf{e}_1\mathbf{e}_2 \cdot \hat{\mathsf{G}}[\Gamma(t,t-\lambda\zeta)\mathbf{R}_n(t-\lambda\zeta)] + \hat{\mathsf{G}}[\Gamma(t,t-\lambda\zeta)\mathbf{R}_n(t-\lambda\zeta)] \cdot \mathbf{e}_2\mathbf{e}_1\end{aligned} \tag{3.83}$$

If we denote the components of $\mathbf{R}_n$ by $r_{ik}^{(n)}$, then Eq. (3.83) becomes

$$\begin{aligned}\mathbf{T}_n(\tau) = &-\frac{1}{G\lambda}\hat{\mathsf{G}}\left[r_{11}^{(n)}(\tau) + 2\Gamma(t,\tau)r_{12}^{(n)}(\tau) + \Gamma^2(t,\tau)r_{22}^{(n)}(\tau)\right]\mathbf{e}_1\mathbf{e}_1 \\ &-\frac{1}{G\lambda}\hat{\mathsf{G}}\left[r_{22}^{(n)}(\tau)\right]\mathbf{e}_2\mathbf{e}_2 - \frac{1}{G\lambda}\hat{\mathsf{G}}\left[r_{33}^{(n)}(\tau)\right]\mathbf{e}_3\mathbf{e}_3 \\ &-\frac{1}{G\lambda}\hat{\mathsf{G}}\left[r_{12}^{(n)}(\tau) + \Gamma(t,\tau)r_{22}^{(n)}(\tau)\right](\mathbf{e}_1\mathbf{e}_2 + \mathbf{e}_1\mathbf{e}_2)\end{aligned} \tag{3.84}$$

where $\tau = t - \lambda\zeta$. Note that Eq. (3.84) consists of integration transforms such as $\hat{\mathsf{G}}[x^M(\tau)y^N(\tau)]$, $\hat{\mathsf{G}}[\Gamma(t,\tau)x^M(\tau)y^N(\tau)]\,\hat{\mathsf{G}}[\Gamma(t,\tau)x^M(\tau)y^N(\tau)]$ and $\hat{\mathsf{G}}\left[\Gamma^2(t,\tau)x^M(\tau)y^N(\tau)\right]$.

3.3.2 Systematic Evaluation of the Integral Transforms

In order to calculate the integral transforms of Eq. (3.84) systematically, we need to find formulas for the integral transform of $x^M(t-\lambda\zeta)y^N(t-\lambda\zeta)$. It is helpful to know that

$$\begin{aligned}x(\tau) &= x(t-\lambda\zeta) = x(t)\cos\lambda\omega\zeta - y(t)\sin\lambda\omega\zeta; \\ y(\tau) &= y(t-\lambda\zeta) = x(t)\sin\lambda\omega\zeta + y(t)\cos\lambda\omega\zeta\end{aligned} \tag{3.85}$$

This equation is the rotation of coordinates $[x(t), y(t)]$ by an angle of $\theta = \lambda\omega\zeta$. For easy calculation, we introduce the complex-valued function of time such that

$$\mathbf{z}(t) \equiv x(t) + \mathrm{i}y(t) = \mathrm{i}\gamma_o e^{-\mathrm{i}\,\omega t} \tag{3.86}$$

Use of this complex notation gives

$$\mathbf{z}(t-\lambda\zeta) = e^{\mathrm{i}\lambda\omega\zeta}\mathbf{z}(t) = \mathrm{i}\gamma_o e^{\mathrm{i}\lambda\omega\zeta}e^{-\mathrm{i}\,\omega t} \tag{3.87}$$

We shall denote the conjugate of $\mathbf{z}(t)$ by $\bar{\mathbf{z}}(t)$. Then, it is obvious that

$$x(t) = \frac{\mathbf{z}(t) + \bar{\mathbf{z}}(t)}{2}; \quad y(t) = \frac{\mathbf{z}(t) - \bar{\mathbf{z}}(t)}{2\mathrm{i}} \tag{3.88}$$

The integral transform of the product $\mathbf{z}^M(t-\lambda\zeta)\,\bar{\mathbf{z}}^N(t-\lambda\zeta)$ is immediately calculated as follows:

$$\hat{\mathsf{G}}\left[\mathbf{z}^M(t-\lambda\zeta)\bar{\mathbf{z}}^N(t-\lambda\zeta)\right] = \mathbf{g}_{M-N}\mathbf{z}^M(t)\bar{\mathbf{z}}^N(t) \tag{3.89}$$

where

$$\mathbf{g}_n \equiv G - G'(n\omega) + \mathrm{i}G''(n\omega) = G - G'_n + \mathrm{i}G''_n \tag{3.90}$$

It should be noted that

$$\mathbf{z}(t)\bar{\mathbf{z}}(t) = x^2(t) + y^2(t) = \gamma_o^2 \tag{3.91}$$

and

$$\mathbf{g}_0 = G; \quad \mathbf{g}_{-n} = \bar{\mathbf{g}}_n \tag{3.92}$$

Note that

$$\hat{\mathsf{G}}\left[x^{2n}(t-\lambda\zeta)\right] = \frac{1}{2^{2n}}\binom{2n}{n} G\gamma_o^{2n} + \frac{1}{2^{2n-1}}\sum_{k=0}^{n-1}\binom{2n}{k}\gamma_o^{2k}\mathrm{Re}\left\{\mathbf{g}_{2\,(n-k)}\mathbf{z}^{2\,(n-k)}(t)\right\} \tag{3.93}$$

where we used Eqs. (3.91) and (3.92) and

$$\binom{N}{k} = \binom{N}{N-k} \tag{3.94}$$

For odd power of $x(t-\lambda\zeta)$, we have

$$\hat{\mathsf{G}}\left[x^{2n+1}(t-\lambda\zeta)\right] = \frac{1}{2^{2n}}\sum_{k=0}^{n}\binom{2n+1}{n-k}\gamma_o^{2\,(n-k)}\,\mathrm{Re}\left\{\mathbf{g}_{2k+1}\mathbf{z}^{2k+1}(t)\right\} \tag{3.95}$$

Similar procedure can be applied to the integral transform of $y^N(t-\lambda\zeta)$:

$$\hat{\mathsf{G}}\left[y^{2n}(t-\lambda\zeta)\right] = \frac{1}{2^{n}}\binom{2n}{n} G\gamma_o^{2n} + \frac{1}{2^{n-1}}\sum_{k=0}^{n-1}\binom{2n}{k}(-1)^{n-k}\,\mathrm{Re}\left\{\mathbf{g}_{2(n-k)}z^{2(n-k)}(t)\right\} \tag{3.96}$$

and

$$\hat{\mathsf{G}}\left[y^{2n+1}(t-\lambda\zeta)\right] = \frac{(-1)^n}{2^{2n}}\sum_{k=0}^{n}\binom{2n+1}{k}(-1)^k\gamma_o^{2k}\mathrm{Im}\left\{\mathbf{g}_{2(n-k)+1}z^{2(n-k)+1}(t)\right\} \tag{3.97}$$

The calculation of $\hat{\mathsf{G}}[x^M(t-\lambda\zeta)y^N(t-\lambda\zeta)]$ can be reduced to that of $\hat{\mathsf{G}}[x^n(t-\lambda\zeta)]$ whenever N is even because

$$\hat{\mathsf{G}}\left[x^M(t-\lambda\zeta)y^{2n}(t-\lambda\zeta)\right] = \hat{\mathsf{G}}\left[x^M(t-\lambda\zeta)\left\{\gamma_o^2 - x^2(t-\lambda\zeta)\right\}^n\right] \tag{3.98}$$

When $M = 2m$, the calculation becomes that of $\hat{\mathsf{G}}[y^n(t-\lambda\zeta)]$ because

$$\hat{\mathsf{G}}\left[x^{2m}(t-\lambda\zeta)y^N(t-\lambda\zeta)\right] = \hat{\mathsf{G}}\left[\left\{\gamma_{\mathrm{o}}^2 - y^2(t-\lambda\zeta)\right\}^m y^N(t-\lambda\zeta)\right] \tag{3.99}$$

Hence, it is sufficient to consider $\hat{\mathsf{G}}[x^n(t-\lambda\zeta)\,y(t-\lambda\zeta)]$. Then, the same procedure gives

$$\begin{aligned}
&\hat{\mathsf{G}}\left[x^{2m}(t-\lambda\zeta)y(t-\lambda\zeta)\right] \\
&\quad = \hat{\mathsf{G}}\left[\left[\gamma_{\mathrm{o}}^2 - y^2(t-\lambda\zeta)\right]^m y(t-\lambda\zeta)\right] \\
&\quad = \sum_{n=0}^{m}\binom{m}{n}\frac{(-1)^n}{2^{2n}}\sum_{k=0}^{n}\binom{2n+1}{n-k}(-1)^k\gamma_{\mathrm{o}}^{2(m-k)}\mathrm{Im}\left\{\mathbf{g}_{2k+1}z^{2k+1}(t)\right\}
\end{aligned} \tag{3.100}$$

and

$$\begin{aligned}
\hat{\mathsf{G}}\left[x^{2m+1}(t-\lambda\zeta)y(t-\lambda\zeta)\right] &= \frac{1}{2^{2m+1}}\sum_{k=0}^{m}\binom{2m+1}{m-k}\gamma_{\mathrm{o}}^{2(m-k)}\,\mathrm{Im}\left\{\mathbf{g}_{2(k+1)}\mathbf{z}^{2(k+1)}(t)\right\} \\
&\quad - \frac{1}{2^{2m+1}}\sum_{k=0}^{m}\binom{2m+1}{m-k}\gamma_{\mathrm{o}}^{2(m-k+1)}\,\mathrm{Im}\left\{\mathbf{g}_{2k}\mathbf{z}^{2k}(t)\right\}
\end{aligned} \tag{3.101}$$

The integration transform including $\Gamma(t,\tau)$ is calculated by

$$\hat{\mathsf{G}}\left[\Gamma(t,\tau)x^M(\tau)y^N(\tau)\right] = x(t)\hat{\mathsf{G}}\left[x^M(\tau)y^N(\tau)\right] - \hat{\mathsf{G}}\left[x^{M+1}(\tau)y^N(\tau)\right] \tag{3.102}$$

and

$$\begin{aligned}
\hat{\mathsf{G}}\left[\Gamma^2(t,\tau)x^M(\tau)y^N(\tau)\right] &= x^2(t)\hat{\mathsf{G}}\left[x^M(\tau)y^N(\tau)\right] - 2x(t)\hat{\mathsf{G}}\left[x^M(\tau)y^N(\tau)\right] \\
&\quad + \hat{\mathsf{G}}\left[x^{M+2}(\tau)y^N(\tau)\right]
\end{aligned} \tag{3.103}$$

It is obvious that all integration transforms needed for the perturbation calculation are expressed by linear combination of $\mathrm{Re}\{\mathbf{g}_n\mathbf{z}^n(t)\}$ or $\mathrm{Im}\{\mathbf{g}_n\mathbf{z}^n(t)\}$. Hence, we have to express them in terms of $x(t)$ and $y(t)$. Equations (3.86) and (3.90) give

$$\begin{aligned}
\mathrm{Re}\left\{\mathbf{g}_{2n}\mathbf{z}^{2n}(t)\right\} &= (-1)^n\left(G - G'_{2n}\right)\gamma_{\mathrm{o}}^{2n}\cos 2n\omega t \\
&\quad + (-1)^n G''_{2n}\gamma_{\mathrm{o}}^{2n}\sin 2n\omega t
\end{aligned} \tag{3.104a}$$

$$\begin{aligned}
\mathrm{Im}\left\{\mathbf{g}_{2n}\mathbf{z}^{2n}(t)\right\} &= (-1)^n g''_{2n}\gamma_{\mathrm{o}}^{2n}\cos 2n\omega t \\
&\quad - (-1)^n\left(G - G'_{2n}\right)\gamma_{\mathrm{o}}^{2n}\sin 2n\omega t
\end{aligned} \tag{3.104b}$$

$$\mathrm{Re}\{\mathbf{g}_{2n+1}\mathbf{z}^{2n+1}(t)\} = (-1)^n\left(G - G'_{2n+1}\right)\gamma_o^{2n+1}\sin(2n+1)\omega t - (-1)^n G''_{2n+1}\gamma_o^{2n+1}\cos(2n+1)\omega t \tag{3.105a}$$

and

$$\mathrm{Im}\{\mathbf{g}_{2n+1}\mathbf{z}^{2n+1}(t)\} = (-1)^n G''_{2n+1}\gamma_o^{2n+1}\sin(2n+1)\omega t + (-1)^n\left(G - G'_{2n+1}\right)\gamma_o^{2n+1}\cos(2n+1)\omega t \tag{3.105b}$$

Although Eqs. (3.104a) and (3.105a) are convenient to obtain a perturbation solution, they are not convenient to check the validity of the conjecture. For this purpose, we can use

$$\begin{aligned}\mathbf{g}_{2n}\mathbf{z}^{2n}(t) &= \left[\left(G - G'_{2n}\right) + \mathrm{i}G''_{2n}\right][x(t) + \mathrm{i}y(t)]^{2n} \\ &= \left[\left(G - G'_{2n}\right) + \mathrm{i}G''_{2n}\right]\sum_{k=0}^{n}\binom{2n}{2k}(-1)^k x^{2(n-k)}(t)y^{2k}(t) \\ &\quad + \left[-G''_{2n} + \mathrm{i}\left(G - G'_{2n}\right)\right]\sum_{k=0}^{n-1}\binom{2n}{2k+1}(-1)^k x^{2(n-k)-1}(t)y^{2k+1}(t)\end{aligned} \tag{3.106}$$

which results in

$$\mathrm{Re}\{\mathbf{g}_{2n}\mathbf{z}^{2n}(t)\} = \left(G - G'_{2n}\right)\sum_{k=0}^{n}\binom{2n}{2k}(-1)^k x^{2(n-k)}(t)y^{2k}(t) - G''_{2n}\sum_{k=0}^{n-1}\binom{2n}{2k+1}(-1)^k x^{2(n-k)-1}(t)y^{2k+1}(t) \tag{3.107a}$$

and

$$\mathrm{Im}\{\mathbf{g}_{2n}\mathbf{z}^{2n}(t)\} = G''_{2n}\sum_{k=0}^{n}\binom{2n}{2k}(-1)^k x^{2(n-k)}(t)y^{2k}(t) + \left(G - G'_{2n}\right)\sum_{k=0}^{n-1}\binom{2n}{2k+1}(-1)^k x^{2(n-k)-1}(t)y^{2k+1}(t) \tag{3.107b}$$

Similarly, we have

$$\begin{aligned}\mathbf{g}_{2n+1}\mathbf{z}^{2n+1}(t) &= \left[\left(G-G'_{2n+1}\right)+\mathrm{i}G''_{2n+1}\right][x(t)+\mathrm{i}y(t)]^{2n+1} \\ &= \left[\left(G-G'_{2n}\right)+\mathrm{i}G''_{2n}\right]\sum_{k=0}^{n}\binom{2n+1}{2k}(-1)^k x^{2(n-k)+1}(t)y^{2k}(t) \\ &\quad+\left[-G''_{2n}+\mathrm{i}\left(G-G'_{2n}\right)\right]\sum_{k=0}^{n}\binom{2n+1}{2k+1}(-1)^k x^{2(n-k)}(t)y^{2k+1}(t)\end{aligned} \tag{3.108}$$

$$\begin{aligned}\mathrm{Re}\left\{\mathbf{g}_{2n+1}\mathbf{z}^{2n+1}(t)\right\} &= \left(G-G'_{2n+1}\right)\sum_{k=0}^{n}\binom{2n+1}{2k}(-1)^k x^{2(n-k)+1}(t)y^{2k}(t) \\ &\quad-G''_{2n+1}\sum_{k=0}^{n}\binom{2n+1}{2k+1}(-1)^k x^{2(n-k)}(t)y^{2k+1}(t)\end{aligned} \tag{3.109a}$$

and

$$\begin{aligned}\mathrm{Im}\left\{\mathbf{g}_{2n+1}\mathbf{z}^{2n+1}(t)\right\} &= G''_{2n+1}\sum_{k=0}^{n}\binom{2n+1}{2k}(-1)^k x^{2(n-k)+1}(t)y^{2k}(t) \\ &\quad+\left(G-G''_{2n+1}\right)\sum_{k=0}^{n}\binom{2n+1}{2k+1}(-1)^k x^{2(n-k)}(t)y^{2k+1}(t)\end{aligned} \tag{3.109b}$$

Now we are equipped with formulas necessary for perturbation calculation.

3.3.3 First-Order Approximation of PTT Model

It is not difficult to show that the second normal stress difference of the PTT model is zero. From Eqs. (3.33) and (3.34), we know that $\mathbf{T}_0$ is given by

$$\mathbf{T}_0 = N_0(x,y)\mathbf{e}_1\mathbf{e}_1+\sigma_0(x,y)(\mathbf{e}_1\mathbf{e}_2+\mathbf{e}_2\mathbf{e}_1) \tag{3.110}$$

where

$$N_0(\tau) = \frac{G'_2}{2}\gamma_o^2+\left(2G'_1-G'_2\right)x^2(\tau)+\left(2G''_1-G''_2\right)x(\tau)y(\tau) \tag{3.111a}$$

and

$$\sigma_0(\tau) = G_1' x(\tau) + G_1'' y(\tau) \tag{3.111b}$$

Then, Eq. (3.79a) means that

$$\mathbf{R}_1(\tau) = N_0^2(\tau)\mathbf{e}_1\mathbf{e}_1 + N_0(\tau)\sigma_0(\tau)(\mathbf{e}_1\mathbf{e}_2 + \mathbf{e}_2\mathbf{e}_1) \tag{3.112a}$$

$$\begin{aligned} r_{11}^{(1)\mathrm{PTT}}(\tau) = {} & \left(\frac{G_2'}{2}\right)^2 \gamma_o^4 + \left[\left(2G_1'' - G_2''\right)^2 + G_2'\left(2G_1' - G_2'\right)\right]\gamma_o^2 x^2(\tau) \\ & + \left[\left(2G_1' - G_2'\right)^2 - \left(2G_1'' - G_2''\right)^2\right] x^4(\tau) + G_2'\left(2G_1'' - G_2''\right)\gamma_o^2 x(\tau) y(\tau) \\ & + 2\left(2G_1' - G_2'\right)\left(2G_1'' - G_2''\right) x^3(\tau) y(\tau) \end{aligned} \tag{3.112b}$$

$$\begin{aligned} r_{12}^{(1)\mathrm{PTT}}(\tau) = {} & \left[\frac{G_1' G_2'}{2} + G_1''\left(2G_1'' - G_2''\right)\right]\gamma_o^2 x(\tau) \\ & + \left[G_1'\left(2G_1' - G_2'\right) - G_1''\left(2G_1'' - G_2''\right)\right] x^3(\tau) \\ & + \left[\frac{G_1' G_2'}{2} + G_1'\left(2G_1'' - G_2''\right) + G_1''\left(2G_1' - G_2'\right)\right]\gamma_o^2 y(\tau) \\ & - \left[G_1'\left(2G_1'' - G_2''\right) + G_1''\left(2G_1' - G_2'\right)\right] y^3(\tau) \end{aligned} \tag{3.112c}$$

and

$$r_{22}^{(1)} = r_{33}^{(1)} = r_{31}^{(1)} = r_{23}^{(1)} = 0 \tag{3.112d}$$

Substitution of Eq. (3.112a) to Eq. (3.84) gives

$$\sigma_1(t) = -\frac{1}{G\lambda}\hat{\mathsf{G}}\left[r_{12}^{(n)}(\tau)\right] \tag{3.113}$$

and

$$N_1(t) = -\frac{1}{G\lambda}\hat{\mathsf{G}}\left[r_{11}^{(n)}(\tau) + 2\Gamma(t,\tau)\, r_{12}^{(n)}(\tau)\right] \tag{3.114}$$

With the help of Eq. (3.112c), Eq. (3.113) becomes

$$\begin{aligned} \sigma_1^{\mathrm{PTT}}(t) = {} & \frac{A_1\left(G_1' - G\right) + \frac{3}{4}A_3\left(G_1' - G_3'\right)}{G\lambda}\gamma_o^2 x(t) \\ & - \frac{A_1 G_1'' + \frac{3}{4}A_3\left(G_3'' - 2G_1''\right)}{G\lambda}\gamma_o^2 y(t) \\ & - \frac{A_3\left(G - \frac{3}{4}G_1' - \frac{1}{4}G_3'\right)}{G\lambda}x^3(t) + \frac{A_3 G_3''\gamma_o^2}{G\lambda}y^3(t) \end{aligned} \tag{3.115}$$

where

$$A_1 = \frac{G_1' G_2'}{2} + G_1''\left(2G_1'' - G_2''\right); \quad A_3 = G_1'\left(2G_1' - G_2'\right) - G_1''\left(2G_1'' - G_2''\right) \tag{3.116}$$

Equation (3.112b) gives

$$\begin{aligned}
N_1^{PTT} = -\frac{2}{G\lambda}\Bigg\{ & \gamma_o^2\left(y(t)\left(G - G_1'\right) + x(t)G_1''\right)\left(\left(2G_1' - G_2'\right)G_1'' + \tfrac{G_2' G_1''}{2} + G_1'\left(2G_1'' - G_2''\right)\right) \\
& + \left(x(t)\left(G - G_1'\right) - y(t)G_1''\right)\left(\tfrac{G_1' G_2'}{2} + \gamma_o^2 G_1''\left(2G_1'' - G_2''\right)\right) \\
& \quad + \left(-2G_1' G_2' G_1'' - G_1'\left(2G_1'' - G_2''\right)\right)\left(y^3(t)\left(G - G_3'\right) - \frac{3}{4}\gamma_o^2 y(t)\left(G_1' - G_3'\right)\right. \\
& \quad \left. + \frac{3}{4}x(t)\gamma_o^2\left(G_1'' - G_3''\right) - x^3(t)G_3''\right) \\
& + \left(G_1'\left(2G_1' G_2'\right) - G_1''\left(2G_1'' - G_x''\right)\right)\left(x^3(t)\left(G - G_3'\right) - \frac{3}{4}x(t)\gamma_o^2\left(G_1' - G_3'\right)\right. \\
& \quad \left. + y^3(t)G_3'' - \frac{3}{4}y\gamma_o^2\left(G_1'' + G_3''\right)\right)
\end{aligned}$$

$$\begin{aligned}
-\frac{1}{G\lambda}\Bigg\{ & \tfrac{1}{4}GG_2''^2\gamma_o^4 + \gamma_o^2 G_2' G_2''\left(x(t)y(t)\left(G - G_2'\right) - \tfrac{\gamma_o^2}{2}G_2' + x^2(t)G_2''\right) \\
& + \gamma_o^2\left(\left(2G_1' - G_2'\right)G_2' + \left(2G_1'' - G_2''\right)^2\right)\left(x^2(t)\left(G - G_2'\right) + \tfrac{\gamma_o^2 G_2'}{2} - x(t)y(t)G_2''\right) \\
& + \left(\left(2G_1' - G_2'\right)^2 - G_2''^2\right)\left\{\begin{array}{l} x^4(t)\left(G - G_4'\right) - x^2(t)\gamma_o^2\left(G_2' - G_4'\right) \\ \quad + \frac{1}{8}\gamma_o^4\left(4G_2' - G_4'\right) \\ -x^3(t)y(t)G_4'' + \frac{1}{2}x(t)y(t)\gamma_o^2\left(-2G_2'' + G_4''\right)\end{array}\right. \\
& + 2\left(2G_1' - G_2'\right)\left(2G_1'' - G_2''\right)\left\{\begin{array}{l} -x(t)y^3(t)\left(G - G_4'\right) + \frac{1}{2}x(t)y(t)\gamma_o^2\left(-G_2' + G_4'\right) \\ \quad + \frac{1}{2}x^2(t)\gamma_o^2\left(G_2'' - 2G_4''\right) + x^4(t)G_4'' \\ \quad + \frac{1}{8}\gamma_o^4\left(-2G_2'' + G_4''\right)\end{array}\right.
\end{aligned}$$

$$\begin{aligned}
+\frac{2}{G\lambda}\Bigg\{ & \gamma_o^2\left(\left(2G_1' - G_2'\right)G_1'' + \tfrac{G_2' G_1''}{2} + G_1'\left(2G_1'' - G_2''\right)\right)\left(x(t)y(t)\left(G - G_2'\right) - \tfrac{\gamma_o^2 G_2'}{2} + x^2(t)G_2''\right) \\
& + \left(\tfrac{G_1' G_2'}{2} + \gamma_o^2 G_1''\left(2G_1'' - G_2''\right)\right)\left(x^2(t)\left(G - G_2'\right) + \tfrac{\gamma_o^2 G_2'}{2} - x(t)y(t)G_2''\right) \\
& + \left(G_1'\left(2G_1' - G_2'\right) - G_1''\left(2G_1'' - G_2''\right)\right)\left\{\begin{array}{l} x^4(t)\left(G - G_4'\right) - \gamma_o^2 x^2\left(G_2' - G_4'\right) \\ \quad + \frac{1}{8}\gamma_o^4\left(4G_2' - G_4'\right) \\ -x^3(t)y(t)G_4'' + \frac{1}{2}x(t)y(t)\gamma_o^2\left(-2G_2'' + G_4''\right)\end{array}\right. \\
& + \left(-2G_1' G_2' G_1'' - G_1'\left(2G_1'' - G_2''\right)\right)\left\{\begin{array}{l} x^3(t)y(t)\left(G - G_4'\right) - x(t)y(t)\gamma_o^2\left(G - \frac{G_2'}{2} - \frac{G_4'}{2}\right) \\ \quad + \gamma_o^4\left(\frac{G_2''}{4} + \frac{G_4''}{8}\right) - x^4(t)G_4'' - x^2(t)\gamma_o^2\left(\frac{G_2''}{2} + G_4''\right)\end{array}\right.
\end{aligned} \tag{3.117}$$

Equations (3.115) and (3.116) show that the conjecture of Eq. (3.2) does not hold for nonseparable constitutive equation although the zeroth-order solution satisfies the conjecture. Similar calculation can be done for the Giesekus model. However, the calculation gives too long equation.

We have applied a perturbation method to nonseparable Maxwell models. Gurnon and Wagner (2012) calculated the power-series solution of the Giesekus model by substitution of assumed solution to the constitutive equation. Their calculation is reduced to solve a set of nonlinear equations of the coefficients of Eq. (3.1). On the other hand, the perturbation method needs not solve a set of nonlinear equations. Hence, it can be said that the perturbation method is more systematic. However, it must be mentioned that both analytical methods give truncated power-series solution whose convergence radius is restricted to small strain amplitude.

Problem 2

[1] Derive Eq. (3.12).
[2] Derive Eqs. (3.21)–(3.24).
[3] Derive Eqs. (3.31) and (3.32).
[4] Derive Eqs. (3.37) and (3.38).
[5] Derive Eqs. (3.51)–(3.55).
[6] Derive Eqs. (3.59)–(3.62).
[7] Derive Eqs. (3.63) and (3.64).
[8] Determine the coefficients of Eq. (3.65) for $N = 3$ and $M = 0$.
[9] Show that Eq. (3.40c) in Chap. 10 is equivalent to Eq. (3.67).
[10] Derive Eqs. (3.69)–(3.72).

4 Semi-analytical Method for LAOS

The analytical methods introduced in previous sections have the limitation in the order of series expansion. Most analytical functions have finite range of convergence. For example, $f(x) = \arctan x$ can be expanded as follows:

$$f(x) = \sum_{k=0}^{\infty} \frac{(-1)^k}{2k+1} x^{2k+1} \tag{4.1}$$

However, this series converges only for $|x| < 1$. Hence, we are worry about the series solutions of the previous section might have a narrow radius of convergence. If our concern is valid, then the analytical solution cannot predict the LAOS behavior of high strain amplitude.

If the purpose of an analytical solution is to use it for the identification of nonlinear parameter of the constitutive equation, then it is sufficient to find the

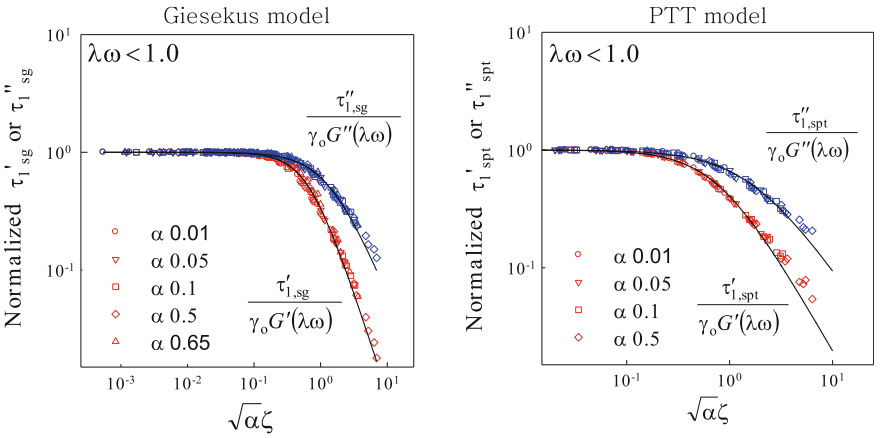

Fig. 11 Superposition of normalized Fourier coefficient of the first harmonic. The *lines* are Eqs. (4.2) and (4.3), and *symbols* are numerical solutions. This figure is redrawn from Bae and Cho (2015)

analytical equations of Fourier coefficients as functions of strain amplitude and frequency. Bae and Cho (2015) invented an idea that circumvents the problem. Their method is a semi-analytical method to find such equations from numerical solutions for various conditions by using the scaling relation addressed in Sect. 2. They checked whether single-mode Giesekus and PTT models obey the strain-frequency superposition or not. They found that τ_1' and τ_1'' of the two models obey the superposition when $\lambda\omega < 1$. This condition agrees with the time–strain separability condition of nonlinear relaxation moduli of the models. Figure 11 indicates that single-mode Giesekus and PTT models show nice superposition when $\tau_1'/(\gamma_o G')$ (or $\tau_1''/(\gamma_o G'')$) is plotted as a function of $\sqrt{\alpha}\zeta$. The superposition is independent of strain amplitude, frequency, and the nonlinear parameter α if $\lambda\omega < 1$. It is not difficult to find the following approximation functions from the superposed data:

$$\tau'_{1,\mathrm{sg}} = \frac{\gamma_o G'_s(\lambda\omega)}{1 + [1.5\sqrt{\alpha}\,\zeta_s(\lambda\omega)]^{1.7}}; \quad \tau''_{1,\mathrm{sg}} = \frac{\gamma_o G''_s(\lambda\omega)}{1 + [0.72\sqrt{\alpha}\,\zeta_s(\lambda\omega)]^{1.4}} \tag{4.2}$$

and

$$\tau'_{1,\mathrm{spt}} = \frac{\gamma_o G'_s(\omega)}{1 + [1.4\sqrt{\alpha}\,\zeta_s(\lambda\omega)]^{1.6}}; \quad \tau''_{1,\mathrm{spt}} = \frac{\gamma_o G''_s(\omega)}{1 + [0.61\sqrt{\alpha}\,\zeta_s(\lambda\omega)]^{1.4}} \tag{4.3}$$

Here, sg and spt imply the single-mode Giesekus and the single-mode PTT models, respectively, and we used the following notations:

$$G_s'(\lambda\omega) = G\frac{\lambda^2\omega^2}{1+\lambda^2\omega^2}; \quad G_s''(\lambda\omega) = G\frac{\lambda\omega}{1+\lambda^2\omega^2} \tag{4.4}$$

and

$$\zeta_s = \gamma_o \cos\delta(\omega) = \gamma_o \frac{G_s'}{\sqrt{\left(G_s'\right)^2 + \left(G_s''\right)^2}} \tag{4.5}$$

Then, the multimode versions are easily obtained as follows:

$$\tau_{1,\Sigma}'(\gamma_o,\omega) = \sum_{k=1}^{N} \tau_{1,s}'(\gamma_o,\lambda_k\omega;G_k); \quad \tau_{1,\Sigma}''(\gamma_o,\omega) = \sum_{k=1}^{N} \tau_{1,s}''(\gamma_o,\lambda_k\omega;G_k) \tag{4.6}$$

Bae and Cho applied Eq. (4.6) to the experimental data of PEO aqueous solution to determine the nonlinear parameter α. Before the fitting, they determined discrete relaxation time spectrum $\{\lambda_k, G_k, N\}$. It is interesting that both numerical solution and semi-analytical equation of Eq. (4.6) for multimode satisfy the strain-frequency superposition of Cho et al. (2010) as shown in Fig. 12.

To check the validity of this semi-analytical method, Bae and Cho compare the Pipkin diagram of the numerical solutions with the values of nonlinear parameter determined from Fig. 12 with experimental data. Figures 13 and 14 are the comparison. As shown in the figures, the semi-analytical method is very effective in determination of the nonlinear parameters of both the Giesekus and the PTT models.

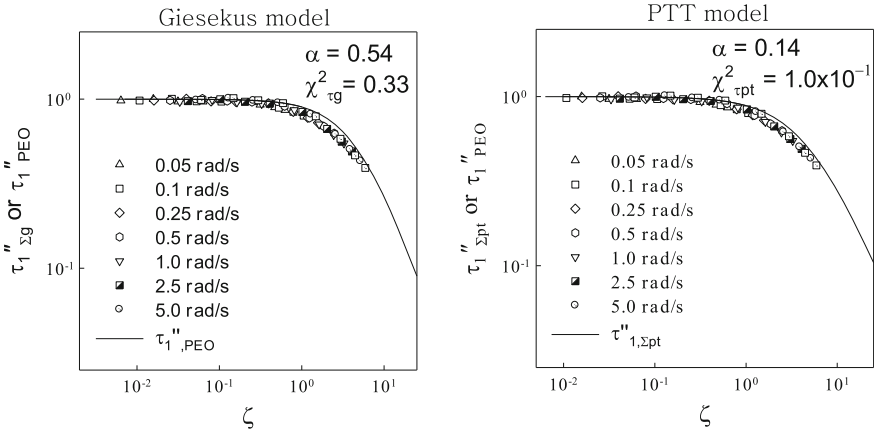

Fig. 12 Superposition of normalized multimode Fourier coefficient of the first harmonic. The *lines* are Eq. (2.6), and *symbols* are experimental data of Cho et al. (2010). This figure is redrawn from Bae and Cho (2015)

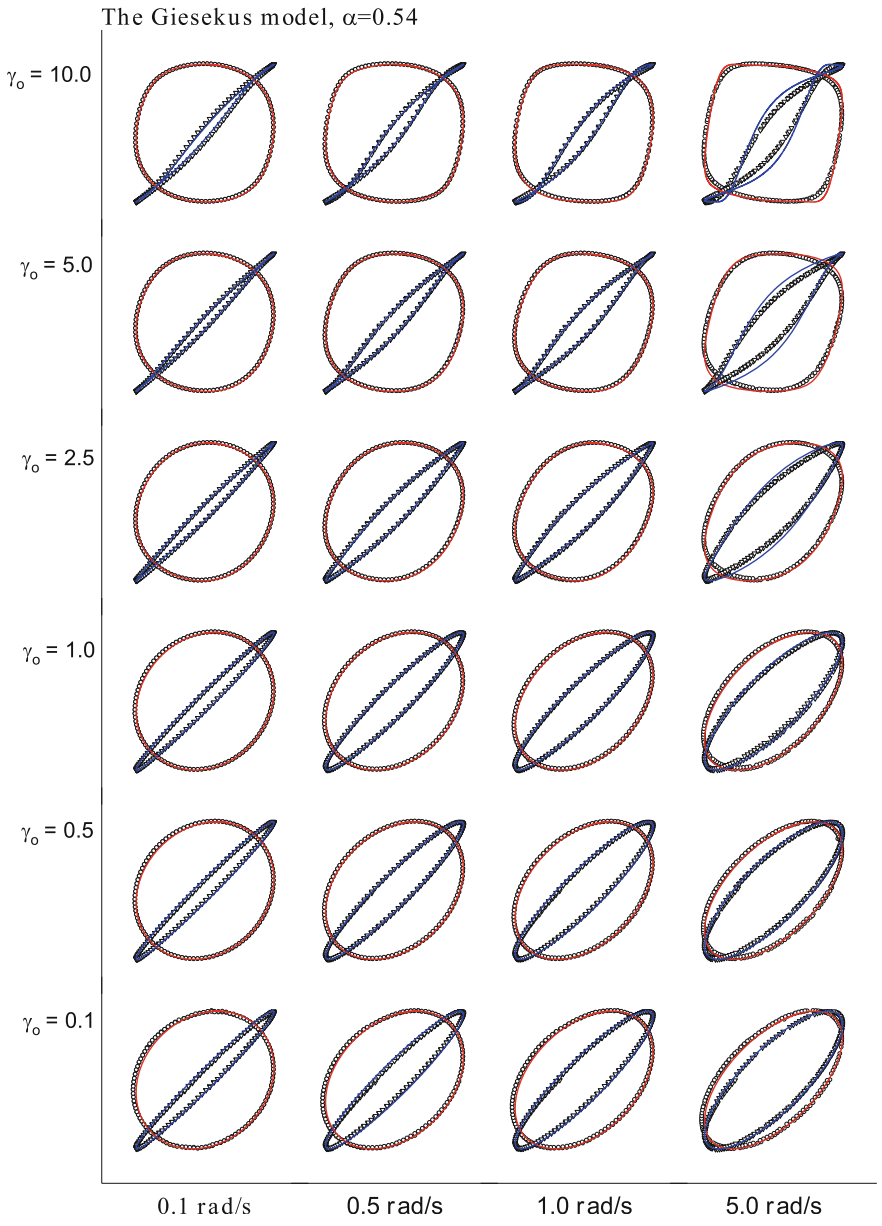

Fig. 13 Comparison of experimental data of PEO aqueous solution and numerical solution of the Giesekus model calculated by the value of $\alpha = 0.54$. This is Fig. 21 of Bae and Cho (2015)

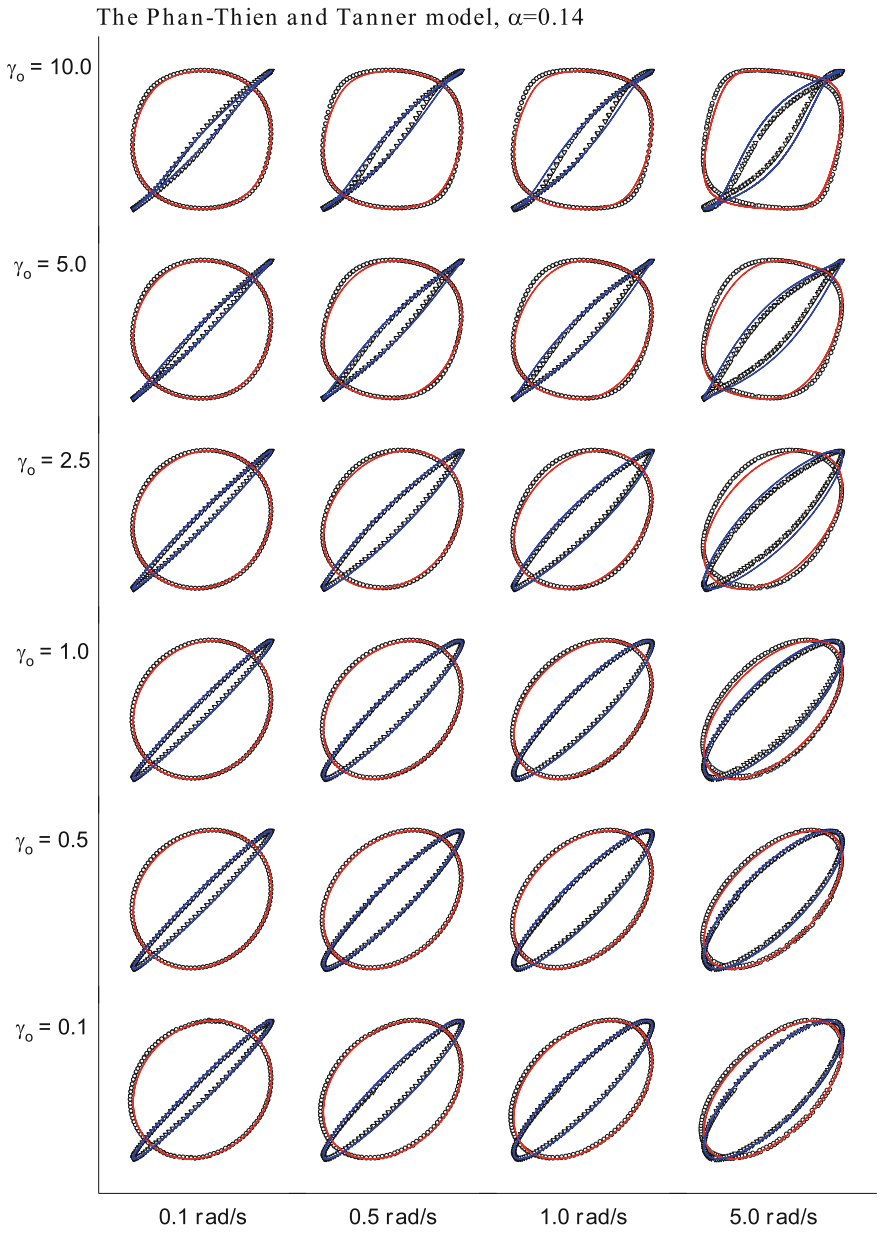

Fig. 14 Comparison of experimental data of PEO aqueous solution and numerical solution of the PTT model calculated by the value of $\alpha = 0.14$. This is Fig. 23 of Bae and Cho (2015)

References

J.-E. Bae, K.S. Cho, Semi-analytical methods for the determination of the nonlinear parameter of nonlinear viscoelastic constitutive equations from LAOS data. J. Rheol. **59**, 525–555 (2015)

J.-E. Bae, M. Lee, K.S. Cho, K.H. Seo, D.G. Kang, Comparison of stress-controlled and strain-controlled rheometers for large amplitude oscillatory shear. Rheol. Acta **52**, 841–857 (2013)

N.A. Bharadwaj, R.H. Ewoldt, The general low-frequency prediction for asymptotically nonlinear material functions in oscillatory shear. J. Rheol. **58**, 891–910 (2014)

M. Boisly, M. Kästner, J. Brummund, V. Ulbricht, Large Amplitude Oscillatory Shear of the Prandtl Element Analysed by Fourier Transform Rheology. Appl. Rheol. **24**, 1–11 (2014)

A. Calin, M. Wilhelm, C. Balan, Determination of the nonlinear parameter (mobility factor) of the Giesekus constitutive model using LAOS procedure. J. Non-Newtonian Fluid Mech. **165**, 1564–1577 (2010)

K.S. Cho, K. Hyun, K.H. Ahn, S.J. Lee, A geometrical interpretation of large amplitude oscillatory shear response. J. Rheol. **49**, 747–758 (2005)

K.S. Cho, K.-W. Song, G.-S. Chang, Scaling relations in nonlinear viscoelastic behavior of aqueous peo solutions under large amplitude oscillatory shear flow. J. Rheol. **54**, 27–63 (2010)

K.S. Cho, J.W. Kim, J.-E. Bae, J.H. Youk, H.J. Jeon, K.-W. Song, Effect of temporary network structure on linear and nonlinear viscoelasticity of polymer solutions. Korea–Aust. Rheol. J. **27**, 151–161 (2015)

C.J. Dimitriou, R.H. Ewoldt, G.H. McKinley, Describing and prescribing the constitutive response of yield stress fluids using large amplitude oscillatory shear stress (LAOStress). J. Rheol. **57**, 27–70 (2013)

B.M. Erwin, S.A. Rogers, M. Cloitre, D. Vlassopoulos, Examining the validity of strain-rate frequency superposition when measuring the linear viscoelastic properties of soft materials. J. Rheol. **54**, 187–195 (2010)

R.H. Ewoldt, Defining nonlinear rheological material functions for oscillatory shear. J. Rheol. **57**, 177–195 (2013)

R.H. Ewoldt, N.A. Bharadwaj, Low-dimensional intrinsic material functions for nonlinear viscoelasticity. Rheol. Acta **52**, 201–219 (2013)

R.H. Ewoldt, G.H. McKinley, On secondary loops in LAOS via self-intersection of Lissajous-Bowditch curves. Rheol. Acta **49**, 213–219 (2010)

R.H. Ewoldt, A.E. Hosoi, G.H. McKinley, New measures for characterizing nonlinear viscoelasticity in large amplitude oscillatory shear. J. Rheol. **52**, 1427–1458 (2008)

R.H. Ewoldt, P. Winter, J. Maxey, G.H. McKinley, Large amplitude oscillatory shear of pseudoplastic and elastoviscoplastic materials. Rheol. Acta **49**, 191–212 (2010)

A.J. Giacomin, J.G. Oakley, Obtaining Fourier series graphically from large amplitude oscillatory shear loops. Rheol. Acta **32**, 328–332 (1993)

A.J. Giacomin, T. Samurkas, J.M. Dealy, A novel sliding plate rheometer for molten plastics. Polym. Eng. Sci. **29**, 499–504 (1989)

A.J. Giacomin, R.B. Bird, L.M. Johnson, A.W. Mix, Large–Amplitude oscillatory shear flow from the co-rotational maxwell model. J. Non-Newtonian Fluid Mech. **166**, 1081–1099 (2011)

A.J. Giacomin, C. Saengow, M. Guay, C. Kolitawong, Padé approximants for large amplitude oscillatory shear flow. Rheol. Acta **54**, 679–693 (2015)

X. Gong, Y. Xu, S. Xuan, C. Guo, L. Zong, W. Jiang, The investigation on the nonlinearity of plasticine-like magnetorehological material under oscillatory shear rheometry. J. Rheol. **56**, 1375–1391 (2012)

A.K. Gurnon, N.J. Wagner, Large amplitude oscillatory shear (LAOS) measurements to obtain constitutive equation model parameters: giesekus model of banding and nonbanding wormlike micelles. J. Rheol. **56**, 333–351 (2012)

E. Helfand, D.C. Pearson, Calculation of the nonlinear stress of polymers in oscillatory shear fields. J. Polym. Sci. Polym. Phys. Ed. **20**, 1249–1258 (1982)

K. Hyun, A study on the nonlinear response of viscoelastic complex fluids under large amplitude oscillatory shear flow, Ph.D. thesis supervised by Prof. S. J. Lee, (Seoul National University, Seoul, 2005)
K. Hyun, M. Wilhelm, Establishing a new mechanical nonlinear coefficient Q from FT-Rheology: first investigation of entangled linear and comb polymer model systems. Macromolecules **42**, 411–422 (2009)
K. Hyun, S.H. Kim, K.H. Ahn, S.J. Lee, Large amplitude oscillatory shear as a way to classify the complex fluids. J. Non-Newtonian Fluid Mech. **107**, 51–65 (2002)
K. Hyun, K.H. Ahn, S.J. Lee, M. Sugimoto, K. Koyama, Degree of branching of polypropylene measured from Fourier-transform rheology. Rheol. Acta **46**, 123–129 (2006)
K. Hyun, E.S. Baik, K.H. Ahn, S.J. Lee, M. Sugimoto, K. Koyama, Fourier–transform rheology under medium amplitude oscillatory shear for linear and branched polymer melts. J. Rheol. **51**, 1319–1342 (2007)
K. Hyun, M. Wilhelm, C.O. Klein, K.S. Cho, J.G. Nam, K.H. Ahn, S.J. Lee, R.H. Ewoldt, G.H. McKinley, A review of nonlinear oscillatory shear tests: analysis and application of large amplitude oscillatory shear (LAOS). Prog. Polym. Sci. **36**, 1697–1753 (2011)
K. Hyun, W. Kim, S.J. Park, M. Wilhelm, Numerical simulation results of the nonlinear coefficient Q from FT-rheology using a single mode pom-pom model. J. Rheol. **57**, 1–25 (2013)
A.I. Isayev, C.M. Wong, Parallel superposition of small- and large-amplitude oscillations upon steady shear flow of polymer fluids. J. Polym. Sci. Polym. Phys. Ed. **26**, 2303–2327 (1988)
M. Kempf, D. Ahirwal, M. Cziep, M. Wilhelm, Synthesis and linear and nonlinear melt rheology of well-defined comb architectures of PS and PpMS with a low and controlled degree of long-chain branching. Macromolecules **46**, 4978–4994 (2013)
H. Kim, K. Hyun, D.-J. Kim, K.S. Cho, Comparison of interpretation methods for large amplitude oscillatory shear response. Korea–Aust. Rheol. J. **18**, 91–98 (2006)
R.G. Larson, *Constitutive equations for polymer melts and solutions* (Butterworths, UK, 1988)
J. Läuger, H. Stettin, Differences between stress and strain control in the non-linear behavior of complex fluids. Rheol. Acta **49**, 909–930 (2010)
X. Li, S.-Q. Wang, X. Wang, Nonlinearity in large amplitude oscillatory shear (LAOS) of different viscoelastic materials. J. Rheol. **53**, 1255–1274 (2009)
H.T. Lim, K.H. Ahn, J.S. Hong, K. Hyun, Nonlinear viscoelasticity of polymer nanocomposites under large amplitude oscillatory shear flow. J. Rheol. **57**, 767–789 (2013)
T. Matsumoto, Y. Segawa, Y. Warashina, S. Onogi, Nonlinear behavior of viscoelastic materials. II. the method of analysis and temperature dependence of nonlinear viscoelastic functions. Trans. Soc. Rheol. **17**, 47–62 (1973)
J.G. Nam, K. Hyun, K.H. Ahn, S.J. Lee, Prediction of normal stresses under large amplitude oscillatory shear flow. J. Non-Newtonian Fluid Mech. **150**, 1–10 (2008)
J.G. Nam, K.H. Ahn, S.J. Lee, K. Hyun, First normal stress difference of entangled polymer solutions in large amplitude oscillatory shear flow. J. Rheol. **54**, 1243–1266 (2010)
T. Neidhöfer, M. Wilhelm, B. Debbaut, Fourier-transform rheology experiments and finite-element simulations on linear polystyrene solutions. J. Rheol. **47**, 1351–1371 (2003)
A. Papon, S. Merabia, L. Guy, F. Lequeux, H. Montes, P. Sotta, D.L. Long, Unique nonlinear behavior of nano-filled elastomers: from the onset of strain softening to large amplitude shear deformations. Macromolecules **45**, 2891–2904 (2012)
E.-K. Park, K.-W. Song, Rheological evaluation of petroleum jelly as a base material in ointment and cream formulations with respect to rubbing onto the human body. Korea–Aust. Rheol. J. **22**, 279–289 (2010)
A.R. Payne, The dynamic properties of carbon black-loaded natural rubber vulcanizates. Part I. J. Appl. Polym. Sci. **6**, 57–63 (1962)
D.S. Pearson, W.E. Rochefort, Behavior of concentrated polystyrene solutions in large-amplitude oscillatory shear fields, J. Polym. Sci., Part B: Polym. Phys. Ed., 20, 83–98 (1982)
W. Pilippoff, Vibrational measurements with large amplitudes. Trans. Soc. Rheol. **10**, 317–334 (1966)

F. Renou, J. Stellbrink, G. Petekidis, Yielding processes in a colloidal glass of soft star-like micelles under large amplitude oscillatory shear (LAOS). J. Rheol. **54**, 1219–1242 (2010)
S.A. Rogers, A sequence of physical processes determined and quantified in LAOS: An instantaneous local 2D/3D approach. J. Rheol. **56**, 1129–1151 (2012)
S.A. Rogers, B.M. Erwin, D. Vlassopoulos, M. Cloitre, A sequence of physical processes and quantified in LAOS: application to a yield stress fluid. J. Rheol. **55**, 435–458 (2011)
C. Saengow, A.J. Giacomin, C. Kolitawong, Exact analytical solution for large-amplitude oscillatory shear flow. Macromol. Theory Simul. **24**, 352–392 (2015)
R. Salehiyan, Y. Yoo, W.J. Choi, K. Hyun, Characterization of morphologies of compatibilized polypropylene/ polystyrene blends with nanoparticles via nonlinear rheological properties from FT-rheology. Macromolecules **47**, 4066–4076 (2014)
E. Senses, P. Akcora, An interface-driven stiffening mechanism in polymer nanocomposites. Macromolecules **46**, 1868–1874 (2013)
H.G. Sim, K.H. Ahn, S.J. Lee, Large amplitude oscillatory shear behavior of complex fluids investigated by a network model: a guide for classification. J. Non-Newtonian Fluid Mech. **112**, 237–250 (2003)
J.W. Swan, R.N. Zia, J.F. Brady, Large amplitude oscillatory microrheology. J. Rheol. **58**, 1–41 (2014)
T.T. Tee, J.M. Dealy, Nonlinear viscoelasticity of polymer melts. J. Rheol. **19**, 595–615 (1975)
D. van Dusschoten, M. Wilhelm, H.W. Spiess, Two-dimensional Fourier transform rheology. J. Rheol. **45**, 1319–1339 (2001a)
D. van Dusschoten, M. Wilhelm, H.W. Spiess, Two-dimensional Fourier transform rheology. J. Rheol. **45**, 1319–1339 (2001b)
I. Vittorias, M. Parkinson, K. Klimke, B. Debbaut, M. Wilhelm, Detection and quantification of industrial polyethylene branching topologies via Fourier-transform rheology, NMR and simulation using the pom-pom model. Rheol. Acta **46**, 321–340 (2007)
M.H. Wagner, R. Rubio, H. Bastian, The molecular stress function model for polydisperse polymer melts with dissipative convective constraint release. J. Rheol. **45**, 1387–1412 (2001)
M.H. Wagner, V.H. Rolón-Garrido, K. Hyun, M. Wilhelm, Analysis of medium amplitude oscillatory shear data of entangled linear and model comb polymer. J. Rheol. **55**, 495–516 (2011)
M. Wilhelm, D. Maring, H.-W. Spiess, Fourier-transform rheology. Rheol. Acta **37**, 399–405 (1998)
M. Wilhelm, P. Reinheimer, M. Ortseifer, High sensitivity Fourier-transform rheology. Rheol. Acta **38**, 349–356 (1999)
M. Wilhelm, P. Reinheimer, M. Ortseifer, T. Neidhöfer, H.W. Spiess, The crossover between linear and nonlinear mechanical behavior in polymer solutions as detected by Fourier-transform rheology. Rheol. Acta **39**, 241–247 (2000)
H.M. Wyss, K. Miyazaki, J. Mattsson, Z. Hu, D.R. Reichman, D.A. Weitz, Strain-rate frequency superposition: a rheological probe of structural relaxation in soft materials. Phys. Rev. Lett. **98**, 238303 (2007)
W. Yu, P. Wang, C. Zhou, General Stress decomposition in nonlinear oscillatory shear flow. J. Rheol. **53**, 215–238 (2009)

Appendix
Functional Derivative

Appendix A: Calculus of Variation

Consider a mapping from a vector space of functions to real number. Such mapping is called *functional*. One of the most representative examples of such a mapping is the action functional of analytical mechanics, A ,which is defined by

$$\mathsf{A}[x(t)] \equiv \int_{t_1}^{t_2} L[x(t), v(t)]\mathrm{d}t \tag{A.1}$$

where t is the independent variable, $x(t)$ is the trajectory of a particle, $v(t) = \mathrm{d}x/\mathrm{d}t$ is the velocity of the particle, and L is the Lagrangian which is the difference of kinetic energy and the potential:

$$L = \frac{m}{2}v^2 - u(x) \tag{A.2}$$

Calculus of variation is the mathematical theory to find the extremal function $\bar{x}(t)$ which maximizes or minimizes the functional such as Eq. (A.1).

We are interested in the set of functions which satisfy the fixed boundary conditions such as $x(t_1) = x_1$ and $x(t_2) = x_2$. An arbitrary element of the function space may be defined from $\bar{x}(t)$ by

$$x(t) = \bar{x}(t) + \varepsilon\eta(t) \tag{A.3}$$

where ε is a real number and $\eta(t)$ is any function satisfying $\eta(t_1) = \eta(t_2) = 0$. Of course, it is obvious that $\bar{x}(t_1) = x_1$ and $\bar{x}(t_2) = x_2$. Varying ε and $\eta(t)$ generates any function of the vector space. Substitution of Eq. (A.3) to Eq. (A.1) gives

$$a(\varepsilon) \equiv \mathsf{A}[\bar{x}(t) + \varepsilon\eta(t)] = \int_{t_1}^{t_2} L\left[\bar{x}(t) + \varepsilon\eta(t), \frac{\mathrm{d}\bar{x}}{\mathrm{d}t} + \varepsilon\frac{\mathrm{d}\eta}{\mathrm{d}t}\right]\mathrm{d}t \tag{A.4}$$

K.S. Cho, *Viscoelasticity of Polymers*, Springer Series
in Materials Science 241, DOI 10.1007/978-94-017-7564-9

From Eq. (A.4), we know that the extremal condition of Eq. (A.1) is equivalent to

$$\left(\frac{\mathrm{d}a}{\mathrm{d}\varepsilon}\right)_{\varepsilon=0} = 0 \tag{A.5}$$

Hence, the introduction of Eq. (A.3) reduces the problems of extremal condition over a function space to those over real number.

Evaluation of Eq. (A.5) can be done by the use of integration by parts:

$$\begin{aligned}\left(\frac{\mathrm{d}a}{\mathrm{d}\varepsilon}\right)_{\varepsilon=0} &= \int_{t_1}^{t_2} \left\{ L_1[\bar{x}(t), \bar{v}(t)]\eta(t) + L_2[\bar{x}(t), \bar{v}(t)]\frac{\mathrm{d}\eta}{\mathrm{d}t} \right\} \mathrm{d}t \\ &= \int_{t_1}^{t_2} \left\{ L_1[\bar{x}(t), \bar{v}(t)] - \frac{\mathrm{d}}{\mathrm{d}t} L_2[\bar{x}(t), \bar{v}(t)] \right\} \eta(t)\mathrm{d}t\end{aligned} \tag{A.6}$$

where

$$L_1 = \frac{\partial}{\partial x} L[x, v]; \quad L_2 = \frac{\partial}{\partial v} L[x, v] \tag{A.7}$$

Since the test function $\eta(t)$ is arbitrary, it is clear that Eq. (A.5) implies

$$\frac{\mathrm{d}}{\mathrm{d}t}\left\{ \frac{\partial}{\partial v} L[x, v] \right\} = \frac{\partial}{\partial x} L[x, v] \tag{A.8}$$

This is the *Euler–Lagrange equation*. Substitution of Eq. (A.2) gives

$$m\frac{\mathrm{d}v}{\mathrm{d}t} = -\frac{\mathrm{d}u}{\mathrm{d}x} \tag{A.9}$$

This is the equation of motion in Newtonian mechanics.

When a binary mixture of fluid is considered, the free energy functional is given in terms of concentration profile $\phi(\mathbf{x})$ as follows:

$$\mathsf{F}[\phi(\mathbf{x})] = \int_{\Omega} f[\phi(\mathbf{x})] + \frac{\gamma}{2}\|\nabla\phi\|^2 \mathrm{d}V \tag{A.10}$$

where $f(\phi)$ is the free energy per unit volume for homogeneous mixture and γ is the material constant representing interfacial tension. Note that if $\phi(\mathbf{x})$ is the concentration of one component, then that of the other component is $1 - \phi(\mathbf{x})$. Thermodynamic theory addresses that the equilibrium concentration minimizes the free energy functional. It is the problem of calculus of variation to determine the

equilibrium concentration profile. As before, we define possible concentration fields by the equilibrium concentration and the test function:

$$\phi(\mathbf{x}) = \bar{\phi}(\mathbf{x}) + \varepsilon\eta(\mathbf{x}) \tag{A.11}$$

The test function $\eta(\mathbf{x})$ is zero on the boundary $\partial\Omega$ of the domain of the mixture fluid. Substitution of Eq. (A.11) to Eq. (A.10) and differentiation with respect to ε give

$$\left(\frac{\partial}{\partial\varepsilon}\mathsf{F}\left[\bar{\phi}(\mathbf{x}) + \varepsilon\eta(\mathbf{x})\right]\right)_{\varepsilon=0} = \int_\Omega \frac{\mathrm{d}f}{\mathrm{d}\phi}\eta(\mathbf{x})\mathrm{d}V + \gamma\int_\Omega \nabla\phi\cdot\nabla\eta\,\mathrm{d}V = 0 \tag{A.12}$$

Application of the divergence theorem to Eq. (A.12) gives

$$\int_\Omega \left[\frac{\mathrm{d}f}{\mathrm{d}\phi} - \gamma\nabla^2\phi\right]\eta(\mathbf{x})\mathrm{d}V = 0 \tag{A.13}$$

Since this equality must be hold for arbitrary domain, we have

$$\frac{\mathrm{d}f}{\mathrm{d}\phi} = \gamma\nabla^2\phi \tag{A.14}$$

This is the Euler–Lagrange equation for scalar field.

It is more convenient to use the notation such that $\delta x(t) \equiv \varepsilon\eta(t)$ for Eq. (A.3) or $\delta\phi(\mathbf{x}) \equiv \varepsilon\eta(\mathbf{x})$ for Eq. (A.11). This notation is called variational notation. Consider a functional defined by

$$\mathsf{A} = \int_{t_1}^{t_2} L[t, q_1(t), \ldots, q_n(t), \dot{q}_1(t), \ldots, \dot{q}_n(t)]\mathrm{d}t \tag{A.15}$$

where $\dot{q}_k(t) = \mathrm{d}q_k/\mathrm{d}t$. The variation of the functional is defined as

$$\delta\mathsf{A} = \mathsf{A}[\mathbf{q}(t) + \delta\mathbf{q}(t), \dot{\mathbf{q}}(t) + \delta\dot{\mathbf{q}}(t)] - \mathsf{A}[\mathbf{q}(t), \dot{\mathbf{q}}(t)] \tag{A.16}$$

where $\mathbf{q}(t) = [q_1(t), \ldots, q_n(t)]$ and $\dot{\mathbf{q}}(t) = [\dot{q}_1(t), \ldots, \dot{q}_n(t)]$ are short notation. It is implied that

$$\delta\dot{q}_k = \frac{\mathrm{d}\delta q_k}{\mathrm{d}t} \tag{A.17}$$

Then, Eq. (A.16) implies that

$$\begin{aligned}\delta \mathsf{A} &= \int_{t_1}^{t_2} \{L[t, \mathbf{q}(t) + \delta\mathbf{q}(t), \dot{\mathbf{q}}(t) + \delta\dot{\mathbf{q}}(t)] - L[t, \mathbf{q}(t), \dot{\mathbf{q}}(t)]\} \mathrm{d}t \\ &= \sum_{k=1}^{n} \int_{t_1}^{t_2} \left[\frac{\partial L}{\partial q_k} \delta q_k + \frac{\partial L}{\partial \dot{q}_k} \delta \dot{q}_k \right] \mathrm{d}t\end{aligned} \tag{A.18}$$

Application of the integration by parts to the second integration gives

$$\delta \mathsf{A} = \sum_{k=1}^{n} \left[\frac{\partial L}{\partial \dot{q}_k} \delta q_k \right]_{t=t_1}^{t=t_2} + \sum_{k=1}^{n} \int_{t_1}^{t_2} \left[\frac{\partial L}{\partial q_k} - \frac{\mathrm{d}}{\mathrm{d}t} \frac{\partial L}{\partial \dot{q}_k} \right] \delta q_k \mathrm{d}t \tag{A.19}$$

Here, we again use the boundary conditions for the variations such that $\delta q_k(t_1) = \delta q_k(t_2) = 0$ for any k. Then, Eq. (A.19) becomes

$$\delta \mathsf{A} = \sum_{k=1}^{n} \int_{t_1}^{t_2} \left[\frac{\partial L}{\partial q_k} - \frac{\mathrm{d}}{\mathrm{d}t} \frac{\partial L}{\partial \dot{q}_k} \right] \delta q_k \mathrm{d}t \tag{A.20}$$

Since we can take δq_k independently, $\delta \mathsf{A} = 0$ implies that for any k,

$$\frac{\partial L}{\partial q_k} - \frac{\mathrm{d}}{\mathrm{d}t} \frac{\partial L}{\partial \dot{q}_k} = 0 \tag{A.21}$$

For a multivariable function $f(x_1, \ldots, x_n)$, the differential of the function is given by

$$\mathrm{d}f = \sum_{k=1}^{n} \frac{\partial f}{\partial x_k} \mathrm{d}x_k \tag{A.22}$$

The stationary condition for the function is that for any k,

$$\frac{\partial f}{\partial x_k} = 0 \tag{A.23}$$

Equation (A.20) is very similar to Eq. (A.22), and the Euler–Lagrange equation (A.21) is also similar to Eq. (A.23). Hence, it can be said that the Euler–Lagrange equation is the condition that the derivative of the functional A becomes zero. This analogy provides a clue to define functional derivative. We shall introduce a generalized derivative called the Gâteaux derivative which is a generalization of directional derivative.

Appendix B: Gâteaux Derivative

Derivative can be considered a linear mapping from the infinitesimal variation of domain to that of image. Consider a real-valued function whose domain is real number, $y = f(x)$. From elementary calculus, we know that

$$\mathrm{d}y = f'(x)\mathrm{d}x \tag{B.1}$$

Note that $\mathrm{d}y$ is the infinitesimal variation of image, while $\mathrm{d}x$ is that of domain. If domain is position vector and image is scalar field, we know that when $y = f(\mathbf{x})$,

$$\mathrm{d}y = \nabla f \cdot \mathrm{d}\mathbf{x} \tag{B.2}$$

The gradient ∇f is the derivative of $f(\mathbf{x})$. As for vector field, $\mathbf{v} = \mathbf{v}(\mathbf{x})$, we know that

$$\mathrm{d}\mathbf{v} = (\nabla \mathbf{v})^T \cdot \mathrm{d}\mathbf{x} \tag{B.3}$$

Then, the tensor $(\nabla \mathbf{v})^T$ is the derivative of the vector field $\mathbf{v}$. In Sect. 5.3, we learned the relation between directional derivative and gradient. Remember that

$$\frac{\mathrm{d}}{\mathrm{d}t} f(\mathbf{x} + t\mathbf{h})\bigg|_{t=0} = \nabla f \cdot \mathbf{h} \tag{B.4}$$

and

$$\frac{\mathrm{d}}{\mathrm{d}t} \mathbf{v}(\mathbf{x} + t\mathbf{h})\bigg|_{t=0} = (\nabla \mathbf{v})^T \cdot \mathbf{h} \tag{B.5}$$

Consider a vector space with a suitable norm which corresponds to the magnitude of vector. The vector space can be a set of numbers, vectors, tensors, or functions. For a mapping F from vector space X to vector space Y, the *Gâteaux derivative* of the mapping is defined as

$$\mathrm{d}_{\mathrm{G}}\mathsf{F}(x; h) = \lim_{\varepsilon \to 0} \frac{\mathsf{F}(x + \varepsilon h) - \mathsf{F}(x)}{\varepsilon} = \left(\frac{\partial}{\partial \varepsilon} \mathsf{F}(x + \varepsilon h) \right)_{\varepsilon = 0} \tag{B.6}$$

where $x \in \mathrm{X}$, $h \in \mathrm{X}$, and $\mathsf{F}(x) \in \mathrm{Y}$. If x is a position vector and the image of F is a real number, then Eq. (B.6) implies the directional derivative in the direction to h. Higher-order Gâteaux derivative can be defined by

$$\mathrm{d}_{\mathrm{G}}^2\mathsf{F}(x; h_1, h_2) = \left(\frac{\partial^2}{\partial \varepsilon_1 \partial \varepsilon_2} \mathsf{F}(x + \varepsilon_1 h_1 + \varepsilon_2 h_2) \right)_{\varepsilon_1 = \varepsilon_2 = 0} \tag{B.7}$$

If F is a mapping from function to real number, the Gâteaux derivative is related to the *functional derivative*. As for the functional of Eq. (A.1), the Gâteaux derivative is given by

$$\mathrm{d}_G\mathsf{A}[x(t);\delta x(t)] = \int_{t_1}^{t_2} \frac{\delta \mathsf{A}}{\delta x(t)}\delta x(t)\mathrm{d}t \tag{B.8}$$

where we used the following notation:

$$\frac{\delta \mathsf{A}}{\delta x(t)} \equiv -u'[x(t)] - m\frac{\mathrm{d}^2 x}{\mathrm{d}^2 t} \text{ with } u'(\xi) = \frac{\mathrm{d}u(\xi)}{\mathrm{d}\xi} \tag{B.9}$$

Analogy to Eqs. (B.4) and (B.5), it can be said that $\delta\mathsf{A}[x(\bullet)]/\delta x(t)$ is the *functional derivative*. Hence, calculus of variation is to find the functional derivative. Then, using this notation, we have

$$\mathrm{d}_\mathrm{G}^2\mathsf{A}[x(t);\delta x(t)] = \int_{t_1}^{t_2}\int_{t_1}^{t_2} \frac{\delta^2 \mathsf{A}}{\delta x(t)\delta x(t')}\delta x(t)\delta x(t')\mathrm{d}t\,\mathrm{d}t' \tag{B.10}$$

Note that a function can be considered as a special case of functional. Using the Dirac delta function, a function $f(t)$ can be represented by

$$f(t) = \int_{-\infty}^{\infty} f(\tau)\delta(\tau - t)\mathrm{d}\tau \equiv \mathsf{F}[f(t)] \tag{B.11}$$

Application of the Gâteaux derivative gives

$$\frac{\delta \mathsf{F}[f(t)]}{\delta f(\tau)} = \frac{\delta f(t)}{\delta f(\tau)} = \delta(t - \tau) \tag{B.12}$$

As for the derivative of a function, we know that

$$\int_{-\infty}^{\infty} f(\tau)\delta'(\tau - t)\mathrm{d}\tau = -\int_{-\infty}^{\infty} f'(\tau)\delta(\tau - t)\mathrm{d}\tau \tag{B.13}$$

We have

$$\frac{\delta f'(t)}{\delta f(\tau)} = -\delta'(t - \tau) \tag{B.14}$$

With the help of Eqs. (B.12) and (B.13), it is obvious that

$$\frac{\delta^2 \mathsf{A}}{\delta x(t)\delta x(t')} = -u''(x(t))\delta(t-t') - m\delta''(t-t') \tag{B.15}$$

Equation (B.6) implies that when $x \in \mathrm{X}$ and $h \in \mathrm{X}$

$$\mathsf{F}(x+h) = \mathsf{F}(x) + \int_0^1 \mathrm{d}_{\mathrm{G}}\mathsf{F}(x+th;h)\mathrm{d}t \tag{B.16}$$

Then, the use of Eq. (B.16) gives the Taylor expansion of F such that

$$\mathsf{F}(x+h) = \mathsf{F}(x) + \mathrm{d}_{\mathrm{G}}\mathsf{F}(x;h) + \frac{1}{2!}\mathrm{d}_{\mathrm{G}}^2\mathsf{F}(x;h) + \cdots + \frac{1}{n!}\mathrm{d}_{\mathrm{G}}^n\mathsf{F}(x;h) + \mathsf{R}_{n+1} \tag{B.17}$$

where

$$\mathsf{R}_{n+1} \equiv \frac{1}{n!}\int_0^1 (1-t)^n \mathrm{d}_{\mathrm{G}}^{n+1}\mathsf{F}(x+th;h)\mathrm{d}t \tag{B.18}$$

Consider the functional of Eq. (2.1) in Chap. 10. Assume that the functional of Eq. (2.1) in Chap. 10 has the following form:

$$\mathbf{e}_i \cdot \overset{\tau=t}{\underset{\tau=-\infty}{\mathsf{T}}}[\mathbf{C}_t(\mathbf{x},\tau)] \cdot \mathbf{e}_k = \int_{-\infty}^{t} P_{ik}[\mathbf{C}_t(\mathbf{x},\tau)]\mathrm{d}\tau \equiv \mathsf{S}_{ik}[\mathbf{C}_t(\mathbf{x},\tau)] \tag{B.19}$$

where $P_{ik}[\mathbf{X}]$ is the ikth component of a tensor-valued function of a tensor $\mathbf{X}$. We know that

$$\begin{aligned}
\mathrm{d}_{\mathrm{G}}\mathsf{S}_{ik}[\mathbf{X}(\tau);\delta\mathbf{X}(\tau)] &= \int_{-\infty}^{t} \frac{\delta \mathsf{S}_{ik}}{\delta X_{ab}(\tau)}\delta X_{ab}(\tau)\mathrm{d}\tau \\
\mathrm{d}_{\mathrm{G}}^2 T'_{ik}[\mathbf{X}(\tau);\delta\mathbf{X}(\tau)] &= \int_{-\infty}^{t}\int_{-\infty}^{t} \frac{\delta^2 \mathsf{S}_{ik}}{\delta X_{ab}(\tau)\delta X_{cd}(\tau')}\delta X_{ab}(\tau)\delta X_{cd}(\tau)\mathrm{d}\tau\,\mathrm{d}\tau' \\
&\vdots
\end{aligned} \tag{B.20}$$

Then, the Taylor expansion of $\mathsf{S}_{ik}[\mathbf{C}_t(\mathbf{x},\tau)]$ about $\mathbf{I} = \mathbf{C}_t(\mathbf{x},t)$ is given by

$$\begin{aligned}\mathsf{S}_{ik}[\mathbf{C}_t(\mathbf{x},\tau)] \approx & \int_{-\infty}^{t} \frac{\delta \mathsf{S}_{ik}}{\delta X_{ab}(\tau)} \left[C_t^{ab}(\mathbf{x},\tau) - \delta_{ab}\right] \mathrm{d}\tau \\ & + \frac{1}{2} \int_{-\infty}^{t} \int_{-\infty}^{t} \frac{\delta^2 \mathsf{S}_{ik}}{\delta X_{ab}(\tau) \delta X_{cd}(\tau')} \left[C_t^{ab}(\mathbf{x},\tau) - \delta_{ab}\right] \left[C_t^{cd}(\mathbf{x},\tau) - \delta_{cd}\right] \mathrm{d}\tau \, \mathrm{d}\tau' \\ & + \cdots \end{aligned} \tag{B.21}$$

This is the derivation of Eq. (2.4) in Chap. 10.

Index

A
Arrhenius equation, 443

B
Bagley correction, 504
Bernstein basis polynomials, 368
Blatz model, 277
Body force, 112
Boltzmann superposition principle, 142, 288
Bond correlation function, 240
Branching parameter, 242
Brownian motion, 211
Bulk modulus, 125

C
Canonical ensemble, 191
Caputo derivative, 329
Carreau-Yasuda model, 135
Cauchy sequence, 11
Cauchy stress, 117
Cayley-Hamilton theorem, 66, 131
Central limit theorem, 184
Chandrasekhar equation, 227
Chapman-Kolmogorov equation, 214
Characteristic function, 180
Characteristic ratio, 249
Chebyshev nodes, 365
Clausius-Duhem inequality, 157
Clausius inequality, 152
Coefficient of variation, 383
Cole-Cole model, 323
Cole-Cole plot, 323
Conditional probability, 181
Cone-and-plate fixture, 303
Configuration, 94
Conformation tensor, 527
Constitutive equation, 113
Contact force, 112
Continuous retardation spectrum, 317
Constraction map, 376
Contravariant base vectors, 30
Convolution theorem, 83
Covariant base vectors, 30
Cox-Merz relation, 505
Creep compliance, 139, 290
Creep ringing, 311
Creep test, 290
Critical molecular weight, 136
Cubic Hermite polynomial, 366
Cumulant generating function, 180
Current configuration, 94

D
Damping function, 519
Davies and Anderssen limit, 425
Deborah number, 286
Deformation gradient, 97
Deformation rate tensor, 103
Deformed configuration, 94
Diffusion wave spectroscopy, 313
Dirac delta function, 138
Discrete fourier transform (DFT), 361
Discrete relaxation time spectrum, 316
Discrete retardation time spectrum, 317
Displacement vector, 99
Double reptation, 474
Dynamic moduli, 294

E
Eight-constant model, 514
End-to-end vector, 239
Engineering strain, 99
Entanglement concentration, 264
Enthalpy, 153

K.S. Cho, *Viscoelasticity of Polymers*, Springer Series
in Materials Science 241, DOI 10.1007/978-94-017-7564-9

Entropy production, 156
Equal a priori probability, 188
Equipartition theorem, 204
Ergodic hyperthesis, 205
Euler-Lagrange equation, 602
Eulerian description, 95
Eulerian objective vectors and tensors, 172
Extended irreversible thermodynamics, 161
Extensional flow, 492

F
Fading memory, 105, 138
Fast Fourier transform (FFT), 314, 394
Finitely extensible nonlinear elastic model (FENE), 270, 379
Finite extensible nonlinear elasticity preaverage (FENE-P), 529
Fick's diffusion law, 215
Final value theorem of Laplace transform, 291
Fixed-point iteration, 415
Flory theorem, 335
Flow direction, 134
Fluctuation-dissipation theorem, 213
Fokker-Planck equation, 187, 223
Fourier Transform Rheology (FT-Rheology), 547
Fractional derivative, 142
Fractional models, 142
Fredholm integral equation of the 1st kind, 406
Freely jointed chain model (FJC), 242
Freely rotating chain model (FRC), 242
Froude number, 133
Fuoss-Kirkwood relation, 398
Functional, 601
Functional derivative, 606

G
Gâteaux derivative, 605
Gaussian distribution function, 184
Generalized Langevin equation, 222
Generalized Maxwell model, 141
Generalized Voigt model, 141
Gibbs free energy, 153
Gradient direction, 134
Gram-Schmidt orthogonalization, 15
Grand canonical ensemble, 193

H
Hamiltonian, 178
Heat conductivity, 118
Heat flux, 118
Helmholtz free energy, 153
Hilbert space, 11
Hindered rotation chain model (HRC), 242
Hookean body, 136
Hydrodynamic interaction, 335
Hydrodynamic screening length, 336

I
Ideal chain, 240
Inaccessible statement of Caratheodory, 152
Incompressible fluid, 132
Incompressible solid, 127
Inertial pressure scale, 133
Infinitesimal strain, 99
Information theory, 191
Internal energy, 119
Internal variables, 143, 161
The intersection condition of coordinate lines, 28
Inverse integration with regularization (IIR), 386
Inverse tensor, 62
Invertible tensor, 62
Isotropic tensor, 69

J
Jaumann time derivative, 174
Jeffreys model, 140
Joint probability density function, 181

K
Kelvin-Voigt model, 138
Kohlrausch-Williams-Watts (KWW) equation, 142
Kramers-Kronig relations, 298
Kronecker's delta, 8

L
Lagrangian description, 95
Lagrangian objective tensors, 172
Laminar flow, 492
Langevin equation, 187, 212
LAOStrain, 563
LAOStress, 563
Large amplitude oscillatory shear (LAOS), 545
Least square method, 363
Left Cauchy-Green tensor, 98
Legendre transform, 154
Levenberg-Marquardt method, 369
Liouville equation, 209, 216
Liouville operator, 217
Lissajous-Bowditch loop (LB loop), 546
Lodge equation, 511
Long-range interaction, 240
Loss modulus, 294

Loss tangent, 300
Lower-convected time derivative, 511
Lower-convective time derivative, 174

M
Marginal distribution function, 181
Mark-Houwink equation, 260
Material coordinate, 94
Material description, 95
Material time derivative, 95
Maxwell distribution, 226
Maxwell model, 137
Mean relaxation time, 297
Memory function, 145
Microcanonical ensemble, 188
Microrheology, 315
Microstate variables, 178
Middle amplitude oscillatory shear (MAOS), 548
Modulus, 125
Molecular stress function model (MSF model), 553
Mooney-Rivlin model, 273
Mooney-Rivlin plot, 273

N
Navier equation, 129
Navier-Stokes equation, 132
Neo-Hookean model, 273
Newtonian fluid, 131
Nonlinear regularization, 414
Norm, 11
Normal equations, 363
N^{th} cumulant, 180
N^{th} order Rivlin-Ericksen tensor, 508

O
Objective time derivatives, 174
Ogden model, 277
Orthogonal tensor, 61
Overlap concentration, 262

P
Pade approximation, 378
Parallel plate fixture, 303
The parallelism of coordinate line, 29
Partition function, 189
Phase angle, 300
Phase space, 178
Piola-Kirchhoff stress of the 1st kind, 117
Piola-Kirchhoff stress of the 2nd kind, 117
Pipkin diagram, 287
Plot of van Gurp and Palmen, 452
Poisson's ratio, 126
Polar decomposition, 97
Post-Widder formula, 411
Power law fluid model, 136
Primitive chain, 347
Principle of causality, 138, 289
Principle of material frame-indifference, 129, 173
Proper transform, 30
Pseudo-inverse, 413
Pseudo inverse matrix, 387
Phan-Thien and Tanner (PTT) model, 533

R
Radius of gyration, 241
Rational thermodynamics, 160
Real chain, 240
Reference configuration, 94
Relative deformation gradient, 105
Relative finger deformation tensor, 106
Relative Piola deformation tensor, 106
Relaxation modulus, 288
Relaxation time spectrum, 142
Retardation time, 139, 140
Retardation time spectrum, 142
Reynolds number, 133
Reynolds transport theorem, 112
Riemann and Liouville derivative, 329
Right Cauchy-Green tensor, 98, 348
Rigid body, 96
Rivlin-Ericksen tensors, 107
Root-mean-square error, 363
Runge phenomenon, 366

S
Secondary critical molecular weight, 441
The second order fluid, 509
Sharda model, 277
Shear flow, 492
Shear modulus, 126
Shear rate, 134
Shear stress, 126
Shear-thinning fluids, 136
Short-range interaction, 240
Simple elongation, 126
Simple shear, 125
Singular value, 387
Singular value decomposition, 387, 413
Small amplitude oscillatory shear (SAOS), 545
Smoluchowski equation, 227, 525
Spatial description, 95

Specific heat capacity, 120
Spin tensor, 103
Standard solid model, 140
State variables, 147
Statistical independence, 182
Steady-state compliance, 293
Stokes-Einstein equation, 213
Stokes flow, 134
Storage modulus, 294
Strain-frequency superposition (SFS), 548, 563
Strain-rate frequency superposition (SRFS), 548, 563
Streamlines, 492
Stress, 112
Stress-controlled and strain-controlled rheometers, 302
Stress decomposition (SD), 547
Stress-optical rule, 348
Stress power, 120
Stress relaxation test, 288
Stress vector, 112, 114
Strouhal number, 133
Sum of state, 189

T
Tangent base vectors, 29
Thermodynamic limit, 201
Thermodynamic process, 147
Tikhonov regularization, 371, 386, 414
Time-strain separable K-BKZ model, 517
Time-temperature superposition, 438
Trouton relation, 506
True stress, 117
Tschoegl model, 277

U
Unit step function, 138
Upper-convective Maxwell model, 168, 512
Upper-convective time derivative, 168

V
Valanis-Landel hypothesis, 274
Valanis-Landel model, 277
Velocity gradient, 102
Viscometric flow, 493
Viscous pressure scale, 133
Voigt model, 138
Vorticity direction, 134

W
Warner's approximation, 379
Weight-average molecular weight, 136
Weissenberg-Rabinowitsch equation, 504
Wick's theorem, 186

Y
Young's modulus, 126

Z
Zero-shear viscosity, 135, 293